CHEMICAL PROFILING OF THE STREET COCKTAIL DRUG 'NYAOPE' IN SOUTH AFRICA USING GAS CHROMATOGRAPHY-MASS SPECTROMETRY (GC-MS)

by

PABALALA MESHACK MTHEMBI

Dissertation submitted in fulfilment of the requirements for the degree
Doctor of Philosophy
(PhD)

in the

Department of Genetics
Faculty of Natural and Agriculture Sciences,

at the University of the Free State
Bloemfontein

September 2020

Promoter: Dr E.M. Mwenesongole
Co-promoters: Prof M.D. Cole Anglia Ruskin University, Cambridge, U.K.
Prof J.P. Grobler

DECLARATION

I, Pabalala Meshack Mthembi declare that the Doctoral research dissertation that I herewith submit at the University of the Free State, is my independent work and that I have not previously submitted it for qualification at another institution of higher education.

_____ _____

Pabalala Meshack Mthembi Date

ACKNOWLEDGEMENTS

- First of all, I would like to thank the South African Police Service – Forensic Science Laboratory, as well the University of the Free State's research bursary fund under the Genetics Department for the financial support.
- A special thanks goes to my supervisor, Dr E.M. Mwenesongole and my co-supervisor Prof Michael D. Cole. Without your guidance and advice, this project would not have been a success. Thank you for being for so patient with me throughout this journey.
- I am grateful to the head of the Genetics department, Prof J.P. Grobler, for his support in disseminating the research at conferences.
- Thank you, Prof M.D. Cole and Anglia Ruskin University, Cambridge, U.K., for the financial support in disseminating the research through publication.
- I am grateful to the South African Police Service Forensic Science Laboratory (SAPS-FSL) for providing us with seized street samples and allowing us to use their resources to conduct the research.
- I am also thankful to Aspen Pharmacare for donating the antiretroviral drugs (efavirenz and nevirapine).
- I thank my colleagues at the SAPS-FSL for their patience and for giving me the preference to run those many samples even when the pressure was upon them to analyse their backlog samples.
- A special thanks goes to Wendy Bebeda for assisting me with the preparation of the blind simulated samples.
- Thank you, Tebogo Golele, for the technical assistance with the instrumentation.
- To my wife Lindiwe and my children, Hlengiwe, Ntsako and Nyiko; thank you for the moral support and giving me the space to work on my studies.

Thanks to the Almighty for giving me strength and wisdom to fulfil my dream.

SUMMARY

The street cocktail drug nyaope, commonly found in South Africa, is a mixture of low-grade heroin, cannabis products, antiretroviral drugs and other materials added as bulking agents. This research led to the development of an analytical method for the identification and profiling of the street cocktail drug nyaope, using gas chromatography – mass spectrometry.

This study determined for the first time the most suitable organic solvent in which the common components of nyaope, namely Δ^9-tetrahydrocannabinol, heroin, caffeine, dextromethorphan, phenacetin and the antiretrovirals efavirenz and nevirapine, which have different chemical characteristics, are stable prior to an analysis of nyaope samples. The main nyaope components, when extracted into tertiary butyl alcohol, exhibited the greatest autosampler stability of up to 72 hours of storage. From these results it can be determined that tertiary butyl alcohol is a suitable solvent for the identification, comparison and profiling of nyaope samples.

With regard to analytical method validation, the method gave acceptable repeatability with the %RSD less than 10% for the 10.0 and 1000.0 mg/L concentration levels for the majority of the components. The linear concentration ranges managed linearity with $r^2 \geq 0.997$. The detection limits varied between 9.90–39.0 pg on column and the limit of quantitation between 30.0–120 pg on column. The method exhibited acceptable recoveries and ruggedness. The method developed is fit for the purpose of quantitative profiling of the major components of nyaope using gas chromatography-mass spectrometry.

The majority of the components in the street cocktail drug nyaope were shown to be stable up to at least 24 hours when stored in a refrigerator. For profiling purposes, samples need to be extracted within 24 hours of seizure in a solvent in which they are stable, such as tertiary butyl alcohol and analysed within 72 hours. At all times the samples need to be protected from light to prevent the photo-decomposition of Δ^9-tetrahydrocannabinol and from moisture to prevent the hydrolysis of diamorphine.

The chemical components of simulated nyaope samples as well as actual seized street nyaope samples were successfully identified and quantitatively determined using gas chromatography – mass spectrometry. The simulated and actual seized street samples were successfully discriminated into original batches using the identified nyaope components and two unsupervised chemometric methods, namely principal component analysis and hierarchical clustering, as well as chromatographic profiles.

Thus, for the first time, a validated analytical method has been developed for the identification, quantitation and profiling of nyaope using gas chromatography – mass spectrometry. The method will assist law enforcement agencies in the identification and comparison of nyaope samples and facilitate the prosecution of illicit drug trafficking offences.

Keywords: Heroin, nyaope, gas chromatography – mass spectrometry.

PUBLICATIONS IN SUPPORT OF THE THESIS

The following outputs have resulted from the work conducted for this study.

Mthembi, P.M.; Mwenesongole, E.M.; Cole, M.D. 2018. Chemical profiling of the street cocktail drug 'nyaope' in South Africa using GC–MS I: Stability studies of components of 'nyaope' in organic solvents. *Forensic Science International*, 292, pp. 115-124.

Mthembi, P.M.; Mwenesongole, E.M.; Cole, M.D. 2019. Chemical profiling of the street cocktail drug 'nyaope' in South Africa using GC–MS II: Stability studies of the cannabinoid, opiate and antiretroviral components during sample storage. *Forensic Science International*, 300, pp. 187-192.

Mthembi, P.M.; Mwenesongole, E.M.; Cole, M.D. 2020.Chemical profiling of the street cocktail drug 'nyaope' in South Africa using GC–MS III: A validated method for drug extraction and GC – MS analysis for the identification and comparison of 'nyaope' samples. *South African Journal of Science*. Submitted.

Oral presentation: Stability studies of components of 'Nyaope' in organic solvents. Analytika conference. Legend Golf and Safari Resort. Mokgophong. South Africa. Awarded 2nd Prize Winner for the presentation by the Analytical Division of SACI (South African Chemical Institute)

TABLE OF CONTENTS

LIST OF FIGURES

(All chemical structures were drawn using ChemDraw Ultra 8 and graphs were produced using Microsoft Excel© 2010).

LIST OF TABLES

APPENDICES

LIST OF ABBREVIATIONS

ABBREVIATIONS RELATING TO ANTIRETROVIRAL DRUGS, CANNABINOIDS AND OPIATES

3-MAM	O^3 Monacetylmorphine
6-MAM	O^6 Monacetylmorphine
ACOD	Acetylcodeine
ARV	Antiretroviral
CBCA	Cannabichromenic acid
CBCM	Cannabichromene
CBCN	Cannabicoumaronone
CBD	Cannabidiol
CBDA	Cannabidiolic Acid
CBE	Cannabielsoin
CBEA	Cannabielsoic acid
CBG	Cannabigerol
CBGA	Cannabigerolic acid
CBL	Cannabicyclol
CBLA	Cannabicyclolic acid
CBN	Cannabinol
CBNA	Cannabinolic acid
CBND	Cannabinodiol
CBNDA	Cannabinodiolic acid
CBT	Cannabitriol
CBV	Cannabivarin
COD	Codeine
DAM	Diamorphine
DTM	Dextromethorphan
EFV	Efavirenz
Δ^8-THC	Δ^8-tetrahydrocannabinol
Δ^9-THC	Δ^9-tetrahydrocannabinol
Δ^9-THCA	Δ^9-tetrahydrocannabinolic acid

GENERAL ABBREVIATIONS

ACA	Acetaminophen
AFLP	Amplified fragment length polymorphism
ANOVA	Analysis of variance
ARV	Antiretroviral
t-BuOH	*tertiary* Butyl Alcohol
CAFF	Caffeine
CCR5	Chemokine Coreceptor Type 5
CD4	Cluster of Differentiation 4
CE	Capillary electrophoresis
CE-PDA	Capillary electrophoresis-photodiode array
COC	Cocaine
COSY	Proton-proton Correlation Spectroscopy
CZE	Capillary zone electrophoresis
CZE-DAD	Capillary zone electrophoresis- diode array detector
CZE-UV	Capillary zone electrophoresis- ultraviolet detection
DCM	Dichloromethane
DFTPP	Decafluorotriphenylphosphine
DNA	Deoxyribonucleic acid
EI	Electron impact
ELISA	Enzyme-linked Immunosorbent Assay
EST- SSR	Expressed sequence tag -simple sequence repeat
ETAC	Ethyl Acetate
ETOH	Ethanol
FDA	Food and Drug Administration
GC-FID	Gas chromatography-flame ionization detection
GC-MS/MS	Gas chromatography tandem mass spectroscopy
GC x GC-FID	Comprehensive two-dimensional gas chromatography- flame ionization detection
GC × GC-MS	Comprehensive two-dimensional gas chromatography-mass spectrometry
GC x GC–TOF–MS	Two-dimensional Gas Chromatography coupled to a time-of-flight MS detector
GC-IRMS	Gas chromatography-Stable isotope ratio-mass spectrometry
GC-MS	Gas chromatography-mass spectrometry
GC-TOFMS	Gas Chromatography – Time of Flight Mass Spectrometry
HCA	Hierarchical cluster analysis

HETP	Height equivalent of a theoretical plate
HEX	Hexane
HIV	Human Immunodeficiency Virus
^{1}HNMR	Proton nuclear magnetic resonance
HPLC	High performance liquid chromatography
HPLC-DAD	High-performance liquid chromatography-diode array detector
HPLC-ESI-MS	High performance liquid chromatography coupled with electrospray mass spectrometry
HPLC–MS/MS	High performance liquid chromatography tandem mass spectrometry
HPLC-UV	High-performance liquid chromatography-Ultraviolet detection
ICH	International Conference on Harmonisation
ICRS	International Chemical Reference Substances
INSTI	integrase strand transfer inhibitors
ISTD	Internal standard
ISS	Intermediate stock solution
ISSR	Inter-simple sequence repeat
ITS2	Internal Transcribed Spacer II
IUPAC	International Union of Pure and Applied Chemistry
LC-MS/MS	Liquid Chromatography tandem Mass Spectrometry
LDA	Linear discriminant analysis
LOD	Limit of Detection
LOQ	Limit of Quantitation
MDA	3,4-Methylenedioxyamphetamine.
MEKC-DAD	Micellar Electrokinetic Chromatography-diode array detector
MEKC-UV	Micellar Electrokinetic Chromatography-Ultraviolet detection
MSD	Mass Selective Detector
MSDS	Material safety data sheet
MTQ	Methaqualone
k-NN	k-nearest neighbor method
NIST	National Institute of Standards and Technology
NMR	Nuclear magnetic resonance
NNRTI	Nonnucleoside Reverse Transcriptase Inhibitor
NRTI	Nonnucleoside; Reverse Transcriptase Inhibitor
PCA	Principal Component analysis
PCR	Polymerase chain reaction
PI	Protease Inhibitors
i-PrOH	*iso*-Propyl Alcohol

NCT	Nicotine
PFTBA	Perfluorotributylamine
PNT	Phenacetin
QA	Quality Assurance
RAPD	Random amplification of polymorphic DNA
RNA	Ribonucleic acid
RRT	Relative retention time
RSD	Relative Standard Deviation
RT	Retention time
SACENDU	South African Community Epidemiology Network on Drug Use
SAHPRA	South African Health Products Regulatory Authority
SAPS	South African Police Services
SAPS-FSL	South African Police Services' Forensic science Laboratory
SADC	Southern African Development Community
SIM	Single ion monitoring
SPME	Solid phase micro extraction
SS	Stock solution
STR	Short tandem repeat
TC	Tetracosane
TOCSY	Total Correlation Spectroscopy
UNODCCP	United Nations Office for Drug Control and Crime Prevention
UNODC	United Nations Office on Drugs and Crime
UHPLC-PDA	Ultra-high-pressure liquid chromatography-Photodiode array
UPLC–MS/MS	Ultra-performance liquid chromatography tandem mass spectrometry
US-DA PLANTS	United States Department of Agriculture Plants Database
US-DEA	United States Drug Enforcement Agency
US-DHHS	United States Department of Health and Human Services
US-FDA	United States Food and Drug Administration
USP	United States Pharmacopeia
UV	Ultraviolet
WHO	World Health Organisation

CHAPTER 1: INTRODUCTION AND LITERATURE REVIEW

1.1 BACKGROUND AND RATIONALE FOR THE CURRENT STUDY

The abuse of illicit drugs such as cocaine, methamphetamine and heroin is a problem that is prevalent in many urban areas in countries around the world, including South Africa. It is estimated that about 35 million people worldwide suffer from disorders related to drug abuse and about 585 000 people died in 2018 as a result of drug abuse (UNODC, 2020). The clampdown on the abuse of illicit drugs through legislation has led to the proliferation of new designer drugs in order to circumvent prosecution. Existing illicit drugs are often reintroduced with new names to disguise them from the authorities. A potent cocktail mixture of low-grade heroin, smoked with cannabis, has been introduced in South Africa as 'nyaope' (Figure 1.1) (Ross, 2013). Nyaope is believed to have originated in the Pretoria townships of Atteridgeville, Soshanguve and Mamelodi between 2000 and 2006, but it is now available in the city's suburbs (Health24, 2014). It has also spread to other parts of South Africa under different street names that are area specific. For instance, in Durban, nyaope is occasionally mixed with antiretroviral drugs and referred to as 'Whoonga' and 'Sugars' (Fihlani, 2011), while in the Western Cape it is called 'Ungah'; it is known as 'Pinch' in Mpumalanga and Limpopo; 'Kataza' in Johannesburg; and 'Plazana' and 'Kwape' in Pretoria (Mokwena and Huma, 2014, GPDPCS-SA, 2015). Nyaope is a cocktail drug that always contains heroin mixed with one or more other psychoactive substances such as cannabis, cocaine, 3,4-methylenedioxyamphetamine (MDA), methaqualone, the antiretroviral (ARV) medication non-nucleoside reverse transcriptase inhibitors (Efavirenz (EFV) and Nevirapine (NVP)), Acetaminophen (ACA), Lidocaine, Phenacetin (PNT), Dextromethorphan, Diazepam and Caffeine (SAPS Fact File, 2013, Khine et al, 2015).

It is believed that nyaope is sometimes also mixed with bulking agents such as bicarbonate of soda, pool cleaner and teething powder to make it last longer, as well as with adulterants such as rat poison (warfarin) to enhance the psychoactive effects (GPDPCS-SA, 2015).

Figure 1.1: Picture of a typical street nyaope sample (Photo by the author)

Recently there has been a media outcry on the abuse of the street cocktail drug nyaope by unemployed South Africans youth (Masombuka, 2013; Health24, 2014; Mokwena and Morojele, 2014). Once addicted to the drug, it becomes almost impossible to break the cycle of use, due to lack of affordable rehabilitation centres (Mokwena and Morojele, 2014). Those that are rehabilitated often relapse because they return to those unfavourable conditions that resulted in the initial use of the drug (Mokwena, 2015).

In South Africa, the abuse of the cocktail drug nyaope has increased in recent years, mainly amongst the youth (Larkan, Van Whyk and Saris, 2010; Shembe, 2013). This often results in these young males turning to theft, losing their jobs and/or dropping out of school (Masombuka, 2013; Grelotti et al, 2014; Mokwena and Huma, 2014; Rough et al, 2014). The nyaope users, who are mostly poor, often resort to criminal activities to sustain their drug habit, which includes stealing anything valuable they can lay their hands on (*ibid*).

Although the drug is widely reported in South Africa, nothing is known of its distribution in neighbouring Mozambique, Zimbabwe, Botswana and Namibia, although there are anecdotal reports that it may have been reported in Malawi (Nyedo, 2020).

Nyaope contains substances that are controlled by the *South African Drugs and Drug Trafficking Act, 1992* (Act 140 of 1992). These substances have been under this legislation from as far back as 1992. The name nyaope itself is a street name and therefore cannot be listed in the Act. The main illicit components of nyaope, heroin and its associated opiates (acetylcodeine, codeine, 6-monoacetylmorphine and morphine), cannabis as well as other illicit drugs (cocaine, 3,4-methylenedioxyamphetamine and methaqualone) are controlled in South Africa. Cannabis, heroin, 3,4-methylenedioxyamphetamine and methaqualone are listed in Part III of Schedule 2 of the *Drugs and Drug Trafficking Act, 1992* (Act 140 of 1992) as undesirable, dependence-producing substances while acetylcodeine, cocaine, codeine, 6-monoacetylmorphine and morphine are listed in Part II of Schedule 2 of the *Drugs and Drug Trafficking Act, 1992* (Act 140 of 1992) as dangerous dependence-producing substances. This legislation prohibits the use, possession, production and commercialization of an undesirable, dependence-producing substance, while the dangerous dependence substances could be produced by anyone in possession of a permit issued by the South African Health Products Regulatory Authority (SAHPRA). These substances are also listed in Schedules 6 and 7 of the *Medicines and Related Substances Act, 1965* (Act 101 of 1965). The other substances believed to be included in the cocktail nyaope mix are only listed as follows in the *Medicines and Related Substances Act, 1965* (Act 101 of 1965):

a) Diazepam in Schedule 5 of the *Medicines and Related Substances Control Act,* 1965 (Act 101 of 1965).

b) Antiretroviral drugs, phenacetin, and anticoagulants in Schedule 4 of the *Medicines and Related Substances Control Act, 1965* (Act 101 of 1965).

c) Caffeine, when intended for injection, in Schedule 3 of the *Medicines and Related Substances Control Act, 1965* (Act 101 of 1965).

d) Acetaminophen (paracetamol) in Schedules 3, 2, 1 and 0 of the *Medicines and Related Substances Control Act, 1965* (Act 101 of 1965).

e) Dextromethorphan and Lidocaine (as a local anaesthetic) in Schedule 2 of the *Medicines and Related Substances Control Act, 1965* (Act 101 of 1965).

Substances listed in Schedules 3 and 4 of the *Medicines and Related Substances Control Act* are only accessible to people who are in possession of a doctor's prescription or a permit from SAHPRA.

Nyaope is an inexpensive cocktail drug with a single dose costing R20,00–R30,00 (circa US$ 2) (Monyakane, 2018). In South Africa, at present, the Criminal Law punishes drugs related offences by a fine or imprisonment. The scale of the nyaope problem is difficult to quantify. At the present time there are few representative surveys on drug use and abuse in South Africa. A recent policy brief summarises the rise in trafficking and abuse of heroin in South Africa (Haysom, 2019), which may be associated with the rise in the abuse of the cocktail drug nyaope. However, there is a growing opinion that to tackle the drug problem in South Africa, including that associated with nyaope, a number of approaches need to be taken (Monyakane, 2018). This includes (i) punishment of those manufacturing, trafficking and distributing the drug. Additionally, a forensic process is proposed towards addressing the nyaope problem (Monyakane, 2018); where (ii) drug users are properly catered for by rehabilitation schemes; (iii) the social circumstances of the drug users are changed; and (iv) implementation of a Public Health Awareness Scheme. Of course, this approach could be applied to many drug problems across the globe.

Anecdotal reports have indicated that nyaope is sometimes mixed with rat poison to make it last longer as well as enhance the psychoactive effects (Health24, 2014; GPDPCS-SA, 2015). Rat poison is mainly a formulation that contains compounds derived from two classes of rodenticide anticoagulants. Coumarins are derived from the woodruff flavour coumarin found in many plants, especially available in higher concentrations in the tonka beans (*Dipteryx odoranta Wild,* Fabaceae) from which it was first isolated (Bovell-Benjamin and Roberts, 2015). Indandiones are mainly derivatives of 1,3-indandione (Pluskota and Koba, 2018). Coumarins and indandiones are also called vitamin K antagonists, because they reduce the synthesis of vitamin K- dependent factors that are necessary for blood coagulation. Coumarins are mainly the 4-hydroxycoumarin derivatives, which are divided into first-generation (warfarins) anticoagulants, namely acenocoumarol, coumatetralyl, coumachlor, phenprocoumon, and warfarin in addition to the second-generation (superwarfarins) namely brodifacoum, bromadiolone, difenacoum, difethialone, and flocoumafen (Grobosch et al, 2006; Marek and Koskinen, 2007; Adamowicz and Kała, 2009; Rother, 2012). Indandiones includes pindone, chlorophacinone and diphacinone (Marek and Koskinen, 2007; Rother, 2012). The structures, common names, International Union of Pure and Applied Chemistry (IUPAC) names empirical formulae and molar masse of coumarin, 4-hydroxycoumarine, 1,3-

indandione , vitamin K and some of the rodenticides are shown in Table 1.1. The substances found in rat poison can easily be detected using gas chromatography- mass spectrometry (GC-MS) that is currently used for routine analysis. The presence of these rodenticides in any of the casework was not reported by the South African Police Service Forensic Science Laboratory (SAPS-FSL). This may be due to the method used for routine drug analysis being unsuitable for the detection of the rodenticides. The non-reporting of the rodenticides suggests that they were either absent or, if present, they were simply not reported by the analyst during normal routine work. These substances are not controlled in terms of the South African drug laws (*Drugs and Drug Trafficking Act*, 1992); as a result, it is normally not required for the analyst to report the presence of the rodenticides. The presence of rat poison in nyaope may result in bleeding in mesenteric blood vessels (Khan and Schell, 2014) which then would cause pain and therefore the need to take more painkiller (heroin). In this manner the abuser would then continue smoking more nyaope. It will be difficult to select particular rodenticides, since they are not reported, and as a result these substances will be excluded from the study.

Table 1.1: Structures, common names, IUPAC names, empirical formulae and molar masses of coumarin, 4-hydroxycoumarine, 1,3-indandione and vitamin K as well as some of the indandione superwarfarin and warfarin rodenticides.

Structure	Common name	IUPAC name	Empirical formula	Molar mass, g/mol
1 Structures of coumarin, 4-hydroxycoumarine, 1,3-indandione and vitamin K				
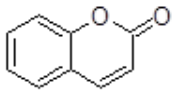	Coumarin	2H-Chromen-2-one	$C_9H_6O_2$	146.14
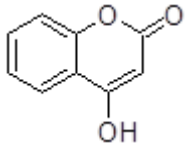	4-Hydroxycoumarine	4-Hydroxy-2H-chromen-2-one	$C_9H_6O_3$	162.14
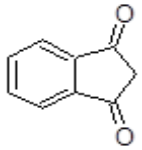	1,3-Indandione	1H-Indene-1,3(2H)-dione	$C_9H_6O_2$	146.14
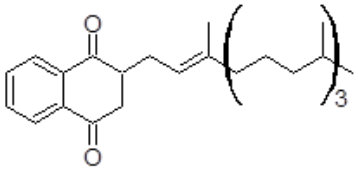	Vitamin K	2-Methyl-3-[(2E,7R,11R)-3,7,11,15-tetramethyl-2-hexadecen-1-yl]-1,4-naphthoquinone	$C_{31}H_{46}O_2$	450.70

Table 1.1 *cont'd*: Structures, common names, IUPAC names, empirical formulae and molar masses of coumarin, 4-hydroxycoumarine, 1,3-indandione and vitamin K as well as some of the indandione superwarfarin and warfarin rodenticides.

Structure	Common name	IUPAC name	Empirical formula	Molar mass, g/mol
2 Structure of warfarins				
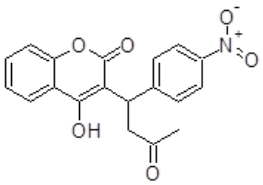	Acenocoumarol	4-Hydroxy-3-[(1S)-1-(4-nitrophenyl)-3-oxobutyl]-2H-chromen-2-one	$C_{19}H_{15}NO_6$	353.33
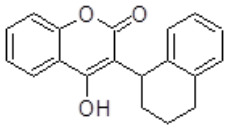	Coumatetralyl	4-Hydroxy-3-(1,2,3,4-tetrahydro-1-napthalenyl)-2H-chromen-2-one	$C_{19}H_{16}O_3$	292.33
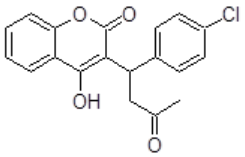	Coumachlor	3-[1-(4-Chlorophenyl)-3-oxobutyl]-4-hydroxy-2H-chromen-2-one	$C_{19}H_{15}ClO_4$	342.77
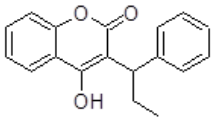	Phenprocoumon	4-Hydroxy-3-(1-phenylpropyl)-2H-chromen-2-one	$C_{18}H_{16}O_3$	280.32
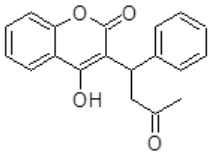	Warfarin	2-Hydroxy-3-(3-oxo-1-phenylbutyl)-4H-chromen-4-one	$C_{19}H_{16}O_4$	308.33

Table 1.1 *cont'd*: Structures, common names, IUPAC names, empirical formulae and molar masses of coumarin, 4-hydroxycoumarine, 1,3-indandione and vitamin K as well as some of the indandione superwarfarin and warfarin rodenticides.

Structure	Common name	IUPAC name	Empirical formula	Molar mass, g/mol
3 Structures of superwarfarins				
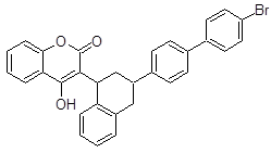	Brodifacoum	3-[3-(4'-Bromo-4-biphenyl)-1,2,3,4-tetrahydro-1-naphthalenyl]-2-hydroxy-4H-chromen-4-one	$C_{31}H_{23}BrO_3$	523.42
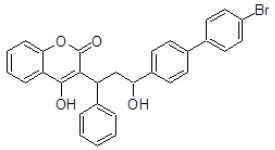	Bromadiolone	3-[(1S,3R)-3-(4'-Bromo-4-biphenylyl)-3-hydroxy-1-phenylpropyl]-4-hydroxy-2h-chromen-2-one	$C_{30}H_{23}BrO_4$	527.41
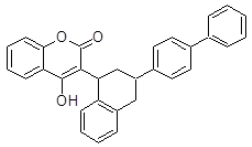	Difenacoum	3-[3-(4-Biphenylyl)-1,2,3,4-tetrahydro-1-naphthalenyl]-4-hydroxy-2H-chromen-2-one	$C_{31}H_{24}O_3$	444.52
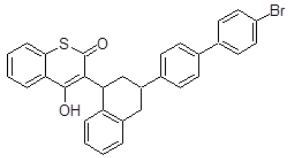	Difethialone	3-[3-(4'-Bromo-4-biphenylyl)-1,2,3,4-tetrahydro-1-naphthalenyl]-4-hydroxy-2H-thiochromen-2-one	$C_{31}H_{23}BrO_2S$	539.48
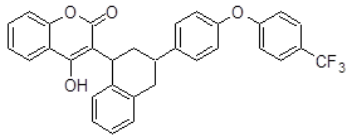	Flocoumafen	4-Hydroxy-3-[3-(4-{[4-(trifluoromethyl)benzyl]oxy}phenyl)-1,2,3,4-tetrahydro-1-naphthalenyl]-2H-chromen-2-one	$C_{33}H_{25}F_3O_4$	542.54

Table 1.1 *cont'd*: Structures, common names, IUPAC names, empirical formulae and molar masses of coumarin, 4-hydroxycoumarine, 1,3-indandione and vitamin K as well as some of the indandione superwarfarin and warfarin rodenticides.

Structure	Common name	IUPAC name	Empirical formula	Molar mass, g/mol
4 Structures of Indandiones				
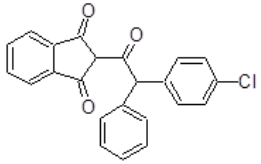	Chlorophacinone	2-[(4-Chlorophenyl)(phenyl)acetyl]-1H-indene-1,3(2H)-dione	$C_{23}H_{15}ClO_3$	374.82
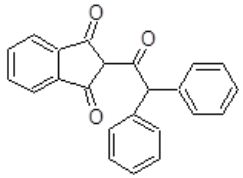	Diphenadione	2-(Diphenylacetyl)-1H-indene-1,3(2H)-dione	$C_{23}H_{16}O_3$	340.37
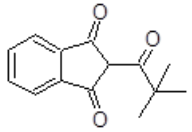	Pindone	2-(2,2-Dimethylpropanoyl)-1H-indene-1,3(2H)-dione	$C_{14}H_{14}O_3$	230.26

The health risks associated with using nyaope are not well investigated, but reports include the restriction of growth and development of neo-nates (Thomas and Velaphi, 2014) and infective endocarditis (Meel and Essop, 2018), which has been misdiagnosed elsewhere as pulmonary tuberculosis or pneumonia (Chambers, 2018). Other problems associated with nyaope use include damaged and infected veins, damaged heart valves, tissue infections, liver failure, kidney disease and lung problems (Recovery Direct, 2019).

1.2 AN OVERVIEW OF ANTRIRETROVIRAL DRUGS

The vast majority of nyaope users are positive for human immunodeficiency virus (HIV) (Meel and Essop, 2018). Nyaope is also reportedly abused by pregnant women, which has detrimental consequences to the unborn babies. The abuse of nyaope mixtures containing antiretroviral (ARV) drugs by pregnant women results in the development of ARV pre-treatment resistance and is associated with abnormal intrauterine growth, neonatal abstinence syndrome, as well as abnormal behaviour for the unborn child (Thomas and Vhelaphi, 2014). The use of ARVs as cutting agents for nyaope has reportedly led to health professionals being robbed or even corrupt officials selling the ARVs (Inciardi et al, 2007; Larkan et al, 2010; Shembe, 2013). Patients who are HIV-positive are also either robbed or sell the ARVs themselves, thereby defaulting on their treatment (*ibid*).

ARVs can be classified into seven classes, namely: nucleoside/nucleotide reverse transcriptase inhibitors (NRTIs), non-nucleoside reverse transcriptase inhibitors (NNRTIs), protease inhibitors (PIs), integrase strand transfer inhibitors (INSTIs), a fusion inhibitor, a Chemokine Coreceptor Type 5 (CCR5) antagonist, and a cluster of differentiation 4 cells (CD4 cells) post-attachment inhibitor. CD4 cells are white blood cells found on the surface of immune cells. The CD4 cell count gives an indication of one's body's ability to defend itself against pathogens, infections and illnesses.

1.2.1 ARV treatment and psychiatric effects

HIV-positive patients are usually treated with a first regimen of antiretrovirals, which is a fixed drug combination of three or four drugs from at least two different classes. The combinations used include either an INSTI with two NRTIs, an NNRTI with two NRTIs, or a boosted PI plus

two NRTIs (Department of Health, 2004; Sogbanmu et al, 2015; Kakande et al, 2015; Meintjies et al, 2017; US-DHHS, 2018). Boosted PIs are PIs in combination with RTV where RTV acts as a booster. This treatment is followed-up by a second line of ARVs, which are a combination of a boosted PI with two NRTIs (*ibid*). Should a third-line regiment be required, a combination of boosted PI with INSTI and NNRTIs is usually employed (*ibid*). Table1.2 lists the structures, common names, IUPAC names, empirical formulae and molecular weights of some of these antiretroviral drugs.

Common psychiatric side-effects of some of these antiretroviral drugs are as follows (Turjanski and Lloyd, 2005; Anagnostopoulos et al, 2013; US-DHHS, 2018):

- Amprenavir causes mood swings
- Atazanavir causes depression and insomnia
- Bictegravir causes insomnia, depression, and suicidality primarily in patients with pre-existing psychiatric conditions.
- Cenicriviroc improves cognitive performance.
- Didanosine causes lethargy, nervousness, anxiety, confusion, sleep disturbances, mood disorders, and psychosis.
- Dolutegravir causes depression or exacerbation of pre-existing depression, anxiety, suicidal ideation or attempted/completed suicide, insomnia, dizziness and headache.
- Doravirine causes sleep disorders and disturbances, dizziness, altered sensorium; depression and suicidality/self-harm.
- Efavirenz causes agitation, depersonalisation, hallucinations, abnormal dreams, mood disorders, depression, antisocial behaviour, psychosis, catatonia, delirium, suicidal ideation, dizziness, somnolence, insomnia or poor sleep quality, impaired concentration, seizures (including absence seizures) and cerebellar dysfunction (tremor, dysmetria, ataxia).
- Elvitegravir causes insomnia, depression, and suicidality primarily in patients with pre-existing psychiatric conditions.
- Emtricitabine causes dizziness, difficulty sleeping, weakness and hallucinations (abnormal dreams).
- Enfuvirtide causes anxiety and depression.
- Indinavir causes mood swings.
- Lamivudine causes insomnia and mood disorders.
- Lopinavir and ritonavir causes mood changes, agitation and anxiety.

- Raltegravir causes increased psychomotor activity, headaches, insomnia, depression and cerebellar dysfunction (e.g. tremor, dysarthria and ataxia).
- Rilpivirine causes depression, suicidality, depressive disorders, suicidal ideation, abnormal dreams/nightmares, headache, dizziness, insomnia and somnolence.
- Saquinavir causes depression, anxiety and sleep disturbances.
- Stavudine causes sleep and mood disorders and delirium.
- Tenofovir causes asthenia, depression, insomnia and anorexia.
- Tipranavir causes insomnia.
- Zalcitabine causes somnolence, impaired, concentration, mood disorders and delirium.
- Zidovudine causes sleep disturbance, vivid dreams, agitation, mania and depression, psychotic symptoms and delirium.

No psychoactive effects have been reported for abacavir, aplaviroc, delavirdine, duranavir, etravirine, fosamprenavir, fostemsavir, ibulizumab, maraviroc, nelfinavir, nevirapine, peptide-T and vicriviroc. As seen above some of the ARVs (efavirenz and emtricitabine) give hallucinogenic effect similar to the illicit drug LSD, which could be the motivation for the use of ARVs as part of the components of the nyaope cocktail drug.

Table 1.2: Structures, common names, IUPAC names, empirical formulae and molar masses of some of the antiretroviral drugs available commercially.

Structure	Common name	IUPAC name	Empirical formula	Molar mass, g/mol
Fusion inhibitors				
-	Enfuvirtide	acetyl-L-tyrosyl-L-threonyl-L-seryl-L-leucyl-L-isoleucyl-L-histidyl-L-seryl-L-leucyl-L-isoleucyl-L-a-glutamyl-L-a-glutamyl-L-seryl-L-glutaminyl-L-asparaginyl-L-glutaminyl-L-glutaminyl-L-a-glutamyl-L-lysyl-L-asparaginyl-L-a-glutamyl-L-glutaminyl-L-a-glutamyl-L-leucyl-L-leucyl-L-a-glutamyl-L-leucyl-L-a-aspartyl-L-lysyl-L-tryptophyl-L-alanyl-L-seryl-L-leucyl-L-tryptophyl-L-asparaginyl-L-tryptophyl-L-phenylalaninamide	$C_{204}H_{301}N_{51}O_{64}$	4492.1
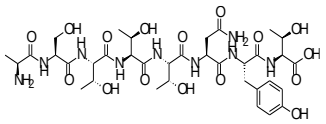	Peptide T	L-alanyl-L-seryl-L-threonyl-L-threonyl-L-threonyl-L-asparaginyl-L-tyrosyl-L-threonine	$C_{35}H_{55}N_9O_{16}$	857.872
CCR5 antagonists				
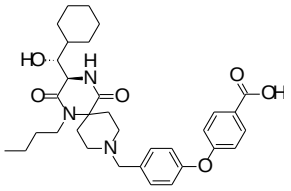	Aplaviroc	4-[4-({(3R)-1-Butyl-3-[(R)-cyclohexyl(hydroxy)methyl]-2,5-dioxo-1,4,9-triazaspiro[5.5]undec-9-yl}methyl)phenoxy]benzoic acid	$C_{33}H_{43}N_3O_6$	577.711

Table 1.2 *cont'd:* Structures, common names, IUPAC names, empirical formulae and molar masses of some of the antiretroviral drugs available commercially.

Structure	Common name	IUPAC name	Empirical formula	Molar mass, g/mol
CCR5 antagonists				
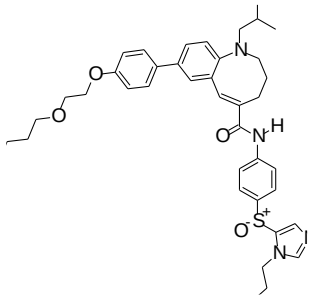	Cenicriviroc	(5E)-8-[4-(2-Butoxyethoxy)phenyl]-1-isobutyl-N-(4-{(S)-[(1-propyl-1H-imidazol-5-yl)methyl]sulfinyl}phenyl)-1,2,3,4-tetrahydro-1-benzazocine-5-carboxamide	$C_{41}H_{52}N_4O_4S$	696.941
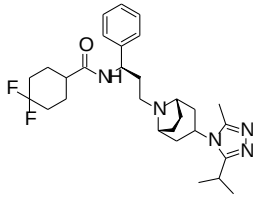	Maraviroc	4,4-Difluoro-N-[(1S)-3-[(3-exo)-3-[3-methyl-5-(1-methylethyl)-4H-1,2,4-triazol-4-yl]-8-azabicyclo[3.2.1]oct-8-yl]-1-phenylpropyl]cyclohexanecarboxamide	$C_{29}H_{41}F_2N_5O$	513.666
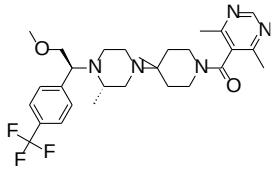	Vicriviroc	(4,6-Dimethyl-5-pyrimidinyl){4-[(3S)-4-{(1R)-2-methoxy-1-[4-(trifluoromethyl)phenyl]ethyl}-3-methyl-1-piperazinyl]-4-methyl-1-piperidinyl}methanone	$C_{28}H_{38}F_3N_5O_2$	533.629

Table 1.2 *cont'd*: Structures, common names, IUPAC names, empirical formulae and molar masses of some of the antiretroviral drugs available commercially.

Structure	Common name	IUPAC name	Empirical formula	Molar mass, g/mol
CD4 post-attachment inhibitors				
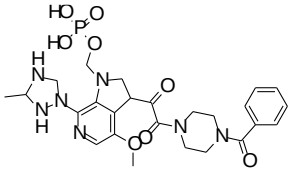	Fostemsavir	{3-[(4-Benzoyl-1-piperazinyl)(oxo)acetyl]-4-methoxy-7-(3-methyl-1H-1,2,4-triazol-1-yl)-1H-pyrrolo[2,3-c]pyridin-1-yl}methyl dihydrogen phosphate	$C_{25}H_{26}N_7O_8P$	583.490
Integrase strand transfer inhibitors				
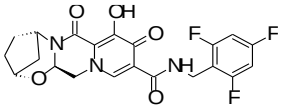	Bictegravir	(1S,11R,13R)-5-Hydroxy-3,6-dioxo-N-(2,4,6-trifluorobenzyl)-12-oxa-2,9-diazatetracyclo[11.2.1.$0^{2,11}$.$0^{4,9}$]hexadeca-4,7-diene-7-carboxamide	$C_{21}H_{18}F_3N_3O_5$	449.380
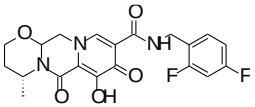	Dolutegravir	(4R,12aS)-N-(2,4-Difluorobenzyl)-7-hydroxy-4-methyl-6,8-dioxo-3,4,6,8,12,12a-hexahydro-2H-pyrido[1',2':4,5]pyrazino[2,1-b][1,3]oxazine-9-carboxamide	$C_{20}H_{19}F_2N_3O_5$	419.379
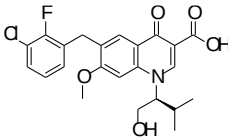	Elvitegravir	6-(3-Chloro-2-fluorobenzyl)-1-[(2S)-1-hydroxy-3-methyl-2-butanyl]-7-methoxy-4-oxo-1,4-dihydro-3-quinolinecarboxylic acid	$C_{23}H_{23}ClFNO_5$	447.884
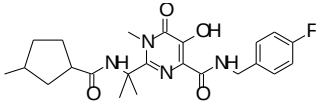	Raltegravir	N-(4-Fluorobenzyl)-5-hydroxy-1-methyl-2-(2-{[(5-methyl-1,3,4-oxadiazol-2-yl)carbonyl]amino}-2-propanyl)-6-oxo-1,6-dihydro-4-pyrimidinecarboxamide	$C_{20}H_{21}FN_6O_5$	444.416

Table 1.2 *cont'd*: Structures, common names, IUPAC names, empirical formulae and molar masses of some of the antiretroviral drugs available commercially.

Structure	Common name	IUPAC name	Empirical formula	Molar mass, g/mol
Non-nucleoside reverse transcriptase inhibitors				
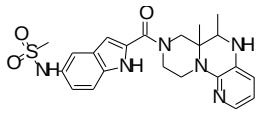	Delavirdine	N-[2-({4-[3-(Isopropylamino)-2-pyridinyl]-1-piperazinyl}carbonyl)-1H-indol-5-yl]methanesulfonamide	$C_{22}H_{28}N_6O_3S$	456.561
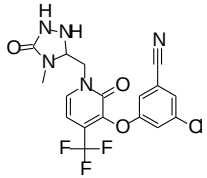	Doravirine	3-Chloro-5-({1-[(4-methyl-5-oxo-4,5-dihydro-1H-1,2,4-triazol-3-yl)methyl]-2-oxo-4-(trifluoromethyl)-1,2-dihydro-3-pyridinyl}oxy)benzonitrile	$C_{17}H_{11}ClF_3N_5O_3$	425.749
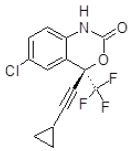	Efavirenz	(4S)-6-Chloro-4-(cycopropylethynyl)-4-(trifluoromethyl)-1,4-dihydro-2H-3,1-benzoxazin-2-one	$C_{14}H_9ClF_3NO_2$	315.68
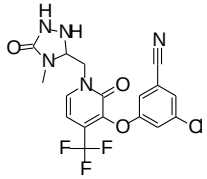	Etravirine	4-({6-Amino-5-bromo-2-[(4-cyanophenyl)amino]-4-pyrimidinyl}oxy)-3,5-dimethylbenzonitrile	$C_{20}H_{15}BrN_6O$	435.277
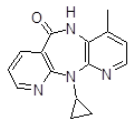	Nevirapine	11-Cyclopropyl-4-methyl-5,11-dihydro-6H-dipyrido[3,2-b:2',3'-e][1,4]diazepin-6-one	$C_{15}H_{14}N_4O$	266.30

Table 1.2 *cont'd*: Structures, common names, IUPAC names, empirical formulae and molar masses of some of the antiretroviral drugs available commercially.

Structure	Common name	IUPAC name	Empirical formula	Molar mass, g/mol
Non-nucleoside reverse transcriptase inhibitors				
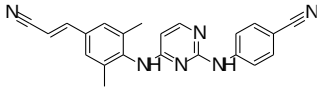	Rilpivirine	4-{[4-({4-[E-2-Cyanovinyl]-2,6-dimethylphenyl}amino)-2-pyrimidinyl]amino}benzonitrile	$C_{22}H_{18}N_6$	366.418
Nucleoside reverse transcriptase inhibitors				
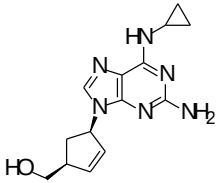	Abacavir	{(1S,4R)-4-[2-Amino-6-(cyclopropylamino)-9H-purin-9-yl]-2-cyclopenten-1-yl}methanol	$C_{14}H_{18}N_6O$	286.332
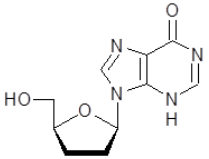	Didanosine	9-[(2R,5S)-5-(hydroxymethyl)tetrahydro-2-furanyl]-1,9-dihydro-6H-purin-6-one	$C_{10}H_{12}N_4O_3$	236.23
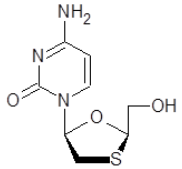	lamivudine	4-Amino-1-[(2R,5S)-2-(hydroxymethyl)-1,3-oxathiolan-5-yl]pyrimidin-2(1H)-one	$C_8H_{11}N_3O_3S$	229.26
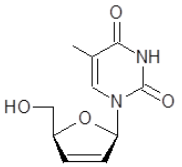	Stavudine	1-[2R,5S)-5-(Hydroxymethyl)-2,5-dihyro-2-furayl]-5-methyl-pyrimidine-2,4(1H,3H)-dione	$C_{10}H_{12}N_2O_4$	224.21

Table 1.2 cont'd: Structures, common names, IUPAC names, empirical formulae and molar masses of some of the antiretroviral drugs available commercially.

Structure	Common name	IUPAC name	Empirical formula	Molar mass, g/mol
Nucleoside reverse transcriptase inhibitors				
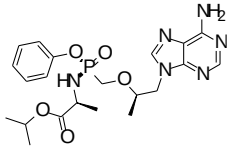	Tenofovir alafenamide	Isopropyl N-[(S)-({[(2R)-1-(6-amino-9H-purin-9-yl)-2-propanyl]oxy}methyl)(phenoxy)phosphoryl]-L-alaninate	$C_{21}H_{29}N_6O_5P$	476.466
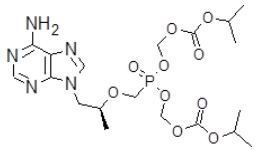	Tenofovir disoproxil	{[(2R)-1-(6-aminopurin-9-yl)propan-2-yl]oxymethyl-(propan-2-yloxycarbonyloxy]methoxy)phosphoryl}oxymethyl propan-2-yl carbonate	$C_{19}H_{30}N_5O_{10}P$	519.44
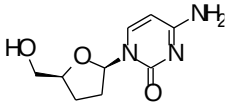	Zalcitabine	1-[(2R,5S)-5-(Hydroxymethyl)tetrahydro-2-furanyl]-4-imino-1,4-dihydro-2-pyrimidinol	$C_9H_{13}N_3O_3$	211.218
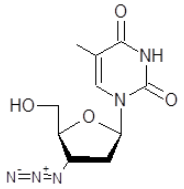	Zidovudine	1-[(2R,4S,5S)-4-Azido-5(hydroxymethyl)tetrahydrofuran-2-yl]-5-methylpyridine-2,4(1H,3H)-dione	$C_{10}H_{13}N_5O_4$	267.24
Protease inhibitors				
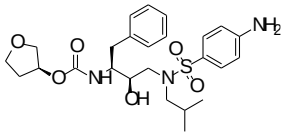	Amprenavir	(3S)-Tetrahydro-3-furanyl [(2S,3R)-4-{[(4-aminophenyl)sulfonyl](isobutyl)amino}-3-hydroxy-1-phenyl-2-butanyl]carbamate	$C_{25}H_{35}N_3O_6S$	505.627

Table 1.2 cont'd: Structures, common names, IUPAC names, empirical formulae and molar masses of some of the antiretroviral drugs available commercially.

Structure	Common name	IUPAC name	Empirical formula	Molar mass, g/mol
Protease inhibitors				
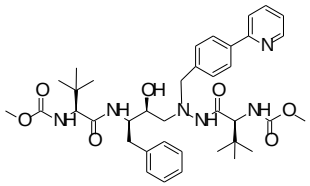	Atazanavir	(3S,8S,9S,12S)-3,12-Bis(1,1-dimethylethyl)-8-hydroxy-4,11-dioxo-9-(phenylmethyl)-6-((4-(2-pyridinyl)phenyl)methyl)-2,5,6,10,13-pentaazatetradecanedioic acid Dimethyl Ester	$C_{38}H_{52}N_6O_7$	704.856
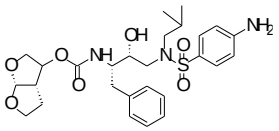	Darunavir	(3R,3aS,6aR)-Hexahydrofuro[2,3-b]furan-3-yl [(2S,3R)-4-{[(4-aminophenyl)sulfonyl](isobutyl)amino}-3-hydroxy-1-phenyl-2-butanyl]carbamate	$C_{27}H_{37}N_3O_7S$	547.664
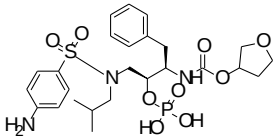	Fosamprenavir	(3S)-Tetrahydro-3-furanyl [(2S,3R)-4-{[(4-aminophenyl)sulfonyl](isobutyl)amino}-1-phenyl-3-(phosphonooxy)-2-butanyl]carbamate	$C_{25}H_{36}N_3O_9PS$	585.607
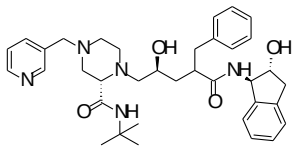	Indinavir	(2S)-1-[(2S,4R)-4-Benzyl-2-hydroxy-5-{[(1S,2R)-2-hydroxy-2,3-dihydro-1H-inden-1-yl]amino}-5-oxopentyl]-N-(2-methyl-2-propanyl)-4-(3-pyridinylmethyl)-2-piperazinecarboxamide	$C_{36}H_{47}N_5O_4$	613.789
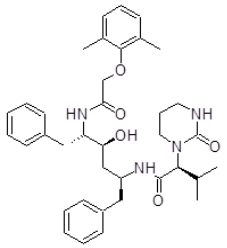	lopinavir	(2S)-N-[(2S,4S,5S)-5-{[(2,6-Dimethylphenoxy)acetyl]amino}-4-hydroxy-1,6-diphenylhexan-2-yl]-3-methyl-2-(2-oxotetrahydropyrimidin-1(2H)-yl)butanamide	$C_{37}H_{48}N_4O_5$	628.81

Table 1.2 *cont'd*: Structures, common names, IUPAC names, empirical formulae and molar masses of some of the antiretroviral drugs available commercially.

Structure	Common name	IUPAC name	Empirical formula	Molar mass, g/mol
Protease inhibitors				
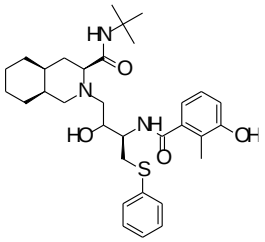	Nelfinavir	(3S,4aS,8aS)-2-[(2R,3R)-2-Hydroxy-3-[(3-hydroxy-2-methylbenzoyl)amino]-4-(phenylsulfanyl)butyl]-N-(2-methyl-2-propanyl)decahydro-3-isoquinolinecarboxamide	$C_{32}H_{45}N_3O_4S$	567.782
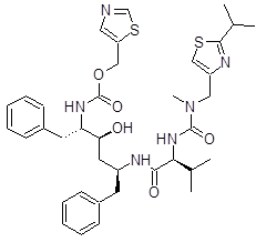	Ritinovir	(1E,2S)-N-[(2S,4S,5S)-4-Hydroxy-5{(E)-[hydroxyl(1,3-thiazol-5-ylmethoxy)methylene]amino}-1,6-diphenyl-2-hexanyl]-2-[(E)-(hydrox{[(2-isopropyl-1,3-thiazol-4-yl)methyl]methyl)amino}methylene)amino]-3-methylbutanamidic acid	$C_{37}H_{48}N_6O_5S_2$	720.95
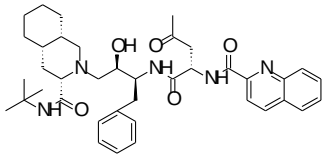	Saquinavir	(1E,2S)-N^1-{(2S,3R)-3-Hydroxy-4-[(3S,4aS,8aS)-3-{(Z)-hydroxy[(2-methyl-2-propanyl)imino]methyl}octahydro-2(1H)-isoquinolinyl]-1-phenyl-2-butanyl}-2-[(2-quinolinylcarbonyl)amino]butanediimidic acid	$C_{38}H_{50}N_6O_5$	670.841
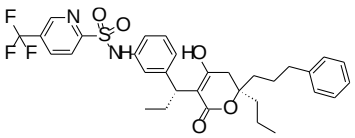	Tipranavir	N-(3-{(1R)-1-[(6R)-4-Hydroxy-2-oxo-6-(2-phenylethyl)-6-propyl-5,6-dihydro-2H-pyran-3-yl]propyl}phenyl)-5-(trifluoromethyl)-2-pyridinesulfonamide	$C_{31}H_{33}F_3N_2O_5S$	602.664

1.2.2 Analysis of ARV drugs

Methods used for the analysis of antiretroviral drugs can also be used for the profiling of these compounds. Liquid chromatographic methods coupled with tandem mass spectrometry appears to be the preferred method for the simultaneous determination of ARVs (Soldin, 2005). The validated methods for the simultaneous quantitation of the antiretroviral drugs include liquid chromatography tandem mass spectrometry (LC-MS/MS) (Shoup et al, 1999; Chi et al, 2002; Crommentuyn et al, 2004; Chang et al, 2005; Colombo et al, 2005; Soldin, 2005; Jung et al, 2007; Huang et al, 2008; Le Saux et al, 2008; Adamowicz and Kała, 2009; Fayet et al, 2009; Martin et al, 2009; Quaranta et al, 2009; Yadav et al, 2009; Brewer et al, 2010; Zhang et al, 2010a; Notari et al, 2012; Sura, Bonthu and Murth, 2013; Vijaya Raju and Appala Raju, 2013; Kromdijk et al, 2013; Kumar et al, 2013; Bhavyasri et al, 2015; Ghosh, Sailaja and Ravikumar, 2015; Penchala et al, 2016; Prathipati, Mandal and Destache, 2016; Prathipati, Mandal and Destache, 2018; Raju et al, 2018; Desai et al, 2019; Penchala et al, 2019; Thimmaraju et al, 2019) and ultra-performance liquid chromatography, coupled with tandem mass spectrometry (UPLC-MS/MS) (Djerada et al, 2013; Fortuna et al, 2013; Ramírez-Ramírez et al, 2018). These methods exhibit good linearity ranges, as indicated in Table 1.3. The linearity range achieved with these methods were orders of magnitude below or equal to the trough concentrations (Table 1.3). Trough concentration is the lowest plasma concentration reached by a drug before a follow-up dose is administered, and is used in therapeutic drug monitoring (André, Widmer and Buclin, 2019).

Table 1.3: Liquid chromatography-tandem mass spectrometry linear range and trough concentrations of antiretroviral drugs.

Compound	Trough Concentration, mg/L	Reference	Linearity Range, mg/L	Reference
Abacavir	0.018	Van Praag et al, 2002	0.0040 – 0.50	Kromdijk et al, 2013
Amprenavir	0.35	Acosta et al, 2012	0.00050 – 0.10	Colombo et al, 2005
Aplaviroc	017	Yeni, et al, 2009	0.00050 – 0.50	Adkison, et al 2006
Atazanavir	0.060	Acosta et al, 2012	0.00050 – 0.10	Colombo et al, 2005
Bictegravir	2.31	Gallant et al, 2017	0.0010 – 0.10	Prathipati, Mandal and Destache, 2018
Cenicriviroc	0.14	Lefebvre et al, 2016	0.0050 – 0.96	Lefebvre et al, 2016
Darunavir	0.025	Acosta et al, 2012	0.0025 – 10.00	Fayet et al, 2009
Delavirdine	0.90	Cheng et al, 1997	0.050 – 10.00	Shoup et al, 1999
Didanosine	0.10	Moyer et al, 1999	0.0010 – 2.00	Rao, Sankar and Rani, 2016
Dolutegravir	0.83 (50 mg dose)	Min et al, 2011	0.0050 – 2.00	Prathipati, Mandal and Destache, 2016
Doravirine	0.27	Calcagno et al, 2011	0.000020 – 0.010	Desai et al 2019
Efavirenz	0.13	Acosta et al, 2012	0.00050 – 0.10	Colombo et al, 2005
Elvitegravir	0.34	Custodio et al, 2014	0.0050 – 2.0	Prathipati, Mandal and Destache, 2016
Emtricitabine	0.077	Benaboud et al, 2011	0.0040 – 0.50	Kromdijk et al, 2013
Enfuvirtide (T-20)	2.24	De Requena et al, 2008	0.010 – 2.00	Chang et al, 2005
Etravirine	0.12	Acosta et al, 2012	0.010 – 4.00	Fayet et al, 2009
Fosamprenavir	0.40	US-DHHS, 2014	0.00050 – 0.20	Thimmaraju, et al, 2019
Fostemsavir	0.055	Nettles et al, 2012	0.0050 – 5.00	Nettles et al, 2012
Indinavir	0.073	Acosta et al, 2012	0.00050 – 0.10	Colombo et al, 2005

Table 1.3 *cont'd*: Liquid chromatography-tandem mass spectrometry linear range and trough concentrations of antiretroviral drugs.

Compound	Trough Concentration, mg/L	Reference	Linearity Range, mg/L	Reference
Lamivudine	0.078	Van Praag et al, 2002	0.0050 – 1.50	Kumar et al, 2013
Lopinavir	0.17	Acosta et al, 2012	0.00050 – 0.10	Colombo et al, 2005
Maraviroc	0.062	Calcagno et al, 2011	0.00050 – 0.50	Brewer et al, 2010
Nelfinavir	8.00	US-DHHS, 2014	0.00050 – 0.10	Colombo et al, 2005
Nevirapine	3.00	Acosta et al, 2012	0.00050 – 0.10	Colombo et al, 2005
Peptide T	-	-	0.10 – 10.0	Soldin, 2005
Raltegravir	0.19	Calcagno et al, 2011	0.0010 – 1.00	Raju & Raju, 2013
Rilpivirine	0.050	Aouri et al, 2017	0.0050 – 2.00	Prathipati, Mandal and Destache, 2016
Ritonavir	0.19	Calcagno et al, 2011	0.00050 – 0.10	Colombo et al, 2005
Saquinavir	0.23	Acosta et al, 2012	0.00050 – 0.10	Colombo et al, 2005
Stavudine	0.12	Van Praag et al, 2002	0.020 – 3.20	Zhang et al, 2010a
Tenofovir	0.056	Benaboud et al, 2011	0.0020 – 0.50	Kumar et al, 2013
Tipranavir	3.90	Acosta et al, 2012	0.10 – 75.0	Crommentuyn et al , 2004
Vicriviroc	0.056	Crawford et al, 2010	0.00050 – 1.00	Crawford et al, 2010
Zalcitabine	0.0020	Adams et al, 1998	0.0020 – 2.00	Volosov et al, 2002
Zidovudine	0.0030	Van Praag et al, 2002	0.0050 – 1.50	Kumar et al, 2013

High-performance liquid chromatography, coupled with electrospray ionisation mass spectrometry (HPLC-ESI-MS), has been developed and validated for the quantitation of plasma concentration of the protease inhibitors darunavir (DRV) and other 11 antiretroviral agents (ritonavir, amprenavir, atazanavir, lopinavir, saquinavir, indinavir, nelfinavir and its metabolite M-8, nevirapine, efavirenz and tipranavir) (D'Avolio et al, 2007). The linearity ranges for the method were below or equal to the trough concentration, except for tipranavir which was above the trough concentration.

Sandwich enzyme-linked immunosorbent assay (ELISA) with absorbance, fluorescence or electrochemical detection has been employed for the quantitation of IBA (US-FDA, 2017). The method involves the use of solid-phase enzyme immunoassay to detect the presence of protein ligand in a liquid sample using antibodies directed against the protein to be measured (*ibid*). The method exhibited linearity range of 0.010 to 2.00 mg/L that was lower than the trough concentration of 5.30 mg/L (*ibid*).

High performance liquid chromatography (HPLC) with ultraviolet (UV) detection has been used to determine 19 ARVs belonging to the three classes, namely nucleoside reverse transcriptase inhibitors (INRTI), non-nucleoside reverse transcriptase inhibitors (INNRTI) and protease inhibitors (PI) (Rebiere et al, 2007). The linear range for the method (10.00 to 100.00 mg/L) was above the trough concentrations for these compounds.

Fourier Transform-Raman spectroscopy has been successfully used for the quantitation of lamivudine (Rao et al, 2017). The limit of detection (15.00 mg/L) for this method was however above the trough concentration for lamivudine.

Gas chromatography-mass spectrometry (GC-MS) has proved to be a valid alternative to Liquid chromatographic methods for the identification and quantitation of efavirenz and nevirapine (Lemmer et al, 2005; Vogel et al, 2010). The limits of detection for efavirenz and nevirapine were 0.026 and 0.027 mg/L in plasma, respectively (Lemmer et al, 2005), which were well below the trough concentration for EFV and NVP. Gas Chromatography–Time of Flight Mass Spectrometry (GC-TOFMS) was used for the quantitation of both efavirenz and nevirapine in wastewater using solid phase extraction (Schoeman et al, 2015). The limits of detection for efavirenz and nevirapine using the GC-TOFMS method were 0.0000078 and 0.0000018 mg/L, respectively. The quantitation limits for efavirenz and nevirapine were

0.000026 and 0.0000060 mg/L, respectively. These limits were at least 4 orders of magnitude lower than the trough concentrations for both compounds (Table 1.3).

LC-MS displays better lower detection limit than GC-MS, but detection limits obtained using both GC-MS and LC-MS were several orders of magnitude below the therapeutic range of NVP (Sichilongo et al, 2014). The LC-MS was not readily available at the time of this research therefore GC-MS was used to analyse nyaope samples.

1.3 AN OVERVIEW ON CANNABIS

Cannabis is believed to have originated earlier than 6000 BC in the grasslands of central Asia confined to the north of the Himalayas in the area between Turkestan, Pakistan and Southern China (Schultes, Hofmann and Rätsch, 2001; Wills, 2003; BBC News, 2005; Carod-Artal, 2013; Clarke and Merlin, 2013). The cultivation of cannabis is reported to have originated in China. Cannabis is cultivated primarily for fibre from the main stalk, narcotic drugs from the flowering parts, and oilseed (Small, 2015). The oilseed is used for human food, livestock feed, nutritional supplements, industrial oils and occasionally as a biofuel (*ibid*). Cannabis plants may have been introduced into Europe at around 1500 BC by nomadic tribes from Central Asia (Schultes, 1970). Arab traders may have introduced cannabis into North Africa at around the 12th century and Southern Africa at around the 13th century (Wills, 2003; BBC News, 2005). The cannabis plant is now distributed worldwide and can be cultivated either outdoor or indoors (hydroponic cultivation) throughout most of the tropic and temperate regions of the world. According to the United Nations Office on Drugs and Crime (UNODC) (2020) cannabis remains the most highly abused drug globally with an estimated 192 million users. The global production of cannabis is estimated to be 4303 tons per annum (UNODC, 2020). Cannabis has over 200 street names, which include the most common names: *Bongo, Buddha-sticks, Dagga, Ganja, Grass, Hemp, Joint-sticks, Kif, Marie-Jeanne, Marihuana, Marijuana, Pot, Sinsemilla, Thai-sticks* and *Weed* (UNODC, 2003; KZN Department of Health, n.d.). In South Africa it is commonly known by the street names *Dagga, Ganja, Grass, Joint, Marijuana, Pot* and *Weed* and *Zol* (DSTV Network, 2016; Drug Wars, n.d.). The main producers of cannabis in the Southern African region are Lesotho, Malawi, Mozambique, South Africa, Swaziland and Tanzania, with South Africa ranked amongst the top producers in the world (Gastrow, 2003). The cannabis produced in these countries illustrated in Figure 1.2 is given street names that

are area specific (Marijuana Genetics Database, 2016). The cannabis produced from Swaziland are named *Swazi rooi* for its characteristically red-coloured, beard-like hair, and *Swazi Skunk*. *Red beards* from the Eastern Cape in South Africa, *Durban Poison* from KwaZulu-Natal in South Africa, *Malawi Gold* (because of its mythical gold colour) from Malawi, *Tanzanian Magic* from Tanzania, *Zambian Copper* from Zambia and *Kariba Surprise* from Zimbabwe. Cannabis has a street value of R1.00 per gram, which makes it easy to access (Drug Wars, n.d.).

Figure 1.2: Pictures of the cannabis varieties (A) *Swazi rooi*, (B) *Swazi Skunk*, (C) *Red beards*, (D) *Durban Poison*, (E) *Malawi Gold*, (F) *Tanzanian Magic*, (G) *Zambian Copper*, and (H) *Kariba Surprise*, produced in Southern Africa

1.3.1 Cannabis plant taxonomy

Cannabis is normally a dioecious plant; that is, male flowers on one plant and the female on another (Cherniak, 1982; Migal, 1991; Moliterni et al, 2004; Bond, 2018). Monoecious plants, called hermaphrodites, in which male and female flowers occur on the same individual plant, do exist (Bond, 2018). The plant is usually wind-pollinated and grows annually from 30 cm to

6 m in height (Schultes et al, 2001). The leaves are palmate, consisting of 5 to 13 separate leaflets, with clusters of flowers (Clarke and Merlin, 2013). In general, the male plant is smaller, sparser in foliage and have a shorter life cycle, while the female plant has a bushy appearance. Male plants are generally taller and slenderer than the female plants are. The stem of the cannabis plant is hollow and four cornered, its surface being covered in anticellular trichomes (hairs), pressed to the stem which curve upward. Unisexual flowers are bored in inflorescences that are terminal at an earlier stage, and terminal or lateral at a later stage. The taxonomical classification of cannabis is indicated in Table 1.4 (US-DA PLANTS, n.d.; Small and Cronquist, 1976; Schultes et al, 2001; Hazekamp, 2007; Clarke and Merlin, 2013).

Table 1.4: Taxonomical classification of cannabis plant

CATEGORY	**TAXON**
Kingdom	*Plant*
Subkingdom	*Tracheobionta*
Superdivision	*Spermatophyta*
Division	*Tracheophyta*
Subdivision	*Pteropsida*
Class	*Angiospermae*
Subclass	*Dicotyledonae*
Superorder	*Dilleniidae*
Order	*Urticales*
Family	*Cannabaceae*
Genus	*Cannabis*
Species	*Cannabis sativa L.*

The cannabis is divided into the drug-type and fibre-type cultivars. Both the drug-type and the fibre-type belong to the species *Cannabis sativa L.* The most popular subspecies for *Cannabis sativa L* proposed by Hillig (2005) are *sativa, indica* and *ruderalis*. Fibre-type

cannabis belongs to the subspecies *sativa*. The subspecies *sativa* can be divided into the variety *sativa* for the cultivated plants and variety *spontanea* for the plants that grow in the wild (Hill, 1983; Small and Cronquist, 1976). The drug-type cannabis belongs to the subspecies *indica* and can be divided into the variety *indica* for the cultivated plants and variety *kafiristanica* for the wild plants (*ibid*). The subspecies *ruderalis* is said to be a class on its own and a plant that grows in the wild with the variety *spontanea* (*ibid*). Cannabis *ruderalis* is an auto-flowering plant that usually has a high concentration of the therapeutic CBD and a low concentration of the intoxicating Δ^9-THC (Seedsman Blog. 2015).

1.3.2 Chemical compounds in cannabis plants

There are more than 545 compounds which include cannabinoids, fatty acids, flavonoids and terpenes, that have been isolated from the plant *Cannabis sativa L* (ElSohly and Gul, 2014; Gould, 2015). The cannabinoids compounds are the only compounds which are of forensic interest and therefore fatty acids, flavonoids and terpenes the focus will not be considered in this research. Among the 545 chemicals there are 104 known cannabinoids, which can be divided into 10 main cannabinoid structural types (Hazekamp, n.d.; Brenneisen, 2007; Flores-Sanchez and Verpoorte, 2008; ElSohly and Gul, 2014; Gould, 2015), namely, 17 cannabigerol (CBG) type; 8 cannabichromene (CBCM) type; 8 cannabidiol (CBD) type; 18 Δ^9-tetrahydrocannabinol (Δ^9-THC) type; 2 Δ^8-tetrahydrocannabinol (Δ^8-THC) type; 3 cannabicyclol (CBL) type; 5 cannabielsoin (CBE) type; 10 cannabinol (CBN) type; 2 cannabinodiol (CBND) type and 9 cannabitriol (CBT) type; as well as 22 miscellaneous types. The 10 cannabinoid structural types are illustrated in Figures 1.3 and 1.4 while the miscellaneous types are illustrated in Figure 1.5 (Flores-Sanchez and Verpoorte, 2008; ElSohly and Gul, 2014).

The most abundant cannabinoids in a cannabis plant are Δ^9-tetrahydrocannabinolic acid (Δ^9-THCA), cannabidiolic acid (CBDA) and cannabinolic acid (CBNA), followed by cannabigerolic acid (CBGA), cannabichrominic acid (CBCA) and cannabinodiolic acid (CBNDA), while the others are minor compounds. Δ^9-THCA is reported to be the most abundant cannabinoid in the drug-type cannabis plant, while CBDA is the major cannabinoid in the fibre-type cannabis plant (Andre, Hausman and Guerriero, 2016). CBCA has been reported to be the most abundant cannabinoid in immature cannabis plants, and its content decline when the plant

reaches a mature stage (De Meijer, Hammond and Sutton, 2009). The cannabinoid acids usually undergo decarboxylation when the plant reaches maturation or is exposed to heat after harvesting and are converted to their decarboxylated form (Flores-Sanchez and Verpoorte, 2008). This implies that Δ^9-tetrahydrocannabinol (Δ^9-THC), cannabidiol (CBD), cannabinol (CBN) cannabigerol (CBG), cannabichromene (CBCM) and cannabinodiol (CBND) will be the most abundant basic compounds.

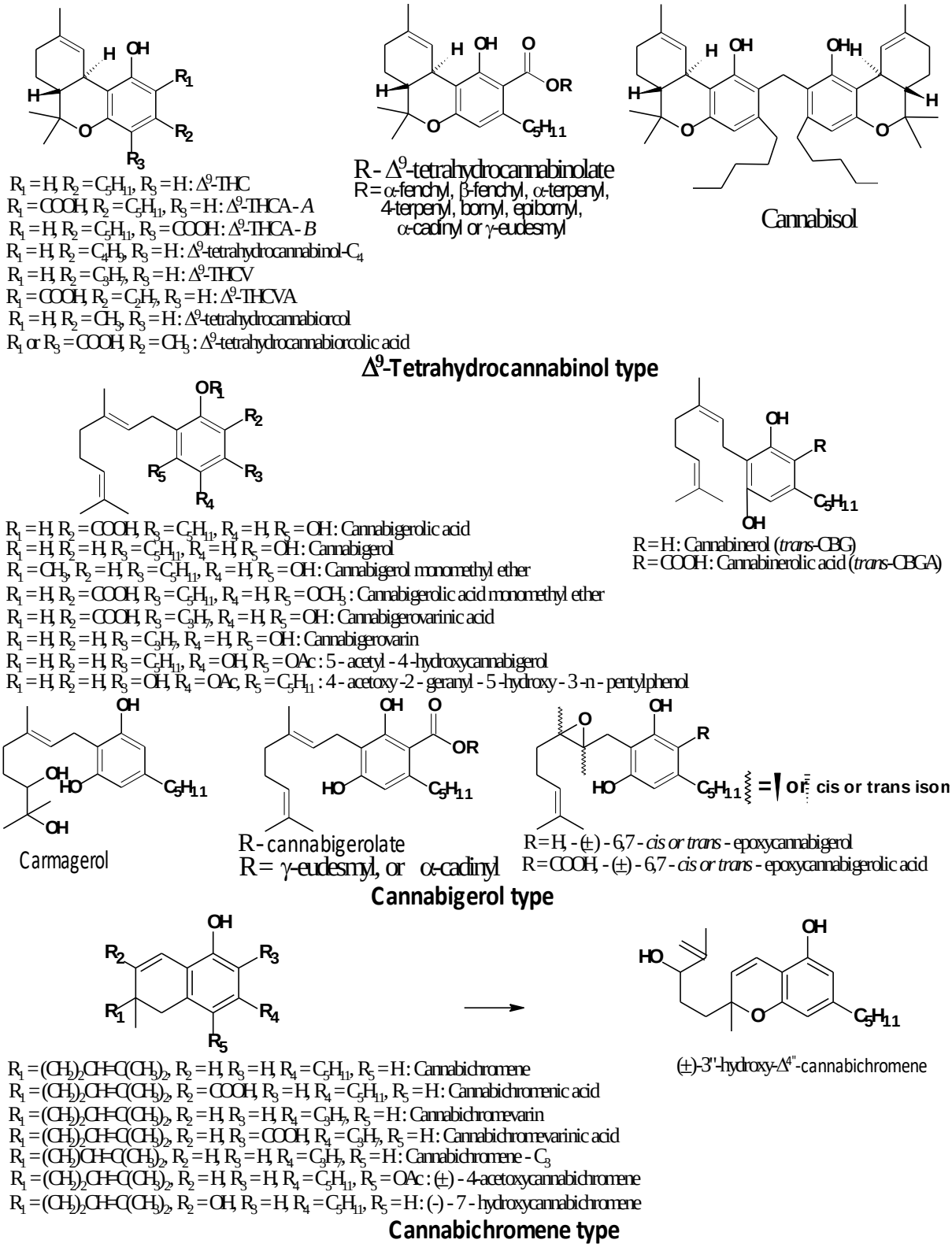

Figure 1.3: Δ9-Tetrahydrocannabinol, cannabigerol and cannabichromene structural types reported to be present in the cannabis plant.

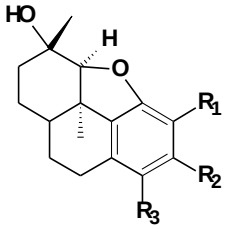

$R_1 = H, R_2 = C_5H_{11}, R_3 = H$, : Cannabielsoin
$R_1 = COOH, R_2 = C_5H_{11}, R_3 = H$, : Cannabielsoic acid A
$R_1 = H, R_2 = C_5H_{11}, R_3 = COOH$, : Cannabielsoic acid B
$R_1 = H, R_2 = C_3H_7, R_3 = H$, : Cannabielsoin-$C_3$
$R_1 = H, R_2 = C_3H_7, R_3 = COOH$, : Cannabielsoic-$C_3$ acid B

Cannabielsoin type

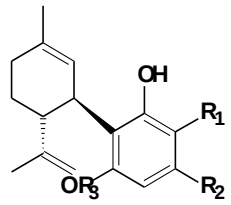

$R_1 = H, R_2 = C_5H_{11}, R_3 = H$, : CBD
$R_1 = COOH, R_2 = C_5H_{11}, R_3 = H$, : CBDA
$R_1 = H, R_2 = C_3H_7, R_3 = H$, : Cannabidivarin
$R_1 = COOH, R_2 = C_3H_7, R_3 = H$, : Cannabidivarinic acid
$R_1 = H, R_2 = C_5H_{11}, R_3 = CH_3$, : Cannabidiol monoethyl ether
$R_1 = H, R_2 = CH_3, R_3 = H$, : Cannabidiorcol
$R_1 = H, R_2 = C_4H_9, R_3 = H$, : Cannabidiol-$C_4$

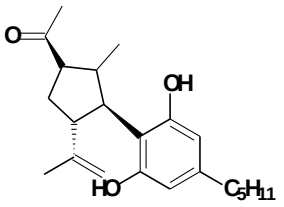

Cannabimovone

Cannabidiol type

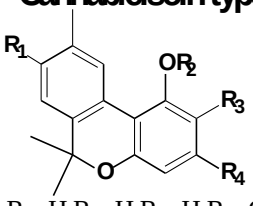

$R_1 = H, R_2 = H, R_3 = H, R_4 = C_5H_{11}$: CBN
$R_1 = H, R_2 = H, R_3 = COOH, R_4 = C_5H_{11}$: CBNA
$R_1 = H, R_2 = H, R_3 = H, R_4 = CH_3$: Cannabiorcol
$R_1 = H, R_2 = H, R_3 = H, R_4 = C_2H_5$: Cannabinol-$C_2$
$R_1 = H, R_2 = H, R_3 = H, R_4 = C_3H_7$: Cannabivarin
$R_1 = H, R_2 = H, R_3 = H, R_4 = C_4H_9$: Cannabinol-$C_4$
$R_1 = H, R_2 = CH_3, R_3 = H, R_4 = C_5H_{11}$: Cannabinol methyl ether
$R_1 = OH, R_2 = H, R_3 = H, R_4 = C_5H_{11}$: 8-hydroxy-CBN
$R_1 = OH, R_2 = H, R_3 = COOH, R_4 = C_5H_{11}$: 8-hydroxy-CBNA

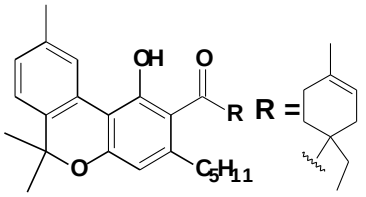

4-terpenyl cannabinolate

Cannabinol type

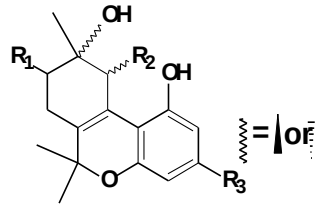

$R_1 = H, R_2 = OH, R_3 = C_5H_{11}$: (+)-*trans*-Cannabitriol
$R_1 = H, R_2 = OH, R_3 = C_5H_{11}$: (-)-*trans*-Cannabitriol
$R_1 = H, R_2 = OH, R_3 = C_5H_{11}$: (-)-*cis*-Cannabitriol
$R_1 = H, R_2 = OH, R_3 = C_3H_7$: ( )-*trans*-Cannabitriol-C_3
$R_1 = H, R_2 = OH, R_3 = C_3H_7$: Cannabitriol-$C_3$ homolgue
$R_1 = H, R_2 = OCH_2CH_3, R_3 = C_5H_{11}$: (-)-*trans*-10-ethoxy-9-hydroxy-$\Delta^{6a(10a)}$-tetrahydrocannabinol
$R_1 = H, R_2 = OCH_2CH_3, R_3 = C_3H_7$: (-)-*trans*-10-ethoxy-9-hydroxy-$\Delta^{6a(10a)}$-tetrahydrocannabivarin
$R_1 = OH, R_2 = OH, R_3 = C_5H_{11}$: 8,9-dihydroxy-$\Delta^{6a(10a)}$-tetrahydrocannabinol

R,R; S,S; R,S or S,R configuration

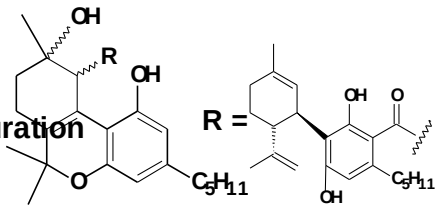

Cannabidiolic acid tetrahydrocannabitriol ester

Cannabitriol type

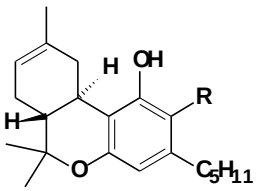

R = H; Δ^8-THC
R = COOH; Δ^8-THCA

Δ^8-Tetrahydrocannabinol type

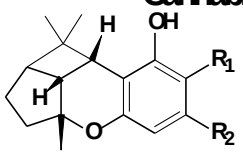

$R_1 = H, R_2 = C_5H_{11}$, : Cannabicyclol
$R_1 = COOH, R_2 = C_5H_{11}$, : Cannabicylolic acid
$R_1 = H, R_2 = C_3H_{11}$, : Cannabicyclovarin

Cannabicyclol type

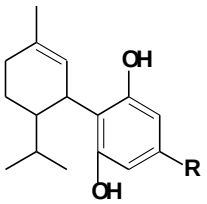

R = C_5H_{11} : cannabinodiol
R = C_3H_7 : cannabinodivarin

Cannabinodiol type

Figure 1.4: Cannabielsoin, cannabidiol, cannabinol, cannabitriol, Δ^8-tetrahydrocannabinol, cannabicyclol and cannabinodiol structural types reported to be present in the cannabis plant.

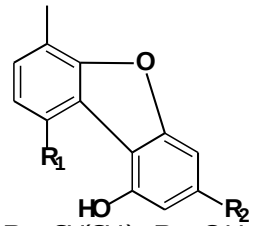

$R_1 = CH(CH_3)_2$, $R_2 = C_5H_{11}$: Cannabifuran
$R_1 = CH(CH_3)=CH_2$, $R_2 = C_5H_{11}$: Dehydrocannabifuran
$R_1 = C(CH_3)_2OH$, $R_2 = C_3H_7$: 8-hydroxy-isohexahydrocannabivarin

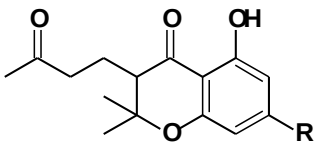

$R = C_5H_{11}$: Cannabichromanone-C_5
$R = C_3H_7$: Cannabichromanone-C_3

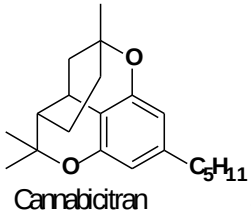

Cannabicitran

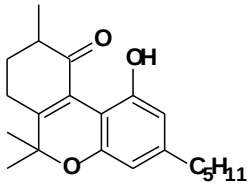

10-OXO-$\Delta^{6a(10a)}$-tetrahydrocannabinol

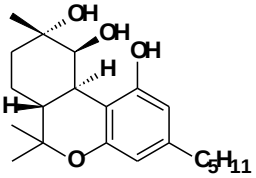

Cannabiripsol

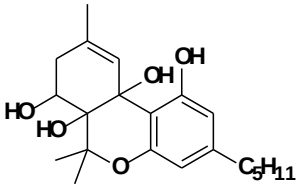

Cannabiterol

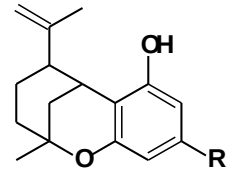

$R = C_3H_7$: (±)-Δ^7-*cis*-isotetrahydrocannabivarin-C_3
$R = C_3H_7$: (-)-Δ^7-*trans*-(1*R*,3*R*,6*R*)-isotetrahydrocannabivarin-C_3
$R = C_5H_{11}$: (-)-Δ^7-*trans*-(1*R*,3*R*,6*R*)-isotetrahydrocannabinol-C_5

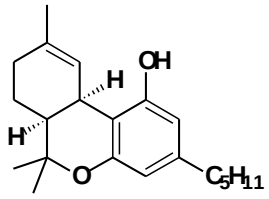

(-)-Δ^9-*cis*-(6a*S*,10a*R*)-tetrahydrocannabinol

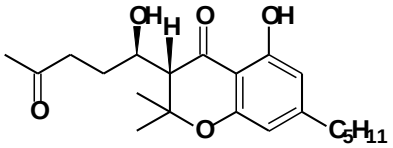

Cannabichromanone-B

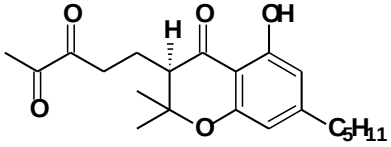

Cannabichromanone-C

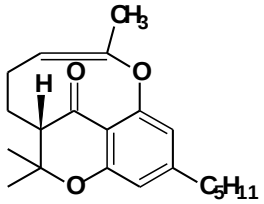

Cannabichromanone-D

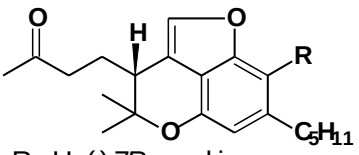

R = H: (-)-7*R*-cannabicoumarone
R = COOH: (-)-7*R*-cannabicoumaronic acid

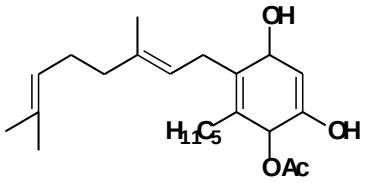

4-acetoxy-2-geranyl-5-hydroxy-3-*n*-pentylphenol

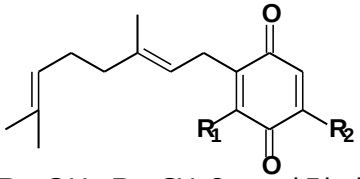

$R_1 = C_5H_{11}$, $R_2 = OH$: 2-geranyl-5-hydroxy-3-*n*-pentyl-1,4-benzoquinone
$R_1 = OAc$, $R_2 = C_5H_{11}$: 4-acetoxy-6-geranyl-3-*n*-pentyl-1,4-benzoquinone

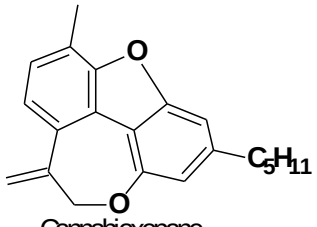

Cannabioxepane

Figure 1.5: Miscellaneous cannabinoids structural types reported to be present in the cannabis plant.

1.3.3 Δ^9-THC nomenclature

The main psychoactive compound in the cannabis plant is Δ^9-THC ((6a*R*,10a*R*)-6a,7,8,10a-tetrahydro-6,6,9-trimethyl-3-pentyl-6*H*-dibenzo[*b,d*]pyran-1-ol) sometimes referred to as Δ^1-THC (Mechoulam and Gaoni, 1967; Gaoni and Mechoulam, 1971; Agurell et al, 1986). The stereochemistry of the two asymmetric centres –C^{10a} and C^{6a}– in cannabidiol (CBD) was deduced to be "trans" from an analysis of the coupling constants of the protons at these centres; therefore, the name (-) Δ^9-trans-tetrahydrocannabinol was assigned (Gaoni and Mechoulam, 1964; Mechoulam R and Gaoni Y 1965). Tetrahydrocannabinol has two well-known isomers, namely Δ^9-THC and Δ^8-THC (sometimes referred to as Δ^6-THC). At least two different numbering systems, shown in Figure 1.6, have been used to identify the various tetrahydrocannabinol isomers (Flemming et al, 2007), namely the "dibenzopyran" system and the "monoterpenoid" system. The designation Δ^9-THC, which is most commonly encountered in present literature is associated with the dibenzopyran system, while the Δ^1-THC designation is associated with the monoterpenoid system. Similarly, the isomers Δ^8-THC and Δ^6-THC are associated with the dibenzopyran system and the monoterpenoid system, respectively. The absolute configuration at both asymmetric centres C^{10a} and C^{6a} in natural (-) Δ^9-THC is the "R R" configuration (Mechoulam and Gaoni, 1967; Rosenqvist and Ottersen, 1975).

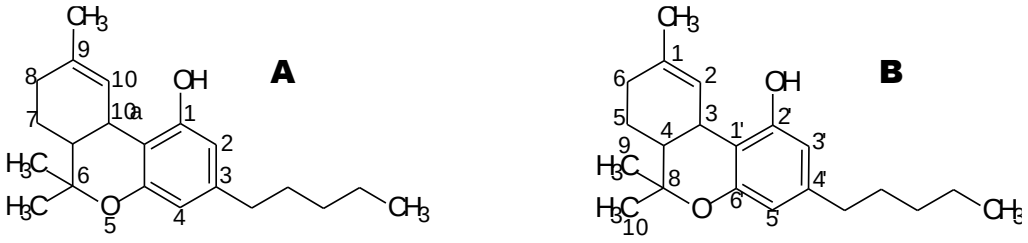

Figure 1.6: The most common numbering systems (A) Dibenzopyran System, (B) Monoterpenoid System, used to identify the various positions within the tetrahydrocannabinol molecule.

Synthetic Δ^9-THC was first successfully produced around 1964 (Mechoulam and Gaoni, 1965). Δ^9-THC is the decarboxylation product of the acid Δ^9-THCA. It has been established that Δ^9-

THCA occurs in two isomeric forms, namely Δ^9-THCA-A and Δ^9-THCA-B as illustrated in Figure 1.7 (Mechoulam et al, 1969).

Figure 1.7: Structures of the tetrahydrocannabinolic acid isomeric forms (A) Δ^9-THCA-A and (B) Δ^9-THCA-B.

The Δ^9-THCA-A has a chelated carboxylic acid group adjacent to the phenolic group. The Δ^9-HCA-B has an unchelated carboxylic acid group on a position which is ortho to the etheric oxygen. Both isomeric forms are psychological in active and are both converted to the active Δ^9-THC on decarboxylation. Literature reports that most cannabis contains the Δ^9-THCA-A isomer (Mechoulam et al, 1969; Rosenqvist and Ottersen, 1975; McPartland et al, 2017). It would also seem to be the preferred molecular structure since steric hindrance from adjacent groups is minimal in the Δ^9-THCA-A, compared to the Δ^9-THCA-B. However, the fact that the Δ^9-THCA-B has been found in a few cannabis samples indicates the possibility that different variants of cannabis may have slightly different biosynthetic pathways. The Δ^9-THCA-B is more stable and therefore readily crystallizes (Rosenqvist and Ottersen, 1975; McPartland et al, 2017). Another cannabis constituent, cannabielsoic acid (CBEA), also occurs in two isomeric forms similarly to Δ^9-THCA illustrated in Figure 1.7.

The concentration of Δ^9-THC determines the potency of cannabis. Δ^8-THC is believed to be as potent as Δ^9-THC, but is usually present in very small amounts in the cannabis plant, and as a result, it does not contribute to the overall potency of cannabis (Agurell et al, 1986, McGilveray, 2005). CBN is said to be about $^1/_{10}$ as potent as Δ^9-THC, whereas CBD is devoid of psychoactive properties (*ibid*). The Δ^9-THC content varies with the different parts of the plant. The flowering tops has the highest (Δ^9-THC content which is about 12%, followed by 2% in the leaves, 0.3% in the stalks and <0.03% in the roots (UNODC, 2009a). The seeds do not contain

Δ^9-THC although detectable amounts of Δ^9-THC can be found on the outside surface of the seeds because of contamination from the bract of the cannabis plant which is Δ^9-THC rich (Grotenhermen, Karus and Lohmeyer, 1998; UNODC, 2009a). This is disputed by Ross et al (2000), who report that small amounts of Δ^9-THC is found inside the seed which is less than 2µg/g for drug-type seeds and less than 0.5 µg/g in fibre-type drug.

Based on the total Δ^9-THC content (Δ^9-THC + Δ^9-THCA), the cannabis plant can be classified as either drug-type or fibre-type. The drug-type cannabis plant material has a total Δ^9-THC content above 0.3%, while the fibre-type cannabis plant has a total Δ^9-THC content up to 0.3% (*ibid*). The ratio of the main cannabinoids Δ^9-THC, CBN and CBD are used to differentiate between the drug-type and fibre-type cannabis plants. Because Δ^9-THC is oxidized partly to CBN after cutting and drying the plant material, the sum of the peak area of Δ^9-THC and CBN is used and divided by the area of CBD. Equation 1.1 illustrates the calculation to differentiate between the drug-type and fibre-type cannabis.

$$\boldsymbol{X} = \frac{[\Delta^{9}\boldsymbol{-THC}]+[\boldsymbol{CBN}]}{[\boldsymbol{CBD}]} \qquad \textbf{1-1}$$

Where [Δ^9-*THC*], *[CBN]* and *[CBD]* is the concentration of Δ^9-THC, CBN and CBD, respectively in the chromatogram.

If the ratio of [THC] + [CBN] to [CBD] is <1, then the cannabis plant is considered to be a fibre type. If the ratio is >1, it is considered a drug type.

The cannabinoids concentration levels in cannabis plant are the lowest during the seedling stage of development, highest prior to flowering stage and intermediate thereafter, up to a stage where deterioration begins (Chandra et al, 2010, De Backer, 2012).

Under the influence of heat, decarboxylation of the cannabinoids acids occurs instantly and completely. When it is required to determine the Δ^9-THC content in marijuana preparations by GC, the resulting THC content represents the total or combined Δ^9-THC and Δ^9-THCA, i.e., Δ^9-THC + Δ^9-Tetrahydrocannabinolic Acid (Δ^9-THCA), the latter being decarboxylated to

Δ^9-THC upon injection into the gas chromatograph. Acid and neutral cannabinoids can be analysed by GC if the sample is silylated prior to injection to prevent decarboxylation.

1.3.4 Psychological effect of cannabis

According to the South African Community Epidemiology Network on Drug Use (SACENDU, 2013) cannabis is the largest drug of abuse amongst youth in South Africa, while nyaope use is on the rise in the Gauteng Province, and stable but high in KwaZulu-Natal. The desired psychoactive effects of cannabis include a sense of well-being, euphoria – a "high" feeling and a pleasurable state of relaxation. Adverse effects include confusion, drowsiness, restlessness, excitement, and hallucinations (Hall and Solowij, 1998; UNODC, 2003; Hall, 2014). Most hallucinogenic plants are alkaloids; however, although Δ^9-THC is a hallucinogen, it does not incorporate a nitrogen atom in its structure and hence it is not an alkaloid.

The cannabinoids CBCM, CBD, CBG, CBN and Δ^9-THC have been reported to all show potent antibacterial activity (Appendino et al, 2008). Essential hemp oils with undetectable levels of the cannabinoids are regarded as having modest antibacterial activity (Novak et al, 2001). Cannabis extracts containing higher CBD ratio to Δ^9-THC show stronger antimicrobial activity (Leizer et al, 2000). The cannabinoid 5-acetyl-4-hydroxycannabigerol is believed to have antileishmanial activity 4-acetoxy-2-geranyl-5-hydroxy-3-n-pentylphenol has antibacterial activity while 8-hydroxycannabinol has antifungal activity (Radwan et al, 2009). The activity of cannabis extracts was shown to be solvent dependant; i.e., methanol extracts show antibacterial activity against *Pseudomonas aeruginosa* and antifungal activity against *Candida albicans,* while petroleum ether extract showed inactivity (Ali et al, 2012).

It is believed that the abuse of cannabis results in both physical and psychologically addiction (Acher et al, 2012; Hall, 2014). The risk of addiction is estimated to be 9% for adult users, which increases to one in every six users if the abuse commenced during adolescence stage (Anthony, 2006; Lopez-Quintero et al, 2011; Hall, 2014).

The abuse of Δ^9-THC, like alcohol, significantly affects the ability to drive in a dose-dependent manner and drivers under the influence of Δ^9-THC drive significantly slower than drivers under the influence of alcohol (Ronen et al, 2008). Unlike alcohol, which causes sleepiness, Δ^9-THC results in increased physical effort and physical discomfort (*ibid*).

1.3.5 Analysis and profiling of cannabis

Several analytical techniques have been described in literature for the identification, quantitation and profiling of cannabis samples. Table 1.5 lists the linearity ranges of some of the different techniques as well as the limit of detection (LOD) and limit of quantitation (LOQ) for Δ^9-THC.

Table 1.5: linearity range, limit of detection and limit of quantitation of Δ^9-THC for different analytical techniques.

Technique	Linearity range, mg/L	Detection limit, mg/L	Quantitation limit, mg/L	Reference
GC-FID	-	0.11 – 0.19	0.34 – 0.56	Ibrahim et al, 2018
GC-MS	0.0010 – 1.00	0.00050	0.024	Kauert et al, 2006
GC-MS/MS	0.0000010 – 0.00024	0.0000010	0.00040	Day, Kuntz and Feldman, 2006
GC x GC-MS	0.00050 – 0.050	0.00050	0.00050	Milman et al, 2010.
HPLC-DAD	0.25 – 50.00	0.062	0.25	Patel, Wene and Fan, 2017
HPLC-CV	0.010 – 200.00	0.15	0.50	Mandrioli et al, 2019
LC-MS	0.0020 – 0.10	0.10	0.0020	Teixeira et al, 2004
LC-MS/MS	0.00050 – 0.020	0.00018	0.00044	König et al, 2011
UPLC-MS/MS	0.00050 – 1.00	0.00020	0.00050	Simões, et al, 2011
NMR	100.00 – 1.00	-	-	Hazekamp, Choi and Verpoorte, 2004

1.3.5.1 Gas chromatographic methods for cannabis analysis

Gas chromatographic methods for the analysis of cannabis are usually hyphenated methods, which includes gas chromatography, coupled with either flame ionisation detection (GC-FID), isotope ratio mass spectroscopy (GC-IRMS), mass spectroscopy (GC-MS), or tandem mass spectroscopy (GC-MS/MS). GC-IRMS, which measures the carbon-13, nitrogen-15, oxygen-18 and hydrogen-2 (D) isotope ratios, is used mainly for the profiling of compounds (UNODC, 2009a; Muccio et al, 2012, Gentile et al, 2015; Cerling et al, 2016). The use of carbon-13 and nitrogen-15 isotopes for the determination of the geographic origin of cannabis plant is hindered by the wide variety of indoor and outdoor conditions under which these plants are

cultivated (Gentile et al, 2015). While the isotope variation of the outdoor cultivated cannabis is well documented, there is limited research on indoor cultivated cannabis (ibid). The method would not be a suitable method for the identification of the different components of nyaope. Although GC-MS/MS is a better method for the identification, quantitation and chemical profiling of cannabis (Day et al, 2006), GC-MS is also a suitable method, since it can be applied to a very large variety of cannabinoids with very high resolution (Brenneisen and ElSohly, 1988; Feng et al, 2000; Cole, 2003; Hewavitharana et al, 2005; Nadulski et al, 2005; Broséus, Anglada and Esseiva, 2010; Fischedick et al, 2010; Hazekamp and Fischedick, 2012; Cadola, Broséus and Esseiva, 2013; Chan, 2014). The GC-MS methods employed have typical linearity ranges as well as LODs and LOQs for Δ^9-THC, illustrated in Table 1.5**.** GC-MS analysis can be conducted in scan mode or single-ion monitoring (SIM) mode. For analytes with known mass spectra and at trace level, SIM mode is the method of choice due to its higher sensitivity. If the analyte is unknown, the scan mode is suitable for the identification of the analyte. Although the use of SIM mode usually gives higher sensitivity, it is not essential in instances where the concentration of the samples encountered have adequate sensitivity when using the scan mode (Hewavitharana et al, 2005).

The chromatographic profiles of cannabis are said to depend on the method of extraction and the nature of the sample (Marchini et al, 2014). Using an optimized solid-phase macro-extraction (SPME) method and two-dimensional gas chromatography-mass spectrometry (GC x GC-MS), the volatile chemical profiles of cannabis-derived products were differentiated greatly, improving compound identification better than one-dimensional profiles (*ibid*).

Gas-chromatograph tandem-mass spectrometry GC-MS/MS has also been applied for the analysis of cannabinoids (Uhl, 1997; Day et al, 2006; Schwilke et al, 2009; Young and Martin, 2010) with typical linearity ranges as well as LODs and LOQs for Δ^9-THC as illustrated in Table 1.5. The gas-chromatography tandem-mass spectrometry (GC-MS/MS) has been shown to give detection limits, which are orders of magnitude lower than those found for liquid-chromatography tandem- mass spectrometry (Day et al, 2006).

GC-FID has been applied successfully for the identification and quantitation of cannabinoids (Pijlman et al, 2005; Fischedick et al, 2010; Ibrahim et al, 2018).

The cannabinoids are mainly available in the cannabis plant in the form of carboxylic acid derivatives and therefore the high temperature involved when samples are introduced into the instrument to enable complete vaporisation of the sample results in the decarboxylation of the cannabinoid acids to the corresponding neutral form. The gas chromatographic quantitation of cannabis therefore measures a total combination of both the acid and the neutral form of the cannabinoids. The decarboxylation of the cannabinoid acids in the injector may be incomplete, resulting in a non-representative analysis of the cannabis samples (Pandohee et al, 2015).The direct analysis of cannabinoids acids using gas chromatographic methods is therefore not possible. To avoid decarboxylation of these acids before gas chromatographic analysis, a derivatisation step by for example silylation, is required. However, the derivatisation step is time consuming and suffers from the difficulty of achieving an effective derivatisation yield for all the components of a complex mixture (Pandohee et al, 2015; Borillea et al, 2017). In addition, the derivatisation products may undergo thermo-degradation in the injector or column (Borillea et al, 2017).

1.3.5.2 Liquid chromatographic methods for cannabis analysis

Liquid chromatographic methods have also been used extensively for the identification, quantitation and profiling of cannabis. The methods includes high-performance liquid chromatography, coupled to either diode array detector (HPLC-DAD) (Swift et al, 2013; Ambach et al, 2014; Peschel and Politi, 2015; Mudge et al, 2017; Patel et al, 2017) or ultraviolet detector (HPLC-UV) (Confidence Analytics, 2018; Zivovinovic et al, 2018; Mandrioli et al, 2019), liquid chromatography coupled with either mass spectrometry (LC-MS) (Teixeira et al, 2004; Teixeira et al, 2007; Gilani and Grinnan, 2019), or tandem mass spectrometry (LC-MS/MS) (Vlase et al, 2010; König et al, 2011; Hudson et al, 2013; Aamir et al, 2016; Aizpurua-Olaizola et al, 2014; Meng et al, 2018); as well as ultra-performance liquid chromatography coupled with tandem mass spectrometry (UPLC-MS/MS) (Young and Martin, 2010; Zhang, Wang and Mo, 2010; Simões, et al, 2011; Wille et al, 2013; Lee et al, 2014; Montesano et al, 2014; Simões, et al, 2014). Typical linearity ranges, LODs and LOQs for Δ^9-THC for each of these liquid chromatographic, are illustrated in Table 1.5. Validated HPLC-DAD methods for the quantitation of cannabinoids reported in literature (Table 1.5) exhibit reasonable linearity range, LOD and LOQ for Δ^9-THC. Using a preconcentration step, which involves an ionic liquid

solvent formation microextraction, coupled with magnetic nano-particle based dispersive micro-solid phase extraction, results in the detection limit that is two orders of magnitude better (Feizbakhsh et al, 2016).

HPLC-UV methods reported in literature exhibit reasonable linearity range, LOD and LOQ for Δ^9-THC (Confidence Analytics, 2018; Zivovinovic et al, 2018; Mandrioli et al, 2019)

Unlike gas chromatographic methods, liquid chromatographic methods do not involve vaporization of the sample and therefore, the methods allow for the analysis of both acidic and neutral forms of the cannabinoids without derivatization. However, the complex composition of the cannabis material leads to a strenuous effort to achieve the separation of major cannabinoids and significant peak overlap occurs (Borillea et al, 2017). Though tandem mass spectrometry helps in resolving the peak overlap issue, characterization of the entire cannabis is still a challenge (Pandohee et al, 2015).

1.3.5.3 Nuclear Magnetic Resonance spectroscopic methods for cannabis analysis

Nuclear Magnetic Resonance (NMR) techniques, which include proton nuclear magnetic resonance (^{1}HNMR) and Proton-Proton Correlation Spectroscopy (COSY) and Total Correlation Spectroscopy (TOCSY), were successfully employed for the identification cannabinoids, taking advantage of the spectroscopic separation power from NMR spectroscopy (Hazekamp et al, 2004; Happyana et al, 2012; Peschel and Politi, 2015; Fowler et al, 2018).

The COSY NMR technique is used for determining the stereochemistry of organic molecules as well as by protein chemists to 'fingerprint' secondary protein structures. TOCSY is similar to COSY in that it analyses proton-proton correlations; however, it has the power to correlate protons beyond two and three bond couplings on the same chain or ring. This provides more structural information and confidence when assigning specific protons to signals.

1.3.5.4 DNA analysis methods for cannabis analysis

The identification and profiling of the cannabis plant can be achieved using DNA analysis in instances where seeds and roots are seized and when Δ^9-THC is not detected with chemical

methods, as well as when the amount of cannabis seized is at trace level (Siniscalco Gigliano, Caputo and Cozzolino, 1997; Linacre and Thorpe, 1998; Siniscalco Gigliano, 1998; Hsieh et al, 2003; Miller-Coyle et al, 2003b). Cannabis cultivation is usually carried out by seed or by cloning propagation of the plants. Seed-propagated cannabis plants are expected to have unique DNA profiles analogous to a human population, while cloned cannabis plants exhibit identical DNA profiles, which allow for tracking of plant material derived from a common genetic lineage (Miller-Coyle et al, 2001). For forensic purposes, DNA analysis can be used for identification of plant material as cannabis, whether cultivated hydroponically or by cloning, as well as determining the origin of the plant (Gilmore, Peakall and Robertson, 2003; Miller-Coyle et al, 2003a). DNA analysis, however, cannot be used to unequivocally differentiate between drug-type and fibre type cannabis (Gilmore et al, 2003). DNA analysis involves amplification of the extracted plant DNA using polymerase chain reaction (PCR). Once PCR amplification of the DNA is done, different methods are then used for the sequencing and thereby create the DNA profiles. Profiling of cannabis plants can be done using the technique amplified fragment-length polymorphism (AFLP) to create a DNA profile for plant varieties (Miller-Coyle et al, 2003a). Random amplification of polymorphic DNA (RAPD) has also been used for profiling cannabis plants which could not be differentiated using chromatographic methods (Gillan et al, 1995). RAPD has an advantage that it requires no previous sequence information but suffers from poor specificity and poor reproducibility, can therefore not be used for routine work and is superseded by polymorphic tests. The first highly polymorphic short tandem repeat (STR) technique, which is highly reproducible, was reported by Hsieh et al (2003). The use of STR DNA markers is reported as the method of choice in forensic investigation, since it is hypervariable and informative for *cannabis sativa* (Gilmore et al, 2003). However, the method cannot differentiate between drug-type and fibre-type cannabis (*ibid*). The identification and profiling of *cannabis sativa L.* for forensic interest was achieved by comparing the sequence of the nuclear ribosomal DNA Internal Transcribed Spacer II (ITS2) (Siniscalco Gigliano et al, 1997; Siniscalco Gigliano, 1998). Both AFLP and STR are believed to have higher discriminating power than RAPD (Miller-Coyle et al, 2003b). Inter-simple sequence repeat (ISSR) amplification has been used for the estimating genetic difference among *cannabis sativa L* samples by studying polymorphic DNA patterns between samples (Kojoma et al, 2002).

1.4 AN OVERVIEW ON HEROIN

The abuse of heroin has increased globally with an estimated production of 722 tons (UNODC, 2020). Heroin is known by the common street names *Boy, Dragon, H, Hairy, Harry, Horse, Joy powder, Junk, Smack, Snow, White lady* and *White stuff*, amongst others (UNODC, 2016). According to the United Nations Office for Drug Control and Crime Prevention (UNODCCP), the street value of heroin was previously R250,00 per gram, which made it inaccessible to the poor, unemployed young adults. Currently, it is sold at R30,00 per 5 milligram; that is, it is sold at a reduced quantity in order to make it easily accessible to this group (Mokwena and Huma, 2014; Drug Wars, n.d.). Heroin is a semi-synthetic product of morphine. Morphine is itself a natural occurring alkaloid that is extracted from the opium poppy plant *Papaver somniferum. L*. *Papaver somniferum* is the medicinal plant which is a source of analgesic narcotic codeine and morphine. The word *papaver* comes from the Greek, meaning "poppy", while *somniferum* is from the Latin and means "to dream" or "induce sleep"; thus, we have "the poppy that produces sleep". The plant species *papaver somniferum* is believed to have evolved from a wild strain *papaver segtigerum* that grows in the coastal areas of the Mediterranean Sea (US-DEA, 1992). The plant species *papaver somniferum* is the only plant that produces opium and was known in Europe at least 4000 years ago. The taxonomical classification of opium is indicated in Table 1.6 (Labanca et al, 2018).

Table 1.6: Taxonomical classification of the opium poppy plant.

CATEGORY	TAXON
Phylym	*Spermatophyta*
Class	*Dicotyledons*
Order	*Papavarales*
Family	*Papaveraceae*
Genus	*Papaver L.*
Species	*Papaver somniferum L.*

Alkaloids derived from opium poppy are referred to as opiates and are usually obtained as a gelatinous juice referred to as opium. Opium extracts usually contain 4–21 wt% morphine, 0.7–3 wt% codeine, 2–8 wt% noscapine, 0.5–1.3 wt% papaverine and 0.2–1 wt% thebaine (Cole, 2003; UNODC, 2003). Opium alkaloids fall into two distinct classes; namely, the phenanthrene group (e.g., morphine) and the benzylisoquinoline group (e.g., papaverine). Alkaloids of the former group are highly addictive and are therefore under full international control. Alkaloids of the latter group possess no addictive liabilities, nor can they be readily converted to addictive substances and are therefore not subject to international control. The main alkaloid morphine was first isolated from the opium poppy by a German pharmacist as early as 1803, and who named it Morpheus after the Greek god. This was followed by the isolation of codeine around 1832 and papaverine around 1848. Morphine and codeine are used clinically as analgesics to reduce pain without a loss of consciousness. Thebaine is without analgesic effect but is of great pharmaceutical value due to its use in the production of semisynthetic opioid morphine analogues such as oxycodone, dihydromorphinone, and hydrocodone (US-DEA, n.d.). Benzylisoquinoline alkaloids that are of pharmaceutical value include noscapine, papaverine and sanguinarine. Papaverine has medicinal value as a vasodilator (Elek and Katz, 1942; Wilson and White, 1986); noscapine is used in the treatment of stroke, as a cough suppressant and a possible anti-cancer agent (Segal, Goldstein and Attinger, 1957; Mahmoudian and Rahimi-Moghaddam, 2009; Mahmoudian et al, 2015), while sanguinarine is a potential antimicrobial, antioxidant, anti-inflammatory and anticancer agent (Godowski, 1989; Mackraj, Govender and Gathiram, 2008; Senchina, Shah and Busch, 2012; Sun et al, 2012; Kalogris et al, 2014; Achkar et al, 2017). Papaverine and noscapine have little to no effect on the human central nervous system, and as such are not considered to be opiates.

1.4.1 Heroin synthesis

Heroin (diacetylmorphine) is the most frequently encountered opiate in a forensic laboratory (US-DEA, n.d.). It is highly abused and has no current accepted medical use in South Africa making it a Schedule III controlled substance. As a narcotic, it is an analgesic (painkiller) and a depressant (sleep inducer). Its effects are some three to six times stronger than morphine, from which it is prepared (UNODC, 2016; US-DEA, n.d.). It is physically addictive and, once the

habit starts, the body develops a "tolerance" for the drug, which means larger dosages are required to get the same effect (*ibid*). A second sign of heroin addiction is withdrawal sickness. When an addict stops using the drug, they may sweat, shake, get chills, develop diarrhoea and nausea, and suffer sharp abdominal and leg cramps (*ibid*).

Heroin is synthesized by the acetylation of morphine using acetic anhydride which often results in the formation of by-products such as 6-monoacetylmorphine (6-MAM) and 3-monoacetylmorphine (3-MAM). Morphine, used in illicit manufacture of heroin, contains codeine which results in the formation acetylcodeine during acetylation. If the morphine used contained impurities such as laudanosine, reticuline, codamine, and laudanine, this will lead to the formation of C1-acetate compounds and the stilbene compounds as neutral impurities (Toske et al, 2006). The neutral impurities can be used to enhance the classification of illicit heroin samples (*ibid*). High-purity heroin only contains acetylcodeine, 6-MAM and 3-MAM as by-products. In addition to these by-products, low-purity heroin samples are most likely to contain codeine, papaverine and noscapine as a result of co-extraction from the opium in addition to the by-products.

The impurities found in street level heroin can be classified into (i) natural occurring substances other than the active ingredient (diamorphine), which are co-extracted from the raw plant; (ii) synthetic by-products; and (iii) cutting agents. The major naturally occurring alkaloids that are found in heroin samples include morphine, codeine, noscapine and papaverine (Cole, 2003; UNODC, 2005). The by-products of the manufacturing process, found in street level heroin, include acetylcodeine, 3-monoacetylmorphine (3-MAM) and 6-monoacetylmorphine (6-MAM). The cutting agents, both diluents and adulterants, are normally added to bulk the sample, reduce the overall production cost, or to enhance the effect of heroin. Diluents are pharmacologically inactive compounds added strictly to increase the bulk of the pharmacologically active ingredient in illicit drugs for distribution. The most common diluents for heroin are lactose, mannitol, corn starch and dextrose. Other diluents occasionally found include inositol, sucrose, sodium bicarbonate (baking soda), sodium carbonate (washing soda), magnesium sulphate (Epsom Salt), sodium chloride, and other starches (US-DEA, n.d.; UNODC, 2005). Adulterants are pharmacologically active compounds which are added either to attempt to increase the effect of the heroin on the body or to fool the pusher and/or addicts into thinking they have better "stuff" than they actually have

purchased. These include substances like acetaminophen, caffeine, phenacetin, dextromethorphan, lidocaine levamisole, and antiretroviral drugs as well as other illicit drugs (Broséus et al, 2015; SAPS Fact File, 2013; UNODC, 2005). Adulterants are normally identified by GC-MS. Table 1.7 lists some of the common adulterants along with the prominent EI mass spectrometric data (UNODC, 2005; Mills III et al, 2006).

Table 1.7: Some of the common adulterants found in heroin samples and associated mass spectroscopic data.

Structure	Common name	IUPAC name	Empirical formula	Molar mass, g/mol	Base peak (shown in bold) and other prominent peaks, m/z
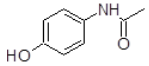	Acetaminophen (Paracetamol)	N-(4-Hydroxyphenyl)acetamide	$C_8H_9NO_2$	151.06	**109** 151, 43, 80, 53
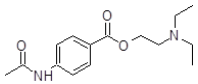	Acetylprocaine	2-(Diethylamino)ethyl 4-acetamidobenzoate	$C_{15}H_{22}N_2O_3$	278.16	**86**, 43,99, 120, 92
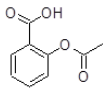	Acetylsalicylic acid (Aspirin)	5-Acetyl-2-hydroxybenzoic acid/ 2-Acetoxybenzoic acid	$C_9H_8O_4$	180.04	**120**, 138, 92, 43, 63, 121, 64
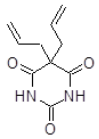	Allobarbital	5,5-Diallyl-2,4,6(1H,3H,5H)-pyrimidinetrione	$C_{10}H_{12}N_2O_3$	208.08	**167**, 124, 80, 141, 106, 193, 179
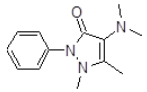	Aminophenazon	4-(Dimethylamino)-1,5-dimethyl-2-phenyl-1,2-dihydro-3H-pyrazol-3-one	$C_{13}H_{17}N_3O$	231.14	**56**, 97, 231, 111, 77
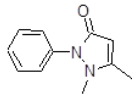	Antipyrine	1,5-Dimethyl-2-phenyl-1,2-dihydro-3H-pyrazol-3-one	$C_{11}H_{12}N_2O$	188.09	**188**, 77, 96, 187, 105, 56, 51
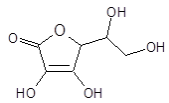	Ascorbic acid	(5R)-5-[(1S)-1,2-Dihydroxyethyl]-3,4-dihydroxy-2(5H)-furanone	$C_6H_8O_6$	176.03	**116**, 85, 43, 119, 71, 101,61, 176
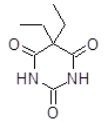	Barbital	5,5-Diethyl-2,4,6(1H,3H,5H)-pyrimidinetrione	$C_8H_{12}N_2O_3$	184.08	**156**, 141, 155, 112, 98, 55, 157
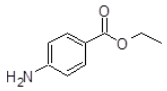	Benzocaine	Ethyl 4-aminobenzoate	$C_9H_{11}NO_2$	165.08	**120**, 165, 92, 137, 65, 121

Table 1.7 *cont'd*: Some of the common adulterants found in heroin samples and associated mass spectroscopic data.

Structure	Common name	IUPAC name	Empirical formula	Molar mass, g/mol	Base peak (shown in bold) and other prominent peaks, m/z
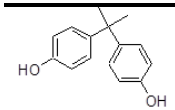	Bisphenol-A	4,4'-(2,2-Propanediyl)diphenol	$C_{15}H_{16}O_2$	228.12	**213**, 228, 119, 214, 91, 65
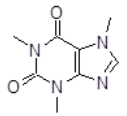	Caffeine	1,3,7-Trimethyl-3,7-dihydro-1H-purine-2,6-dione	$C_8H_{10}N_4O_2$	194.08	**194**, 109, 67, 82, 55, 193)
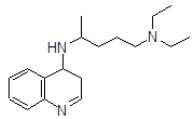	Chloroquine	N^4-(7-Chloro-4-quinolinyl)-N^1,N^1-diethyl-1,4-pentanediamine	$C_{18}H_{26}ClN_3$	319.18	**86**, 319, 58, 99, 247, 179, 126
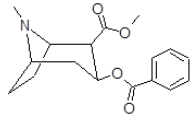	Cocaine	Methyl (2S,3R)-3-(benzoyloxy)-8-methyl-8-azabicyclo[3.2.1]octane-2-carboxylate	$C_{17}H_{21}NO_4$	303.14	**82**, 182, 83, 77,94, 105,96, 303
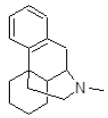	Dextromethorphan	(9α,13α,14α)-3-Methoxy-17-methylmorphinan	$C_{18}H_{25}NO$	271.19	**271**, 59, 150, 214, 270, 171, 128
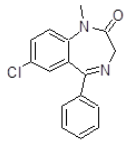	Diazepam	7-Chloro-1-methyl-5-phenyl-1,3-dihydro-2H-1,4-benzodiazepin-2-one	$C_{16}H_{13}ClN_2O$	284.07	**256**, 283, 284, 255, 285, 221, 77,165, 151
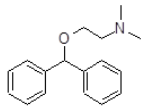	Diphenhydramine	**2**-(Diphenylmethoxy)-N,N-dimethylethanamine	$C_{17}H_{21}NO$	255.16	**58**, 73, 165, 152, 167, 166
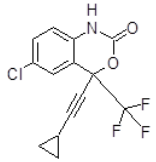	Efavirenz	(4S)-6-Chloro-4-(cyclopropylethynyl)-4-(trifluoromethyl)-1,4-dihydro-2H-3,1-benzoxazin-2-one	$C_{14}H_9ClF_3NO_2$	315.03	**246**, 243, 180, 248, 167 245, 315, 182, 224

Table 1.7 *cont'd*: Some of the common adulterants found in heroin samples and associated mass spectroscopic data.

Structure	Common name	IUPAC name	Empirical formula	Molar mass, g/mol	Base peak (shown in bold) and other prominent peaks, m/z
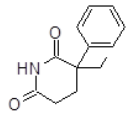	Gluthetimide	3-Ethyl-3-phenyl-2,6-piperidinedione	$C_{13}H_{15}NO_2$	217.11	**189**, 117, 132, 160, 115 91, 217
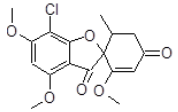	Griseofulvin	(2S,6'R)-7-Chloro-2',4,6-trimethoxy-6'-methyl-3H,4'H-spiro[1-benzofuran-2,1'-cyclohex[2]ene]-3,4'-dione	$C_{17}H_{17}ClO_6$	352.07	**352**, 310, 138, 215, 214, 321, 354, 69
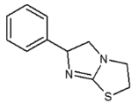	Levamisole	(6S)-6-Phenyl-2,3,5,6-tetrahydroimidazo[2,1-b][1,3]thiazole	$C_{11}H_{12}N_2S$	204.072	**204,** 148, 203, 101, 73, 127, 121
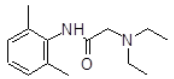	Lidocaine	(lignocaine) N-(2,6-Dimethylphenyl)-N^2,N^2-diethylglycinamide	$C_{14}H_{22}N_2O$	234.17	**86**, 58, 234, 72, 120, 77, 118
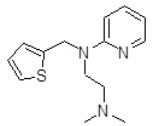	Methaprilene	N,N-Dimethyl-N'-(2-pyridinyl)-N'-(2-thienylmethyl)-1,2-ethanediamine	$C_{14}H_{19}N_3S$	261.13	**97**, 58, 191, 72, 261, 203, 119
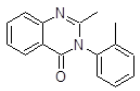	Methaqualone	2-Methyl-3-(2-methylphenyl)-4(3H)-quinazolinone	$C_{16}H_{14}N_2O$	250.11	**235**, 250, 233, 236, 91, 76, 132
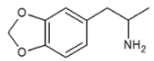	3,4-methylenedioxyamphetamine	1-(1,3-Benzodioxol-5-yl)-2-propanamine	$C_{10}H_{13}NO_2$	179.22	**44,** 136, 135, 77, 51, 81, 179
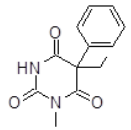	Methylphenobarbitone	5-Ethyl-1-methyl-5-phenyl-2,4,6(1H,3H,5H)-pyrimidinetrione	$C_{13}H_{14}N_2O_3$	246.10	**218**, 117, 118, 146, 115, 103, 91, 219
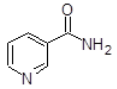	Nicotinamide	6-Aminonicotinamide	$C_6H_6N_2O$	122.05	**122**, 78, 106, 51, 44, 79, 94

Table 1.7 *cont'd*: Some of the common adulterants found in heroin samples and associated mass spectroscopic data.

Structure	Common name	IUPAC name	Empirical formula	Molar mass, g/mol	Base peak (shown in bold) and other prominent peaks, m/z
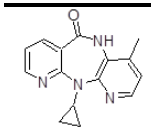	Nevirapine	11-Cyclopropyl-4-methyl-5,11-dihydro-6H-dipyrido[3,2-b:2',3'-e][1,4]diazepin-6-one	$C_{15}H_{14}N_4O$	266.12	**265**, 251, 133, 266, 134, 237, 78, 52
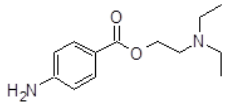	Procaine	2-(Diethylamino)ethyl 4-aminobenzoate	$C_{13}H_{20}N_2O_2$	236.15	**86**, 99, 120, 164, 65, 92, 58
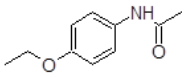	Phenacetin	(1E)-N-(4-Ethoxyphenyl) ethanimidic acid	$C_{10}H_{13}NO_2$	179.09	**108**, 109, 179, 137, 80, 81, 53
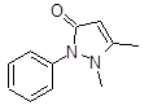	Phenazon	1,5-Dimethyl-2-phenyl-1,2-dihydro-3H-pyrazol-3-one	$C_{11}H_{12}N_2O$	257.14	**228**, 72, 68, 214, 55, 99, 69, 257, 242
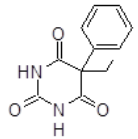	Phenobarbital	5-Ethyl-5-phenyl-2,4,6(1H,3H,5H)-pyrimidinetrione	$C_{12}H_{12}N_2O_3$	232.08	**204**, 117, 232, 161, 146, 174, 103
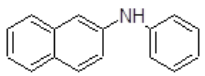	N-Phenyl-2-Naphthylamine	N-Phenyl-2-naphthalenamine	$C_{16}H_{13}N$	218.10	**219**, 218, 217, 220, 108, 115, 109, 216
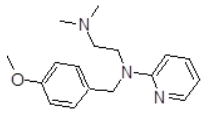	Pyrilamine	N-(4-Methoxybenzyl)-N',N'-dimethyl-N-(2-pyridinyl)-1,2-ethanediamine	$C_{17}H_{23}N_3O$	285.18	**121**, 58, 78, 72, 215, 285, 91
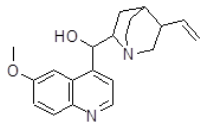	Quinine	(8α,9R)-6'-Methoxycinchonan-9-ol	$C_{20}H_{24}N_2O_2$	324.18	**136**, 79, 81, 117, 189, 55, 95, 324
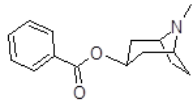	Tropacocaine	8-Methyl-8-azabicyclo[3.2.1]oct-3-yl benzoate	$C_{15}H_{19}NO_2$	245.32	**124**, 82, 94, 77, 245, 105, 67, 140

Table 1.7 *cont'd*: Some of the common adulterants found in heroin samples and associated mass spectroscopic data.

Structure	Common name	IUPAC name	Empirical formula	Molar mass, g/mol	Base peak (shown in bold) and other prominent peaks, m/z
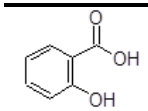	Salicylic acid	2-hydroxybenzoic acid	$C_7H_6O_3$	138.03	**92,** 120, 64, 138, 63, 65, 80
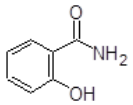	Salicylamide	salicylamide	$C_7H_7NO_2$	137.05	**120**, 137, 92, 65, 121, 64, 93
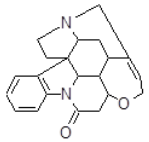	Strychnine	(1R,11S,18S,20R,21R,22S)-12-oxa-8,17-diazaheptacyclo[15.5.2.$0^{1,18}$.$0^{2,7}$.$0^{8,22}$.$0^{11,21}$.$0^{15,20}$]tetracosa-2,4,6,14-tetraen-9-one	$C_{21}H_{22}N_2O_2$	334.17	**334**, 335, 120, 162, 107, 130, 161, 143, 144
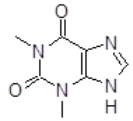	Theophylline	1,3-Dimethyl-3,7-dihydro-1H-purine-2,6-dione	$C_7H_8N_4O_2$	180.06	**180**, 95, 68, 53, 123, 67, 96, 151
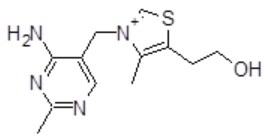	Thiamine	5-(2-Hydroxyethyl)-3-[(6-imino-2-methyl-1,6-dihydro-5-pyrimidinyl)methyl]-4-methyl-1,3-thiazol-3-ium chloride	$C_{12}H_{17}ClN_4OS$	300.08	**112**, 122, 264, 143, 113, 233, 85, 45
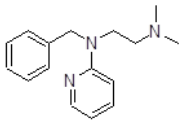	Tripelennamine	N-Benzyl-N',N'-dimethyl-N-(2-pyridinyl)-1,2-ethanediamine	$C_{16}H_{21}N_3$	255.17	**58**, 91, 197, 72, 185, 65, 79, 255
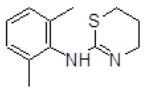	Xylazine	N-(2,6-Dimethylphenyl)-5,6-dihydro-4H-1,3-thiazin-2-amine	$C_{12}H_{16}N_2S$	220.10	**205**, 220, 145, 130, 177, 77, 91, 103

1.4.2 Heroin common trafficking routes

Opium is produced mainly in four regions, namely Afghanistan, Colombia, Mexico and Myanmar/Lao People's Democratic Republic. The Afghanistan region cultivates and produces about 84% of the world's illicit opium according to the UNODC (2020). According to the UNODC's Afghan Opiate Trade Project (AOTP) (UNODC, 2015), the heroin produced from the largest producer, Afghanistan, is trafficked to all the countries of the world except South America. Afghanistan is not only the largest producer of opium, it is also the world's leading heroin producer accounting for about 70% (UNODC, 2020). Once the heroin is produced in those different regions, it is trafficked throughout the world. The trafficking route of heroin and/or opium from the four regions of origin are illustrated in Figure 1.8.

There are three main routes through which opium and/or heroin produced from Afghanistan is trafficked. These routes includes the so-called "Balkan route", which crosses the Islamic Republic of Iran, mostly via Pakistan, to Turkey, Greece and Bulgaria across South East Europe to the western European states. The Balkan route is said to branch into a recently identified route, the Caucasus route, which moves from Afghanistan through the Caucasus across Central Asia to the Russian Federation. The Balkan route is said to be the single largest heroin trafficking route in the world, accounting for about 58% of the heroin seizures (UNDOC, 2020).The second route is the northern route, which mainly runs through Tajikistan and Kyrgyzstan (or Uzbekistan or Turkmenistan) to Kazakhstan and the Russian Federation. The push-back by law enforcement agencies is said to force traffickers from the Balkan route to the third trafficking route, the southern route, where enforcement is lacking (Bruwer, 2017). The southern route goes from Afghanistan through Pakistan and Iran, and transits East African states, especially Kenya, Tanzania and Zanzibar to Asia, Europe, South Africa and West Africa. From West Africa heroin is trafficked to Asia, Canada and the United States of America. Most of the heroin reaches South Africa through this route. Some of the heroin is distributed in the local markets while the rest is transited to West Africa. Because of the efficient transport infrastructure, the majority of the heroin seized in South Africa are those trafficked by land from the neighbouring countries, such as Mozambique (Bruwer, 2017). The heroin, from Afghanistan, that reaches Canada and China is trafficked through the southern route through South East Asia.

The heroin produced in Myanmar/Lao People's Democratic Republic is distributed using two main routes. The first route goes from Myanmar to China, and the second route transits South East Asia to Australia and New Zealand.

The heroin produced from Mexico is mainly trafficked to the United States of America, while the heroin from Colombia is trafficked to both South America and the United States of America.

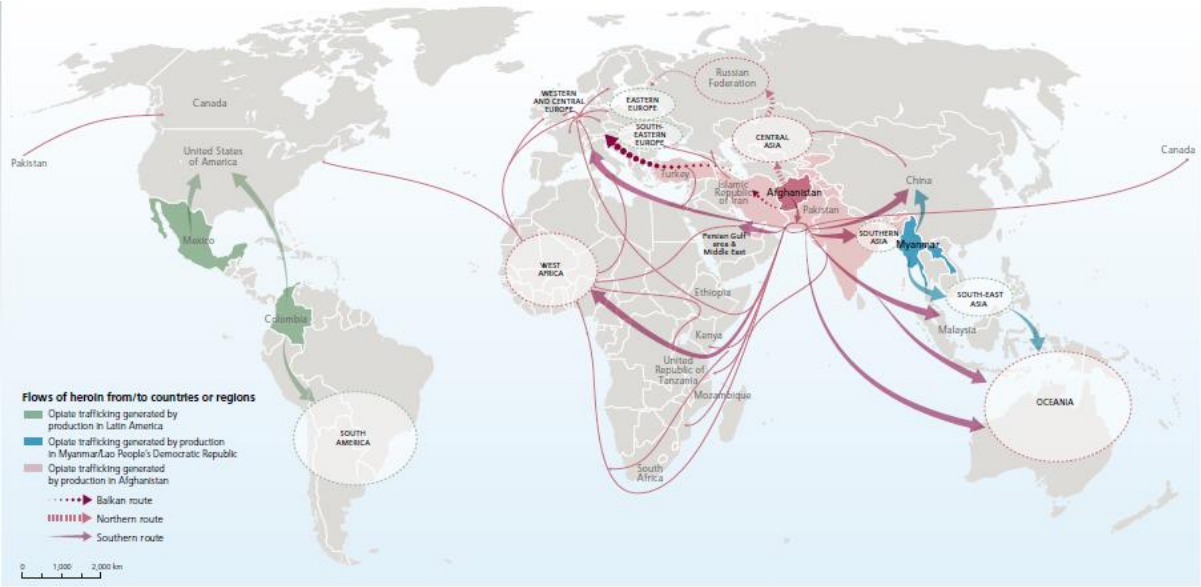

Figure 1.8: Typical heroin trafficking routes from the four opium producing regions. Source: https://www.unodc.org/unodc/en/data-and-analysis/aotp.html

1.4.3 Heroin: common methods of abuse

The abuse of heroin, that of smoking and ingesting heroin tablets, is reported to have emerged in the Far East around 1920 and spread to the United States and other parts of the world (UNODC, 1953). The heroin tablets generally contained caffeine, cinchona alkaloid (quinine, cinchonine, or cinchonidine), strychnine and aspirin as psychoactive compounds, as well as the diluents starch, cane sugar or milk sugar (*ibid*). Another method of heroin abuse, that of inhaling the heroin smoke that is released when the heroin powder and tablets, is heated in a foil paper, developed around 1950 in Hong Kong (Strang, Griffiths and Gossop, 1997). This method of inhaling the heroin smoke is referred to as 'chasing the dragon'. The

procedure is believed to have spread to South East Asia around 1970, and to other parts of Europe and the rest of the world around 1980. The development of the street drug nyaope in South Africa, which is mainly a combination of heroin and cannabis, may have been influenced by the fact that heroin smoking is usually done with cigarettes, and since cannabis is also abused by smoking. The abuse of heroin by injecting it intravenously was first reported around 1950 in Hong Kong, although this was not a preferred method of abuse (Strang et al, 1997). A very bizarre method of heroin abuse by injection has been developed in South Africa, known as 'Bluetoothing'. Heroin is injected by a user and then their blood is drawn and shared with other users. Although the blood transfusions can induce psychoactive effects of warmness and wellbeing, this may just represent a placebo effect, since the amount of heroin injected will be so diluted that it will have an insignificant effect on the secondary user (Sifile, 2017). The 'Bluetoothing' method is prevalent amongst the nyaope users. The abuse of heroin in the nyaope cocktail drug in South Africa resulted in a massive increase in cases encountered at the SAPS-FSL, as shown in Figure 1.9 (SAPS-FSL data 2009–2017). It is reported that South Africa is has the largest heroin consumer market on the African continent (Eligh, 2020).

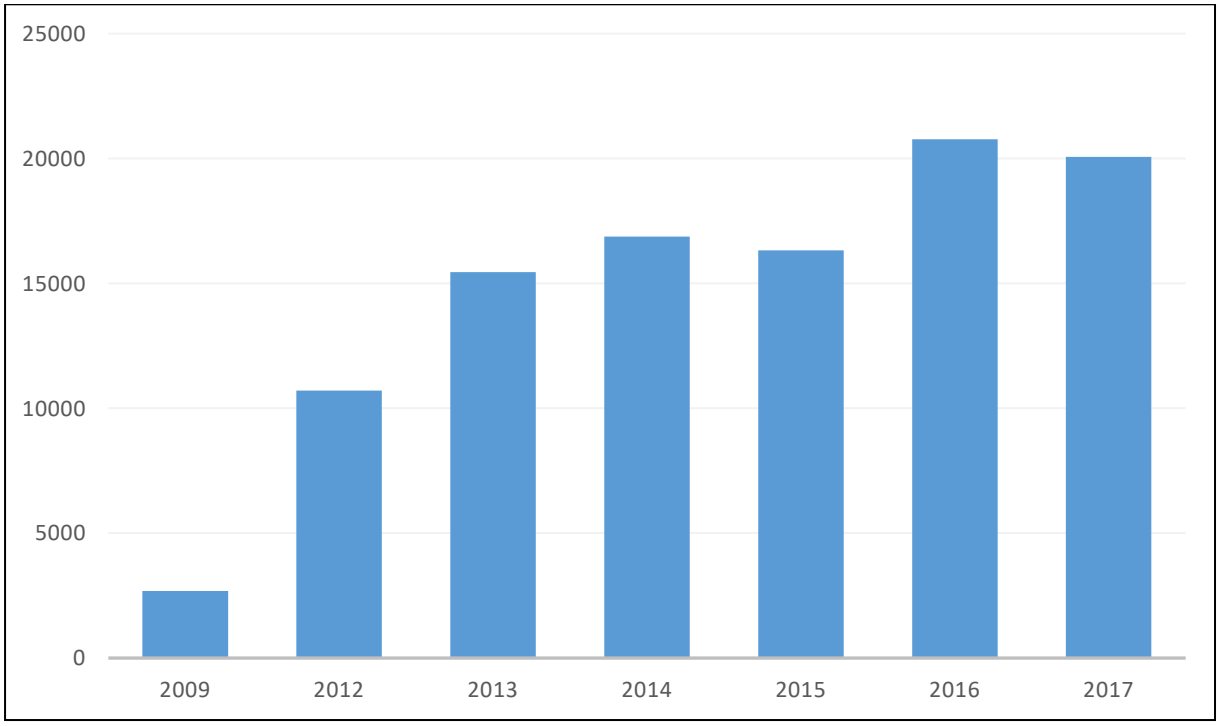

Figure 1.9: Graph showing the number of heroin containing cases analysed by the SAPS-FSL in the period 2009 to 2017.

1.4.4 Analysis and profiling of heroin

A number of analytical methods have been reported in literature for the identification, quantitation and profiling of heroin. The analytical methods include the capillary electrophoresis (CE) methods, gas chromatographic (GC) methods, liquid chromatographic (LC) methods and nuclear magnetic resonance spectrometry (NMR) methods. The CE methods include capillary zone electrophoresis-diode array detector (CZE-DAD), capillary zone electrophoresis-ultraviolet detection (CZE-UV), micellar electrokinetic chromatography-diode array detector (MEKC-DAD) and micellar electrokinetic chromatography-ultraviolet (MEKC-UV) (Wernly and Thormann, 1991; Wernly and Thormann, 1992; Hyotylainen, Sirén and Riekkola, 1996; Taylor, Low and Reid, 1996; Boone et al, 1999; UNODC, 2005; Krishna, Srinath and Sankar, 2008). The GC and LC methods are discussed in Sections 1.4.4.1 and 1.4.4.2, respectively. The NMR methods include proton Nuclear Magnetic Resonance (1H NMR), one-dimensional total-correlation spectroscopy (1D TOCSY) 1H NMR and two-dimensional diffusion-ordered spectroscopy (2D DOSY) 1H NMR (Neville, Ekiel and Smith, 1987; Hays et al, 2000; Suryaprakash et al, 2000; Hays, 2005; Balayssac et al, 2014; Zhong et al, 2018). Very little literature is available for the quantitative analysis of heroin using NMR, since the technique is used mainly for the structural elucidation of organic compounds. The limit of detection, limit of quantitation and linear ranges of heroin (diamorphine) for some of these methods are illustrated in Table 1.8. The heroin detection limit for both the CE and NMR methods shown in Table 1.8 indicates these techniques to be inferior in detecting trace amounts of heroin when compared to GC and LC techniques.

Table 1.8: Linearity range, limit of detection and limit of quantitation of heroin for different analytical techniques.

Technique	Linearity range, mg/L	Detection limit, mg/L	Quantitation limit, mg/L	Reference
CZE-DAD	0.15	0.0080	-	Krishna, Srinath and Sankar, 2008
GC x GC-TOFMS	0.0050 – 1.00	0.0016 (assumed)	0.0050 (assumed)	Guthery et al, 2009
GC-FID	7.70 – 1000.00	2.20	7.30	Yuksel, 2020
GC-MS	0.020 – 1.50	0.00040	0.0013	Bravo, Gonzalez and Benites, 2011
HPLC-DAD	5.00 – 120.00	0.16	0.54	Elbardisy et al, 2019
HPLC-UV	0.010 – 1.20	-	0.010	Rop et al, 1987
LC-MS	0.0050 – 0.20	0.0025	0.0050	Jones et al, 2013
LC-MS/MS	0.0020 – 0.89	0.00096	0.0025	Karinen et al, 2009
MEKC-DAD	$25 \times 10^{-1} – 1.0 \times 10^{1}$	$\pm 1.0 \times 10^{-1}$	-	Wernly and Thormann, 1992
MEKC-UV	-	0.52	0.88	Hyotylainen, Sirén and Riekkola, 1996
NMR	-	1.10	20.00	Balayssac et al, 2014
UPLC-MS/MS	0.00000070 – 0.0010	0.00000021	0.00000070	Boleda, Galceran and Ventura, 2007

1.4.4.1 Gas chromatographic methods for heroin analysis

Gas chromatographic methods that has been used for the identification, quantitation and profiling of heroin includes gas chromatography coupled with flame ionisation detection (GC-FID) (Janhunen and Cole, 1999; Zhang et al, 2004; Esseiva et al, 2005; UNODC, 2005; Dufey et al, 2007; Chan, Tan and Wong, 2012a; Yuksel, 2020); gas chromatography-coupled with isotope ratio mass spectroscopy (GC-IRMS)(Ihle and Schmidt, 1996; Besacier et al, 1997; Ehleringer et al, 1999; UNODC, 2005); gas chromatography-coupled mass spectrometry (GC-MS) (Klemenc, 2001; Cole, 2003; Zhang et al, 2004; UNODC, 2005; Morello et al, 2010; Bravo, Gonzalez and Benites, 2011; Chan, Tan and Wong, 2012a); and two-dimension gas chromatography coupled to either flame ionisation detector (GC x GC–FID) (Mitrevski, Wynne and Marriott, 2011; Marriott and Mitrevski, 2014), or time-of-flight mass-spectrometry detector (GC x GC-TOFMS) (Gröger et al, 2008; Guthery et al, 2010; Mitrevski et al, 2011; Marriott and Mitrevski 2014). GC-IRMS is useful for the determination of the origin of the

heroin samples using the abundances of the carbon-13 and nitrogen-15 isotopes. Both the GC-MS and GC x GC techniques offer comparable LODs and LOQs to other techniques listed in Table 1.8 while GC-FID is somewhat inferior to these techniques. GC x GC methods offers high peak capacity, enhanced signal, and structured chromatograms compared to the traditional one dimensional gas chromatography (Murray, 2012), but limited in its application, mainly because of the unavailability of standardized methodology, complex data interpretation and consistency of results (Gruber et al, 2018). Quantitation using GC x GC is not so simple, compared to GC-FID and/or GC-MS, because the analyte response is compromised by the multiple modulated peaks (*ibid*).

1.4.4.2 Liquid chromatographic methods for heroin analysis

Liquid chromatographic methods that have been employed for the analysis of heroin include high performance liquid chromatography (HPLC) as well as liquid chromatography (LC). HPLC methods have been employed with either diode array detection (HPLC-DAD) (Cole, 2003; UNODC, 2005), or ultraviolet detection (HPLC-UV) (Rop et al, 1987; UNODC, 2005). LC methods have been employed coupled to either a mass spectrometer (LC-MS) (Jones et al, 2013), or to a tandem-mass spectrometer (LC-MS/MS) (Dams et al, 2001; Gergov et al, 2009; Karinen et al, 2009; Moreno-Vicente et al, 2015). High-performance liquid chromatographic methods employed include ultra-high-performance liquid chromatography-photodiode array (UHPLC-PDA) (Lurie et al, 2013; Elbardisy et al, 2019) and ultra-performance liquid chromatography tandem–mass spectrometry (UPLC–MS/MS) (Boleda, Galceran and Ventura, 2007; Lurie and Toske 2008). High- performance liquid chromatographic methods exhibited better LODs and LOQs for heroin compared to the other methods listed in Table 1.8.

1.5 PROFILING OF ILLICIT DRUGS

Profiling of illicit drugs is a tool that can be used by law enforcement agencies to provide evidence in a court of law, for medico-legal purposes, or for intelligence purposes, i.e., profiling is either evidence based, or intelligence based. For the evidence in court, profiling is used to link different cases or individuals as well as instances when the main focus is a single case or an individual. In cases where intelligence gathering is required, profiling assists law

enforcement agencies to identify drug trafficking patterns and take steps to disrupt them. Profiling assists law-enforcement officers to achieve the following (UNODC, 2001):

- A link between different drug seizures and consequently, between drug dealers and/or drug users;
- Classify materials from different drug seizures into batches of related samples;
- Establish distribution networks and trafficking patterns either locally, regionally or internationally; and
- Determine the source, including the geographic origin of such drugs

Profiling of illicit drugs can be used to assist law enforcement decision makers and to guide police investigations. In order for this to be realised, there has to be a close collaboration between the laboratory analyst and the police officials on the ground. Both parties must ensure that there is a common understanding on issues like the correct handling of the seized drug exhibit material for profiling, the limitations of the drug profiling process and the information that is expected from the analyst. Illicit drug profiling can be achieved by either investigating the chemical components or the physical properties of the street drug, or both.

1.5.1 Physical profiling of illicit drugs

The physical properties include packaging material, insignia, or whether the drug is sold as powdery or hard, solid material. As an example, heroin street samples seized by the SAPS are usually packaged either in straws or capsules in the KwaZulu-Natal Province (Figure 1.10), while the heroin is usually wrapped in pieces of plastic in the Gauteng Province. Therefore, this could be used to classify the heroin seizure according to the province that they were found. The packaging material have different colours which could be used to classify the seizure within a province according to a specific region and or a particular drug peddler who packaged the drug. Physical properties alone will not be sufficient, since some of the street drugs have similar packaging and may contain similar markings. A combination of both physical and chemical profiling will enhance the classification of the street drug seizures. This information may be used for evidential purposes or as a source of intelligence to identify the samples with common history. The strength of evidence gathered by linking different seizures

through profiling is dependent on the closeness of their relationship as well as the frequency of the particular pattern of the profile.

Figure 1.10: Pictures of some of the typical packaging material for street heroin samples (Photos are by the author).

1.5.2 Chemical profiling of illicit drugs

Chemical profiling considers the chemical components of the illicit drugs, which includes (i) naturally occurring drugs like cannabis, cathinone, cocaine, mescaline, opium, psilocin and psilocybin; (ii) semi-synthetic drugs like heroin and lysergide; as well as (iii) synthetic drugs like amphetamine, methamphetamine, methaqualone and methylenedioxyamphetamine. The chemical components of seized street samples may contain, in addition to the drug itself, the following, depending upon the origin of the drug:

- Naturally occurring components found in the plant that are extracted together with the illicit drug during processing;
- Synthetic by-products that are formed during the synthesis process of both semi-synthetic and synthetic illicit drugs;
- Adulterants that are pharmacologically active compounds added at different stages of the drug chain by peddlers trying to enhance the effect of the drug; and
- Diluents that are pharmacologically inactive compounds added merely to increase the bulk of the drug and in turn maximize their profit.

Published literature has shown that the chemical profiling of any substance can be conducted by considering the following (UNODC, 2001; 2005; Lyengar and Hadi, 2014; McCord et al, 2018):

- the major organic components of the drug;
- trace organic components available in addition to the drug;
- occluded solvents during the processing of the drug;
- trace elements;
- Isotope abundances in the drug; and
- DNA analysis of plant-based drugs.

1.5.2.1 The chemical profiling using the major organic components of nyaope

The street cocktail drug nyaope has been shown from the SAPS-FSL casework analysis to contain mainly a mixture of naturally occurring drug (cannabis), the semi-synthetic drug (heroin) and synthetic drugs (antiretroviral drugs and adulterants such as acetaminophen, phenacetin, diazepam and dextromethorphan). Other illegal drugs such as cocaine, methaqualone and MDA, as mentioned in Section 1.1, have been identified in these samples. For the nyaope component heroin, the major components are usually extracted together with the heroin precursor, morphine, from the opium plant and includes codeine, papaverine, noscapine and thebaine. For the nyaope component cannabis, the major components include Δ^9-tetrahydrocannabinol, cannabinol, cannabidiol, cannabichromene, cannabigerol, tetrahydrocannabivarin and cannabivarin, which are present as part of the more than 100 cannabinoids in the natural plant. Profiling of the cannabinoids using major components can be achieved by quantifying these major components. For heroin the levels of the components have been studied extensively and therefore by calculating the ratios of these levels and comparing them to available database it is possible to establish the geographic origin of the heroin samples (UNODC, 2005; Collins et al, 2007). Due to cloning of cannabis samples the geographic origin of cannabis using only the natural occurring cannabinoids may not be easy. The chromatographic profiles of the major components present can also be used to group related samples into batches in instances where geographic origin is not necessary, i.e. in instances where the comparison between seized samples is sufficient. The identity of the

components can be visually matched and chemometric methods applied to their concentration profiles in order to classify the samples.

1.5.2.2 The chemical profiling of illicit drugs using occluded solvents

In any synthetic process, trace amount of the solvents used are usually occluded within the crystal lattice of the solid sample. For the synthetic compounds like heroin, the solvent used in the synthesis process is said to be unique to a particular region (South East Asia, South West Asia, Mexico, or South America) (Collins et al, 2007). These solvents can be identified using simple techniques such as headspace gas chromatography-mass spectrometry. The identification of these solvents can help law enforcement agencies to monitor which solvents are purchased where, and by whom, in order to link the street sample to a region and also to the clandestine laboratory operator.

1.5.2.2 The chemical profiling of illicit drugs using synthesis by-products

Synthesis processes always result in the formation by-products, for the heroin synthesis, there are more than 100 known synthesis by-products (Toske et al, 2006). The quantitation of some of these by products like acetylcodeine, 3-monoacetylmorphine and 6-monoacetylmorphine using chromatographic techniques discussed in Section 1.4.4 is usually used for the profiling of heroin. The identification of all the other by-products can assist in classifying the related heroin samples further into batches (Toske et al, 2006; Collins et al, 2007).

1.5.2.3 The chemical profiling of illicit drugs using trace elemental impurities

Trace element analysis is also a powerful tool that can be used for the analysis and classification of the street nyaope product. The trace elements present in naturally occurring drugs are due to contamination from the soil the plant was cultivated; therefore it is possible to link the drug to a particular region. Synthetic and semi-synthetic components would offer a challenge to link to a particular region, since the source of contamination is usually unknown. Inductively-coupled plasma atomic-emission spectrometry (ICP-AES), inductively-coupled mass spectrometry (ICP-MS), laser ablation inductively-coupled mass spectrometry

(LA-ICP-MS), ICP-OES have been employed for the elemental analysis in both cannabis (Jones and Nelson, 2017; Shimandzu, 2017), and heroin (Bora, Merdivan and Hamamci, 2002; Licsandru, Nacea and Boscencu, 2012; Liu et al, 2014). Profiling using trace element analysis has been conducted using Neural Network Analysis, Principal Component Analysis, Canonical Discriminant Analysis, Discriminant function analysis and k-nearest neighbours (Anderson et al, 1999; Berry, 2015) as well as hierarchical cluster analysis (Myors et al, 1998). These methods can be successfully applied to the analysis and classification of the street drug nyaope. The limitation for the trace elemental profiling of the street nyaope sample would be the lack of database for the variety of analytes available in such samples.

1.5.2.4 The chemical profiling of illicit drugs using isotopic abundances

Another powerful tool for the classification of natural occurring drugs is the isotopic abundance analysis (UNODC, 2005; Cerling et al, 2016; Casale et al, 2019). The abundances of the isotopes carbon-13, nitrogen-15 and oxygen-18 relative to the most abundant isotopes are usually determined using GC-IRMS mentioned in Section 1.3.5.1. Isotope abundances analysis is mainly useful for the determination of the geographic origin of drugs. Isotopic abundances measurement are therefore limited to naturally occurring drugs and would be a challenge to classify a complex sample like nyaope, which contains a mixture of natural occurring, semi-synthetic and synthetic drugs. Apart from this limitation, the technique is not readily available to forensic analysts, due to the cost of the instrumentation and extensive training required to master the technique.

1.5.2.5 The chemical profiling of illicit drugs using DNA

Forensic DNA or DNA profiling of both human and non-human DNA is one of the powerful tools used in unambiguously resolving criminal cases (Lyengar and Hadi, 2014; McCord et al, 2018; Amorim, 2019). The analysis of non-human DNA from cats, dogs, plants, viruses and bacteria has been shown to be of great forensic evidential value in solving criminal cases (*ibid*). The identification and profiling of plant-derived drugs can be achieved by using validated chemistry-based DNA analysis methods to determine the genetic diversity of the substances (Weedn, Rodgers and Henry, 1998; SWGDAM, 2016; McCord et al, 2018). DNA

profiling can be used for the determination of geographic origin of the naturally occurring drugs like cannabis, cathinone, cocaine, mescaline, opium, psilocin and psilocybin. Several DNA analysis techniques have been described in literature for the identification and profiling of *cannabis sativa* (Siniscalco Gigliano et al, 1997; Linacre and Thorpe, 1998; Siniscalco Gigliano, 1998; Hsieh et al, 2003; Miller-Coyle et al, 2003b), *papaver somniferum* plants that produce the opiates drugs (Saunders et al, 2001; Hari, Sharma and Sharma, 2009; Darokar et al, 2014; Mičianová et al, 2017; Sharma et al, 2019; Vašek et al, 2020; Young et al, 2020) and *psilocybe* mushrooms that produce the hallucinogenic drugs psilocin and psilocybin (Lee, Cole and Linacre, 2000; Lee, 2001; Linacre, Cole and Lee, 2002; Nugent and Saville, 2004). The *papaver somniferum* DNA can be extracted and classified from heroin street samples (Marciano et al, 2018), which suggests that drugs synthesised for precursors that are of plant origin may be subjected to DNA analysis. The identification and profiling of the DNA analysis have also been applied to the spores of the *psilocybe* mushrooms in grow kits to detect the illegal cultivation of these hallucinogenic mushrooms (Gambaro et al, 2016). It is also possible to extract plant DNA from woody material using chemistry-based methods to obtain amplifiable DNA material (Paranaiba et al, 2020). DNA analysis involves the extraction of the plant DNA followed by amplification of the extracted DNA using a chemical process known as polymerase chain reaction (PCR). Once PCR amplification of the DNA is done, different techniques are then used for the sequencing and thereby create the DNA profiles. DNA sequencing techniques reported in literature for the profiling of plant-based drugs include amplified fragment length polymorphism (AFLP) (Lee et al, 2000; Saunders et al, 2001; Miller-Coyle et al, 2003a), expressed sequence tag -simple sequence repeat (EST-SSR) (Vašek et al, 2020), inter-simple sequence repeat (ISSR) (Kojoma et al, 2002; Hari et al, 2009; Sharma et al, 2019), random amplification of polymorphic DNA (RAPD) (Gillan et al, 1995; Lee, 2001; Darokar et al, 2014) and short tandem repeat (STR) (Gilmore et al, 2003; Hsieh et al, 2003; Mičianová et al, 2017; Young et al, 2020). Sequence analysis is, however, a very laborious technique, which requires very expensive facilities (Kojoma et al, 2002).

1.5.3 Choice of the analytical technique for nyaope profiling

The profiling of nyaope requires a process that seeks to extract information from the drug samples in order to determine whether there is a link between the sample seizures. The

author is not aware of any literature for the profiling of the cocktail drug nyaope. Both physical and chemical method could be used for the profiling of nyaope. The physical methods need to be used in combination with the chemical methods for the identification of the nyaope samples. Physical information includes the area where the seizure was made, the type of sample (solid vs powder) and the packaging material. The information that can be obtained from packaging material includes the type, colour, shape and fingerprint of anyone who handled the packaging material. A database of these physical properties would need to be created in order to be able to link the seizures to a particular area, users and/dealers. For this work we will focus mainly on the chemical profiling of nyaope. The method mentioned in Sections 1.2.2, 1.3.5 and 1.4.4 can be used for the chemical identification and profiling of street nyaope samples. The liquid chromatographic tandem mass spectrometry method appears to be the most appropriate method of analysis; however, this requires very expensive instrumentation that is not always available in many financially strapped laboratories in the SADC region. On the other hand, the GC-MS technique is readily available in many laboratories for routine work; therefore, a method that uses this technique will be much more beneficial. GC-MS has been widely used for the analysis of illicit drugs (UNODC, 2005; Suurkuusk, 2010; Mwenesongole et al, 2013; Kuleya et al, 2014). Suitable internal standards used in the GC-MS methods for the analysis of illicit drugs have included deuterated analogues as well as eicosane (C_{20}) and teracosane (C_{24}) *[ibid]*. As illustrated in Tables 1.5 and 1.8, GC-MS gives linearity ranges as well as well as LODs and LOQs for both Δ^9-THC and DAM, which is comparable to those given by the liquid chromatographic methods. It is, therefore, a suitable method for the identification, quantitation and profiling of nyaope samples. Since decarboxylation of the acidic cannabinoids occurs during GC-MS analysis, total Δ^9-THC is measured rather than both Δ^9-THC and Δ^9-THCA.

The pH and pKa values of some of the drugs identified in the cocktail drug nyaope are given in Table 1.9. The cocktail drug nyaope contains both acidic (acetaminophen, heroin, lidocaince nevirapine) and basic (caffeine, cocaine, codeine, efavirenz, diazepam, 3,4-methylenedioxyamphetamine, 6-monoacetylmorphine, methaqualone, noscapine, papaverine, Δ^9-tetrahydrocannabinol) drugs. Acetaminophen has a phenolic group and is weakly acidic, even though its pKa value is 9.8. Methaqualone is an alkaloid comprising a nitrogen atom with a lone pair of electrons; and therefore, it is basic, even though the pKa

value is 2.5. All these nyaope components are volatile under GC-MS conditions without the need for derivatization and therefore GC-MS is suitable for the identification and quantification of street nyaope samples. The identity and the proportion of these nyaope components, once established using GC-MS, can be used to link different sample seizures.

Table 1.9: The pH and pKa values of some of the components of the street cocktail drug nyaope.

Compound	pH	pKa
6-Monoacetylmorphine	-	8.19[a]
Acetaminophen	5.5 -6.5[b]	9.38[c]
Caffeine	6.9[d]	14.0[e]
Cocaine	>7.0[d]	8.61[d]
Codeine	9.8[f]	6.05[d]
Efavirenz	-	10.2[d]
Diazepam	6.8[g]	3.4[d]
Heroin	4.8[h]	7.6[i]
lidocaine	6.09[j]	7.95[i]
Methaqualone	>7.0[d]	2.5[i]
3,4-Methylenedioxyamphetamine	-	9.67[i]
Nevirapine	-	2.8[d]
Noscapine	7.0[d]	7.8[d]
Papaverine	-	8.07[d]
Δ^9-Tetrahydrocannabinol	-	10.6[d]

References: [a]Avdeef et al, 1996; [b]Lewis Sr, 2007; [c]Dastmalchi, Rashidi and Rassi, 1995; [d]O'Neil, 2017; [e]Sigma-Aldrich, n.d.; [f]US-NTP, 1992; [g]Posner, 2012; [h]Ciccarone and Harris, 2015; [i]Moffatt, Osselton and Widdop, 2011; [j]Frank and Lalonde, 2012.

1.6 AN OVERVIEW OF SOLVATION

Chemical analysis frequently involves dissolution of a drug prior to using an instrumental method. A solvent in which the components of nyaope are soluble and stable is necessary for the profiling of impurities since chemical degradation of the sample and/or artefact formation may result in erroneous chemical profiles of the nyaope samples (Aalberg et al, 2005). For a sample to dissolve in a solvent, there has to be intermolecular interaction between the sample molecules and the solvent molecules (Reichardt and Welton, 2011). Solvation describes the interaction between the solvent and the dissolved solute. Solvents that form a strong interaction with the solute will favourably dissolve the solute. The interaction between the solvent and solute involves the formation of intermolecular forces, also known as Van der Waal's forces. The forces include dispersion interaction (dipole-induced dipole, instantaneous dipole-induced dipole), dipole interaction, dielectric interaction and hydrogen bonding.

1.6.1 Eluotropic strength of common solvents

The polarity of the solvent determines the strength of the solvent to elute a solute from an adsorbent. The eluting power of solvents is referred to as the eluotropic strength of the solvents. Eluotropic strength is measured by determining the retention time of a constant adsorbent. The eluting power of the solvent as well as the polarity of the solvent increases with decreasing retention time of the sample. The adsorbents frequently used are oxides such as aluminium oxide and silica, which gives identical eluotropic strengths. Solvents with high eluotropic strength and polarity are polar, while low eluotropic strength is characteristic of nonpolar solvents.

1.6.2 Solubility evaluation

The solubility parameter, δ, also known as the Hildebrand solubility parameter, is often used to estimate the solubility of nonpolar or slightly polar substances without hydrogen bonding in organic solvents. The Hildebrand solubility parameter describes the amount of energy required to evaporate one-unit volume of a liquid (Hildebrand and Scott, 1964). Liquids with a similar solubility parameter are more likely to be miscible (Moghaloo et al, 2018). The Hildebrand solubility parameter is defined by Equation 1.2 (Welker, 2012):

$$\boldsymbol{\delta = \sqrt{E_{coh}} = \frac{\Delta H_{vap} - RT}{V_m}} \qquad \textbf{1-2}$$

Where E_{coh}, is the cohesive energy density difined by Equation 1.3;

$$\boldsymbol{E_{coh} = \frac{\Delta U_{vap}}{V_m}} \qquad \textbf{1-3}$$

ΔH_{vap} is the molar heat of vaporisation;

ΔU_{vap} is the molar energy;

R is the universal gas constant;

T is the absolute temperature; and

V_m is the molar volume.

The solvent properties reported in literature (Snyder and Kirkland, 1979 Barwick, 1997) that is used for the selection of an extraction solvent is given in Table 1.10.

Table 1.10*:* Solvent properties that can be used for the selection of the extraction solvents arranged in order of increasing eluotropic strength.

Solvent	Eluotropic property, ε^o	Boiling point, °C	Dielectric constant, ε	Kamlet – Taft Parameters			Polarity, P'	Refractive Index,	Solubility parameter, δ	Viscosity, cP
				α	β	π*				
n-Pentane	0.00	36	1.84	-	-	-	0.0	1.3575		0.22
n-Hexane	0.01	69	1.88	0.00	0.00	-1.23	0.1	1.3749	30.9	0.30
n-Heptane	0.01	98	1.92	-	-	-	0.2	1.3876		0.40
Carbon tetrachloride	0.18	77	2.24	0.00	0.10	0.21	1.6	1.4602	8.55	0.90
Xylene	0.26	138	2.30	-	-	-	2.5	1.4930	8.83	0.60
Toluene	0.29	110	2.40	0.00	0.11	0.49	2.4	1.4969	8.93	0.55
Diethyl ether	0.38	35	4.30	0.00	0.47	0.24	2.8	1.3524	7.53	0.24
Chloroform	0.40	61	4.80	0.20	0.10	0.69	4.1	1.4430	9.16	0.53
Dichloromethane	0.42	40	8.90	0.13	0.10	0.73	4.1	1.4242	9.88	0.41
Acetone	0.56	56	-	0.08	0.48	0.62	5.1	1.3587	9.62	0.30
Dioxane	0.56	101	2.20	0.00	0.37	0.49	4.8	1.4224	10.13	1.20

Source: Kamlet – Taft parameters (Reichardt and Welton, 2011); Hilderband parameter (Rohrschneider, 1973); Boiling point, Dielectric constant, Polarity, Viscosity (t-BUOH MSDS, n.d.; Snyder and Kirkland, 1979); Eluotropic series for hydrophilic alumina adsorbents (Rohrschneider, L. 1973; Snyder and Kirkland, 1979; Caude and Jardy, 1998; Reichardt and Welton 2011); Refractive index Refractive index at the average D-line of sodium (16969 cm^{-1}) at 20 °C (Wiley online library)

Table 1.10 cont'd: Solvent properties that can be used for the selection of the extraction solvents arranged in order of increasing eluotropic strength.

Solvent	Eluotropic property, ε^o	Boiling point, ^oC	Dielectric constant, ε	Kamlet – Taft Parameters			Polarity, P'	Refractive Index,	Solubility parameter, δ	Viscosity, cP
				α	β	π*				
Tetrahydrofuran	0.57	66	7.60	0.00	0.55	0.55	4.0	1.4072	-	0.46
Ethyl acetate	0.58	77	6.00	0.00	0.45	0.45	4.4	1.3724	8.91	0.43
Acetonitrile	0.65	82	37.5	0.19	0.40	0.66	5.8	1.3441	12.11	0.34
n-Butanol	0.70	118	17.5	0.84	0.84	0.47	3.9	1.3993	11.60	2.60
t-Butanol	0.70	82	10.9	0.42	0.93	0.41	4.1	1.4050		3.38
Isopropanol	0.82	82	20.3	0.76	0.84	0.48	3.9	1.3772	11.44	1.90
Ethanol	0.88	78	24.6	0.86	0.75	0.54	4.3	1.3614	12.78	1.08
Dimethyl sulfoxide	0.75	189	4.70	0.00	0.76	1.00	7.2	1.4793	-	2.00
Methanol	0.95	65	32.7	0.98	0.66	0.60	5.1	1.3284	14.50	0.54
Water	>>1	100	80.0	1.17	0.47	1.09	10.2	1.3330	23.53	0.89

Source: Kamlet – Taft parameters (Reichardt and Welton, 2011); Hilderband parameter (Rohrschneider, 1973); Boiling point, Dielectric constant, Polarity, Viscosity (t-BUOH MSDS, n.d. ; Snyder and Kirkland, 1979); Eluotropic series for hydrophilic alumina adsorbents (Rohrschneider, L. 1973; Snyder and Kirkland, 1979; Caude and Jardy, 1998; Reichardt and Welton 2011); Refractive index Refractive index at the average D-line of sodium (16969 cm^{-1}) at 20 ^oC (Wiley online library.

1.6.3 Solvent selection

The use of solvents that need to be avoided when making a selection includes: (a) flammable solvents due to their low boiling point and low viscosity; hydrocarbon solvents which are usually more flammable than multi-halogenated solvents; (b) toxic solvents, which includes solvents which are suspected carcinogens (aromatic and chlorinated solvent); (c) reactive solvents, which have a tendency of reacting with the solute.

Since nyaope contains both acidic and basic compounds, different solvents from an eluotropic series will be tested for the extraction of the main nyaope components in order to find the most suitable solvent. The use of a tertiary alcohol such as 2-methyl-propan-2-ol has been reported in literature (Kuleya et al, 2014). The study of both solvent stabilities and storage stabilities of the nyaope components, which are the cannabinoids (THCV, CBV, CBD, Δ^9-THC and CBN), opiates (ACOD, diamorphine and 6-MAM), the antiretroviral drugs (EFV and NVP) as well as the other adulterants (caffeine, dextromethorphan and phenacetin) need to be conducted in order to ensure proper profiling of the street drug nyaope.

1.6.3.1 Stability of the components of nyaope in solvents

However, although methanol is believed to be a more efficient solvent for the extraction of cannabinoids (Smith and Vaughan, 1971) it facilitates the hydrolysis of diamorphine to form 6-monacetylmorphine (6-MAM) (Huizer and Poortman, 1989). Methanolic extracts, therefore, result in the immediate decomposition of diamorphine (Varshney, 2002; Hong et al, 2014). On the other hand, whilst chloroform is a suitable solvent for diamorphine since it dissolves the drug quantitatively over a wide concentration range, is compatible with instrumental analysis and does not degrade diamorphine, it is known to facilitate the breakdown of cannabinoids (Hong et al, 2014, Turner and Henry, 1975). Some solvents may not be suitable for either diamorphine or Δ^9-THC because they do not dissolve the drugs quantitatively over a wide concentration range, while others may be unsuitable for subsequent analysis. In short, a wide range of factors have to be considered in the choice of solvent for drug analysis. Both efavirenz and nevirapine are shown to be stable in methanol when stored for 24 hours at ambient temperature (Rezk, Tidwell and Kashuba, 2002; Kappelhoff et al 2003). The adulterants caffeine and phenacetin, also used as cutting agents

in nyaope, have previously been shown to be stable in methanol for at least 24 hours of storage at ambient temperature (Sena et al, 2017). The adulterant dextromethorphan has been reported to be stable in acetonitrile after 8 hours of storage (Goyal, 2013).

1.6.3.2 Storage stability of the components of nyaope

Long term storage of cannabis in ethanol extracts is known to degrade the active ingredient Δ^9-tetrahydrocannabinol to the oxidation product cannabinol (Carbone, 2010) while diamorphine, on the other hand, hydrolyses to 6-monacetylmorphine and ultimately morphine due to interaction with water present in the solvent (Barrett, Dyssegaard and Shaw, 1992; Wijesekera, Abeysinghe and Pathirana, 1994; Brenneisen and Hasler, 2002; Hutchinson and Somogyi, 2002). Under long-term storage (five weeks) DAM was reported to undergo degradation (an average of 17.0%) when stored in a refrigerator (Wijesekera, Abeysinghe and Pathirana, 1994). When stored at ambient temperature it degraded by an average of 23.3% (*ibid*).

There have been a number of studies of individual components of nyaope under different storage conditions. Under long-term storage, cannabis, in the absence of direct light, has been shown to degrade to a lesser extent when stored at 4 ^oC than at 22 ^oC (Turner, Hadley and Fetterman, 1973a). The active ingredient Δ^9-tetrahydrocannabinol (Δ^9-THC) degrades to the less potent cannabinol (CBN) (Carbone, 2010; Turner and Elsohly, 1979); cannabidiol (CBD) degrades to menthane carboxylic acid (Mechoulam and Hanuš, 2002); while tetrahydrocannabivarin (THCV) which is a propyl homolog of Δ^9-THC (Turner, Hadley and Fetterman, 1973b; Bailey and Gagné, 1975) degrades to cannabivarin (CBV), which is itself a homologue of CBN.

Table 1.11 displays the structures and the possible degradation products of cannabinoids (CBD, THCV and Δ^9-THC), and CBN), opiates (ACOD, diamorphine and 6-MAM), ARVs (EFV and NVP) and adulterants (acetaminophen, caffeine, dextromethorphan and PNT) found in the cocktail drug nyaope.

Table 1.11: Structures of some of the nyaope compounds and their possible degradation products.

Component	Degradation product/s			
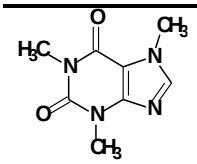	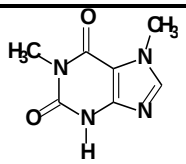	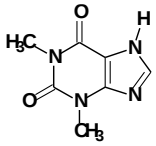		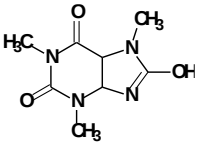
Caffeine	Paraxanthine	Theophylline	Theobromine	1,3,7-Trimethyloric acid
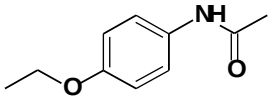	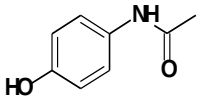	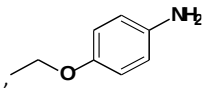		
Phenacetin	Acetaminophen	*p*-Phenetidine		
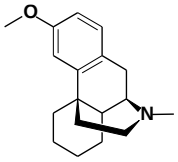	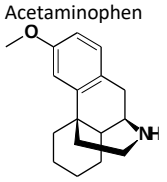	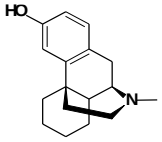		
Dextromethorphan	3-Methoxymorphinan	17-Methylmorphinan-3-ol		
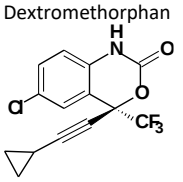	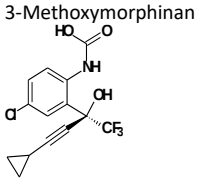	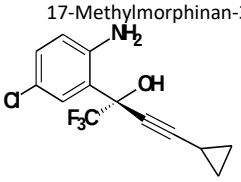	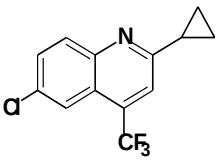	
Efavirenz	Carbamic acid derivative	Efavirenz amino alcohol	Quinoline derivative	
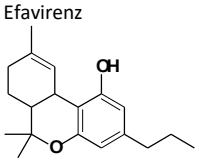	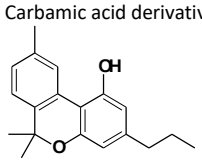			
Tetrahydrocannabivarin	Cannabivarin			
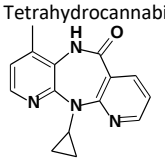	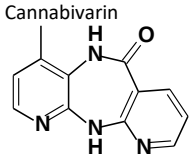	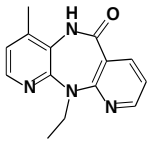		
Nevirapine	Descyclopropyl nevirapine	Ethyl nevirapine		
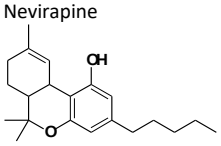	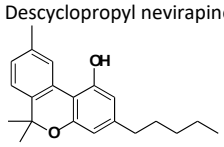			
Δ^9-Tetrahydrocannabinol	Cannabinol			
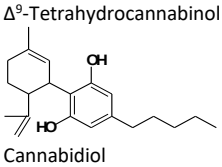	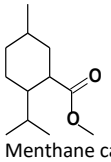	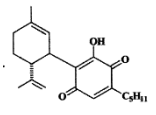	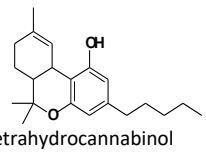	
Cannabidiol	Menthane carboxylic acid	Hyroxyquinone	Δ^9-Tetrahydrocannabinol	
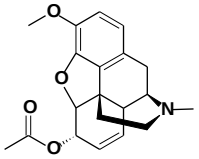	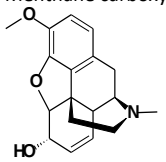	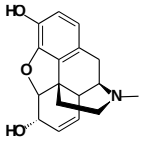		
Acetylcodeine	Codeine	Morphine		
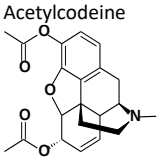	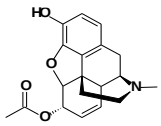			
Diamorphine	6-Monoacetylmorphine	Morphine		

ACOD is a synthetic impurity of illicit heroin usually present at concentration levels of 15–20% relative to DAM and ranges up to 45% (Sione, 1985). ACOD undergoes hydrolysis to codeine (COD) and subsequently to MOR (O'Neal and Poklis, 1997; Staub et al, 2001). EFV was shown to be stable in methanol for at least 7 days and undergoes degradation after 24 hours of storage when exposed to UV light (Hamrapurkar et al, 2010). EFV undergoes hydrolysis to an intermediate carbamic acid ({4-Chloro-2-[(1S)-3-cyclopropyl-1-hydroxy-1-(triflouromethyl) prop-2-yn-1yl]phenyl}carbamic acid), which subsequently forms efavirenz amino alcohol ((2S)-2-(2-amino-5-chlorophenyl)-4-cyclopropyl-1,1,1-trifluorobut-3-yn-2-ol) and carbon dioxide (Maurin et al, 2002). The alcohol may undergo cyclization to form the quinoline derivative (6-chloro-2-cyclopropyl-4-(trifluoromethyl) quinoline (De Aquino-Ribeiro, 2007).The potential degradation products of NVP are reported to be ethyl nevirapine and descyclopropyl nevirapine (Aparna et al, 2010). EFV stock solutions in methanol and NVP stock solution in dimethyl sulfoxide were reported to be stable after 24 hours of storage at ambient temperatures, and 24 and 36 months of storage, respectively, at -20 ^{o}C (Kappelhoff et al 2003). EFV and NVP were reported to be stable after 3 months of storage at 4 ^{o}C and 20 ^{o}C, while EFV and NVP were only stable up to 50 and 70 days, respectively when stored at ambient temperatures (D'Avolio et al, 2010). NVP has been shown to be relatively stable when exposed to humidity, UV light and heat up to 2 days of storage (Navaneethan, Karunakaran and Elango, 2012) as well as in acetonitrile up to 48 hours of storage (Reddiah et al, 2013).

Caffeine was reported to undergo radical induced degradation to 1,3,7-trimethyluric acid (Telo and Viera, 1997) and undergoes oxidation to paraxanthine, theophylline and theobromine (Chung and Cha, 1997). Caffeine was reported to be stable at room temperature for 24 hours and at -20 ^{o}C for 12 weeks (three months) of storage (Alvi and Hammami, 2011). Caffeine was also reported to undergo minimum degradation in freeze-dried urine stored 4 ^{o}C for 18 months (Ventura et al, 2003). Dextromethorphan (DTM) undergoes hydrolysis via N-demethylation to form 3-methoxymorhinan, and O-demethylation to form 17–methylmorhinan-3-ol (Daal et al, 2008; Raju et al, 2013). DTM is an adulterant in nyaope has been shown to be stable when exposed to humidity for at least 7 days (Raju et al, 2013) and was shown to be stable in methanol/water for 2 months at 4 ^{o}C, for 48 hours at ambient temperature and 96 days at -20 ^{o}C (Zhang et al, 2010b). Phenacetin (PNT) was reported to

undergo hydrolysis to p-phenetidine and deethylation to form acetaminophen (Watanabe et al, 2010). PNT in methanol was shown to be stable after a long-term storage (20 days) at -20 ^{o}C (Ma et al, 2015).

1.7 ANALYTICAL METHOD VALIDATION

Analytical method validation is the process of confirming through laboratory tests that an analytical method is suitable for what it is intended for. A reliable calibration model is the one that contains between seven and ten concentration levels with at least eight to ten replicates (Lavagnini and Magno, 2007). Quantitative drugs analysis requires that the following set of validation parameters as suggested by the UNODC and ICH (ICH, 2005; UNODC, 2009b) be tested:

Accuracy (bias) (under within laboratory repeatability and within laboratory reproducibility conditions); Limit of detection (LOD); Limit of quantitation (LOQ); Linearity and Range; Precision (only within laboratory repeatability and intermediate precision (within laboratory reproducibility)); Recovery; Ruggedness; Specificity/selectivity; and Stability Uncertainty of measurement.

For our purpose the following key parameters for quantitative validation of selected compounds in the drug sample will be conducted using guidelines as suggested by the ICH, FDA and UNODC (ICH, 2005; UNODC, 2009b; FDA, 2018) as well as published literature (Thompson, Ellison and Wood, 2002; Skoog et al, 2004; Lavagnini and Magno, 2007; Bonfilio et al, 2012; González et al, 2014):

- Linearity
- Limit of detection and limit of quantitation
- Accuracy and precision (Repeatability and Intermediate Precision)
- Ruggedness
- Selectivity
- Recovery

1.7.1 The evaluation of the linearity of the analytical method

Linearity range is the range over which the instrumental response obtained is directly proportional to the concentration of analyte in the sample. The linearity will be estimated using standard IUPAC methods (Thompson et al, 2002; UNODC, 2005). Linearity will be assessed using calibration graphs and considered linear if the correlation coefficients (r^2) exceeds or equals 0.99. The t-Test and F-Test will also be used to assess linearity.

1.7.2 The evaluation of the limit of detection and the limit of quantitation of the analytical method

Limit of detection (LOD) – the lowest amount of analyte in a sample which can be detected but not necessarily quantitated as an exact value. It is the lowest concentration level that can be determined statistically different from a blank at a specified level of confidence.

Limit of quantitation (LOQ) – This is the lowest concentration level at which quantitative results may be determined with acceptable accuracy and precision.

In order to determine LOD and LOQ, it is recommended to determine the calibration curve slope using reference sample solutions with concentrations in the vicinity of the DL (Bonfilio et al, 2012). Equations 1.4 and 1.5 will be used for the determination of LOD and LOQ respectively.

$$\boldsymbol{LOD = \frac{3.3 \times \sigma \times C_{IS}}{s}} \qquad \textbf{1-4}$$

$$\boldsymbol{LOQ = \frac{10 \times \sigma \times C_{IS}}{s}} \qquad \textbf{1-5}$$

Where σ = standard error,

- S = slope of the regression line, and
- C_{IS}= concentration of the internal standard = 0.018

1.7.3 Accuracy and precision

1.7.3.1 The evaluation of the accuracy of the analytical method

Accuracy (under within laboratory repeatability and within laboratory reproducibility conditions) is the closeness of a result or the mean of a set of measurements to the true value. It is common to estimate accuracy by analysing samples spiked at three different concentrations (low, medium, high) covering the working range. Methods reported in literature (ICH, 2005; Araujo, 2009) for the determination of accuracy include:

a) Measuring the analyte in a particular reference material and comparing the result with the certified value.

b) Measuring the analyte in blank matrix samples spiked with known analytical concentrations and determining the percentage of recovery.

c) Comparing the results from the method under validation with those from a reference method.

d) Determining the analytical concentration in the sample by means of the standard addition technique.

e) Accuracy may be inferred once precision, linearity and specificity have been established.

The first method will be used in this study by calculating the accuracy using the Equation 1.6:

$$\%\boldsymbol{Accuracy} = \frac{\boldsymbol{Measured\ concentration}}{\boldsymbol{actual\ concentration}} \times \mathbf{100} \qquad \textbf{1-6}$$

1.7.3.2 The evaluation of the precision of the analytical method

Precision is a measure of the closeness of the analytical results obtained from a series of replicate measurements of the same measure under the conditions of the method. Intra-

assay precision (repeatability) is when the same analyst analyses samples on the same day with the same instrument or materials in the same laboratory. The acceptance criteria for repeatability are %RSD equal or less than 15% for the higher concentration and less than or equal to 20% for the lower concentration (González et al, 2014; FDA, 2018). Intermediate precision (within laboratory reproducibility) is when the analysis is carried out: on different days, by different analysts, using different instruments, etc. The precision of an analytical method is usually expressed in standard deviation, variance or coefficient of variance (relative standard deviation). Precision is assessed by calculating relative standard deviation (% RSD) for Intra-assay precision (repeatability). For the Intermediate precision, five replicate analyses will be performed for five days. The within-group (W) precision and between-group (B) precision is calculated using Equations 1.7 and 1.8, respectively by one-way ANOVA (Group = Day) (Skoog et al, 2004).

$$\%\boldsymbol{RSD_W} = \frac{\sqrt{\boldsymbol{MSW}}}{\boldsymbol{X}} \times \mathbf{100} \qquad \textbf{1-7}$$

$$\%\boldsymbol{RSD_B} = \frac{\sqrt{(\boldsymbol{MSB}-\boldsymbol{MSW})/\boldsymbol{n}}}{\boldsymbol{X}} \times \mathbf{100} \qquad \textbf{1-8}$$

If MSB < MSW, set $\%RSD_B = 0$

Where,

X = Grand mean of all observations

n = Number of observations in group

- *MSW* = mean of squares within group
- *MSB* = mean of squares between groups

1.7.4 The evaluation of the ruggedness of the analytical method

According to the United States Pharmacopia, ruggedness is a measure of reproducibility of the test results obtained by the analysis of the samples under a variety of conditions such as different laboratories, analysts, instruments, lots of reagents, elapsed assay times, assay temperatures, or days (USP, 2005). Ruggedness will be evaluated by determining the repeatability (RSD) of the responses of the two different instruments when analysing five replicate analyses at low, medium and high concentration levels, for five consecutive days,, using the developed method (USP, 2005; Dejaegher and Heyden, 2007; Burns, Danzer and Townshend, 2009; César and Pianetti, 2009). The acceptance criteria for repeatability are %RSD equal to or less than 15% for the higher concentration and less than or equal to 20% for the lower concentration (ICH, 2005; González et al, 2014; FDA, 2018).

1.7.5 The evaluation of the selectivity of the analytical method

Some authors consider selectivity and specificity as different terms, as the term 'selective' refers to a method that produces different responses for different chemical entities or analytes, while specificity is the ability to assess, unequivocally, the analyte in the presence of components that may eventually be found with the analyte (ICH, 2005). Typically these might include impurities, degradants, matrix, etc. (*ibid*). However, both selectivity and specificity are considered one and the same for other authors (Taverniers, De Loose and Van Bockstaele, 2004).

Selectivity can be assessed in several ways. The first is a comparison between a matrix without analyte and a matrix with this analyte added. In this case, the interfering compounds present should not affect the assay result (ICH, 2005). The %RSD of spiked samples at the limit of detection concentration level is considered and should be less than or equal to 20% (FDA, 2018).

1.7.6 The evaluation of the recovery of the analytical method

Recovery is said to be of less importance in method validation as long as accuracy, precision, LOQ and LOD are acceptable (Hartmann et al, 1998; Shah et al, 2000; Peters and Maurer, 2002; Peters, Drummer and Musshoff, 2007). Recovery is the detector response obtained

from an amount of the analyte added to and extracted from the matrix, compared to the detector response for the true concentration of the pure authentic standard (seized materials). Recovery can be calculated using Equation 1.9 (Thompson et al, 1999; Bonfilio et al, 2012).

$$\%\boldsymbol{Recovery} = \frac{\boldsymbol{Measured\ Concentration}}{\boldsymbol{Added\ concentration}} \times \mathbf{100} \qquad \textbf{1-9}$$

An alternative approach is the standard addition technique, which is used when it is not possible to prepare a blank sample (solution without the analyte being present). In this case, the recovery is calculated by Equation 1.10 (*ibid*).

$$\%\boldsymbol{Recovery} = \frac{\boldsymbol{Measured\ Spiked\ Concentration - Measured\ Unspiked\ Concentration}}{\boldsymbol{Added\ concentration}} \times \mathbf{100} \qquad \textbf{1-10}$$

1.7.7 The stability of the analytes

Stability is the extent to which the analytes are stable during the whole analytical procedure, including storage before and after analysis.

1.8 STATISTICAL TREATMENT OF DATA

Previously, the statistical treatment of data for profiling of illicit drugs was done using both unsupervised and supervised chemometric methods. Supervised chemometric methods are methods where objects are classified into predefined groups. Unsupervised chemometric methods are classification methods where objects are classified into groups without prior knowledge of the groups to be expected (Hibbert, 2016). Unsupervised methods reported in literature are mainly principal component analysis (PCA) and hierarchical cluster analysis (HCA) for the profiling of both heroin (Chan, Tan and Wong, 2012c; Esseiva et al, 2005; Fischedick et al, 2010; Klemenc, 2001) and cannabis (Ahmad, Muniandy and Hassan, 2005;

Broséus et al, 2010; Chan, 2014). HCA is reported to offer information pertaining to the explicit relationship of the samples and deduce the number of mistakenly grouped sample units directly from the dedrogram (Chan, 2014).

Supervised methods reported include linear discriminant analysis (LDA), k-nearest neighbor method (k-NN) and artificial neural networks (Dams et al, 2001; Esseiva et al, 2005; Janhunen and Cole, 1999). Unsupervised methods are reportedly not the most suitable for determining the origin of a new sample that needs to be classified. As a result, a combination of supervised and unsupervised methods was suggested (Dams et al, 2001). Profiling of cannabis using principal component analysis for a large data set is reported to be more appropriate than cluster analysis (Ahmed et al, 2005). Two unsupervised chemometric methods, namely (i) principal component analysis (PCA) and (ii) agglomerative hierarchical clustering (HCA), were used in this research for the statistical treatment of data using the XLSTAT software (Addinsoft, 2019).

1.8.1 Basic statistics

The basic statistics used in the chemometric treatment of data include the mean, standard deviation, variance, covariance as well as correlation matrices described below.

1.8.1.1 The mean of a data set

In any data set, the spread of the data can be expressed by the mean of the data set. The mean of a data set is a central tendency of the data set, i.e. the data elements on the left-hand side of the mean are balanced by the data elements to the right of the mean. For a sample that is made up of the data set X = {x_1, x_2, …, x_n}, the mean of the data can be calculated using Equation 1.11:

$$\overline{\boldsymbol{x}} = \frac{\sum_{i=1}^{n} \boldsymbol{x_i}}{\boldsymbol{n}} \qquad \textbf{1-11}$$

Where, x_i is the *i*th data, $\bar{x}$ is the mean and n is the number of data elements.

1.8.1.2 The standard deviation of a data set

The major disadvantage of the mean is that it can be affected by outliers and therefore can be biased. Standard deviation can be used as a better estimate of how the data are spread out using the Equation 1.12:

$$\boldsymbol{s = \sqrt{\frac{\sum_{i=1}^{n}(x_i - \bar{x})^2}{(n-1)}}} \qquad \textbf{1-12}$$

Where *s* is the standard deviation, $\bar{x}$ is the mean, x_i is the *i*th data, and n is the number of data elements.

1.8.1.3 The variance of a data set

Another measure of the spread of data that are used in statistics is the variance. For the data set mentioned above the variance can be calculated using Equation 1.13:

$$\boldsymbol{var(X) = \frac{\sum_{i=1}^{n}(x_i - \bar{x})^2}{n-1} = \frac{\sum_{i=1}^{n}(x_i - \bar{x})(x_i - \bar{x})}{n-1}} \qquad \textbf{1-13}$$

Where *var(X)* is the variance, $\bar{x}$ is the mean, x_i is the *i*th data element, and n is the number of data elements.

1.8.1.4 The covariance matrix of a data set

Standard deviation and variance are used to determine the spread of data only in 1-dimension; that is, one calculates the standard deviation for each dimension of the data set independently of the other dimensions. In order to determine the spread of data between more than 1-dimensions, covariance is used. For a 2-dimensional data set Y = {x,y}, the covariance will be between two variable x and y, i.e. $covar(x, y)$. The formula for covariance

is very similar to the formula for variance; that is, the covariance between two variables x and y is given by Equation 1.14:

$$\boldsymbol{covar(x,y) = \frac{\sum_{i=1}^{n}(x_i-\bar{x})(y_i-\bar{y})}{n-1}} \qquad \textbf{1-14}$$

Where $covar(x,y)$ is the covariance between x and y, $\bar{x}$ and $\bar{y}$ are the means for variables x and y, respectively, x_i and y_i are the *i-th* data elements, and n is the number of data elements.

For an n-dimensional data set, the covariance will be a measure of variance between the variables x_i and x_j; that is $covar(x_i, x_j)$, where $i \neq j$. If $i = j$, then the covariance is nothing else but the measure of the variance between the variables x_i and x_j. It is often convenient to represent the covariance values in a covariance matrix. The covariance matrix is constructed such that the diagonal components are the variance, and the other components are the covariances. The n x n matrix is usually a square matrix, as illustrated in Equation 1.15:

$$\boldsymbol{C} = \begin{pmatrix} \boldsymbol{var(x_1,x_1)} & \boldsymbol{covar(x_1,x_2)} & \cdots & \boldsymbol{covar(x_1,x_n)} \\ \boldsymbol{covar(x_2,x_1)} & \boldsymbol{var(x_2,x_2)} & & \boldsymbol{covar(x_2,x_n)} \\ \vdots & & \ddots & \vdots \\ \boldsymbol{covar(x_n,x_1)} & \boldsymbol{covar(x_2,x_2)} & \cdots & \boldsymbol{var(x_n,x_n)} \end{pmatrix} \qquad \textbf{1-15}$$

1.8.2 Agglomerative Hierarchical Clustering

Agglomerative Hierarchical cluster analysis is a process where a data set is separated according to dissimilarity into smaller groups, followed by linking the data belonging to a particular group base on the distance between the data using single linkage, complete linkage or average linkage. No single linkage is better than the other, although the average linkage is said to be a compromise between single and complete linkage (Bratchell, 1989; Yim and Randeen, 2015). Hierarchical cluster analysis can be agglomerative or divisive. Agglomerative clustering involves the initial separation of each data set into its own cluster, followed by

linking the sets that are close to one another according to a set distance. Divisive clustering, on the other hand, involves the initial clustering of all the data sets into one large cluster, followed by gradual separation of the data sets into smaller clusters and linking the sets that are close to one another as per a set distance. The divisive clustering method is seldom used due to its complex computation algorithm (Yim and Ramdeen, 2015). Some of the distance measures used for continuous variables include the Chord distance, Euclidean distance, Mahalanobis distance, Manhattan distance and Minkowski distance with the Euclidean distance, defined by Equation 1.16, being the most used in numerical data analysis (Spencer, Bates Prins and Beckom, 2010; Hassan, Aickelin and Wagner, 2014; Brereton, 2015; Shirkhorshidi, Aghabozorgi and Wah, 2015). The Chord distance, Euclidean distance, Mahalanobis distance, Manhattan distance and Minkowski distance are defined by Equations 1.16, 1.18, 1.19, 1.20 and 1.21, where x_i and y_i are two vectors in *n*-dimensional space:

$$\boldsymbol{d_{Chord} = \left(2 - 2\frac{\sum_{i=1}^{n} x_i y_i}{\|x\|_2 \|y\|_2}\right)^{1/2}} \quad \textbf{1-16}$$

Where $\|x\|_2$ is the L^2-norm and is defined by Equation 1.17:

$$\boldsymbol{\|x\|_2 = \sqrt{\sum_{i=1}^{n} x_i^2}} \quad \textbf{1-17}$$

$$\boldsymbol{d_{Eucl} = \left(\sum_{i=1}^{n} |x_i - y_i|^2\right)^{1/2}} \quad \textbf{1-18}$$

$$\boldsymbol{d_{Mah} = \sqrt{(x-y)S^{-1}(x-y)^T}} \quad \textbf{1-19}$$

Where x and y are a pair of objects and S is the covariance matrix of the data set, T is the transpose:

$$\boldsymbol{d_{Man} = (\sum_{i=1}^{n} |x_i - y_i|^2)^{1/2}} \quad \textbf{1-20}$$

$$\boldsymbol{d_{Min} = (\sum_{i=1}^{n} |x_i - y_i|^q)^{1/q}} \quad \textbf{1-21}$$

where q ≥1. The Hamming distance used for categorical variables in a data set is given in Equation 1.22 (Spencer et al, 2010; Hassan, Aickelin and Wagner, 2014):

$$\boldsymbol{d_H = \sum_{i=1}^{n} |x_i - y_i|,} \quad \textbf{0-22}$$

where $d_H = \begin{cases} 0 \; if \; x = y \\ 1 \; if \; x \neq y \end{cases}$ and x_i and y_i are two vectors in n-dimensional space.

The distance measure that is used which incorporate both the continuous and categorical variables is the heterogeneous Euclidean overlap metric (HEOM) defined by the Equation 1.23 (Wilson and Martinez, 1997; Spencer et al, 2010):

$$\boldsymbol{HEOM(x, y) = \sqrt{\sum_{i=1}^{n} d_i(x_i, y_i)^2},} \quad \textbf{1-23}$$

Where $d_i(x_i, y_i)$ is defined by Equation 1.24;

$$\boldsymbol{d_i(x, y) = \begin{cases} 1 & if \; x \; or \; y \; is \; unknown, else \\ overlap(x, y), if \; i \; is \; nominal, else \\ rn\_ \; diff_i(x, y) \end{cases},} \quad \textbf{1-24}$$

The function $overlap\ (x, y)$ is defined by Equation 1.25 and the range normalized difference $rn\_diff_i(x, y)$ is defined by Equation 1.26:

$$\boldsymbol{overlap\ (x, y) = \begin{cases} 0 \; if \; x = y \\ 1 \; if \; x \neq y \end{cases},} \quad \textbf{1-25}$$

$$rn\_diff_i(x, y) = \frac{|x-y|}{range} \quad \textbf{1-26}$$

Generally, the evaluation measures in classification methods are determined from a matrix called the confusion matrix, which consists of correctly and incorrectly classified objects for each class (Costa et al, 2007). For a binary classification, confusion matrix (Table 1.12) yields four outcomes, namely true positive (TP), false positive (FP), true negative (TN) and false negative (FN).

- True positive (TP): correct positive classification of the data set when a positive dataset is present
- False positive (FP): incorrect positive classification of the data set when a positive dataset is absent
- True negative (TN): correct negative classification of the dataset when the actual class of the dataset was false.
- False negative (FN): incorrect negative classification of the data set when the actual class of the dataset was true.

Table 1.12: A typical confusion matrix for a binary classification.

		Classification	
		Positive	Negative
Detected	Positive	TP	FP
	Negative	TN	FN

The evaluation measures derived from the confusion matrix are accuracy, error rate, sensitivity, specificity and F-score (García, Mollineda and Sánchez, 2008; Ali, Neagu and Trundle, 2019). Accuracy (Equation 1.27) is defined as the total correct positive classifications divided by the number of dataset. Error rate (Equation 1.28) is defined as the total incorrect negative classifications divided by the number of data sets. Sensitivity (Equation 1.29), also referred to as recall, is defined as the correct positive classification divided by the number of positives. Specificity or precision (Equation 1.30) is defined as the number of correct positive

classifications divided by the total number of correct positive classifications. F-score (Equation 1.31) is defined as the weighted average of specificity and sensitivity.

$$\boldsymbol{Accuracy = \frac{TP+TN}{TP+TN+FP+FN} = 1 - Error\ rate} \quad \textbf{1-27}$$

$$\boldsymbol{Error\ rate = \frac{FP+FN}{TP+TN+FP+FN}} \quad \textbf{1-28}$$

$$\boldsymbol{Sensitivity = \frac{TP}{TP+FN}} \quad \textbf{1-29}$$

$$\boldsymbol{Specificity = \frac{TP}{TP+FP}} \quad \textbf{1-30}$$

$$\boldsymbol{Fscore = 2\frac{(Sensitivity \times sepecificity)}{(sensitivity+Specificity)}} \quad \textbf{1-31}$$

The success of classification increases with increasing accuracy, sensitivity, specificity or F-score and decreases with increasing error rate. The most common and intuitive evaluation measures are accuracy and error rate. A maximum accuracy of 1.00 indicates that the classification is completely successful while a minimum accuracy of 0.0 indicates that the classification completely failed. Conversely a minimum error rate of 0.0 indicates that the classification was successful while a maximum error rate of 1.00 indicates that the classification was successful. The accuracy that is ≥ 0.54 is believed to indicate the best success of the classification (Fawcett, 2004.), thus an error rate that is ≤ 0.46 indicates the best success of the classification."

Agglomerative hierarchical classification usually assumes that the data set is characterized by an n x n distance matrix (Hennig, 2008). The method makes the assumption that the data

points are in a metric space and thus the measure of similarity/dissimilarity between data points, say x and y, is determined by calculating the distance d between x and y, using any of the distance measures Euclidean, Manhattan, Minkowski and the Hamming distance. The distance measure used is expected to satisfy the following criteria (Hennig, 2008; XLSTAT, 2019):

- $d(x, y) = d(y, x)$: Symmetry property
- $d(x, y) \geq 0$: Non negativity property
- $d(x, y) = 0 \; if \; x = y$: Identity property
- $d(x, z) \geq d(x, y) + d(y, z)$: Inequality property

Hierarchical clustering begins by calculating distance between each pair of objects, resulting in a symmetric matrix where the diagonal has zero values since the distance between an object and itself is zero. The results of the hierarchical clustering is represented in a tree graph called a dendrogram, with vertical lines representing the grouping of the clusters as well as the distance between two joining clusters. The proximity between objects is measured by determining the similarity or the dissimilarity of the measured distance. The software used in this research uses the dissimilarity measure (XLSTAT, 2019).

1.8.3 Principal Component analysis

Principal component analysis (PCA) is an unsupervised chemometric method that uses an orthogonal transformation to convert a set of data consisting of variables that might be correlated into a set of values of uncorrelated variables called principal components (Chandra Paul, Al Suman and Sultan, 2013). For a data set that consists of m variables and n units, PCA generate an mxn matrix (covariance matrix) and seeks to establish a linear combination of the columns of the matrix with maximum variance (Bro and Smilde, 2014; Jolliffe and Cadima, 2016). Since principal component analysis is defined by variances, which itself depends on units of measurements, the covariance matrix is likely to change when the unit of measurement of one of the variable changes (Jolliffe and Cadima, 2016). To mitigate this feature, the data elements are standardised by subtracting the mean from each data element and divide by the standard deviation, as illustrated in Equation 1.32:

$$z = \frac{x_i - \bar{x}}{s} \qquad \textbf{1-32}$$

The covariance matrix derived from the standardised data elements is referred to as a correlation matrix. The correlation matrix is not affected by any change in units of measurement and therefore is regarded as appropriate choice for data sets with different changes of scale for each of the variables in the data set (Jolliffe and Cadima, 2016). The generated covariance/correlation matrices are used to determine eigenvalues and corresponding eigenvectors related to a new linear combination called principal components. Eigenvectors are nonzero vectors that undergo the linear transformation by scalar factors. The corresponding scalar factors are referred to as eigenvalues. Each eigenvector represents one principal component. The eigenvectors represent the dimensions in PCA, and the corresponding eigenvalues represent the scaling factor, length, size or robustness of the eigenvectors (Hyvärinen, 1970; Strang and Aarikka, 1986). The eigenvector with the highest eigenvalue represents the first principal component and it has the maximum variance (Hyvärinen, 1970). The principal components with eigenvalues greater than 1.00 account for at least as much variability as can be explained by one variable, whereas those components with eigenvalues below 1.00 account for less variability than does a single variable (Floyd and Widaman, 1995). The principal components with eigenvalues greater than 1.00 are sufficient to explain the variability of the data set (Kaiser, 1970). The principal components with a factor loading ≥ 0.300 is considered to account for at least as much variability as can be explained by one variable (*ibid*). The principal components that account for a total of 70% or more variability are considered to be sufficient to explain the variability of the data set (Jolliffe and Cadima, 2016). The elements of the principal components referred to as scores are used in a cluster plot to illustrate the similarity/dissimilarity of the data (Wold, Esbensen and Geladi, 1987; Ringnér, 2008; Bro and Smilde, 2014; Jolliffe and Cadima, 2016). The similarity/dissimilarity of the data points are established using Euclidean or Mahalanobis distance (Chandra Paul, Al Suman and Sultan, 2013; Brereton, 2015). The following assumptions are made when conducting a PCA:

(i) There is a linear combination between two variables measured by the covariance. A high covariance value represents high redundancy, conversely a low covariance value represents a low redundancy. High redundancy indicates that the data are highly correlated, while low redundancy indicates that the data are uncorrelated (Figure 1.11). A positive non-zero value indicates a positive correlation and a negative non-zero value indicates a negative correlation, while a zero covariance indicates that the variables are uncorrelated (Shlens, 2005).

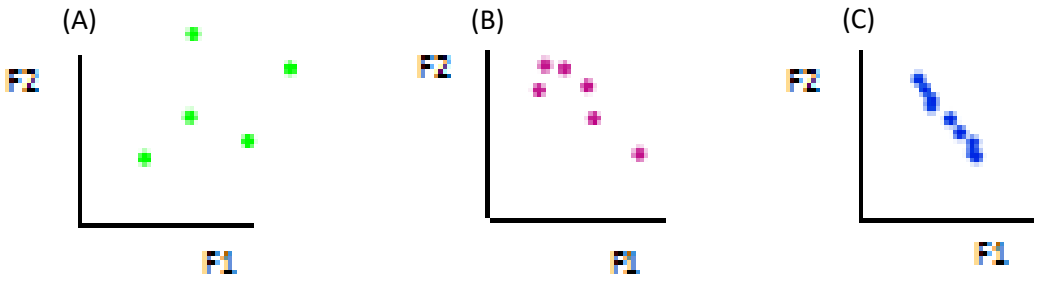

Figure 1.11: Diagrams of typical PCA plot illustrating (A) low redundancy, (B) normal redundancy and (C) high redundancy (Adapted from Shlens, 2005).

(ii) The principal components are orthogonal. Orthogonility is evaluated using a correlation (covariance) matrix. When the covariance matrix is equal to its transpose, their product is an identity matrix, implying that the principal components are orthogonal.

(iii) Large variance has significant dynamics, i.e. principal components with associated large variance have interesting dynamics and explain the variance of the data set, while those with lower variance represents noise. For example, in drug sample mixtures with different components, the concentration of each component and/or the number of different components per sample may define the variability of the sample. If the concentration has the large variance, it would be regarded as the first principal component and the variable one is capturing, since it explains the variance of the data set. The number of components would have lower variance and therefore regarded as the unwanted variance (noise). The principal components can be reduced to those components with large variance. The relevant information is larger than random noise and that the magnitude of the

variation of random noise seems to level off quite linearly with the number of components. The scree plot is used to evaluate this assumption which indicates an exponential decline towards zero of the eigenvalues of the principal components.

1.9 AIM OF THE RESEARCH

The aim of this project was to develop an analytical method for the chemical profiling of the major components present in the street cocktail drug nyaope, which is abused mainly in South Africa, by the analysis of seized samples using instrumental methods. The study aims to show that clustering techniques can be used to determine the relationship between nyaope samples.

The main objectives were:

1. Selection of the major psychoactive substances found in the street cocktail drug nyaope based on the data collected from the South African Police Services (SAPS) database of drug seizures in the area of interest.

2. Development and validation of an analytical methodology for the simultaneous identification and quantitation of selected major components found in nyaope extracted into an organic solvent followed by instrumental analysis.

3. Identification and quantitation of the cocktail components in the street nyaope samples seized by the South African Police Services and demonstration of the appropriateness of clustering techniques for the samples using two unsupervised methods, namely principal component analysis (PCA) and hierarchical cluster analysis (HCA).

CHAPTER 2: EXPERIMENTAL PROCEDURES

This chapter outlines the experimental procedures that were used in this research. The chemicals and standards used in the stability studies (Chapter 3) and analytical method validation (Chapter 4) are presented. The instrumental technique used during the study, the procedures used during stability studies in Chapter 3, as well as the procedures followed during analytical method validation in Chapter 4 are introduced.

2.1 CHEMICALS USED FOR THE STUDY

Dichloromethane (Distol-Pesticide residue grade) and hexane (HPLC grade) were purchased from Fischer Chemicals; absolute ethanol (Analytical reagent 99.9%) and tertiary butyl alcohol (ACS, Reag. Ph Eur) from Merck; eicosane, ethyl acetate (Chromasolv for HPLC ≥ 99%) and tetracosane (99%) from Sigma-Aldrich; and isopropanol (AR grade) from Associated Chemical Enterprise. Solvents were used as received without further purification. Efavirenz 600 mg tablets (PHD item 41047) and nevirapine 200 mg tablets (PHD item 41071) were both donated by Aspen Pharmacare. Cannabis and heroin street samples seized by the South African Police Services (SAPS) were used in this study. Certified reference Standards in 1 mL ampoules for Δ^9-tetrahydrocannabinol and heroin (diamorphine) base, both 1000.0 mg/L were purchased from Ceriliant-Sigma Aldrich. Caffeine and phenacetin were purchased from the US-Pharmacopeia as USP powder reference standards, while the reference material efavirenz and nevirapine were purchased from WHO International Chemical Reference Substances as an ICRS powder reference substance.

2.2 PREPARATION OF INTERNAL STANDARDS

The internal standard (ISTD) , tetracosane, was prepared at a final concentration of 20.0 mg/L in each of the solvents under study, i.e. dichloromethane (DCM), ethanol (ETOH), ethyl acetate (ETAC), hexane (HEX), isopropanol (i-PrOH) and tertiary butyl alcohol t-BuOH). The internal standard solution was then used to dissolve the drug samples prior to the stability tests.

2.3 SAMPLE PREPARATION

Street cannabis and heroin samples seized by the SAPS were used to prepare simulated nyaope samples. The simulated samples were prepared by mixing the heroin street sample, cannabis street sample, efavirenz tablet sample and nevirapine tablet sample, to mimic as closely as possible a typical street nyaope sample. The heroin street samples were determined to contain caffeine, diamorphine, dextromethorphan, acetylcodeine, 6-mono-acetylmorphine, noscapine, papaverine and phenacetin using GC-MS during routine casework at the SAPS Forensic Science Laboratory (SAPS-FSL). The simulated nyaope samples were homogenized by grinding, using a mortar and pestle. Blind simulated nyaope samples used to evaluate the validated analytical method, as discussed in Chapter 5, were also prepared by mixing a heroin street sample, a cannabis street sample, an efavirenz tablet sample and a nevirapine tablet sample in different combinations and proportions, to mimic as closely as possible a typical street nyaope sample. Three different groups of blind simulated nyaope samples were prepared and homogenised by grinding, using a mortar and pestle. The samples were then further divided into six sub-samples from each group to give a total of 18 blind simulated nyaope samples. Each sample was then weighed (mass given in Table 2.1) and extracted with 3 mL of the internal standard solution in a 20 mL head space vial.

2.4 HE INSTRUMENT PARAMETERS AND SYSTEM SUITABILITY

2.4.1 Temperature program

GC-MS analysis was carried out using an Agilent Technologies system consisting of a gas chromatograph (GC), Agilent 7890A, and mass selective (MS) detector (Agilent 5975 CVL MSD) with an auto sampler 7683B series (1 µL injection). Chromatographic separation was performed on a computer controlled auto sampler used with a fused-silica capillary column HP-5MS (30 m x 0.25 mm, film thickness 0.25 µm; J&W Scientific, Folsom, CA, USA). Splitless injection, with a solvent delay of 2.4 min, was used at 280 ^{o}C. The GC oven temperature programme consisted of an initial temperature of 100 ^{o}C for 0.4 min, raised to 290 ^{o}C at a rate of 60 ^{o}C/min, held at 290 ^{o}C for 2.4 min then raised to reach 316 ^{o}C at 60 ^{o}C/min and held for 3 min. The total run time was 9.40 minutes. High-purity helium (99.9995%) was used as the carrier gas, at a flow rate of 1 mL/min. The MS parameters used was performed as follows:

the interface temperature (280 ^{o}C), the inlet temperature (250 ^{o}C), the ion-source temperature (230 ^{o}C), electron impact ionization (EI) at 70 eV and the mass spectrometer (quadrupole) used in scan mode. The spectra were recorded in the scan range of mass particles (m/z) from 35 to 550 amu, at a scan time of 1 scan/sec (scan rate).

2.4.2 System suitability

Prior to analysis, confirmation that the instrument met quality assurance (QA) standards was achieved using a system suitability test according to the SAPS-FSL protocol (SAPS-FSL, 2017). The column efficiency was evaluated by analysing a Grob mixture containing decane, 1–octanol, undecane, nonanal, 2,3-dimethyiphenol, 2-ethylhexanoic acid, 2,5-dimethylbenzamine, decanoic acid methyl ester, undecanoic acid methyl ester, N-cyclohexylcyclohexanamine and dodecanoic acid methyl ester. The alkanes (decane and undecane) an; the fatty acid methyl esters (decanoic acid methyl ester, undecanoic acid methyl ester, N-cyclohexylcyclohexanamine and dodecanoic acid methyl ester) all measure column efficiency. The alcohol (1-octanol) and the phenol (2,3-dimethyiphenol) measure the presence of hydrogen-bonding sites (exposed silanols). The aldehyde (nonanal) measures saturated aldehyde adsorption by means other than hydrogen-bonding. The amine (dicyclohexylamine) measures irreversible adsorption. The acid/base pairs (2,6-dimethylphenol/2,6-dimethylaniline) and (2-ethylhexanoic acid/dicyclohexylamine) measure acid/base surface characteristics (Grob Jr, Grob, and Grob, 1978) The Grob mixture was analysed using a temperature program that consisted of an initial temperature of 35 °C for 1 min, raised to 110 °C at a rate of 10 °C/min, and then raised to 280 °C at a rate of 15 °C/min, and held for 5 min. To evaluate the Grob mixture, a line is drawn from the tip of the first peak (decane) to the tip of the ninth peak (undecanoic acid methyl ester). The height of each peak is then determined as a percentage of the height of the drawn line. The measurement of the peak height and the height of the drawn line must be taken at the same position on the horizontal axis. The acceptance criteria are a percentage of 20% or more for alcohol, aldehyde, phenol and amine as well as a percentage of 5% or more for the acid in the Grob mixture. The separation power of the column was reflected by the Trennzahl (TZ_e) values. The Trennzahl values were calculated by dividing the distance between neighbouring peaks (decanoic acid methyl ester, undecanoic acid methyl ester and dodecanoic acid methyl ester)

by the sum of the peak widths at half height (Equations 2.1 and 2.2) and are an indication of the resolution of a column.

$$TZ_{e1} = \frac{D_1}{d_1+d_2} \qquad \textbf{2-1}$$

$$TZ_{e2} = \frac{D_2}{d_2+d_3} \qquad \textbf{2-2}$$

where :

D_1 is the distance between the decanoic acid methyl ester and undecanoic acid methyl ester peaks

D_2 is the distance between the undecanoic acid methyl ester and dodecanoic acid methyl ester peaks

d_1 is the width of the decanoic acid methyl ester peak at half height

d_2 is the width of the undecanoic acid methyl ester peak at half height.

d_3 is the width of the dodecanoic acid methyl ester peak at half height.

The distance between neighbouring peaks is related to the retention time of each peak, which is a function of temperature (selectivity). Peak widths are related to the efficiency of a column, which is a function of the number of theoretical plates (N), and the height equivalent of a theoretical plate (HETP). N is a function of the length of the column, and HETP is a function of the flow rate, and thickness of the stationary phase (gas chromatography).

The tuning of the mass selective detector (MSD) was performed using the internal standard perfluorotributylamine (PFTBA). The calibration ions generated from the PFTBA in the EI ionization mode were 69 lower mass, 218.90 middle mass, and 502 higher mass.

An air leak in the GC-MS instrumentation can impact the performance of the chromatography negatively and is monitored by an air/water check software supplied by the manufacturer (Agilent Technologies). An air/water check was performed by leaking PFTBA into the MSD.

The abundance of the 69 amu fragment of PFTBA is taken as 100% (base peak), and the abundances of the other ions are expressed as percentages of the base peak. Accepted criteria as set by the manufacturer of the GC-MS instrumentation (Agilent Technologies) are water < 20% and nitrogen < 10%. When the calculated percentages of water and nitrogen fall within these limits, the instrument is suitable for the analysis of samples, provided that the instrument passes the tune specifications and Grob evaluation.

The mass spectrum was evaluated by analysing 5 ng/µL of decafluorotriphenylphosphine (DFTPP) and determining the percentage intensity of m/z values 51, 69, 127, 198, 275 365 and 442. The acceptance criteria are when the percentage intensities is between the minimum and maximum percentage intensities for each m/z value (Table 1) (Ferry, 2016). DFTPP contained 2 ng/mL of methaqualone to evaluate the sensitivity. The acceptance criteria are a signal-to-noise ratio of 20:1 (SAPS-FSL, 2017). (The signal-to-noise (S/N) ratio of 20:1 is an operational value set by the SAPS-FSL to be above 10 times signal-to-noise, based on data acquired over the years which shows that when the system passes all other set criteria, the methaqualone S/N ratio is always above 20:1).

Table 2.1: Minimum and maximum percentage intensities for evaluation of mass spectrum.

m/z value	Minimum % intensity	Maximum % intensity
51	20	50
69	17	51
127	35	61
198	95	100
275	16	32
365	0.5	5
442	85	100

2.5 TABILITY STUDIES

2.5.1 Solvent stability studies

The method used for the sample preparation is a modification of the methods reported in literature (Ahmad, Muniandy and Hassan, 2005; UNODC, 2009b). Homogenised simulated nyaope samples ranging between 10 mg and 22 mg were mixed with 10 mL of the internal standard solution in a 20 mL head space vial. The mixture was sonicated for 15 minutes, filtered and the solution divided into seven 1mL portions in amber GC-MS vials representing each of the time intervals, 0, 1, 6, 8, 24, 48 and 72 hours. Each of the vials was analysed in triplicate without further dilution. 100% of each of the solvents t-BuOH, DCM, ETOH, ETAC, HEX and iPrOH were used for the extraction of the simulated nyaope. The mass of the samples used in the study is shown in Table 2.2.

Table 2.2: Masses of the homogenised simulated nyaope samples and ISTD used in the solvent stability study.

Solvent	Mass of nyaope, mg	Mass of TC, mg
100% t-BuOH	18.1	20.3
100% DCM	16.3	23.6
100% ETAC	11.9	20.9
100% ETOH	20.4	21.1
100% HEX	21.7	20.6
100% i-PrOH	11.4	22.7

On the basis of the results for the simulated nyaope samples, tests were carried out on actual seized street samples of nyaope in selected solvents. Street samples were ground into a fine powder using a mortar and pestle. Separate aliquots of the homogenised street sample ranging from 10 mg to 24 mg were weighed into a 20 mL vial and mixed with 1 mL of each of the t-BuOH, DCM and i-PrOH internal standard solution. The mass of samples used in the study is shown in Table 2.3. The mixture was sonicated for 15 minutes, filtered and the

solution divided into seven 100 µL portions in inserts placed in amber GC-MS vials representing each of the time intervals. Each of the vials was analysed in triplicate without further dilution.

Table 2.3: Masses of the homogenised street nyaope samples and ISTD used in the solvent stability study.

Solvent	Mass of nyaope, mg	Mass of TC, mg
100% t-BuOH	10.3	20.3
100% DCM	15.5	23.6
100% i-PrOH	14.5	22.7

To test the stability of the drugs in the solvent, samples were analysed after each of the storage time interval at room temperature. The GC-MS analysis was performed using different vials for each time interval to minimise sample evaporation due to a perforated vial septum. The volume of sample in each vial was, however, kept the same.

2.5.1 Storage stability studies

The simulated nyaope samples were homogenised by grinding using a mortar and pestle. Each powdered nyaope sample was then divided into aliquots ranging from 10.0–11.9 mg. To obtain data at t=0, 10.2 mg of the homogenised samples was weighed into a 15 mL head space vial. 3 mL of the internal standard solution was added, and the vial sealed. The mixture was then sonicated for 15 minutes [30, 31]. The residue was filtered off and the eluate divided into three 800 µL portions into an amber GC-MS vial, representing each of the triplicate analyses. The remainder of the aliquoted homogenised samples (Table 2.4) ranging between 10.0 mg to 11.9 mg were weighed into clear glass bottles. The sample bottles were placed in (i) an opaque paper bag and stored in a desiccator in a refrigerator (±4 ^{o}C), (ii) in a desiccator at room temperature in the dark, (iii) in a desiccator under direct laboratory light, (iv) in an uncontrolled environment in a locker (ambient), (v) in an opaque paper bag and stored in a freezer at -70 ^{o}C and (vi) in an opaque paper bag and stored in a desiccator in a freezer

at -70 °C. The simulated samples were subsequently extracted and analysed after storage intervals of 0,24 hours, 72 hours and 1 , 2 and 3 weeks.

Table 2.4: Mass of simulated samples used for each time interval under the different storage conditions.

Time , hours	Mass of samples in a fridge, mg	Mass of samples in the dark, mg	Mass of samples in laboratory light, mg	Mass of samples in ambient environment, mg	Mass of samples in a freezer, mg	Mass of samples in a freezer and desiccator, mg
0	10.2	10.2	10.2	10.2	10.8	11.6
24	10.4	10.3	10.3	10.2	10.9	11.7
72	10.2	10.5	10.4	10.3	10.7	11.9
168 (1 week)	10.6	10.3	10.1	10.2	10.9	11.7
336 (2 weeks)	10.2	10.5	10.3	10.2	11.2	11.8
504 (3 weeks)	10.1	10.2	10.5	10.4	10.9	11.6
Average	10.3	10.3	10.3	10.3	10.9	11.7
Standard deviation	0.183	0.137	0.141	0.084	0.167	0.117
%RSD	1.78	1.32	1.37	0.82	1.54	1.00

2.6 ANALYTICAL METHOD VALIDATION

2.6.1 Preparation of working solutions

Drug standards of the major components of nyaope, namely caffeine (CAFF), diamorphine (DAM), efavirenz (EFV), nevirapine (NVP), phenacetin (PNT) and Δ^9-tetrahydrocannabinol (Δ^9-THC), which were available at the time of this research, were selected for the analytical method validation study. Tertiary butyl alcohol shown to be the suitable solvent for the identification, comparison and profiling of nyaope samples (Mthembi et al, 2018), was used during the analytical method validation. 1 mL of stock solution in methanol for Δ^9-tetrahydrocannabinol (Δ^9-THC) and acetonitrile for diamorphine (DAM) were placed in an amber GC-MS vial and evaporated to dryness under nitrogen and re-dissolved in 1 mL of the ISTD to give 1000.0 mg/L stock solution (SS). The powder standards were prepared by weighing accurately 50 mg, which was dissolved in 50 mL internal standard solution to give a final concentration of 1000.0 mg/L. The masses were 51.8 mg, 50.2 mg, 49.9 mg and 52.7 mg for phenacetin (PNT), caffeine (CAFF), efavirenz (EFV) and nevirapine (NVP), respectively, resulting in the respective concentrations of 1036.0, 1000.0, 998.0 and 1050.0 mg/L. 100 µL of SS was transferred to a new amber GC-MS vial, 900 µL of ISTD was added to obtain 1000 µL of a working solution (ISS). 100 µL of ISS were transferred to a new amber GC-MS vial, 900 µL of ISTD was added to obtain 1000 µL of a 10.0 mg/L working solution (ISS-1). 100 µL of ISS-1 was transferred to a new amber GC-MS vial, 900 µL of ISTD was added to obtain 1 000 µL of a 1.0 mg/L working solution (ISS-2). Other dilutions were made as indicated in Table 2.5.

Table 2.5: Dilutions of the working solutions used in the study.

Concentration, mg/L	Working solution	ISTD	Total volume
0	0	200 µL ISTD	200 µL
1.0	200 µL ISS-2	0	1000 µL
2.5	50 µL ISS-1	150 µL ISTD	200 µL
5.0	100 µL ISS-1	100 µL ISTD	200 µL
7.5	150 µL ISS-1	50 µL ISTD	200 µL
10.0	200 µL ISS-1	0	200 µL
25.0	50 µL ISS	150 µL ISTD	200 µL
50.0	100 µL ISS	100 µL ISTD	200 µL
75.0	150 µL ISS	50 µL ISTD	200 µL
100.0	200 µL ISS	0	200 µL
250.0	50 µL SS	150 µL ISTD	200 µL
500.0	100 µL SS	100 µL ISTD	200 µL
750.0	150 µL SS	50 µL ISTD	200 µL
1000.0	200 µL SS	0	200 µL

2.6.2 The evaluation of the linearity of the analytical method

A range of working solutions of PNT, CAFF, EFV, NVP, DAM and Δ^9-THC with concentrations 1.0, 2.5, 5.0, 7.5, 10.0, 25.0, 50.0, 75.0, 100.0, 250.0, 500.0, 750.0, 1000.0 mg/L were prepared and 10 replicate measurements were performed at each of the concentration levels (Lavagnini and Magno, 2007). A calibration curve was created by plotting average response ratio versus concentration. Linearity was assessed using the calibration graph and considered linear if the correlation coefficients (r^2) exceeded or equalled 0.99 (UNODC, 2005). The t-Test and F-Test were also used to assess linearity. Excel analysis of data variance (ANOVA) was used to calculate the t-Test and the F-Test for linearity.

The hypothesis for both t-test and F-test used for the evaluation of linearity was as follows:

- H_o = No linear relationship between x and y
- H_1 = There is a linear relationship between x and y

if $t_{calc} > t_{crit}$ and $F_{calc} > F_{crit}$ then H_o reject and H_1 is accepted.

2.6.3 The evaluation of the limit of detection and the limit of quantitation of the analytical method

A working solutions of PNT, CAFF, EFV, NVP, DAM and Δ^9-THC with concentrations 1.0, 2.5, 5.0, 10.0 and 50.0 mg/L in the vicinity of the limit of detection (Bonfilio et al, 2012) were prepared. The standards were analysed in ten replicate measurements. The limit of detection and quantitation was determined by regression analysis of the response ratios for the concentration for phenacetin, caffeine, efavirenz, nevirapine, diamorphine and Δ^9-THC. Regression statistics was used to determine the slope and standard error used in Equations 2.3 and 2.4 to calculate the detection limits and quantitation limits.

$$\boldsymbol{LOD = \frac{3.3 \times \sigma \times C_{IS}}{s}} \qquad \textbf{2-3}$$

$$\boldsymbol{LOQ = \frac{10 \times \sigma \times C_{IS}}{s}} \qquad \textbf{2-4}$$

where σ = standard error,

S = slope of the regression line, and

C_{IS}= concentration of the internal standard = 18.0 mg/L.

2.6.4 Accuracy and precision

2.6.4.1 The evaluation of the accuracy the analytical method

Accuracy was evaluated by preparing drug standard mixtures of PNT, CAFF, EFV, NVP, DAM and Δ^9-THC with concentrations 10.0, 100.0 and 1000.0 mg/L, representing the low, medium and high concentration levels, respectively. The standards were then analysed in ten replicate analyses. The peak area ratio of each analyte was determined for each replicate analysis by dividing the response ratio of the analyte by response ratio of the internal standard. The peak are ratios were then used to determine the measured concentration from the calibration curve.

The percentage accuracy was calculated using Equation 2.5 for each of the analyte at each concentration level and replicate measurement. The average accuracy was calculated and used to evaluate the accuracy. The acceptance criteria for accuracy are the average percentage accuracy of between 80% and 120% (Peters et al, 2007; González et al 2014; Kadiana et al, 2016).

$$\%\boldsymbol{Accuracy} = \frac{\boldsymbol{Measured\ concentration}}{\boldsymbol{actual\ concentration}} \times \mathbf{100} \qquad \textbf{2-5}$$

Accuracy was also evaluated by determining back-calculated accuracy expressed as %Bias. The drug standard mixtures were analysed concurrently with the linearity determination and the concentrations for the three levels (10.0, 100.0 and 1000.0 mg/L) were back-calculated using the calibration curve and Equation 2.6. The acceptance criteria for accuracy is a %Bias less than or equal to 15% for the higher concentration and less than or equal to 20% for the lower concentration (Rigdon, A. 2016; Zabell, Lytle and Julian, 2016).

$$\%\boldsymbol{Bias} = \frac{|\boldsymbol{Measured\ concentration - Actual\ concentration}|}{\boldsymbol{Actual\ concentration}} \times \mathbf{100} \qquad \textbf{2-6}$$

2.6.4.2 The evaluation of the precision of the analytical method

Precision ((under within laboratory repeatability and intermediate precision (within laboratory reproducibility)) was evaluated by preparing drug standard mixtures of PNT, CAFF, EFV, NVP, DAM and Δ^9-THC with concentrations 10.0, 100.0 and 1000.0 mg/L, representing the low, medium and high concentration levels, respectively. The standards were then analysed in ten replicate analyses. The precision of an analytical method is usually expressed in standard deviation, variance or coefficient of variance (relative standard deviation). The peak area ratio of each analyte was determined for each replicate analysis by dividing the response ratio of the analyte by response ratio of the internal standard. Precision was assessed by calculating relative standard deviation (%RSD) for Intra-assay precision (repeatability). The acceptance criteria for repeatability are %RSD equal or less than 15% for the higher concentration and less than or equal to 20% for the lower concentration. For the Intermediate precision, five replicate analyses of the calibration mixture at the low, medium and high concentration levels was performed using two instruments over five consecutive days. The within group (W) precision and between group (B) precision are calculated using Equations 2.7 and 2.8, respectively by one-way ANOVA (Group = Day) (Skoog et al, 2004):

$$\%\boldsymbol{RSD_W} = \frac{\sqrt{\boldsymbol{MSW}}}{\boldsymbol{X}} \times \mathbf{100} \qquad \textbf{2-7}$$

$$\%\boldsymbol{RSD_B} = \frac{\sqrt{(\boldsymbol{MSB}-\boldsymbol{MSW})/\boldsymbol{n}}}{\boldsymbol{X}} \times \mathbf{100} \qquad \textbf{2-8}$$

if MSB < MSW, set $\%RSD_B = 0$

where,

X = Grand mean of all observations

n = Number of observations in group

MSW = mean of squares within group

MSB = mean of squares between groups

2.6.5 The evaluation of the ruggedness of the analytical method

Drug standard mixtures of PNT, CAFF, EFV, NVP, DAM and Δ^9-THC with concentrations 10.0, 100.0 and 1000.0 mg/L, representing the low, medium and high concentration levels, respectively, were prepared. The standards were then analysed in five replicate analyses on two different instruments over five consecutive days to determine repeatability in the two instruments (Thompson et al, 2002). The peak area ratio of each analyte was determined for each replicate analysis by dividing the response ratio of the analyte by the response ratio of the internal standard. The relative standard deviation (%RSD) amongst the replicate analyses was calculated in order to evaluate ruggedness. The acceptance criteria for ruggedness are %RSD equal or less than 15% for the higher concentration (1000.0 mg/L), and less than or equal to 20% for the lower concentration (10.0 mg/L) (ICH, 2005; González et al, 2014; FDA, 2018).

2.6.6 The evaluation of the selectivity of the analytical method

Blank samples as well as working solutions analysed in ten replicate measurements as described in section 2.6.2, for the generation of the calibration curve was used to evaluate selectivity. The peak area ratio of each analyte was determined for each replicate analysis by dividing the response ratio of the analyte with the response ratio of the internal standard. The relative standard deviation (%RSD) amongst the replicate analyses was calculated in order to evaluate selectivity. The acceptance criteria are the lack of interference in the blank samples at the retention time(s) of the analyte(s) and the internal standard, as well as the resolution of the individual peaks of the components in the working solutions (ICH, 2005; FDA, 2018). Furthermore, the %RSD of the peak areas of the analytes at the LOD concentration level should be less than or equal to 20% (ICH, 2005; FDA, 2018).

2.6.7 The evaluation of the recovery of the analytical method

Recovery was evaluated using the standard addition method. Homogenised street samples containing CAFF, DAM and Δ^9-THC between 10.4 and 16.49 mg (Table 2.6) were weighed into amber headspace vials and extracted with each of the solvents t-BuOH, DCM, ETAC, i-PrOH, ETOH and HEX. Five replicate analyses were performed on each of the solvent extracts. A

separate set of homogenised street samples containing CAFF, DAM and Δ^9-THC between 11.3 and 16.68 mg (Table 2.6) was spiked with the reference standard mixture containing DAM, EFV, CAFF, PNT and Δ^9-THC with concentrations as shown in Table 2.6. The spiked samples were extracted with each of the solvents t-BuOH, DCM, ETAC, i-PrOH, ETOH and HEX and 5 replicate analyses were performed on each of the solvent extracts. The street recovery for EFV, PNT was calculated using Equation 2.9 (Bonfilio et al, 2012):

$$\%\boldsymbol{Recovery} = \frac{\boldsymbol{Measured\ Concentration}}{\boldsymbol{Added\ concentration}} \times \mathbf{100} \qquad \textbf{2-9}$$

The standard addition technique was used to calculate the percentage recovery for CAFF, DAM and Δ^9-THC using Equation 2.10 (*ibid*):

$$\%\boldsymbol{Recovery} = \frac{\boldsymbol{Measured\ Spiked\ Concentration - Measured\ Unspiked\ Concentration}}{\boldsymbol{Added\ concentration}} \times \mathbf{100} \qquad \textbf{2-10}$$

Table 2.6 : Sample quantities used in the different solvents for recovery studies.

Solvent	Mass of spiked sample, mg	Mass of un-spiked, mg	Concentration, mg/L
t-BuOH	13.99	15.6	17.0
DCM	16.68	12.8	17.0
ETAC	11.82	16.49	17.0
i-PrOH	11.84	10.4	17.0
ETOH	12.46	12.1	13.0
HEX	11.3	14.0	10.0

CHAPTER 3: RESULTS AND DISCUSSION – STABILITY STUDIES

This chapter discusses stability studies conducted on street nyaope samples to determine what precautionary steps need to be taken to prevent degradation of the samples and ensure more efficient profiling of the samples. Section 3.1 discusses autosampler stabilities for 72 hours of the nyaope extracts in different solvents. Long-term stability studies conducted over a period of 21 days are discussed in Section 3.2.

3.1 SOLVENT STABILITY STUDIES

The samples, after extraction with pure solvents (dichloromethane (DCM), ethanol (ETOH), ethyl acetate (ETAC), isopropanol (i-PrOH), hexane and tertiary butyl alcohol (t-BuOH)) were analysed using GC-MS in the presence of the internal standard tetracosane (TC), as explained in Sections 2.4.1 and 2.5.1. Figures 3.1 and 3.2 show typical chromatograms of the simulated nyaope sample and an actual seized street nyaope sample, respectively. The peak areas of TC and each of the target compounds, acetylcodeine (ACOD), caffeine (CAFF), cannabidiol (CBD), cannabinol (CBN), diamorphine (DAM), dextromethorphan (DTM), efavirenz (EFV), 6-monoacetylmorphine (6-MAM), nevirapine (NVP), nicotine (NCT), noscapine (NOSC), papaverine (PPV), phenacetin (PNT), tetrahydrocannabivarin (THCV) and Δ^9–tetrahydrocannabinol (Δ^9–THC) were determined from total ion chromatograms. The retention times (RT) of the individual components for the simulated nyaope samples as well as the components for actual seized street nyaope samples are given in Tables 3.1 and 3.2, respectively. DAM and Δ^9-THC were identified on the basis of their retention time and mass spectral data using certified reference material and ACOD, CAFF, CBD, CBN, EFV, 6-MAM, NVP and PNT were identified on the basis of their retention time and mass spectral data using USP reference standards, while NCT, α-caryophyllene, α-humelene, α/β -selinene, neophyltadiene, palmitic acid, phytol, (Z,Z,Z)-9,12,15-octadecatrienoic acid, CBV, 4,8,13-duvatriene-1,3-diol, cannabicyclol, THCV, CBV, CBCM, CBCN, CBG, vitamin E and β/γ-sitosterol were identified using the NIST library.

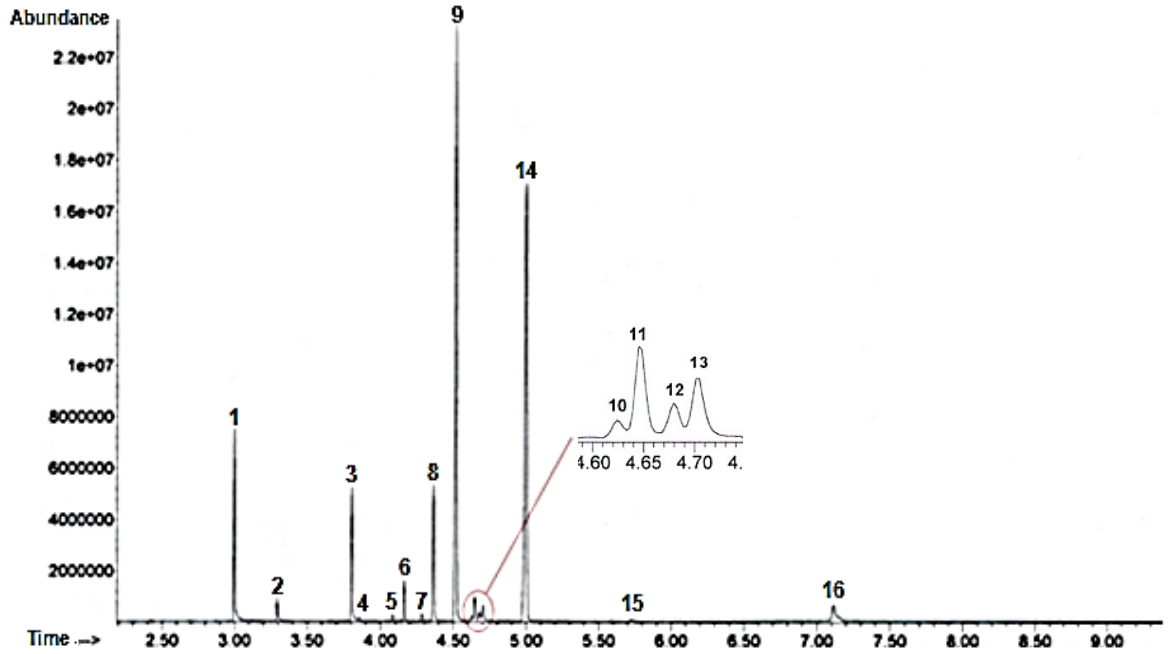

Figure 3.1: Typical total ion chromatograph for the simulated nyaope samples where (1) phenacetin; (2) caffeine; (3) EFV; (4) dextromethorphan; (5) tetrahydrocannabivarin; (6) tetracosane; (7) cannabidiol; (8) NVP; (9) Δ^9-THC; (10) cannabigerol; (11) acetylcodeine; (12) cannabinol; (13) 6-monoacetylmorphine; (14) diamorphine; (15) papaverine and (16) noscapine.

Table 3.1: Retention times and relative retention times of individual components for the simulated nyaope sample.

Component	Retention time (minutes)	Relative retention time (tetracosane = 1.000)
Phenacetin	3.002	0.720
Caffeine	3.297	0.791
Efavirenz	3.809	0.914
Dextromethorphan	3.859	0.926
Tetrahydrocannabivarin	4.088	0.981
Tetracosane/IS	4.167	1.000
Cannabidiol	4.291	1.030
Nevirapine	4.369	1.048
Δ^9-tetrahydrocannabinol	4.524	1.086
Cannabigerol	4.631	1.111
Acetylcodeine	4.652	1.116
Cannabinol	4.685	1.124
6-monoacetylmorphine	4.709	1.130
Diamorphine	5.006	1.201
Papaverine	5.735	1.376
Noscapine	7.120	1.709

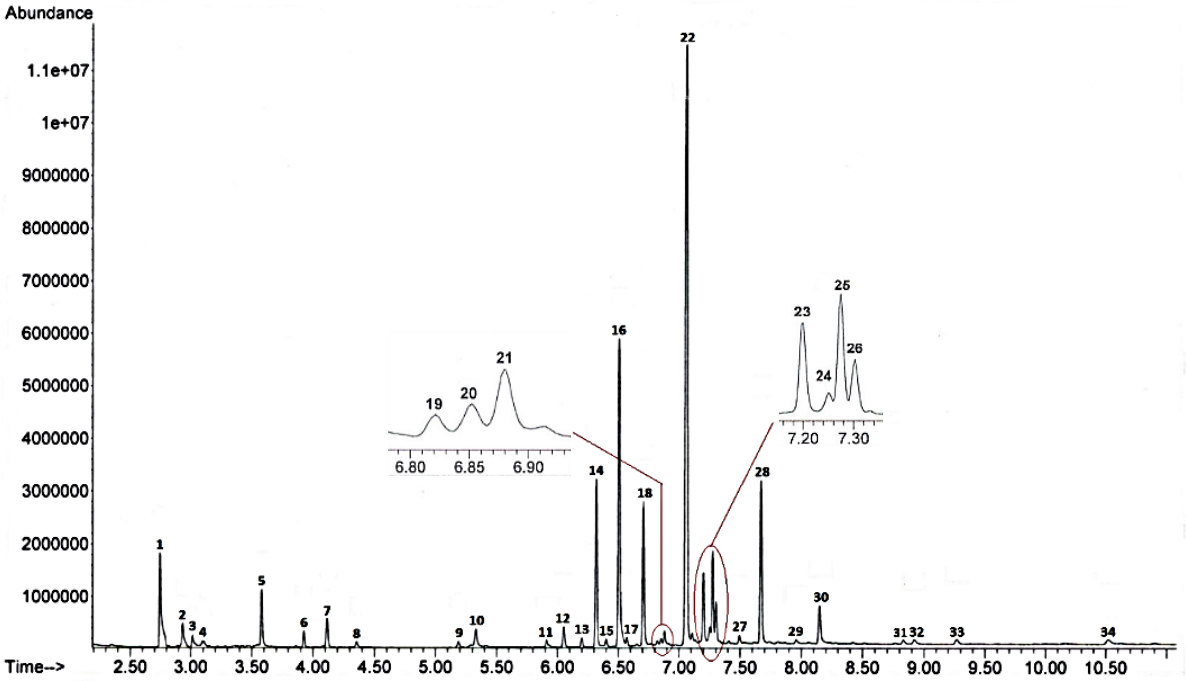

Figure 3.2. Typical total ion chromatograph for an actual seized street nyaope samples where (1) nicotine; (2) α-caryophyllene; (3) α-humelene; (4) α/β-selinene; (5) phenacetin; (6) neophyltadiene; (7) caffeine; (8) palmitic acid (9) phytol; (10) (Z,Z,Z)-9,12,15-octadecatrienoic acid; (11) cannabivarol; (12) 4,8,13-duvatriene-1,3-diol; (13) cannabicyclol; (14) tetrahydrocannabivarin; (15) cannabichromene; (16) internal standard tetracosane; (17) cannabivarin (18) cannabidiol; (19) nevirapine; (20) cannabicoumaronone; (21) unknown (22); Δ^9-tetrahydrocannabinol; (23) cannabigerol; (24) acetylcodeine; (25) cannabinol; (26) 6-monoacetylmorphine; (27) heneicosane; (28) diamorphine; (29) squalene; (30) 11-butyl docosane; (31) unknown; (32) triacontane; (33) vitamin E and (34) β/γ-sitosterol.

Table 3.2: Retention times and relative retention times of individual components for the actual seized street nyaope sample.

Component	Retention time, minutes	Relative retention time (tetracosane = 1.000)
Nicotine	2.746	0.422
α-Caryophyllene	2.934	0.451
α-Humelene	3.015	0.463
α/β-selinene	3.094	0.475
Phenacetin	3.580	0.550
Neophyltadiene	3.927	0.603
Caffeine	4.115	0.632
Palmitic acid	4.356	0.669
Phytol	5.187	0.797
(Z,Z,Z)-9,12,15-octadecatrienoic acid	5.330	0.819
Cannabivarol	5.912	0.908
4,8,13-Duvatriene-1,3-diol	6.053	0.930
Cannabicyclol	6.201	0.953
Tetrahydrocannabivarin	6.320	0.971
Cannabichromene	6.400	0.983
Tetracosane	6.509	1.000
Cannabivarin	6.572	1.010
Cannabidiol	6.708	1.031
Nevirapine	6.822	1.048
Cannabicoumaronone	6.853	1.053
Unknown	6.881	1.057
Δ^9-Tetrahydrocannabinol	7.062	1.085
Cannabigerol	7.200	1.106
Acetylcodeine	7.252	1.114
Cannabinol	7.276	1.118
6-Monoacetylmorphine	7.304	1.122
Heneicosane	7.496	1.152
Diamorphine	7.673	1.179
Squalene	7.959	1.223
11-Butyl docosane	8.150	1.252
Unknown	8.832	1.357
Triacontane	8.922	1.371
Vitamin E	9.269	1.424
β/γ-Sitosterol	10.520	1.616

The GC-MS analyses were performed in triplicate. Relative response ratios for each target compound in each replicate measurement were calculated by dividing the peak area of the target compound with the peak area of the internal standard (Aalberg et al, 2005). The averages of these response ratios were calculated, and the normalised average response ratio was determined using Equation 3.1:

$$R_N = ABS\,(100 - \frac{R_i}{R_0} \times 100) \qquad 3\text{-}1$$

where R_N is the normalised average response ratio, *ABS* is absolute value, R_i is the relative response ratio at the time T_i, and R_0 is the relative response ratio for the initial injection.

The ratio of CBN to Δ^9-THC was calculated by dividing the peak area response of CBN with the peak area response of Δ^9-THC. CBN is a degradation product for Δ^9-THC; therefore, an increase in the ratio CBN to Δ^9-THC indicates an increase in the amount of CBN and a decrease in the amount of Δ^9-THC, and suggests that the latter is decomposing. CBN can also be formed from the corresponding cannabinolic acid (CBNA), itself a degradation product of Δ^9-tetrahydrocannabinolic acid (Δ^9-THCA). 6-MAM is the degradation product for DAM, and the ratio of 6-MAM to DAM was calculated in a similar manner where an increase in the ratio indicates an increase in the amount of 6-MAM and a decrease in the amount of DAM.

The degradation products of the major components of nyaope are shown in Section 1.6.3.2 (Table 1.11). The degradation product acetaminophen, of phenacetin, is itself one of the adulterants of street nyaope observed in casework at the South African Police Forensic Science Laboratory (SAPS-FSL). The CAFF degradation products (paraxanthine, theophylline, theobromine and 1,3,7-trimethyloric acid), PNT degradation products (acetaminophen and phenetidine), as well as DTM degradation products (3-methoxymorphinan and 17-methylmorphinan-3-ol), although present in the NIST library used were not detected in the simulated nyaope sample. The EFV degradation products (carbamic acid derivative, efavirenz amino alcohol and quinoline derivative), NVP degradation products (descyclopropyl nevirapine and ethyl nevirapine) and the CBD degradation products (menthane carboxylic acid and hyroxyquinone derivative) were not present in the NIST library used and could therefore not be identified.

The results for individual solvents are discussed in order of decreasing suitability for extraction and storage stability of the target compounds using pure solvents. On the basis of the data around the stability of simulated nyaope samples (Mthembi et al, 2018) tertiary butyl alcohol, dichloromethane and isopropanol were selected for extraction and storage stability studies for the actual seized street nyaope samples. Based on prior analysis (ibid) and NIST library hits, the street nyaope sample tested was tentatively identified to contain NCT, α-caryophyllene, α-humelene, α/ β -selinene, PNT, neophyltadiene, CAFF, palmitic acid, phytol, (Z,Z,Z)-9,12,15-octadecatrienoic acid, cannabivarol (CBV), 4,8,13-duvatriene-1,3-diol, cannabicyclol (CBL), THCV, cannabivarin (CBV), CBD, NVP, cannabichromene (CBCM), cannabicoumaronone (CBCN), Δ^9-THC, cannabigerol (CBG), ACOD, CBN, 6-MAM, DAM, vitamin E and β/γ-sitosterol.

The stabilities for the monitored components in both simulated nyaope samples and actual seized street samples extracted with pure solvents are summarised in Tables 3.3 and 3.4, respectively, where 1 denotes a decrease of 0–15% and considered stable; 2 denotes a decrease of 15–30% and considered moderately stable; and 3 denotes a loss above 30% and considered unstable (Saar et al, 2012).

Table 3.3: Summarised stability of the main nyaope components monitored in pure solvents.[1]

Time, hours	Compound	Dichloromethane		Ethanol	Ethyl acetate	hexane	Isopropanol		Tertiary alcohol	butyl
		simulated sample	*street sample*	simulated sample	simulated sample	simulated sample	*simulated sample*	*street sample*	*simulated sample*	*street sample*
	NCT	*nd*	1	*Nd*	*nd*	*nd*	*nd*	1	*nd*	1
	PNT	1	1	1	1	1	1	1	1	1
	CAFf	1	1	1	1	1	1	2	1	1
	EFV	1	*nd*	1	1	1	1	*nd*	1	*nd*
	DTM	1	*nd*	1	1	1	1	*nd*	3	*nd*
	THCV	1	1	1	1	1	1	1	1	1
	CBD	1	1	1	1	1	1	1	1	1
1	NVP	1	1	1	1	1	1	1	1	2
	Δ^9-THC	1	1	1	1	1	1	1	1	1
	ACOD	1	1	1	1	1	1	1	1	2
	CBN	1	1	1	1	1	1	1	1	1
	6-MAM	1	1	1	1	1	1	1	1	1
	DAM	1	1	1	1	1	1	1	1	1
	PPV	1	*nd*	1	2	1	2	*nd*	1	*nd*
	NOSC	1	*nd*	1	1	1	1	*nd*	1	*nd*
	NCT	*nd*	1	*Nd*	*nd*	*nd*	*nd*	2	*nd*	1
	PNT	1	1	1	2	2	1	2	2	1
	CAFf	1	1	1	1	1	1	2	1	1
	EFV	1	*nd*	1	1	1	1	*nd*	1	*nd*
	DTM	1	*nd*	1	1	1	1	*nd*	2	*nd*
	THCV	1	1	1	1	1	1	1	1	1
	CBD	1	1	1	1	1	1	1	2	2
6	NVP	1	1	1	1	1	1	1	1	3
	Δ^9-THC	1	1	1	1	1	1	1	1	1
	ACOD	1	1	1	1	1	1	1	1	3
	CBN	1	1	1	1	1	1	1	1	1
	6-MAM	1	1	1	1	1	1	1	1	1
	DAM	1	1	1	1	1	1	1	1	1
	PPV	1	*nd*	1	3	1	2	*nd*	1	*nd*
	NOSC	1	*nd*	1	1	1	1	*nd*	1	*nd*
	NCT	*nd*	1	*nd*	*nd*	*nd*	*nd*	2	*nd*	1
	PNT	1	1	1	2	2	1	2	2	1
	CAFf	1	1	1	1	1	1	2	1	1
	EFV	1	*nd*	1	1	1	1	*nd*	1	*nd*
	DTM	1	*nd*	1	1	1	1	*nd*	2	*nd*
	THCV	1	1	1	1	1	1	1	1	1
	CBD	1	1	1	1	1	1	1	2	2
8	NVP	1	1	1	1	1	1	1	1	3
	Δ^9-THC	1	1	1	1	1	1	1	1	1
	ACOD	1	1	1	1	1	1	1	1	3
	CBN	1	1	1	1	1	1	1	1	1
	6-MAM	1	1	1	1	1	1	1	1	1
	DAM	1	1	1	1	1	1	1	1	1
	PPV	2	*nd*	2	2	2	1	*nd*	1	*nd*
	NOSC	1	*nd*	1	2	1	1	*nd*	1	*nd*

[1]*where 1 denotes a change of 0–15% and considered stable, 2 denotes a change of 16–30% and considered moderately stable and 3 denotes a change above 30% and considered unstable (Saar et al, 2012).*

nd = not detected

Table 3.3 *contn'd*: Summarised stability of the main nyaope components monitored in pure solvents.[1]

Time, hours	Compound	Dichloromethane		Ethanol	Ethyl acetate	hexane	Isopropanol		Tertiary butyl alcohol	
		simulated sample	***street sample***	**simulated sample**	**simulated sample**	**simulated sample**	***simulated sample***	***street sample***	***simulated sample***	***street sample***
	NCT	*nd*	2	*nd*	*nd*	*nd*	*nd*	3	*nd*	1
	PNT	1	1	1	1	2	1	3	1	1
	CAFf	1	2	1	1	1	1	3	1	1
	EFV	1	*nd*	1	1	1	1	*nd*	1	*nd*
	DTM	1	*nd*	2	1	1	1	*nd*	2	*nd*
	THCV	1	1	2	1	2	1	2	1	1
	CBD	1	1	2	1	3	1	2	1	2
24	NVP	1	1	1	1	1	1	3	1	3
	Δ^9-THC	1	1	2	1	2	1	1	1	1
	ACOD	2	1	1	1	2	1	1	1	3
	CBN	1	1	1	1	2	1	2	1	1
	6-MAM	3	1	2	2	3	2	2	1	1
	DAM	1	1	1	1	1	1	1	1	1
	PPV	1	*nd*	1	*1*	1	1	*nd*	1	*nd*
	NOSC	1	*nd*	1	*1*	1	1	*nd*	1	*nd*
	NCT	*nd*	2	*nd*	*nd*	*nd*	*nd*	3	*nd*	2
	PNT	1	3	2	1	2	1	3	1	3
	CAFf	1	1	1	1	2	1	3	1	2
	EFV	1	*nd*	1	1	1	1	*nd*	1	*nd*
	DTM	1	*nd*	3	2	3	3	*nd*	2	*nd*
	THCV	2	1`	2	2	1	2	2	1	1
	CBD	2	1	2	2	1	2	3	1	1
48	NVP	1	1	1	1	3	1	3	1	1
	Δ^9-THC	2	1	1	2	2	3	1	1	1
	ACOD	3	1	1	1	1	2	3	1	2
	CBN	1	1	1	2	1	1	3	2	1
	6-MAM	2	1	2	3	2	3	3	1	1
	DAM	2	1	1	1	1	1	2	1	1
	PPV	1	*nd*	3	2	1	2	*nd*	1	*nd*
	NOSC	1	*nd*	1	2	1	1	*nd*	1	*nd*
	NCT	*nd*	2	*nd*	*nd*	*nd*	*nd*	3	*nd*	1
	PNT	2	3	3	1	3	2	3	2	3
	CAFf	1	2	3	2	2	3	3	3	1
	EFV	2	*nd*	3	1	3	1	*nd*	1	*nd*
	DTM	3	*nd*	3	3	3	3	*nd*	2	*nd*
	THCV	2	1	3	1	3	1	2	1	1
	CBD	3	1	3	1	3	1	2	2	1
72	NVP	1	1	3	1	3	1	3	1	1
	Δ^9-THC	3	1	3	2	3	2	1	1	1
	ACOD	2	1	3	1	3	2	2	1	2
	CBN	1	1	3	1	3	1	3	1	1
	6-MAM	2	1	3	1	3	1	3	1	1
	DAM	1	1	3	1	3	1	1	1	1
	PPV	1	*nd*	3	1	3	1	*nd*	1	*nd*
	NOSC	1	*nd*	3	3	3	3	*nd*	2	*nd*

[1]*where 1 denotes a change of 0–15% and considered stable; 2 denotes a change of 16–30% and considered moderately stable; and 3 denotes a change above 30% and considered unstable (Saar et al, 2012).*

nd = not detected

Table 3.4: Summarised stabilities for the CBN to Δ^9-THC and 6-MAM to DAM ratios for pure solvents.[2]

Time, hours	Compound	Dichloromethane		Ethanol	Ethyl acetate	hexane	Isopropanol		Tertiary butyl alcohol	
		simulated sample	*street sample*	simulated sample	simulated sample	simulated sample	*simulated sample*	*street sample*	*simulated sample*	*street sample*
1	CBN/ Δ^9-THC	1	1	1	1	1	1	1	1	1
	6-MAM/ DAM	1	1	1	1	1	1	1	1	1
6	CBN/ Δ^9-THC	1	2	1	1	1	1	1	1	1
	6-MAM/ DAM	1	1	1	2	1	1	1	2	1
8	CBN/ Δ^9-THC	1	2	1	1	1	1	1	1	1
	6-MAM/ DAM	1	1	1	2	1	1	1	2	1
24	CBN/ Δ^9-THC	1	2	1	1	1	1	1	1	1
	6-MAM/ DAM	2	2	2	3	3	1	1	2	1
48	CBN/ Δ^9-THC	3	1	2	1	1	2	3	1	1
	6-MAM/ DAM	1	1	2	3	2	3	3	2	1
72	CBN/ Δ^9-THC	3	1	1	2	1	2	3	1	1
	6-MAM/ DAM	1	1	3	1	2	2	3	2	1

[2]The stabilities are summarised in the Tables 3 and 4 above , where 1 denotes a change of 0–15% and considered stable; 2 denotes a change of 16–30% and considered moderately stable; and 3 denotes a change above 30% and considered unstable (Saar et al, 2012) .

Figure 3.3 is the plot of the normalised relative response ratio vs injection time for the ratio of CBN to Δ^9-THC and 6-MAM to DAM for the actual seized street nyaope samples extracted with each of the solvents t-BuOH, DCM and i-PrOH. Plots of the normalised relative response ratio against injection time for the ratio of CBN to Δ^9-THC and 6-MAM to DAM as well as the responses to the compounds CAFF, DTM, EFV, NVP and PNT were prepared for the simulated nyaope samples extracted with each of the pure solvents as shown in Figures 3.4 and 3.5.

3.1.1 The stability of nyaope components in tertiary butyl alcohol

Tertiary butyl alcohol (t-BuOH) was shown to be the better solvent in which the main components of nyaope are more stable, as illustrated in Figures 3.3, 3.4 and 3.5. Stabilities shown in Tables 3.3 and 3.4 indicate that the target compounds THCV, CBD, CBN, Δ^9-THC, 6-MAM and DAM are stable after 72 hours of storage in both simulated and actual seized street nyaope samples. The ratios CBN to Δ^9-THC and 6-MAM to DAM confirm the stability of CBN, Δ^9-THC, 6-MAM and DAM during 72 hours of storage. While NVP and ACOD present in simulated nyaope samples indicate stability after 72 hours of storage, a definitive conclusion cannot be made regarding their stability in actual seized street nyaope samples. Results for NVP and ACOD in actual seized street nyaope samples range from stable to unstable within the same storage time period. This may either be due to the fact that these components are present at a very low amount and therefore the response is susceptible to instrument background interference, or due to interaction with other compounds within the street samples. PNT and CAFF are stable for 72 hours of storage in simulated nyaope samples while in the actual seized street samples, PNT is stable for 24 hours of storage and CAFF is stable for 48 hours of storage. Both CAFF and PNT are present at a very low amount and therefore the response is susceptible to background interference.

EFV, present only in simulated nyaope sample, was shown to be stable for 72 hours of storage, while DTM is shown to be unstable after 24 hours of storage. DTM was present at a very low amount and therefore the response is susceptible to instrument background interference. NCT, present only in actual seized street nyaope sample, was found to be stable for 72 hours of storage. The stability of the target compounds in t-BuOH is to be expected since it is an unreactive solvent (Chemindustry.ru, n.d.; Reeve, Erikson and Aluotto, 1979). Both PPV and NOSC are present in low abundance only in the simulated nyaope sample but were shown to

be stable for 72 hours of storage. From this it is clear that tertiary butyl alcohol is the suitable solvent for the extraction of the compounds ACOD,CAFF, CBD, CBN, DAM, EFV, 6-MAM, NOSC, NVP, PNT, PPV, Δ^9-THC and THCV with the subsequent instrumental analysis performed within 72 hours.

Solvent	Tertiary butyl alcohol	Dichloromethane	Isopropanol
6 - MAM/DAM	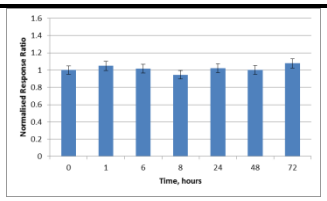	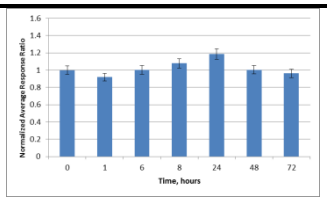	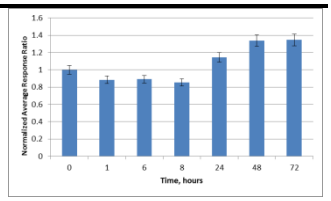
CBN/Δ^6-THC	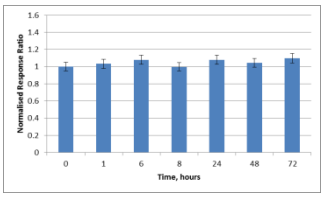	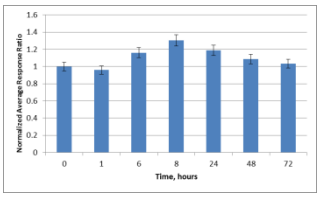	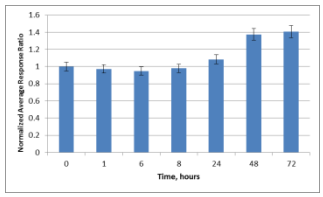

Figure 3.3: Plot of normalized average response ratios of 6-MAM to DAM and CBN to Δ^9-THC for actual seized street nyaope samples extracted with t-BuOH, DCM and i-PrOH respectively.

Solvent	Tertiary butyl alcohol	Dichloromethane	Ethyl acetate	isopropanol	Ethanol	Hexane
6 - MAM/DAM	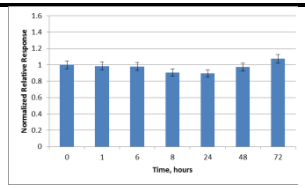	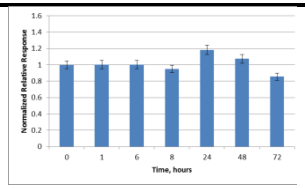	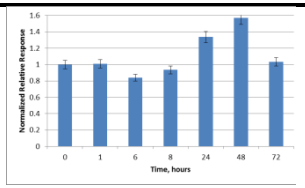	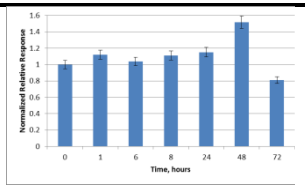	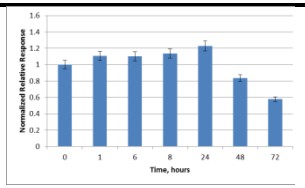	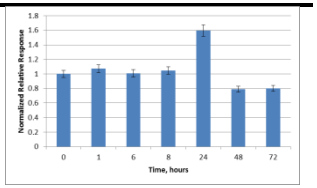
CBN/Δ^6-THC	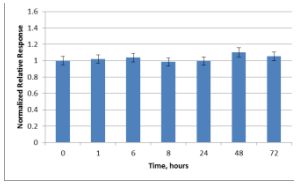	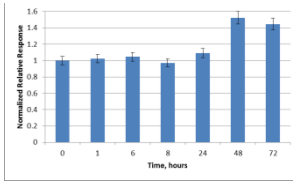	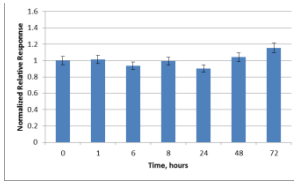	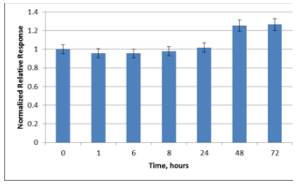	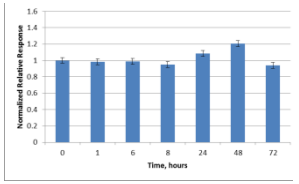	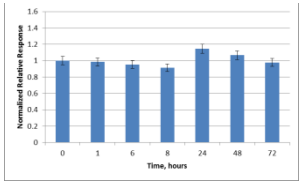

Figure 3.4: Plot of normalized average response ratio vs time of 6-MAM to DAM and CBN to Δ^9-THC ratios for simulated nyaope samples extracted with t-BuOH, DCM, ETAC, i-PrOH, ETOH and hexane, respectively.

Solvent	Efavirenz	Nevirapine	Phenacetin	Caffeine	Dextromethorphan
t-BuOH	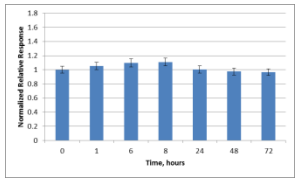	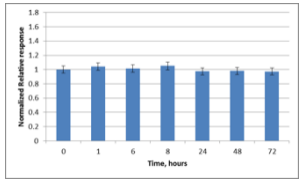	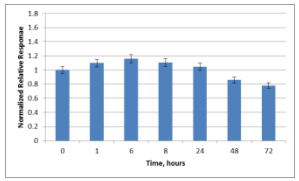	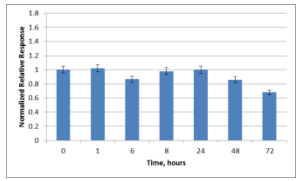	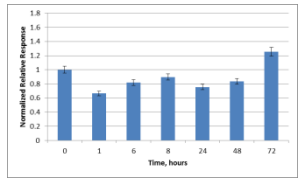
DCM	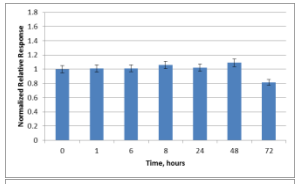	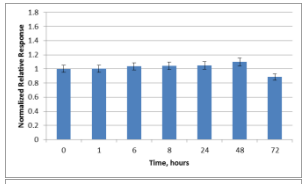	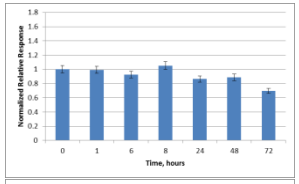	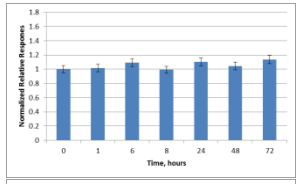	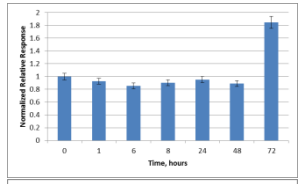
ETAC	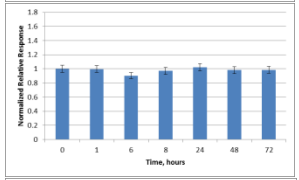	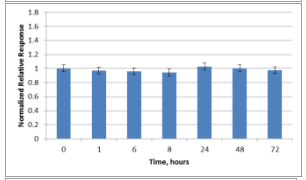	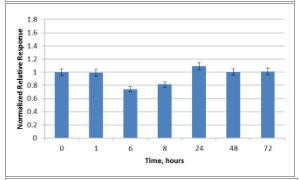	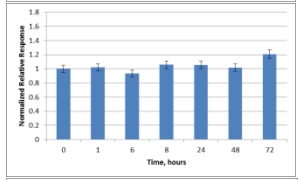	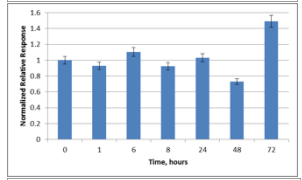
i-PrOH	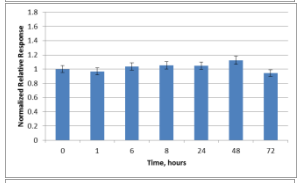	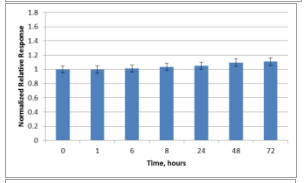	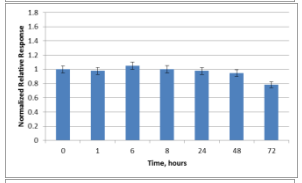	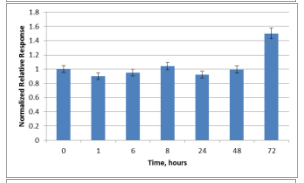	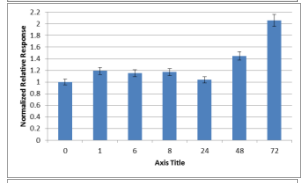
ETOH	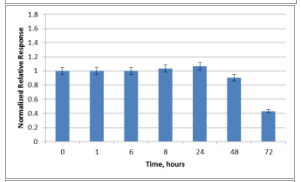	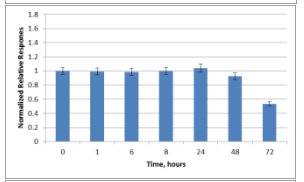	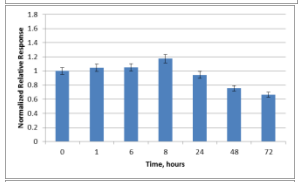	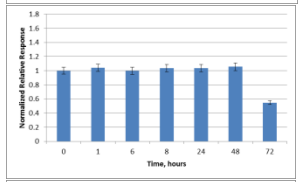	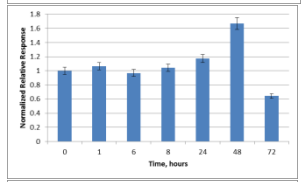
Hexane	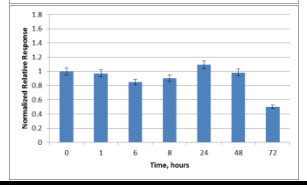	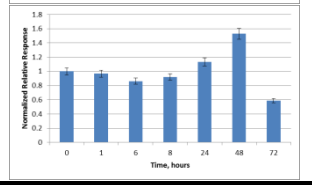	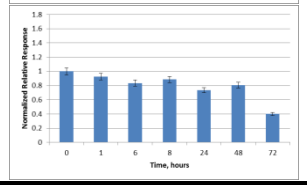	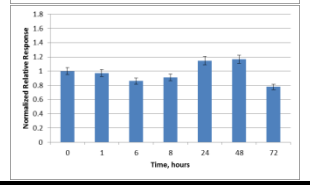	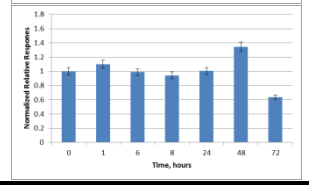

Figure 3.5: Plot of normalized average response ratio vs time for EFV, NVP, PNT, CAFF and DTM for simulated nyaope samples extracted with t-BuOH, DCM, ETAC, I-PrOH, ETOH and hexane.

3.1.2 The stability of nyaope components in dichloromethane

The solvent in which the samples were second-most stable after t-BuOH was DCM. The results for the extraction of simulated nyaope samples as well as actual seized street nyaope samples with DCM are shown in Tables 3.3 and 3.4. In both simulated and actual seized street nyaope samples CAFF, THCV, NVP, 6-MAM, DAM are shown to be stable for the 72 hours of storage. The ratio 6-MAM to DAM confirms the stability of DAM and 6-MAM in both simulated and actual seized street nyaope samples. CBN and Δ^9-THC are shown to be stable for 72 hours of storage in the actual seized street nyaope sample. Although CBN is shown to be stable for the 72 hours of storage in simulated nyaope samples, the ratio of CBN to Δ^9-THC only confirms stability in actual seized street nyaope samples and shows both CBN and Δ^9-THC to be stable for 24 hours of storage in simulated nyaope samples. DCM contains hydrochloric acid, as a result of photocatalytic breakdown of the DCM, which facilitates the decomposition of Δ^9-THC to form CBN. PNT is stable for 72 in simulated nyaope samples while only stable for 24 hours in the actual seized street nyaope sample. This may be due to the fact that PNT is present at a very low amount and therefore the response is susceptible to background interference. CBD and ACOD were both stable for 72 hours in actual seized street samples, while ACOD was found to be moderately stable for 24 hours and CBD was only stable for 48 hours in simulated nyaope samples. EFV, PPV and NOSC, which are only present in simulated nyaope sample, were shown to be stable for 72 hours of storage, while DTM is shown to be stable for 48 hours of storage. NCT, present only in actual seized street nyaope sample, was found to be stable for 72 hours of storage. As a highly volatile solvent, dichloromethane easily evaporates from the GC-MS sample vials (Aalberg et al, 2005). This may limit its use for the identification, profiling and quantitation of nyaope samples.

3.1.3 The stability of nyaope components in ethyl acetate

The results for the extraction of simulated nyaope samples with ETAC are shown in Tables 3.3 and 4. ETAC was found to be the third-best solvent and performed nearly as well as DCM. The target compounds CAFF, CBN, DAM, EFV, 6-MAM, NVP, PNT, Δ^9-THC and THCV are shown to be stable for 72 hours of storage. The ratio CBN to Δ^9-THC confirms the stability of CBN and

Δ^9-THC, while the ratio 6-MAM to DAM indicates DAM and 6-MAM to be unstable after 24 hours of storage. 6-MAM showed an increase after 24 hours of storage while diamorphine showed a slight decrease, which suggests that DAM undergoes hydrolysis in ETAC. ETAC is hygroscopic (Tan, Melius and Ziegler, 1982) and therefore absorbs moisture that facilitates the hydrolysis of DAM. The water content in ETAC is said to be a maximum of 0.1% W/W (Jubilant Life sciences, n.d.). NOSC, present only in the simulated nyaope sample, was shown to be moderately stable for 48 hours of storage. PPV, found only in the simulated nyaope sample, was found to be unstable after just 6 hours of storage. DTM is shown to be unstable after 48 hours of storage.

3.1.4 The stability of nyaope components in isopropanol

The solvent that followed after ETAC and DCM was i-PrOH and gave better stabilities than ETOH and hexane. The results for the extraction of simulated nyaope samples as well as actual seized street nyaope samples with i-PrOH are shown in Tables 3.3 and 3.4. In both simulated and actual seized street nyaope samples, only THCV is stable for 72 hours of storage. ACOD, CBD and PNT are stable in simulated nyaope samples for 72 hours of storage, whereas ACOD and CBD were found to be unstable after 24 hours of storage in actual seized street nyaope samples. PNT, CAFF and NVP are stable for 8 hours of storage in actual seized street samples. While Δ^9-THC is shown to be stable for 72 hours of storage in both simulated and actual seized street nyaope samples, the ratio CBN to Δ^9-THC only confirms the stability for 72 hours of storage in simulated nyaope samples and indicates Δ^9-THC and CBN to be only stable for 24 hours of storage in actual seized street nyaope samples. The ratio 6-MAM to DAM shown in Table 3.4 indicates 6-MAM and DAM to be unstable after 24 hours of storage for the street samples. This is to be expected, since the water found in i-PrOH facilitates the hydrolysis of DAM to form 6-MAM and subsequently morphine. However, morphine was not detected in any of the samples studied, which suggests that it may have been present at the level lower than the detection limit (25 ng/mL)(Cone et al, 2006). The target compound found only in simulated nyaope sample EFZ was found to be stable for 72 hours of storage ,while DTM was found to be unstable after 24 hours of storage. PPV, found only in the simulated nyaope sample, was found to be moderately stable for 72 hours of storage. NOSC, present only in the

simulated nyaope sample, was found to be stable for 48 hours of storage. The target compound NCT found only in the actual seized street nyaope sample was found to be stable after 8 hours of storage.

3.1.5 The stability of nyaope components in ethanol

Ethanol has previously been found to be a suitable solvent for the extraction of DAM (Hong et al, 2014). However, the water in ethanol will facilitate the hydrolysis of DAM to 6-MAM and subsequently morphine. Morphine was not detected in any of the ETOH extracts, suggesting it may have been present at levels that are below detection limit. The results for the extraction of simulated nyaope samples with ETOH are shown in Tables 3.3 and 3.4. The target compounds ACOD, PNT, CAFF, CBD, CBN, DAM, EFV, 6-MAM, NVP, Δ^9-THC and THCV were found to be stable for 48 hours of storage. The ratio 6-MAM to DAM confirms the stability of DAM and 6-MAM for 48 hours of storage, while the ratio CBN to Δ^9-THC indicates CBN and Δ^9-THC to be stable for 72 hours of storage. NOSC present only in the simulated nyaope sample, was shown to be stable for 48 hours of storage. DTM and PPV, present only in the simulated nyaope sample, were shown to be unstable after 24 hours of storage.

3.1.6 The stability of nyaope components in hexane

The results for the extraction of simulated nyaope samples with hexane are shown in Tables 3.3 and 3.4. CAFF was the only compound shown to be stable after 72 hours of storage. The target compounds ACOD, CBN, DAM, EFV, PNT, Δ^9-THC and THCV are all stable to moderately stable up to 48 hours of storage. The ratio CBN to Δ^9-THC indicates CBN and Δ^9-THC to be stable for 72 hours of storage, while the ratio 6-MAM to DAM indicates DAM and 6-MAM to be unstable after 24 hours of storage. CBD was found to be unstable after 24 hours of storage. DTM and NVP were shown to be stable for 24 hours of storage. Both PPV and NOSC are present in low abundance only in the simulated nyaope sample but were shown to be stable for 48 hours of storage. Hexane is a non-polar solvent with low eluent strength and therefore not expected to extract the more polar DAM and 6-MAM.The extraction with non-polar hexane may be good for Δ^9-THC but not suitable for the more polar DAM and its adulterants. Hexane was the solvent that exhibited the least stability for the target compounds.

3.2 STORAGE STABILITY STUDIES

Storage stability studies for simulated and street nyaope samples were analysed as explained in Sections 2.4.1 and 2.5.2 using t-BuOH as the extraction solvent. The GC-MS analysis was done with the internal standard tetracosane. The compounds ACOD, cannabivarin (CBV), CAFF, CBD, CBN, DAM, DTM, EFV, 6-MAM, NVP, PNT, Δ^9-THC and THCV were monitored during the study. The response area of the total ion chromatograph of each peak of interest was used to evaluate the stability of the samples under the respective storage conditions. In particular, the relative response factor (RRF), which is the ratio of the peak area of the sample to the peak area of the internal standard, was calculated using Equation 3.2 (Aalberg et al, 2005):

$$RRF = \frac{A_{IS}}{A_S} \qquad 3\text{-}2$$

where A_s is the peak area of the sample, A_{IS} is the peak area of the internal standard.

The samples were analysed in triplicate and average response ratio was calculated using Equation 2. Different weights were used for each storage period therefore the RRF was calculated using Equation 3.3:

$$RRF = \frac{A_S}{m_S \times A_{IS}} \qquad 3\text{-}3$$

where A_S is the average response peak area of the sample, A_{IS} is the average response peak area of the internal standard and m_s is the mass of the sample.

The percentage normalized average response ratio ($\%R_N$) of the RF of the injection after storage time T_x to the initial injection at T_0 was calculated using Equation 3.4:

$$\%R_N = \frac{A_x \times m_0}{A_0 \times m_x} \times 100 \qquad 0\text{-}4$$

where A_x is the average response peak area of the injection after storage time T_x, A_0 is the average response peak area of the initial injection, m_x and m_0 are the respective masses.

The normalized average response ratios, R_N, for ACOD, CBV, CAFF, CBD, CBN, DAM, DTM, EFV, 6-MAM, NVP, PNT, Δ^9-THC and THCV were determined using Equation (4) with TC as an internal standard. Degradation of drug substances of 10–15% is considered acceptable (Szepesi, Gazdag and Mihalyfi, 1989); degradation between 5% and 20% has been accepted as reasonable for validation of chromatographic assays (Carr and Wahlich, 1990; Blessy et al, 2014). The percentage normalized response between of 85% and 115% was considered stable in this study. Compounds with percentage normalised response between 85% and 100% exhibit a percentage decomposition of 15% or less, while the percentage normalised response above 100% and below 115% indicates an increase with regard to degradation products of 15% or less. Tables 5 to 7 lists the percentage normalized responses of ACOD, CAFF, CBD, CBN, CBV, DTM, DAM, EFV, 6-MAM, NVP, PNT, Δ^9-THC and THCV used to evaluate their stabilities for each of the storage conditions and periods.

3.2.1 The stability of acetylcodeine in different storage conditions

The percentage normalised average response ratios for the different storage conditions and period for ACOD are shown in Table 3.5. ACOD was shown to be stable for 504 hours (21 days) when stored in the freezer at -70 ^{o}C, with and without desiccant. ACOD was shown to be stable for 336 hours (14 days) when stored in the dark with a desiccant, 168 hours (7 days) when stored in the fridge at ± 4^{o}C with a desiccant and at ambient condition and unstable when exposed to laboratory light. ACOD, a synthetic impurity of illicit heroin usually present at concentration levels of 15–20% relative to DAM and ranging up to 45% (Sione, 1986), undergoes hydrolysis to codeine and subsequently to morphine shown in Figure 1.9 (O'Neal and Poklis, 1997; Staub et al, 2001). The ACOD degradation products codeine and morphine shown in Figure 1.9 were not detected in the samples analysed, probably because the degradation products were absent or present at levels that are below the detection limit of the method.

Table 3.5: Percentage normalised average response ratios (n = 3) of ACOD, CBD, CAFF, CBN and Δ^9-THC under different storage conditions.

Compound	Time, hours	0	24		72		168		336		504	
	Storage condition			%RSD		%RSD		%RSD		%RSD		%RSD
ACOD	Freezer	100,0	101,1	1,90	105,0	0,09	113,6	6,80	110,5	8,12	98,6	3,85
	Freezer-desiccator	100,0	93,4	5,84	88,4	7,44	93,9	4,77	111,6	9,06	105,2	8,28
	Fridge	100,0	94,9	6,11	88,8	8,95	88,1	6,45	80,3	8,02	107,5	6,48
	Dark	100,0	95,3	3,71	87,2	3,80	88,6	7,32	89,0	6,36	121,5	5,02
	Light	100,0	151,0	15,50	113,0	14,37	75,8	8,29	121,0	21,86	136,9	20,95
	Ambient	100,0	89,3	6,09	94,3	6,14	85,6	5,70	83,5	5,15	112,3	5,59
CAFF	Freezer	100,0	101,3	0,60	103,0	7,83	123,1	6,19	106,4	1,51	86,4	1,68
	Freezer-desiccator	100,0	101,9	14,94	97,9	12,80	80,7	4,29	78,0	19,73	131,3	11,50
	Fridge	100,0	89,1	5,69	86,7	10,54	91,3	7,87	88,2	7,37	94,6	7,05
	Dark	100,0	91,6	5,94	84,5	6,66	89,1	7,34	94,4	8,09	106,2	7,33
	Light	100,0	87,0	7,39	96,2	8,05	79,4	6,29	92,2	5,89	98,4	6,74
	Ambient	100,0	85,0	6,05	91,2	6,53	85,7	7,29	82,7	6,90	93,1	6,17
DTM	Freezer	100,0	99,5	13,00	115,9	11,23	138,3	15,40	114,7	11,30	112,0	8,94
	Freezer-desiccator	100,0	104,7	34,76	129,8	44,21	112,2	22,45	192,2	12,54	106,0	8,81
	Fridge	100,0	99,3	2,50	93,8	4,62	98,7	1,90	90,4	0,14	146,2	1,74
	Dark	100,0	105,5	4,43	96,5	1,56	98,5	3,79	103,1	1,62	171,0	4,50
	Light	100,0	103,4	3,37	102,2	4,75	84,1	4,11	97,1	1,71	140,6	3,14
	Ambient	100,0	102,4	2,71	106,1	6,61	92,8	4,39	96,6	3,68	141,2	6,85
CBN	Freezer	100,0	102,4	3,96	89,3	5,55	99,8	5,82	94,4	1,99	101,8	3,27
	Freezer-desiccator	100,0	105,2	9,23	116,9	4,80	100,7	7,25	109,1	4,18	101,0	19,38
	Fridge	100,0	96,7	8,31	89,1	10,13	85,6	6,61	93,4	6,03	118,1	7,18
	Dark	100,0	99,4	4,29	87,8	5,86	90,5	8,83	104,6	7,05	146,5	6,44
	Light	100,0	95,1	5,54	95,2	5,82	77,1	6,02	85,8	4,71	106,9	4,94
	Ambient	100,0	95,1	7,18	91,6	6,05	90,5	7,11	90,7	4,86	134,5	5,87
Δ^9-THC	Freezer	100,0	100,7	4,08	101,1	2,31	81,8	18,42	85,4	15,53	118,0	2,11
	Freezer-desiccator	100,0	105,1	4,46	106,9	8,75	113,0	11,15	117,0	8,49	99,3	15,47
	Fridge	100,0	93,5	8,06	85,5	9,12	83,3	8,38	79,5	7,70	75,6	7,74
	Dark	100,0	91,8	6,23	85,1	7,91	84,4	12,40	81,9	9,46	82,1	7,67
	Light	100,0	60,5	7,55	66,3	7,84	64,3	9,42	96,1	6,62	88,2	6,38
	Ambient	100,0	88,7	8,47	85,9	7,70	83,7	8,59	72,6	5,47	76,2	7,19

3.2.2 The stability of caffeine in different storage conditions

The percentage normalised average response ratios for the different storage conditions and period for CAFF are shown in Table 3.5. Caffeine was reported to undergo radical induced degradation to 1,3,7-trimethyluric acid (Telo and Viera, 1997) and undergoes oxidation to

paraxanthine, theophylline and theobromine (Chung and Cha, 1997). CAFF was shown to be stable for 504 hours (21 days) in the fridge and in the dark, 168 hours (7 days) at ambient condition, 72 hours when stored in the freezer both with and without desiccant and under laboratory light. The degradation product of caffeine, 1,3,7-trimethyluric acid, paraxanthine, theophylline and theobromine, shown in Figure 1.9, was not identified. The caffeine degradation products were not identified either because they were absent or present at levels that are below the detection limit of the method.

3.2.3 The stability of cannabinol in different storage conditions

The percentage normalised average response ratios for the different storage conditions and period for CBN are shown in Table 3.5. CBN was shown to be stable for 504 hours (21 days) when stored in the freezer without desiccant, 336 hours (14 days) when stored in the fridge, in the dark and ambient condition, 72 hours when stored under laboratory light, 24 hours when stored in the freezer with desiccant. CBN is a degradation product of Δ^9-THC and it is expected to increase with the decrease of Δ^9-THC, as observed previously (Turner et al, 1973a; Harvey, 1974; Repka et al, 2006; Lindholst, 2010; Trofin et al, 2012). The increase in CBN for the samples stored under laboratory light is illustrated in the total ion chromatograms in Figure 3.7 after 0, 24 hours, 72 hours, 168 hours (7 days), 336 hours (14 days) of storage. The chromatograms illustrating similar increases for the samples stored (i) in the fridge, (ii) in the dark and at ambient condition are given in Appendix Ia–Id. The extent of the increase becomes greater from the samples stored in the refrigerator, followed by samples stored in the dark and at room temperature, and then those stored under laboratory light.

3.2.4 The stability of Δ^9-tetrahydrocannabinol in different storage conditions

The percentage normalised average response ratios for the different storage conditions and period for Δ^9-THC are shown in Table 3.5. Δ^9 -THC undergoes oxidation in the presence of light to form the less potent cannabinol (CBN) (Carbone et al, 2010). The degradation results in the decrease of Δ^9-THC under all storage conditions, as illustrated in Figure 3.7, as well as Appendix Ia–Id for the sample storage up to 336 hours (14 days). CBN is a degradation product of Δ^9-THC and it is expected to increase with the decrease of THC, as observed previously

(Turner et al, 1973a; Harvey, 1990; Repka et al, 2006; Lindholst, 2010; Trofin et al, 2012). Δ^9-THC was shown to be stable for 168 hours (7 days) if stored in the freezer with desiccant; up to 72 hours in the freezer with no desiccant, in the fridge, in the dark and at ambient condition; and unstable when exposed to laboratory light. The extent of the increase becomes greater from the samples stored in the freezer, followed by those stored in the refrigerator, in the dark and at ambient condition, and then those stored under laboratory light.

3.2.5 The stability of dextromethorphan in different storage conditions

The percentage normalised average response ratios for the different storage conditions and period for DTM are shown in Table 3.5. DTM undergoes hydrolysis via N-demethylation to form 3-methoxymorhinan and O-demethylation to form 17–methylmorhinan-3-ol (Daal et al, 2008; Raju et al, 2013). Although DTM has been shown to be stable for at least 7 days when exposed to humidity (Raju et al, 2013); for 2 months in methanol/water at ±4 ^{o}C; for 48 hours at ambient temperature and 96 days at -20 ^{o}C (Zhang et al, 2010b), it was shown in this study to be stable for 336 hours (14 days) when stored in the refrigerator at ± 4^{o}C, in the dark and at ambient condition; 72 hours when stored under laboratory light and in the freezer with no desiccant. Surprisingly, the samples stored in the freezer with a desiccant was shown to be stable for only 24 hours.

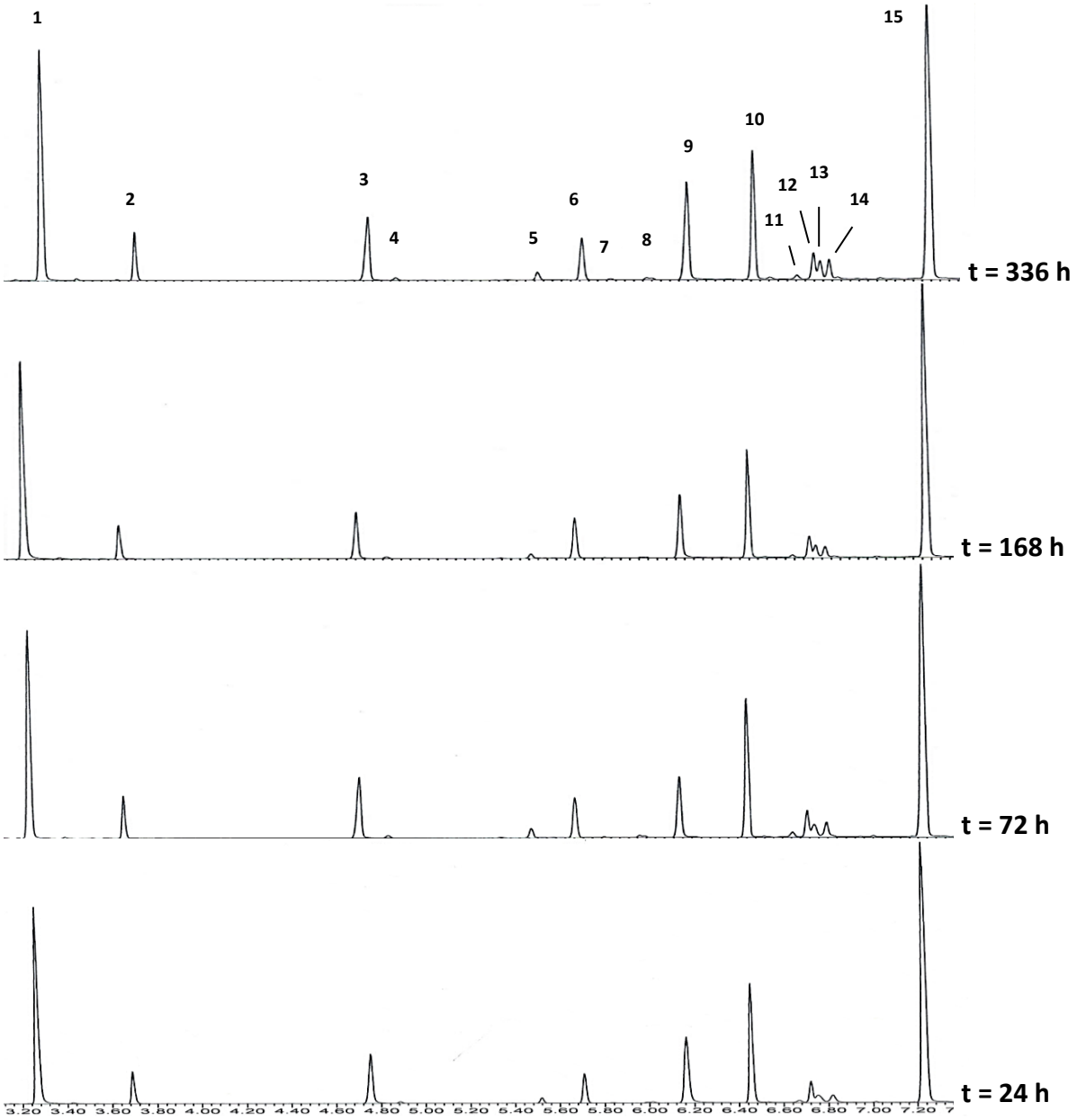

Figure 3.6: Total ion chromatographs for the samples stored under laboratory light after t = 0, 24 hours, 72 hours, 168 hours and 336 hours of storage where (1) phenacetin, (2) caffeine, (3) efavirenz, (4) dextromethorphan, (5) tetrahydrocannabivarin, (6) tetracosane (IS), (7) cannabivarin (8) cannabidiol (9)nevirapine; (10) Δ^9-tetrahydrocannabinol; (11) cannabigerol, (12) acetylcodeine, (13) cannabinol, (14) 6-monoacetylmorphine, (15) diamorphine.

3.2.6 The stability of cannabivarin in different storage conditions

The percentage normalized average response for the different storage conditions and period for CBV is listed in Table 3.6. CBV was shown to be stable for 336 hours (14 days) when stored in the freezer without desiccant, 24 hours in the freezer with a desiccant and in the fridge, and unstable in all other storage conditions. CBV is a degradation product of THCV; therefore expected to increase, as illustrated in Figure 3.7, as well as Appendix Ia–Id for all the storage conditions up to 336 hours (14 days). The samples stored in the freezer at -70 ^{o}C display minimum degradation, followed by samples stored at ± 4^{o}C at room temperature in the dark in a desiccator and those stored at ambient condition. The samples stored at room temperature in a desiccator under laboratory light showed the greatest increase in CBV. Samples stored in the dark was shown to be unstable, although expected to show more or less similar stabilities to the samples stored in the fridge.

3.2.7 The stability of tetrahydrocannabivarin in different storage conditions

The percentage normalized average response for the different storage conditions and period for THCV is listed in Table 3.6. THCV was shown to be stable in the freezer without desiccant and at ambient condition up to 336 hours (14 days), 168 hours (7 days) in the freezer with desiccant, 72 hours under laboratory light and up to 24 hours in a fridge and unstable in the dark. THCV is a homolog of Δ^9-THC and is therefore expected to undergo degradation pathway similar to Δ^9-THC to form cannabivarin a homolog of cannabinol (Δ^9-THC degradation product) (Turner et al, 1973b; Bailey and Gagné, 1975). The decrease in THCV as a result of degradation is illustrated in Figure 3.7 as well Appendix Ia–Id for the all storage conditions up to 336 hours (14 days). The samples showed better stabilities for the storage in the freezer. Surprisingly, the samples stored under laboratory light showed better stabilities than samples stored in the fridge and in the dark.

Table 3.6: Percentage normalised average response ratios (n = 3) of CBV, THCV, DAM and 6-MAM under different storage conditions.

Compound	Time, hours	0	24		72		168		336		504	
	Storage condition			%RSD		%RSD		%RSD		%RSD		%RSD
CBV	Freezer	100.0	84,8	7,99	95,3	13,21	96,2	9,90	104,6	4,10	123,6	9,35
	Freezer-desiccator	100,0	106,1	11,82	116,3	3,67	119,6	10,53	181,0	4,15	131,9	2,14
	Fridge	100,0	102,0	20,01	73,8	15,33	133,2	24,13	165,4	18,51	218,4	25,31
	Dark	100,0	143,6	1,45	129,8	26,06	139,9	24,82	208,5	24,27	285,2	22,62
	Light	100,0	138,6	28,49	119,2	23,27	97,7	23,39	195,0	21,74	260,6	26,23
	Ambient	100,0	148,6	36,41	112,5	23,02	133,2	23,87	182,9	19,47	240,2	10,71
THCV	Freezer	100,0	93,2	10,88	103,3	9,48	91,7	16,85	100,4	14,80	124,0	3,46
	Freezer-desiccator	100,0	105,5	6,86	104,1	3,17	106,1	10,05	121,9	13,04	113,1	16,72
	Fridge	100,0	85,7	2,39	73,3	6,11	98,1	10,64	98,5	8,91	134,2	12,42
	Dark	100,0	123,4	13,87	89,3	10,53	100,1	4,97	116,2	13,62	155,5	11,11
	Light	100,0	112,0	13,93	93,3	15,97	61,7	4,81	92,3	13,20	117,5	14,40
	Ambient	100,0	110,0	13,07	99,2	12,51	88,0	17,58	89,1	20,95	134,8	11,44
DAM	Freezer	100,0	109,2	5,50	103,2	5,22	93,3	5,82	95,9	5,76	90,5	3,99
	Freezer-desiccator	100,0	92,4	8,13	87,7	1,87	91,9	0,62	89,3	6,45	90,7	7,15
	Fridge	100,0	85,4	1,58	83,1	7,83	80,2	5,60	73,1	4,29	59,8	4,37
	Dark	100,0	81,1	3,74	79,6	4,01	81,9	4,55	77,9	5,24	68,5	4,65
	Light	100,0	153,1	4,69	112,2	5,62	96,9	4,99	146,2	5,02	194,2	2,93
	Ambient	100,0	75,4	5,95	82,9	4,37	79,1	6,24	71,7	4,44	61,9	4,24
6-MAM	Freezer	100,0	108,3	7,13	144,5	1,92	159,7	7,21	140,0	10,08	131,9	6,78
	Freezer-desiccator	100,0	139,0	11,77	119,7	17,97	106,8	15,24	149,1	12,90	168,0	14,46
	Fridge	100,0	146,8	17,73	106,7	15,72	109,8	16,98	107,0	16,20	173,2	13,93
	Dark	100,0	153,2	15,44	102,7	11,20	110,6	14,40	150,5	21,22	205,0	16,98
	Light	100,0	103,4	21,41	95,2	12,64	82,3	22,37	110,9	20,00	137,5	17,21
	Ambient	100,0	144,6	20,60	112,5	17,74	111,9	20,26	148,4	21,23	214,6	19,57

3.2.8 The stability of diamorphine in different storage conditions

The percentage normalised average response ratios for the different storage conditions and period for DAM are shown in Table 3.6. DAM undergoes hydrolysis to form 6-MAM and then morphine (Barrett et al, 1992; Hutchinson and Somogyi, 2002). DAM was shown to be stable for 504 hours (21 days) when stored in the freezer with and without desiccant; 24 hours when stored in the fridge; and unstable for all the other storage conditions. The samples stored at ambient temperature are expected to be unstable, since they are exposed to moisture in the environment, which facilitates the hydrolysis of DAM. Samples stored in a desiccator, on the other hand, are protected from the moisture in the surrounding and therefore expected to

show better stability. Surprisingly, samples stored in the dark with a desiccant was shown to be unstable. The results show that DAM degradation commences just after 24 hours of storage for all the storage conditions, as was observed previously (Omar et al, 1989). Diamorphine (DAM) long-term storage of DAM (five weeks) was reported to undergo minimum degradation (an average of 17.0%) when stored in a refrigerator than when stored at ambient temperature (an average of 23.3%) (Wijesekera, Abeysinghe and Pathirana, 1994). The degradation of 17.0% and 23.3% is regarded as unstable on the basis of the acceptable 5–15% degradation (Szepesi, Gazdag and Mihalyfi, 1989). The decrease in DAM as a result of degradation is illustrated in Figure 3.7 as well in Appendix Ia–Id for the all storage conditions up to 336 hours (14 days).

3.2.9 The stability of 6-monoacetylmorphine in different storage conditions

The normalised average response ratios for the different storage conditions and period for 6-MAM are shown in Table 3.6. 6-MAM, which is the hydrolysis product of diamorphine (Sibley, 1996), increase from 24 hours of storage (Barrettet al, 1992; Wijesekera, Abeysinghe and Pathirana, 1994) under all storage conditions. The increase of 6-MAM is not expected to be massive since in turn it undergoes degradation to form morphine (Figure 1.9). The increase in 6-MAM is illustrated in Figure 3.7, as well Appendix Ia–Id for the all storage conditions up to 336 hours (14 days). The results for the 24 hours storage for the sample in the refrigerator, in the dark and ambient conditions showed an increase in 6-MAM. The increase maybe as a result of the degradation of the DAM present in the sample since 6-MAM is a degradation product of DAM. 6-MAM was shown to be stable for 336 hours (14 days) for the samples stored in the refrigerator, 168 hours (7 days) for samples stored in the dark and ambient conditions, and 72 hours for the samples stored under laboratory light.

3.2.10 The stability of cannabidiol in different storage conditions

The percentage normalised average response ratios for the different storage conditions and period for CBD are shown in Table 3.7. CBD was shown to be stable for 336 hours (14 days) when stored in the freezer without a desiccant, 168 hours (7 days) when stored in the freezer with desiccant, 24 hours when stored in the fridge, in the dark and at ambient condition and

unstable under laboratory light. CBD undergoes acid catalysed degradation to Δ^9-THC and Δ^8-THC (Mechoulam and Hanuš, 2002; Merrick et al, 2016), menthane carboxylic acid and undergoes oxidation to quinone (Figure 1.9) (Mechoulam and Hanuš, 2002). The samples stored in the freezer at -70 ^oC showed better stability, followed by samples stored in the refrigerator at ± 4^oC, in the dark in a desiccator, and at ambient condition, while samples stored in a desiccator and exposed to laboratory light showed greater degradation. The degradation products Δ^8-THC and menthane carboxylic acid were not detected in the samples analysed, probably because either the method used is not suitable, or that these products were available at a level below the detection limit of the method.

3.2.11 The stability efavirenz in different storage conditions

The normalised average response ratios for the different storage conditions and period for EFV are shown in Table 3.7. On the basis of 10–15% stability, the EFV was shown to be stable for 504 hours (21 days) in the freezer with and without a desiccant, up to 72 hours when stored under laboratory light and 24 hours when stored at ambient conditions and in the dark. EFV was shown to be unstable when stored in the refrigerator at 4 ^oC which may be due to interaction with other components in the nyaope sample. EFV stock solutions in methanol were reported to be stable after 24 hours of storage at ambient temperatures and 24 months of storage at -20 ^oC (Kappelhoff et al, 2003). EFV was reported to be stable after 3 months of storage at ± 4^oC and ± 20^oC; and after 50 days when stored at ambient temperatures (D'Avolio et al, 2010). EFV is said to undergo hydrolysis to an intermediate carbamic acid ({4-Chloro-2-[(1S)-3-cyclopropyl-1-hydroxy-1-(triflouromethyl) prop-2-yn-1yl]phenyl}carbamic acid), which subsequently forms efavirenz amino alcohol ((2S)-2-(2-amino-5-chlorophenyl)-4-cyclopropyl-1,1,1-trifluorobut-3-yn-2-ol) and carbon dioxide (Figure1.9) (Maurin et al, 2002).

3.2.12 The stability of nevirapine in different storage conditions

The percentage normalised average response ratios for the different storage conditions and period for NVP are shown in Table 3.7. NVP was shown to be stable for 504 hours (21 days) in the freezer with or without a desiccant, up to 72 hours under laboratory light and unstable under the other storage conditions. The potential degradation products of NVP are reported

to be ethyl nevirapine and descyclopropyl nevirapine, shown in Figure 1.9 (Aparna et al, 2010). NVP decreases under all storage conditions after 24 hours of storage. NVP stock solution in dimethyl sulfoxide were reported to be stable after 24 hours of storage at ambient temperatures, and 36 months of storage, at -20 ^{o}C (Kappelhoff et al, 2003). NVP was reported to be stable after 3 months of storage at ±4 ^{o}C and ±20 ^{o}C and 70 days when stored at ambient temperatures (D'Avolio et al, 2010). Nevirapine is shown to be relatively stable when exposed to humidity, UV light and heat up to 2 days of storage (Navaneethan et al, 2012, as well as in acetonitrile up to 48 hours of storage (Reddiah et al, 2013).

3.2.13 The stability of phenacetin in different storage conditions

The percentage normalised average response ratios for the different storage conditions and period for PNT are shown in Table 3.7. PNT was shown to be stable for 504 hours (21 days) when stored in the freezer without desiccant, 72 hours when stored in the freezer with a desiccant and unstable for all other storage conditions. PNT undergoes hydrolysis to form p-phenetidine and deethylation to form acetaminophen (Watanabe et al, 2010). The degradation products acetaminophen and p-phenetidine, however, were not identified in the samples analysed, probably because they were absent or present at the level that is below the detection limit. The samples stored in the freezer showed better stability than the samples in all the other storage conditions. PNT in methanol was shown to be stable after a long-term storage (20 days) at -20 ^{o}C (Ma et al, 2015).

Table 3.7: Percentage normalised average response ratios (n = 3) of CBD, EFV, NVP and PNT under different storage conditions.

Compound	Time, hours	0	24		72		168		336		504	
	Storage condition			%RSD		%RSD		%RSD		%RSD		%RSD
CBD	Freezer	100,0	88,5	10,18	98,7	2,53	87,5	18,25	110,2	12,31	144,7	3,67
	Freezer-desiccator	100,0	104,4	6,54	107,7	7,77	114,4	12,47	127,6	22,77	125,0	17,94
	Fridge	100,0	104,0	18,97	64,0	14,97	96,2	9,97	113,4	13,66	108,2	9,22
	Dark	100,0	98,8	9,18	75,7	11,64	101,4	12,10	104,6	12,57	177,1	8,67
	Light	100,0	138,6	0,11	119,2	2,07	97,7	3,51	195,0	0,57	260,6	4,08
	Ambient	100,0	96,3	18,13	83,0	9,86	76,0	11,19	114,1	11,00	158,7	15,88
EFV	Freezer	100,0	106,5	2,40	104,8	4,12	113,2	4,68	115,8	2,72	115,1	3,67
	Freezer-desiccator	100,0	105,3	1,96	98,1	1,51	106,7	3,78	100,0	5,01	98,1	6,74
	Fridge	100,0	79,2	4,14	71,8	6,36	81,0	2,17	87,9	3,61	103,0	2,65
	Dark	100,0	88,5	2,70	81,6	1,78	72,1	2,59	82,9	3,31	105,5	2,50
	Light	100,0	88,6	1,51	92,4	2,39	63,4	2,01	86,6	2,19	87,3	4,04
	Ambient	100,0	92,0	3,69	84,0	1,34	71,0	2,77	70,9	2,75	80,8	2,81
NVP	Freezer	100,0	84,8	2,29	87,8	1,33	98,0	5,10	95,6	4,47	87,4	1,90
	Freezer-desiccator	100,0	94,7	2,44	103,9	1,62	93,7	3,24	96,6	4,95	97,3	4,52
	Fridge	100,0	58,1	11,44	50,3	14,27	65,6	8,76	96,0	8,43	111,1	9,72
	Dark	100,0	73,4	6,47	57,6	8,83	79,5	9,24	72,0	9,22	98,0	8,48
	Light	100,0	89,7	6,38	96,7	6,62	63,6	9,42	96,2	8,04	124,9	7,84
	Ambient	100,0	70,3	7,32	74,4	7,71	66,9	7,81	75,9	6,45	81,7	5,95
PNT	Freezer	100,0	93,8	5,67	96,6	5,42	110,2	5,32	102,7	2,74	87,8	4,10
	Freezer-desiccator	100,0	105,9	8,86	89,0	7,88	82,3	4,14	52,5	0,70	129,0	5,95
	Fridge	100,0	81,4	7,76	83,7	11,20	89,8	7,48	88,6	7,87	66,1	8,31
	Dark	100,0	81,9	6,95	81,1	7,10	91,2	6,52	93,4	8,75	73,3	7,50
	Light	100,0	83,5	8,04	88,2	8,57	79,7	11,32	85,7	6,28	66,3	8,17
	Ambient	100,0	79,6	6,82	88,2	6,56	86,3	7,71	83,3	7,73	66,1	6,88

CHAPTER 4: RESULTS AND DISCUSSION – ANALYTICAL METHOD VALIDATION

The chapter discusses the analytical method validation parameters evaluated in this research. These are linearity, limit of detection (LOD), limit of quantitation (LOQ), accuracy and precision (repeatability and intermediate precision), stability, ruggedness, selectivity and recovery. Since sample stability in different solvents ahead of analysis were discussed extensively in Chapter 3, it will not be discussed in this chapter.

4.1 THE EVALUATION OF THE LINEARITY OF THE ANALYTICAL METHOD

Working solutions with the concentrations shown in Table 4.1 were prepared as discussed on section 2.6.1. Ten replicates injections were made using the GC-MS method described in Section 2.4.1. The peak area ratios and mean peak area ratios for Δ^9-THC in the working solutions are given in Table 4.2.

Table 4.1: Concentrations in mg/L of the working solutions.

CAFF	DAM	EFV	NVP	PNT	Δ^9-THC
1.00	1.00	0.998	1.05	1.04	1.00
2.50	2.50	2.50	2.64	2.59	2.50
5.00	5.00	4.95	5.27	5.18	5.00
7.50	7.50	7.49	7.91	7.77	7.50
10.00	10.00	9.98	10.50	10.36	10.00
25.00	25.00	25.00	26.40	25.90	25.00
50.00	50.00	49.50	52.70	51.80	50.00
75.00	75.00	74.90	79.10	77.70	75.00
100.00	100.00	99.80	105.00	103.60	100.00
250.00	250.00	250.00	264.00	259.00	250.00
500.00	500.00	495.00	527.00	518.00	500.00
750.00	750.00	749.00	791.00	777.00	750.00
1000.00	1000.00	998.00	1050.00	1036.00	1000.00

Table 4.2: Peak area ratios for the Δ^9-THC in the mixture of PNT, CAFF, EFV, NVP, Δ^9-THC and DAM reference standards.

Conc.mg/L / Replicate	1.00	2.50	5.00	7.50	10.00	25.00	50.00	75.00	100.00	250.00	500.00	750.00	1000.00
1	0,035	0,140	0,272	0,326	0,486	1,778	2,628	3,363	4,501	14,792	19,001	28,629	42,573
2	0,042	0,157	0,243	0,313	0,512	1,474	2,613	3,615	4,432	14,185	22,860	32,549	39,857
3	0,036	0,119	0,250	0,303	0,511	1,512	2,660	4,172	5,353	10,546	19,274	29,899	37,951
4	0,035	0,146	0,232	0,229	0,610	2,095	2,556	3,934	4,574	17,456	21,730	22,637	41,712
5	0,033	0,190	0,265	0,331	0,565	1,268	2,893	3,705	3,813	12,052	21,641	31,861	40,672
6	0,038	0,159	0,251	0,297	0,568	1,733	2,516	3,762	4,306	13,897	25,513	31,259	39,387
7	0,039	0,148	0,282	0,262	0,565	2,046	2,545	3,616	5,360	12,667	19,955	33,409	42,533
8	0,044	0,155	0,244	0,320	0,538	1,547	2,779	3,302	4,655	13,001	19,853	30,390	40,413
9	0,033	0,157	0,228	0,351	0,569	1,712	2,646	3,602	4,812	10,851	18,186	28,992	35,103
10	0,034	0,160	0,273	0,313	0,549	2,044	2,297	3,545	4,601	12,970	24,343	24,635	42,527
Mean	0,037	0,153	0,254	0,304	0,547	1,721	2,613	3,662	4,641	13,242	21,236	29,426	40,273
STDV	0,004	0,018	0,018	0,035	0,036	0,161	0,159	0,255	1,024	1,792	2,048	3,784	1,742
%RSD	10,33	11,71	7,18	11,61	6,63	7,88	6,07	6,97	19,46	11,31	9,08	14,98	3,98

The mean peak area ratio of each of the 10 replicate analyses was determined and the deviation from the mean was evaluated by using %RSD. The acceptance criteria are a %RSD of 20% or less (Karnes and March, 1993; SOFT/AAFS, 2006; Elliott, Stephen and Paterson, 2018). The peak area ratios and mean peak area ratios for the rest of the components in the working solutions are given in Appendices II-a to II-e. The calibration plots of average peak area ratio against concentration to evaluate linearity for CAFF, DAM, EFV, NVP PNT and Δ^9-THC are shown in Figure 4.1.

Regression analysis was performed on all the peak area ratios using Microsoft Excel 2010 in order to determine if there were any outliers. The presence of an outlier can either increase or decrease the correlation coefficient depending on which side it occur in relation to the other data points (Suchowski, 2001). Furthermore, outliers increases the estimate of the variance and therefore makes the F-statistics too large. The increase or decrease on the correlation coefficient as well as a large F-statistics increase the risk of an incorrect decision when evaluating linearity. Outliers were eliminated from the data by using residual plots, where a residual data point that is ≥ 2 or ≤ -2 was considered an outlier (Lavagnini and Mas, 2007). The residual plot in Figure 4.2 for CAFF, DAM, EFV, NVP PNT and Δ^9-THC indicates that the data at 250.00 mg/L lies outside the limit and are therefore an outlier. Peak area ratio at 250.00 mg/L were omitted in all the standards and the data are plotted without an outlier in Figure 4.3, while the respective residual plots, which demonstrate that there is no further outliers, are given in Figure 4.4.

The calibration curve is considered linear if the correlation coefficient (r^2) is ≥ 0.99 (UNODC, 2005). The correlation coefficients (r^2) for the calibration curves of CAFF, DAM, EFV, NVP, PNT and Δ^9-THC were ≥ 0.99, as shown in Table 4.3. The correlation coefficient (r^2) for DAM showed better improvement, while only a minimal increase was observed for CAFF, EFV, NVP, PNT and Δ^9-THC, after omitting the outlier. This indicates that calibration curves are linear for CAFF, DAM, EFV, NVP, PNT and Δ^9-THC and the analytical method is linear in the range 1.00 mg/L to 1000.00 mg/L. A random distribution of data in the residual plot implies that the calibration is linear, while data following a particular pattern imply non-linear calibration curve (Thompson, 2005; Bonfilio et al, 2012). The residual plots for CAFF, DAM, EFV, NVP, PNT and Δ^9-THC with outliers shown in Figure 4.2 display a particular pattern, indicating a deviation from linearity due to the presence of an outlier, while the residual plots for CAFF,

EFV, NVP, PNT and Δ^9-THC without outlier shown in Figure 4.4 displays a random distribution of data, proving that the analytical method is linear in the given range. Table 4.4 is a typical output of the analysis of variance (ANOVA) in Excel for DAM, which was used to calculate the t-Test (one-tail) and the F-Test to evaluate linearity. Similar ANOVA output for PNT, CAFF, EFV, NVP and Δ^9-THC are used to calculate the *t*-Test (one-tail) and the F-Test shown in Table 4.3.

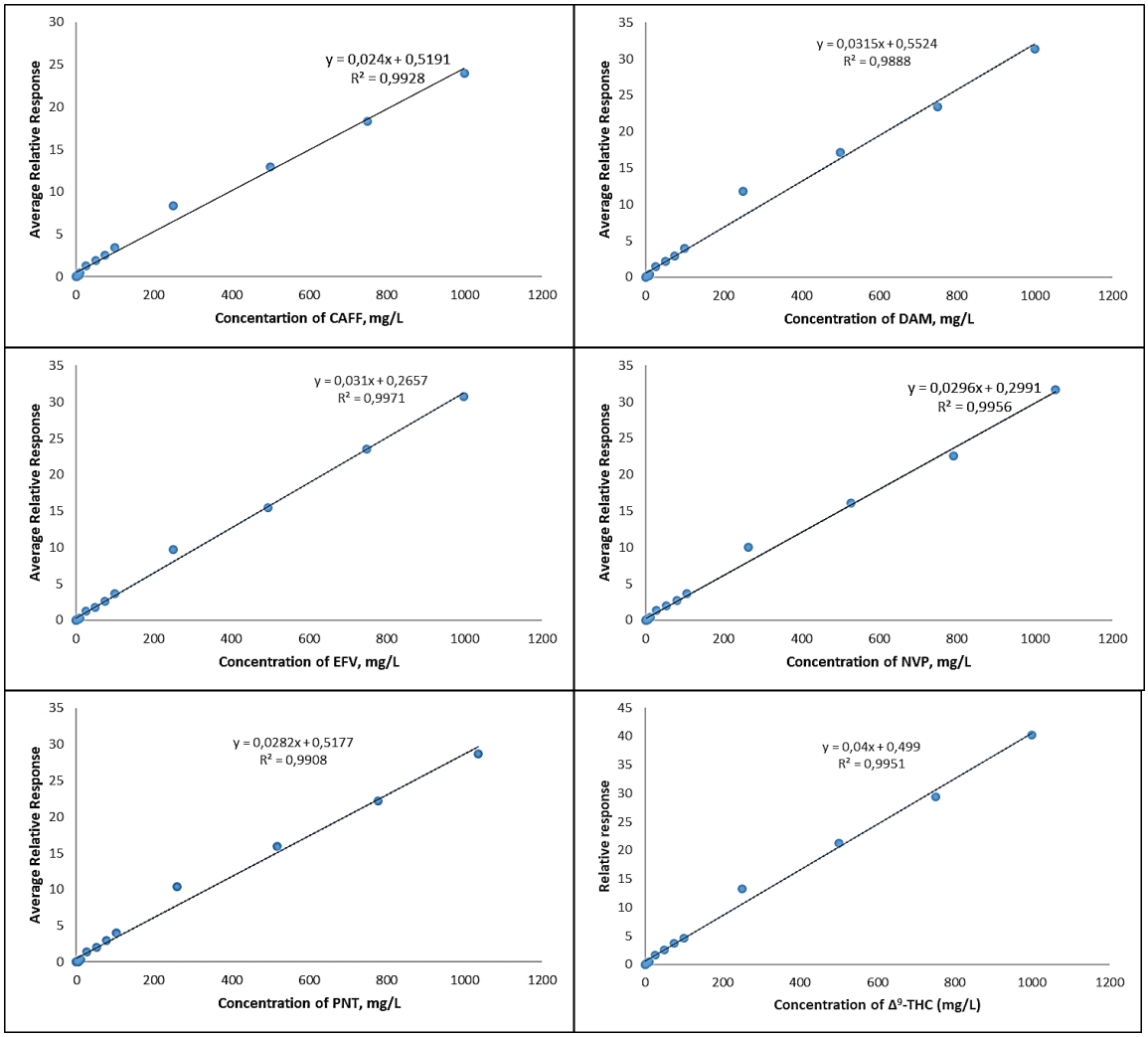

Figure 4.1: Plot of average peak area ratio vs concentration for CAFF, DAM, EFV, NVP, PNT and Δ^9-THC reference standards, respectively, with outlier.

Table 4.3: Summarised linearity data for CAFF, DAM, EFV, NVP, PNT and Δ^9-THC.

Analyte	Linearity range , mg/L	r^2	Regression equation	t	F
CAFF	1.00 to 1000.00	0.9975	$y = 23.941x + 0.3916$	2.180	574.6
DAM	1.00 to 1000.00	0.9981	$y = 31.360x + 0.3174$	2.135	985.3
EFV	0.998 to 998.00	0.9995	$y = 30.924x + 0.1477$	2.077	956.8
NVP	1.05 to 1050.00	0.9987	$y = 29.494x + 0.1671$	2.080	871.1
PNT	1.04 to 1036.00	0.9970	$y = 28.051x + 0.3403$	2.143	789.2
Δ^9-THC	1.00 to 1000.00	0.9988	$y = 39.912x + 0.3106$	2.126	1595

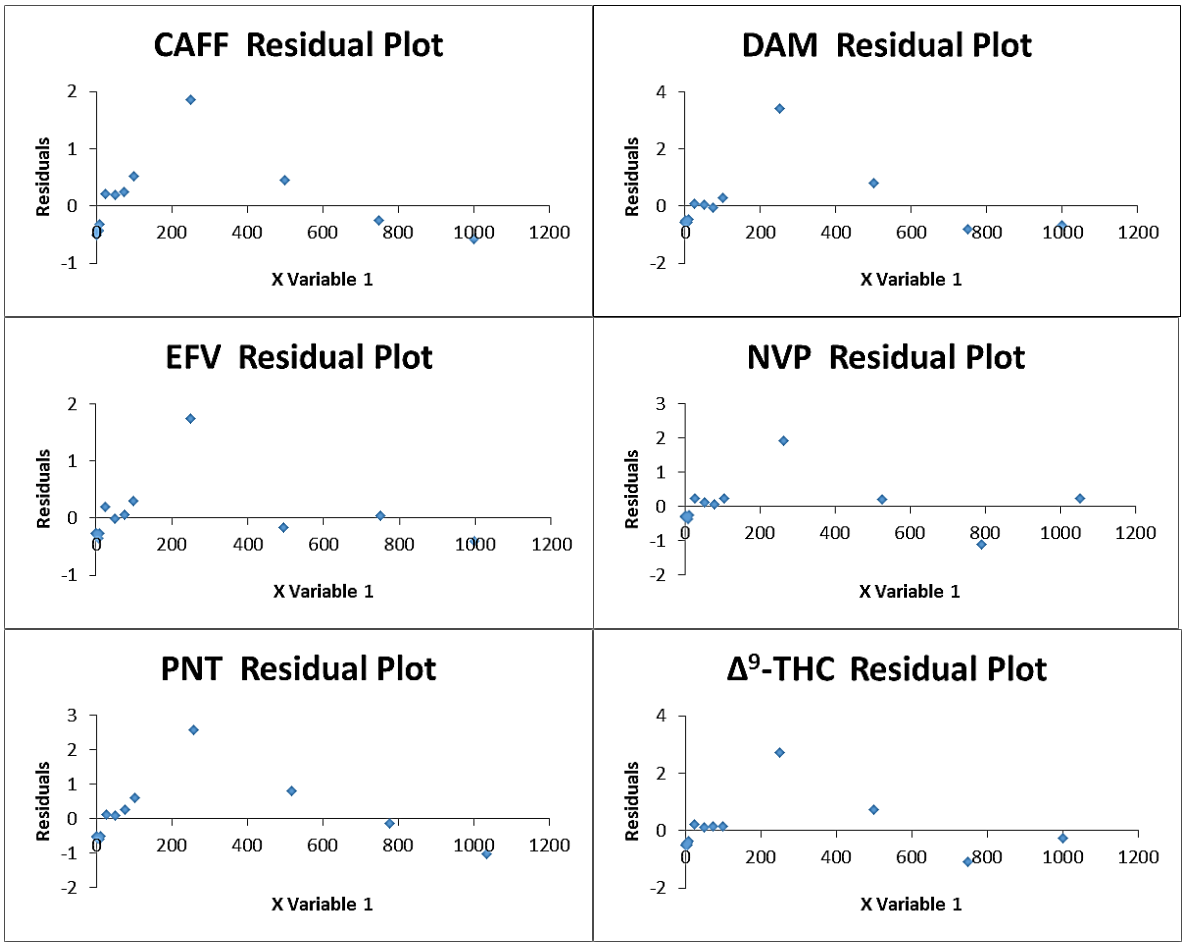

Figure 4.2: Residual plots for CAFF, DAM, EFV, NVP, PNT and Δ^9-THC reference standards, with outlier.

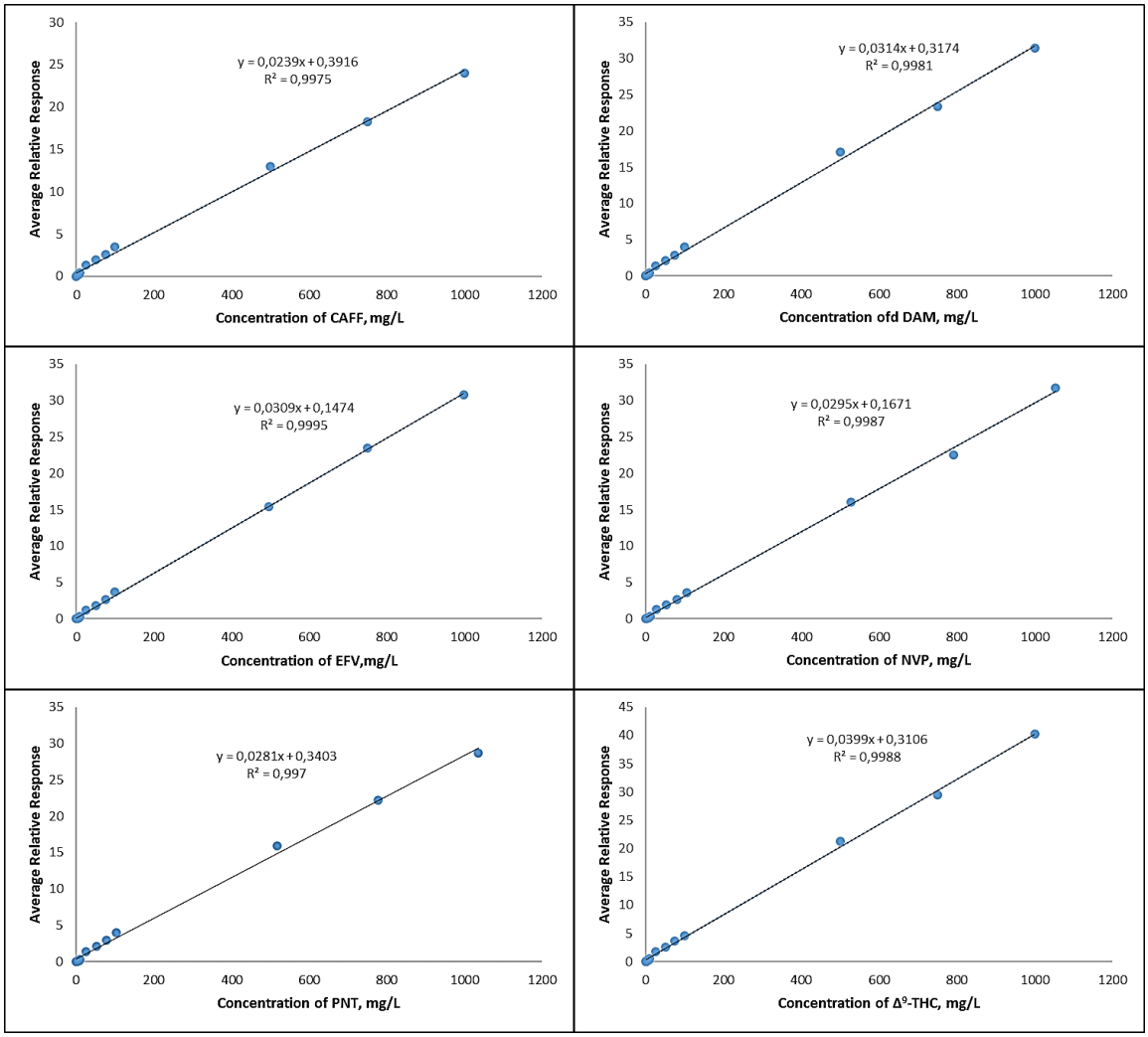

Figure 4.3: Plot of average peak area ratio vs concentration CAFF, DAM, EFV, NVP, PNT and Δ^9-THC reference standards, respectively, without outlier.

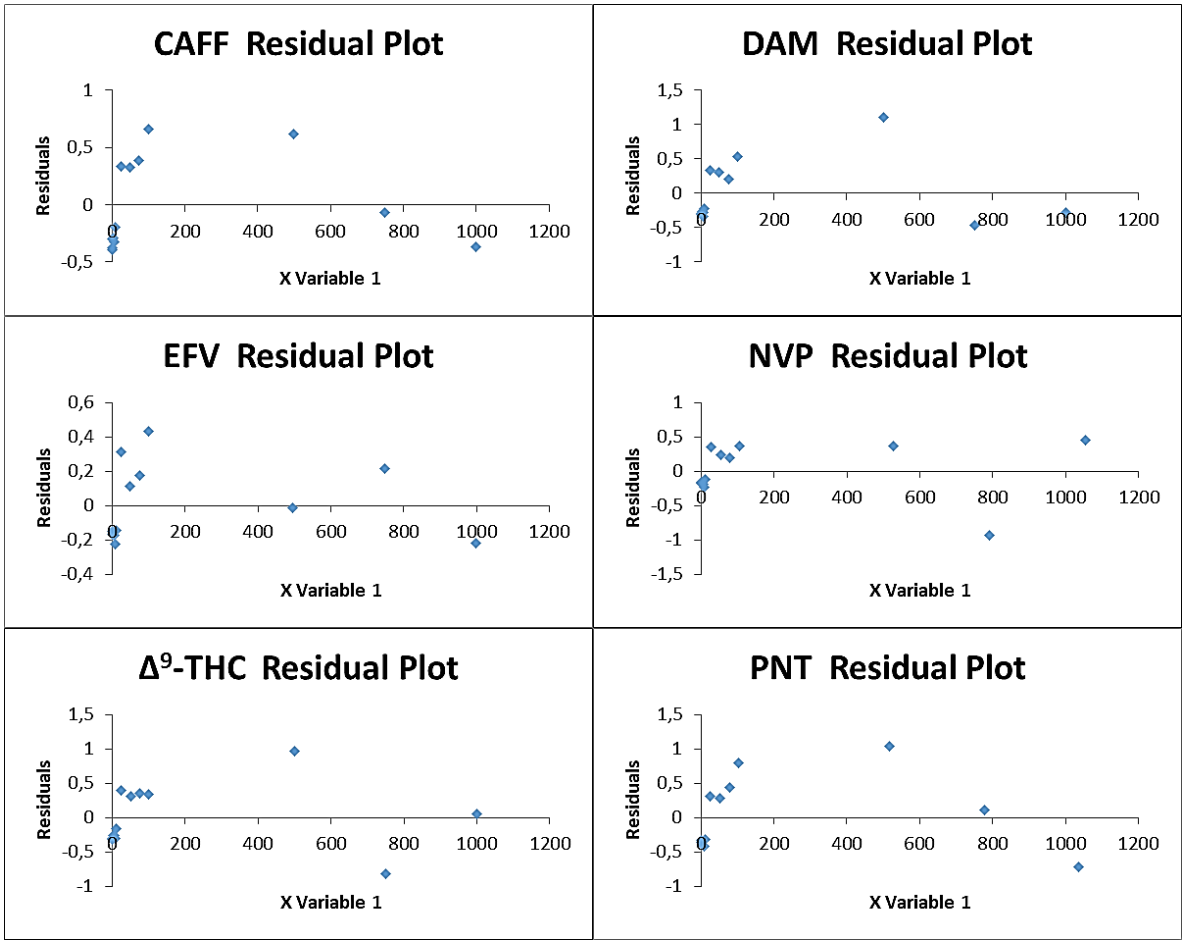

Figure 4.4: Residual plots for CAFF, DAM, EFV, NVP, PNT and Δ^9-THC reference standards, without outlier.

Table 4.4: Typical ANOVA output for DAM.

F-Test Two-Sample for Variances			t-Test: Two-Sample Assuming Unequal Variances		
	Variable 1	Variable 2		Variable 1	Variable 2
Mean	6.410844	0.194308	Mean	6.410844	0.194308
Variance	110.0795	0.111718	Variance	110.0795	0.111718
Observations	13	13	Observations	13	13
df	12	12	Hypothesized Mean Difference	0	
F	985.3325		Df	12	
P(F<=f) one-tail	5E-16		t Stat	2.13524	
F Critical one-tail	2.686637		P(T<=t) one-tail	0.027024	
			t Critical one-tail	1.782288	
			P(T<=t) two-tail	0.054048	
			t Critical two-tail	2.178813	

To evaluate the linearity using the t-Test and the F-test we state the null hypothesis using 95% confidence level as the threshold (Santer et al, 2000; Skoog et al, 2004):

H_o = No linear relationship between x and y

H_1 = There is a linear relationship between x and y

If the calculated t-value (t_{calc}) and F-value (F_{calc}) are less than the corresponding critical values (t_{crit} and F_{crit}), then the null hypothesis is rejected, that is there is a significant linear relationship between x and y i.e., y=mx +c.

t_{crit} = 1.782 with 12 degrees of freedom (95%)

F_{crit} = 2.687 with 12 degrees of freedom (95% confidence level)

Therefore, from the data shown in Table 4.3, $t_{calc} > t_{crit}$ and $F_{calc}>F_{crit}$; we reject the **H_o**. Sufficient proof to accept a linear relationship between x and y exists since; therefore, the calibration curve is linear.

4.2 THE EVALUATION OF THE LIMIT OF DETECTION AND THE LIMIT OF QUANTITATION OF THE ANALYTICAL METHOD

A range of working solutions with concentrations shown in Table 4.5 for CAF, DAM, EFV, NVP, PNT and Δ^9-THC, were prepared as discussed in Section 2.6.3. Five replicate measurements were conducted using GC-MS and the mean response of the 5 replicates were used to draw a calibration plot of average relative response against concentration, shown in Figure 4.5. The residual plots for the CAF, DAM, EFV, NVP, PNT and Δ^9-THC concentrations are shown in Figure 4.6. The residual plots shown in Figure 4.6 indicate that there are no outliers for the data. The limits of detection (LOD) and quantitation (LOQ) were determined by regression analysis of the response ratios. The regression statistics for DAM used to determine the slope and standard error are shown in Table 4.6. Similar regression statistics for PNT, CAFF, EFV, NVP and Δ^9-THC are used to determine the data shown in Table 4.7. The regression analysis of each of the data was used to calculate the detection limits and quantitation limits in the Equations 2.3 and 2.4, respectively, given in Section 2.6.3.

Table 4.5: Concentrations in mg/L of CAFF, DAM, EFV, NVP, PNT and Δ^9-THC working solutions used for LOD and LOQ determination.

CAFF	DAM	EFV	NVP	PNT	Δ^9-THC
1.00	1.00	0.998	1.05	1.04	1.00
2.50	2.50	2.50	2.64	2.59	2.50
5.00	5.00	4.95	5.27	5.18	5.00
10.00	10.00	9.98	10.50	10.36	10.00
50.00	50.00	49.50	52.70	51.80	50.00

Table 4.6: Typical regression statistics for DAM.

Regression Statistics	
Multiple R	0.999739
R Square	0.999478
Adjusted R Square	0.999348
Standard Error	0.0221444
Observations	6

ANOVA

	df	*SS*	*MS*	*F*	*Significance F*
Regression	1	3.523421	3.523421	7662.491	1.02E-07
Residual	4	0.001839	0.00046		
Total	5	3.52526			

	Coefficients	*Standard Error*	*t Stat*	*P-value*	*Lower 95%*	*Upper 95%*	*Lower 95.0%*	*Upper 95.0%*
Intercept	-0.00364	0.010442	-0.34894	0.744727	-0.03263	0.025347	-0.03263	0.025347
X Variable 1	43.63871	0.498525	87.53565	1.02E-07	42.25459	45.02284	42.25459	45.02284

Table 4.7: LOD and LOQ of the components PNT, CAFF, EFV, NVP, Δ^9-THC and DAM.

	Standard error	slope	LOD(mg/L)	LOQ (mg/L)
Caffeine	0.013392	37.8742	0.021	0.064
Diamorphine	0.010442	43.63871	0.014	0.043
Efavirenz	0.01146	36.62379	0.019	0.056
Nevirapine	0.011864	37.70615	0.019	0.057
Phenacetin	0.027081	41.15575	0.039	0.12
Δ^9-THC	0.008745	52.24967	0.0099	0.030

The detection limits for CAFF, DAM, EFV, NVP, PNT and Δ^9-THC were 0.021, 0.014, 0.019, 0.019, 0.039 and 0.0099 mg/L, respectively. Multiplying the concentration with the volume injected (1 µL), indicates that the detection limits were 21.0, 14.0, 19.0, 19.0, 39.0 and 9.90 pg on column, respectively. The limit of quantitation for CAFF, DAM, EFV, NVP, PNT and Δ^9-THC were 0.064, 0.043, 0.056, 0.057, 0.12 and 0.030 mg/L, respectively. The limit of quantitation was therefore 64.0, 43.0, 56.0, 57.0, 120 and 30.0 pg on column, respectively. The LOD and LOQ for CAFF, DAM, PNT and Δ^9-THC obtained in this research was lower than those reported in literature (Weigel et al, 2004; Rahim et al, 2011; Chan, Tan and Wong, 2012b; Florian-Ramírez, Garzón-Méndez and Parada-Alfonso, 2012; Gumbi et al, 2017), while the LOD and LOQ for EFV and NVP were comparable (Lemmer et al, 2005). Therefore, the GC-MS analysis is sensitive enough for the quantitative analysis and profiling of nyaope samples.

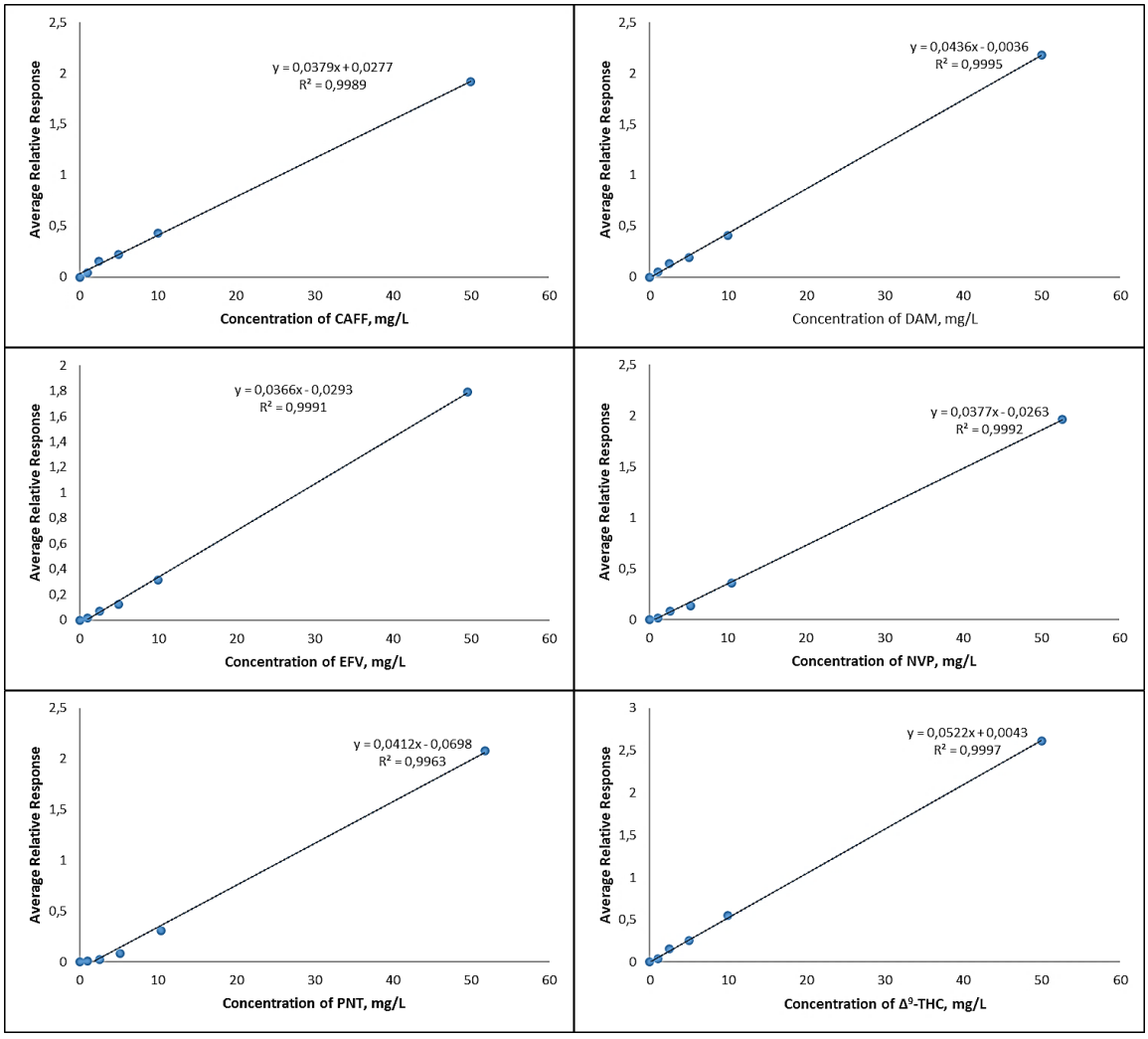

Figure 4.5: Plot of average peak area ratio vs concentration for CAFF, DAM, EFV, NVP, PNT and Δ^9-THC reference standards used for LOD and LOQ determination.

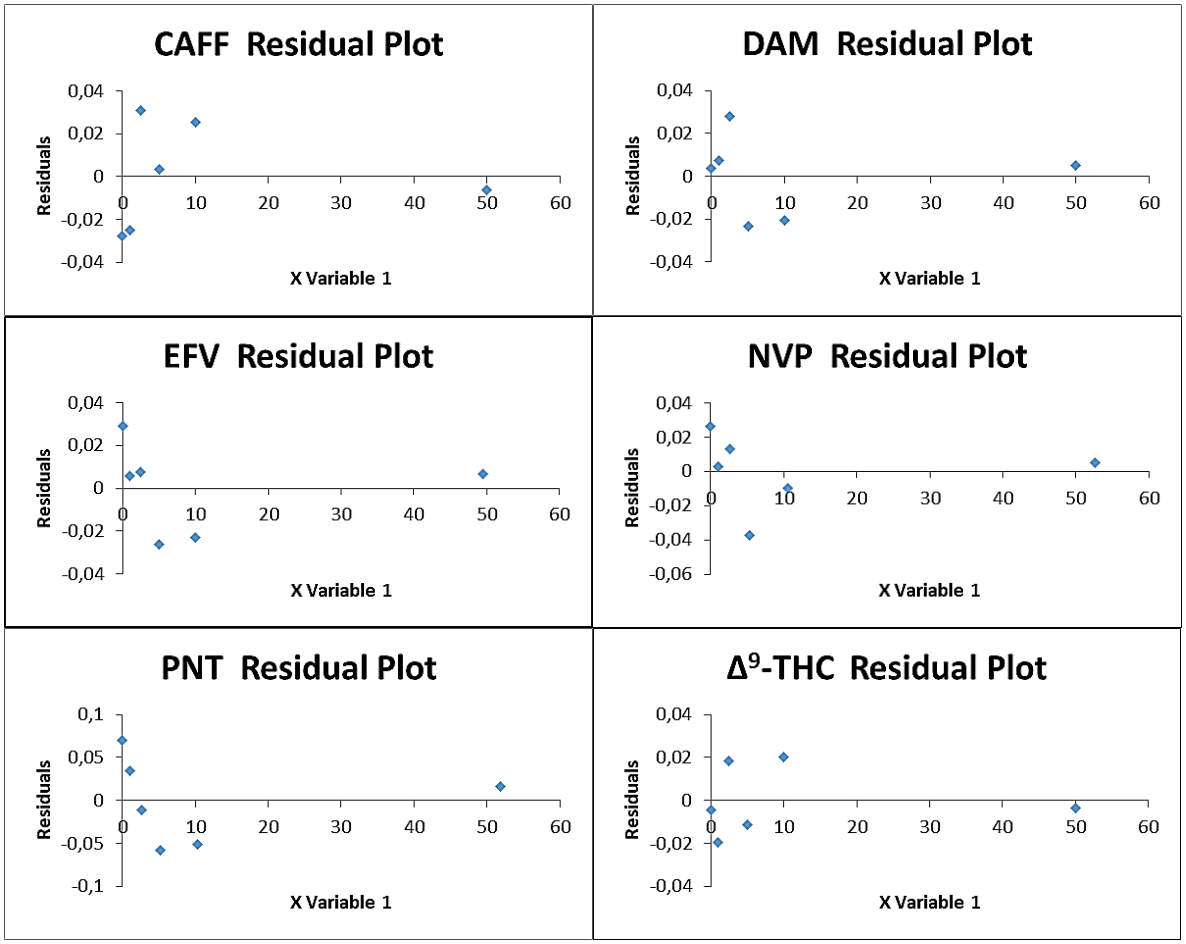

Figure 4.6: Residual plots for CAFF, DAM, EFV, NVP, PNT and Δ^9-THC reference standards used for LOD and LOQ determination.

4.3 ACCURACY AND PRECISION

4.3.1 The evaluation of the accuracy of the analytical method

Accuracy was evaluated using drug standard mixtures of CAFF, EFV, DAM, NVP, PNT and Δ^9-THC with concentrations 10.0, 100.0 and 1000.0 mg/L, representing the low, medium and high concentration levels, respectively (ICH, 2005; Araujo, 2009) as explained in Section 2.6.4. The average response ratios for CAFF, EFV, DAM, NVP, PNT and Δ^9-THC were used in Equation 2.5 to calculate percentage accuracy shown in Table 4.8. The acceptance criteria are percentage accuracy that is between the accepted limits of 80–120% (Peters et al, 2007; González et al, 2014; Kadiana et al, 2016). The percentage accuracy was above 100% for the high concentration level in all the components and above 80% for the lower concentration level; thus, the accuracy of the analytical method is acceptable.

Table 4.8: Average percentage accuracy (n = 10) as well %Bias for PNT, CAFF, EFV, NVP, Δ^9-THC and DAM reference standards at three different concentration levels.

Analyte	Control level (mg/L)	Average %Accuracy	%RSD	%Bias
	Low (10.00)	106	2,46	6,35
CAFF	Medium (100.00)	101	1,79	6,46
	High (1000.00)	106	4,00	11,49
	Low (10.00)	95	7,53	1,81
DAM	Medium (100.00)	97	13,64	8,95
	High (1000.00)	107	5,14	4,79
	Low (10.00)	93	13,35	6,69
EFV	Medium (100.00)	112	8,56	1,03
	High (1000.00)	107	3,56	9,24
	Low (10.00)	88	4,63	1,09
PNT	Medium (100.00)	101	9,34	3,70
	High (1000.00)	106	5,36	0,23
	Low (10.00)	97	16,29	11,97
NVP	Medium (100.00)	82	14,89	3,70
	High (1000.00)	103	3,95	6,82
	Low (10.00)	104	6,63	1,99
Δ^9-THC	Medium (100.00)	97	13,75	14,42
	High (1000.00)	108	3,98	5,41

The average response ratios for CAFF, EFV, DAM, NVP, PNT and Δ^9-THC were also used in Equation 2.6 to calculate percentage bias shown in Table 4.8. The acceptance criteria is percentage bias less than or equal to 15% for the higher concentration and less than or equal to 20% for the lower concentration (Rigdon, A. 2016; Zabell, Lytle and Julian, 2016). The percentage bias was less than 15% for all the concentration levels in all the components and thus the accuracy of the analytical method is acceptable.

4.3.2 The evaluation of the precision of the analytical method

Precision under within laboratory repeatability was evaluated by conducting ten replicate analyses of CAFF, DAM, EFV, NVP, PNT and Δ^9-THC drug standards, at three concentration levels 10.0, 100.0 and 1000.0 mg/L (ICH, 2005). The average response ratio calculated as described in Section 2.6.4 was used to determine relative standard deviation (%RSD) amongst the ten replicate analyses in order to evaluate repeatability. The acceptance criteria for repeatability are %RSD equal to, or less than 15% for the higher concentration level, and less than, or equal to 20% for the lower concentration level (ICH, 2005; González et al, 2014; FDA, 2018). The results are shown in Table 4.9 and the %RSD obtained for the high concentration levels were less than 10% for all analytes. For the lower concentration level, the analyses gave %RSD less than 10% for CAFF, DAM, EFV, NVP and Δ^9-THC while PNT gave %RSD of 15.78%, which is less than 20%. The acceptance criteria are met for all the analytes used; therefore, the analytical method is repeatable.

Intermediate precision was evaluated by conducting five replicate analyses of CAFF, DAM, EFV, NVP, PNT and Δ^9-THC drug standards, at three concentration levels 10.0, 100.0 and 1000.0 mg/L on two different instruments (Thompson et al, 2002; UNODC, 2009b) as explained in Section 2.6.4.2. Table 4.10 shows ANOVA data for PNT used in Equations 2.7 and 2.8 in Section 2.6.4.2 to calculate the within-group precision ($\%RSD_W$) and the between-group precision ($\%RSD_B$), given in Table 4.11.

The %RSD for both within-group and between-group precision were all less than or equal to the 15% limit (Peters et al, 2007; UNODC, 2009b; González et al, 2014; FDA 2018) for all the components at high concentration level in both instruments. The %RSD for the within-group precision were less than 20% for the components at low concentration level for both instruments. For the between-group, the %RSD were less than 20% for the components at low concentration level for both instruments.

Table 4.9: Average peak area ratios (n = 10) for CAFF, DAM, EFV, NVP, PNT and Δ^9-THC reference standards at three different concentration levels.

Analyte	Control level (mg/L)	Average Peak Area Ratio	%RSD
	Low (10.00)	0.433 ± 0.011	2.46
CAFF	Medium (100.00)	3.36 ± 0.06	1.79
	High (1000.00)	27.4 ± 1.097	4.00
	Low (10.00)	0.408 ± 0.031	7.70
DAM	Medium (100.00)	4.98 ± 0.044	0.89
	High (1000.00)	32.7 ± 2.78	8.51
	Low (10.00)	0.384 ± 0.021	5.55
EFV	Medium (100.00)	4.53 ± 0.027	0.59
	High (1000.00)	40.6 ± 1.762	4.34
	Low (10.00)	0.421 ± 0.023	5.52
PNT	Medium (100.00)	4.55 ± 0.04	0.89
	High (1000.00)	39.6 ± 1.858	4.69
	Low (10.00)	0.35 ± 0.055	15.78
NVP	Medium (100.00)	3.75 ± 0.053	1.40
	High (1000.00)	31.4 ± 1.239	3.95
	Low (10.00)	0.506 ± 0.024	4.80
Δ^9-THC	Medium (100.00)	5.94 ± 0.052	0.88
	High (1000.00)	30.8 ± 2.755	8.95

Table 4.10 : Single Factor ANOVA for PNT at low concentration level.

Groups	*Count*	*Sum*	*Average*	*Variance*
Column 1	5	0.863715	0.172743	0.001833
Column 2	5	1.557594	0.311519	0.000214
Column 3	5	1.377965	0.275593	0.000228
Column 4	5	1.561253	0.312251	0.000135
Column 5	5	1.567177	0.313435	8.34E-05

ANOVA

Source of Variation	*SS*	*df*	*MS*	*F*	*P-value*	*F crit*
Between Groups	0.073166	4	0.018291	36.67801	6.05E-09	2.866081
Within Groups	0.009974	20	0.000499			
Total	0.08314	24				

Table 4.11: The within group (W) precision and between group (B) %RSD for the components CAFF, DAM, EFV, PNT, NVP and Δ^9-THC.

		Instrument 1		Instrument 2	
Analyte	**Control level (mg/L)**	**$\%RSD_W$**	**$\%RSD_B$**	**$\%RSD_W$**	**$\%RSD_B$**
	Low (10.00)	2.84	5.79	16.83	8.85
CAFF	Medium (100.00)	2.31	1.54	2.36	5.36
	High (1000.00)	6.09	6.91	3.62	5.77
	Low (10.00)	6.14	5.57	11.10	15.01
DAM	Medium (100.00)	4.34	5.87	2.87	8.48
	High (1000.00)	6.38	0.45	2.98	7.89
	Low (10.00)	3.09	9.51	3.55	14.21
EFV	Medium (100.00)	2.75	3.38	1.07	2.50
	High (1000.00)	7.32	7.22	2.87	5.28
	Low (10.00)	3.92	5.52	3.78	13.39
NVP	Medium (100.00)	2.93	2.90	1.82	2.46
	High (1000.00)	10.78	14.96	1.33	8.31
	Low (10.00)	8.06	21.53	2.80	15.19
PNT	Medium (100.00)	2.08	2.67	2.52	4.11
	High (1000.00)	5.55	7.41	4.20	5.43
	Low (10.00)	3.90	7.29	4.05	6.04
Δ^9-THC	Medium (100.00)	3.50	6.04	0.73	3.42
	High (1000.00)	6.43	8.66	2.43	5.71

4.4 THE EVALUATION OF THE RUGGEDNESS OF THE ANALYTICAL METHOD

Five replicate analyses of the reference standard mixture at three concentration levels were performed on two different instruments for five consecutive days (Thompson et al, 2002; Bonfilio et al 2012). Ruggedness was tested by evaluating the peak areas and the retention time (Dejaegher and Heyden, 2007; César and Pianetti, 2009).

Peak areas are evaluated by calculating peak area ratios and determining the %RSD. The %RSD for the different analyses is given in Table 4.12. The peak area ratios for CAFF, DAM, EFV, NVP, PNT and Δ^9-THC at the different concentration levels for five days are given in Appendices III-

a to III-f. The acceptance criteria are a %RSD equal to or less than 15% for the high concentration level and %RSD equal to or less than 20% for the low concentration level. The %RSD for all concentration levels were all less than or equal to 15%, except CAFF for instrument 2 and PNT for instrument 1 on day 1 at low concentration level, which gave %RSD greater than 20%, as well as NVP on day 2 at high concentration level, which gave %RSD greater than 15% for instrument 2. Above-limit results can be considered to be an anomaly. The acceptance criteria are met for most of the analytes used; therefore, the analytical method is robust.

The average peak area ratios (PAR) for the five replicate analyses for each day were determined. The pooled average peak area ratios (PPAR) for the five days, given in Table 4.13, were used for the F-test and t-test (two-tailed). The ANOVA statistical analysis gave F_{calc} = 0.514 (low concentration level), 0.079 (medium concentration level) and 0.011 (high concentration level), with the corresponding p-values = 0.490, 0.784 and 0.917. The F_{calc} for all concentration levels is less than the F_{crit} = 4.965. The t_{calc} = 0.830 (low concentration level), 0.428 (medium concentration level) and -0.095 (high concentration level), with corresponding p values = 0.445, 0.686 and 0.928. The t_{calc} for all concentration levels is less than t_{crit} = 2.571. This demonstrates that there were no significant differences amongst the peak area ratios for the two instruments over five days.

Retention time (RT) was evaluated for ruggedness by determining the average retention time for each of the replicate analyses over five days for each concentration level. The pooled average relative retention time (RRT) over five days was determined for each component and the result is given in Table 4.13. Treatment of the data using ANOVA (single factor), as well as t-test (paired two samples for means) gave Fcalc = 0.029 (low concentration level), 0.008 (medium concentration level) and 0.040 (high concentration level) with the corresponding p-values = 0.867, 0.928 and 0.845. The Fcalc for all concentration levels is less than the Fcrit = 4.965. The tcalc = -2.658 (low concentration level), -0.824 (medium concentration level) and -2.800 (high concentration level), with corresponding p values = 0.045, 0.448 and 0.038. The tcalc for all concentration levels is less than tcrit = 2.571. The results indicate that there is no significant difference between the retention times of the two instruments over the five days. Therefore the analytical method can be applied successfully using different instruments.

Table 4.12: Average percentage RSD (n = 5) for CAFF, DAM, EFV, NVP, PNT and Δ^9-THC reference standards at three different concentration levels.

		Day 1		Day 2		Day 3		Day 4		Day 5	
Analyte	Control level (mg/L)	Instrument 1	Instrument 2	Instrument 1	Instrument 2	Instrument 1	Instrument 2	Instrument 1	Instrument 2	Instrument 1	Instrument 2
	Low (10.00)	1.11	30.3	4.03	1.48	3.89	2.50	1.91	7.40	1.26	9.11
CAFF	Medium (100.00)	3.75	3.54	1.98	2.04	2.33	1.55	1.35	1.86	0.89	1.85
	High (1000.00)	2.64	1.87	7.16	4.17	10.4	6.48	3.79	1.43	2.84	0.68
	Low (10.00)	4.56	8.22	4.51	14.1	5.15	3.62	7.27	5.87	2.06	12.3
DAM	Medium (100.00)	6.02	2.21	5.37	2.47	3.53	3.33	2.89	3.17	3.18	3.07
	High (1000.00)	1.18	2.65	6.64	2.75	5.70	4.20	7.89	2.03	8.02	2.42
	Low (10.00)	1.72	5.82	4.63	3.42	4.44	4.03	1.56	1.14	1.12	3.05
EFV	Medium (100.00)	4.38	1.00	4.01	1.37	1.06	1.38	1.45	0.34	1.10	0.96
	High (1000.00)	2.71	1.46	13.12	1.87	6.99	5.61	7.38	0.91	4.64	0.81
	Low (10.00)	1.83	4.97	4.43	4.20	5.12	3.60	4.78	1.93	2.24	4.22
NVP	Medium (100.00)	4.00	0.46	3.91	0.55	2.18	0.42	2.00	3.99	1.68	0.84
	High (1000.00)	2.61	0.47	16.68	1.91	3.64	2.15	7.19	0.94	9.04	0.69
	Low (10.00)	24.8	2.83	4.69	3.00	5.48	4.28	3.73	1.58	2.91	2.20
PNT	Medium (100.00)	3.26	4.05	2.40	2.81	0.83	1.72	1.38	0.80	1.53	1.46
	High (1000.00)	3.44	2.25	7.70	2.38	8.38	8.27	3.58	1.96	2.86	0.57
	Low (10.00)	4.66	2.97	1.22	1.27	5.98	3.40	3.29	6.68	2.73	3.98
Δ^9-THC	Medium (100.00)	6.13	0.44	2.70	0.59	2.70	0.98	1.21	0.71	2.00	0.82
	High (1000.00)	1.49	0.53	12.12	1.45	6.99	4.70	5.95	1.41	3.41	1.37

Table 4.13: Pooled average peak area ratios (PPAR) and relative retention time (RRT) for the two instruments.

Concentration level, mg/L	Low (10.00)				Medium (100.00)				High (1000.00)			
Instrument	1		2		1		2		1		2	
	PPAR	RRT	PPAR	RRT	PPAR	RRT	PPAR	RRT	PPAR	RRT	PPAR	RRT
PNT	0.277	0.578	0.387	0.601	3.289	0.663	3.975	0.603	23.578	0.584	21.954	0.611
CAFF	0.390	0.650	0.455	0.672	2.901	0.652	3.339	0.674	22.677	0.663	20.322	0.684
EFV	0.428	0.826	0.356	0.839	3.975	0.832	3.648	0.845	26.443	0.851	22.999	0.862
NVP	0.414	1.086	0.346	1.091	3.858	1.093	3.703	1.098	24.069	1.113	22.760	1.127
Δ^9-THC	0.546	1.148	0.482	1.179	4.966	1.151	4.694	1.184	19.581	1.156	27.452	1.203
DAM	0.418	1.298	0.232	1.380	4.016	1.301	3.015	1.382	19.338	1.308	21.165	1.400

4.5 THE EVALUATION OF THE SELECTIVITY OF THE ANALYTICAL METHOD

The absence of interference signal in blank samples was used to evaluate selectivity (UNODC, 2005; Mannocchi et al, 2015; FDA, 2018) also demonstrating that there is no co-elution of the analytes in the presence of other components and internal standard (FDA, 2018). The chromatogram of the sample spiked with a mixture of the CAFF, PNT, EFV, NVP, Δ^9-THC, and DAM reference standards with the internal standard tetracosane (TC) shown in Figure 4.7 demonstrate a clear separation of the peaks, i.e. no co-elution of the analytes. The chromatograms of ten replicate blank analyses shown in Appendix IV demonstrate the absence of interference signal at the retention time of the analytes CAFF, DAM, EFV, NVP, PNT and Δ^9-THC. The analytical method was determined to be selective for CAFF, PNT, EFV, NVP, Δ^9-THC and DAM, since no interferences were indicated in the blank samples. The ten replicate analyses performed for evaluating repeatability in Section 4.3 were also used to evaluate selectivity. The acceptance criteria are a %RSD equal to or less than 20% for the low concentration level (FDA, 2018). The %RSD at the lower concentration level for the components CAFF, DAM, EFV, NVP, PNT and Δ^9-THC were all less than 20% and therefore the analytical method was considered selective.

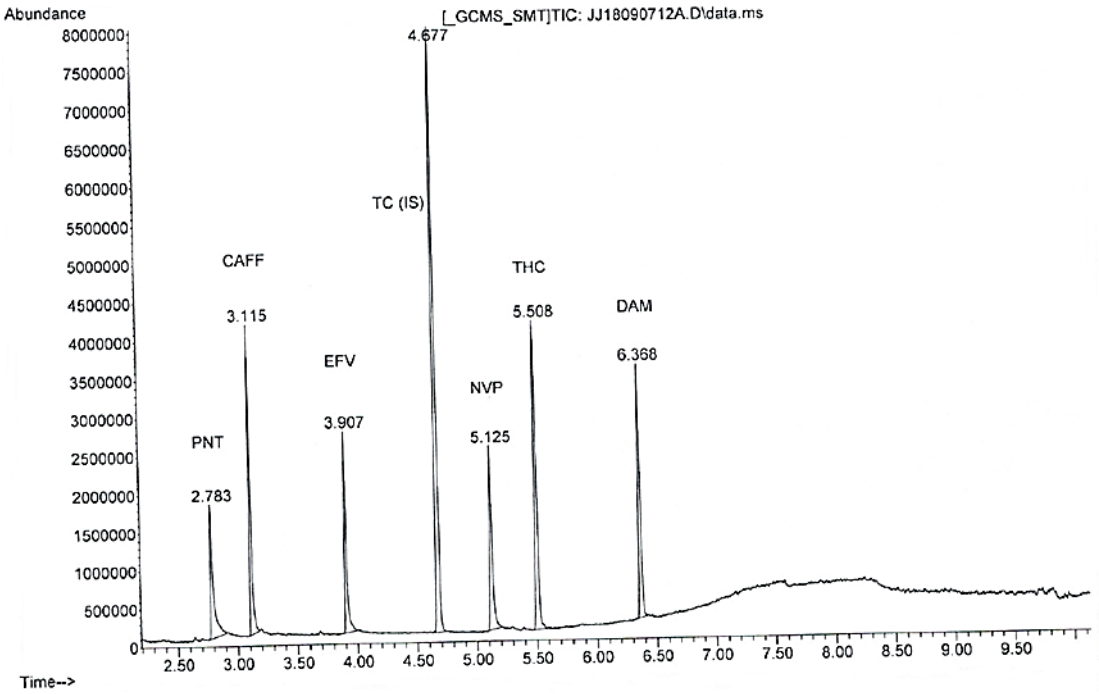

Figure 4.7: Chromatogram of the GCMS analysis of a mixture of PNT, CAFF, EFV, TC (IS), NVP, Δ^9-THC and DAM reference standards.

4.6 THE EVALUATION OF THE RECOVERY OF THE ANALYTICAL METHOD

Street samples containing CAFF, DAM and Δ^9-THC were spiked with the reference standard mixture in a 3 mL internal standard solvent to give a final concentration shown in the Table 4.14. Equations 2.9 and 2.10 were used to calculate the percentage recoveries shown in Table 4.15 as explained in paragraph 2.6.7.

Table 4.14: Sample quantities and concentrations used in the different solvents for recovery studies.

solvent	Mass of spiked sample, mg	Mass of un-spiked sample, mg	Concentration, mg/L
t-BuOH	13.99	15.6	17.00
DCM	16.68	12.8	17.00
ETAC	11.82	16.49	17.00
i-PrOH	11.84	10.4	17.00
ETOH	12.46	12.1	13.00
HEX	11.3	14.0	10.00

Table 4.15: Percentage recoveries of the components CAFF, PNT, EFV, NVP, Δ^9-THC and DAM in different solvents.

	t-BuOH	DCM	ETAC	i-PrOH	ETOH	HEX
CAFF	160	166	166	135	206	97
DAM	98	321	135	30	32	47
EFV	202	189	292	243	232	151
NVP	60	56	103	75	106	74
PNT	116	98	161	137	127	52
Δ^9-THC	160	142	164	129	238	100

The recoveries for PNT were acceptable for t-BuOH, DCM, ETAC, i-PrOH and ETOH, while there is poor recovery where HEX is used as a solvent. CAFF displayed recoveries above 100% for all the solvents except hexane, which showed 97% recovery. Δ^9-THC recoveries of 58–105% have been reported to be acceptable (Simões, et al, 2014). The Δ^9-THC and EFV recoveries achieved in this research were above 100% for all the solvents studied. NVP showed acceptable recoveries for ETAC and ETOH, with poor recoveries for the solvents t-BuOH, DCM, i-PrOH and hexane. DAM showed acceptable recoveries for the solvents t-BuOH, DCM and ETAC,

with poor recoveries for i-PrOH, ETOH and hexane. ETAC showed better recoveries, followed by DCM and then t-BuOH ETOH and i-PrOH. Hexane exhibited the least recoveries for the target compounds. It is important to note that there is no minimum established value for recovery, since a low recovery could be suitable for a certain analyte if the sensitivity of the detection technique is high enough (González et al, 2014). Recoveries above 100%, ranging from 106 to 292% were observed, which may be due to a number of factors, including the loss of sensitivity during analysis, increased concentration of the analyte due to partial evaporation of the solvent before analysis (Bogusz et al, 1998; Mwenesongole, 2015) or errors during the extraction process. Low recoveries of DAM in i-PrOH, ETOH and HEX (30–47%). This can be due to the degradation of DAM through hydrolysis in these solvents or loss during extraction (Mwenesongole, 2015). As discussed in section 1.7.6, the method is acceptable since the precision and accuracy of the method was found to be acceptable (Hartmann et al, 1998; Shah et al, 2000; Peters and Maurer, 2002; Peters et al, 2007).

CHAPTER 5: RESULTS AND DISCUSSION- APPLICATION OF THE VALIDATED ANALYTICAL METHOD

In order to investigate the validity of the analytical method for nyaope sample identification, quantitation and comparison, both simulated and casework samples (seized street samples) of nyaope were investigated. The comparison of samples within a batch and between batches using chromatograms and mass spectrometric data were investigated.

5.1 CALIBRATION CURVES

Drug standards available during analytical method validation, as discussed in chapter 4, were caffeine (CAFF), diamorphine (DAM), efavirenz (EFV), nevirapine (NVP), phenacetin (PNT) and Δ^9-tetrahydrocannabinol (Δ^9-THC). Therefore, only these standards were used to generate calibration curves for the quantitation of both simulated and actual seized street samples. Triplicate analyses of working solutions consisting of a mixture of CAFF, DAM, EFV, NVP, PNT and Δ^9-THC were conducted, and the average peak area ratios were determined as discussed in Section 3.1. The calibration plots of average peak area ratio against concentration for CAFF, DAM, EFV, NVP, PNT and Δ^9-THC are shown in Figure 5.1. Regression analysis was performed on the peak area ratios using Microsoft Excel 2010, and the linearity data summarised in Table 5.1 showed a correlation coefficient > 0.99 for all the components. This confirms the observation made in Section 4.1 that the analytical method used for the research resulted in a linear detector response. Regression analysis yielded an equation that describes the best fit of the line through the data points, with the form:

$$\boldsymbol{y = mx + c} \qquad \text{5-1}$$

The concentration of an unknown is calculated using the equation below:

$$\boldsymbol{C_x = \frac{y-c}{m} \times C_{IS}} \qquad \text{5-2}$$

where:

y = response ratio for the sample = $\frac{peak\ area\ of\ the\ sample}{peak\ area\ of\ the\ internal\ standard}$

m = the slope of the regression line

c = intercept of the regression line with the y-axis

C_x = concentration of the unknown sample

C_{IS} = concentration of internal standard

Concentrations of the major components CAFF, DAM, EFV, NVP, PNT and Δ^9-THC in both the simulated nyaope samples and casework samples were calculated using Equation 5.1:

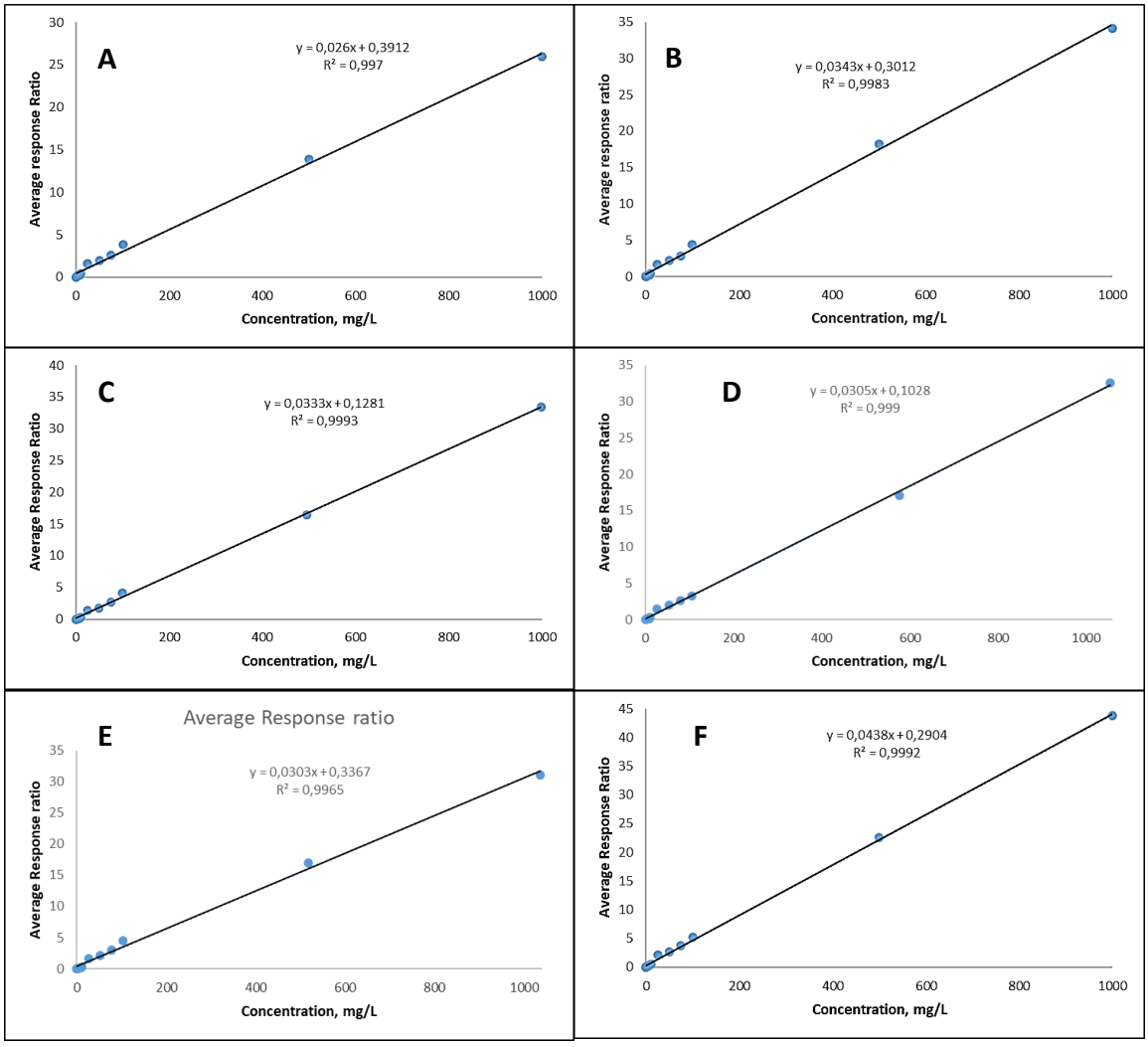

Figure 5.1: Calibration curves for the determination of (A) CAFF, (B) DAM, (C) EFV, (D) NVP, (E) PNT and (F) Δ^9-THC in nyaope samples by GC-MS analysis.

Table 5.1: Summarised linearity data for CAFF, DAM, EFV, NVP, PNT and Δ^9-THC.

Standard	r^2	Regression equation
CAFF	0.9970	$y = 0.0260x + 0.391$
DAM	0.9983	$y = 0.0343x + 0.301$
EFV	0.9993	$y = 0.0333x + 0.128$
NVP	0.9991	$y = 0.0305x + 0.103$
PNT	0.9965	$y = 0.0303x + 0.337$
Δ^9-THC	0.9992	$y = 0.0438x + 0.290$

5.2 IDENTIFICATION OF COMPONENTS

The compounds acetaminophen (ACA), acetylcodeine (ACOD), bulnesol, caffeine (CAFF), cannabichromene (CBCM), cannabicoumaronone (CBCN), cannabidiol (CBD), cannabigerol (CBG), cannabinol (CBN), cannabivarin (CBV), caryophyllene, cocaine (COC), codeine (COD), diamorphine (DAM), dextromethorphan (DTM), efavirenz (EFV), 6-monoacetylmorphine (6-MAM), methaqualone (MTQ), nevirapine (NVP), nicotine (NCT), nonacosane, phenacetin (PNT), Δ^9-tetrahydrocannabinol (Δ^9-THC), tetrahydrocannabivarin (THCV) and vitamin E were the major components identified in the analysis of simulated and actual seized street nyaope samples. The components COC, DAM, MTQ, and Δ^9-THC were identified on the basis of their relative retention time (RRT) and mass spectral data using certified reference material. CAFF, EFV, NVP and PNT were identified on the basis of their RRT and mass spectral data using USP reference standards. A typical chromatogram of reference standards CAFF, DAM, EFV, NVP, PNT and Δ^9-THC, in comparison with the chromatogram of the simulated nyaope sample, is displayed in Figure 5.2. ACA, ACOD, bulnesol, caryophyllene, CBCM, CBD, CBG, CBN, CBV, 6-MAM, NCT, THCV and vitamin E were identified by comparing the experimental mass spectral data with the NIST mass spectral library. The mass spectra of the components as well as the proposed fragmentation patterns for the components EFV and NVP are displayed in Figure 5.3. Similar mass spectral data as well as fragmentation patterns of the components ACA, ACOD, CAFF, CBCM, CBD, CBN, COC, CBV, DAM, EFV, 6-MAM, MTQ, NCT, NVP, PNT, Δ^9-THC, THCV and vitamin E are displayed in Appendix V a-c. The retention times (RT) and RRT of the individual components identified in both simulated and actual seized street nyaope samples are given in Table 5.2. The mass spectra, in comparison with the NIST standards for the

components ACA, ACOD, CAFF, CBCM, CBD, CBN, COC, CBV, DAM, EFV, 6-MAM, MTQ, NCT, NVP, PNT, Δ^9-THC, THCV and vitamin E, are displayed in Appendix VI a-f.

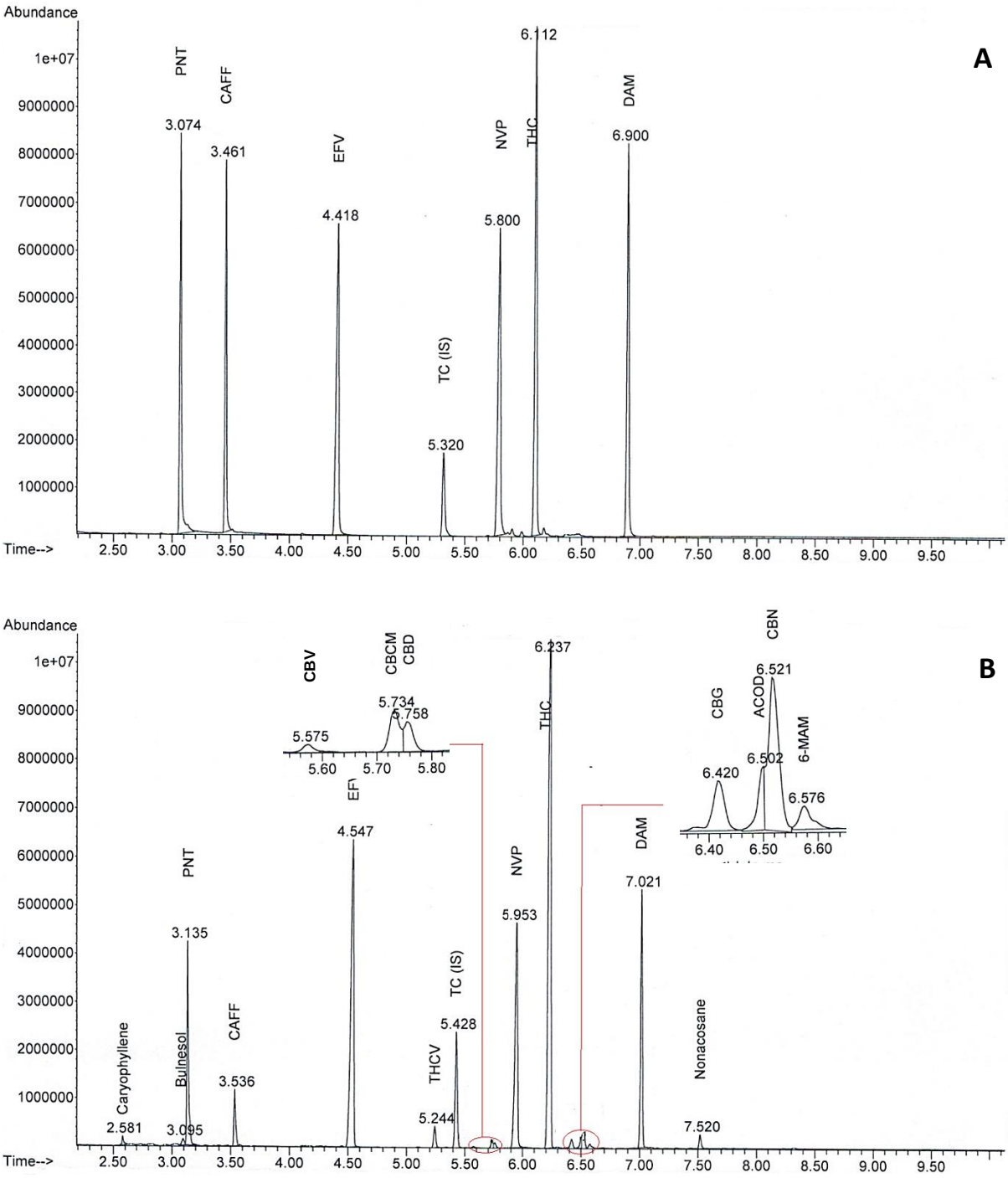

Figure 5.2: Chromatograms of (A) reference standards CAFF, DAM, EFV, NVP, PNT and Δ^9-THC, in comparison with (B) simulated nyaope samples.

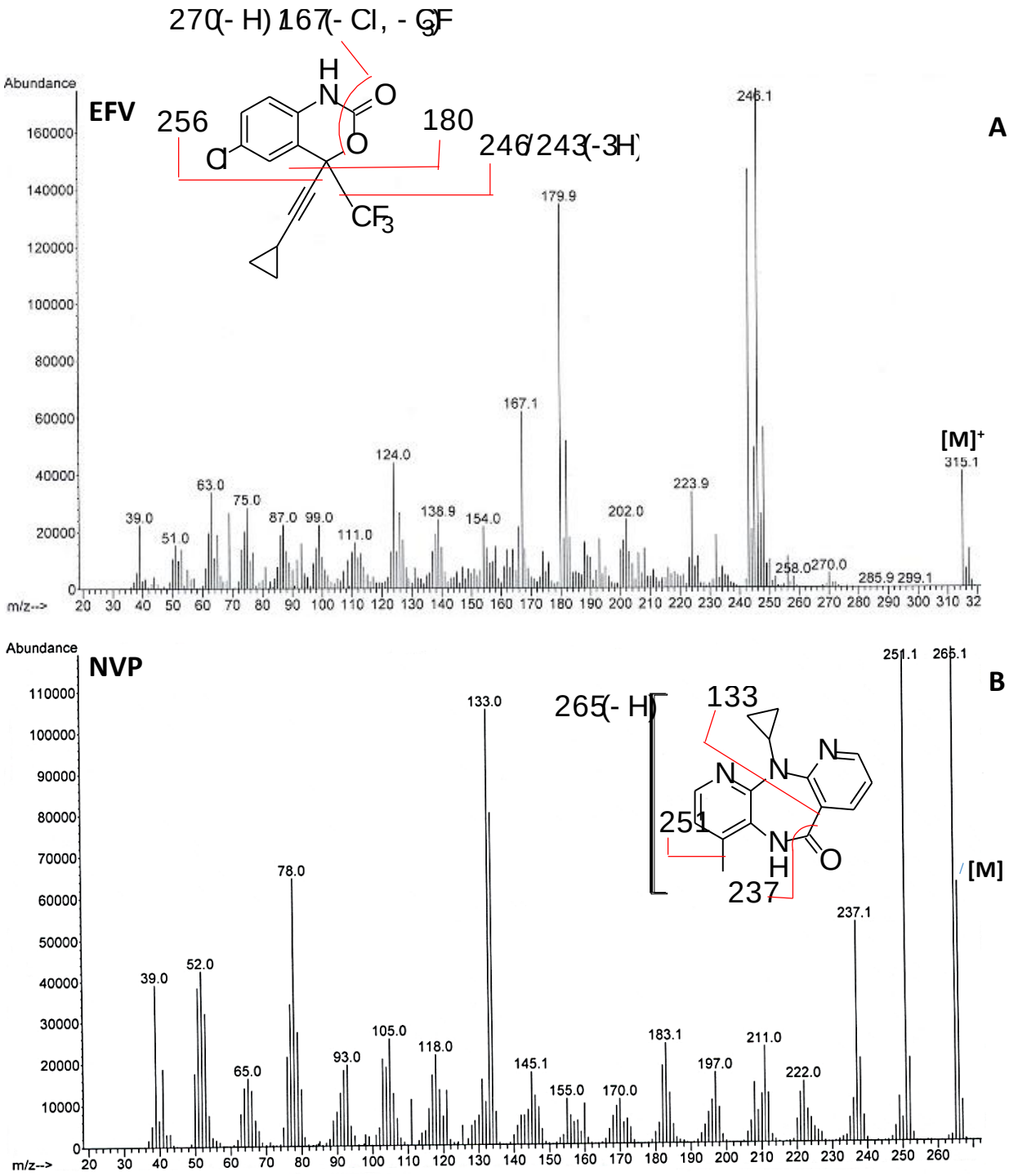

Figure 5.3: EI mass spectra of (A) EFV and (B) NVP as well as proposed fragmentation patterns.

Table 5.2: Retention time and relative retention time for the compounds identified in the analysis of simulated and actual seized street samples of nyaope.

	Retention time	RRT of samples (TC = 1.000)	RRT of standards (TC = 1.000)
NCT	2.41	0.44	-
Caryophyllene	2.58	0.48	-
Bulnesol	3.10	0.57	-
PNT	3.13	0.58	0.59
ACA	3.19	0.59	-
CAFF	3.53	0.65	0.65
EFV	4.54	0.83	0.83
DTM	4.66	0.86	-
MTQ	4.78	0.87	0.87
COC	4.89	0.90	0.89
THCV	5.24	0.97	-
TC (IS)	5.43	1.00	-
CBV	5.57	1.03	-
CBCM	5.73	1.06	-
CBD	5.75	1.06	-
CBCN	5.93	1.09	-
COD	5.95	1.09	-
NVP	5.95	1.10	1.09
Δ^9-THC	6.23	1.15	1.15
CBG	6.41	1.18	-
ACOD	6.50	1.20	-
CBN	6.52	1.20	
6-MAM	6.57	1.21	
DAM	7.02	1.29	1.30
Nonacosane	7.52	1.38	
Vitamin E	8.67	1.60	

From the relative retention times it is clear that NVP and COD would co-elute. This may be the reason why COD is not detected in the simulated nyaope samples containing NVP. The mass spectrum of NVP (A) in comparison with that of COD (B), as shown in Figure 5.5, however, does not show the COD prominent m/z ions of 162, 214 and 228, indicating that COD was absent from the samples, and therefore co-elution in these samples can be ruled out.

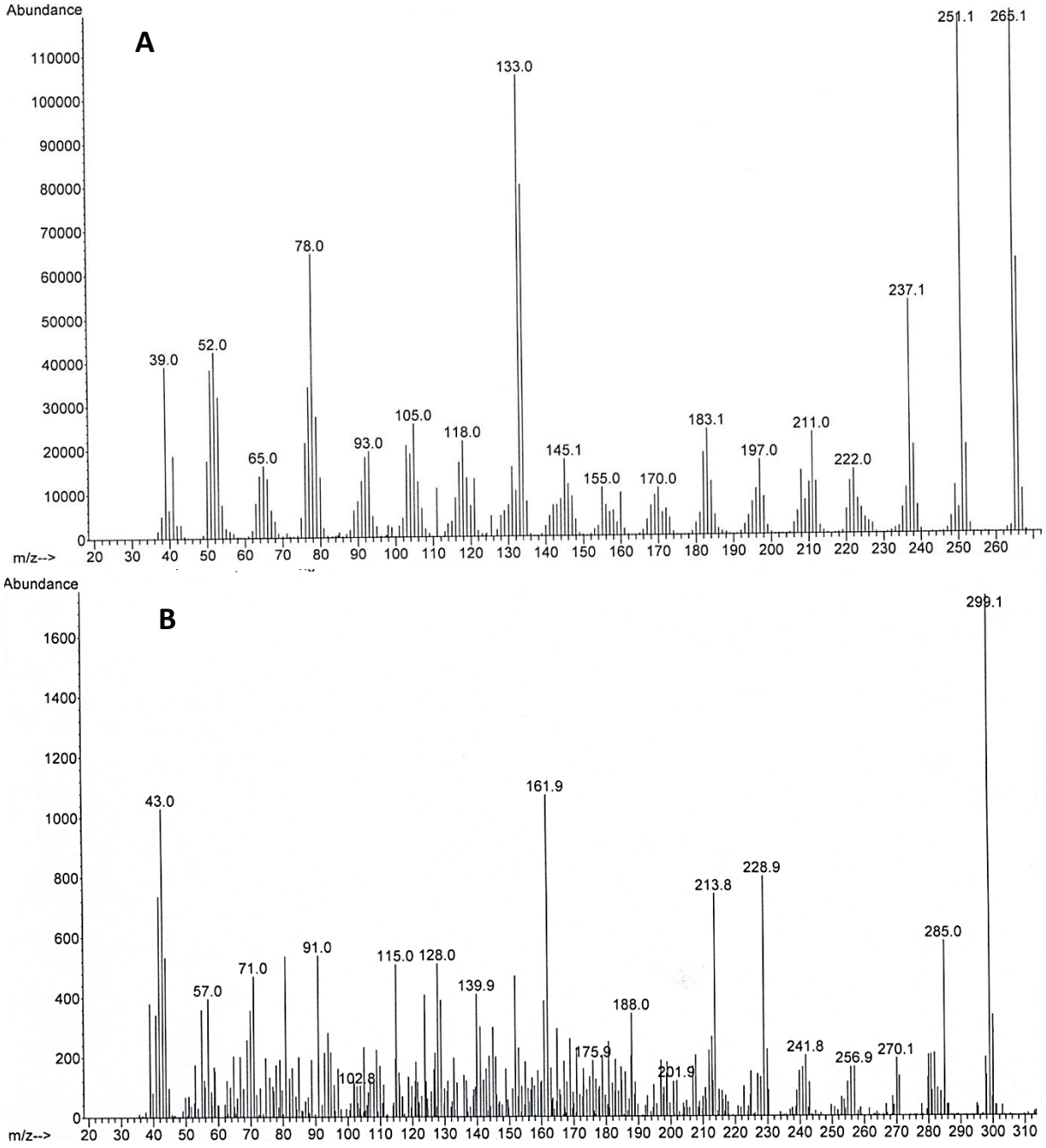

Figure 5.4: EI Mass spectrum of NVP (A) in comparison with the mass spectrum of COD (B).

5.3 SIMULATED NYAOPE SAMPLES

The 18 blind simulated nyaope samples prepared as described in Section 2.3 were weighed and marked S1–S18, as indicated in Table 5.3. The samples with mass shown in Table 5.3 were extracted with 3 mL of the internal standard solution in a 20 mL head space vial. Each of the 18 blind simulated samples, S1–S18, were analysed in triplicate using the GC-MS method described in Section 2.4, without dilution, after storage intervals of 0, 24, 48 and 72 hours on the autosampler in order to confirm the stability observed in Section 3.1.

Table 5.3: The masses of the simulated nyaope samples used for the study.

Sample	Mass (mg)	Sample	Mass (mg)
S1	12.4	**S10**	12.6
S2	12.5	**S11**	12.6
S3	12.7	**S12**	12.4
S4	13.5	**S13**	13.3
S5	12.3	**S14**	12.6
S6	12.5	**S15**	13.1
S7	13.9	**S16**	13.3
S8	13.3	**S17**	12.8
S9	12.8	**S18**	12.7

5.3.1 Discrimination of the simulated nyaope samples based on identified components

The components ACOD, CAFF, CBCM, CBD, CBG, CBN, CBV, caryophyllene, DAM, EFV, 6-MAM, nonacosane, NVP, PNT, THCV and Δ^9-THC were identified in the analysis of the samples S1, S2, S6, S7, S12 and S13. All these components except CBD and PNT were also identified in the analysis of the samples S4, S9, S10, S16, S17 and S18. Bulnesol, together with all the components except NVP and PNT, were identified in the analysis of the samples S3, S5, S8, S11, S14 and S15. Based on the identified components, the samples S1, S2, S6, S7, S12 and S13 were from the same batch and grouped as Class 1; the samples S3, S5, S8, S11, S14 and

S15 were from the second batch and grouped as Class 2; and the samples S4, S9, S10, S16, S17 and S18 were from the third batch and grouped as Class 3. Therefore it is possible to discriminate nyaope samples based on the components identified in the samples.

5.3.2 Stability evaluation of identified components based on average response ratios

Normalised average response ratios were determined in a similar manner as discussed in Section 3.1 in order to evaluate the stabilities of the main components in both simulated nyaope samples and actual seized street samples. The stabilities of the main components in simulated nyaope samples are summarised in Table 5.4 for the simulated samples, where 1 denotes a decrease of 0–15% and considered stable; 2 denotes a decrease of 15–30% and considered moderately stable; and 3 denotes a loss above 30% and is considered unstable (Saar et al, 2012). As indicated in Table 5.4, the components CAFF, CBCM, CBD, CBN, CBV, DAM, EFV, NVP, PNT Δ^9-THC and THCV were stable for the 72 hours of autosampler storage in all the samples as observed previously (Mthembi et al, 2018), except for the samples CBCM and CBD in the sample S1, which was unstable after 24 hours of storage. It is known that Δ^9-THC degrades to CBN, THCV degrades to CBV by oxidation (Turner and Elsohly, 1979; Carbone et al, 2010), while DAM will hydrolyse to 6-MAM and ultimately morphine (Barrett et al, 1992; Hutchinson and Somogyi, 2002). Therefore, the ratios CBV/THCV, CBN/ Δ^9-THC and 6-MAM/DAM can be used as a measure of stability of the components THCV, CBV, CBN, DAM, 6-MAM and Δ^9-THC. If the ratios CBN/Δ^9-THC, CBV/THCV and 6-MAM/DAM yield a value of 1, 2 or 3, then the sample can be considered to be stable, moderately stable, or unstable, respectively. The ratios CBV/THCV and CBN/Δ^9-THC demonstrate that the samples were stable for 72 hours of storage for all the samples except for the S1 samples which was showed to be moderate stable and S18 which was showed to be unstable after 48 hours of storage. The ratios confirms the stability of THCV, CBV, CBN and Δ^9-THC in the simulated nyaope samples except for S18. 6-MAM was, however, shown to be stable for 72 hours of storage in the samples S3, S4, S5, S8, S9, S10, S11, S14, S15, S16, S17 and S18 only; and unstable after 24 hours for samples S1, S2, S6, S7, S12 and S13. The components CBCM, CBD and 6-MAM were present in low abundance in all the samples and are susceptible to instrumental

background effect, which may explain the instability of these compounds. Furthermore 6-MAM undergoes degradation to morphine which may explain its instability.

Table 5.4: Summarised stability of the components in the different simulated nyaope samples.[1]

Time (hours)	Compound	S1	S2	S3	S4	S5	S6	S7	S8	S9	S10	S11	S12	S13	S14	S15	S16	S17	S18
24	PNT	1	1	nd	nd	nd	1	1	nd	nd	nd	nd	1	1	nd	nd	nd	nd	nd
	CAFF	1	1	1	1	1	1	1	1	1	1	1	1	1	1	1	1	1	1
	EFV	1	1	1	1	1	1	1	1	1	1	1	1	1	1	1	1	1	1
	THCV	2	1	1	1	1	1	1	1	1	1	1	1	1	1	1	1	1	1
	CBV	3	1	1	1	1	1	1	1	1	1	1	1	2	1	1	1	1	2
	CBV/THCV	2	1	1	1	1	1	1	1	1	1	1	1	1	1	1	1	1	1
	CBCM	3	1	1	1	1	1	1	1	1	1	1	2	2	2	1	1	1	1
	CBD	2	1	3	nd	1	1	1	1	nd	nd	2	1	1	1	1	nd	nd	nd
	NVP	1	1	nd	1	nd	1	1	nd	1	1	nd	1	1	nd	nd	1	1	1
	Δ^9-THC	1	1	1	1	1	1	1	1	1	1	1	1	1	1	1	1	1	1
	ACOD	1	1	1	1	2	2	1	1	1	1	1	2	1	2	1	1	1	1
	CBN	2	1	1	1	1	1	1	1	1	1	1	1	1	1	1	1	1	1
	CBN/Δ^9-THC	1	1	1	1	1	1	1	1	1	1	1	1	1	1	1	1	1	1
	6-MAM	2	2	1	1	1	1	1	1	1	1	1	3	1	1	1	1	1	1
	6-MAM/DAM	1	2	1	1	1	1	1	1	1	1	1	3	2	1	1	1	1	1
	DAM	1	1	1	1	1	1	1	1	1	1	1	1	1	1	1	1	1	1
48	PNT	1	1	nd	nd	nd	1	1	nd	nd	nd	nd	1	1	nd	nd	nd	nd	nd
	CAFF	1	1	1	1	1	1	1	1	1	1	1	1	1	1	1	1	1	1
	EFV	1	1	1	1	1	1	1	1	1	1	1	1	1	1	1	1	1	1
	THCV	2	1	2	1	1	1	1	1	1	1	1	1	1	1	1	1	1	2
	CBV	3	1	1	1	1	1	1	1	1	1	1	1	1	1	1	1	1	2
	CBV/THCV	2	1	1	1	1	1	1	1	2	1	1	1	1	1	1	1	1	3
	CBCM	3	1	2	1	2	1	1	1	1	1	1	1	1	1	1	1	1	2
	CBD	2	1	2	nd	3	1	1	1	nd	nd	2	1	1	1	1	nd	nd	nd
	NVP	1	1	nd	1	nd	1	1	nd	1	1	nd	1	1	nd	nd	1	1	1
	Δ^9-THC	1	1	2	1	2	1	1	1	2	1	1	1	1	1	1	1	1	2
	ACOD	2	1	1	1	2	2	2	2	1	1	2	2	2	2	3	1	3	1
	CBN	3	1	2	1	2	1	1	1	3	1	1	1	1	1	1	1	1	2
	CBN/ Δ^9-THC	2	1	1	1	1	1	1	1	1	1	1	1	1	1	1	1	1	1
	6-MAM	3	2	1	1	1	2	2	1	1	1	1	2	2	1	1	1	1	1
	6-MAM/DAM	3	2	1	1	1	2	3	1	1	1	1	3	3	1	1	1	1	1
	DAM	1	1	1	1	1	1	1	1	1	1	1	1	1	1	1	1	1	1
72	PNT	1	1	nd	nd	nd	2	1	nd	nd	nd	nd	1	1	nd	nd	nd	nd	nd
	CAFF	1	1	1	1	1	1	1	1	1	1	1	1	1	1	1	1	1	1
	EFV	1	1	1	1	1	1	1	1	1	1	1	1	1	1	1	1	1	1
	THCV	1	1	2	1	1	1	1	1	1	1	1	1	1	1	1	1	1	1
	CBV	2	1	1	1	2	1	1	1	1	1	1	1	1	1	1	1	1	3
	CBV/THCV	1	1	1	1	1	1	1	1	1	1	1	1	1	1	1	1	1	2
	CBCM	2	1	1	1	1	1	1	1	1	1	1	1	1	1	1	1	1	2
	CBD	2	1	2	nd	3	1	1	1	nd	nd	2	1	1	1	1	nd	nd	nd
	NVP	1	1	nd	1	nd	1	1	nd	1	1	nd	1	1	nd	nd	1	1	1
	Δ^9-THC	1	1	2	1	2	1	1	1	2	1	1	1	1	1	1	1	1	2
	ACOD	2	1	1	2	1	2	1	2	1	1	1	2	1	2	1	1	2	1
	CBN	2	1	2	1	2	1	1	1	1	1	1	1	2	1	1	1	1	2
	CBN/Δ^9-THC	1	1	1	1	1	1	1	1	1	1	1	1	1	1	1	1	1	1
	6-MAM	3	2	2	1	1	2	2	1	1	1	1	3	2	1	2	1	1	1
	6-MAM/DAM	3	2	1	1	1	2	3	1	1	1	1	3	3	1	2	1	1	1
	DAM	1	1	2	1	1	1	1	1	1	1	1	1	1	1	1	1	1	1

[1] *Where 1 denotes a change of 0–15% and considered stable, 2 denotes a change of 16– 30% and considered moderately stable and 3 denotes a change above 30% and considered unstable (Saar et al, 2012).*

nd = not detected

The average peak area ratios (PAR) for the three replicate analyses for each of the time intervals t =0, 24, 48 and 72 hours were determined for each of the 18 simulated nyaope

samples. Pooled average peak area ratios (PPAR) were determined by averaging the PARs at t = 0, 24, 48 and 72 hours. The PAR and the PPAR of the sub-samples S2 from Class 1, for the time intervals t =0, 24, 48 and 72 hours are given in Table 5.5. The PAR and the PPAR of the 18 simulated nyaope sapmles for the time intervals t =0, 24, 48 and 72 hours respectively are shown in Appendix VII a - d. ANOVA statistical analysis for the sub-samples S2, using the F-test (single factor) gave Fcalc = 0.0106, which is less than the critical value (Fcrit = 2.798), with the corresponding p-value = 0.998. The Fcalc, Fcrit and the corresponding p-values for the samples S1 – S18 are given in Table 5.6. The Fcalc values for all the samples were less than the corresponding Fcrit values, which show that there was no significant difference amongst the peak area ratios for the simulated nyaope sub-samples over the 72 hours of autosampler storage, confirming the stability of these sample for the time period.

Table 5.5: Average peak area ratios and the pooled average peak area ratios for the simulated nyaope sample, S2, at t = 0, 24, 48 and 72 hours of autosampler storage.

	0	24 h	48 h	72 h	PPAR	SD	%RSD (n = 4)
PNT	1,316	1,306	1,214	1,058	1,223	0,120	9,77
CAFF	0,445	0,438	0,424	0,415	0,430	0,014	3,16
EFV	3,939	3,967	3,965	3,646	3,879	0,156	4,02
THCV	0,203	0,215	0,210	0,188	0,204	0,012	5,84
CBV	0,025	0,027	0,029	0,023	0,026	0,003	10,24
CBCM	0,088	0,097	0,094	0,079	0,089	0,008	8,64
CBD	0,052	0,053	0,052	0,052	0,052	0,001	1,55
NVP	1,520	1,560	1,488	1,357	1,481	0,088	5,94
Δ^9-THC	6,003	6,184	6,496	6,134	6,205	0,209	3,37
ACOD	0,088	0,085	0,108	0,101	0,096	0,011	11,27
CBN	0,336	0,352	0,345	0,295	0,332	0,026	7,69
6-MAM	0,065	0,079	0,082	0,077	0,076	0,007	9,43
HER	2,234	2,217	2,168	2,142	2,190	0,043	1,95

Table 5.6: The F_{calc}, F_{crit} and corresponding p-values for the peak area ratios of each of the simulated nyaope samples S1–S18.

Class1				Class 2				Class 3			
Sample	**F_{Calc}**	**F_{Crit}**	**p-value**	**Sample**	**F_{Calc}**	**F_{Crit}**	**p-value**	**Sample**	**F_{Calc}**	**F_{Crit}**	**p-value**
S1	0.0106	2.798	0.998	**S3**	0.0206	2.839	0.996	**S4**	0.00237	2.839	1.000
S2	0.00554	2.798	0.999	**S5**	0.0166	2.839	0.997	**S9**	0.0171	2.839	0.997
S6	0.000231	2.798	1.000	**S8**	0.00073	2.839	1.000	**S10**	0.000242	2.839	1.000
S7	0.000578	2.798	1.000	**S11**	0.00173	2.839	1.000	**S16**	0.00581	2.839	0.999
S12	0.000427	2.798	1.000	**S14**	0.00110	2.839	1.000	**S17**	0.000616	2.839	1.000
S13	0.000267	2.798	1.000	**S15**	0.00241	2.839	1.000	**S18**	0.0199	2.839	0.996

The PPAR of simulated nyaope samples from Class 1, Class 2 and Class 3 are given in Tables 5.7, 5.8 and 5.9, respectively. ANOVA statistical analysis using the F-test (single factor) gave F_{calc} = 0.0268 < F_{crit} = 2.342, F_{calc} = 0.0461 < F_{crit} = 2.368 and F_{calc} = 0.0429 < F_{crit} = 2.368, respectively, with the corresponding p-values = 1.000, 0.999 and 0.999. The F_{calc} values for all the samples were less than the corresponding F_{crit} values, which demonstrates that there was no significant difference amongst the peak area ratios for the samples belonging to the same group over the 72-hour autosampler storage.

Table 5.7: Pooled average peak area ratios for the simulated nyaope samples from Class 1(S1, S2, S6, S7, S12 and S13).

	Class 1					
Sample	**S1**	**S2**	**S6**	**S7**	**S12**	**S13**
PNT	1,188	1,223	1,401	1,366	1,341	1,589
CAFF	0,378	0,430	0,379	0,371	0,388	0,419
EFV	3,742	3,879	4,206	2,678	3,609	5,357
THCV	0,205	0,204	0,195	0,227	0,204	0,188
CBV	0,021	0,026	0,024	0,028	0,025	0,023
CBCM	0,076	0,089	0,086	0,099	0,080	0,078
CBD	0,051	0,052	0,048	0,060	0,051	0,059
NVP	2,595	1,481	1,432	1,265	1,318	2,218
Δ^9-THC	6,235	6,205	6,118	7,017	6,323	6,332
ACOD	0,103	0,096	0,107	0,110	0,085	0,093
CBN	0,290	0,332	0,330	0,376	0,356	0,340
6-MAM	0,068	0,076	0,086	0,080	0,080	0,082
DAM	2,022	2,190	2,508	2,504	2,475	2,444

Table 5.8: Pooled average peak area ratios for the simulated nyaope samples from Class 2 (S3, S5, S8, S11, S14 and S15).

	Class 2					
Sample	**S3**	**S5**	**S8**	**S11**	**S14**	**S15**
CAFF	0,524	0,443	0,598	0,576	0,505	0,565
EFV	7,452	4,536	7,974	8,845	7,882	6,785
THCV	0,107	0,113	0,126	0,108	0,111	0,124
CBV	0,014	0,013	0,016	0,013	0,015	0,015
CBCM	0,168	0,165	0,204	0,176	0,180	0,198
CBD	0,044	0,039	0,055	0,046	0,047	0,042
Δ^9-THC	7,962	7,614	8,682	8,092	8,179	8,880
ACOD	0,094	0,090	0,108	0,106	0,103	0,086
CBN	0,836	0,801	1,035	0,880	0,999	1,043
6-MAM	0,270	0,231	0,322	0,307	0,274	0,306
DAM	1,953	1,561	2,315	2,279	1,927	2,187

Table 5.9: Pooled average peak area ratios for the simulated nyaope samples from Class 3 (S4, S9, S10, S16, S17 and S18).

	Class 3					
Sample	**S4**	**S9**	**S10**	**S16**	**S17**	**S18**
CAFF	0,233	0,120	0,207	0,149	0,207	0,173
EFV	4,931	3,670	3,930	3,609	5,474	4,430
THCV	0,210	0,210	0,184	0,198	0,217	0,196
CBV	0,026	0,025	0,022	0,026	0,026	0,023
CBCM	0,086	0,085	0,075	0,097	0,091	0,080
NVP	2,288	1,936	1,884	1,947	1,525	1,720
Δ^9-THC	3,047	3,028	2,745	3,129	3,171	2,950
ACOD	0,073	0,047	0,065	0,056	0,064	0,056
CBN	0,251	0,221	0,216	0,238	0,250	0,216
6-MAM	0,435	0,256	0,315	0,325	0,414	0,296
DAM	0,659	0,322	0,563	0,413	0,603	0,467

5.3.3 Comparison of chromatographic profiles between different batches of simulated nyaope samples over a 72-hour period

The chromatograms of the components from the three different batches (first batch (S1), second batch (S14) and third batch (S17)) were generated to compare the profiles of the compounds in these samples. An example of the chromatograms of the samples S1, in comparison with the samples S14 and S17 at t= 0, is displayed in Figure 5.6. The chromatograms displaying the comparison of S1 to S17 and S14 at t= 24, 48 and 72 hours, respectively are shown in Appendix VIII a - d. From these chromatograms it was demonstrated that the profiles between the batches can be differentiated even after 72 hours of autosampler storage.

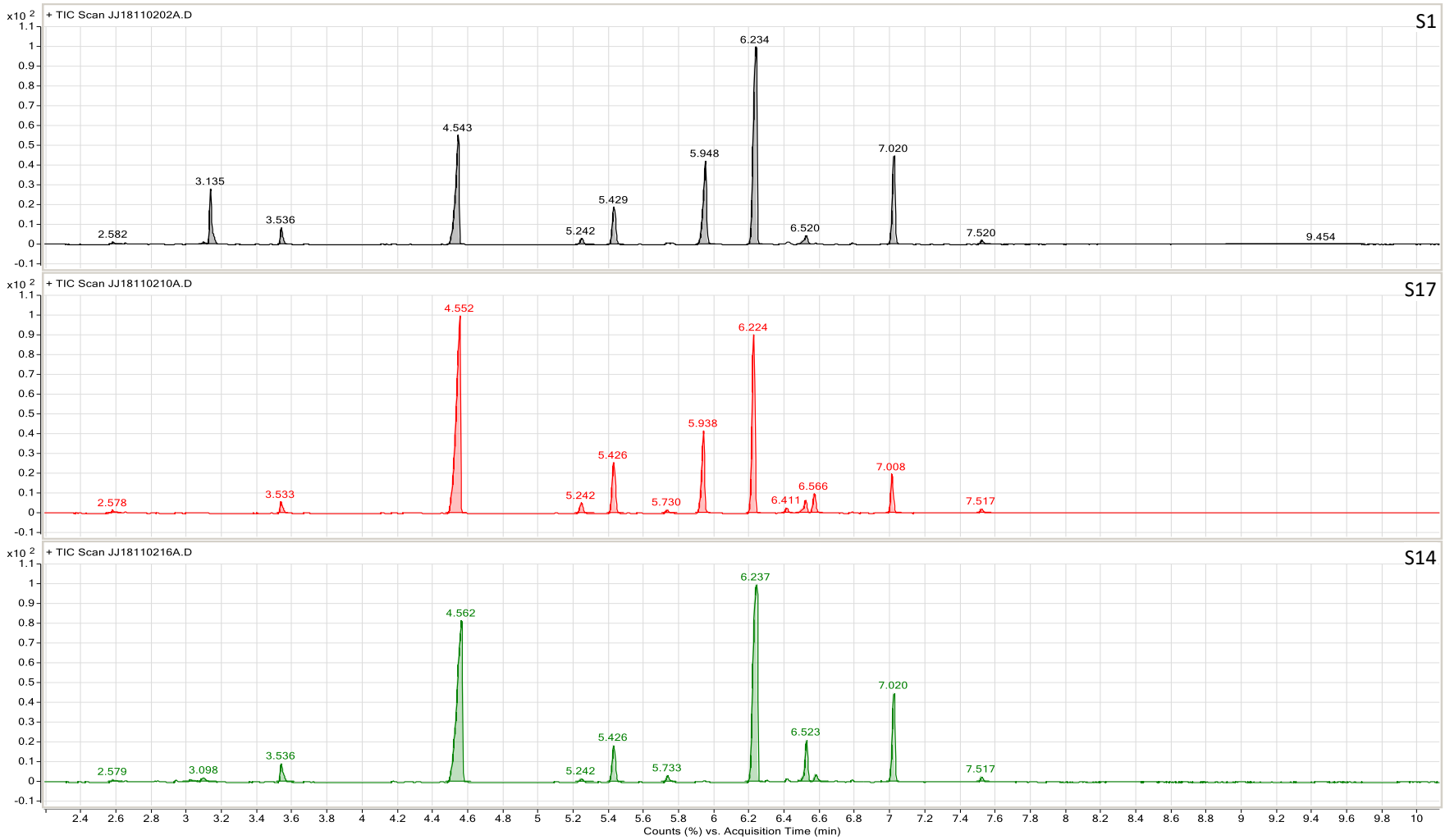

Figure 5.5: **Chromatograms showing the comparison of the samples for S1, S17 and S14 respectively at t=0 where identifications were: (2.582) caryophyllene, (3.135) phenacetin, (3.536) caffeine, (4.543) efavirenz, (5.242) tetrahydrocannabivarin, (5.429) tetracosane IS, (5.733) cannabichromene, (5.948) nevirapine, (6.234) Δ^9-THC, (6.411) cannabigerol, (6.520) cannabinol, (7.020) diamorphine, (7.520) nonacosane, (9.454) unknown in the first chromatogram (S1).**

5.3.4 Comparison of chromatographic profiles between simulated nyaope samples from the same batch over a 72-hour period

Chromatograms of members from the same group were compared to one another in order to determine whether samples from the same parent batch could be discriminated after 0, 24, 48, 72 hours of autosampler storage. An example of the chromatograms' comparing samples within the first batch (S1, S7, S13, S12, S6 and S2) is displayed in Figure 5.7. The chromatograms comparing samples within the second batch (S3, S5, S8, S11, S14 and S15) and within the third batch (S4, S9, S10, S16, S17 and S18) after 0, 24, 48 and 72 hours of autosampler storage are shown in Appendix IXa-c. From these chromatograms it was demonstrated that the profiles within the parent batch cannot be differentiated, even after 72 hours of autosampler storage. This confirms the stability of the components of nyaope up to 72 hours of autosampler storage when extracted with tertiary butyl alcohol as observed in Section 3.1.

5.3.5 Comparison of chromatographic profiles of a sub-sample within a batch in simulated nyaope samples over a 72-hour period

Chromatograms from one member of each of the three batches were compared at t= 0, 24, 48 and 72-hour time intervals to demonstrate whether or not the components could be identified over the 72-hour time period and whether their proportion changed or not. The chromatograms of the sample S1 from the first batch were compared after t= 0, 24, 48 and 72 hours and the profiles are displayed in Figure 5.8. Similar comparison of the samples S14 from the second batch and S17 from the third batch after t= 0, 24, 48 and 72 hours are displayed in Appendix X a-c. The %RSD for the PPAR was found to be < 20% for all the components in the 18 samples which indicates that the PAR of these components did not change significantly over the 72 hours' time period once extracted from the nyaope samples into the tertiary butyl alcohol. From these chromatographic profiles it was demonstrated that each component of the simulated nyaope sample can be identified and that their relative proportions do not change over a 72-hour time period once extracted from nyaope into tertiary butyl alcohol. This confirms the stability of these components up to 72 hours of

autosampler storage once extracted into tertiary butyl alcohol, as observed previously in Section 3.1.

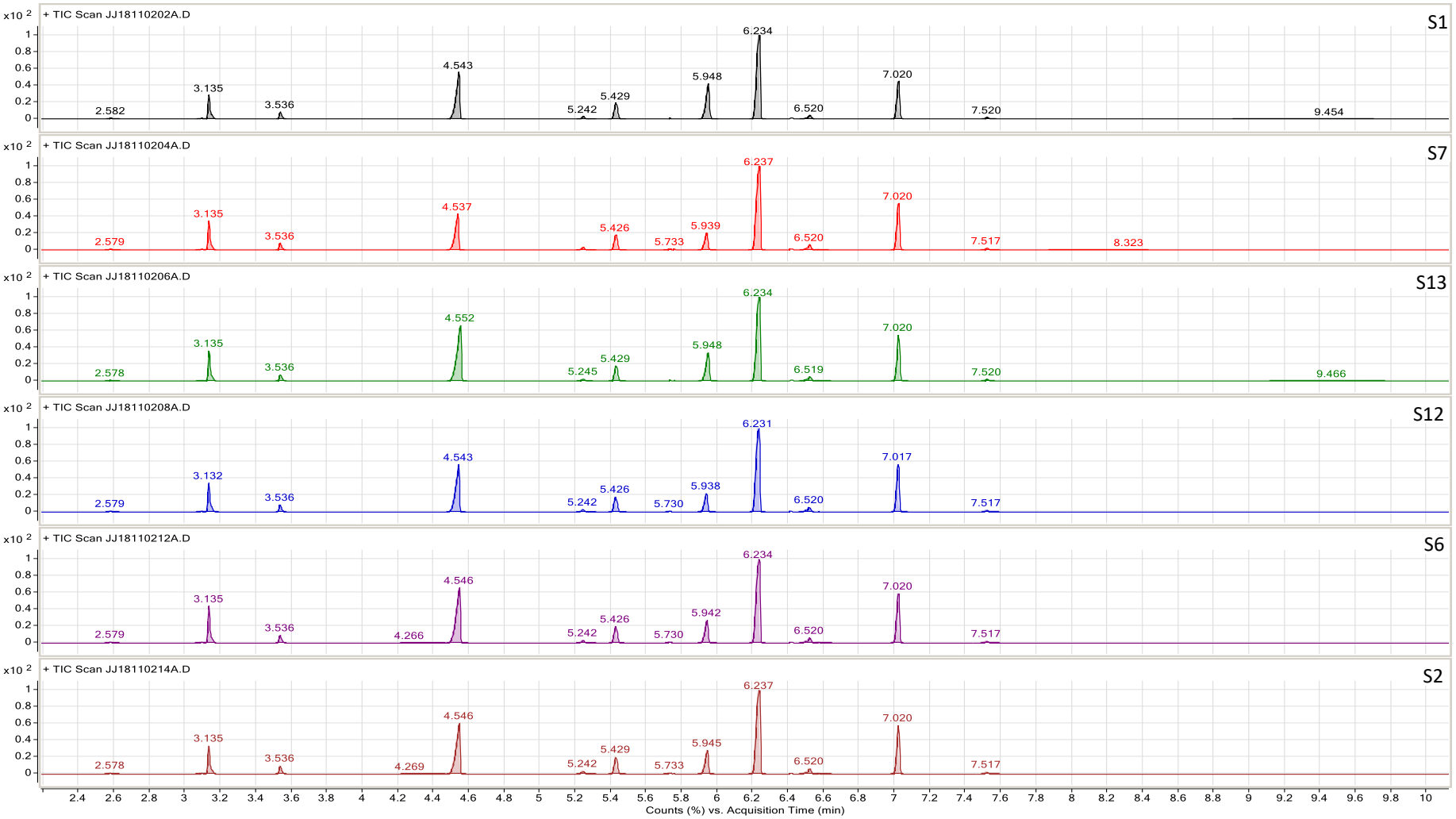

Figure 5.6: **Chromatograms showing the comparison of the samples S1, S7, S13, S12, S6 and S2 respectively within the same batch at t=0 where identifications were: (2.582) caryophyllene, (3.135) phenacetin, (3.536) caffeine, (4.543), efavirenz, (5.242) tetrahydrocannabivarin, (5.429) tetracosane IS, (5.733) cannabichromene, (5.948) nevirapine, (6.234) Δ^9-THC, (6.520) cannabinol, (7.02) diamorphine, (7.520) nonacosane and (9.454) unknown in the first chromatogram (S1).**

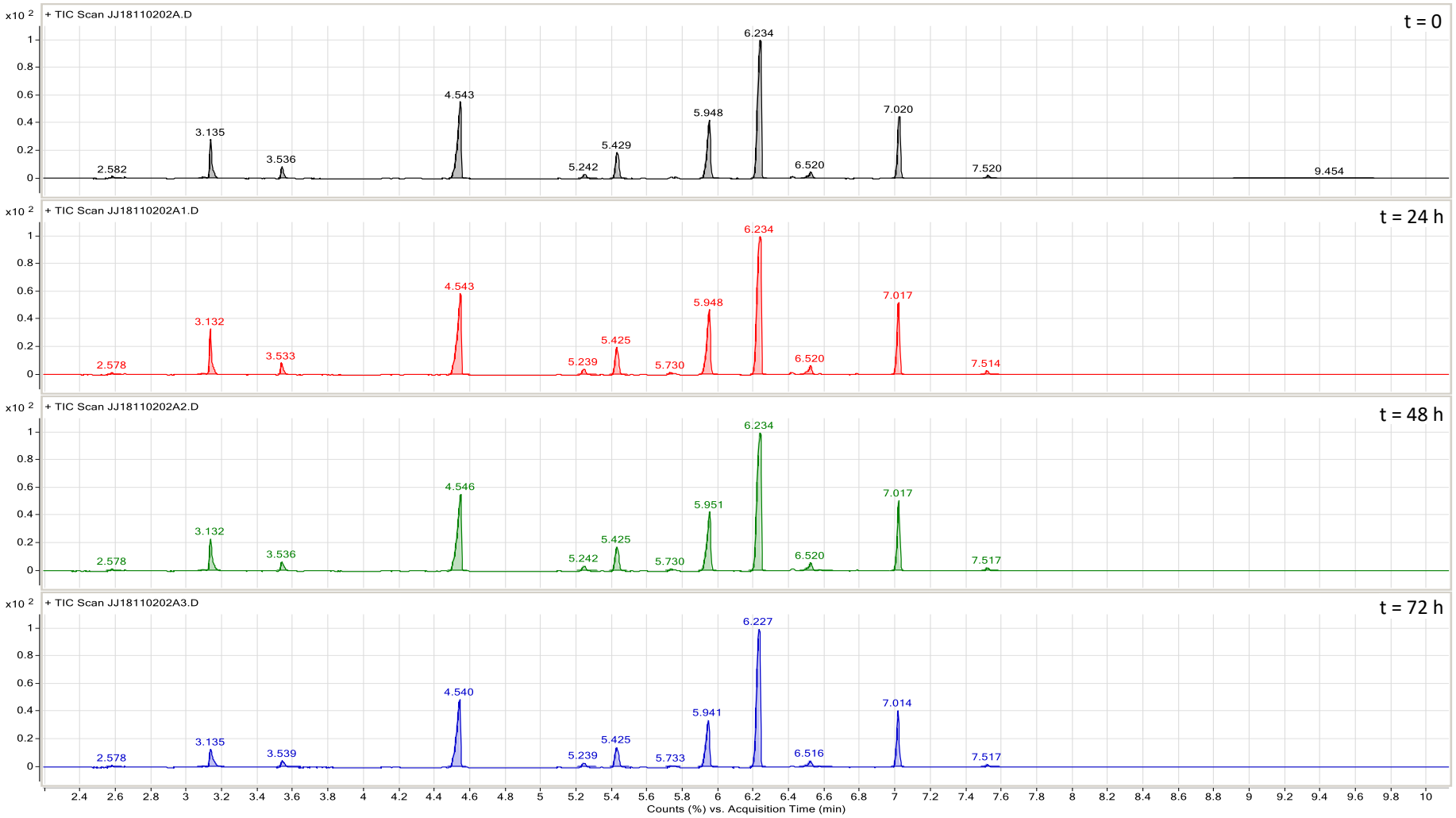

Figure 5.7: Chromatograms comparing samples of S1 after 0, 24, 48 and 72 hours respectively where identifications were: (2.582) caryophyllene, (3.135) phenacetin, (3.536) caffeine, (4.543), efavirenz, (5.242) tetrahydrocannabivarin, (5.429) tetracosane IS, (5.733) cannabichromene, (5.948) nevirapine, (6.234) Δ^9-THC, (6.520) cannabinol, (7.02) diamorphine, (7.520) nonacosane and (9.454) in the first chromatogram (t=0).

5.3.6 Concentration profiles of CAFF, DAM, EFV, NVP PNT and Δ^9-THC in simulated nyaope samples over a 72 hour period

Triplicate analyses of the 18 simulated nyaope samples were conducted and the average peak-area ratios were determined as discussed in Section 3.1. The calibration data given in Section 5.1 were used to determine the concentrations of CAFF, DAM, EFV, NVP PNT and Δ^9-THC using Equation 5.2. The concentrations were determined for each of the time intervals 0, 24, 48 and 72 hours, for each of the components CAFF, DAM, EFV, NVP PNT and Δ^9-THC. The difference in concentrations between the time intervals was evaluated using %RSD. Pooled average concentration was used to determine the %RSD, shown in Table 5.10. The average %RSD was found to be < 10% for all the components (CAFF, DAM, EFV, NVP, PNT and Δ^9-THC) in the 18 samples, which indicates that the concentrations of these components did not change significantly over the 72-hour time period once extracted from the nyaope samples into the tertiary butyl alcohol. This suggests that the components CAFF, DAM, EFV, NVP PNT and Δ^9-THC were stable for the 72 hours of autosampler stability, confirming the observation made in Section 3.1.

Table 5.10: Average concentrations (n = 4) of the components CAFF, DAM, EFV, NVP, PNT and Δ^9-THC in the simulated samples S1 – S18 (mg/L).

	CAFF					DAM					EFV					NVP					PNT					THC				
Time, hours	0	24	48	72	**%RSD**	0	24	48	72	**%RSD**	0	24	48	72	**%RSD**	0	24	48	72	**%RSD**	0	24	48	72	**%RSD**	0	24	48	72	**%RSD**
S1	0.28	0.30	0.29	0.28	**2.99**	1.56	1.60	1.53	1.52	**2.31**	3.19	3.51	3.35	3.39	**3.91**	2.54	2.56	2.45	2.48	**2.00**	0.99	1.07	1.09	1.11	**4.96**	2.82	2.89	2.76	2.91	**2.41**
S2	0.36	0.35	0.36	0.33	**3.49**	1.70	1.68	1.64	1.59	**2.74**	3.50	3.50	3.48	3.40	**1.34**	1.52	1.53	1.50	1.50	**0.97**	1.08	1.11	1.13	1.10	**1.91**	2.92	2.89	2.88	2.91	**0.70**
S6	0.26	0.28	0.28	0.29	**4.21**	1.75	1.77	1.73	1.74	**1.14**	3.57	3.69	3.63	3.73	**1.85**	1.37	1.41	1.40	1.45	**2.27**	1.23	1.28	1.29	1.34	**3.47**	2.63	2.63	2.64	2.69	**1.03**
S7	0.31	0.27	0.28	0.28	**5.55**	1.74	1.83	1.78	1.74	**2.53**	2.39	2.51	2.49	2.49	**2.14**	1.23	1.28	1.28	1.28	**2.02**	1.30	1.22	1.27	1.30	**2.99**	3.16	3.14	3.16	3.21	**0.95**
S12	0.29	0.30	0.29	0.29	**1.78**	1.80	1.81	1.76	1.69	**3.18**	3.08	3.24	3.15	3.17	**2.12**	1.26	1.34	1.30	1.29	**2.60**	1.18	1.25	1.22	1.25	**2.67**	2.65	2.79	2.79	2.79	**2.48**
S13	0.34	0.35	0.34	0.34	**1.69**	1.73	1.81	1.76	1.75	**2.00**	4.40	4.63	4.42	4.40	**2.47**	2.08	2.12	2.10	2.10	**0.86**	1.44	1.48	1.45	1.51	**2.23**	2.78	2.86	2.78	2.78	**1.44**
S4	< QL	< QL	< QL	< QL	**< QL**	0.54	0.53	0.53	0.52	**1.72**	4.27	4.08	4.13	4.14	**1.96**	2.19	2.15	2.16	2.14	**1.00**	nd	nd	nd	nd	**nd**	1.40	1.37	1.42	1.40	**1.55**
S9	< QL	< QL	< QL	< QL	**< QL**	0.25	0.24	0.23	0.22	**5.07**	3.43	3.36	3.42	3.31	**1.70**	1.97	1.95	1.93	1.90	**1.42**	nd	nd	nd	nd	**nd**	1.49	1.47	1.46	1.45	**1.13**
S10	< QL	< QL	< QL	< QL	**< QL**	0.47	0.46	0.45	0.42	**4.42**	3.50	3.42	3.47	3.34	**2.10**	1.86	1.86	1.83	1.76	**2.67**	nd	nd	nd	nd	**nd**	1.32	1.28	1.26	1.26	**2.14**
S16	< QL	< QL	< QL	< QL	**< QL**	0.35	0.32	0.32	0.30	**6.59**	3.30	3.22	3.26	3.10	**2.71**	1.97	1.90	1.92	1.86	**2.44**	nd	nd	nd	nd	**nd**	1.48	1.45	1.45	1.44	**1.33**
S17	< QL	< QL	< QL	< QL	**< QL**	0.46	0.48	0.46	0.44	**3.58**	4.34	4.36	4.52	4.27	**2.41**	1.47	1.47	1.47	1.48	**0.40**	nd	nd	nd	nd	**nd**	1.32	1.38	1.36	1.43	**3.48**
S18	< QL	< QL	< QL	< QL	**< QL**	0.39	0.40	0.38	0.37	**3.11**	4.01	3.96	3.91	3.97	**0.95**	1.80	1.75	1.72	1.77	**1.84**	nd	nd	nd	nd	**nd**	1.42	1.38	1.40	1.41	**1.21**
S3	0.48	0.50	0.50	0.50	**1.54**	1.67	1.62	1.55	1.57	**3.41**	6.48	6.36	6.33	5.40	**8.07**	nd	nd	nd	nd	**nd**	nd	nd	nd	nd	**nd**	4.20	3.83	3.95	3.92	**3.93**
S5	0.37	0.36	0.37	0.37	**1.17**	1.36	1.37	1.32	1.31	**2.20**	4.15	4.07	4.02	3.40	**8.82**	nd	nd	nd	nd	**nd**	nd	nd	nd	nd	**nd**	3.94	3.87	3.76	3.76	**2.35**
S8	0.58	0.59	0.57	0.58	**1.62**	1.90	1.77	1.77	1.72	**4.37**	6.64	6.69	6.51	5.52	**8.67**	nd	nd	nd	nd	**nd**	nd	nd	nd	nd	**nd**	4.54	4.43	4.23	4.23	**3.49**
S11	0.55	0.57	0.57	0.53	**3.77**	1.82	1.76	1.71	1.70	**3.22**	7.31	7.27	7.14	5.93	**9.55**	nd	nd	nd	nd	**nd**	nd	nd	nd	nd	**nd**	3.86	4.07	3.77	3.72	**3.97**
S14	0.45	0.47	0.47	0.45	**2.04**	1.48	1.53	1.42	1.43	**3.51**	6.54	6.56	6.51	5.49	**8.38**	nd	nd	nd	nd	**nd**	nd	nd	nd	nd	**nd**	4.05	4.05	3.81	3.79	**3.66**
S15	0.53	0.54	0.54	0.54	**1.42**	1.77	1.71	1.67	1.67	**2.86**	5.64	5.58	5.54	4.68	**8.54**	nd	nd	nd	nd	**nd**	nd	nd	nd	nd	**nd**	4.36	4.41	4.26	4.27	**1.66**

< QL = below quantitation limit
nd = not detected

5.3.7 Chemometric treatment of simulated nyaope data

Two unsupervised chemometric methods, principal component analysis (PCA) and hierarchical clustering (HCA), were used for the analysis of average concentrations of CAFF, DAM, EFV, NVP PNT and Δ^9-THC using the XLSTAT software (Addinsoft, 2019). The average concentration of CAFF, DAM, EFV, NVP, PNT and Δ^9-THC for each of the 18 simulated nyaope samples at each of the time intervals t= 0, 24, 48, and 72 hours, were analysed with both HCA and PCA.

5.3.7.1 Hierarchical clustering analysis of simulated nyaope samples

HCA, using agglomerative clustering and unweighted linkage, was conducted on the average concentration of CAFF, DAM, EFV, NVP PNT and Δ^9-THC for each of the 18 simulated nyaope samples at each of the time interval t= 0, 24, 48, and 72 hours. Hierarchical clustering analysis performed on the simulated nyaope samples using Euclidean distance and average linkage indicated that the data can be clustered into three classes, namely (i) Class 1 associated with sample S2, (ii) Class 2 associated with sample S3, and (ii) Class 3 associated with sample S18. The classes were each made up of six samples. The matrix generated for the samples at t = 0, 24, 48 and 72 hours are shown in Table 5.11. The matrices have zero values on the diagonal and are symmetric. As discussed in Section 1.8.3, the symmetric matrix indicates that the HCA method was suitable in discriminating the simulated nyaope samples into different classes. The matrices demonstrate that there was a maximum distance between Class 2 and Class 3, and a minimum distance between Class 1 and Class 3.

Table 5.11: Matrices showing distances between central objects at t = 0, 24, 48 and 72 hours for the simulated nyaope samples S2, S3 and S18.

		t = 0				t = 24h	
Class	**1 (S2)**	**2 (S3)**	**3 (S18)**	**Class**	**1 (S2)**	**2 (S3)**	**3 (S18)**
1 (S2)	0	3.74	2.37	**1 (S2)**	0	3.56	2.35
2 (S3)	3.74	0	4.35	**2 (S3)**	3.56	0	4.07
3 (S18)	2.37	4.35	0	**3 (S18)**	2.35	4.07	0
		t = 48h				**t = 72h**	
Class	**1 (S2)**	**2 (S3)**	**3 (S18)**	**Class**	**1 (S2)**	**2 (S3)**	**3 (S18)**
1 (S2)	0	3.58	2.33	**1 (S2)**	0	2.92	2.34
2 (S3)	3.58	0	4.12	**2 (S3)**	2.92	0	3.63
3 (S18)	2.33	4.12	0	**3 (S18)**	2.34	3.63	0

The dendrograms of the simulated nyaope samples analysed at each of the time interval t= 0, 24, 48, and 72 hours of autosampler storage as shown in Figure 5.8 demonstrate that HCA has successfully discriminated the simulated nyaope samples. The simulated samples were discriminated into the first batch (S1, S2, S6, S7, S12 and S13), the second batch (S3, S5, S8, S11, S14 and S15), and the third batch (S4, S9, S10, S16, S17 and S18), similar to the observation made with chromatographic profiles. The HCA further demonstrated that the simulated nyaope samples can still be discriminated even after 72 hours of autosampler storage which confirms that the samples are the stable for 72 hours once extracted into tertiary butyl alcohol.

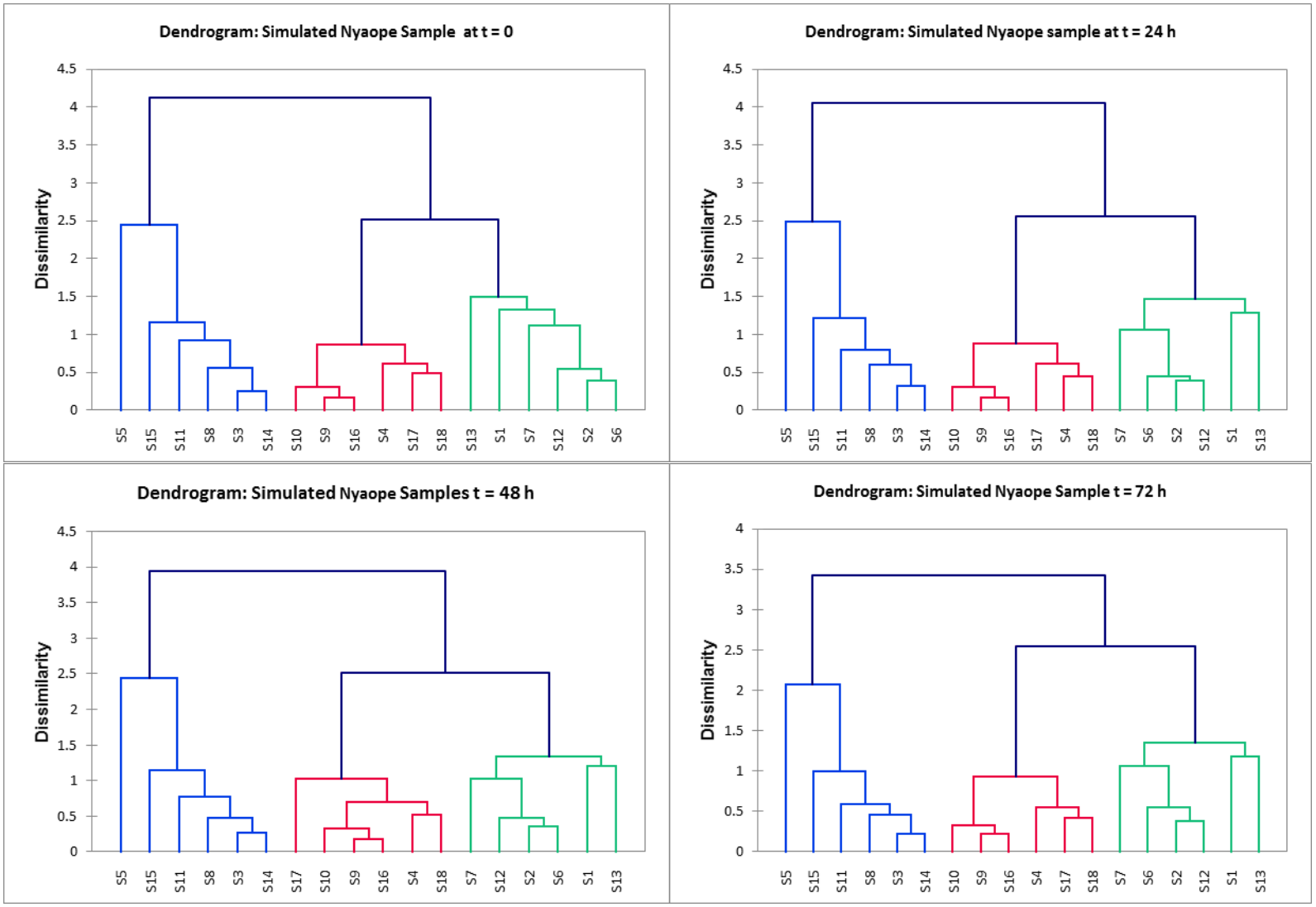

Figure 5.8: Dendrogram of the simulated nyaope samples S1–S18 analysed by HCA using unweighted linkage and Euclidean distance for the time interval t = 0, 24, 48 and 72 hours, respectively.

5.3.7.2 Principal Component Analysis of simulated nyaope samples

PCA analysis was conducted on the average concentration of CAFF, DAM, EFV, NVP PNT and Δ^9-THC for each of the 18 simulated nyaope samples at each of the time interval t= 0, 24, 48, and 72 hours. In order to show that the PCA method is appropriate for the discrimination of the samples by demonstrating that (i) there is a linear combination between the principal components, (ii) the principal components are orthogonal, and (iii) the variance can be explained by the components with large variance. The correlation matrices for the time interval t = 0, 24, 48 and 72 hours are shown in Table 5.12. All the values are different from zero, with a significant level $\alpha = 0.95$ (two-tailed), which indicates that there is a linear correlation between the variables. A positive correlation was observed between CAFF and DAM, CAFF and EFV, CAFF and PNT; CAFF and Δ^9-THC, DAM and EFV, DAM and PNT, DAM and Δ^9-THC; EFV and Δ^9-THC; NVP and PNT, PNT and Δ^9-THC. A negative correlation was observed between CAFF and NVP, DAM and NVP, EFV and NVP, EFV and PNT, NVP and Δ^9-THC. The same correlation pattern is observed up to 72 hours of autosampler storage. The transpose of these correlation matrices are identical to the matrices themselves; as a result, their product is an identity matrix. This proves that the principal components are orthogonal. The principal component analysis indicates that there are six principal components, F1, F2, F3, F4, F5 and F6 that explain the variability of the variables CAFF, DAM; EFV, NVP, PNT and Δ^9-THC. The scree plot for the time interval 0, 24 48 and 72 hours is shown in Figure 5.9. Each plot displays an exponential decline towards zero for the principal components F1, F2, F3, F4, F5 and F6. The plots also indicate that the principal components F1 and F2 show the largest variances, while F3, F4, F5 and F6 show low variances.

The eigenvalues and variability (%) are shown in Table 5.13 and indicates values greater than 1.00 for the principal components F1 and F2, with variability of 65.63% and 28.76% (t = 0). The total percentage (94.39%) is more than the minimum 70%; therefore, F1 and F2 are sufficient to explain the variability of the data set. The factor loadings (coefficients) are shown in Table 5.14. Considering values greater than 0.300, the principal component F1 explains the variable of CAFF, DAM; EFV, NVP and Δ^9-THC; F2 explains the variability of DAM, EFV and PNT; while F3 only explains the variability of EFV. This further demonstrates that the first two principal components F1and F2 are sufficient to explain the variability of the data set. The

assumptions mentioned in Section 1.8.6 are satisfied and therefore the performance of the method is acceptable.

Table 5.12: Pearson correlation matrices at t = 0, 24, 48 and 72 hours for the components CAFF, DAM, EFV, NVP PNT and Δ^9-THC in the simulated nyaope samples S1 – S18.

			t = 0							t = 24h				
Variables	CAFF	DAM	EFV	NVP	PNT	Δ^9 -THC	Variables	CAFF	DAM	EFV	NVP	PNT	Δ^9 -THC
CAFF	**1**	**0.908**	**0.642**	**-0.776**	**0.137**	**0.974**	CAFF	**1**	**0.877**	**0.703**	**-0.758**	**0.125**	**0.978**
DAM	**0.908**	**1**	**0.339**	**-0.533**	**0.516**	**0.839**	DAM	**0.877**	**1**	**0.349**	**-0.468**	**0.564**	**0.835**
EFV	**0.642**	**0.339**	**1**	**-0.757**	**-0.520**	**0.642**	EFV	**0.703**	**0.349**	**1**	**-0.756**	**-0.453**	**0.666**
NVP	**-0.776**	**-0.533**	**-0.757**	**1**	**0.368**	**-0.840**	NVP	**-0.758**	**-0.468**	**-0.756**	**1**	**0.408**	**-0.816**
PNT	**0.137**	**0.516**	**-0.520**	**0.368**	**1**	**0.019**	PNT	**0.125**	**0.564**	**-0.453**	**0.408**	**1**	**0.047**
Δ^9 -THC	**0.974**	**0.839**	**0.642**	**-0.840**	**0.019**	**1**	Δ^9 -THC	**0.978**	**0.835**	**0.666**	**-0.816**	**0.047**	**1**
			t = 48h							**t = 72h**			
Variables	CAFF	DAM	EFV	NVP	PNT	Δ^9 -THC	Variables	CAFF	DAM	EFV	NVP	PNT	Δ^9 -THC
CAFF	**1**	**0.874**	**0.667**	**-0.776**	**0.122**	**0.977**	CAFF	**1**	**0.884**	**0.595**	**-0.771**	**0.125**	**0.981**
DAM	**0.874**	**1**	**0.303**	**-0.475**	**0.566**	**0.842**	DAM	**0.884**	**1**	**0.290**	**-0.471**	**0.556**	**0.858**
EFV	**0.667**	**0.303**	**1**	**-0.759**	**-0.498**	**0.616**	EFV	**0.595**	**0.290**	**1**	**-0.645**	**-0.437**	**0.512**
NVP	**-0.776**	**-0.475**	**-0.759**	**1**	**0.399**	**-0.823**	NVP	**-0.771**	**-0.471**	**-0.645**	**1**	**0.412**	**-0.801**
PNT	**0.122**	**0.566**	**-0.498**	**0.399**	**1**	**0.069**	PNT	**0.125**	**0.556**	**-0.437**	**0.412**	**1**	**0.089**
Δ^9 -THC	**0.977**	**0.842**	**0.616**	**-0.823**	**0.069**	**1**	Δ^9 -THC	**0.981**	**0.858**	**0.512**	**-0.801**	**0.089**	**1**

Values in bold are different from 0 with a significance level alpha=0.95 (two-tailed)

Table 5.13: Eigenvalues, percentage variability and percentage cumulative variance of the principal components F1, F2, F3, F4, F5 and F6 of the simulated nyaope samples S1–S18 at t = 0, 24, 48 and 72 hours.

	t =0			t = 24h			t = 48h			t = 72h		
PC	Eigen-value	Variability (%)	Cumulative variance (%)	Eigen-value	Variability (%)	Cumulative variance (%)	Eigen-value	Variability (%)	Cumulative variance (%)	Eigen-value	Variability (%)	Cumulative variance (%)
F1	3.938	65.63	65.63	3.918	65.29	65.29	3.886	64.77	64.77	3.780	63.01	63.01
F2	1.725	28.76	94.39	1.737	28.96	94.25	1.783	29.71	94.48	1.745	29.08	92.08
F3	0.236	3.93	98.31	0.259	4.32	98.57	0.251	4.18	98.66	0.392	6.54	98.62
F4	0.079	1.31	99.63	0.070	1.17	99.74	0.063	1.05	99.71	0.068	1.13	99.75
F5	0.016	0.27	99.90	0.009	0.15	99.89	0.010	0.17	99.88	0.008	0.14	99.89
F6	0.006	0.10	100.00	0.007	0.11	100.00	0.007	0.12	100.00	0.007	0.11	100.00

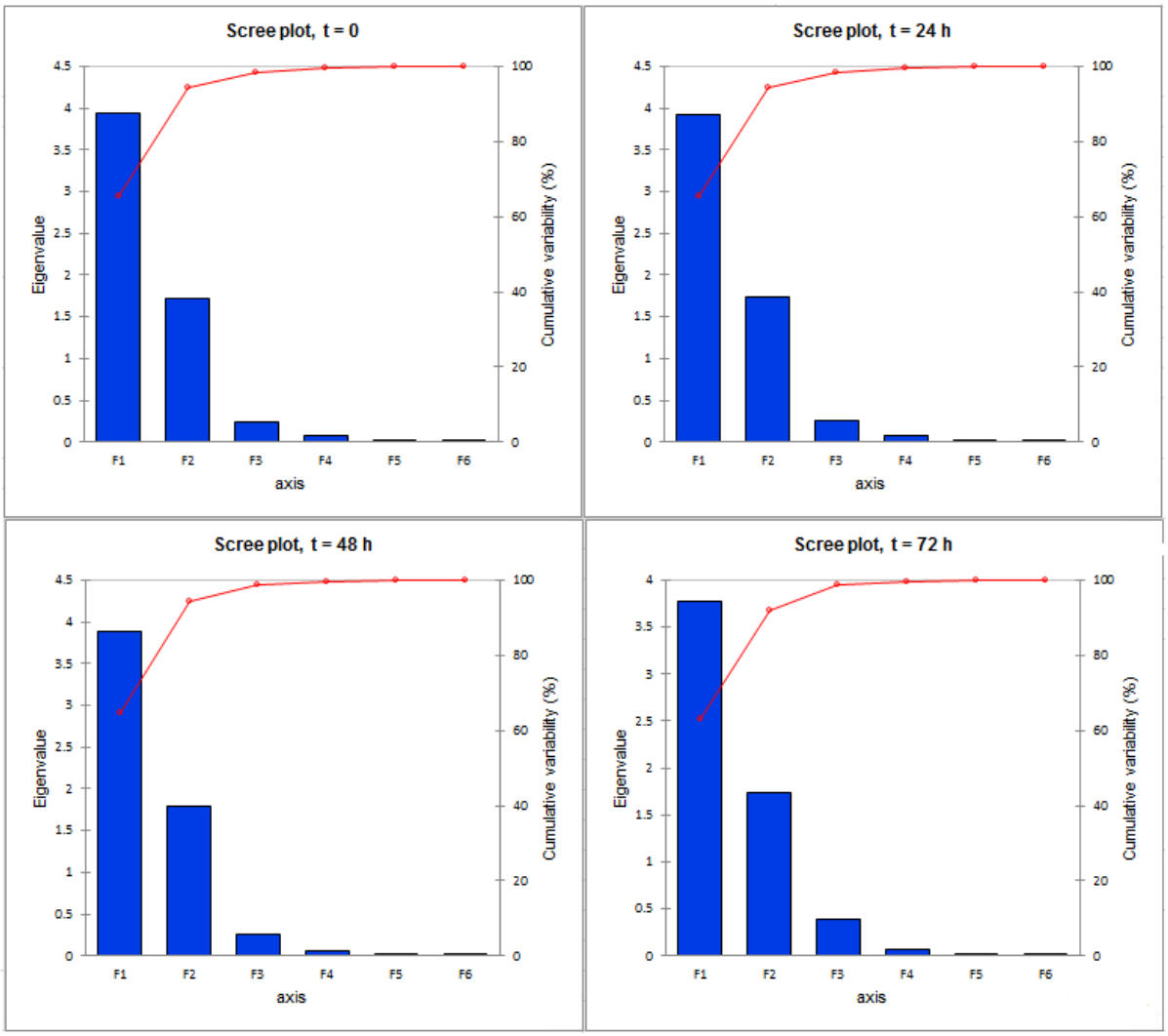

Figure 5.9: Principal component analysis scree plot at t = 0, 24, 48, 72 hours for the simulated nyaope samples S1 – S18.

Table 5.14: Principal components Loadings (coefficients) and their percentage contributions for the components CAFF, DAM, EFV, NVP PNT and Δ^9-THC in the simulated nyaope samples S1 – S18.

	t = 0												t = 24h											
	CAFF		DAM		EFV		NVP		PNT		Δ^9 -THC		CAFF		DAM		EFV		NVP		PNT		Δ^9 -THC	
PC	Loading	% Contr.	Loading	% Contr.	Loading	% Contr.	Loading	% Contr.	Loading	% Contr.	Loading	% Contr.	Loading	% Contr.	Loading	% Contr.	Loading	% Contr.	Loading	% Contr.	Loading	% Contr.	Loading	% Contr.
F1	**0.975**	24.12	**0.819**	17.05	**0.758**	14.60	**-0.887**	19.97	-0.049	0.06	**0.976**	24.20	**0.980**	24.52	**0.801**	16.37	**0.783**	15.67	**-0.864**	19.04	-0.030	0.02	**0.977**	24.39
F2	0.195	2.20	**0.563**	18.39	**-0.531**	16.34	0.326	6.17	**0.986**	56.40	0.091	0.48	0.161	1.49	**0.594**	20.29	**-0.474**	12.94	**0.381**	8.35	**0.990**	56.36	0.099	0.57
F3	0.035	0.53	0.047	0.93	**0.371**	58.56	0.273	31.60	0.086	3.15	-0.111	5.22	0.046	0.82	0.004	0.01	**0.395**	60.35	0.285	31.45	0.081	2.51	-0.112	4.86
F4	0.082	8.61	-0.020	0.49	-0.068	5.87	0.181	41.44	-0.115	16.76	0.145	26.83	0.084	10.12	-0.030	1.29	-0.068	6.63	0.166	38.98	-0.106	15.96	0.138	27.02
F5	0.012	0.92	0.087	47.16	-0.023	3.20	0.008	0.38	-0.061	23.16	-0.064	25.18	-0.004	0.21	0.071	56.56	-0.010	1.05	0.012	1.56	-0.047	25.14	-0.037	15.49
F6	-0.063	63.62	0.032	15.97	0.009	1.42	0.005	0.44	-0.005	0.46	0.034	18.08	0.066	62.84	-0.019	5.49	-0.015	3.36	-0.007	0.63	0.001	0.00	-0.044	27.68

	t = 48h												t = 72h											
PC	CAFF		DAM		EFV		NVP		PNT		Δ^9 -THC		CAFF		DAM		EFV		NVP		PNT		Δ^9 -THC	
PC	Loading	% Contr.	Loading	% Contr.	Loading	% Contr.	Loading	% Contr.	Loading	% Contr.	Loading	% Contr.	Loading	% Contr.	Loading	% Contr.	Loading	% Contr.	Loading	% Contr.	Loading	% Contr.	Loading	% Contr.
F1	**0.981**	24.74	**0.799**	16.43	**0.754**	14.63	**-0.875**	19.72	-0.029	0.02	**0.975**	24.45	**0.987**	25.74	**0.830**	18.22	**0.672**	11.96	**-0.849**	19.06	0.010	0.00	**0.973**	25.02
F2	0.157	1.39	**0.595**	19.83	**-0.526**	15.53	**0.369**	7.62	**0.988**	54.79	0.122	0.84	0.125	0.90	**0.551**	17.38	**-0.533**	16.30	**0.404**	9.36	**0.982**	55.32	0.115	0.75
F3	0.042	0.70	0.033	0.42	**0.389**	60.35	0.266	28.20	0.097	3.79	-0.128	6.53	0.003	0.00	0.050	0.64	**0.512**	66.84	0.288	21.09	0.149	5.63	-0.151	5.79
F4	0.086	11.78	-0.028	1.20	-0.054	4.55	0.164	42.62	-0.102	16.44	0.121	23.40	0.084	10.34	-0.026	0.96	-0.035	1.77	0.183	49.17	-0.104	16.07	0.121	21.68
F5	-0.008	0.70	0.076	57.98	-0.012	1.44	0.010	0.98	-0.050	24.96	-0.037	13.94	0.010	1.22	0.064	48.10	-0.013	2.02	0.009	0.97	-0.042	21.18	-0.047	26.51
F6	0.066	60.69	-0.017	4.13	-0.016	3.50	-0.008	0.85	0.000	0.00	-0.047	30.84	0.064	61.80	-0.031	14.70	-0.009	1.12	-0.005	0.35	0.011	1.80	-0.036	20.24

%Contr. = percentage contribution

Values in bold are the most significant factor loadings

Figure 5.10 displays the observation axis of the 18 simulated nyaope samples analysed after 0, 24, 48 and72 hours of autosampler storage. As indicated in Figure 5.10, PCA has discriminated samples into the first batch consisting of the samples S1, S2, S6, S7, S12 and S13; the second batch consisting of the samples S3, S5, S8, S11, S14 and S15; and the third batch consisting of the samples S4, S9, S10, S16, S17and S18. These are the same batches observed using chromatographic profiles (Sections 5.3.3, 5.3.4 and 5.3.5), as well HCA clustering. The PCA further demonstrated that the simulated nyaope samples can still be discriminated even after 72 hours of autosampler storage which confirms that the samples are stable for 72 hours once extracted into tertiary butyl alcohol.

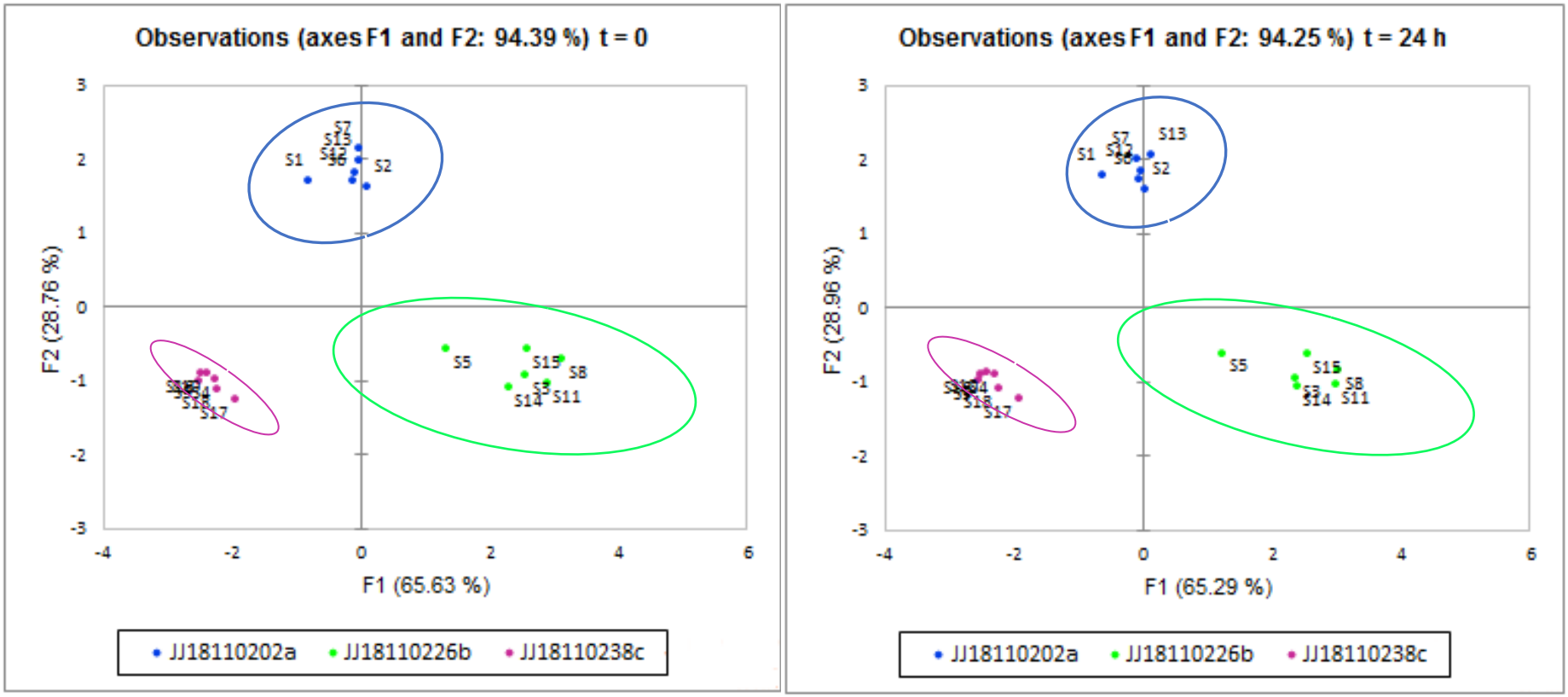

Figure 5.10: Observation axis for the simulated nyaope samples S1–S18 analysed by PCA for the time interval t = 0 and 24 hours, respectively.

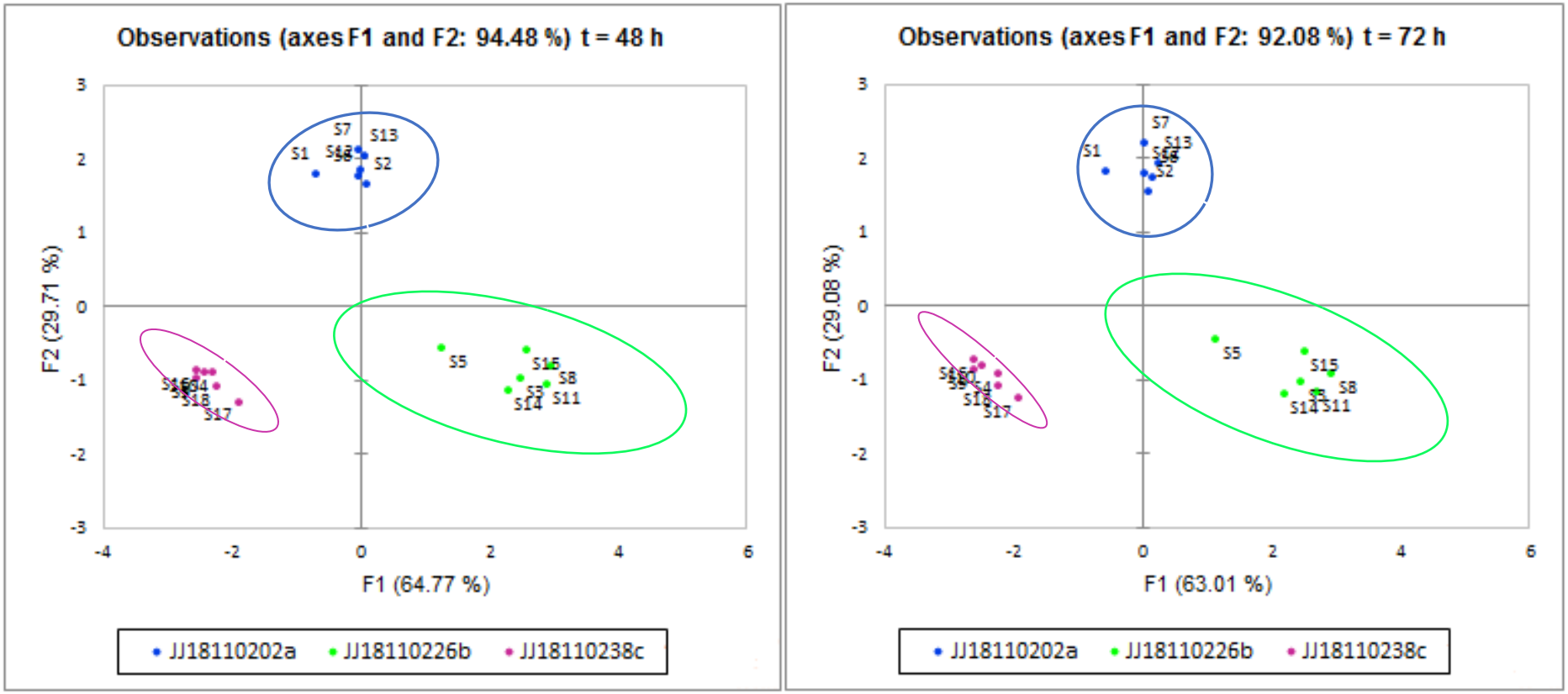

Figure 5.10 *cont'd*: Observation axis for the simulated nyaope samples S1–S18 analysed by PCA for the time interval t = 48 and 72 hours, respectively.

5.3.8 Compound identification – stability of retention time of simulated samples

The RRT of the individual components ACOD, CAFF, CBCM, CBD, CBG, CBN, CBV, DAM, EFV, 6-MAM, NVP, PNT, Δ^9-THC and THCV was determined for the 18 simulated nyaope samples. The relatively standard deviation for the relative retention times (RRT) of these compounds shown in Table 5.15 are all below 0.5%, illustrating the stability of this parameter. Identification of components of nyaope can therefore be made on the basis of RRT and the mass spectrum of each separated compound.

Table 5.15: Relative retention times of individual components for the simulated nyaope samples S1 – S18 (tetracosane IS = 1.000).

	S1	S2	S6	S7	S12	S13	S4	S9	S10	S16	S17	S18	S3	S5	S8	S11	S14	S15	Aver	SD	%RSD
PHEN	0.58	0.58	0.58	0.58	0.58	0.58	-	-	-	-	-	-	-	-	-	-	-	-	0.58	0.0005	**0.0948**
CAFF	0.65	0.65	0.65	0.65	0.65	0.65	0.65	0.65	0.65	0.65	0.65	0.65	0.65	0.65	0.65	0.65	0.65	0.65	0.65	0.000373	**0.0588**
EFV	0.84	0.84	0.84	0.84	0.84	0.84	0.84	0.84	0.84	0.84	0.84	0.84	0.84	0.84	0.84	0.84	0.84	0.84	0.84	0.001795	**0.2202**
THCV	0.97	0.97	0.97	0.97	0.97	0.97	0.97	0.97	0.97	0.97	0.97	0.97	0.97	0.97	0.97	0.97	0.97	0.97	0.97	0.000416	**0.0443**
CBV	1.03	1.03	1.03	1.03	1.03	1.03	1.03	1.03	1.03	1.03	1.03	1.03	1.03	1.03	1.03	1.03	1.03	1.03	1.03	0.000229	**0.023**
CBCM	1.06	1.06	1.06	1.06	1.06	1.06	1.06	1.06	1.06	1.06	1.06	1.06	1.06	1.06	1.06	1.06	1.06	1.06	1.06	0.000229	**0.0223**
CBD	1.06	1.06	1.06	1.06	1.06	1.06	-	-	-	-	-	-	1.06	1.06	1.06	1.06	1.06	1.06	1.06	0.001027	**0.1013**
NVP	1.10	1.10	1.10	1.09	1.10	1.10	1.10	1.09	1.09	1.09	1.09	1.09	-	-	-	-	-	-	1.10	0.000745	**0.0711**
Δ^9-THC	1.15	1.15	1.15	1.15	1.15	1.15	1.15	1.15	1.15	1.15	1.15	1.15	1.15	1.15	1.15	1.15	1.15	1.15	1.15	0.001599	**0.1432**
CBG	1.18	1.18	1.18	1.18	1.18	1.18	1.18	1.18	1.18	1.18	1.18	1.18	1.18	1.18	1.18	1.18	1.18	1.18	1.18	0.000731	**0.0637**
ACOD	1.20	1.20	1.20	1.20	1.20	1.20	1.20	1.20	1.20	1.20	1.20	1.20	1.20	1.20	1.20	1.20	1.20	1.20	1.20	0.000687	**0.0591**
CBN	1.20	1.20	1.20	1.20	1.20	1.20	1.20	1.20	1.20	1.20	1.20	1.20	1.20	1.20	1.20	1.20	1.20	1.20	1.20	0.000687	**0.0589**
6-MAM	1.21	1.21	1.21	1.21	1.21	1.21	1.21	1.21	1.21	1.21	1.21	1.21	1.21	1.21	1.21	1.21	1.21	1.21	1.21	0.000803	**0.0683**
DAM	1.29	1.29	1.29	1.29	1.29	1.29	1.29	1.29	1.29	1.29	1.29	1.29	1.29	1.29	1.29	1.29	1.29	1.29	1.29	0.001181	**0.0941**

5.4 ACTUAL SEIZED STREET NYAOPE SAMPLES

Five actual seized street nyaope samples marked A (LAB25142), B (LAB25209), C (LAB34000), D (LAB379599) and E (LAB503909) as displayed in Figure 5.11 were homogenised as described in Section 2.3. The homogenised street samples were then further divided into three sub-samples each to give a total of 15 samples marked A1, A2, A3, B1, B2, B3, C1, C2, C3, D1, D2, D3 E1, E2, and E3, with corresponding laboratory numbers indicated in Table 5.12. The samples with masses shown in Table 5.16 were extracted with 3 mL of the mixed internal standard and tertiary butyl alcohol solution in a 20 mL head space vial. The samples were analysed in triplicate using the GC-MS method described in Section 2.4 without dilution, after storage intervals of 0, 24, 48 and 72 hours on the autosampler to confirm observations made in Section 3.1.

Figure 5.11: Pictures of actual seized street nyaope samples A, B, C, D and E respectively (Photos are by the author).

Table 5.16: The masses of the actual seized street nyaope samples used in the study.

Sample	Mass (mg)	Sample	Mass (mg)
A1 (2514202)	36.7	**D1 (37959902)**	31.6
A2 (2514204)	38.2	**D2 (37959904)**	34.1
A3 (2514206)	38.5	**D2 (37959906)**	34.5
B1 (2520902)	29.4	**E1 (50390902)**	37.6
B2 (2520904)	29.8	**E2 (50390904)**	38.2
B3 (2520906)	32.4	**E3 (50390906)**	37.9
C1 (3400002)	22.5		
C2 (3400004)	22.3		
C3 (3400006)	22.5		

The five samples analysed contained the components CAFF, CBCM, CBN, NCT, Δ^9-THC and THCV. Sample A, C, D and E contained ACOD, COD, DAM and 6-MAM in addition to these components. Methaqualone was identified in sample A, B and D only. Interestingly, sample B, although submitted as nyaope, did not contain DAM or any of the opiate-related substances (ACOD, COD, 6-MAM). The sample contained cannabinoids and methaqualone, confirming the existence of a popular method of a mixture of cannabis and methaqualone in South Africa called the 'white pipe'. ACA and DTM were only identified in sample A, while vitamin E was identified in both samples D and E. The components identified in the actual seized street nyaope samples are summarised in Table 5.17.

Table 5.17: Components identified in the samples A (LAB25142), B (LAB25209), C (LAB34000), D (LAB379599) and E (LAB503909) respectively.

Sample number / Component	LAB25142	LAB25209	LAB34000	LAB379599	LAB503909
bulnesol	×	√	×	×	×
acetaminophen	√	×	×	×	×
acetylcodeine	×	×	√	√	×
caffeine,	√	√	√	√	√
cannabichromene	√	√	√	×	×
cannabicoumaronone	×	√	√	×	×
cannabidiol	×	×	×	√	×
cannabigerol	√	√	×	√	×
cannabinol	√	√	×	×	×
cannabivarin	×	√	×	×	×
cocaine	×	×	√	×	×
codeine	×	×	×	√	×
diamorphine	√	×	√	√	√
methaqualone	×	√	×	√	√
6-monoacetylmorphine	√	×	√	√	√
nicotine	×	√	×	√	√
nonacosane	√	√	×	√	×
tetrahydrocannabivarin	√	√	√	√	×
Δ^9-THC	√	√	√	√	√
Vitamin E	×	×	×	√	×

√ = detected

× = not detected

5.4.1 Stability evaluation of identified components based on average response ratios

Normalised average response ratios were determined in a similar manner as discussed in Section 3.1 in order to evaluate the stabilities of the main components in actual seized street nyaope samples. The stabilities of the main components are summarised in Table 5.18 for the actual seized street samples, where 1 denotes a decrease of 0– 5% and considered stable; 2 denotes a decrease of 15–30% and considered moderately stable; and 3 denotes a loss above 30% and considered unstable (Saar et al, 2012).

The components CAFF, THCV, CBV, Δ^9-THC, CBN and DAM were found to be stable after 72 hours of autosampler storage, confirming the observation made previously in Section 3.1. The component ACA, identified only in sample A (Table 5.17), was shown to be moderately stable in two out of the three sub-samples of A. The third sample of A was shown to be unstable after 48 hours of storage. NCT was shown to be stable for 72 hours in all the sub-samples of B, D and E and unstable after 24 hours in samples A and C where the abundance is very low and therefore affected by background response. DAM (identified in samples A, C, D, and E), DTM (identified only in the sample A), COC (identified only in sample C), MTQ (identified in samples A, B and D) and vitamin E (identified in sample D and E) as indicated in Table 5.17, were all stable for 72 hours. CAFF, THCV, and Δ^9-THC were stable up to 72 hours for all the samples. The ratios CBV/THCV confirms the stability of THCV for the samples A, B and C and indictes THCV and CBV to be unstable after 24 hours in D. This may be because CBV was present at low abundance in sample D and therefore affected by background. The ratio CBN/Δ^9-THC does not confirm the stability of Δ^9-THC. This may be because CBN was present in low abundance in those samples and therefore affected by background response. ACOD was shown to be stable for 72 hours while COD was shown to be stable up to 72 hours only in sample A.

Table 5.18: Summarised stability of selected components in the actual seized street nyaope samples A (A1, A2, A3), B (B1, B2, B3), C (C1, C2, C3), D (D1, D2, D3) and E (E1, E2, E3).[2]

Time (hours)	Compound	A1	A2	A3	B1	B2	B3	C1	C2	C3	D1	D2	D3	E1	E2	E3
24	**NCT**	3	1	1	1	1	1	3	1	3	1	1	1	1	1	1
	ACA	2	1	1	nd	nd	nd	nd	nd	nd	nd	nd	nd	nd	nd	nd
	CAFF	1	1	1	1	1	1	1	1	1	1	1	1	1	1	1
	DTM	1	1	1	nd	nd	nd	nd	nd	nd	nd	nd	nd	nd	nd	nd
	MTQ	1	1	2	1	1	1	nd	nd	nd	1	1	1	nd	nd	nd
	COC	nd	nd	nd	nd	nd	nd	1	1	1	nd	nd	nd	nd	nd	nd
	THCV	1	1	1	1	1	1	1	1	1	1	1	1	1	1	1
	CBV	1	1	1	1	1	1	1	1	1	3	3	1	nd	nd	nd
	CBV/THCV	1	1	1	1	1	1	1	1	1	3	3	1	nd	nd	nd
	COD	2	1	1	nd	nd	Nd	2	2	1	2	2	1	2	2	1
	Δ^9-THC	1	1	1	1	1	1	1	1	1	1	1	1	1	1	1
	ACOD	1	1	1	nd	nd	nd	1	2	1	1	1	2	1	1	1
	COD/ACOD	2	1	1	nd	nd	nd	2	2	2	2	2	3	1	2	2
	CBN	2	1	3	1	1	1	2	1	2	1	3	3	nd	nd	nd
	CBN/THC	2	2	3	1	1	1	2	1	1	1	3	3	nd	nd	nd
	6-MAM	3	2	1	nd	nd	nd	2	1	1	2	3	1	1	1	1
	6-MAM/DAM	1	1	2	nd	nd	nd	2	1	1	2	3	1	1	1	1
	DAM	1	1	1	nd	nd	nd	1	1	1	1	1	1	1	1	1
	TOCO	nd	nd	nd	nd	nd	nd	nd	nd	nd	1	1	1	1	1	1
48	**NCT**	3	2	2	1	1	1	3	1	1	1	1	1	1	1	1
	ACA	1	2	1	nd	nd	nd	nd	nd	nd	nd	nd	nd	nd	nd	nd
	CAFF	1	1	1	1	1	1	1	1	1	1	1	1	1	1	1
	DTM	1	1	1	nd	nd	nd	nd	nd	nd	nd	nd	nd	nd	nd	nd
	MTQ	1	1	1	1	1	1	nd	nd	nd	1	1	1	nd	nd	nd
	COC	nd	nd	nd	nd	nd	nd	1	1	1	nd	nd	nd	nd	nd	nd
	THCV	1	1	1	1	1	1	1	1	1	1	1	1	1	1	1
	CBV	1	1	1	1	1	1	2	1	1	3	3	1	nd	nd	nd
	CBV/THCV	1	1	1	1	1	1	2	1	2	3	3	1	nd	nd	nd
	COD	1	1	1	nd	nd	nd	2	3	2	2	2	1	2	1	1
	Δ^9-THC	1	1	1	1	1	1	2	1	1	1	1	1	1	1	1
	ACOD	1	1	1	nd	nd	nd	1	1	1	2	1	2	1	1	1
	COD/ACOD	1	1	1	nd	nd	nd	1	3	1	3	2	2	2	1	1
	CBN	1	1	3	1	1	1	1	1	1	1	1	2	nd	nd	nd
	CBN/THC	1	2	3	1	1	1	1	1	1	1	1	2	nd	nd	nd
	6-MAM	1	3	2	nd	nd	nd	2	1	1	1	1	1	1	1	1
	6-MAM/DAM	2	3	2	nd	nd	nd	2	1	1	2	2	1	1	1	1
	DAM	1	1	1	nd	nd	nd	1	1	1	1	1	1	1	1	1
	TOCO	nd	nd	nd	nd	nd	nd	nd	nd	nd	1	1	1	1	1	1

nd = not detected

[2] Where 1 denotes a change of 0–15% and considered stable, 2 denotes a change of 16–30% and considered moderately stable and 3 denotes a change above 30% and considered unstable (Saar et al, 2012).

Table 5.18 *cont'd*: Summarised stability of selected components in the actual seized street nyaope samples A (A1, A2, A3), B (B1, B2, B3), C (C1, C2, C3), D (D1, D2, D3) and E (E1, E2, E3).[2]

Time (hours)	Compound	A1	A2	A3	B1	B2	B3	C1	C2	C3	D1	D2	D3	E1	E2	E3
72	**NCT**	1	3	2	1	1	1	3	1	1	1	1	1	1	1	1
	ACA	2	2	3	nd	nd	nd	nd	nd	nd	nd	nd	nd	nd	nd	nd
	CAFF	1	1	1	1	1	1	1	1	1	1	1	1	1	1	1
	DTM	1	1	1	nd	nd	nd	nd	nd	nd	nd	nd	nd	nd	nd	nd
	MTQ	1	1	1	1	1	1	nd	nd	nd	1	1	1	nd	nd	nd
	COC	nd	nd	nd	nd	nd	nd	1	1	1	nd	nd	nd	nd	nd	nd
	THCV	2	1	1	1	1	1	1	1	1	1	1	2	1	3	1
	CBV	1	1	1	1	1	1	1	1	1	3	3	2	nd	nd	nd
	CBV/THCV	2	2	2	1	1	1	2	2	2	3	3	2	nd	nd	nd
	COD	1	1	1	nd	nd	nd	2	3	2	2	3	2	1	1	2
	Δ^9-THC	1	1	1	1	1	1	1	1	1	1	1	1	1	1	1
	ACOD	1	1	1	nd	nd	nd	2	1	1	1	1	1	1	1	1
	COD/ACOD	1	1	1	nd	nd	nd	1	2	1	2	3	2	2	1	1
	CBN	1	2	2	1	1	1	1	1	1	1	1	2	nd	nd	nd
	CBN/THC	1	2	3	1	1	1	1	2	1	1	3	2	nd	nd	nd
	6-MAM	1	3	3	nd	nd	nd	2	2	1	1	1	1	2	2	1
	6-MAM/DAM	1	3	2	nd	nd	nd	2	2	1	1	1	1	1	1	1
	DAM	1	1	1	nd	nd	nd	1	1	1	1	1	1	1	1	1
	TOCO	nd	nd	nd	nd	nd	nd	nd	nd	nd	2	1	1	1	1	1

nd = not detected

[2] Where 1 denotes a change of 0–15% and considered stable, 2 denotes a change of 16–30% and considered moderately stable and 3 denotes a change above 30% and considered unstable (Saar et al, 2012).

The average peak area ratios (PAR) for the three replicate analyses for each of the time intervals t =0, 24, 48 and 72 hours was determined for the selected components of each of the 15 sub-samples from the 5 actual seized street nyaope samples. Pooled average peak area ratios (PPAR) were determined by averaging the PARs at t = 0, 24, 48 and 72 hours. The PAR and the PPAR of the sub-samples A1 form sample A, for the time intervals t =0, 24, 48 and 72 hours are given in Table 5.19. The PAR and the PPAR of the 15 sub-samples for the time intervals t =0, 24, 48 and 72 hours respectively are shown in Appendix XI a - d. ANOVA statistical analysis for the sub samples A1, using the F-test (single factor) gave $F_{calc} = 0.0132 < F_{crit} = 2.866$ with the corresponding p-value = 0.998. The F_{calc}, F_{crit} and the corresponding p-values for the samples A1–A3, B1–B3, C1–C3, D1–D3 and E1–E3 are given in Table 5.20. The F_{calc} values for all the samples were less than the corresponding F_{crit} values, which demonstrates that there was no significant difference amongst the peak area ratios for the

simulated nyaope sub-samples over the 72 hours of autosampler storage, confirming the stability of these samples for the time period.

The PPAR of the actual seized street nyaope samples A (LAB25142), B (LAB25209), C (LAB34000), D (LAB37959902B) and E (LAB503909) are given in Table 5.21. ANOVA statistical analysis using the F-test (single factor) gave $F_{calc} = 0.000861 < F_{crit} = 3.354$, $F_{calc} = 0.00729 < F_{crit} = 3.555$, $F_{calc} = 0.146 < F_{crit} = 3.316$, $F_{calc} = 0.0429 < F_{crit} = 3.285$ and $F_{calc} = 0.00120 < F_{crit} = 3.403$ respectively, with the corresponding p-values = 0.999, 0.993, 0.863, 0.996 and 0.999. The F_{calc} values for all the samples were less than the corresponding F_{crit} values, which demonstrates that there were no significant difference amongst the peak area ratios for the samples belonging to the same group over the 72-hour autosampler storage.

Table 5.19: Average peak area ratios and the pooled average peak area ratios of the individual components in the actual seized street nyaope sample, A1, at t = 0, 24, 48 and 72 hours of autosampler storage.

Component	0	24	48	72	PPAR	SD	%RSD (n = 4)
NCT	0,077	0,117	0,105	0,074	0,093	0,021	22.59
ACA	0,193	0,241	0,085	0,200	0,180	0,066	36.94
CAFF	0,288	0,292	0,284	0,264	0,282	0,012	4.38
THCV	1,464	1,446	1,576	1,230	1,429	0,144	10.11
CBV	0,137	0,143	0,165	0,109	0,139	0,023	16.67
Δ^9-THC	13,089	12,655	12,850	11,073	12,417	0,913	7.35
ACOD	0,279	0,262	0,222	0,203	0,241	0,035	14.55
CBN	1,057	1,045	1,213	0,880	1,049	0,136	13.00
6-MAM	1,653	1,576	1,744	1,437	1,602	0,130	8.12
DAM	0,544	0,533	0,573	0,453	0,526	0,051	9.75

Table 5.20: The F_{calc}, F_{crit} and corresponding p-values for the average peak area ratios of each of the actual seized street nyaope samples A (A1, A2, A3), B (B1, B2, B3), C (C1, C2, C3), D (D1, D2, D3) and E (E1, E2, E3).

A (LAB25142)				B (LAB25209)				C (LAB34000)			
Sample	**F_{Calc}**	**F_{Crit}**	**p-value**	**Sample**	**F_{Calc}**	**F_{Crit}**	**p-value**	**Sample**	**F_{Calc}**	**F_{Crit}**	**p-value**
A1	0.0132	2.866	0.998	**B1**	0.00782	3.009	0.999	**C1**	0.00312	2.839	1.000
A2	0.0181	2.866	0.997	**B2**	0.00124	3.009	1.000	**C2**	0.00218	2.839	1.000
A3	0.00292	2.866	1.000	**B3**	0.00254	3.009	1.000	**C3**	0.0178	2.839	0.997
D (LAB379599)				**E (LAB503909)**							
Sample	**F_{calc}**	**F_{crit}**	**p-value**	**Sample**	**F_{calc}**	**F_{crit}**	**p-value**				
D1	0.156	2.816	0.925	**E1**	0.00330	2.901	1.000				
D2	0.138	2.816	0.937	**E2**	0.0186	2.901	0.996				
D3	0.130	2.816	0.942	**E3**	0.00884	2.901	0.999				

Table 5.21: Pooled average peak area ratios for the actual seized street nyaope samples A (LAB25142), B (LAB25209), C (LAB34000), D (LAB379599) and E (LAB503909).

Component	A			B			C			D			E		
NCT	0,093	0,081	0,081	0,236	0,221	0,241	0,009	0,013	0,019	0,410	0,369	0,428	0,090	0,101	0,103
ACA	0,180	0,119	0,170	0,048	0,045	0,065	0,980	1,277	1,483	*nd*	*nd*	*nd*	*nd*	*nd*	*nd*
CAFF	0,282	0,281	0,292	*nd*	*nd*	*nd*	*nd*	*nd*	*nd*	0,631	0,603	0,597	1,048	1,054	1,016
COC	*nd*	*nd*	*nd*	*nd*	*nd*	*nd*	0,100	0,107	0,200	*nd*	*nd*	*nd*	*nd*	*nd*	*nd*
MTQ	*nd*	*nd*	*nd*	0,117	0,107	0,132	*nd*	*nd*	*nd*	0,041	0,039	0,039	*nd*	*nd*	*nd*
THCV	1,429	1,448	1,467	0,293	0,262	0,288	0,060	0,083	0,091	0,057	0,055	0,054	0,009	0,009	0,008
CBV	0,139	0,147	0,156	0,146	0,134	0,147	0,023	0,031	0,032	0,043	0,042	0,042	*nd*	*nd*	*nd*
COD	*nd*	*nd*	*nd*	*nd*	*nd*	*nd*	0,028	0,040	0,046	0,013	0,012	0,012	0,023	0,023	0,022
Δ^9-THC	12,417	12,794	12,899	3,067	2,833	3,063	0,911	1,143	1,254	1,489	1,420	1,407	0,363	0,364	0,351
ACOD	0,241	0,263	0,259	*nd*	*nd*	*nd*	0,221	0,295	0,344	0,214	0,203	0,200	0,321	0,322	0,310
CBN	1,049	1,068	1,138	1,882	1,767	1,906	0,143	0,169	0,195	0,296	0,282	0,279	*nd*	*nd*	*nd*
6-MAM	1,602	1,560	1,675	*nd*	*nd*	*nd*	0,521	0,692	0,842	0,253	0,241	0,239	0,729	0,729	0,703
DAM	0,526	0,471	0,531	*nd*	*nd*	*nd*	3,584	4,636	5,513	2,693	2,572	2,545	3,813	3,834	3,692
TOCO	*nd*	*nd*	*nd*	*nd*	*nd*	*nd*	*nd*	*nd*	*nd*	0,064	0,061	0,060	0,057	0,057	0,055

nd = undetected

5.4.2 Comparison of chromatographic profiles between different actual seized street nyaope samples over a 72-hour period

The chromatograms of the actual seized street nyaope samples analysed after t = 0, 24, 48 and 72 hours of autosampler storage were generated for each of the samples A, B, C, D and E. The chromatogram of one member of each of the batches A, B, C, D and E were compared at the same time interval to determine whether the samples from different parent batches could be discriminated from one another. The comparative chromatograms at t = 0 of each of the samples A, B, C, D and E are displayed in Figures 5.12. The chromatograms displaying the comparison of each of the samples A, B, C, D and E at t =0, 24, 48 and 72 hours, respectively are shown in Appendix XII a–d. From these chromatograms it was demonstrated that the chromatographic profiles can be used to differentiate street nyaope samples, even after 72 hours of autosampler storage after extraction into tertiary butyl alcohol.

5.4.3 Comparison of chromatographic profiles between actual seized street nyaope samples from the same batch over a 72-hour period

Chromatograms of members of the same group were compared to determine whether samples from the same parent batch could be discriminated after 0, 24, 48 and 72 hours of autosampler storage. This would also demonstrate that the batch from which the sub samples were prepared was homogeneous. Chromatograms of the three sub-samples of the parent batch A at t = 0 is displayed in Figure 5.13. The chromatograms comparing samples within the parent groups B, C, D and E at t = 0 are shown in Appendix XIII a–c. From these chromatograms it was demonstrated that the profiles within the same parent batch cannot be differentiated. This demonstrates that the samples were homogeneous before extraction with tertiary butyl alcohol.

5.4.4 Comparison of chromatographic profiles of sub-samples within a batch in actual seized street nyaope samples over a 72 hour period

Chromatograms from one member of each of the three batches were compared at t= 0, 24, 48- and 72-hour time intervals to demonstrate whether the components could be identified over the 72-hour period and whether their proportion changed or not. The chromatograms

of one member from the sample A were compared after t= 0, 24, 48 and 72 hours' time interval and the profiles are displayed in Figure 5.14. Similar comparison of the samples B, C, D and E at t= 0, 24, 48 and 72 hours' time interval are displayed in Appendix XIV a–e. The %RSD of the PAR was found to be < 20% for the major components in the 15 samples which indicates that the PAR of these components did not change significantly over the 72 hours' time period once extracted from the nyaope samples into the tertiary butyl alcohol. From these chromatographic profiles it was demonstrated that each component of the actual seized street nyaope sample can be identified and that their relative proportions do not change over a 72 hour time period once extracted from nyaope into tertiary butyl alcohol. This confirms the stability of these components up to 72 hours of autosampler storage once extracted into tertiary butyl alcohol, as observed previously in Section 3.1.

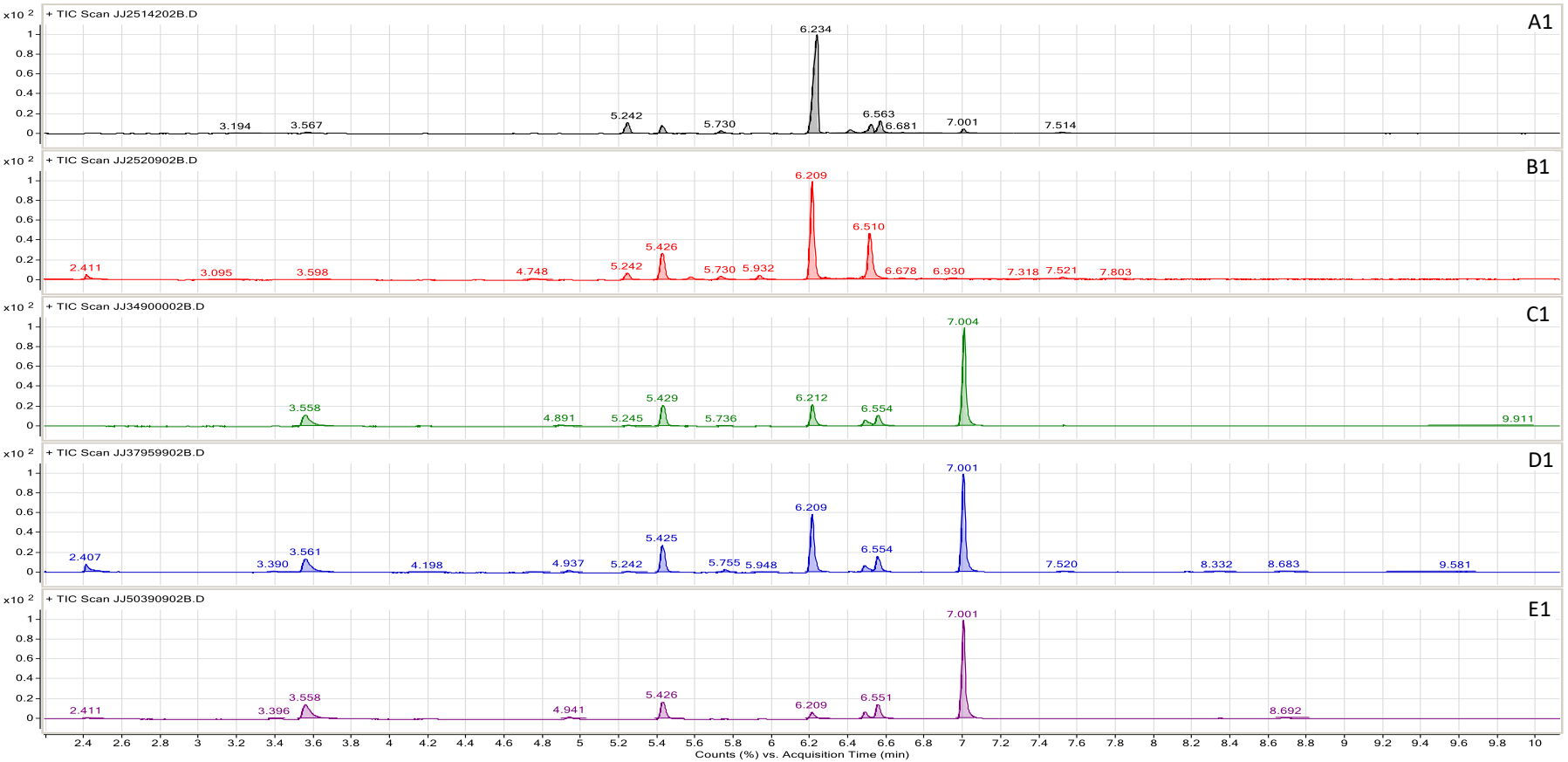

Figure 5.12: Chromatograms showing the samples for A1, B1, C1, D1 and E1 respectively at t = 0 where identifications were For A1: (3.194) acetaminophen, (3.564) caffeine, (5.242) tetrahydrocannabivarin, (5.429) tetracosane IS, (5.730) cannabichromene, (6.234) Δ^9-THC, (6.411) cannabigerol, (6.517) cannabinol, (6.563) 6-monoacetylmorphine, (6.681) unknown, (7.001) diamorphine and (7.514) nonacosane; For B1: (2.411) nicotine, (3.098) bulnesol, (3.616) caffeine, (4.754) methaqualone, (5.242) tetrahydrocannabivarin, (5.426) tetracosane IS, (5.575) cannabivarin, (5.733) cannabichromene, (5.935) cannabicoumaronone, (6.212) Δ^9-THC, (6.411) cannabigerol, (6.513) cannabinol, (6.681) unknown, (6.933) unknown, (7.517) nonacosane; For C1 (3.558) caffeine, (4.891) cocaine, (5.245) tetrahydrocannabivarin, (5.429) tetracosane IS, (5.736) cannabichromene, (5.935) cannabicoumaronone, (6.212) Δ^9-THC, (6.489) acetylcodeine, (6.554) 6-monoacetylmorphine, (7.004) diamorphine; For D1 (2.407) nicotine, (3.390) unknown, (3.561) caffeine, (4.198) unknown, (4.937) methaqualone, (5.242) tetrahydrocannabivarin, (5.425) tetracosane IS, (5.755) cannabidiol, (5.948) codeine, (6.209) Δ^9-THC, (6.485) acetylcodeine, (6.554) 6-monoacetylmorphine, (7.001) diamorphine, (7.520) nonacosane, (8.332) unknown, (8.683) unknown, (9.581) unknown; For E1 (2.411) nicotine, (3.396) unknown, (3.558) caffeine, (4.941) methaqualone, (5.426) tetracosane IS, (6.209) Δ^9-THC, (6.551) 6-monoacetylmorphine, (7.001) diamorphine, (8.692) unknown.

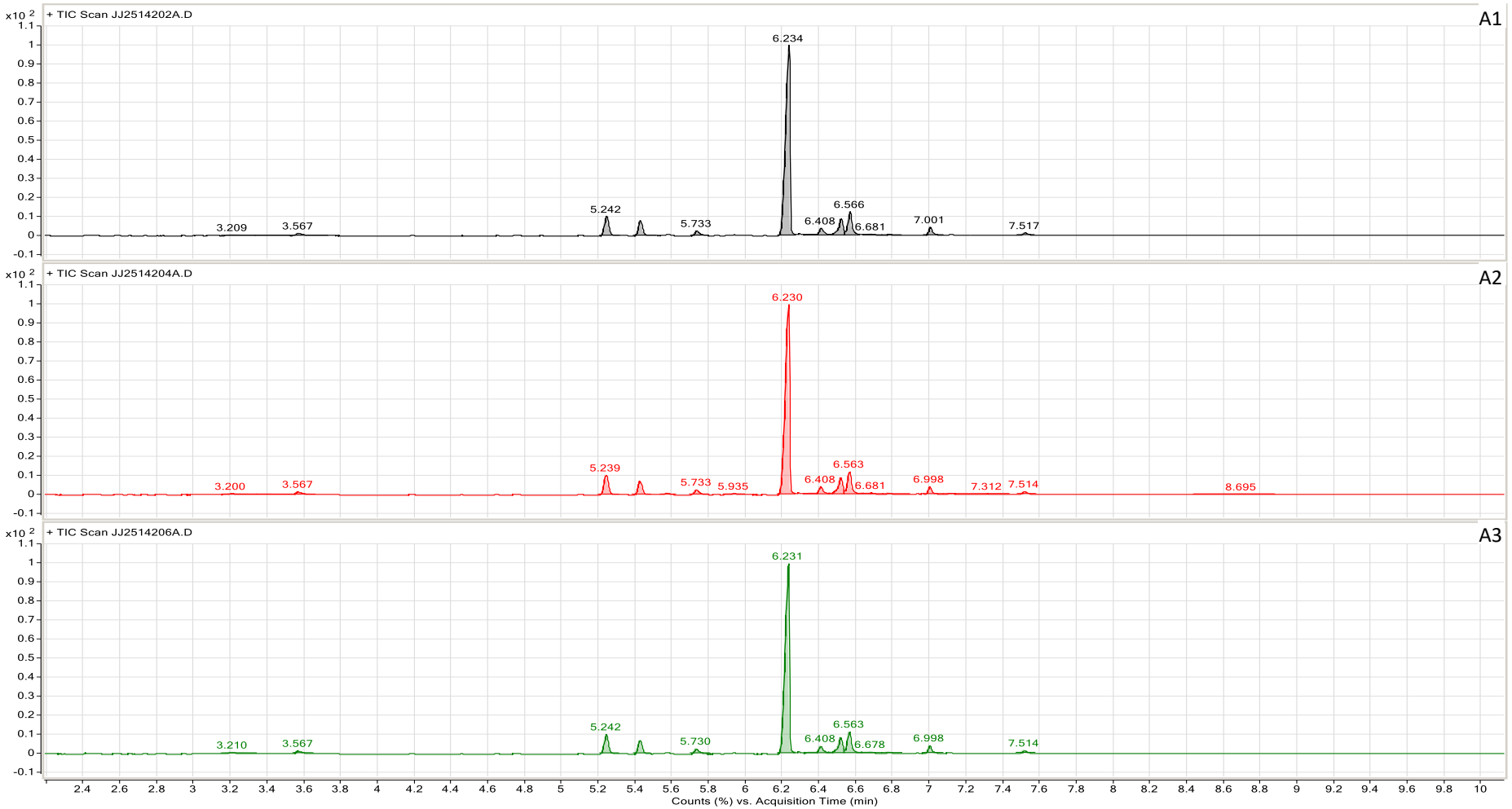

Figure 5.13: Chromatograms showing the three sub-samples for sample A (A1, A2, A3) at t = 0 where identifications were: (3.209) acetaminophen, (3.567) caffeine, (5.242) tetrahydrocannabivarin, (5.429) tetracosane IS, (5.733) cannabichromene, (6.234) Δ^9-THC, (6.408) cannabigerol, (6.517) cannabinol, (6.566) 6-monoacetylmorphine, (6.681) unknown, (7.001) diamorphine and (7.517) nonacosane in the first chromatogram (A1).

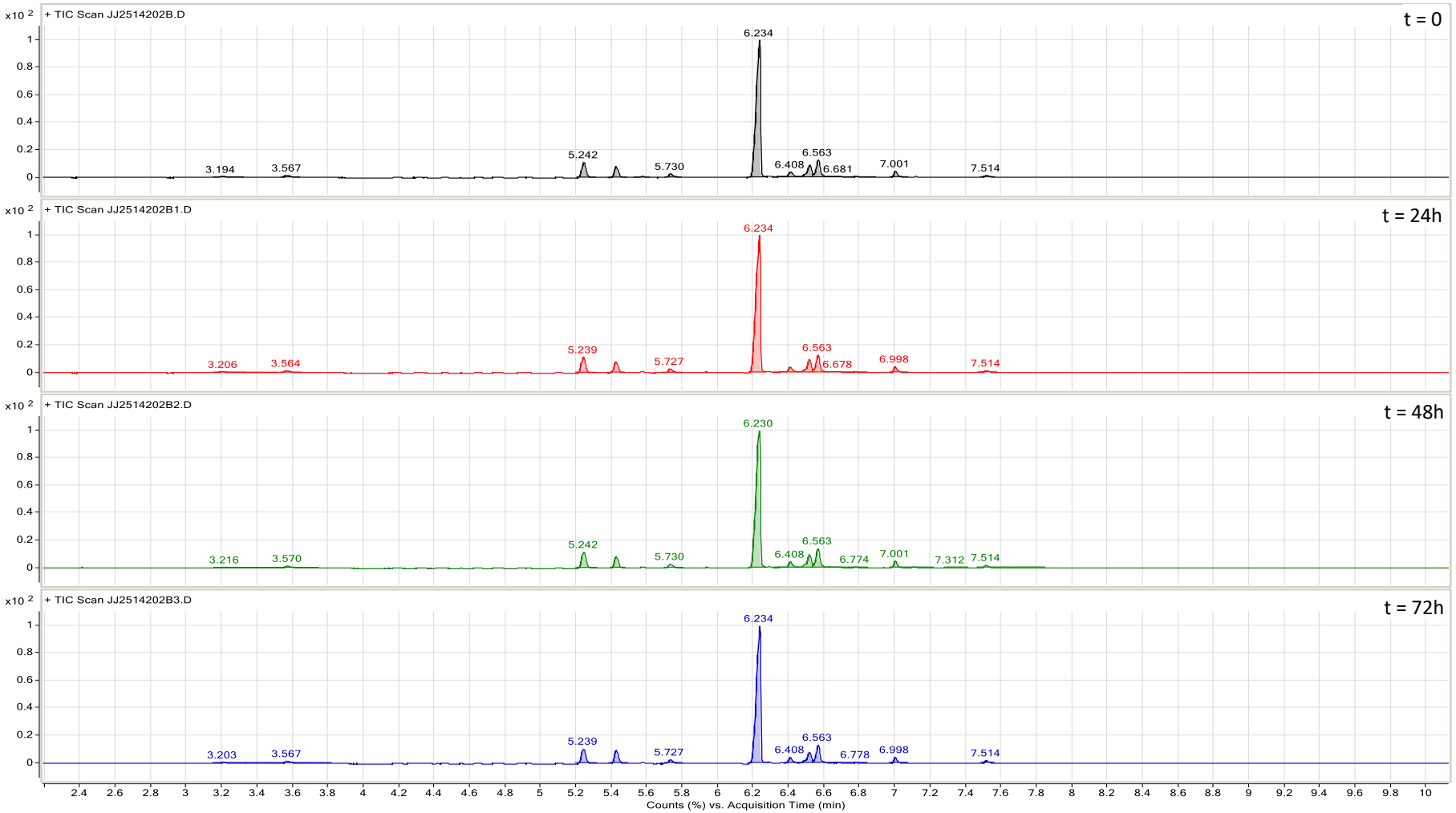

Figure 5.14: Chromatograms for the sub-sample A1 after 0, 24, 48 and 72 hours respectively where identifications were: (3.194) acetaminophen, (3.567) caffeine, (5.242) tetrahydrocannabivarin, (5.429) tetracosane IS, (5.730) cannabichromene, (6.234) Δ^9-THC, (6.408) cannabigerol, (6.517) cannabinol, (6.563) 6-monoacetylmorphine, (6.681) unknown, (7.001) diamorphine and (7.514) nonacosane in the first chromatogram (t = 0).

5.4.5 Concentrations profiles of CAFF, DAM and Δ^9-THC in actual seized street nyaope samples over a 72-hour period

Concentrations of the major components CAFF, DAM and Δ^9-THC in samples A, B, C, D and E shown in Table 5.22 were calculated using Equation 5.2. The CAFF concentration for sample B was below the quantitation limit (6.36×10^{-2} mg/L). The pooled average concentration for each time interval of the three sub-samples in a batch was used to calculate the average %RSD, shown in Table 5.22 to determine if the concentrations are significantly different. The average %RSD was found to be < 10% for all the components (CAFF, DAM and Δ^9-THC) in the samples A, B, C, D and E, except for CAFF in sample B, whose concentration was below the quantitation limit. This indicates that there is no significant difference between the concentrations of a particular component over a 72-hour period once extracted into tertiary butyl alcohol. This suggests that all the components were stable for the 72 hours of autosampler stability. The average %RSD of CAFF in sample B was > 5%. Since CAFF was below the quantitation limit, it may be affected by the background response and not necessarily unstable. The average concentration of CAFF, DAM and Δ^9-THC for each of the 15 sub-samples at each of the time interval t= 0, 24, 48 and 72 hours, were analysed with each of HCA and PCA chemometric methods mentioned in Section 5.3.3.

Table 5.22: Average concentrations (n = 4) of the components CAFF, DAM and Δ^9-THC in the actual seized street nyaope samples A (A1, A2, A3), B (B1, B2, B3), C (C1, C2, C3), D (D1, D2, D3) and E (E1, E2, E3) (mg/L).

	CAFF					**DAM**					**THC**				
	0	**24**	**48**	**72**	**%RSD**	**0**	**24**	**48**	**72**	**%RSD**	**0**	**24**	**48**	**72**	**%RSD**
A1	< QL	< QL	< QL	< QL	**< QL**	0.21	0.20	0.21	0.21	**4.00**	5.48	4.97	5.21	5.25	**4.00**
A2	< QL	< QL	< QL	< QL	**< QL**	0.18	0.16	0.17	0.15	**7.78**	5.36	4.91	4.88	4.99	**4.43**
A3	< QL	< QL	< QL	< QL	**< QL**	0.23	0.19	0.19	0.19	**9.67**	5.57	5.40	5.10	4.94	**5.41**
B1	< QL	< QL	< QL	< QL	**< QL**	nd	nd	nd	nd	**nd**	1.44	1.39	1.32	1.32	**4.34**
B2	< QL	< QL	< QL	< QL	**< QL**	nd	nd	nd	nd	**nd**	1.29	1.25	1.13	1.14	**6.56**
B3	< QL	< QL	< QL	< QL	**< QL**	nd	nd	nd	nd	**nd**	1.42	1.37	1.25	1.27	**6.18**
C1	0.70	0.70	0.69	0.69	**1.47**	3.53	3.42	3.44	3.38	**2.52**	0.42	0.43	0.41	0.40	**3.92**
C2	0.70	0.70	0.68	0.68	**1.45**	3.22	3.11	3.08	3.07	**2.16**	0.45	0.43	0.39	0.39	**7.16**
C3	0.78	0.76	0.77	0.78	**1.20**	3.91	3.69	3.80	3.70	**2.74**	0.55	0.52	0.49	0.50	**4.82**
D1	0.44	0.42	0.42	0.42	**2.19**	2.10	2.08	2.11	2.03	**1.67**	0.87	0.85	0.78	0.84	**4.70**
D2	0.44	0.44	0.44	0.43	**0.88**	2.02	1.97	1.97	1.90	**2.45**	0.80	0.80	0.77	0.79	**1.71**
D3	0.45	0.45	0.45	0.46	**0.96**	2.22	2.17	2.21	2.13	**1.93**	0.95	0.89	0.91	0.92	**2.98**
E1	0.82	0.80	0.81	0.81	**0.94**	2.87	2.82	2.82	2.79	**1.10**	0.11	0.10	0.10	0.10	**6.36**
E2	0.79	0.77	0.78	0.78	**1.01**	2.99	2.93	2.94	2.85	**1.91**	0.11	0.10	0.09	0.11	**9.39**
E3	0.81	0.78	0.79	0.79	**1.78**	2.99	2.91	3.00	2.92	**1.57**	0.14	0.13	0.13	0.14	**3.36**

< QL = below quantitation limit
nd = not detected

5.4.6 Chemometric treatment of simulated nyaope data

The two unsupervised chemometric methods mentioned in 5.3.7 were also used for the analysis of average concentrations of CAFF, DAM and Δ^9-THC of the actual seized street nyaope samples. The average concentrations of CAFF, DAM and Δ^9-THC for each of the 15 sub-samples at each of the time interval t= 0, 24, 48 and 72 hours were analysed with each of HCA and PCA.

5.4.6.1 Hierarchical Cluster Analysis of actual seized street nyaope samples

Analysis using agglomerative hierarchical clustering (HCA), Euclidean distance and unweighted average linkage, was conducted on the average concentration of CAFF, DAM and Δ^9-THC for the 15 sub-samples at each of the time interval t= 0, 24, 48 and 72 hours. The matrix generated for the samples at t = 0, 24, 48 and 72 hours are shown in Table 5.23. The matrices have zero values on the diagonal and are symmetric. As discussed in Section 1.8.2, the symmetric matrix indicates that the HCA method was suitable to discriminate the actual seized street nyaope samples into different classes. The results of the hierarchical clustering analysis performed on the actual seized street nyaope samples are indicated in the dendrogram in Figure 5.15. The results demonstrate that HCA has successfully discriminated samples, confirming that the samples A1, A2 and A3 were from the first batch A; the samples B1, B2, and B3 were from the second batch B; the samples D1, D2, and D3 were from the fourth batch D; and the samples E1, E2 and E3 were from the fifth batch E. The variation within the samples from the third batch C was too great to cluster them together, but sufficiently different from the others to distinguish them from the samples from the batches A, B, D and E. The variation is maybe as a result of concentration difference due to errors during the extraction process of the samples. The HCA further demonstrated that the actual seized street nyaope samples can still be discriminated even after 72 hours of autosampler storage. The matrices indicate that there was a maximum distance between Class 1 and Class 3 and a minimum distance between Class 2 and Class 3.

Table 5.23: Matrices showing distances between central objects at t = 0, 24, 48 and 72 hours for the actual seized street nyaope samples A1, B3 and C1.

		t = 0				t = 24h	
Class	**1 (A1)**	**2 (B3)**	**3 (C1)**	**Class**	**1 (A1)**	**2 (B3)**	**3 (C1)**
1 (A1)	0	4.07	5.68	**1 (A1)**	0	3.61	5.17
2 (B3)	4.07	0	2.80	**2 (B3)**	3.61	0	2.68
3 (C1)	5.68	2.80	0	**3 (C1)**	5.17	2.68	0
		t = 48h				**t = 72h**	
Class	**1 (A3)**	**2 (B3)**	**3 (C1)**	**Class**	**1 (A2)**	**2 (B3)**	**3 (C1)**
1 (A3)	0	3.85	5.31	**1 (A2)**	0	3.72	5.22
2 (B3)	3.85	0	2.66	**2 (B3)**	3.72	0	2.62
3 (C1)	5.31	2.66	0	**3 (C1)**	5.22	2.62	0

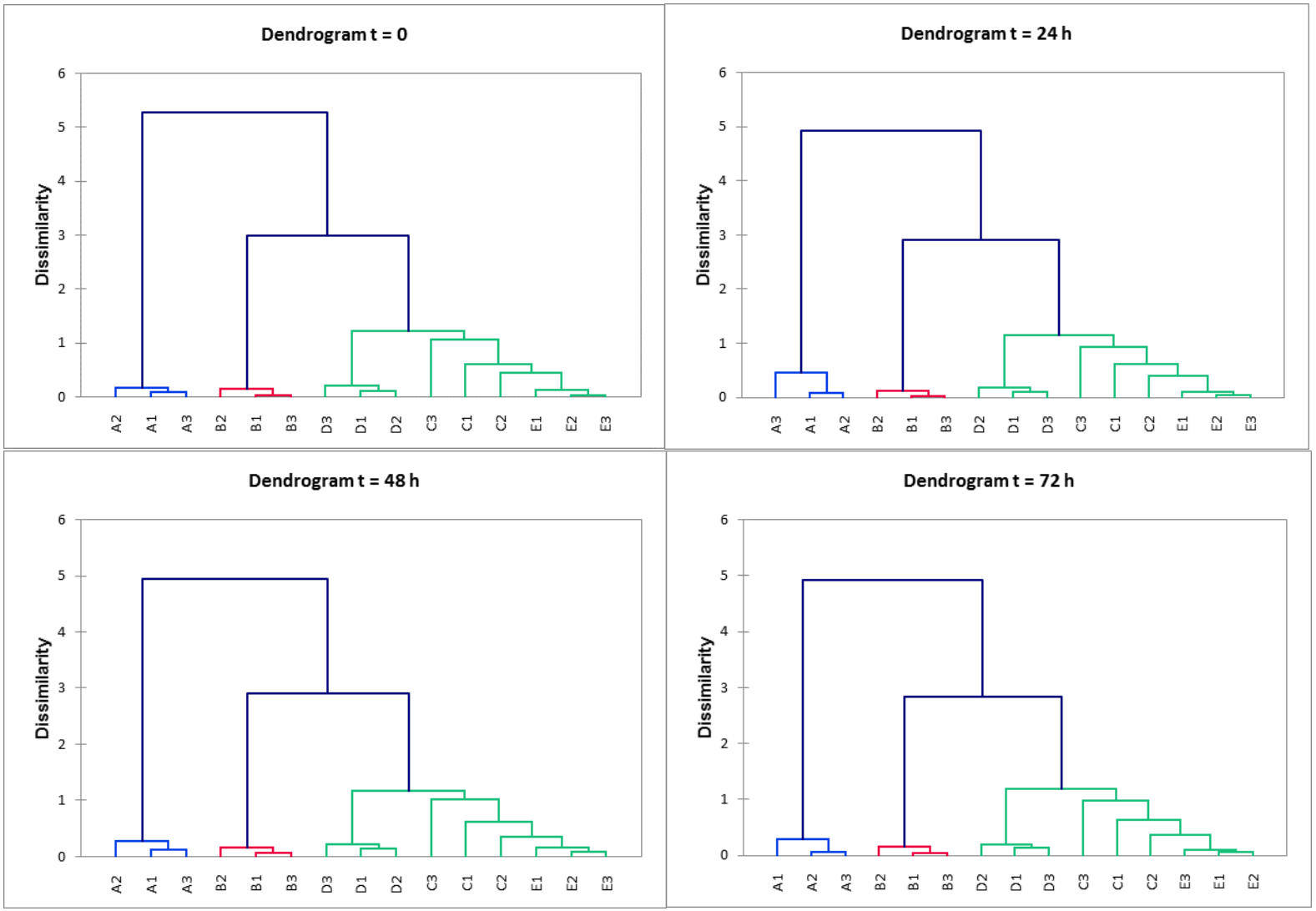

Figure 5.15: Dendrogram of the actual seized street nyaope samples A (A1, A2, A3), B (B1, B2, B3), C (C1, C2, C3), D (D1, D2, D3) and E (E1, E2, E3) analysed by HCA using unweighted linkage and Euclidean distance for the time interval t = 0, 24, 48 and 72 hours, respectively.

5.4.6.1 Principal Component Analysis of actual seized street nyaope samples

The correlation matrices for the time interval t = 0, 24 48 and 72 hours are shown in Table 5.24 for the actual seized street nyaope samples. All the values are different from zero with a significant level α = 0.95 (two-tailed), which indicates that there is a linear correlation between the variables. A positive correlation was observed between CAFF and DAM, while negative correlation between CAFF and Δ^9-THC as well as DAM and Δ^9-THC was observed. The same correlation pattern is observed up to 72 hours of autosampler storage. The transpose of these correlation matrices will yield matrices that are identical to the original matrices themselves. As a result, the product of the transpose and the original matrix would yield an identity matrix. This proves that the principal components are orthogonal. The principal component analysis indicates that there are three principal components, F1, F2 and F3 that explains the variability of the variables CAFF, DAM and Δ^9-THC. The scree plots for the actual seized street nyaope samples at time interval 0, 24 48 and 72 hours are shown in Figure 5.16. Each plot displays an exponential decline towards zero for the principal components F1, F2 and F3. The plots also indicate that the principal component F1 exhibits the largest variances, while F2 and F3 show low variances. The assumptions mentioned in Section 1.8.4 are satisfied and therefore the performance of the method is acceptable.

The eigenvalues and variability (%) are shown in Table 5.25 and indicate a value greater than 1.00 for the principal component F1, with variability of 86.61%, which is more than the minimum 70%. The principal component F1 is sufficient to explain the variability of the data set. The factor loadings (coefficients) for the actual seized street nyaope samples are shown in Table 5.26. Considering values greater than 0.300, the principal components F1 explain the variable of CAFF, DAM and Δ^9-THC, while F2 only explains the variability of Δ^9-THC. Therefore, the first principal component F1 is sufficient to explain the variability of the data set.

Table 5.24: Pearson correlation matrices at t = 0, 24, 48 and 72 hours for the components CAFF, DAM and Δ^9-THC in actual seized street nyaope samples A, B, C, D and E.

t = 0				t = 24h			
Variables	CAFF-T1	DAM-T1	THC-T1	Variables	CAFF_T2	DAM-T2	THC=T2
CAFF-T1	**1**	**0.982**	**-0.716**	CAFF_T2	**1**	**0.986**	**-0.723**
DAM-T1	**0.982**	**1**	**-0.688**	DAM-T2	**0.986**	**1**	**-0.700**
THC-T1	**-0.716**	**-0.688**	**1**	THC=T2	**-0.723**	**-0.700**	**1**
t = 48h				**t = 72h**			
Variables	CAFF-T3	DAM-T3	THC-T3	Variables	CAFF-T4	DAM-T4	THC-T4
CAFF-T3	**1**	**0.983**	**-0.710**	CAFF-T4	**1**	**0.984**	**-0.710**
DAM-T3	**0.983**	**1**	**-0.686**	DAM-T4	**0.984**	**1**	**-0.687**
THC-T3	**-0.710**	**-0.686**	**1**	THC-T4	**-0.710**	**-0.687**	**1**

Values in bold are different from 0 with a significance level alpha=0.95

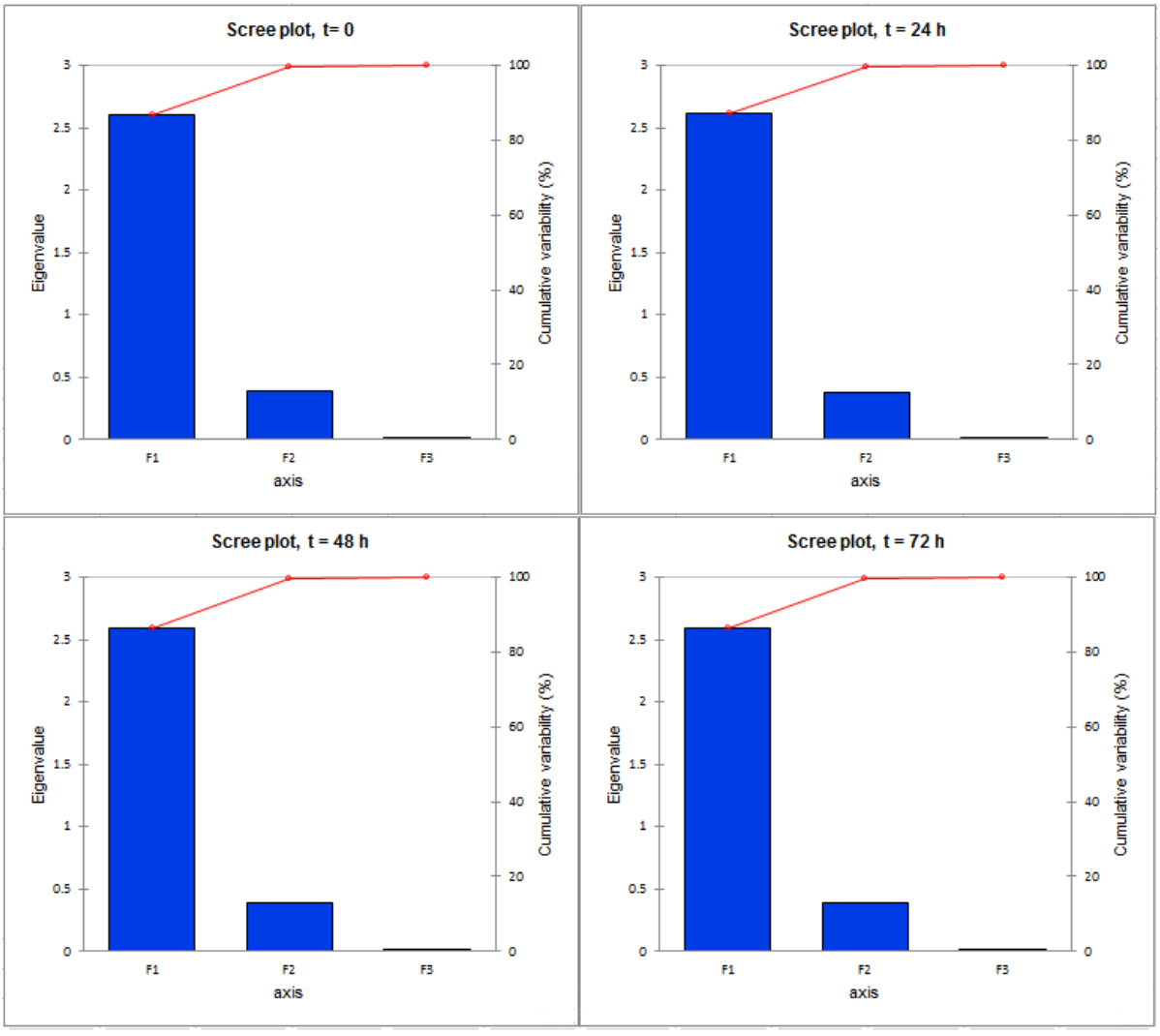

Figure 5.16: Principal component analysis scree plot at t = 0, 24, 48, 72 hours for the actual seized street nyaope samples A, B, C, D and E.

Table 5.25: Eigenvalues, percentage variability and percentage cumulative variance of the principal components F1, F2 and F3 of the actual seized street nyaope samples A, B, C, D and E at t = 0, 24, 48 and 72 hours.

	t = 0			t = 24h			t = 48h			t = 72h		
	Eigen-value	Variability (%)	Cumulative %	Eigen-value	Variability (%)	Cumulative %	Eigen-value	Variability (%)	Cumulative %	Eigen-value	Variability (%)	Cumulative %
F1	2.598	86.61	86.61	2.614	87.12	87.12	2.595	86.49	86.49	2.595	86.51	86.51
F2	0.384	12.80	99.41	0.373	12.42	99.54	0.389	12.97	99.46	0.389	12.98	99.49
F3	0.018	0.59	100.00	0.014	0.46	100.00	0.016	0.54	100.00	0.015	0.51	100.00

Table 5.26: Principal components factor Loadings (coefficients) and their percentage contributions for the components CAFF, DAM and Δ^9-THC in actual seized street nyaope samples at t = 0 and 24 h.

	t = 0						t = 24h					
	CAFF		DAM		Δ^9 -THC		CAFF		DAM		Δ^9 -THC	
PC	Loadings	% Contr.	Loadings	% Contr.	Loadings	% Contr.	Loadings	% Contr.	Loadings	% Contr.	Loadings	% Contr.
F1	**0.973**	36.42	**0.964**	35.74	**-0.851**	27.84	**0.974**	36.27	**0.966**	35.71	**-0.856**	28.02
F2	0.211	11.60	0.251	16.40	**0.526**	71.99	0.212	12.02	0.245	16.11	**0.517**	71.86
F3	0.096	51.98	-0.092	47.86	0.005	0.17	0.084	51.70	-0.081	48.18	0.004	0.12
	t = 48h						**t = 72h**					
	CAFF		DAM		Δ^9 -THC		CAFF		DAM		Δ^9 -THC	
PC	Loadings	% Contr.	Loadings	% Contr.	Loadings	% Contr.	Loadings	% Contr.	Loadings	% Contr.	Loadings	% Contr.
F1	**0.972**	36.43	**0.964**	35.85	**-0.848**	27.72	**0.972**	36.43	**0.965**	35.86	**-0.848**	27.70
F2	0.215	11.89	0.249	15.95	**0.530**	72.16	0.216	11.94	0.249	15.87	**0.530**	72.19
F3	0.092	51.67	-0.089	48.21	0.004	0.12	0.089	51.62	-0.086	48.26	0.004	0.11

%Contr. = percentage contribution

Values in bold are the most significant factor loadings

The results of the PCA analysis conducted for each of the individual time intervals t = 0, 24, 48, and 72 hours are shown in the observation axis in Figure 5.17. As indicated in Figure 5.17, PCA has discriminated samples, confirming the samples A1, A2 and A3 were from the same batch A; the samples B1, B2 and B3 were from the second batch B; the samples D1, D2 and D3 were from the fourth batch D; and the samples E1, E2 and E3 were from the fifth batch E. The samples of the third batch C could not be classed and were shown as individual groups C1, C2 and C3. The PCA further demonstrated that the simulated nyaope samples can still be discriminated even after 72 hours of autosampler storage.

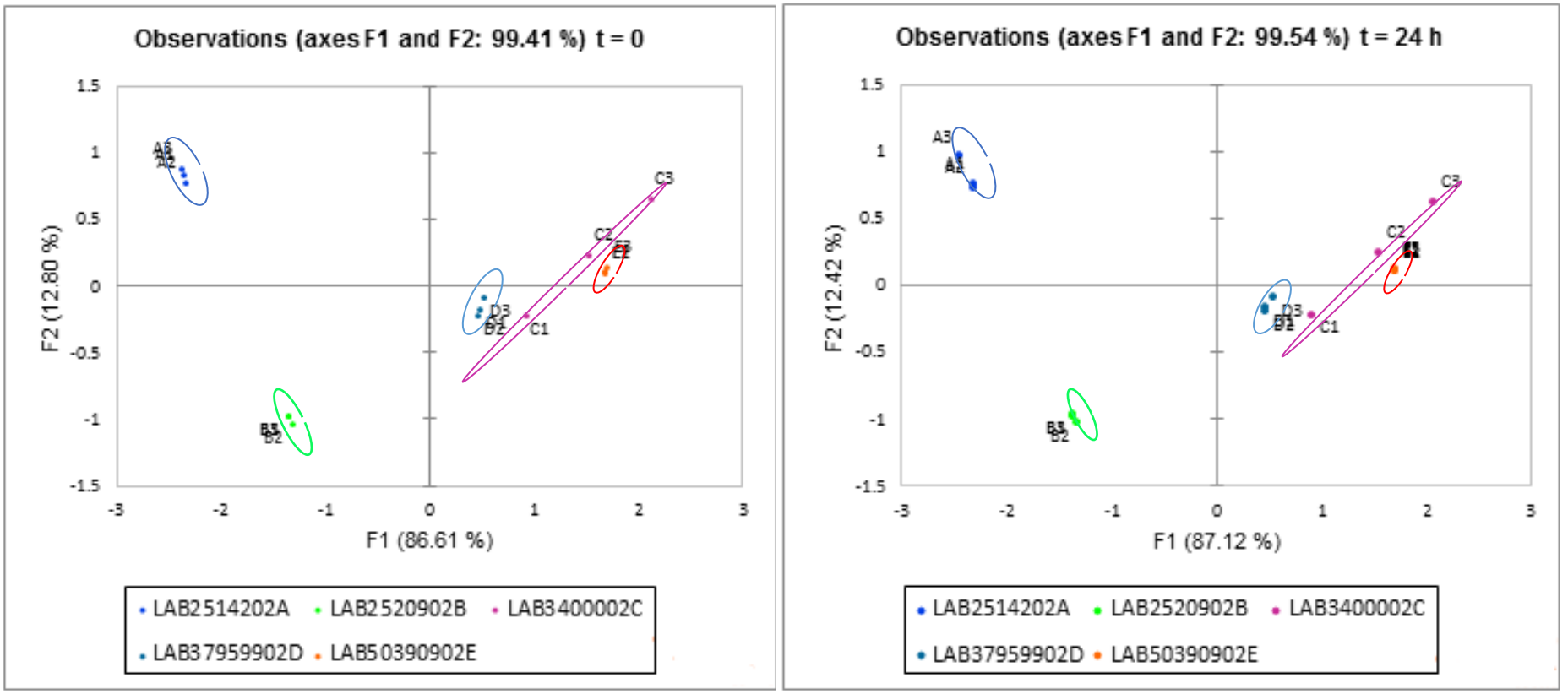

Figure 5.17: Observation axis for the actual seized street nyaope samples A (A1, A2, A3), B (B1, B2, B3), C (C1, C2, C3), D (D1, D2, D3) and E (E1, E2, E3 analysed by PCA for the time interval t = 0 and 24 hours.

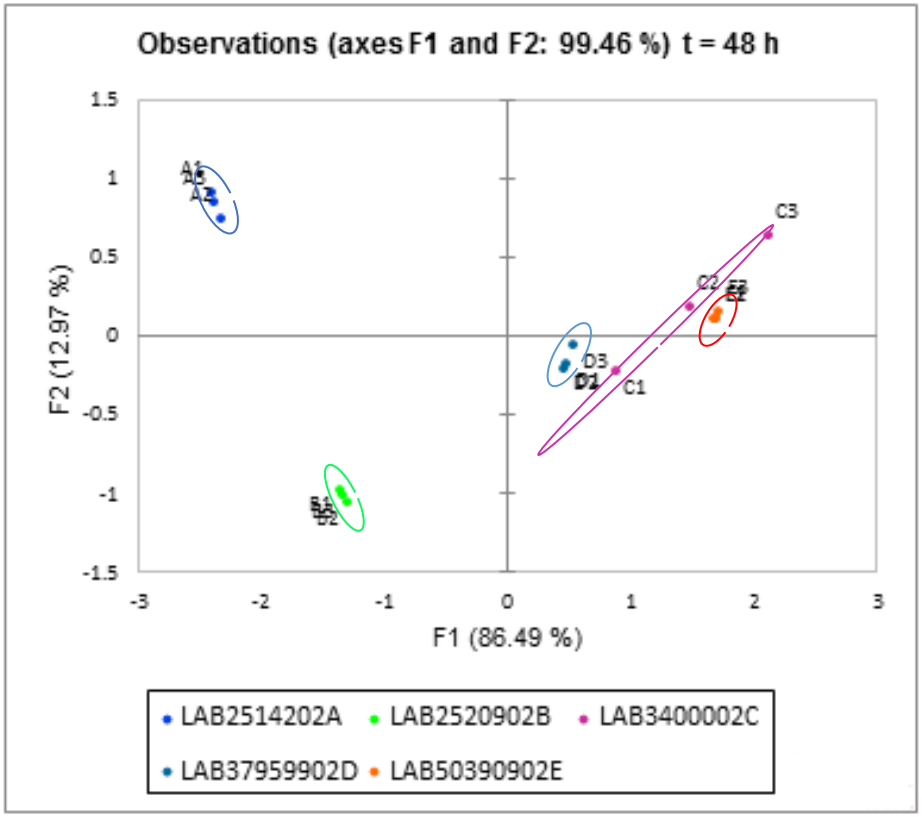

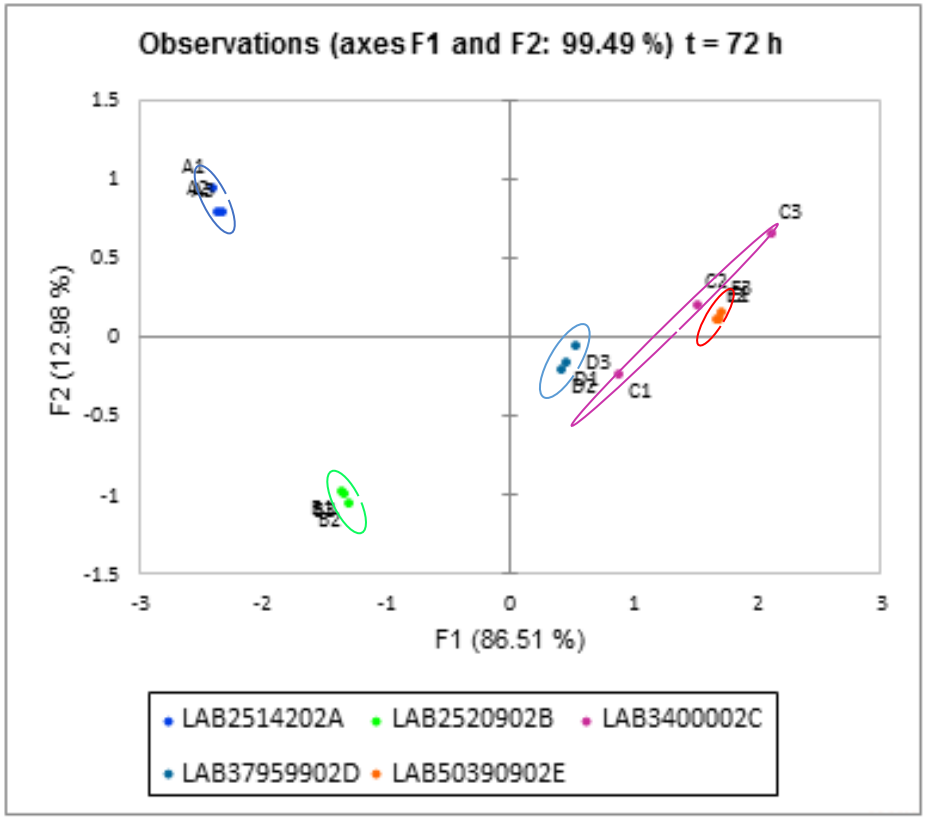

Figure 5.17 *cont'd*: Observation axis for the actual seized street nyaope samples A (A1, A2, A3), B (B1, B2, B3), C (C1, C2, C3), D (D1, D2, D3) and E (E1, E2, E3analysed by PCA for the time interval t = 48 and 72 hours

5.4.7 Compound identification – stability of relative retention times for actual seized street samples

The RRT of the individual components ACOD, CAFF, CBCM, CBD, CBG, CBN, CBV, DAM, EFV, 6-MAM, NVP, PNT, Δ^9-THC and THCV were determined for the 15 sub-samples from the 5 actual seized street nyaope samples. The relative standard deviations for the relative retention times of these compounds shown in Table 5.27 are all below 0.5%, illustrating the stability of this parameter. Identification of components of nyaope can therefore be made on the basis of retention time and the mass spectrum of each separated compound.

Table 5.27: Relative retention times of individual components for the actual seized street nyaope samples A (A1, A2, A3), B (B1, B2, B3), C (C1, C2, C3), D (D1, D2, D3) and E (E1, E2, E3).

	A1	A2	A3	B1	B2	B3	C1	C2	C3	D1	D2	D3	E1	E2	E3	Aver	SD	%RSD
NCT	0.445	0.445	0.445	0.445	0.445	0.445	0.445	0.445	0.445	0.444	0.444	0.444	0.445	0.445	0.445	0.445	0.00037	0.0824
ACA	0.589	0.592	0.591	Nd	nd	nd	nd	nd	nd	nd	nd	nd	nd	nd	nd	0.591	0.00150	0.2542
CAFF	0.657	0.658	0.658	0.663	0.667	0.668	0.656	0.656	0.654	0.656	0.655	0.654	0.656	0.656	0.655	0.658	0.00439	0.6671
DTM	0.856	0.856	0.856	nd	nd	nd	nd	nd	nd	nd	nd	nd	nd	nd	nd	0.856	0.00011	0.0124
MTQ	0.876	0.876	0.876	0.875	0.876	0.876	nd	nd	nd	0.875	0.875	0.874	nd	nd	Nd	0.876	0.00092	0.1052
COC	nd	nd	nd	nd	nd	nd	0.902	0.901	0.901	nd	nd	nd	nd	nd	nd	0.901	0.00046	0.0515
THCV	0.966	0.966	0.966	0.966	0.966	0.966	0.967	0.967	0.967	0.967	0.967	0.966	0.969	0.967	0.968	0.967	0.00085	0.0882
TC	1.000	1.000	1.000	1.000	1.000	1.000	1.001	1.000	1.000	1.000	1.001	1.000	1.000	1.000	1.001	1.000	0.00034	0.0344
CBV	1.028	1.027	1.027	1.027	1.027	1.027	1.029	1.028	1.028	1.027	1.028	1.027	nd	nd	nd	1.028	0.00060	0.0585
CBCM	1.056	1.056	1.056	1.056	1.056	1.056	1.057	1.057	1.057	1.057	1.058	1.056	1.060	1.060	1.060	1.057	0.00148	0.1398
CBD	nd	nd	nd	nd	nd	nd	1.060	1.060	1.060	1.061	1.061	1.060	nd	nd	nd	1.060	0.00040	0.0375
CBCO	nd	nd	nd	1.094	1.093	1.093	nd	nd	nd	nd	nd	nd	nd	nd	nd	1.094	0.00011	0.0097
COD	1.094	1.094	1.094	nd	nd	nd	1.096	1.096	1.095	1.096	1.096	1.095	1.096	1.096	1.096	1.095	0.00078	0.0708
THC	1.149	1.149	1.148	1.144	1.144	1.144	1.145	1.144	1.144	1.144	1.145	1.145	1.144	1.144	1.144	1.145	0.00172	0.1504
CBG	1.181	1.181	1.181	1.182	1.181	1.181	1.182	1.182	1.182	1.181	1.182	1.181	nd	nd	nd	1.181	0.00045	0.0379
ACOD	1.196	1.197	1.196	nd	nd	nd	1.196	1.196	1.195	1.195	1.196	1.195	1.195	1.195	1.195	1.196	0.00068	0.0572
CBN	1.201	1.201	1.201	1.200	1.200	1.200	1.199	1.198	1.198	1.198	1.199	1.198	1.198	1.198	1.197	1.199	0.00134	0.1117
6-MAM	1.210	1.210	1.210	nd	nd	nd	1.208	1.208	1.208	1.208	1.208	1.208	1.208	1.207	1.208	1.208	0.00093	0.0768
DAM	1.290	1.290	1.290	nd	nd	nd	1.291	1.291	1.292	1.290	1.291	1.291	1.291	1.291	1.291	1.291	0.00043	0.0336
Vitamin E	nd	nd	nd	nd	nd	nd	nd	nd	nd	1.600	1.600	1.599	1.601	1.599	1.600	1.600	0.00072	0.0447

nd = not detected

CHAPTER 6: CONCLUSIONS AND FUTURE WORK

The main objectives of this research as mentioned Section 1.9 were:

1. Selection of the major psychoactive substances found in the street cocktail drug nyaope based on the data collected from the South African Police Services (SAPS) database of drug seizures in the area of interest.
2. Development and validation of an analytical methodology for the simultaneous identification and quantitation of selected major components found in nyaope extracted into an organic solvent followed by instrumental analysis.
3. Identification and quantitation of the cocktail components in the street nyaope samples seized by the South African Police Services and demonstration of the appropriateness of clustering techniques for the samples using two unsupervised methods, namely principal component analysis (PCA) and hierarchical cluster analysis (HCA).

The first objective was investigated in Chapter 3, the second was investigated in Chapters 3 and 4, respectively, while the third objective was investigated in Chapter 5. The conclusions in Section 6.1 discuss how these objectives have been met. Section 6.2 outlines the future work and recommendations.

6.1 CONCLUSIONS

This section presents a summary of the findings made during solvent stability studies in Chapter 3 (Section 6.1.1), storage stability studies in Chapter 3 (Section 6.1.2), analytical method validation in Chapter 4 (Section 6.1.3), and the application of the validated analytical method in Chapter 5 (Section 6.1.4).

6.1.1 Solvent stability

Nyaope, a street drug commonly found in South Africa, is a mixture of low-grade heroin, cannabis products, antiretroviral drugs and other materials added as bulking agents. It is a highly physiologically addictive substance which is smoked by users. Little work has been

published on the chemical analysis and profiling of nyaope. Sample preparation prior to chromatographic or spectrometric analysis normally involves dissolution of the sample in an organic solvent. This study determined the most suitable organic solvent in which the common components of nyaope, namely Δ^9-tetrahydrocannabinol, diamorphine, caffeine, dextromethorphan, phenacetin and the antiretrovirals efavirenz and nevirapine, which have different chemical characteristics, are stable prior to analysis of nyaope samples. Individual seized street samples of cannabis (Δ^9-tetrahydrocannabinol), heroin (diamorphine) and antiretrovirals were mixed to mimic a nyaope sample and dissolved in the organic solvents dichloromethane, ethanol, ethyl acetate, hexane, isopropanol and tertiary butyl alcohol. In addition, actual seized street nyaope samples, not mixed with any other drugs, were extracted with selected solvents (dichloromethane, isopropanol and tertiary butyl alcohol). This study has shown that the major components of nyaope are the most stable in tertiary butyl alcohol stored in amber vials at room temperature. The nyaope components caffeine, cannabinol, diamorphine, efavirenz, 6-monoacetylmorphine, nevirapine, phenacetin, Δ^9-tetrahydrocannabinol and tetrahydrocannabivarin were stable up to 72 hours of autosampler stability for both simulated and actual seized street nyaope samples extracted with dichloromethane, ethyl acetate and tertiary butyl alcohol. Dichloromethane is a highly volatile solvent and therefore easily evaporates from the GC-MS sample vials. Furthermore, it contains hydrochloric acid that facilitates the decomposition of Δ^9-tetrahydrocannabinol to form cannabinol, which makes tertiary butyl alcohol the more suitable solvent. In order of suitability for extraction and autosampler stability, tertiary butyl alcohol was the most suitable solvent, followed by dichloromethane, ethyl acetate, isopropanol, ethanol, and lastly hexane. With the exception of dextromethorphan, all the components studied can be extracted with tertiary butyl alcohol, dichloromethane, ethyl acetate, isopropanol or ethanol, provided instrumental analysis is performed within 72 hours. This would allow for the identification, quantitation and profiling of nyaope using GC-MS. Samples prepared for the profiling of nyaope can therefore be extracted with tertiary butyl alcohol with subsequent instrumental analysis performed within 72 hours of preparation. Using this data, it is possible to identify the components of a nyaope sample and in principle establish possible links between drug seizures.

6.1.2 Storage stability

Both simulated and actual seized street nyaope samples were homogenized and transferred into glass bottles and extracted with tertiary butyl alcohol and analysed after the storage interval of 0, 24 hours, 72 hours and 1, 2 and 3 weeks. Samples were first placed in a desiccator and then stored at room temperature in the dark and under laboratory light, in a refrigerator at ±4 ^{o}C and at -70 ^{o}C. Acetylcodeine and the adulterants caffeine, dextromethorphan, efavirenz, nevirapine and phenacetin were shown to undergo minimum degradation for the 3 weeks (21 days) of storage under all storage conditions. A fourth set of samples was placed in an uncontrolled environment in a cabinet (without being placed in a desiccator) that mimics the storage conditions of samples received by the South African Police Services' Forensic Science laboratory (SAPS-FSL). Samples stored in a desiccator at ±4 ^{o}C and at room temperature in the dark showed minimal degradation of tetrahydrocannabivarin, Δ^9-tetrahydrocannabinol and diamorphine. The samples stored in a desiccator under laboratory light showed a greater degradation of tetrahydrocannabivarin, Δ^9-tetrahydrocannabinol and a minimal degradation of diamorphine, while samples stored in the uncontrolled environment showed greater degradation of diamorphine and minimal degradation of Δ^9-tetrahydrocannabinol. The results justify that the samples for profiling should be stored in the dark protected from light and moisture, such as in a desiccator, for a maximum of 21 days for qualitative analysis.

For profiling purposes, samples need to be extracted within 24 hours of seizure in solvent such as t-BuOH, as established in Section 3.2. If the samples are extracted into t-BuOH, it needs to be analysed within 72 hours, as established in Section 3.2. The drug markers for the profiling of cannabis include Δ^9-THC and THCV and for opiates include DAM and ACOD. This study demonstrated that when mixed together in nyaope, with the addition of the antiretrovirals, decomposition of the main components starts within 24 hours. The implications of this are that in order to profile the drug, the samples need to be protected from light at all times to prevent the photo-decomposition of Δ^9-THC, and from moisture to prevent the hydrolysis of DAM. The extracts in t-BuOH must be prepared immediately the drug is seized, and these need to be analysed within 72 hours, as established in 3.1. If drug identification only is required, the drugs are qualitatively present in the samples for a considerably longer period, longer than 21 days.

A further implication for drug profiling is that if two drug samples have matching chemical profiles, then it is likely that they came from a once larger batch, because it is extremely unlikely that two unrelated samples would decompose to give the same profile if they were seized, extracted and analysed under identical conditions. On the other hand, if two samples have different chemical profiles, it does not mean that they were from a once larger sample, or that they were not. The time of seizure and conditions of storage prior to analysis would impact on the drug profile, therefore, it is not possible to draw a conclusion if the necessary precautions are not taken before hand. In terms of policing and forensic science this study means that, for nyaope, decisions around whether an identification is required, or a profile is to be generated, must be made at a very early stage in the case, in order to take the necessary precautions when the samples are seized. Forensic practitioners must be aware of the requirements of the law enforcement agencies ahead of time. This may require changes in the way that nyaope cases are handled and processed by law enforcement agencies.

6.1.3 Analytical method validation

Drug standards available during the analytical method validation, and therefore used to generate calibration curves as discussed in Chapter 4, were caffeine (CAFF), diamorphine (DAM), efavirenz (EFV), nevirapine (NVP), phenacetin (PNT) and Δ^9-tetrahydrocannabinol (Δ^9-THC). Triplicate analyses of working solutions consisting of a mixture of CAFF, DAM, EFV, NVP PNT and Δ^9-THC were conducted, and the average peak area ratios were determined as discussed in Section 3.1. The accuracy and precision for the analytical method were assessed for the 10.0, 100.0 and 1000.0 mg/L concentration levels and found to be acceptable. The accuracy was above 100% for the high concentration level in all the components and above 80% for the lower concentration level. The analyses gave precision (%RSD) less than 10% for all concentration levels for CAFF, DAM, EFV, NVP and Δ^9-THC. PNT gave %RSD of 15.78% for the lower concentration level and %RSD less than 10% for the higher concentration levels. The analytical method was found to be linear for CAFF, DAM, EFV, NVP, PNT and Δ^9-THC in the concentration range 1.00 mg/L to 1000.00 mg/L. The linear concentration ranges for the nyaope components CAFF, DAM, EFV, NVP, PNT and Δ^9-THC managed linearity with $r2 \geq 0.997$. The detection limits (LOD) for CAFF, DAM, EFV, NVP, PNT and Δ^9-THC were 21.0, 14.0, 19.0, 19.0, 39.0 and 9.90 pg on column, respectively. The limit of quantitation for CAFF, DAM, EFV,

NVP, PNT and Δ^9-THC were 64.0, 43.0, 56.0, 57.0, 120 and 30.0 pg on column, respectively. The analytical method gave acceptable selectivity, with %RSD less than 20% for low concentration level (10.00 mg/L). The %RSD for the components CAFF, DAM, EFV, NVP, PNT and Δ^9-THC at all concentration levels were all less than or equal to 15% for the ruggedness test and hence was acceptable. The solvent ETAC showed better recoveries, followed by DCM and then t-BuOH, ETOH, i-PrOH and hexane. Therefore, the analytical method is fit for the purpose of quantitative profiling of major components of nyaope using the GC-MS technique.

6.1.4 Application of the validated analytical method

Subsequent to the analytical method validation, the developed analytical method was successfully applied to both simulated and five actual seized street nyaope samples. The major components of nyaope, including the antiretroviral drugs efavirenz and nevirapine, were identified in the simulated samples. Chemical components PNT, CAFF, EFV, NVP, Δ^9-THC and DAM for the cocktail drug nyaope were successfully identified and quantitatively determined, using GC-MS in both simulated samples. It was, however, interesting that whilst antiretrovirals have been reported to be present in nyaope, in the five actual seized street nyaope samples analysed, the antiretrovirals efavirenz and nevirapine were not identified. It may be that they were below the detection limit of the instrument or that they were indeed absent. However, the analytical method does provide for the determination of these antiretrovirals where they are present at concentrations above the detection threshold. It should, however, be noted that other antiretrovirals cannot be detected by GC-MS, but that LC-MS is a more suitable method for their detection. However, LC-MS is not currently readily available to the SAPS-FSL. The majority of the target compounds were stable up to 72 hours of storage for both simulated and actual seized street nyaope samples in tertiary butyl alcohol. The nyaope components ACA, COD, THCV, DTM, COC, NCT, MTQ, CBV, CBN, ACOD, 6-MAM, TOCP and NCP were qualitatively identified in the actual seized street nyaope samples using GC-MS. Both quantitative and qualitative profiles of major components of nyaope can be achieved satisfactorily using the GC-MS technique. This would allow for the identification, quantitation and profiling of nyaope using GC-MS.

Using two unsupervised chemometric methods as well as chromatographic profiles, it was demonstrated that each compound of interest can be identified and that their relative

proportions do not change over a 72-hour period once extracted from nyaope, into tertiary butyl alcohol, confirming previous work (Section 3.1). When each of the samples from the same batch for both simulated and actual seized street nyaope samples were analysed, it was found that the chromatographic profiles relating to each batch could be discriminated from one another. It was reported that for a small number of samples, HCA gives better results than PCA (Ahmad et al, 2005). This study, however, indicates that both HCA and PCA gave similar results for the small samples in both simulated and actual seized street nyaope samples.

Samples prepared as soon as possible after seizure (within 24 hours), for the profiling of nyaope can therefore be reliably extracted with tertiary butyl alcohol, with subsequent instrumental analysis performed within 72 hours of preparation. The study has shown, for the first time, that it is possible to reliably identify the components of nyaope samples and establish possible links between drug seizures. The analytical method can therefore be employed for the chemical profiling of the street drug nyaope. Provided that the samples are correctly seized and stored as discussed in Section 3.2, extracted into tertiary butyl alcohol and analysed within 72 hours of preparation as determined in Section 3.1, this study demonstrated that quantitative comparisons of nyaope samples can be made. This means that law enforcement agencies in the Southern African Development Community (SADC) and beyond have, for the first time, the ability to analyse nyaope and compare forensic science data. This will allow distribution and trafficking routes to be identified and will assist in the determination of the origins of this drug type. It does, however, require that decisions be made about how the samples will be treated prior to any investigative activity. It has been shown in Section 3.2 that the extraction of the drugs for analysis should be made as soon as possible after samples are seized, which requires planning before any police action.

This analytical method assists law enforcement and public health officials in a number of ways. It assists the law enforcement agencies in the identification and comparison of nyaope samples. It allows the establishment, for the first time, of a database on the composition of nyaope. It allows the exchange of analytical data between jurisdictions, provided that the necessary quality control protocols are in place. It also facilitates the prosecution of trafficking offences. In terms of public health, it allows determination of the drugs present in nyaope

and better public health information to be disseminated amongst the users of nyaope. In turn they may choose, having this information, to avoid using this drug cocktail.

6.2 FUTURE WORK

In Section 1.2 it was discussed that ARV compounds are high-molecular weight compounds, which cannot be identified using GC-MS, with the exception of efavirenz and nevirapine. It was further discussed that liquid chromatographic methods, coupled with tandem mass spectrometry, would be suitable methods for the analysis of the ARV compounds that cannot be identified using GC-MS. Therefore, future work should involve the development and validation of LC-MS/MS or UPLC-MS/MS (not readily available to SAPS-FSL) methods for the quantitation and profiling of antiretroviral components, as well as cannabinoids and opiates, in nyaope.

Solid-phase micro-extraction (SPME) has been used for the preconcentration and analysis of cannabinoids such as cannabinol, cannabidiol and Δ^9-tetrahydrocannabinol in urine samples, and achieved the Δ^9-tetrahydrocannabinol detection limit that is two orders of magnitude better than the liquid-liquid extraction used in this research (Feizbakhsh et al, 2016). It will, therefore, be worthwhile to consider using SPME in order to improve the detection limit of the nyaope analytes (codeine, morphine, noscapine, papaverine) which were not detected in most of the samples analysed. Furthermore, extraction using SPME and headspace analysis has been used successfully for cannabis classification using volatile profiles (Marchini et al, 2014), which would present an alternative method for the classification of the nyaope samples.

As discussed in Section 1.5.1, the semi-synthetic component of nyaope (heroin) and the synthetic components (other illicit drugs), may have occluded solvents within their crystal lattice. The occluded solvent can shed some light as to the synthesis process used, and consequently assist in linking the street samples as well as the determination of the geographic origin of the heroin sample. Therefore, the identification of occluded solvents in nyaope sample may be worth investigating in order to further the nyaope samples classify.

Stability studies conducted in this research used pure solvents such as tertiary butyl alcohol, isopropyl alcohol, ethanol, dichloromethane, ethyl acetate and hexane. A combination of

both polar and nonpolar solvents to improve the extraction of both acidic and basic components of nyaope could be considered for future work. Considering green chemistry, supercritical CO_2 could be considered for the extraction of the major components and not the minor components of nyaope. The stability of the nyaope extracts was conducted only in autosampler storage condition. It would be worthwhile in future work to include different storage conditions such refrigerator storage and freezer storage.

GC-MS analysis using single-ion monitoring (SIM) mode is said to be more sensitive than the scan mode in the analysis of substances at trace level. The current research was conducted in scan mode to identify unknown compounds; furthermore, the major components studied had adequate sensitivity samples (Hewavitharana et al, 2005). In order to improve the identification of the nyaope components available at trace level and thereby improve the discrimination of the street samples, it would be worthwhile to consider GC-MS analysis using SIM mode.

Analysis of the actual seized street nyaope samples was done for only five samples; therefore it would be worthwhile to analyse a large number of samples from different areas using the validated method to obtain a better understanding of the suitability of the classification methods used in this research. Furthermore, a concentration profile of a large number of nyaope samples would assist in the determination of the average concentration of the major components in street nyaope samples.

The classification conducted in this research did not seek to establish the origin of any of the components of nyaope. Future work to try and establish the origin of the components of nyaope would be worthwhile.

The chemical profiling of cannabis to determine the geographic origin using instances where seeds and roots are seized and when Δ^9-THC is not detected, as well as when the amount of cannabis seized is at trace level has been reported to be successful (Siniscalco Gigliano et al, 1997; Linacre and Thorpe, 1998; Siniscalco Gigliano, 1998; Hsieh et al, 2003; Miller-Coyle et al, 2003b). The extraction and classification of *papaver somniferum* DNA from heroin street samples have been reported to be possible (Marciano et al, 2018). Nyaope contains mainly the opiate drugs (diamorphine, codeine) and cannabis; therefore, chemical profiling using DNA analysis would be worth investigating for laboratories that have access to this technique.

The chemical profiling conducted in this research was done considering only the organic components of the street drug nyaope. As discussed in Section 1.5.1, chemical profiling using the trace elemental impurity profiling of nyaope would be a topic worth investigating.

In order to derive maximum benefit on the profiling of nyaope samples it is important that samples are packaged and delivered to the laboratory as soon as the seizure is made. It would be beneficial to train law enforcement officers on the proper handling of the samples required for profiling, from the packaging, storage before delivery, to the forensic lab and importance of delivering the samples as soon as possible after seizure. In addition, once at the forensic lab, proper storage conditions need to be adhered to, followed by analysis within 24 hrs for profiling purposes.

REFERENCES

Aalberg, L.; Andersson, K.; Bertler, C.; Cole, M.D.; Finnon, Y.; Huizer, H.; Jalava, K.; Kaa, E.; Lock, E.; Lopes, A.; Poortman-van der Meer, A.; Sippola, E.; Dahleń, J. 2005. Development of a harmonised method for the profiling of amphetamines. II. Stability of impurities in organic solvents. *Forensic Science International*, 149, 231–241.

Aamir, M.; Hafeez, A.; Ijaz, A.; Khan, S.A.; Chaudhry, N.; Ahmed, N. 2016. Development and validation of a liquid chromatography – tandem mass spectrometry method for cannabis detection in hair of chronic cannabis users under surveillance. *Pakistan Journal of Pathology*, 27(2), 61–70.

Acher, D. 2012. Is Marijuana Adictive (online). https://www.psychologytoday.com/blog/reading-between-the-headlines/201205/is-marijuana-addictive [Accessed on 2016-05-19].

Achkar, I.W.; Mraiche, F.; Mohammad, R.M; Udddin, S. 2017. Anticancer potential of sanguinarine for various human malignancies. *Future Medicinal Chemistry*, 9(9), 933–950.

Acosta, E.P.; Limoli, K.L.; Trinh, L.; Parkin, N.T.; King, J.R.; Weidler, J.M.; Ofotokun, I.; Petropoulos, C.J. 2012. Novel Method To Assess Antiretroviral Target Trough Concentrations Using In Vitro Susceptibility Data. *Antimicrobial Agents and Chemotherapy*, 56 (11), 5938–5945.

Adamowicz, P.; Kała. M. 2009. LC-MS and LC-MS/MS determination of six anticoagulant rodenticides in blood. *Problems of Forensic Sciences*, LXXVII, 53–63.

Adams, J.M.; Shelton, M.J.; Hewitt, R.G.; Deremer, M.; Difrancesco, R.; Grasela, T.H.; Morse, G.D. 1998. Zalcitabine Population Pharmacokinetics: Application of Radioimmunoassay. *Antimicrobial Agents and Chemotherapy*, 42(2), 409–413.

Addinsoft 2019. *XLSTAT statistical and data analysis solution*. New York, USA. https://www.xlstat.com [Accessed on 2020-04-09].

Adkison, K.K.; Shachoy-Clark, A.; Fang, L.; Lou, Y.; Otto, V R.; Berrey, M.M.; Piscitelli, S.C. 2006. The effects of ritonavir and lopinavir/ritonavir on the pharmacokinetics of a novel CCR5 antagonist, aplaviroc, in healthy subjects. *British Journal of Clinical Pharmacology,* 62(3), 336–344.

Agurell, S.; Halldin, M.; Lindgren, J.-E.; Ohlsson, A.; Widman, M.; Gillepsie. H.; Hollister, L. 1986. Pharmacokinetics and Metabolism of Δ^1-Tetrahydrocannabinol and Other Cannabinoids with Emphasis on Man. *Pharmacological Reviews*, 88(1), 21–43.

Ahmad, U.K.; Muniandy, Y.; Hassan, M.S. 2005. Physical Analysis and Chemical Profiling of Illicit Herbal Cannabis using Multivariate Analysis. *Malaysian Journal of Forensic Sciences*, 5(1), 26–34.

Aizpurua-Olaizola, O.; Omar, J.; Navarro, P.; Olivares, M.; Etxebarria, N.; Usobiaga, A. 2014. Identification and quantification of cannabinoids in *Cannabis Sativa L*. plants by high performance liquid chromatography-mass spectrometry. *Analytical and Bioanalytical Chemistry*, 406(29), 7549–7560.

Ali, E.M.M.; Almagboul, A.Z.I.; Khogali, S.M.E.; Gergeir, U.M.A. 2012. Antimicrobial activity of *Cannabis sativa. L*. Chinese Medicine 3, 61–64.

Ali, N.; Neagu, D.; Trundle, P. 2019. Evaluation of k.nearest neighbour classifier performance for heterogeneous data sets. *SN Applied Sciences*, 1, 1559. https://doi.org/10.1007/s42452-019-1356-9 [Accessed on 202-03-20].

Alvi, S.N.; Hammami, M.M. 2011. Validated HPLC Method for Determination of Caffeine Level in Human Plasma using Synthetic Plasma: Application to Bioavailability Studies. *Journal of Chromatographic Science*, 49, 292–296.

Ambach, L.; Penitschka, F.; Broillet, A.; Konig, S.; Weinmann, W.; Bernhard, W. 2014. Simultaneous quantification of delta-9-THC, THC-acid A, CBN and CBD in seized drugs using HPLC-DAD. *Forensic Science International*, 243, 107–111.

Amorim, A. 2019. Nonhuman forensic genetics. *Forensic Science International: Genetics Supplement Series*, 7, 44–46.

Anagnostopoulos, A.; Rotger, M.; Aouri, M.; Kuster, S.P.; Telenti, A.; Décosterd, L.A.; Günthard, H.F. 2013. Efavirenz intoxication due to a new CYP2B6 constellation. *Antiviral Therapy*, 18, 739–743.

Anderson, K.A.; Magnuson, B.A.; Tschirgi, M.L.; Smith, B. 1999. Determining the Geographic Origin of Potatoes with Trace Metal Analysis Using Statistical and Neural Network Classifiers. *Journal of Agricultural and Food Chemistry*, 47, 1568–1575.

Andre, C.M.; Hausman, J. F.; Guerriero, G. 2016. *Cannabis sativa*: The Plant of the Thousand and One Molecules. *Frontiers in Plant Science*, 7, 19. https://doi.org/10.3389/fpls.2016.00019 [Accessed on 2019-01-07].

André, P.; Widmer, N.; Buclin, T. 2019. Therapeutic drug monitoring (TDM) https://www.revmed.ch/contentrevmed/download/246079/2326082 [Accessed on 2019-11-29].

Anthony, J.C. 2006. The epidemiology of cannabis dependence. In Cannabis dependence: Its nature, consequences and treatment. *9780521814478*. pp. 58–105. DOI https://doi.org/10.1017/CB09780511544248.006 [Accessed on 2016-05-31].

Aouri, M.; Barcelo, C.; Guidi, M.; Rotger, M.; Cavassini, M.; Hizrel, C.; Buclin, T.; Decosterd, L. A.; Csajka, C.; the Swiss HIV Cohort Study. 2017. Population pharmacokinetics and pharmacogenetics analysis of rilpivirine in HIV-1-infected individuals. *Antimicrobial Agents and Chemotherapy* 61(1), e00899-16. https://doi.org/10.1128/AAC.00899-16 [Accessed on 2019-11-12].

Aparna, P.; Rao, S.V.; Thomas, K.M.; Mukkanti, K.; Badarinadh Gupta, P.; Rangarao, K.; Narayan, G.K.; Sandip, T.; Upendra, K. 2010. Identification, isolation, and characterization of potential degradation products in a triple combination lamivudine, zidovudine, and nevirapine tablet for oral suspension. *Pharmazie*, 65, 331–335.

Appendino, G.; Gibbons, S.; Giana, A.; Pagani, A.; Grassi, G.; Stavri, M.; Smith, E.; Rahman, M. M. 2008. Antibacterial Cannabinoids from *Cannabis sativa*: A Structure-Activity Study. *Journal of Natural Products*, 71(8), 1427–1430.

Araujo, P. 2009. Key aspects of analytical method validation and linearity evaluation. *Journal of Chromatography B*, 877, 2224–2234.

Avdeef, A.; Barrett, D.A.; Shaw, P.N.; Knaggs, R.D.; Davis, S.S. 1996. Octanol-, Chloroform-, and Propylene Glycol Dipelargonat-Water Partitioning of Morphine-6-glucuronide and Other Related Opiates. *Journal of Medicinal Chemistry*, 39(22), 4377–4381.

Bailey, K.; Gagné, D. 1975. Distinction of synthetic cannabidiol, cannabichromene and cannabivarin by GLC using on-column methylation. *Journal of Pharmaceutical Sciences*, 64(10), 1719–1720.

Balayssac, S.; Retailleau, E.; Bertrand, G.; Escot, M.-P.; Martino, R.; Malet-Martino, M.; Gilard, V. 2014. Characterization of heroin samples by 1H NMR and 2D DOSY 1H NMR. *Forensic Science International*, 234, 29–38.

Barrett, D.A., Dyssegaard, A.L.P.; Shaw, P.N. 1992. The effect of temperature and pH on the deacetylation of diamorphine in aqueous solution and in human plasma. *Journal of Pharmacy and Pharmacology*, 44, 606–608.

Barwick, V. J. 1997. Strategies for solvent selection — a literature review. *TrAC Trends in Analytical Chemistry*, 16 (6), pp. 293–309.

BBC News. *"Timeline: the use of cannabis"*. June 16, 2005. [Accessed on 2019-02-12].

Benaboud, S.; Pruvost, A.; Coffie, P.A.; Ekoue´vi, D.K.; Urien, S.; Arrive´, E.; Blanche, S.; The´odoro, F.; Avit, D.; Dabis, F.; Tre´luyer, J.-M.; Hirt, D. 2011. Concentrations of Tenofovir and Emtricitabine in Breast Milk of HIV-1-Infected Women in Abidjan, Côte d'Ivoire, in the ANRS 12109 TEmAA Study, Step 2. *Antimicrobial Agents and Chemotherapy*, 55(3), 1315–1317.

Berry, J.E. 2015. Trace metal analysis by laser ablation-inductively coupled plasma-mass spectrometry and x-ray K-edge densitometry of forensic samples. Graduate Theses and Dissertations. 14675. http://lib.dr.iastate.edu/etd/14675 [Accessed on 2018-05-07].

Besacier, F.; Guilluy, R.; Brazier, J.L.; Chaudron-Thozet, H.; Girard, J.; Lamotte, A. 1997. Isotopic analysis of ^{13}C as a tool for comparison and origin assignment of seized heroin samples. *Journal of Forensic Science*, 42(3), 429–433.

Bhavyasri, K.; Balaram, V.M.; Nageswarao, R.; Rambabu, D.; Ajitha, M.; Challa, B. 2015. Quantification of Etravirine in Rat Plasma by LC-MS/MS and Application to a Pharmacokinetic Study. *Journal of Scientific Research & Reports*, 8(4), 1–10.

Blessy, M.; Patel, R.D.; Prajapati, P.N.; Agrawal, Y.K. 2014. Development of forced degradation and stability indicating studies of drugs—A review. *Journal of Pharmaceutical Analysis*, 4(3), 159–165.

Bogusz, M.; Wijsbeek, J.; Franke, J.P.; De Zeeuw R.A.; Gierz, J. 1985. Impaét of Biological Matrix, Drug Concentration, and Method of Isolation on Detectability and Variability of Retention Index Values in Gas Chromatography. *Journal of Analytical Toxicology*, 9(2), 49–54.

Boleda, M.R.; Galceran, M.T.; Ventura, F. 2007. Trace determination of cannabinoids and opiates in wastewater and surface waters by ultra-performance liquid chromatography–tandem mass spectrometry. *Journal of Chromatography A*, 1175, 38–48.

Bond, C. 2018. Are Cannabis Plants Monecious or Dioecious? In Maximum yield. https://www.maximumyield.com/are-cannabis-plants-monecious-or-dioecious/2/5095 [Accessed on 2019-01-28].

Bonfilio, R.; Cazedey, E.C.L.; De Arańjo, M.B.; Salgado, H.R.N. 2012. Analytical Validation of Quantitative High-Performance Liquid Chromatographic Methods in Pharmaceutical Analysis: A Practical Approach. *Critical Reviews in Analytical Chemistry*, 42, 87–100.

Boone, C.M.; Waterval, J.C.M.; Lingeman, H.; Ensing, K.; Underberg, W.J.M. 1999. Capillary electrophoresis as a versatile tool for the bioanalysis of drugs – a review. *Journal of Pharmaceutical and Biomedical Analysis*, 20 (6), 831–863.

Bora, T.; Merdivan, M.; Hamamci, C. 2002. Levels of Trace and Major Elements in Illicit Heroin. *Journal of Forensic Sciences*, 47(5), 959–963.

Bovell-Benjamin, A.C.; Roberts, J. 2015. Chapter 13 – naturally occurring toxicants: presence in selected commonly consumed fruits. In Martín-Belloso, O.; Keener, L.; Astley, S.B.; Braun, S. McMahon, H.; Lelieveld, H (Eds), *Regulating Safety of Traditional and Ethnic Foods*. Academic Press, Cambridge, 247–282.

Bratchell, N. 1989. Cluster analysis. *Chemometrics and Intelligent Laboratory Systems*, 6, 105–125.

Bravo, F.; Gonzalez, D.; Benites, J. 2011. Development and validation of a solid-phase extraction gas chromatography-mass spectrometry method for the simultaneous quantification of opioid drugs in human whole blood and plasma. *Journal of the Chilean Chemical Society*, 56(3), 799–802.

Brenneisen, R. 2007. Chemistry and Analysis of Phytocannabinoids and Other Cannabis Constituents. In ElSohly, M.A. (Ed), *Marijuana and the cannabinoids.* Humana Press Inc., Totowa, New Jersey. 17–49.

Brenneisen, R.; ElSohly, M.A. 1988, Chromatographic and spectroscopic profiles of Cannabis of different origins: Part I. *J. Forensic Sci*., 33, 1385–1404.

Brenneisen, R.; Hasler, F. 2002. GC/MS Determination of Pyrolysis Products from Diacetylmorphine and Adulterants of Street Heroin Samples. *Journal Forensic Science*, 47(4), 1–4.

Brereton, R.G. 2015. The Mahalanobis distance and its relationship to principal component scores. *Journal of Chemometrics*, 29, 143–45.

Brewer, E.; Felix, T.; Clarke, P.; Edgington, A.; Muirhead, D. 2010. An LC-MS-MS method for quantitative determination of maraviroc (UK-427,857) in human plasma, urine and cerebrospinal fluid. *Biomedical Chromatography*, 24(12), 1316–1323.

Borillea, B.T.; González, M.; Steffens, L.; Ortiz, R. S.; Limberger, R.P. 2017. *Cannabis sativa*: A systematic review of plant analysis. *Drug Analytical Research*, 01, 1–23.

Bro, R.; Smilde, A. K. 2014. Principal component analysis, *Analytical Methods*, 6, pp. 2812–2831.

Broséus, J.; Anglada, F.; Esseiva, P. 2010. The differentiation of fibre- and drug type Cannabis seedlings by gas chromatography/mass spectrometry and chemometric tools. *Forensic Science International,* 200, 87–92.

Broséus, J.; Gentile, N.; Pont, F. B.; Gongora, J.M.G.; Gasté L.; Esseiva, P. 2015. Qualitative, quantitative and temporal study of cutting agents for cocaine and heroin over 9 years. *Forensic Science International,* 257, 307–313.

Bruwer, C. 2017. Heroin trafficking through South Africa: why here and why now? August 15, 2017 4.01pm SAST. https://theconversation.com/heroin-trafficking-through-south-africa-why-here-and-why-now-81627 [Accessed on 2020-04-29].

Burns, D.T.; Danzer, K.; Townshend, A. 2009. A Tutorial Discussiom of the use of the terms "Robust" and "Rugged" and the Associated Characteristics of "Robustness" and "Ruggedness" ab used in Descriptions of Analytical Procedures. *Journal of the Association of Public Analysts,* 37, 40–60.

Cadola, L.; Broséus, J.; Esseiva, P. 2013. Chemical profiling of different hashish seizures by gas chromatography-mass spectrometry and statistical methodology: A case report. *Forensic Science International*, 232, e24–e27.

Calcagno, A.; Nozza, S.; Bonora, S.; Castagna, A.; Gonzalez de Requena, D.; D'Avolio, A.; Lazzarin, A.; Di Perri, G. 2011. Pharmacokinetics of the raltegravir/maraviroc/etravirine combination. *Journal of Antimicrobial Chemotherapy*, 66(8), 1932–1934.

Carbone, M.; Castelluccio, F.; Daniele, A.; Sutton, A.; Ligresti, A.; Di Marzo, V.; Gavagnin, M. 2010. Chemical characterisation of oxidative degradation products of Δ^9-THC. *Tetrahedron*, 66(49), 9497–9501.

Carod-Artal, F.J. 2013. Psychoactive plants in ancient Greece. *Neurosciences and History*, 1(1), 28–38.

Carr, G.P.; Wahlich, J.C. 1990. A practical approach to method validation in pharmaceutical analysis. *Journal of Pharmacy and Biomedical Analysis*, 86, 613–618.

Casale, J.F.; Casale E.; Collins, M.; Morello, D. 2019. Stable Isotope Analyses of Heroin Seized from the Merchant Vessel Pong Su. *Journal of Forensic Sciences*, 51(3), 603–606.

Caude, M.; Jardy, A. 1998. Normal-Phase Liquid Chromatography, in Handbook of HPLC. Katz, E.; Eksteen, R.; Schoenmaker, P.; Miller, N. (Eds.). *Chromatographic Science Series, Vol. 78.* Marcel Dekker Inc. New York. pp. 325–363. ISBN-0-8247-9444-3

Cerling, T.E.; Barnette, J.E.; Bowen, G.J.; Chesson, L.A.; Ehleringer, J.R.; Remien, C.H.; Shea, P.; Tipple, B.J.; West, J.B. 2016. Forensic Stable Isotope Biogeochemistry. *Annual Review of Earth and Planetary Sciences*, 44, 175–206.

César, I.C.; Pianetti, G.A. 2009. Robustness evaluation of the chromatographic method for the quantitation of lumefantrine using Youden's test. *Brazilian Journal of Pharmaceutical Sciences*, 45(2), 235–240.

Chambers, D. 2018. 10 die after destroying their hearts by mainlining nyaope. TimesLive South Africa. https://www.timeslive.co.za/news/south-africa/2018-07-02-10-die-after-destroying-their-hearts-by-mainlining-nyaope/ [Accessed on 2019-06-06].

Chan, K.-W. 2014. Validating a gas chromatography-mass spectrometric method and sample classification procedure for cannabis profiling using cannabinoids from case samples, *Australian Journal of Forensic Sciences*, 46(4), 424–432. http://dx.doi.org/10.1080/00450618.2014.882985 [Accessed on 2016-03-30].

Chan, K.-W.; Tan, G.-H.; Wong, R.C.S. 2012a. Chemometric procedures for analyzing trace organic impurities present in street doses of heroin via a constant weight approach. Australian *Journal of Forensic Sciences*, 44(3), 299–309.

Chan, K.-W.; Tan, G.-H.; Wong, R.C.S. 2012b. Gas chromatographic method validation for the analysis of major components in illicit heroin seized in Malaysia. *Science and Justice*, 52, 9–16.

Chan, K.-W.; Tan, G.-H.; Wong, R.C.S. 2012c. Investigation of illicit heroin seized in Malaysia: physical characteristics and chemical profiling. *Australian Journal of Forensic Sciences*, 44(4), 353–369.

Chandra, S.; Lata, H.; Mehmedic, Z.; Khan, I.A.; ElSohly, M.A. 2010. Assessment of cannabinoids content in micropropagated plants of *Cannabis sativa* and their comparison with conventionally propagated plants and mother plant during developmental stages of growth. *Planta Medicine*, 76(7), 743–750.

Chandra Paul, L.; Al Suman, A.; Sultan, N. 2013. Methodological Analysis of Principal Component Analysis (PCA) Method. *International Journal of Computational Engineering & Management*, 16(2), 32–38.

Chang, D.; Kolis, S.J.; Linderholm, K.H.; Julian, T. F.; Nachi, R.; Dzerk, A.M.; Lin. P.P.; Lee, J.W.; Bansal, S.K. 2005. Bioanalytical method development and validation for a large peptide HIV fusion inhibitor (Enfuvirtide, T-20) and its metabolite in human plasma using LC-MS/MS. *Journal of Pharmaceutical and Biomedical Analysis*, 38(3), 487–496.

Chemindustry.ru. *Product information* http://chemindustry.ru/tert-Butanol.php [Accessed on 2017-12-28].

Cheng, C.-L.; Smith, D.E.; Carver, P.L.; Cox, S.R.; Watkins, P.B.; Blake, D.S.; Kauffman, C.A.; Meyer, K.M.; Amidon, G.L.; Stetson, P.L. 1997. Steady-state pharmacokinetics of delavirdine in HIV-positive patients: Effect on erythromycin breath test. *Clinical Pharhmacology & Therapeutics,* 61, 531–543.

Cherniak, L. 1982. *The great books of Cannabis, Vol. I: Book II*. Cherniak/Damele Publishing Co., Oakland, CA.

Chi, J.; Jayewardene, A.I.; Stone, J.A.; Matoya, T.; Aweeka, F.T. 2002. Simultaneous determination of five HIV protease inhibitors nelfinavir, indinavir, ritonavir, saquinavir and amprenavir in human plasma by LC-MS/MS. *Journal of Pharmaceutical and Biomedical Analysis*, 30(3), 675–684.

Chung, W.-G.; Cha, Y.-N. 1997. Oxidation of Caffeine to Theobromine and Theophylline is Catalysed Primarily by Flavin-Containing Monooxygenase in Liver Microsomes. *Biochemical and Biomedical Research ommunications*, 235, pp. 685–688.

Ciccarone, D.; Harris, M. 2015. Fire in the vein: Heroin acidity and its proximal effect on users' health. *International Journal of Drug Policy*, 26(11), 1103–1110.

Clarke, R.C.; Merlin, M.D. 2013. *Cannabis: evolution and ethnobotany*. University of California Press. Berkeley, Los Angeles and London.

Cole, M.D. 2003. *The Analysis of Controlled Substances*. Cambridge, UK. John Wiley & Sons, Ltd.

Collins, M.; Huttunen, J.; Evans, I.; Robertson J. 2007. Illicit drug profiling: the Australian experience. *Australian Journal of Forensic Sciences*, 39(1), 25–32.

Colombo, S.; Beguin, A.; Telenti, A.; Biollaz, J.; Buclin, T.; Rochat, B.; Decosterd, L.A. 2005. Intracellular measurements of anti-HIV drugs indinavir, amprenavir, saquinavir, ritonavir, nelfinavir, lopinavir, atazanavir, efavirenz and nevirapine in peripheral blood mononuclear cells by liquid chromatography coupled to tandem mass spectrometry. *Journal of Chromatography B*, 819, 259–276.

Cone, E.J.; Heir, H.A.; Caplan, Y.H.; Gourlay, D. 2006. Evidence of Morphine Metabolism to Hydromorphone in Pain Patients Chronically Treated with Morphine. *Journal of Analytical Toxicology*, 30, 1–5.

Confidence Analytics, LLC. 2018. Eight Cannabinoids by HPLC-UV. Method Application Note. https://www.conflabs.com/wp-content/uploads/2018/03/EIght-Cannabinoids-by-HPLC-UV-v1.1.pdf [Accessed on 2019-12-03].

Costa, E.P.; Lorena, A.C.; Carvalho, A.C.P.L.F.; Freitas, A.A. 2007. A review of performance evaluation measures for hierarchical classifiers. In: Drummond, C.; Elazmeh, W.; Japkowicz, N and Macskassy, S.A. (Eds), *Proceedings of the 2007 AAAI Workshop Evaluation Methods for Machine Learning I*I, AAAI Press, pp. 1–6. ISBN 978-1-57735-332-4 (KAR id: 14562).

Crawford, K.W.; Li, C.; Keung, A.; Su, Z.; Hughes, M.D.; Greaves, W.; Kuritzkes, D.; Gulick, R.; Flexner, C. 2010. Pharmacokinetic/pharmacodynamic modelling of the antiretroviral activity of the ccr5 antagonist vicriviroc in treatment experienced HIV-infected subjects (ACTG PROTOCOL 5211). *Journal of Acquired Immune Deficiency Syndrome*, 53(5), 598–605.

Crommentuyn, K.M.L.; Rosing, H.; Hillebrand, M.J.X.; Huitema, A.D.R.; Beijnen, J.H. 2004. Simultaneous quantification of the new HIV protease inhibitors atazanavir and tipranavir in human plasma by high-performance liquid chromatography coupled with electrospray ionisation tandem mass spectrometry. *Journal of Chromatography B*, 804(2), 359–367.

Custodio, J.M.; Rhee, M.; Shen, G.; Ling, K.H.J.; Kearney, B.P.; Ramanathan S. 2014. Pharmacokinetics and Safety of Boosted Elvitegravir in Subjects with Hepatic Impairment. *Antimicrobial Agents and Chemotherapy*, 58(5), 2564–2569.

Daal, Y.; Cherkaoui, S.; Doffey-Lazeyras, F.; Dayer, P.; Desmeules, J.A. 2008. Development and validation of a chemical hydrolysis method for dextromethorphan and dextrophan

determination in urine samples: Application to the assessment of CYP2D6 activity in fibromyalgia patients. *Journal of Chromatography B*, 861, 56–63.

Dams, R.; Benijts, T.; Lambert, W.T.; Massart, D.L.; De Leenheer, A.P. 2001. Heroin impurity profiling: trends throughout a decade of experimenting. *Forensic Science International*, 123, 81–88.

Dams, R.; Murphy, C.M.; Choo, R.E.; Lambert, W.E.; De Leenheer, A.P.; Huestis, M.A. 2003. LC-Atmospheric Pressure Chemical Ionization-MS/MS Analysis of Multiple Illicit Drugs, Methadone, and Their Metabolites in Oral Fluid Following Protein Precipitation. *Analytical Chemistry*, 75(4), February 15, pp. 798–804.

Darokar, M.P.; Dhawan, S.S.; Shukla, A.K.; Thul, S.T.; Lal, R.K.; Shasany, A.K.; Khanuja, S.P.S. 2014. Assessment of genetic relatedness among selected cultivars of opium poppy (*Papaver Somniferum L*.) through DNA profiling. *Acta Horticulture*, 1036, 2–28.

Dastmalchi, S.; Rashidi, M.; Rassi, M. 1995. Simultaneous determination of the pKa and octanol/water partition coefficient (Pm) of acetaminophen. *Journal of School of Pharmaceutical Medicine and Science, Tehran University*, 4, 7–14.

Day, D.; Kuntz, D.J.; Feldman, M. 2006. Detection of THCA in Oral Fluid by GC-MS-MS. *Journal of Analytical Toxicology*, 30, 645–650.

D'Avolio, A.; Siccardi, M.; Sciandra, M.; Lorena, B.; Bonora, S.; Trentini, L.; Di Perri, G. 2007. HPLC–MS method for the simultaneous quantification of the new HIV protease inhibitor darunavir, and 11 other antiretroviral agents in plasma of HIV-infected patients. *Journal of Chromatography B*, 859, 234–240.

D'Avolio, A.; Simiele, M. Siccardi, M.; Baietto, L.; Sciandra, M.; Bonora, S.; Di Perri,G. 2010. HPLC–MS method for the quantification of nine anti-HIV drugs from dry plasma spot on glass filter and their long term stability in different conditions. *Journal of Pharmaceutical and Biomedical Analysis*, 52, 774–780.

De Aquino Ribeiro, J.A.; De Campos, L.M.; Alves, R.J.; Lages, G.P.; Pianetti, G.A. 2007. Efavirenz related compounds preparation by hydrolysis procedure: setting reference standards for chromatographic purity analysis. *Journal of Pharmaceutical and Biomedical Analysis*, 43, 298–303.

De Backer, B.; Maebe, K.; Verstraete, A.G.; Charlier, C. 2012. Evolution of the Content of THC and Other Major Cannabinoids in Drug-Type Cannabis Cuttings and Seedlings During Growth of Plants. *Journal of Forensic Science*, 57(4), 918–922.

Dejaegher, B.; Heyden, Y.V. 2007. Ruggedness and robustness testing. *Journal of Chromatography A*, 1158, 138–157.

De Meijer, E.P.M.; Hammond, K.M.; Sutton, A. 2009. The inheritance of chemical phenotype in *Cannabis sativa L.* (IV): cannabinoid-free plants. *Euphytica*, 168, 95–112.

Department of Health (South Africa). 2004. Anti-Retroviral Therapy in South Africa - A pocket guide of the prevention and management of Side Effects and Drug Interactions. http://www.hst.org.za/sites/default/files/art_pocketguide.pdf [Accessed on 2016-03-05].

De Requena, D.G.; Bonora, S.; Castagna, A.; Hasson, H.; Marucco, D.A.; D'Avolio, A.; Sciandra, M.; Trentini, L.; Calcagno, A.; Lazzarin, A.; Di Perri, G. 2008. Pharmacokinetic and pharmacodynamic determinants of early virological response to enfuvirtide-based regimens in HIV-positive patients. *Journal of Antimicrobial Chemotherapy*, 62, 384–387.

Desai, R.; Roadcap, B.; Goykhman, D.; Woolf, E. 2019. Determination of doravirine in human plasma using liquid- liquid extraction and HPLC-MS/MS. *Bioanalysis*, 11(16). https://doi.org/10.4155/bio-2019-0116 [Accessed on 2019-11-25].

Djerada, Z.; Feliu, C.; Tournois, C.; Vautier, D.; Binet, L.; Robinet, A.; Marty, H.; Gozalo, C.; Lamiable, D.; Millart, H. 2013.Validation of a fast method for quantitative analysis of elvitegravir, raltegravir, maraviroc, etravirine, tenofovir, boceprevir and 10 other antiretroviral agents in human plasma samples with a new UPLC-MS/MS technology. *Journal of Pharmaceutical and Biomedical Analysis*, 86, 100–111. https://doi.org/10.1016/j.jpba.2013.08.002 [Accessed on 2019-11-25]

Drug Wars. http://www.drugaware.co.za/index2.html [Accessed on 2016-05-23].

DSTV Network: Carte Blanche. Hiting the streets- SA's Top Drugs. 08 May 2016. http://carteblanche.dstv.com/street-drugs/ [Accessed on 2016-05-23].

Dufey, V.; Dujourdy, L.; Besacier, F.; Chaudron, H. 2007. A quick and automated method for profiling heroin samples for tactical intelligence purposes. *Forensic Science International*, 169, 108–117.

Ehleringer, J.R. and others. 1999. Geo-location of heroin and cocaine by stable isotope ratios. *Forensic Science International*, 106(1), 27–35.

Elbardisy, H.M.; Foster, C.W.; Cumba, L.; Antonides, L.H.; Gilbert, N.; Schofield, C.J.; Belal, T.S.; Talaat, W.; Sutcliffe, O.B.; Daabeesg, H.G.; Banks, C.E. 2019. Analytical determination of heroin, fentanyl and fentalogues using high-performance liquid chromatography with diode array and amperometric detection. *Analytical Methods*, 11, 1053–1063.

Elek, S.R.; Katz, L.N. 1942. Some clinical uses of papaverine in heart disease. *Journal of the American Medical Association*, 120(6), 434–441.

Eligh, J. 2020. A shallow flood: The diffusion of heroin in Eastern and Southern Africa. Global initiative Against Transnational Organised Crime. https://globalinitiative.net/wp-content/uploads/2020/05/A-Shallow-Flood-The-Diffusion-of-Heroin-in-Eastern-and-Southern-Africa-GITOC.pdf [Accessed on 2020-08-07].

Elliott, S. P.; Stephen, D. W. S.; Paterson, S. 2018. The United Kingdom and Ireland association of forensic toxicologists' forensic toxicology laboratory guidelines. *Science & Justice*, 58, pp. 335–345.

ElSohly, M.A.; Gul, W. 2014. Constituents of *Cannabis Sativa*. In Pertwee, R. (Ed), *Handbook of Cannabis.* Oxford University Press. New York, United States of America. 3-22.

Esseiva, P.; Anglada, F.; Dujourdy, L.; Taroni, F.; Margot, P.; Du Pasquier, E.; Dawson, M.; Roux, C.; Doble, P. 2005. Chemical profiling and classification of illicit heroin by principal component analysis, calculation of inter sample correlation and artificial neural networks. *Talanta*, 67, 360–367.

Fawcett, T. 2004. ROC Graphs: Notes and Practical Considerations for Researchers. *HP Laboratories [Online]*. Available at: http://binf.gmu.edu/mmasso/ROC101.pdf Accessed 2020-12-21].

Fayet, A.; Beguin, A.; Zanolari, B.; Cruchon, S.; Guignard, N.; Telenti, A.; Cavassini, M.; Gunthard, H.F.; Buclin, T.; Biollaz, J.; Rochat, B.; Decosterd, L.A. 2009. A LC-tandem MS assay for the simultaneous measurement of new antiretroviral agents: Raltegravir, maraviroc, darunavir and etravirine. *Journal Chromatography B: Analytical Technologies in the Biomedical and Life Sciences* 877 (11–12), 1057–1069.

FDA (Food and Drug Administration). 2018. Bioanalytical Method Validation Guidance for Industry.

Feizbakhsh, R.; Ebrahimi, M.; Davoodnia, A. 2016. Preconcentration and analysis of cannabinoid compounds (THC-9, CBN, CBD) in urine samples by IL-ISFME/D-ì-SPE/HPLC-DAD. *International Journal of Medical Research & Health Sciences*, 5(1), 235–244.

Feng, S.; ElSohly, M.A.; Salamone, S.; Salem, M.Y. 2000. Simultaneous Analysis of Δ9-THC and its Major Metabolites in Urine, Plasma, and Meconium by GC-MS Using an Immunoaffinity Extraction Procedure. *Journal of Analytical Toxicology*, 24, 395–402.

Ferry, M. A. 2016. Tuning for Agilent GC/MS Systems. *Optimize.* https://www.spexcertiprep.com/knowledge-base/files/Optimize_201601.pdf [Accessed 2020-11-17].

Fihlani, P. 2011. *BBC News*, Durban, 28 February. https://www.bbc.com/news/world-africa-12389399 [Accessed on 2019-03-30].

Fischedick, J.T.; Hazekamp, A.; Erkelens, T.; Choi, Y.H.; Verpoorte, R. 2010. Metabolic fingerprinting of *Cannabis sativa L.*, cannabinoids and terpenoids for chemotaxonomic and drug standardization purposes. *Phytochemistry*, 71, 2058–2073.

Flemming, T.; Muntendam, R.; Steup, C.; Kayser, O. 2007. Chemistry and Biological Activity of Tetrahydrocannabinol and its Derivatives. *Bioactive Heterocycles IV, Topics in Heterocyclic Chemistry,* 10, 1–42.

Flores-Sanchez, I.J.; Verpoorte, R. 2008. Secondary metabolism in cannabis. *Phytochem Rev*., 7, 615–639.

Florian-Ramírez, N.M.; Garzón-Méndez, W.F.; Parada-Alfonso, F. 2012. Chromatography - Biochemicals, Narcotics and Essential Oils, Dr. Bekir Salih (Ed). ISBN: 978-953-51-0295-3, InTech, Available from: http://www.intechopen.com/books/gas-chromatography-biochemicals-narcotics-andessential-oils/gas-chromatography-in-forensic-chemistry-cannabinoids-content-in-marijuana-leaves-cannabissativa-l- [Accessed on 2018-11-16].

Floyd, F.J.; Widaman, K.F. 1995. Factor analysis in the development and refinement of clinical assessment instruments. *Psychological Assessment*, 7, 286–299.

Fortuna, S.; Ragazzoni, E.; Lisi, L.; Di Giambenedetto, S.; Fabbiani, M.; Navarra, P. 2013. Validation of an UPLC-MS/MS Method for Quantitative Analysis of Raltegravir in Human Plasma Samples. *Therapeutic Drug Monitoring*, 35(2), 258–263.

Fowler, F.; Voyer, B.; Marino, M.; Finzel, J.; Veltri, M.; Wachter, N.M.; Huang, L. 2015. Rapid screening and quantification of synthetic cannabinoids in herbal products with NMR spectroscopic methods. *Analytical Methods*, 7, 7907–7916.

Frank, S.G.; Lalonde, D.H. 2012. How acidic is the lidocaine we are injecting, and how much bicarbonate should we add? *Canadian Journal of Plastic Surgery*, 20(2), 71–73.

Gallant, J.; Lazzarin, A.; Mills, A.; Orkin, C.; Podzamczer, D.; Tebas, P.; Girard, P.-M.; Brar, I.; Daar, E.S.; Wohl, D.; Rockstroh, J.; Wei, X.; Custodio, J.; White, K.; Martin, H.; Cheng, A.; Quirk, E. 2017. Bictegravir, emtricitabine, and tenofovir alafenamide versus dolutegravir, abacavir, and lamivudine for initial treatment of HIV-1 infection (GS-US-380-1489): a double-blind, multicentre, phase 3, randomised controlled non-inferiority trial. *The Lancet*. http://dx.doi.org/10.1016/S0140-6736(17)32299-7 [Accesed on 2019-11-12].

Gambaro, V.; Roda, G.; Visconti, G.L.; Arnoldi, S.; Casagni, E.; Dell'Acqua, L.; Fare, F.; Paladino, E.; Rusconi, C.; Arioli, S.; Mora, D. 2016. DNA-based taxonomic identification of basidiospores in hallucinogenic mushrooms cultivated in "grow-kits" seized by the police: LC-UV quali-quantitative determination of psilocybin and psilocin. *Journal of Pharmaceutical and Biomedical Analysis*, 125, 427–432.

Gaoni, Y.; Mechoulam, R. 1971. Isolation and structure of Δ^1 -tetrahydrocannabinol and other neutral cannabinoids from hashish. *Journal of the American Chemical Society*, 93(1), 217–224.

Gaoni, Y.; Mechoulam R. 1964. Isolation, Structure, and Partial Synthesis of an Active Constituent of Hashish. *Journal of the American Chemical Society*, 86(8), 1646–1647.

García, V.; Mollineda, R.A.; Sánchez, J.S. 2008. On the k-NN performance in a challenging scenario of imbalance and overlapping. *Pattern Analysis and Application*, 11, 269–280.

Gastrow, P. 2003. Mind-blowing: The cannabis trade in Southern Africa. Institute for Security Studies, Cape Town. Unpublished paper. https://www.issafrica.org/uploads/CANNABIS.PDF [Accessed on 2016-05-05].

Gauteng Province Department of Community Safety, Republic of South Africa (GPDPCS-SA). 2015. Drug abuse. http://www.gautsafety.gpg.gov.za/Documents/drug%20abuse.pdf [Accessed on 2016-04-29].

Gentile, N.; Siegwolf, R.T.W.; Esseiva, P.; Doyle, S.; Zollinger, K.; Delémont, O. 2015. Isotope ratio mass spectrometry as a tool for source inference in forensic science: A critical review. *Forensic Science International*, 251, 139–158.

Gergov, M.; Nokua, P.; Vuori, E.; Ojanperā, I. 2009. Simultaneous screening and quantification of 25 opioid drugs in post-mortem blood and urine by liquid chromatography-tandem mass spectrometry. *Forensic Science International*, 186, 36–43.

Ghosh, S.; Sailaja, A.; Ravikumar, B.V.V. 2015. Analytical method development and validation of etravirine in its bulk dosage form by using Reverse Phase High Performance Liquid Chromatography method as per International Conference on Harmonisation guidelines. Asian *Journal of Pharmaceutical and Clinical Research*, 8(2), 147–150.

Gilani, A. Grinnan, S. 2019 Quantitative Analysis of 16 Cannabinoids with Complete Baseline Separation of D8 and D9 THC Utilizing the Triple Quad LCMS-8050. Shimanzu Application news no. SSI-LCMC-108. https://www.ssi.shimandzu.com

Gillan, R.; Cole, M.D.; Linacre, A.; Thorpe, J.W.; Watson, N.D. 1995. Comparison of *Cannabis sativa* by random amplification of polymorphic DNA (RAPD) and HPLC of cannabinoids: a preliminary study. *Science and Justice*, 35, 169–177.

Gilmore, S.; Peakall, R.; Robertson, J. 2003. Short tandem repeat (STR) DNA markers are hypervariable and informative in *Cannabis sativa:* implication for forensic investigation. *Forensic Science International*, 131, 65–74.

Godowski, K.C. 1989. Antimicrobial action of sanguinarine. *Journal of Clinical Dentistry*, 1(4), 96–101.

González, O.; Blanco, M.E.; Iriarte, G.; Bartoloméd, L.; Maguregui, M.I.; Alonso, R.M. 2014. Bioanalytical chromatographic method validation according to current regulations, with a special focus on the non-well defined parameters limit of quantification, robustness and matrix effect. *Journal of Chromatography A*, 1353, 10–27.

Gould, J. 2015. The cannabis crop. *Nature*, 525, S2–S3.

Goyal, T. 2013. A novel stability indicating HPLC method for simultaneous estimation of guaiphenesin, chlorpheneramine maleate & dextromethorphan HBr. *International Journal of Pharmaceutical Sciences and Research,* 4, 4435–4441.

Grelotti, D.J.; Closson, E.F.; Smit, J.A.; Mabude, Z.; Matthews, L.T.; Safren, S.A.; Bangsberg, D.R.; Mimiaga, M.J. 2014. Whoonga: Potential Recreational Use of HIV Antiretroviral Medication in South Africa*. AIDS Behav*, 18, 511–518.

Grob Jr, K.; Grob, G.; Grob, K. 1978. Comprehensive, standardized quality test for glass capillary columns. *Journal of Chromatography A*, 156 (1), 1–20.

Grobosch, T.; Angelow, B.; Schönberg, L.; Lampe, D. 2006. Acute Bromadiolone Intoxication. *Journal of Analytical Toxicology*, 30, 281–286.

Gröger, Th.; Schäffer, M.; Pütz, M.; Ahrens, B.; Drew, K.; Eschner, M.; Zimmermann, R. 2008. Application of two-dimensional gas chromatography combined with pixel-based chemometric processing for the chemical profiling of illicit drug samples. *Journal of Chromatography A*, 1200, 8–6.

Grotenhermen, F.; Karus, M.; Lohmeyer, D. 1998. THC limits for food: A scientific study. *Journal of the International Hemp Association*, 5(2), 101–105.

Gruber, B.; Weggler, B.A.; Jaramillo, R.; Murrell, K.A.; Piotrowski, P.K.; Dorman, F.L. 2018. Comprehensive two-dimensional gas chromatography in forensic science: A critical review of recent trends. *Trends in Analytical Chemistry,* 105, 292–301.

Gumbi, B.P.; Moodley, B.; Birungi, G.; Ndungu, P.G. 2017. Detection and quantification of acidic drug residues in South African surface water using gas chromatography-mass spectrometry. *Chemosphere*, 168, 1042–1050.

Guthery, B.; Bassindale, A.; Pillinger, C.T.; Morgan, G.H. 2009. The detection of various opiates and benzodiazepines by comprehensive two-dimensional gas chromatography/time-of-flight mass spectrometry. *Rapid Communication in Mass Spectrometry*, 23, 340–348.

Guthery, B.; Bassindale, T.; Bassindale, A.; Pillinger, C.T.; Morgan, G.H. 2010. Qualitative drug analysis of hair extracts by comprehensive two-dimensional gas chromatography/time-of-flight mass spectrometry. *Journal of Chromatography A*, 1217, 4402–4410.

Hall, W.; Solowij, N. 1998. Adverse effects of cannabis. *The Lancet*, 352, 1611–1616.

Hall, W. 2014. What has research over the past two decades revealed about the adverse health effects of recreational cannabis use? Addiction, 110, 19–35.

Hamrapurkar, P.D.; Patil, P.S.; Phale, M.D.; Shah, N.; Pawar, S.B. 2010. Optimization and Validation of RP-HPLC Stability-Indicating Method for Determination of Efavirenz and its Degradation Products. *International Journal of Applied Science and Engineering*, 8, 155–165.

Happyana, N.; Agnolet, S.; Muntendam, R.; Van Dam, A.; Schneider, B.; Kayser, O. 2012. Analysis of cannabinoids in laser micro dissected trichomes of medicinal *Cannabis sativa* using LCMS and cryogenic NMR. *Phytochemistry*, 87, 51–59.

Hari, S.; Sharma, A.; Sharma, V. 2009. Molecular characterization of opium poppy (*Papaver somiferum*) germplasm. *American Journal of Infectious Diseases*, 5(2), 155–160.

Harvey, D.J. 1990. Stability of cannabinoids in dried samples of cannabis dating from around 1896-1905. *Journal of Ethnopharmacology*, 28, 117–128.

Hartmann, C.; Smeyers-Verbeke, J.; Massart, D. L.; McDowall, R. D. 1998. Validation of bioanalytical chromatographic methods. *Journal of Pharmaceutical and Biomedical Analysis*, 17(2), 193–218.

Hassan, D.; Aickelin, U.; Wagner, C. 2014. Comparison of Distance Metrics for Hierarchical Data in Medical Databases. arXiv preprint arXiv:1409.1055. https://arxiv.org/pdf/1409.1055.pdf [Accessed on 2019-12-30]

Hays, P.A.; Remaud, G.S.; Jamin, E.; Martin, Y.-L. 2000. Geographic origin determination of heroin and cocaine using site-specific isotopic ratio deuterium NMR. *Journal of Forensic Science*, 45(3), 552–562.

Hays, P.A. 2005. Proton nuclear magnetic resonance spectroscopy (NMR) methods for determining the purity of reference drug standards and illicit forensic drug seizures. *Journal of Forensic Science*, 50, 1342–1360.

Haysom, S. 2019. Hiding in plain sight: Heroin's stealthy takeover of South Africa. ENACT Heroin Policy Brief. https://enactafrica.org/research/policy-briefs/hiding-in-plain-sight-heroins-stealthy-takeover-of-south-africa [Accessed on 2019-04-10].

Hazekamp, A. n.d. Cannabis review 2008–2009. https://www.oregon.gov/pharmacy/Imports/Marijuana/StaffInfo/CannabisReview.pdf [Accessed on 2016-02-05].

Hazekamp, A. 2007. Cannabis; extracting the medicine. Leiden (the Netherlands): Universiteit Leiden, Thesis. pp. 181.

Hazekamp, A.; Choi, Y.H.; Verpoorte, R. 2004. Quantitative Analysis of Cannabinoids from *Cannabis sativa* Using 1H-NMR. *Chemical and Pharmaceutical Bulletin*, 52(6), 718–721.

Hazekamp, A.; Fischedick, J.T. 2012. Cannabis – from cultivar to chemovar. *Drug Testing and Analysis*, 4, 660–667.

Health24. 2014. Is nyaope South Africa's worst drug? https://www.health24.com/Lifestyle/Street-drugs/News/Street-drug-nyaope-classified-as-illegal-20140403 [Accessed on 2016-03-19].

Hennig, C. 2008. Dissolution point and isolation robustness: Robustness criteria for general cluster analysis methods. *Journal of Multivariate Analysis*, 99, 1154–1176.

Heroin. https://www.unodc.org/documents/data-and-analysis/tocta/5.Heroin.pdf [Accessed on 2020-04-29].

Hewavitharana, A.K.; Golding, G.; Tempany, G.; King, G.; Holling, N. 2005. Quantitative GC-MS Analysis of Δ9-Tetrahydrocannabinol in Fiber Hemp Varieties. *Journal of Analytical Toxicology*, 29, 258–260.

Hibbert, D.B. 2016. Vocabulary of concepts and terms in chemometrics (IUPAC Recommendations 2016). *Pure and Applied Chemistry*, 88(4), 407–443.

Hildebrand J. H.; Scott, R. L. 1964. *Solubility of Non-Electrolytes, 3rd ed.*, Dover, New York,

Hill, R.J. 1983. Marijuana, *Cannabis sativa L. Regulatory Horticulture, Weed Circular 5*, 9(1-2), 57–66.

Hillig, K.W. 2005. Genetic evidence for speciation in Cannabis (Cannabaceae). *Genetic Resources and Crop Evolution*, 52, 161–180.

Hong, L.; Wen-song, Z.; Ping, F.; Hong-mei, Y.; De-qiang, J.; Shao-peng, L.; Zhi-qiang L.; Can-peng, L. 2014. The study on the stability of heroin standard in organic solvents (Abstract). *Forensic Sci. Tech*, 39(3), 3.

Hsieh, H.-M.; Hou, R.-J.; Tsai, L.-C.; Wei, C.-S.; Liu, S.-W.; Huang, L.-H.; Kuo, Y.C.; Linacre, A.; Lee, J.C. 2003. A highly polymorphic STR locus in *Cannabis sativa*. *Forensic Science International*, 131, 53–58.

Huang, Y.; Gandhi, M.; Greenblatt, R.M.; Gee, W.; Lin, E.T.; Messenkoff, N. 2008.Sensitive analysis of anti-HIV drugs, efavirenz, lopinavir and ritonavir, in human hair by liquid chromatography coupled with tandem mass spectrometry. *Rapid Communication Mass Spectrometry,* 22(21): 3401–3409.

Hudson, J.; Hutchings, J.; Wagner, R.; Harper, C.; Friel, P. 2013. Cannabinoids quantification using an Agilent 6430 LC/MS/MS. Application Note 5991-2521EN Forensic www.agilent.co/chem [Accessed on 2019-11-24].

Huizer, H.; Poortman, A. J. 1989. Some Aspects of the Gas Chromatographic (GC) Analysis of Heroin. United Nations Scientific and Technical Notes. SCITEC/5. https://www.unodc.org/pdf/scientific/SCITEC_5.pdf [Accessed 2016-06-02].

Hutchinson, M.R.; Somogyi, A.A. 2002. Diacetylmorphine degradation to 6-monoacetylmorhine and morphine in cell culture: its implications for in vitro studies. *European Journal of Pharmacology*, 453, 27–32.

Hyotylainen, T.; Sirén, H.; Riekkola, M.L. 1996. Determination of morphine analogues, caffeine and amphetamine in biological fluids by capillary electrophoresis with the marker technique. *Journal of Chromatography A*, 735(1-2), 439–447.

Hyvärinen, l. 1970. *Principal component analysis.* In: *Mathematical Modeling for Industrial Processes. Lecture Notes in Operations Research and Mathematical Systems (Economics, Computer Science, Information and Control), vol 19.* Springer, Berlin, Heidelberg. https://doi.org/10.1007/978-3-642-87427-7_6 [Accessed on 2020-01-08].

Ibrahim, E.A.; Gul, W.; Gul, S.W.; Stamper, B.J.; Hadad, G.M.; Abdel-Salam, R.A.; Ibrahim, A.K.; Ahmed, S.A.; Chandra, S.; Lata, H.; Radwan, M.M.; ElSohly M.A. 2018. Determination of acid and neutral cannabinoids in extracts of different strains of *Cannabis sativa* using GC-FID. *Planta Medica*, 84(04), 250–259.

Ihle, E.; Schmidt, L. 1996. Multielement isotope analysis on drugs of abuse. Possibility for their origin assignment. *Isotopes in Environmetal and Health Studies*, 32, 226–228.

Inciardi, J.A.; Surratt, H.L.; Kurtz, S.P.; Cicero, T.J. 2007. Mechanisms of prescription drug diversion among drug-involved club- and street-based populations. *Pain Med*., 8(2), 171–183.

International Conference on Harmonisation (ICH), ICH Harmonised Tripartite Guideline Stability Testing of New Drug Substances and Products Q1A(R2). 2003. http://www.ich.org/fileadmin/Public_Web_Site/ICH_Products/Guidelines/Quality/Q1A_R2/Step4/Q1A_R2__Guideline.pdf [Accessed on 2016-03-18].

International Conference on Harmonisation (ICH), ICH Harmonised Tripartite Guideline: Validation of Analytical Procedures: Text And Methodology, Q2(R1). 2005. http://www.ich.org/zfileadmin/Public_Web_Site/ICH_Products/Guidelines/Quality/Q2_R1/Step4/Q2_R1__Guideline.pdf [Accessed on 2016-03-18].

Janhunen, K.; Cole M.D. 1999. Development of a predictive model for batch membership of street samples of heroin. *Forensic Science International*, 102, 1–11.

Jolliffe I.T.; Cadima J. 2016.Principal component analysis: a review and recent developments. *Philosophical Transactions of the Royal Society A*, 374: 20150202. http://dx.doi.org/10.1098/rsta.2015.0202 [Accessed on 2020-01-08].

Jones, C.; Nelson, J. 2017. Multi-Element Analysis of Cannabis using the Agilent 7800 ICP-MS. Application Note. Food safety. Agilent Technologies, USA. www.agilent.com/chem [Accessed on 2018-05-07].

Jones, J.M.; Raleigh, M.D.; Pentel, P.R.; Harmon, T.M.; Keyler, D.E.; Remmel, R.P.; Birnbauma, A.K. 2013. Stability of heroin, 6-monoacetylmorphine, and morphine in biological samples and validation of an LC–MS assay for delayed analyses of pharmacokinetic samples in rats. *Journal of Pharmaceutical and Biomedical Analysis*, 74, 291–297.

Jubilant life sciences. Technical data sheet. www.jubl.com [Accessed on 2019-07-17].

Jung, B.H.; Rezk, N.L.; Bridges, A.S.; Corbert, A.H.; Kashuba, A.D.W. 2007. Simultaneous determination of 17 antiretroviral drugs in human plasma for quantitative analysis with liquid chromatography-tandem mass spectrometry. *Biomedical Chromatography*, 21(10), 1095–2011.

Kadiana, N.; Raju, K.S.R.; Rashid, M.; M. Malika, Y.; Taneja, I.; Wahajuddin, M. 2016. Comparative assessment of bioanalytical method validation guidelines for pharmaceutical industry. *Journal of Pharmaceutical and Biomedical Analysis*, 126, 83–97.

Kaiser, H.F. 1970. A second generation Little Jiffy. *Psychometrika*, 35, 401–415.

Kakande, B.; Isaacs, T.; Muloiwa, R.; Dlamini, S.; Lehloenya, R. 2015. Case Report: Stevens-Johnson syndrome following a single double dosing of nevirapine-containing regimen once in an HIV-infected woman on long-term antiretroviral therapy. [version 1; referees: 1 approved, 2 approved with reservations]. *F1000Research*, 4, 175. (doi: 10.12688/f1000research.6715.1) http://dx.doi.org/10.12688/f1000research.6715.1 [Accessed on 2016-03-05].

Kalogris, C.; Garulli, C.; Pietrella, L.; Gambini, V.; Pucciarelli, S.; Lucci, C.; Tilio, M.; Zabaleta, M. E.; Bartolacci, C.; Andreani, C.; Giangrossi, M.; Iezzi, M.; Belletti, B.; Marchini, C.; Amici, A. 2014. Sanguinarine suppresses basal-like breast cancer growth through dihydrofolate reductase inhibition. *Biochemical Pharmacology*, 90(3), 226–234.

Kappelhoff, B.S.; Rosinga, H.; Huitemaa, A.D.R.; Beijnen, J. H. 2003. Simple and rapid method for the simultaneous determination of the non-nucleoside reverse transcriptase inhibitors efavirenz and nevirapine in human plasma using liquid chromatography. *Journal of Chromatography B*, 792, 353–362.

Karinen, R.; Andersen, J.M.; Ripel, Å.; Hasvold, I.; Hopen, A.B.; Mørland, J.; Christophersen, A.S. 2009. Determination of Heroin and Its Main Metabolites in Small Sample Volumes of Whole Blood and Brain Tissue by Reversed-Phase Liquid Chromatography–Tandem Mass Spectrometry. *Journal of Analytical Toxicology*, 33, 345–350.

Karnes, H.T.; March, C. 1993. Precision, Accuracy and Data Acceptance Criteria in Biopharmaceutical Analysis. *Pharmaceutical Research*, 10(10), 1420–1426.

Kauert, G.F.; Iwersen-Bergmann, S.; Toennes, S.W. 2006. Assay of Δ9-Tetrahydrocannabinol (THC) in Oral Fluid--Evaluation of the OraSure Oral Specimen Collection Device. *Journal of Analytical Toxicology*, 30, 274–277.

Khan, S.A; Schell, M.M. 2014. Anticoagulant rodenticides (Warfarin and Congeners). MSD Veterinary Manual https://www.msdvetmanual.com/toxicology/rodenticides-poisoning/anticoagulant-rodenticides-wafarin-and-congeners [Accessed on 2020-08-18].

Khine, A.A.; Mokwena K.E. Huma, M.; Fernandes, L. 2015. Identifying the composition of street drug Nyaope using two different mass spectrometer methods. *African Journal of Drug & Alcohol Studies,* 14(1), 49–56.

Kiprono, P.C.; Kaberia, F.; Keriko, J.M.; Karanja, J.N. 2000. The *in vitro* Anti-Fungal and Anti-Bacterial Activities of ß-Sitosterol from *Senecio lyratus* (Asteraceae). *Zeitschrift für Naturforschung C*, 55c, 485–488.

Klemenc, S. 2001. In common batch searching of illicit heroin samples – evaluation of data by chemometrics methods. *Forensic Science International*, 115, 43–52.

Kojoma, M.; Iida, O.; Makino, Y.; Sekita, S.; Satake, M. 2002. DNA fingerprinting of *Cannabis sativa* using inter-simple sequence repeat (ISSR) amplification. *Planta Medica*, 68, 60–63.

König, S.; Aebi, B.; Lanz, S.; Gasser, M.; Weinmann W. 2011. On-line SPE LC-MS/MS for the quantification of Δ9-tetrahydrocannabinol (THC) and its two major metabolites in human peripheral blood by liquid chromatography tandem mass spectrometry. *Analytical and Bioanalytical Chemistry,* 400(1), 9–6.

Krishna, M.V.; Srinath, M.; Sankar, D.G. 2008. Principles and Applications of Capillary Electrophoresis in New Drug Discovery. *Current Trends in Biotechnology and Pharmacy*, 2(1), 142–155.

Kromdijk, W.; Pereira, S.A.; Rosing, H.; Mulder, J.W.; Beijnen, J.H.; Huitema, A.D.R. 2013. Development and validation of an assay for the simultaneous determination of zidovudine, abacavir, emtricitabine, lamivudine, 239enofovir and ribavirin in human plasma using liquid chromatography-tandem mass spectrometry. *Journal of Chromatography B*, 919–920, 43–51.

Kuleya, C.; Hall, S.; Gautam, L.; Cole, M.D. 2014. An optimised gas chromatographic-mass spectrometric method for the chemical characterisation of benzylpiperazine and 1-arylpiperazine based drugs. *Analytical Methods*, 6, 156–163.

Kumar, V.R.; Reddy, B.P.; Kumar, B.R.; Sreekanth, K.; Babu, K.N. 2013. High throughput LC-MS/MS method for simultaneous determination of zidovudine, lamivudine and nevirapine in human plasma. *Journal of Chromatography B,* 921–922, 9–14.

KZN Department of Health (South Africa). Marijuan facts for teens. n.d. http://www.kznhealth. gov.za/mental/marijuana.pdf [Accessed on 2016-05-23].

Labanca, F.; Ovesná, J.; Milella, L. 2018. Papaver somniferum L. taxonomy, uses and new insight in poppy alkaloid pathways. *Phytochemistry Reviews*, 17, 853–871.

Larkan, F.; Van Whyk, B.; Saris, J. 2010. Of remedies and poisons: recreational use of antiretroviral drugs in the social imagination of South African carers. *African Sociology Review*, 14 (2), 62–73.

Lavagnini, I.; Magno, F. 2007. A statistical overview on univariate calibration, inverse regression, and detection limits: application to gas chromatography/mass spectrometry technique. *Mass Spectrometry Reviews*, 26, 1–18.

Le Saux, T.; Chhun, S.; Ret, E.; Launay, O.; Weis, L.; Viard, J.-P.; Pons, G.; Julien, V. 2008. Quantification of seven nucleoside/nucleotide reverse transcriptase inhibitors in human plasma by high-performance liquid chromatography with tandem mass-spectrometry. *Journal of Chromatography B*, 865 (1 – 2), 81–90.

Lee, J.C.-I.; Cole, M.; Linacre, A. 2000. Identification of members of the genera Panaeolus and Psilocybe by a DNA test: a preliminary test for hallucinogenic fungi. *Forensic Science International,* 112, 123–133.

Lee, J.C.-I. 2001. Towards A Molecular Approach for the Identification of Fungal Taxa that Contain Psilocybin. PhD Thesis, Universlty of Strathclyde.

Lee, R.; Saussereau, E.; Lacroix, C.; Wood, M. 2014. Quantitative Analysis of Cannabinoids in Whole Blood Using UPLC-MS/MS for Forensic Laboratories. Waters application note 720004700EN. http://www.waters.com [Accessed on 2019-11-26].

Lefebvre, E.; Moyle, G.; Reshef, R.; Richman, L.P.; Thompson, M.; Hong, F.; Chou, H.-I.; Hashiguchi, T.; Plato, C.; Poulin, D.; Richards, T.; Yoneyama, H.; Jenkins, H.; Wolfgang, G.; Friedman, S.L. 2016a. Antifibrotic Effects of the Dual CCR2/CCR5 Antagonist cenicriviroc in Animal Models of Liver and Kidney Fibrosis. *PLOS ONE*, 11(6): e0158156. doi:10.1371/journal.pone.0158156

Leizer, C.; Ribnicky, D.; Poulev, A.; Dushenkov, S.; Raskin, I. 2000. The Composition of Hemp Seed Oil and Its Potential as an Important Source of Nutrition. *Journal of Nutraceuticals, Functional and Medical Foods*, 2(4), 35–54.

Lemmer, P.; Schneider, S.; Schuman, M.; Omes, C.; Arendt, V.; Toyari, J.-C.; Fundira, L.; Wennig, R. 2005. Determination of Nevirapine and Efavirenz in Plasma Using GC/MS in Selected Ion Monitoring Mode. *Therapeutic Drug Monitoring*, 27(4), 521–525.

Lewis Sr, R.J. 2007. *Hawley's Condensed Chemical Dictionary*. 15th ed. John Wiley & Sons, Inc. New York, NY, p. 11. pH-ACA.

Licsandru, A.; Nacea, V.; Boscencu, R. 2012. Microwave Assisted Digestion of Heroin Street Samples for Trace Metals Analysis by Inductively Coupled Plasma Mass Spectrometry. *(Revista de Chimie) REV. CHIM. (Bucharest),* 63(1), 86–90.

Linacre, A.; Thorpe, J. 1998. Detection and identification of cannabis by DNA. *Forensic science International*, 91, 71–76.

Linacre, A.; Cole, M.; Lee, J.C.-I. 2002. Identifying the presence of 'magic mushrooms' by DNA profiling. *Science & Justice*, 42(1), 50–54.

Lindholst, C. 2010. Long term stability of cannabis resin and cannabis extracts. Australian *Journal of Forensic Sciences Pages*, 42(3), 181–190.

Liu, C.; Hua, Z.; Bai, Y.; Liu, Y. 2014. Profiling and classification of illicit heroin by ICP-MS analysis of inorganic elements. *Forensic Science International*, 239, 37–43.

Lopez-Quintero, C.; Perez de los Cobos, J.; Hasin, D.S.; Okuda, M.; Wang, S.; Grant, B.F.; Blanco, C. 2011. Probability and predictors of transition from first use to dependence on nicotine, alcohol, cannabis, and cocaine: Results of the National Epidemiologic Survey on Alcohol and Related Conditions (NESARC). *Drug and Alcohol Dependence*, 115, 120–130.

Lurie, I.S.; Driscoll, S.E.; Cathapermal, S.S.; Panicker, S. 2013. Determination of heroin and basic impurities for drug profiling by ultra-high-pressure liquid chromatography. *Forensic Science International,* 231, 300–305.

Lurie, I.S.; Toske, S.G. 2008. Applicability of ultra-performance liquid chromatography–tandem mass spectrometry for heroin profiling, *J. Chromatogr. A*, 1188, 322–326.

Lyengar, A.; Hadi, S. 2014. Use of non-human DNA analysis in forensic science: A mini review. *Medicine, Science and the Law*, 54(1), 41–50.

Ma, J.; Wang, S.; Zhang, M.; Zhang, Q.; Zhou, Y.; Lin, C.; Lin, G.; Wang, X. 2015. Simultaneous determination of bupropion, metroprolol, midazolam, phenacetin, omeprazole and tolbutamide in rat plasma by UPLC-MS/MS and its application to cytochrome P450 activity study in rats. *Biomedical Chromatography*, 29, 1203–1212.

Mackraj, I.; Govender T.; Gathiram, P. 2008. Sanguinarine. *Cardiovascular Therapeutics*, 26 75–83.

Mahmoudian, M.; Rahimi-Moghaddam, P. 2009. The Anti-Cancer Activity of Noscapine: A Review. *Recent Patents on Anti-Cancer Drug Discovery*, 4(1), 92–97.

Mahmoudian, M.; Rezvani, M.; Rohani, M.; Benaissa, F.; Jalili, M.; Ghourchian, S. 2015. A novel effect of Noscapine on patients with massive ischemic stroke: A pseudo-randomized clinical trial. *Iranian Journal of Neurology*, 14(1), 12–16.

Mandrioli, M.; Tura, M.; Scotti, S.; Toschi, T.G. 2019. Fast Detection of 10 Cannabinoids by RP-HPLC-UV Method in *Cannabis sativa L. Molecules,* 24, 2113. http://dx.doi.org/10.3390/molecules24112113 [Accessed on 2019-11-21].

Mannocchi, G.; Pantano, F.; Tittarelli, R.; Catanese, M.; Ronchi, F.U.; Busardò, F.P. 2015. Development and Validation of a GC-MS Method for the Detection and Quantification of Clotiapine in Blood and Urine Specimens and Application to a Postmortem Case. International *Journal of Analytical Chemistry*, 2015, Article ID 972480, 5 pages. https://doi.org/10.1155/2015/972480 [Accessed on 2019-09-06].

Marchini, M.; Charvoz, C.; Dujourdy, L.; Baldovini, N.; Filippi, J.-J. 2014. Multidimensional analysis of cannabis volatile constituents: identification of 5, 5-dimethyl-1 vinylbicyclo[2.1.1]hexane as a volatile marker of hashish, the resin of *Cannabis sativa L. Journal of Chromatography A,* 1370, 200–215.

Marciano, M.A.; Panicker, S. X.; Liddil, G.D.; Lindgren, D.; Sweder, K.S. 2018.Development of a Method to Extract Opium Poppy (*Papaver Somniferum L.*) DNA from Heroin. *Scientific Repoerts,* 8 (1), 2590– 2599. https://doi.org/10.1038/s41598-018-20996-9 [Accessed XXXX].

Marek, L.J.; Koskinen, W.C. 2007. Multiresidue Analysis of Seven Anticoagulant Rodenticides by High-Performance Liquid Chromatography/Electrospray/Mass Spectrometry. J. *Agric. Food Chem.*, 55, 571–576.

Marijuana Genetics Database. 2016. Marijuana Genetics of Africa http://www.marijuanagenetics.com/africangenetics.html [Accessed on 2016-05-11].

Marriott, P.; Mitrevski, B., 2014. Innovative solutions for enhanced illicit drugs profiling using comprehensive two-dimensional gas chromatography and mass spectrometry technologies. Monograph Series 50. www.ndlerf.gov.au/publications/monograps/monograph-50 [Accessed on 2016-04-30].

Martin, J.; Deslandes, G.; Dailly, E.; Renaud, C.; Reliquet, V.; Raffic, F.; Jolliet, P. 2009. A liquid chromatography–tandem mass spectrometry assay for quantification of nevirapine, indinavir,

atazanavir, amprenavir, saquinavir, ritonavir, lopinavir, efavirenz, tipranavir, darunavir and maraviroc in the plasma of patients infected with HIV. *Journal of Chromatography B*, 877, 3072–3082.

Masombuka, J. 2013. Children's addiction to the drug "NYAOPE" in Soshanguve Township: Parents' experiences and support needs. University of South Africa, Pretoria. Thesis. 154 p.

Maurin, M.B.; Rowe, S.M.; Blom, K.; Pierce M.E. 2002. Kinetics and mechanism of hydrolysis of efavirenz. *Pharmaceutical Research*, 19(4), 517–521.

McCord, B.; Gauthier, Q.; Cho, S.; Roig, M.; Gibson-Daw, G.; Young, B.; Taglia, F.; Zapico, S.C.; Mariot, R.F.; Lee, S.B.; Duncan, G. 2018. Forensic DNA Analysis. Analytical Chemistry. DOI: 10.1021/acs.analchem.8b05318

McGilveray, I.J. 2005. Pharmacokinetics of cannabinoids. *Pain Research and Management*, 10(Suppl A), 15A–22A.

McPartland, J.M.; McDonald, C.; Young, M.; Grant, P. S.; Fukert, D.P.; Glass M. 2017. Affinity and Efficacy Studies of Tetrahydrocannabinolic Acid A at Cannabinoid Receptor Types One and Two. *Cannabis and Cannabinoid Research*, 2(1), 87–95.

Mechoulam, R.; Hanuš, L. 2002. Review: Cannabidiol: an overview of some chemical and pharmacological aspects. Part I: chemical aspects. *Chemistry and Physics of Lipids*, 121, 35–43.

Mechoulam, R.; Gaoni, Y. 1967. Absolute configuration of Δ^1 -tetrahydrocannabinol, the major active constituent of hashish. *Tetrahedron Letters*, 8(12), 1109–1111.

Mechoulam, R.; Ben-Zvi, Z.; Yagnitinsky, B.; Shani, A. 1969. A new tetrahydrocannabinolic acid. *Tetrahedron Letters*, 10, 2339–2341.

Meel, R.; Essop, M.R. 2018. Striking increase in the incidence of infective endocarditis associated with recreational drug abuse in urban South Africa. *South African Medical Journal*, 108(7), 585–589.

Meintjies, G.; Moorhouse, M.A.; Carmona, S.; Davies, N.; Dlamini, S.; van Vuuren, C.; Manzini, T.; Mathe, M.; Moosa, Y.; Nash, J.; Nel, J.; Pakade, Y.; Woods, J.; van Zyl, G.; Conradie, F.; Venter, F. 2017. Adult antiretroviral therapy guidelines. *South African Journal of HIV Medicine*, 18(1), a776. DOI: https://doi.org/10.4102/sajhivmed.v18i1.776 [Accessed on 2019-1-14].

Meng, Q.; Buchanan, B.; Zuccolo, J.; Poulin, M-M.; Gabriele, J.; Baranowski, D.C. 2018. A reliable and validated LC-MS/MS method for the simultaneous quantification of 4 cannabinoids in 40 consumer products. *PLoS ONE*, 13(5), e0196396. https://doi.org/10.1371/journal.pone.0196396 [Accessed on 2019-11-21].

Merrick, J.; Lane, B.; Sebree, T.; Yaksh, T.; O'Neill, C.; Banks, S.L. 2016. Identification of Psychoactive Degradants of Cannabidiol in Simulated Gastric and Physiological Fluid. *Cannabis and Cannabinoid Research,* 1(1), 102–115.

Mičianová, V.; Ondreičková, K.; Muchová, D.; Klčová, L.; Hudcovicová, M.; Havrlentová, M.; Mihálik, D.; Kraic, J. 2017. Forensic application of EST-derived STR markers in opium poppy. *Biologia,* 72, 587–594. https://doi.org/10.1515/biolog-2017-0076.

Migal N.D. 1991. Genetics of polymorphic sex evolution in hemp. *Genetika*, 27, 1561–1569. (Translated in *Soviet Genetics*, March 1992: 1095–1102).

Miller-Coyle, H.; Ladd, C.; Palmbach, T.; Lee, H.C. 2001. The green revolution: botanical contributions to forensics and drug enforcement. *Croat. Med. J.,* 42, 340–345.

Miller-Coyle, H.; Sutler, G.; Abrams, S.; Hanniman, J.; Neylon, S.; Ladd, C.; Palmbach, T.; Lee, H.C. 2003a. A simple DNA extraction method for Marijuana samples used in amplified fragment length polymorphism (AFLP) analysis. *Journal of Forensic Science*, 48, 343–347.

Miller-Coyle, H.; Palmbach, T.; Juliano, N.; Ladd, C.; Lee, H.C. 2003b. An overview of DNA methods for the identification and individualization of marijuana. *Croatian Medical Journal*, 44(3), 315–321.

Milman, G.; Barnes, A.J.; Lowe, R.H.; Huestis, M.A. 2010. Simultaneous quantification of cannabinoids and metabolites in oral fluid by two-dimensional gas chromatography mass spectrometry. *Journal of Chromatography A*, 1217(9), 1513–1521.

Mills III, T.; Roberson, J.C.; Matchett, C.C.; Simon, M.J.; Burns, M.D.; Ollis Jr., R.J. 2006. Instrumental Data for Drug Analysis. 3rd Ed. Taylor & Francis Group, LLC. *Mass Spectra Indices of Drugs*, 6, 4409–4460.

Min, S.; Sloan, L.; DeJesus, E.; Hawkins, T.; McCurdy, L.; Song, I.; Stroder, R.; Chen, S.; Underwood, M.; Fujiwara, T.; Piscitelli, S.; Lalezari, J. 2011. Antiviral activity, safety, and pharmacokinetics/pharmacodynamics of dolutegravir as 10-day monotherapy in HIV-1-infected adults. *AIDS*, 25(14), 1737–1745.

Mitrevski, B.; Wynne, P.; Marriott, P.J. 2011. Comprehensive two-dimensional gas chromatography applied to illicit drug analysis. *Analytical and Bioanalytical Chemistry*, 401, 2361–2371.

Moffatt, A.C.; Osselton, M.D.; Widdop, B. (eds). 2011. *Clarke's analysis of drugs and poisons in pharmaceuticals, body fluids and postmortem material. Volume 2*. 4th ed. London, Pharmaceutical Press.

Mokwena, K.; Morojele, N. 2014. Unemployment and unfavourable social environment as contributory factors to nyaope use in three provinces of South Africa. *African Journal for Physical, Health Education, Recreation and Dance, Supplement*, 1(2), 374–384.

Mokwena, K.E.; Huma, M. 2014. Experiences of 'nyaope' users in three provinces of South Africa. African Journal for Physical, Health Education, Recreation and Dance, (Supplement 1:2), pp.352-363.

Mokwena K. 2015. "Consider our plight": a cry for help from nyaope users, Health SA Gesondheid. http://dx.doi.org/10.1016/j.hsag.2015.09.001 [Accessed on 2016-03-16].

Moliterni, V.M.C.; Cattivelli, L.; Ranalli, P.; Mandolino, G. 2004. The sexual differentiation of *Cannabis sativa L.*: A morphological and molecular study. *Euphytica*, 140, 95–106.

Montesano, C.; Johansen, S.S.; Nielsen, M.K.K. 2014. Validation of a method for the targeted analysis of 96 drugs in hair by UPLC–MS/MS. *Journal of Pharmaceutical and Biomedical Analysis,* 88, 295–306.

Monyakane, M.M-E.M. 2018. A Rehabilitative South African Criminal Law Response to Nyaope, Drug Addiction: A Recommendation for Health Oriented Nyaope Drug Weaning. *Research in Pediatrics & Neonatology*, 3(1), 206–214.

Morello, D.R.; Cooper, S.D.; Panicker, S.; Casale, J.F., 2010. Signature Profiling and Classification of Illicit Heroin by GC-MS Analysis of Acidic and Neutral Manufacturing Impurities. *J. Forensic Sci*., 55(1), 42–49.

Moreno-Vicente, R.; Fernández-Nieva, Z.; Navarro, A.; Gascón-Crespí, I.; Farré-Albadalejo, M.; Igartua, M.; Hernández, R.M.; Pedraz, J.L. 2015.Development and validation of a bioanalytical method for the simultaneous determination of heroin, its main metabolites, naloxone and naltrexone by LC-MS/MS in human plasma samples: Application to a clinical trial of oral administration of a heroin/naloxone formulation. *Journal of Pharmaceutical and Biomedical Analysis*, 114, 105–112.

Moyer, T.P.; Temesgen, Z.; Enger, R.; Estes, L.; Charlson, J.; Oliver, L.; Wright, A. 1999. Drug Monitoring of Antiretroviral Therapy for HIV-1 Infection: Method Validation and Results of a Pilot Study. *Clinical Chemistry,* 45(9), 1465–476.

Mthembi, P.M.; Mwenesongole, E.M.; Cole, M.D. 2018. Chemical profiling of the street cocktail drug 'Nyaope' in South Africa using GC-MS. I: Stability studies of components of 'Nyaope' in organic solvents. *Forensic Science International,* 292, 115–124.

Mthembi, P.M.; Mwenesongole, E.M.; Cole, M.D. 2019. Chemical profiling of the street cocktail drug 'nyaope' in South Africa using GC–MS II: Stability studies of the cannabinoid, opiate and antiretroviral components during sample storage. *Forensic Science International*, 300, 187–192.

Muccio, Z.; Wöckel, C.; An, Y.; Jackson, G.P. 2012. Comparison of Bulk and Compound-Specific δ13C Isotope Ratio Analyses for the Discrimination Between Cannabis Samples. *Journal of Forensic Science*, 57(3), 757–764.

Mudge, E.M.; Murch, S.J.; Brown, P. 2017. Leaner and greener analysis of cannabinoids. *Analytical and Bioanalytical Chemistry*, 409, 3153–3163.

Murray, J.A. 2012. Qualitative and quantitative approaches in comprehensive two-dimensional gas chromatography. *Journal of Chromatography A*, 1261, 58–68.

Mwenesongole, E.M. 2015. Simultaneous Detection of Drugs of Abuse in Waste Water Using Gas Chromatography-Mass Spectrometry. Thesis. 278 p.

Myors, R.B.; Crisp, P.T.; Skopec, S.V.; Wells, R.J. 2001. Investigation of heroin profiling using trace organic impurities. *Analyst*, 126, 679–689.

Myors, R.; Wells, R.J.; Skopec, S.V.; Crisp, P.; Iavetz, R.; Skopec, Z.; Ekangaki, A.; Robertson, J. 1998. Preliminary investigation of heroin fingerprinting using trace element concentrations. *Analytical Communication*, 35, 403–410.

Nadulski, T.; Sporkert, F.; Schnelle, M.; Stadelmann A.M.; Roser, P.; Schefter, T.; Pragst, F. 2005. Simultaneous and Sensitive Analysis of THC, 11-OH-THC, THC-COOH, CBD, and CBN by GC-MS in Plasma after Oral Application of Small Doses of THC and Cannabis Extract. *Journal of Analytical Toxicology*, 29, 782–789.

National Toxicology Program, Institute of Environmental Health Sciences, National Institutes of Health (US-NTP). 1992. National Toxicology Program Chemical Repository Database. Research Triangle Park, North Carolina.

Navaneethan, G.; Karunakaran, K.; Elango, K.P. 2012. Development and application of stability-indicating HPLC method for the determination of nevirapine and its impurities in combination drug product. *Acta Chromatographica*, 24(4), 575–587.

Nettles, R.E.; Schürmann, D.; Zhu, L.; Stonier, M.; Huang, S.-P.; Chang, I.; Chien, C.; Krystal, M.; Wind-Rotolo, M.; Ray, N.; Hanna, G.J.; Bertz, R.; Grasela, D. 2012. Pharmacodynamics, Safety, and Pharmacokinetics of BMS-663068, an Oral HIV-1 Attachment Inhibitor in HIV-1–Infected Subjects. *The Journal of Infectious Diseases*, 206, 1002–1011.

Neville, G.A.; Ekiel, I.; Smith, I.C.P. 1987. High-resolution proton magnetic resonance spectra of morphine and its three O-acetyl derivatives. *Magnetic Resonance in Chemistry*, 25(1), 31–35.

Notari, S.; Sergi, M.; Montesano, C.; Ivanovic, J.; Narciso, P.; Pucillo, L. P.; Ascenzi, P. 2012. Simultaneous Determination of Lamivudine, Lopinavir, Ritonavir, and Zidovudine Concentration in Plasma of HIV-Infected Patients by HPLC-MS/MS. *IUBMB Life*, 64(5,) 443–449.

Novak, J.; Zitterl-Eglseer, K.; Deans, S.G.; Franz, C.M. 2001. Essential oils of different cultivars of *Cannabis sativa L.* and their antimicrobial activity. *Flavour and Fragrance Journal*, 16, 259–262.

Nugent, K.G.; Saville, B.J. 2004. Forensic analysis of hallucinogenic fungi – a DNA-based approach. *Forensic Science International,* 140, 147–157.

Nyedo, E. 2020. Drugs are killing Malawi youths but why are we silent? *Nyasa Times*. https://www.nyasatimes.com/drugs-are-killing-malawi-youths-but-why-are-we-silent/ [Accessed on 2020-02-20].

Omar, O.A.; Hoskin, P.J.; Johnston, A.; Hanks, G.W.; Turner, P. 1989. Diamorphine stability in aqueous solution for subcutaneous infusion. *Journal of Pharmacy and Pharmacology*, 41(4), 275–277.

O'Neal, C.L.; Poklis, A. 1997. Simultaneous Determination of Acetylcodeine, Monoacetylmorphine, and Other Opiates in Urine by GC-MS. *Journal of Analytical Toxicology,* 21, 427–432.

O'Neil, M.J. (ed). 2017. *The Merck Index – An Encyclopedia of Chemicals, Drugs, and Biologicals.* 13th ed. Cambridge, UK: Royal Society of Chemistry.

Pandohee, J.; Holland, B.J.; Li, B.; Tsuzuki, T.; Stevenson, P.G.; Barnett, N.W.; Pearson, J.R.; Jones, O.A.H.; Conlan, X.A. 2015. Screening of cannabinoids in industrial-grade hemp using two-dimensional liquid chromatography coupled with acidic potassium permanganate chemiluminescence detection: Liquid Chromatography. *Journal of Separation Science*, 38, 2024–2032.

Paranaiba, R.T.F.; Carvalho, C.B.V.; Paiva, R.S.; Trindade, B.R.; Barros, M.G.; Souza, E.P.; Gontijo, A.B.; Silveira, D. 2020. DNA from wood – A simple approach facing a challenging

matrix – A preliminary study. *Forensic Science International*, 314, http://dx.doi.org/10.1016/j.forsciint.2020.110371 [Accessed om 2020-07-16].

Patel, B.; Wene, D.; Fan, Z.T. 2017. Qualitative and quantitative measurement of cannabinoids in cannabis using modified HPLC/DAD method. *Journal of Pharmaceutical and Biomedical Analysis*, 146, 15–23.

Penchala, S.D.; Fawcett, S.; Else, L.; Egan, D.; Amar, A.; Elliot, E.; Challenger, E.; Back, D.; Boffito, M.; Khoo, S. 2016. The Development and Application of a Novel LC-MS/MS Method for the Measurement of Dolutegravir, Elvitegravir and Cobicistat in Human Plasma. *Journal of chromatography B.* http://dx.doi.org/10.1016/j.jchromb.2016.05.040 [Accessed XXXX].

Penchala, S.D.; Alagaratnam, J.; Challenger, E.; Amara, A.; Else, L.; Winston, A.; Khoo, S. 2019. The development and validation of a novel LC-MS/MS method for the quantification od Cenicriviroc in human plasma and cerebrospinal fluid. *Biomedical chromatography*, e4711 https://doi.org/10.1002/bmc.4711 [Accessed XXXX].

Peschel, W.; Politi, M., 2015. 1H NMR and HPLC/DAD for *Cannabis sativa L.* chemotype distinction, extract profiling and specification. *Talanta*, 140, 150–165.

Peters, F.T.; Maurer, H.H. 2002. Bioanalytical method validation and its implications for forensic and clinical toxicology – A review. *Accreditation and Quality Assurance*, 7, 441–449.

Peters, F.T.; Drummer, O.H.; Musshoff, F. 2007. Validation of new methods. *Forensic Science International*, 165, 216–224.

Pijlman, F.T.A.; Rigter, S.M.; Hoek, J.; Goldschmidt, H.M.J.; Niesink, R.J.M. 2005. Strong increase in total delta-THC in cannabis preparations sold in Dutch coffee shops. *Addiction Biology*, 10, 171–180.

Pluskota, R.; Koba, M. 2018. Indandione and Its Derivatives - Chemical Compounds with High Biological Potential. *Mini Review Medicinal Chemistry*, 18(15), 1321–1330.

Posner, L.P. 2012. Midazolam and Diazepam – What's the Difference? Proceedings of the NAVC Conference – Large Animals https://www.vetfolio.com/learn/article/midazolam-and-diazepam-whats-the-difference [Accessed on 2020-08-20].

Prathipati, P.K.; Mandal, S.; Destache, C.J. 2016. Simultaneous quantification of tenofovir, emtricitabine, rilpivirine, elvitegravir and dolutegravir in mouse biological matrices by LC-MS/MS and its application to a pharmacokinetic study. *Journal of Pharmaceutical and Biomedical Analysis*, 129, 473–481.

Prathipati, P.K.; Mandal S.; Destache, C.J. 2018. Development and validation of LC–MS/MS method for quantification of bictegravir in human plasma and its application to an intracellular uptake study. *Biomedical Chromatography,* e4379. https://doi.org/10.1002/bmc.4379 [Accessed on 2019-11-14].

Quaranta, S.; Woloch, C.; Paccou, A.; Giocanti, M.; Solas, C.; Lacarelle, B. 2009. Validation of an electrospray ionization LC-MS/MS method for quantitative analysis of raltegravir, etravirine, and 9 other antiretroviral agents in human plasma samples. *Therapeutic Drug Monitoring*, 31(6), 695–702.

Radwan, M.M.; ElSohly, M.A.; Slade, D.; Ahmed, S.A.; Khan, I.A.; Ross, S.A. 2009. Biologically Active Cannabinoids from High-Potency *Cannabis sativa*. *Journal of Natural Products*, 72, 906–911.

Rahim, A.A.; Saad, B.; Osman, H.; Hashim, N.; Yahya, S.; Talib, K.M. 2011. Simultaneous determination of diethylene glycol, diethylene glycol monomethyl ether, coumarin and caffeine in food items by gas chromatography. *Food Chemistry*, 126, 1412–1416.

Raju, T.V.R.; Kumar, N.A.; Kumar, S.R.; Reddy, A.M.; Rao, N.S.; Rao, I.M. 2013. Development and Validation of a Stability-Indicating RP-HPLC Method for the Simultaneous Estimation of Guaifenesin and Dextromethorphan Impurities in Pharmaceutical Formulations. *Chromatography Research International*, 2013, 12 pages. doi:10.1155/2013/315145

Raju, V.A.; Ramana, M.V.; Principal, T.S.; Rajinikanth K.N.; Kumar, V.K.; Raju, N.A. 2018. Bioanalytical method development and validation for simultaneous determination of bictegravir, 247enofovir and emtricitabine in human plasma by LCMS/MS. *World Journal of Pharmacy and Pharmaceutical Sciences*, 7(12), 441–463.

Ramírez-Ramírez, A.; Sánchez-Serrano, E.; Loaiza-Flores, G.; Plazola-Camacho, N.; Rodríguez-Delgado, R.G.; Figueroa-Damián, R.; Domínguez-Castro, M.; Lŏpez-Martínez, M.; Flores-García, Z.; Hernández-Pineda, J. 2018. Simultaneous quantification of four antiretroviral drugs in breast milk samples from HIV-positive women by an ultra-high performance liquid chromatography tandem mass spectrometry (UPLC-MS/MS) method. *PloS ONE*, 13(1), e0191236. https://doi.org/10.1371/journal.pone.0191236 [Accessed on 2019-11-20].

Rao, M.C.S.; Reddy, R.C.K.; Sekhar, K.B.C.; Reddy, Y.V.R. 2017. FT-Raman Spectroscopy with chemometric Methods for Quantification of Lamivudine Form II and Lamivudine Form I. Asian *Journal of Chemistry*, 29(8), 1735–1742.

Rao, T.N.; Sankar, G.G.; Rani, L.J. 2016. High throughput LC-MS/MS method for the quantitation of didanosine in human plasma by solid phase extraction using 96 well plate format. *World Journal of Pharmacy and Pharmaceutical Sciences*, 5(3), 781–798.

Rebiere, H.; Mazel, B.; Civade, C.; Bonnet, P., 2007. Determination of 19 antiretroviral agents in pharmaceuticals or suspected products with two methods using high-performance liquid chromatography. *Journal of Chromatography B*, 850, 376–383.

Recovery Direct, Cape Town's Top Whoonga/Nyaope Rehab Centre. https://www.recoverydirect.co.za/drug/whoonga-addiction/ [Accessed on 2019-06-06].

Reddiah, Ch. V.; Devi, P.R.; Mukkanti, K.; Srinivasu, P. 2013. Stability indicating HPLC method for impurities estimation of nevirapine in extended release tablet dose. *Pharmacophore,* 4(2), 50–58.

Reeve, W.; Erikson, C.M.; Aluotto, P.F. 1979. A new method for the determination of the relative acidities of alcohols in alcoholic solutions. The nucleophilicities and competitive reactivities of alkoxides and phenoxides. *Canadian Journal of Chemistry*, 57, 2747–2754.

Reichardt, C.; Welton, T. 2011. *Solvents and Solvent Effects in Organic Chemistry. 4th Ed.*, Wiley-VCH Verlag GmbH & Co. KGaA, Weinheim.

Repka, M.A.; Munjal, M.; ElSohly, M.A.; Ross S.A. 2006. Research Temperature Stability and Bioadhesive Properties of Δ^9-Tetrahydrocannabinol Incorporated Hydroxypropylcellulose Polymer Matrix Systems. *Drug Development and Industrial Pharmacy*, 32(1), 21–32. doi:10.1080/03639040500387914.

Republic of South Africa [RSA]. 1965. *Medicines and Related Substances Act no. 101 of 1965*. Pretoria: Government Printers.

Republic of South Africa [RSA]. 1992. *The Drugs and Drug Trafficking Act no. 140 of 1992*. Pretoria: Government Printers.

Rigdon, A. 2016. The Practical Chemist Calibration Part II- Evaluating your curves. *Cannabis industry journal [Online]*. https://cannabisindustryjournal.com/column/calibration-part-ii-evaluating-your-curves/[Accessed on 2020-01-04].

Ringnér, M. 2008.What is principal component analysis? *Nature Biotechnology*, 26 (3), 303–304.

Rohrschneider, L. 1973. Solvent characterization by gas-liquid partition coefficients of selected solutes. *Analytical Chemistry*, 45 (7), 1241–1247.

Ronen, A.; Gershon, P.; Drobiner, H.; Rabinovich, A.; Bar-Hamburger, R.; Mechoulam, R.; Cassuto, Y.; Shinar, D. 2008. Effects of THC on driving performance, physiological state and subjective feelings relative to alcohol. *Accident Analysis and Prevention*, 40, 926–934.

Rop, P.P.; Fornaris, M.; Salmon, T.; Burle, J.; Bresson, M. 1997. Concentrations of Heroin, 06-Monoacetylmorphine, and Morphine in a Lethal Case Following an Oral Heroin Overdose. *Journal of Analytical Toxicology*, 21, 232–235.

Rosenqvist, E.; Ottersen, T. 1975. The crystal and molecular structure of D^9-tetrahydrocannabinolic acid B. *Acta Chemica Scandinavia B*, 29, 379–384.

Ross, W. 2013. South Africa's craze for heroin-marijuana cocktail. BBC News, Soweto. 18 September. https://www.bbc.com/news/world-africa-24137003 [Accessed 2019-03-31].

Ross, S.A.; Mehmedic, Z.; Murphy, T.P.; ElSohly, M.A. 2000. GC-MS Analysis of the Total Δ^9-THC Content of Both Drug- and Fiber-Type Cannabis Seeds. *Journal of Analytical Toxicology*, 24, 715–717.

Rother, H.-A. 2012. Analysis: Improving poisoning diagnosis and surveillance of street pesticides. *South African Medical Journal*, 102(6), 485–488.

Rough, K.; Dietrich, J.; Essien, T.; Grelotti, D.J.; Bansberg, D.R.; Gray, G.; Katz, I.T. 2014. Whoonga and the Abuse and Diversion of Antiretrovirals in Soweto, South Africa. *AIDS Behav*, 18, 1378–1380.

Saar, E.; Gerostamoulos, D.; Drummer, O.H.; Beyer, B. 2012. Assessment of the stability of 30 antipsychotic drugs in stored blood specimens. *Forensic Science International,* 215, 152–158.

Santer, B.D.; Wigley, T.M.L.; Boyle, J.S.; Gaffen, D.J.; Hnilo, J.J.; Nychka, D.; Parker, D.E.; Taylor, K.E. 2000. Statitical significant of trends and trend differences in layer-average atmospheric temperature time series. *Journal of Geophysical Research*, 105(D6), 7337–7356.

Saunders, J.A.; Pedroni, M.J.; Penrose, L.D.J.; Fist, A.J. 2001. AFLP Analysis of opium poppy. *Crop Science*, 41, 1596–1601.

Schoeman, C.; Mashiane, M.; Dlamini, M.; Okonkwo, O.J. 2015. Quantification of Selected Antiretroviral Drugs in a Wastewater Treatment Works in South Africa Using GC-TOFMS. *Journal of Chromatography & Separation Techniques*, 6(4), 272. doi:10.4172/2157-7064.1000272.

Schultes, R.E. 1970. The Botanical and Chemical Distribution of Hallucinogens. *Annual Review of Plant Physiology,* 21, 571–598.

Schultes, R.E.; Hofmann, A.; Rätsch, C. 2001. *Plants of the Gods: Their Sacred, Healing, and Hallucinogenic Powers*. 2nd ed. Healing Arts Press Rochester, Vermont.

Schwilke, E.W.; Schwope, D.M.; Karschner, E.L.; Lowe, R.H.; Darwin, W.D.; Kelly, D.L.; Goodwin, R.S.; Gorelick, D.A.; Huestis, M.A. 2009. Δ9-Tetrahydrocannabinol (THC), 11-Hydroxy-THC, and 11-Nor-9-carboxy-THC Plasma Pharmacokinetics during and after Continuous High-Dose Oral THC. *Clinical Chemistry*, 55(12), 2180–2189.

Scientific Working Group on DNA Analysis Methods (SWGDAM). 2016. Validation Guidelines for DNA Analysis Methods.

Seedsman Blog. 2015. Cannabis Ruderalis – Seedsman Blog. https://blog.seedsman.com/cannabis-ruderalis/ [Accessed on 2019-01-14].

Segal, M.S.; Goldstein, M.M.; Attinger, E.O. 1957. The Use of Noscapine (Narcotine) as an Antitussive Agent. *Diseases of the Chest*, 32(3), 305–309.

Sena, L. C. S.; Matos, H. R.; Dórea, H. S.; Pimentel, M. F.; de Santana, D. C. A. S.; de Santana, F. J. M. 2017. Dispersive liquid-liquid microextraction based on solidification of floating organic drop and high-performance liquid chromatography to the analysis of cocaine's major adulterants in human urine. *Toxicology*, 376, 102–112.

Senchina, D.S.; Shah, N.B.; Busch, M G. 2012. Effects of Berberine, Chelerythrine, and Sanguinarine on Proliferation in Four Human Immortalized Cell Lines. *Journal of the Iowa Academy of Science*, 119(1-4), 22–27.

Shah, V. P.; Midha, K. K.; Findlay, J. W. A.; Hill, H. M.; Hulse, J. D.; McGilveray, I. J.; McKay, G.; Miller, K. J.; Patnaik, R. N.; Powell, M. L.; Tonelli, A.; Viswanathan, C. T.; Yacobi, A. 2000. Bioanalytical Method Validation—A Revisit with a Decade of Progress. *Pharmaceutical Research*, 17(12), 1551–1557.

Sharma, P.; Joshi, A.; Rajamani, G.; Jain, D.; Choudahary, R.S.; Dadheech, A.; Sharma, D.; Rajoriya, S.; Sharma, G. 2019. ISSR-Based Molecular Characterization of Opium poppy (*Papaver somniferum L.)* Genotypes. *International Journal of Current Microbiology and Applied Sciences*, 8(9), 2540–2545.

Shembe, Z.T. 2013. The effects of whoonga on the learning of affected youth in Kwa-Dabeka Township. Thesis, 123 p.

Shimandzu Excellence in Science. 2017. Application News No. ICP-006. Inductively Coupled Plasma Mass Spectrometry. Analysis of Heavy Metal Contaminants in Cannabis Flower using

the Shimadzu ICPMS-2030. https://www.ssi.shimadzu.com/sites/ssi.shimadzu. com/files/Products/literature/ICP/006_CannabisICPMS.pdf [Accessed on 2018-05-14].

Shirkhorshidi, A.S.; Aghabozorgi, S.; Wah, T.Y. 2015. A Comparison Study on Similarity and Dissimilarity Measures in Clustering Continuous Data. *PLoS ONE*, 10(12), e0144059. doi:10.1371/journal.pone.0144059. https://journals.plos.org/plosone/ article?id=10.1371/journal.pone.0144059 [Accessed on 2019-12-19]

Shlens, J. 2005. A Tutorial on Principal Component Analysis. http://www.cs.cmu,edu/~elaw/papers/pca.pdf [Accessed on 2020-03-22].

Shoup, R.E.; Ren, X.; Johnson, A.P.; Gray, D.A.; Evarts, S.; Gill, L.; Beato, B.D. 1999. Simultaneous Determination of Six Protease/Reverse Transcriptase Inhibitors in Human Plasma Utilizing LC/MS/MS. *Current Separations,* 18(1), 17–22.

Sibley, J.A. 1996. Formation of O-6-acetylmorphine in the 'homebake' preparation of heroin. *Forensic Science International*, 77, 159–167.

Sichilongo, K.; Chinyama, M.; Massele, A.; Ventoc, S. 2014. Comparative chromatography-mass spectrometry studies on the antiretroviral drug nevirapine. Analytical performance characteristics in human plasma determination. *Journal of Chromatography B*, 945– 946, 101–109.

Sifile, L. 2017. Bluetooth drug high 'impossible' NEWS [Accessed on 2019-02-25].

Sigma-Aldrich Product Information sheet https://www.sigmaaldrich.com/content/dam/sigma-aldrich/docs/Sigma-Aldrich/Product_Information_Sheet/c0750pis.pdf Accessed on 2020-07-22].

Simões, S.S.; Silva, I.; Ajenjo, A.C.; Dias, M.J. 2011.Qualitative and quantitative analysis of THC, 11-hydroxy-THC and 11-nor-9-carboxy-THC in whole blood by ultra-performance liquid chromatography/tandem mass spectrometry. *Rapid Communications in Mass Spectrometry*, 25(18), 2603–2610.

Simões, S.S.; Silva, I.; Ajenjo, A.C.; Dias, M.J. 2014. Validation and application of an UPLC-MS/MS method for the quantification of synthetic cannabidids in urine samples of seized material from the Portuguese market. *Forensic Science International*, 243, 117–125.

Siniscalco Gigliano, G. 1998. Identification of *Cannabis sativa L.* (Cannabiceae) using restriction profiles of the Internal Transcribed Spacer II (ITS2). *Science and Justice*, 38, 225–230.

Siniscalco Gigliano, G.; Caputo, P.; Cozzolino, S. 1997. Ribosomal DNA analysis as a tool for the identification of *Cannabis sativa L.* specimens of forensic interest. Science and Justice, 37, 171-174.

Sione, W.H. 1986. Clandestine drug synthesis. *Medical Research Review*, 6(1), 41–74.

Skoog D.A., West D.M., Holler F.J., Crouch S.R. 2004. *Fundamentals of Analytical Chemistry.* 8th ed., Chapter 7 p. 163. Brooks/Cole – Thomson Learning Inc. Toronto.

Small, E. 2015. Evolution and Classification of *Cannabis sativa* (Marijuana, Hemp) in Relation to Human Utilization. *Botanical Review*, 81, 189–294. https://doi.org/10.1007/s12229-015-9157-3 [Accessed on 2019-01-07].

Small, E.; Cronquist, A. 1976. A practical and natural taxonomy for Cannabis. *Taxon*, 25, 405–435

Smith, R.N.; Vaughan, C.G. 1971.The decomposition of acidic and neutral cannabinoids in organic solvents. *J. Pharm. Pharmac*, 29, 286–290.

Snyder, L. R.; Kirkland, J. J. 1979. *Introduction to Modern Liquid Chromatography 2nd ed.*, Wiley-Interscience, John Wiley & Sons, Inc. New York.

SOFT / AAFS Forensic Laboratory Guidelines – 2006.

Sogbanmu, O.O.; Adeniyi, O.V.; Fuentes, Y.O.; Ter Goon, D., 2015. Very early virological failure and drug resistance mutations in a woman on antiretroviral therapy in Eastern Cape, South Africa: a case report. *Journal of Medical Case Reports*, 9, 106 (DOI 10.1186/s13256-015-0557-0). http://www.jmedicalcasereports.com/content/pdf/s13256-015-0557-0.pdf [Accessed on 2016-03-05].

Soldin. S.J. 2005. Anti-retroviral Analyss by Mass Spectrometry. US Patent US 2005/0032042 A1.

South African Community Epidemiology Network on Drug Use (SACENDU) – Monitoring Alcohol and Drug Abuse Treatment Admissions in South Africa February 2014, Phase 34 January to June 2013. http://www.mrc.ac.za/adarg/sacendu/ Sacenduphase34.pdf [Accessed on 2016-04-16].

South African Police's (SaPS). 2013. Forensic Fact File no. 9.

South Afrcan Police's Forensic Science laboratory (SAPS-FSL). 2017. Maintenance and Monitoring of GC-MS instrumentation.

Spencer, M.S.; Bates Prins, S.C.; Beckom, M.S. 2010. Heterogeneous Distance Measures and Nearest-Neighbor Classification in an Ecological setting. *Distance and Neighbors in an Ecological Setting*, 22(2), 108–123.

Staub, C.; Marset, M.; Mino, A.; Mangin, P. 2001. Detection of Acetylcodeine in Urine as an Indicator of Illicit Heroin Use: Method Validation and Results of a Pilot Study. *Clinical Chemistry,* 47(2), 301–307.

Strang, J.; Griffiths, P.; Gossop, M. 1997. Hroin smoking by 'chasing the dragon': Origins and history. *Addiction*, 92(6), 673–783.

Strang, G.; Aarikka, K. 1986. *Introduction to applied mathematics. Vol. 16*. 4th ed. Wellesley-Cambridge Press, Massachusetts.

Sun, M.; Liu. C.; Nadiminty, N.; Lou, W.; Zhu, Y.; Yang, J.; Evans, C.P.; Zhou, Q.; Gao, A.C. 2012. Inhibition of Stat3 activation by sanguinarine suppresses prostate cancer cell growth and invasion. *Prostate,* 72(1), 82–89.

Sura, H.; Bonthu, S.; Murthy, T.E.G.K. 2013. Quantization of Didanosine in Human Plasma using High-Performance Liquid Chromatography–Tandem Mass Spectrometry. *Journal of Advanced Pharmacy Education & Research*, 3 (3), 187–195.

Suryaprakash, N.; Azoury, M.; Goren, Z.; Jelinek, R. 2000. Identification of heroin in street doses using 1D-TOCSY nuclear magnetic resonance. *Journal of Forensic Science*, 45(5), 963–967.

Suurkuusk, G. 2010. Validation of the Gas Chromatographic method for THC, CBD and CBN determination. Thesis, 40p.

Swift, W.; Wong, A.; Li, K.M.; Arnold, J.C.; McGregor, I.S. 2013. Analysis of Cannabis Seizures in NSW, Australia: Cannabis Potency and Cannabinoid Profile. *PLoS ONE*, 8(7), e70052. doi:10.1371/journal.pone.0070052.

Szepesi, G.; Gazdag, M.; Mihalyfi, K. 1989. Selection of High-performance liquid chromatographic methods in pharmaceutical analysis. *Journal of Chromatography*, 464, 265–278.

Tan, B.; Melius, P.; Ziegler, P. 1982. A Simple Gas Chromatographic Method for the Study of Organic Solvents: Moisture Analysis, Hygroscopicity, and Evaporation. *Journal of Chromatographic Science*, 20, 213–217.

Taverniers, I.; De Loose, M.; Van Bockstaele, E. 2004. Trends in quality in the analytical laboratory. II. Analytical method validation and quality assurance. *Trends in Analytical Chemistry*, 23(8), 535–552.

Taylor, R.B.; Low, A.S.; Reid, R.G. 1996. Determination of opiates in urine by capillary electrophoresis. *Journal of Chromatography B: Biomedical Sciences and Applications*, 675(2), 213–223.

Teixeira, H.; Proenc, P.; Castanheira, A.; Santos, S.; Lo´pez-Rivadullac, M.; Corte-Real, F.; Marquesa, E.P.; Vieira, D.N. 2004. Cannabis and driving: the use of LC–MS to detect Δ9-tetrahydrocannabinol (Δ^9-THC) in oral fluid samples. *Forensic Science International*, 146S, S61–S63.

Teixeira, H.; Verstraete, A.; Proenc, P.; Corte-Real, F.; Monsanto, P.; Vieira, D.N. 2007. Validated method for the simultaneous determination of Δ^9-THC and Δ^9-THC-COOH in oral fluid, urine and whole blood using solid-phase extraction and liquid chromatography–mass spectrometry with electrospray ionization. *Forensic Science International*, 170, 148–155.

Telo, J.P.; Vieira, A.J.S.C. 1997. Mechanism of free radical oxidation of caffeine in aqueous solution. *J. Chem. Soc., Perkin Trans*, 2, 1755–1757.

Tert-Butyl Alcohol MSDS (t-BUOH MSDS). n.d. [Online]. Available at: http://www.microkat.gr/msdspd90-99/tert-Butyl%20alcohol.html [Accessed on 2020-04-24].

Thimmaraju, M.K.; Mondal, P.; Venu, K.; Babu, G.S.; Rajkumar, G.; Padmaja, B. 2019. Quantification of fosamprenavir in spiked human plasma using liquid chromatography–electrospray ionization–tandem mass spectrophotometry – application to pharmacokinetic study. *Egyptian Pharmaceutical Journal*, 18(2), 149–159.

Thomas, R.; Velaphi, S., 2014. Abuse of antiretroviral drugs combined with addictive drugs by pregnant women is associated with adverse effects in infants and risk of resistance. *South African Journal of Child Health (SAJCH),* 8(2), 78–79.

Thompson, M. 2005. Is my calibration linear. AMC technical brief. The Royal society of Chemistry. https://www.rsc.org/images/calibration-linear-technical-brief-3_tcm18-214846.pdf [Accessed on 2016-10-18].

Thompson, M. Ellison, S.L.R.; Wood, R. 2002. Harmonized guidelines for single laboratory validation of methods of analysis (IUPAC Technical Report). *Pure and Applied Chemistry*, 74(5), 835–855.

Thompson, M.; Ellison, S.L.R.; Fajgelj, A.; Willetts, P.; Wood, R. 1999. Harmonised Guidelines for the Use of Recovery Information in Analytical Measurement (IUPAC Technical Report). *Pure and Applied Chemistry*, 71 (2), 337–348.

Toske, S.G.; Cooper, S.D.; Morello, D.R.; Hays, P.A.; Casale, J.F.; Casale, E. 2006. Neutral Heroin Impurities from Tetrahydrobenzylisoquinoline Alkaloids. *Journal of Forensic Science*, 51(2), 308–320.

Trofin, I.G.; Dabija, G.; Vaireanu, D.-I.; Filipescu, L. 2012. Long - term Storage and Cannabis Oil Stability. *Revista de Chimie – Bucharest*, 63(3), 293–297.

Turjanski, N.; Lloyd, G.G. 2005. Psychiatric side-effects of medications: recent developments. *Advances in Psychiatric Treatment*, 11, 58–70.

Turner, C.E.; Elsohly, M.A. 1979. Constituents of *Cannabis sativa L.* XVI. A possible decomposition pathway of Δ9-tetrahydrocannabinol to cannabinol. *Journal of Heterocyclic Chemistry*, 16, 1667–1668.

Turner, C.E.; Hadley, K.W.; Fetterman, P.S.; Doorenbos, N.J.; Quimby, M.W.; Waller, C. 1973a. Constituents of *Cannabis sativa L.* IV: Stability of Cannabinoids in Stored Plant Material. *Journal of Pharmaceutical Sciences*, 62(10), 1601–1605.

Turner, C.E.; Hadley, K.W.; Fetterman, P.S. 1973b. Constituents of *Cannabis sativa L.* VI: Propyl Homologs in Samples of Known Geographical Origin. *Journal of Pharmaceutical Sciences*, 62 (10), 1739–1741.

Turner, C. E. Henry, J. T. 1975. Constituents of Cannabis sativa L. IX: Stability of synthetic and naturally occurring cannabinoids in chloroform. *Journal of Pharmaceutical Sciences*, 64 (2), 357–359.

U.S. Department of Health and Human Services (US-DHHS) (of America). 2014. Panel on Antiretroviral Guidelines for Adults and Adolescents. Guidelines for the Use of Antiretroviral Agents in Adults and Adolescents with HIV. Available at: http://www.aidsinfo.nih.gov/ContentFiles/AdultandAdolescentGL.pdf [Accessed on 2019-11-11].

U.S. Department of Justice Drug Enforcement Administration (US-DEA). n.d. Basic Training program for Forensic Drug Chemists.

U.S. Department of Justice Drug Enforcement Administration (US-DEA). 1992. Opium Poppy' Cultivation and Heroin Processing in Southeast Asia.

Uhl, M. 1997. Determination of drugs in hair using GC-MS/MS. *Forensic Science International*, 84, 281–294.

United Nation Office on Drugs and Crime (UNODC). 1953. The Mysterious Heroin Pills for Smoking. https://www.unodc.org/unodc/en/data-and-analysis/bulletin/bulletin1953-01-01_2_page012.html [Accessed on 2020-02-15].

United Nations Office for Drug Control and Crime Prevention (UNODCCP). 1999. South Africa Country Profile on Drugs and Crime http://www.unodc.org/pdf/southafrica/sadrug.pdf [Accessed on 2015-07-27].

United Nations Office on Drugs and Crime (UNODC). 2001. Drug Characterization/Impurity Profiling; Backgound and Concepts. 14 p. (ST/NAR/32/Rev.1).

United Nations Office on Drugs and Crime (UNODC). 2003. Terminology and Information on Drugs. 2nd ed. 73 p. Sales No. E.03.XI.14, ISBN 92-1-148163-5.

United Nations Office on Drugs and Crime (UNODC).2005. Methods for impurity profiling of heroin and cocaine. 81 p. (ST/NAR/35).

United Nations Office on Drugs and Crime (UNODC). 2009a. Recommended Methods for the Identification and Analysis of Cannabis and Cannabis Products, 47 p. (ST/NAR/40).

United Nations Office on Drugs and Crime (UNODC). 2009b. Guidance for the Validation of Analytical Methodology and Calibration of Equipment used for Testing of Illicit Drugs in Seized Materials and Biological Specimens, 67 p. (ST/NAR/41).

United Nations Office on Drugs and Crime (UNODC). 2015. Afghan Opitate Trafficking through the Southern Route. Vienna.

United Nations Office on Drugs and Crime (UNODC). 2016. *Terminology and Information on Drugs*. 3rd ed. 69 p.

United Nations Office on Drugs and Crime (UNODC). 2020. World Drug Report. https://wdr.unodc.org/wdr2020/field/WDR20_Booklet_3.pdf [Accessed on 2020-07-02].

United States Department of Agriculture Plants Database (USDA PLANTS). Natural Resources conservation service (NRCS). n.d. https://plants.usda.gov/java/Classification_Servlet?source=display&classid=CASA3 [Accessed on 2019-01-09].

United States Department of Health and Human Services (US-DHHS) (of America). 2018. Panel on Antiretroviral Guidelines for Adults and Adolescents. Guidelines for the Use of Antiretroviral Agents in Adults and Adolescents with HIV. http://www.aidsinfo.nih.gov/ContentFiles/AdultandAdolescentGL.pdf [Accessed on 2019-09-05].

United States Food and Drug Administration (US-FDA). 2017. Ibalizumab-Treatment of HIV-1 infection in heavily treatment experienced adults with multidrug resistant HIV-1 infection failing current antiretroviral therapy, in combination with other antiretroviral(s). Clinical Pharmacology and Biopharmaceutics Review(s). Center for Drug Evaluation and Research. Application note no. 761065Orig1s000. https://accessdata.fda.gov/drugsatfda_docs/nda/2018/7610650rig1s000ClinPharmR.pdf [Accessed on 2019-11-13].

United States Pharmacopoeia (USP). 2005. USP29–NF24 Page 3050. http://www.pharmacopeia.cn/v29240/usp29nf24s0_c1225.html [Accessed on 2019-11-13].

Van Praag, R.M.E.; Van Weert, E.C.M.; Van Heeswijk, R.P.G.; Zhou, X.-J.; Sommadossi, J.-P.; Jurriaans, S.; Lange, J.M.A.; Hoetelmans, R.M.W.; Prins, J.M. 2002. Stable Concentrations of Zidovudine, Stavudine, Lamivudine, Abacavir, and Nevirapine in Serum and Cerebrospinal Fluid during 2 Years of Therapy. *Antimicrobial Agents and Chemotherapy*, 46(3), 896–899.

Varshney, K. M. 2002. HPTLC study of the stability of heroin in methanol. *Journal of Planar Chromatography*, 15, 46–49.

Vašek, J.; Čílová, D.; Melounová, M.; Svoboda, P.; Vejl, P.; Štikarová, R.; Vostrý, L.; Kuchtová, P.; Ovesná, J. 2020. New EST-SSR Markers for Individual Genotyping of Opium Poppy Cultivars (*Papaver somniferum* L.). *Plants*, 9(1), 10–12.

Ventura, R.; Jimenez, C.; Closas, N.; Segura, J.; De la Torre, R. 2003. Stability studies of selected doping agents in urine: caffeine. *Journal of Chromatography B*, 795, 167–177.

Vijaya Raju, A.D.; Appala Raju, N. 2013. Dawley Development and Validation of a LC-MS/MS Method for the Determination of Raltegravir in Sprague Rat Serum and Its Application to Pharmacokinetic Study. *American Journal of Biomedical Sciences*, 5(3), 197–207.

Vlase, L.; Popa, D.-S.; Zaharia, D.; Loghin, F. 2010. High-throughput toxicological analysis of Δ9-THC and 11-nor-9-carboxy-Δ9-THC by LC/MS/MS. *Romanian Journal of Legal Medicine*, 2, 133–140.

Vogel, M.; Bertram, N.; Wasmuth, J.C.; Emmelkamp, J.; Rockstroh, J.K.; Reichel, C. 2010. Determination of Nevirapine in Plasma by GC–MS. *Journal of Chromatographic Science*, 48, 91–94.

Volosov, A.; Alexander, C.; Ting, L.; Soldin S.J. 2002. Simple rapid method for quantification of antiretrovirals by liquid chromatography-tandem mass-spectrometry. *Clinical Biochemistry*, 35, 99–103.

Watanabe, A.; Fukami, T.; Takahashi, S.; Kobayashi, Y.; Nakagawa, N.; Nakajima, M.; Yokoi, T. 2010. Arylacetamide Deacetylase Is a Determinant Enzyme for the Difference in Hydrolase Activities of Phenacetin and Acetaminophen. *Drug Metabolism and Disposition*, 38(9), 1532–1537.

Weedn, V.W.; Rodgers, G.S.; Henry, B.E. 1998. DNA Testing in the Forensic Laboratory. *Laboratory Medicine*, 29(8), 484–489. https://academic.oup.com/labmed/article_abstract/29/8/484/2504067 [Accessed on 2020-0717].

Weigel, S.; Berger, U.; Jensen, E.; Kallenborn, R.; Thoresen, H.; Huhnerfuss, H. 2004. Determination of selected pharmaceuticals and caffeine in sewage and seawater from Tromsø/Norway with emphasis on ibuprofen and its metabolites. *Chemosphere*, 56, 583–592.

Welker, R. W. 2012. Basics and Sampling of Particles for Size Analysis and Identification, in *Developments in Surface Contamination and Cleaning: Detection, Characterization, and Analysis of Contaminants*, pp. 1 – 80. Available at https://doi.org/10.1016/B978-1-4377-7883-0.00001-8 [Accessed on 2020-04-24].

Wernly, P.; Thormann, W. 1991. Analysis of illicit drugs in human urine by micellar electrokinetic capillary chromatography with on-column fast scanning polychrome absorption detection. *Analytical Chemistry*, 63(24), 2878–2882.

Wernly, P.; Thormann, W. 1992. Drug of abuse confirmation in human urine using stepwise solid-phase extraction and micellar electrokinetic capillary chromatography. *Analytical Chemistry*, 64(18), 2155–2159.

Wille, S.M.R.; Di Fazio, V.; Ramírez-Fernandez, M.; Kummer, N.; Samyn, N. 2013. Driving Under the Influence of Cannabis: Pitfalls, Validation, and Quality Control of a UPLC-MS/MS Method for the Quantification of Tetrahydrocannabinol in Oral Fluid Collected With StatSure, Quantisal, or Certus Collector. *Therapeutic Drug Monitoring*, 35(1), 101–111.

Wijesekera, A.R.L.; Abeysinghe, D.M.U.J.; Pathirana, K.C. 1994. Studies on the degradation of heroin. *Forensic Science International*, 67(3), 10 August, 147–154.

Wills, S. 2003. Cannabis Use and Abuse by Man: An Historical Perspective. In *Cannabis: the genus Cannabis.— Medicinal and aromatic plants: industrial profiles; volume 4.* Brown, D.T. (Ed). Harwood Academic Publishers. pp. 1–27.

Wilson, D.R.; Martinez, T.R. 1997. Improved Heterogeneous Distance Functions. *Journal of Artificial Intelligence Research*, 6, 1–34.

Wilson, R. F.; White, C. W. 1986. Intracoronary papaverine: an ideal coronary vasodilator for studies of the coronary circulation in conscious humans. *Circulation*, 73(3), 444–451.

XLSTAT. 2019. XLSTAT Help Documentation. https://cdn.xlstatl.com/helpcentersfdc/ XLSTAT_HELP_EN.pdf [Accessed on 2020-04-09].

Yadav, M.; Mishra, T.; Singhal, P.; Goswami, S.; Shrivastav, P.S. 2009. Rapid and Specific Liquid Chromatographic Tandem Mass Spectrometric Determination of Tenofovir in Human Plasma and its Fragmentation Study. *Journal of Chromatographic Science*, 47, 140–148.

Yeni, P.; LaMarca, A.; Berger, D.; Cimoch, P.; Lazzarin, A.; Salvato, P.; Smaill, F.M.; Teofilo, E.; Madison, S.J.; Nichols, W.G.; Adkison, K.K.; Bonny, T.; Millard, J.; McCarty D.; the EPIC (CCR100136) study team. 2009. Antiviral activity and safety of aplaviroc, a CCR5 antagonist, in combination with lopinavir/ritonavir in HIV-infected, therapy-naive patients: results of the EPIC study (CCR100136). *HIV Medicine*, 10, 116–124.

Yim, O.; Ramdeen, K.T. 2015. Hierarchical Cluster Analysis: Comparison of Three Linkage Measures and Application to Psychological Data. *The Quantitative Methods for Psychology*, 11(1), 8–21.

Young, M.S.; Martin, J.T. 2010. Optimized SPE for UPLC/MS/MS and GC/MS/MS Determination of THC and its Metabolites in Urine and Blood. Waters Application note 720003738EN 2010. http://www.waters.com [Accessed on 2019-11-26].

Young, B.; Roman, M.G.; LaRue, B.; Gangitano, D.; Houston, R. 2020. Evaluation of 19 short tandem repeat markers for individualization of *Papaver Somniferum. Science and Justice*, 60(3), 253–262.

Yuksel, B.2020. Quantitative GC-FID analysis of heroin for seized drugs. The Annals of Clinical and Analytical Medicine. doi:10.4328/ACAM.6139 https://bayrakol.org/en/about-acam/publish-online/item/2138-quantitative-gc-fid-analysis-of-heroin-for-seized-drugs [Accessed on 2020-01-15].

Zabell, A. P. R.; Lytle, F. E.; Julian, R. K. A. 2016. Proposal to improve calibration and outlier detection in high-throughput mass spectrometry. *Clinical Mass Spectrometry*, 2, 25–33.

Zhang, D.; Shi, X.; Yuan, Z.; Ju, H. 2004. Component Analysis of Illicit Heroin samples with GC/MS and Its Application in Source Identification. *Journal of Forensic Sciences*, 49(1), 81–86.

Zhang, A.; Wang, Q.; Mo, S. 2010. Simultaneous determination of Δ^9-tetrahydrocannabinol, cannabidiol and cannabinol in edible oil using ultra performance liquid chromatography-tandem mass spectrometry. *Se Pu*, 28(11), 1015–1019.

Zhang, L.-J., Yao, Y.-M., Sun, J.-J.; Chen, J.; Jia, X.-F.; Shen, F.; Lu, H.-Z. 2010a. An LC–MS/MS Method for Simultaneous Quantification of Seven Anti-HIV Medicines in Plasma of HIV-infected Patients. *Pharmaceutica Analytica Acta*, 1, 102. doi:10.4172/2153-2435.1000102

Zhang, W.; Han, F.; Guo, P.; Zhao, H.; Lin, Z.J.; Huang, M.-Q.; Bertelsen, K.; Weng, N. 2010b. Simultaneous determination of tolbutamide, omeprazole, midazolam and dextromethorphan in human plasma by LC–MS/MS—A high throughput approach to evaluate drug–drug interactions. *Journal of Chromatography B*, 878, 1169–1177.

Zhong, Y.; Huang, K.; Luo, Q.; Yao, S.; Liu, X.; Yang, N.; Lin, C.; Luo, X. 2018. The Application of a Desktop NMR Spectrometer in Drug Analysis. *International Journal of Analytical Chemistry*, 10.1155/2018/3104569, 1–7. https://doi.org/10.1155/2018/3104569 . [Accessed on 2020-04-21].

Zivovinovic, S.; Alder, R.; Allenspach, M.D.; Steuer, C. 2018. Determination of cannabinoids in *Cannabis sativa L.* samples for recreational, medical, and forensic purposes by reversed-phase liquid chromatography-ultraviolet detection. *Journal of Analytical Science and Technology*, 9, 27. https://doi.org/10.1186/s40543-018-0159-8 [Accessed on 2019-11-26].

APPENDIX I Total ion chromatographs for the samples stored under different storage conditions and analysed after t = 0, 24, 72, 168 and 336 hours of storage.

APPENDIX I-a: Total ion chromatographs for the samples stored in a refrigerator and analysed after t = 0, 24, 72, 168 and 336 hours of storage where identifications were (1) phenacetin, (2) caffeine, (3) efavirenz, (4) dextromethorphan, (5) tetrahydrocannabivarin, (6) tetracosane (IS), (7) cannabivarin (8) cannabidiol (9) nevirapine; (10) Δ^9-tetrahydrocannabinol; (11) cannabigerol, (12) acetylcodeine, (13) cannabinol, (14) 6-monoacetylmorphine, (15) diamorphine.

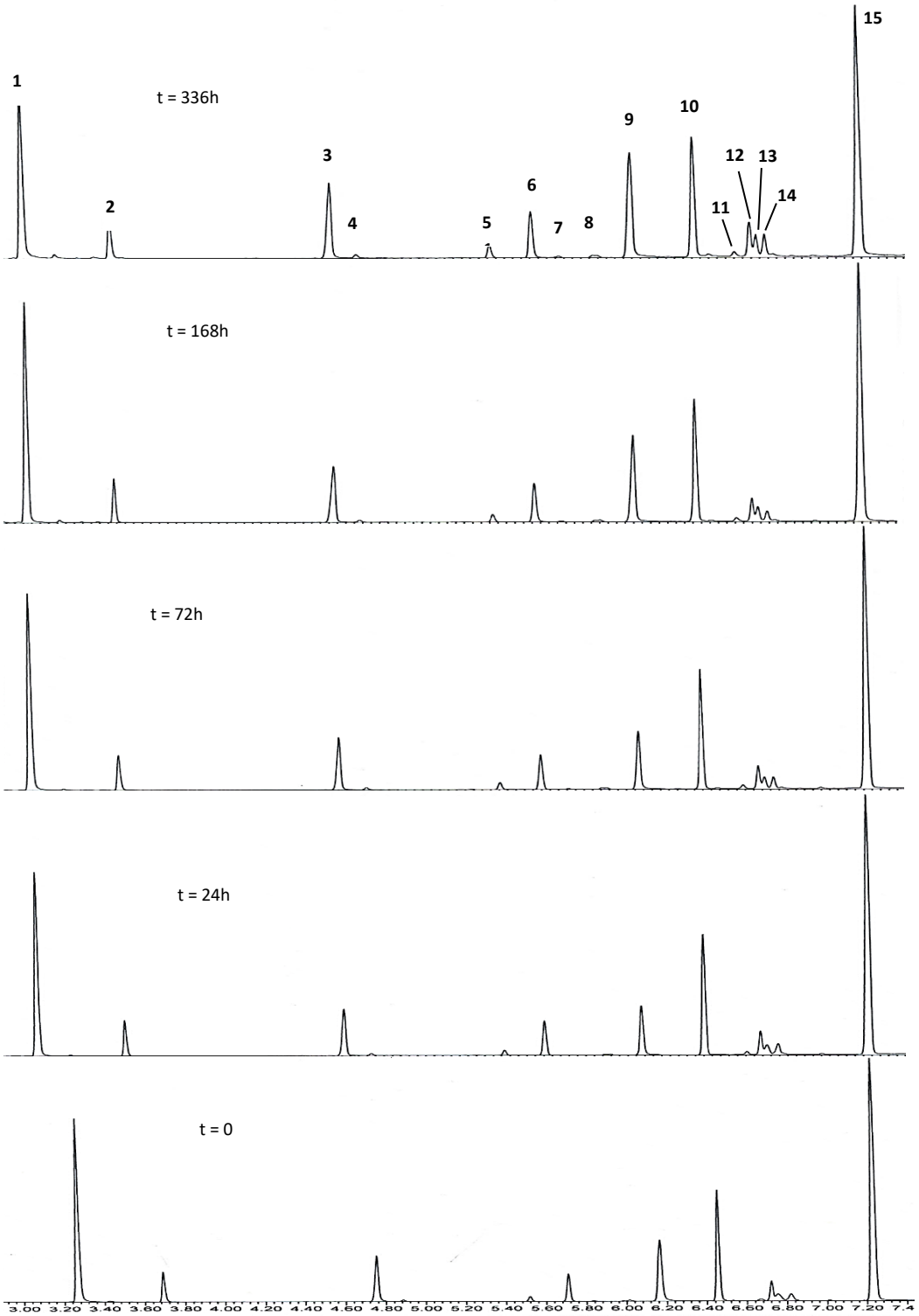

APPENDIX I-b: Total ion chromatographs for the samples stored in the dark and analysed after t = 0, 24, 72, 168 and 336 hours of storage where identifications were (1) phenacetin, (2) caffeine, (3) efavirenz, (4) dextromethorphan, (5) tetrahydrocannabivarin, (6) tetracosane (IS), (7) cannabivarin (8) cannabidiol (9) nevirapine; (10) Δ^9-tetrahydrocannabinol; (11) cannabigerol, (12) acetylcodeine, (13) cannabinol, (14) 6-monoacetylmorphine, (15) diamorphine.

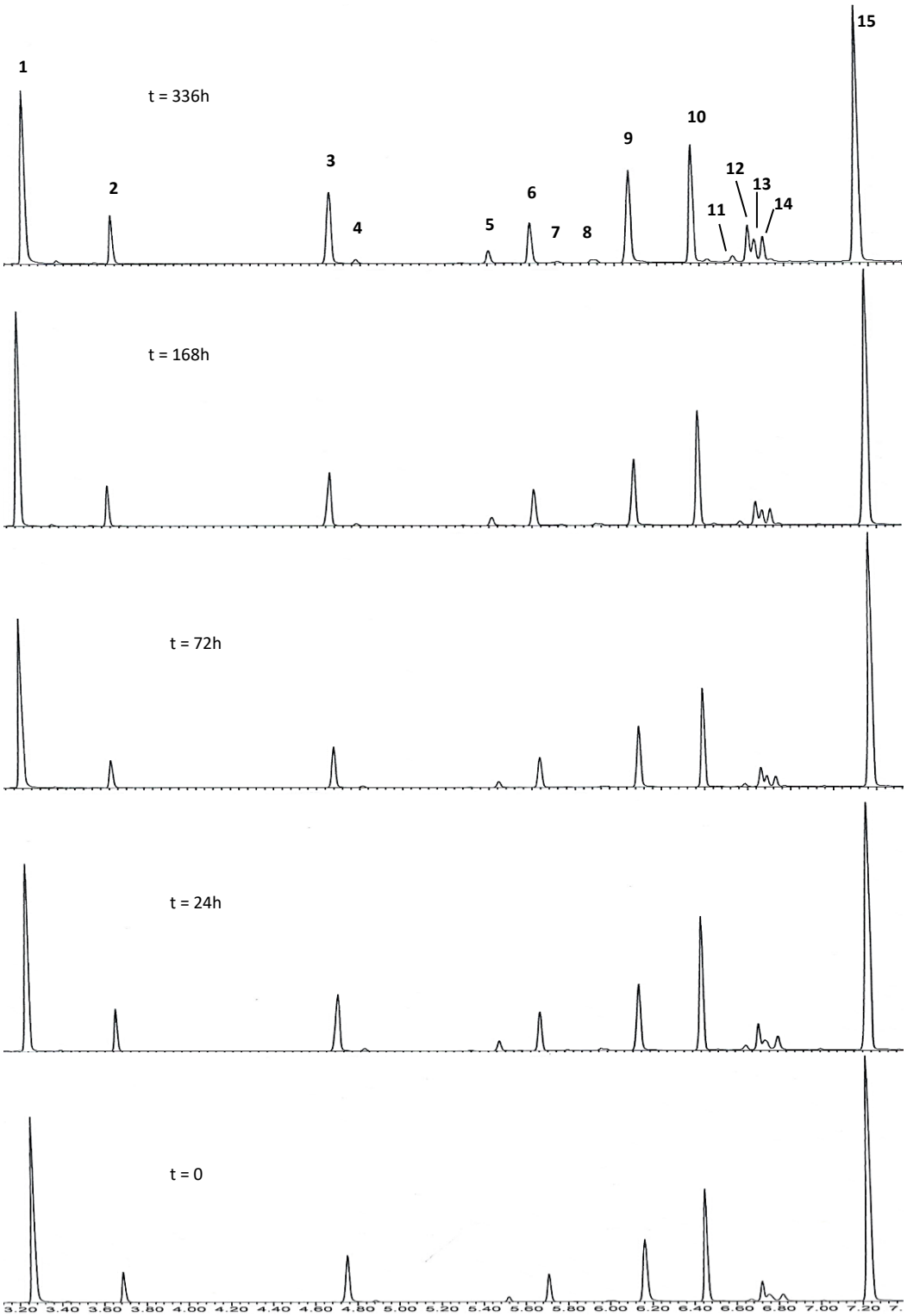

APPENDIX I-c: Total ion chromatographs for the samples stored under laboratory light and analysed after t = 0, 24, 72, 168 and 336 hours of storage where identifications were (1) phenacetin, (2) caffeine, (3) efavirenz, (4) dextromethorphan, (5) tetrahydrocannabivarin, (6) tetracosane (IS), (7) cannabivarin (8) cannabidiol (9) nevirapine; (10) Δ^9-tetrahydrocannabinol; (11) cannabigerol, (12) acetylcodeine, (13) cannabinol, (14) 6-monoacetylmorphine, (15) diamorphine.

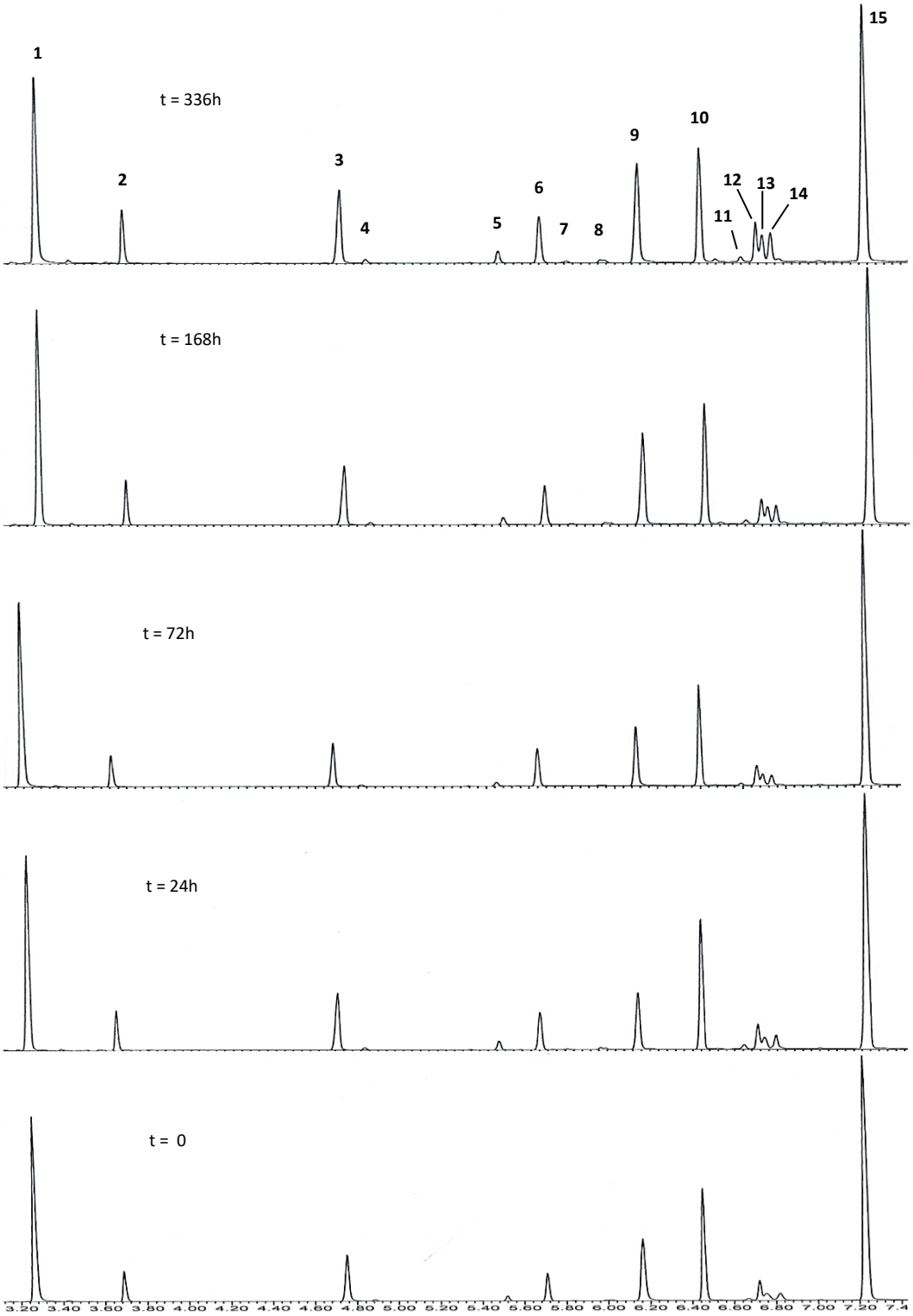

APPENDIX I-d: Total ion chromatographs for the samples stored at ambient conditions and analysed after t = 0, 24, 72, 168 and 336 hours of storage where identifications were (1) phenacetin, (2) caffeine, (3) efavirenz, (4) dextromethorphan, (5) tetrahydrocannabivarin, (6) tetracosane (IS), (7) cannabivarin (8) cannabidiol (9)nevirapine; (10) Δ^9-tetrahydrocannabinol; (11) cannabigerol, (12) acetylcodeine, (13) cannabinol, (14) 6-monoacetylmorphine, (15) diamorphine.

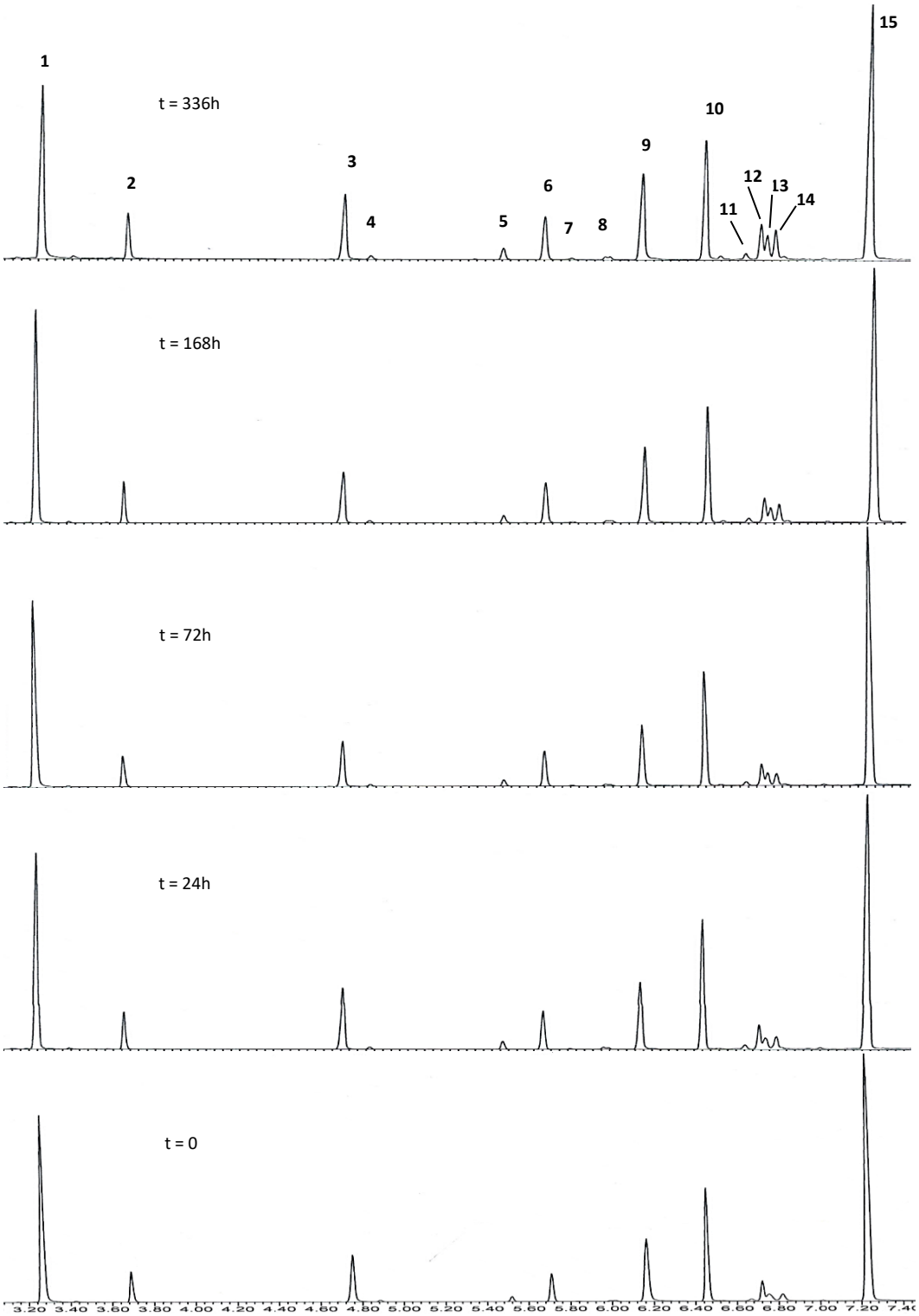

APPENDIX II Peak area ratios of the mixture of PNT, CAFF, EFV, NVP, Δ^9-THC and DAM reference standards.

APPENDIX II-a: Peak area ratios for the PNT in the mixture of PNT, CAFF, EFV, NVP, Δ^9-THC and DAM reference standards

Conc.mg/L / Replicate	1.04	2.59	5.18	7.77	10.36	25.90	51.80	77.70	103.60	259.00	518.00	777.00	1036.00
1	0.004687	0.051504	0.082042	0.114584	0.26814	1.277564	1.637057	3.005759	3.842309	11.77396	14.93047	22.97691	31.92889
2	0.017301	0.036096	0.132974	0.119637	0.210274	1.181839	2.064592	2.800989	4.276837	10.47179	16.98292	25.45555	31.79987
3	0.004226	0.024742	0.109809	0.117591	0.360557	1.098954	2.152301	2.74679	4.322894	8.995667	15.71532	21.00205	28.40834
4	0.002982	0.033031	0.074764	0.139418	0.320112	1.634085	2.132578	3.12244	3.06512	12.11256	14.28051	19.44314	29.24571
5	0.00547	0.02699	0.093373	0.13444	0.303243	1.524129	2.010898	3.005474	3.324357	9.791222	14.80621	23.04023	27.30591
6	0.009967	0.014335	0.059454	0.129327	0.291601	1.176248	2.257736	2.968167	3.907965	10.5662	17.83009	21.85883	27.55385
7	0.005947	0.02054	0.09049	0.103447	0.29489	1.723012	2.116976	3.010558	3.570398	10.25473	16.95831	27.61955	30.02144
8	0.006503	0.016336	0.053946	0.15375	0.302426	1.429035	2.133902	2.982449	4.971143	10.53649	16.35238	21.03121	27.24057
9	0.003318	0.017776	0.055938	0.183345	0.307295	1.433755	2.227635	3.029838	4.602755	10.54699	15.58826	20.1306	23.39556
10	0.010008	0.014997	0.102573	0.159202	0.39641	1.222964	2.045125	2.89354	4.47907	8.807565	15.64747	19.92219	29.83756
Mean	0.007041	0.025635	0.085536	0.135474	0.305495	1.370158	2.07788	2.9566	4.036285	10.38572	15.90919	22.24803	28.67377
STDV	0.004351	0.01179	0.0256	0.024212	0.049773	0.211407	0.172573	0.112347	0.601116	1.043036	1.114349	2.608646	2.516067
%RSD	61.79709	45.99266	29.92876	17.8718	16.29274	15.42941	8.305251	3.799881	14.8928	10.04299	7.004435	11.72529	8.774804

APPENDIX II-b: Peak area ratios for the CAFF in the mixture of PNT, CAFF, EFV, NVP, Δ^9-THC and DAM reference standards

Conc.mg/L / Replicate	1.00	2.50	5.00	7.50	10.00	25.00	50.00	75.00	100.00	250.00	500.00	750.00	1000.00
1	0.053577	0.154138	0.207939	0.21913	0.346539	1.270647	1.771916	2.897016	4.166995	10.23686	14.86651	21.86056	26.4621
2	0.045968	0.184907	0.249937	0.234108	0.407378	1.141237	1.974849	2.478401	3.159433	10.79079	13.69879	15.90747	26.6234
3	0.050075	0.136869	0.234971	0.220592	0.527446	1.076007	1.898936	2.471565	3.836031	8.551075	12.82443	14.10955	28.25785
4	0.034937	0.148705	0.197101	0.228844	0.483588	1.60813	1.981887	2.452383	4.083297	9.561354	12.38712	17.18169	25.86837
5	0.028505	0.107224	0.2284	0.272187	0.404196	1.44113	1.866789	2.61707	3.901155	10.18282	12.57191	14.61228	25.34216
6	0.047008	0.160991	0.234003	0.26752	0.412696	1.198369	1.978784	2.484098	3.801901	11.37733	13.72824	14.63182	26.20431
7	0.038838	0.149168	0.206094	0.23778	0.406036	1.596702	1.858258	2.564608	3.801657	10.75592	16.43586	17.85844	25.85488
8	0.037626	0.171386	0.182612	0.254386	0.397001	1.382066	2.043675	2.605041	4.063575	10.10371	12.92903	13.55165	25.03067
9	0.03512	0.165547	0.200496	0.286058	0.429756	1.347555	1.986096	2.580388	3.794796	10.02688	15.17866	13.85961	25.38289
10	0.032299	0.150805	0.263221	0.275991	0.501862	1.170824	1.788581	2.540236	3.738426	8.764565	13.73094	13.72898	25.19818
Mean	0.040395	0.152974	0.220477	0.249659	0.43165	1.323267	1.914977	2.569081	3.834727	10.03513	13.83515	15.73021	26.02248
STDV	0.008279	0.021009	0.025591	0.024631	0.055388	0.185512	0.091889	0.129396	0.278495	0.881953	1.299935	2.6158	0.952844
%RSD	20.49528	13.73353	11.60727	9.865894	12.83171	14.01924	4.798452	5.036674	7.262455	8.788653	9.395888	16.62915	3.66162

APPENDIX II-c: Peak area ratios for the EFV in the mixture of PNT, CAFF, EFV, NVP, Δ^9-THC and DAM reference standards

Conc.mg/L / Replicate	1.00	2.50	4.95	7.49	9.98	24.95	49.50	74.85	99.80	249.50	495.00	748.50	998.00
1	0.007369	0.054032	0.129686	0.136472	0.294615	1.203704	1.80988	2.461161	3.565169	10.94522	12.54205	22.84216	32.20676
2	0.025217	0.078877	0.147619	0.146931	0.258934	1.042044	1.825407	2.459285	3.764622	9.068353	14.18679	25.80053	34.90831
3	0.010938	0.056956	0.141887	0.150801	0.38455	1.000522	1.710683	3.01911	3.886349	7.975589	13.54089	22.43905	29.17301
4	0.010874	0.064305	0.117149	0.151843	0.340228	1.574487	1.870854	2.565184	2.708026	13.03227	15.94503	19.42163	28.23591
5	0.00972	0.072474	0.117218	0.162874	0.262093	1.289923	1.789114	2.592417	2.980934	9.197576	16.27516	23.94681	30.56187
6	0.021258	0.073726	0.119323	0.132138	0.314625	1.022392	1.847557	2.695635	4.40465	10.2335	16.04603	26.26877	30.17124
7	0.009744	0.08955	0.110133	0.176415	0.320856	1.496566	1.752697	2.708542	3.278837	9.189447	16.87224	28.54139	33.43832
8	0.021977	0.074118	0.106488	0.16112	0.270172	1.203391	1.833375	2.56741	4.132464	8.462275	17.26236	22.6821	30.42887
9	0.006526	0.061584	0.102524	0.151204	0.333348	1.194947	1.854627	2.679239	4.264823	9.581741	16.35847	21.75017	26.15602
10	0.008895	0.070415	0.164074	0.163852	0.354719	1.267262	1.610067	2.642803	3.683765	9.65405	15.36688	21.3935	32.6427
Mean	0.013252	0.069604	0.12561	0.153365	0.313414	1.229524	1.790426	2.639079	3.666964	9.734002	15.43959	23.50861	30.7923
STDV	0.006815	0.010672	0.019903	0.013261	0.041853	0.191027	0.08001	0.160149	0.550501	1.42834	1.53175	2.686027	2.594671
%RSD	51.42855	15.33181	15.84492	8.646907	13.3538	15.53668	4.46878	6.068357	15.01244	14.67371	9.920924	11.42572	8.426363

APPENDIX II-d: Peak area ratios for the NVP in the mixture of PNT, CAFF, EFV, NVP, Δ^9-THC and DAM reference standards

Conc.mg/L / Replicate	1.05	2.64	5.27	7.91	10.54	26.35	52.70	79.05	105.40	263.50	527.00	790.50	1054.00
1	0.011434	0.096625	0.115094	0.169697	0.349711	1.252676	1.967292	2.492204	3.512024	11.30672	12.36774	23.8731	33.75004
2	0.012119	0.077896	0.144005	0.173119	0.336251	1.143757	1.904378	2.902089	4.170951	11.18825	15.8271	23.87998	32.58991
3	0.014527	0.061975	0.121296	0.174078	0.357749	1.12882	2.249179	2.541186	4.411694	7.705913	16.02721	23.02595	29.87734
4	0.010393	0.076596	0.113603	0.170786	0.381471	1.470538	1.729305	2.621836	3.040031	12.84322	16.50432	17.1132	34.15234
5	0.028143	0.083594	0.137291	0.198237	0.376665	1.372136	1.959228	2.669819	3.07305	9.0079	16.50861	24.11787	31.67651
6	0.018447	0.09096	0.149636	0.181421	0.368246	1.26936	2.245131	2.755485	3.48519	9.625469	18.72898	24.18391	30.24862
7	0.017997	0.093219	0.162559	0.178913	0.372258	1.539587	1.996395	2.74808	3.715766	9.150164	17.29951	22.81178	33.06017
8	0.018954	0.082493	0.132438	0.177385	0.349247	1.152918	1.935048	2.571628	3.566073	11.49223	14.68861	23.36367	31.48964
9	0.010705	0.108964	0.132879	0.17998	0.340261	1.189068	1.954992	2.765053	3.778624	7.793753	15.77531	22.50219	27.22367
10	0.019124	0.090361	0.144288	0.128197	0.379941	1.50181	1.717595	2.823464	3.642607	9.972913	17.02855	20.61503	32.96935
Mean	0.016184	0.086268	0.135309	0.173181	0.36118	1.302067	1.965854	2.689084	3.639601	10.00865	16.07559	22.54867	31.70376
STDV	0.005509	0.012844	0.015629	0.017747	0.016736	0.157482	0.176912	0.131831	0.425517	1.680186	1.687998	2.183515	2.107676
%RSD	34.03838	14.88812	11.5504	10.2479	4.633744	12.09476	8.999258	4.902451	11.69132	16.78734	10.50038	9.683563	6.648031

APPENDIX II-e: Peak area ratios for the Δ^9-THC in the mixture of PNT, CAFF, EFV, NVP, Δ^9-THC and DAM reference standards

Conc. mg/L / Replicate	1.00	2.50	5.00	7.50	10.00	25.00	50.00	75.00	100.00	250.00	500.00	750.00	1000.00
1	0.034953	0.140207	0.272052	0.325619	0.48631	1.778332	2.628069	3.363188	5.738233	16.0931	24.17532	35.16549	42.57267
2	0.042369	0.156789	0.242875	0.312997	0.511592	1.473698	2.613083	3.614939	3.928375	18.60892	24.36363	24.81101	39.85673
3	0.035672	0.119192	0.250476	0.302772	0.510596	1.511816	2.659555	4.171753	5.62553	13.12869	19.27421	24.01773	44.58324
4	0.035395	0.145874	0.232059	0.229376	0.609734	2.094745	2.556007	3.933625	7.168949	15.80691	21.72981	24.99953	45.81749
5	0.032888	0.190193	0.265386	0.331352	0.564955	1.2682	2.892785	3.704824	5.213516	15.37237	21.64123	24.97843	44.90905
6	0.038238	0.158976	0.251442	0.296531	0.568275	1.732928	2.51616	3.761827	4.30646	18.15997	25.51312	23.92131	44.92663
7	0.038525	0.14763	0.282423	0.261513	0.564964	2.04643	2.544832	3.616135	6.582596	16.2158	22.6046	26.09842	43.59032
8	0.04406	0.155403	0.244417	0.31965	0.537771	1.547431	2.778815	3.30179	4.655369	16.39706	19.85306	24.09495	44.71259
9	0.03347	0.156542	0.22837	0.350829	0.568895	1.711727	2.646129	3.602405	4.811709	13.05778	21.9787	24.09257	44.54957
10	0.033728	0.160262	0.273181	0.312529	0.549016	2.043538	2.297464	3.544764	4.601448	15.66769	24.3427	20.39425	42.5268
Mean	0.03693	0.153107	0.254268	0.304317	0.547211	1.720885	2.61329	3.661525	5.263218	15.85083	22.54764	25.25737	43.80451
STDV	0.003816	0.017921	0.018268	0.035335	0.036307	0.27753	0.1585	0.255186	1.024176	1.792112	2.048222	3.784493	1.741591
%RSD	10.33385	11.70518	7.184551	11.61134	6.634871	16.12717	6.065169	6.969395	19.45911	11.30611	9.083975	14.98372	3.975825

APPENDIX II-f: Peak area ratios for the diamorphine in the mixture of PNT, CAFF, EFV, NVP, Δ^9-THC and DAM reference standards.

Conc. , mg/L / Replicate	1.00	2.50	5.00	7.50	10.00	25.00	50.00	75.00	100.00	250.00	500.00	750.00	1000.00
1	0.054484	0.112035	0.18088	0.226864	0.387723	1.436618	2.057128	2.713057	3.602075	12.12833	15.28302	24.2309	34.5988
2	0.062714	0.181987	0.193995	0.225999	0.359376	1.306923	1.924797	3.127951	4.174658	10.886	17.14246	26.2498	33.94221
3	0.046473	0.143993	0.179268	0.175314	0.394405	1.017577	2.126553	2.720093	4.642293	10.28708	16.81131	23.60066	30.84983
4	0.042248	0.12313	0.1687	0.203108	0.475248	1.854716	2.274618	2.759138	3.451709	11.84655	17.32252	17.62402	31.25695
5	0.042831	0.123314	0.172107	0.269731	0.4	1.428255	2.035136	2.928365	3.604344	11.66917	17.35751	25.60531	31.90753
6	0.048951	0.114533	0.214839	0.219721	0.421705	1.374575	2.586495	2.966291	3.108391	13.73158	18.87431	24.94867	30.41795
7	0.053668	0.135171	0.206805	0.159059	0.429126	1.651949	2.336719	2.979058	2.944856	12.24685	17.61354	23.83082	28.93321
8	0.045754	0.14008	0.192721	0.219263	0.40656	1.440357	2.121116	2.635635	4.647588	13.43023	16.71343	24.47739	30.84274
9	0.027989	0.122343	0.181957	0.272534	0.432504	1.205121	2.506072	2.851101	4.862377	9.569762	14.72591	23.4579	27.67158
10	0.050075	0.136548	0.221957	0.211533	0.413547	1.594673	1.863527	3.096253	4.804734	12.61372	19.18847	19.64254	33.5007
Mean	0.047519	0.133313	0.191323	0.218313	0.412019	1.431076	2.183216	2.877694	3.984302	11.84093	17.10325	23.3668	31.39215
STDV	0.009196	0.0202	0.018146	0.035521	0.031006	0.234707	0.238668	0.168782	0.728396	1.310601	1.376857	2.686033	2.184525
%RSD	19.35334	15.15236	9.484277	16.27087	7.52545	16.40075	10.93195	5.865185	18.28165	11.0684	8.050265	11.49508	6.958827

APPENDIX III Peak area ratios for PNT, CAFF, EFV, NVP, Δ^9-THC and DAM in the reference standards mixture at three different concentration level.

APPENDIX III-a: Peak area ratios for the caffeine in the mixture of PNT, CAFF, EFV, NVP, Δ^9-THC and DAM reference standards at three different concentration level.

	Day 1		Day 2		Day 3		Day 4		Day 5	
Control Level (mg/L)	**Instrument 1**	**Instrument 2**	**Instrument 1**	**Instrument 2**	**Instrument 1**	**Instrument 2**	**Instrument 1**	**Instrument 2**	**Instrument 1**	**Instrument 2**
Low (10.00)	0.357789	0.420338	0.429247	0.415148	0.408929	0.380217	0.371719	0.446167	0.393105	0.473533
	0.363931	0.715718	0.392046	0.420594	0.439087	0.401632	0.360957	0.507432	0.402417	0.397780
	0.360955	0.416785	0.394941	0.418968	0.420659	0.400507	0.380677	0.446800	0.395599	0.485297
	0.362500	0.708355	0.389867	0.430729	0.394967	0.405144	0.372069	0.510441	0.401281	0.411696
	0.353992	0.411996	0.398929	0.426865	0.417490	0.393045	0.374131	0.443297	0.405258	0.476595
Average	0.359833	0.534638	0.401006	0.422461	0.416226	0.396109	0.371911	0.470828	0.399532	0.448980
Standard deviation	0.003983	0.161990	0.016148	0.006263	0.016195	0.009918	0.007103	0.034830	0.005023	0.040914
%RSD	1.106936	30.298898	4.026799	1.482554	3.890802	2.503746	1.909980	7.397641	1.257308	9.112710
Medium (100.00)	3.084664	3.764210	2.776595	3.341166	2.826611	3.245481	2.911412	3.429382	2.827881	3.163174
	3.139472	3.495476	2.837933	3.392315	3.006851	3.202273	2.927678	3.313822	2.850310	3.297815
	2.898323	3.758327	2.909484	3.238337	2.894657	3.163747	2.930063	3.384330	2.856799	3.157419
	2.924091	3.517547	2.913722	3.241653	2.896926	3.255818	2.862274	3.268329	2.859475	3.176660
	2.911095	3.674413	2.870495	3.334495	2.861578	3.141605	2.845239	3.342473	2.898335	3.169152
Average	2.991529	3.641995	2.861646	3.309593	2.897325	3.201785	2.895333	3.347667	2.858560	3.192844
Standard deviation	0.112101	0.128914	0.056733	0.067367	0.067605	0.049744	0.039093	0.062226	0.025472	0.059113
%RSD	3.747271	3.539666	1.982531	2.035507	2.333349	1.553622	1.350220	1.858800	0.891070	1.851425
High (1000.00)	23.024968	21.667413	18.135421	19.743452	21.355994	19.406658	23.596786	19.424432	22.467234	19.320929
	22.817459	22.396056	18.924818	19.816577	22.546930	19.286627	24.885130	19.845412	23.899183	19.543318
	22.907257	22.589594	21.455498	18.855017	22.151738	19.607625	23.727618	19.343782	23.492968	19.284396
	21.777252	22.688464	21.035096	19.725182	22.672561	21.836336	25.106804	19.953281	23.541238	19.228911
	23.385567	22.613623	19.337640	21.161329	27.482350	21.835087	22.950685	19.415888	24.248884	19.469686
Average	22.782500	22.391030	19.777695	19.860311	23.241914	20.394467	24.053405	19.596559	23.529902	19.369448
Standard deviation	0.602036	0.418656	1.415468	0.827208	2.425574	1.320660	0.912695	0.280777	0.667843	0.131925
%RSD	2.642537	1.869747	7.156888	4.165131	10.436207	6.475580	3.794451	1.432789	2.838275	0.681100

APPENDIX III- b: Peak area ratios for the diamorphine in the mixture of PNT, CAFF, EFV, NVP, Δ^9-THC and DAM reference standards at three different concentration level.

	Day 1		Day 2		Day 3		Day 4		Day 5	
Control Level (mg/L)	**Instrument 1**	**Instrument 2**	**Instrument 1**	**Instrument 2**	**Instrument 1**	**Instrument 2**	**Instrument 1**	**Instrument 2**	**Instrument 1**	**Instrument 2**
Low (10.00)	0.326978	0.232357	0.425185	0.170896	0.422130	0.267392	0.399717	0.237235	0.475943	0.212050
	0.353346	0.284184	0.386469	0.190558	0.430803	0.285706	0.389642	0.253898	0.458246	0.179357
	0.365274	0.260376	0.398351	0.224737	0.395144	0.283282	0.453979	0.229761	0.452738	0.206314
	0.362325	0.277151	0.380660	0.246217	0.391972	0.295654	0.411496	0.261454	0.454541	0.162262
	0.364926	0.284179	0.386517	0.215955	0.382440	0.279864	0.454945	0.230962	0.465664	0.166766
Average	0.354570	0.267649	0.395436	0.209673	0.404498	0.282379	0.421956	0.242662	0.461427	0.185350
Standard deviation	0.016161	0.021996	0.017831	0.029457	0.020820	0.010235	0.030667	0.014249	0.009509	0.022731
%RSD	4.558037	8.218292	4.509171	14.049079	5.147022	3.624668	7.267854	5.872070	2.060832	12.263741
Medium (100.00)	3.835638	3.348916	3.454627	3.011159	4.381881	3.248961	4.123310	2.833407	4.129696	2.717738
	4.445608	3.173878	3.436790	3.050760	4.024093	3.176956	4.193572	3.002761	4.018337	2.506252
	3.938112	3.200842	3.462504	3.174943	4.129254	3.110275	3.967035	2.827876	3.869835	2.639711
	4.230311	3.207151	3.651912	3.171295	4.098974	3.120422	4.230945	2.958098	4.157499	2.611687
	4.258775	3.281447	3.884008	3.049200	4.294239	3.368090	3.990149	3.023575	4.184201	2.561340
Average	4.141689	3.242447	3.577968	3.091472	4.185688	3.204941	4.101002	2.929144	4.071914	2.607346
Standard deviation	0.249519	0.071650	0.192097	0.076213	0.147557	0.106588	0.118520	0.093000	0.129401	0.079983
%RSD	6.024583	2.209760	5.368874	2.465268	3.525273	3.325729	2.890014	3.174979	3.177890	3.067603
High (1000.00)	20.132397	24.275991	18.12026	20.177939	18.252487	22.424846	18.262496	19.101650	18.188832	19.740664
	19.638516	23.495738	17.33013	21.064547	18.538029	21.363796	21.462304	18.955341	20.173693	20.006291
	19.962119	22.827790	18.94915	21.760042	18.102876	21.800357	19.133452	19.907218	20.092339	19.817982
	19.764911	23.102387	20.2774	21.133432	18.108352	23.791980	19.516014	19.219197	18.777079	20.205402
	20.189425	22.781283	20.07396	20.755783	20.605493	22.829478	17.454902	19.622823	22.331167	18.954048
Average	19.937474	23.296638	18.95018	20.978349	18.721447	22.442091	19.165834	19.361246	19.912622	19.744877
Standard deviation	0.235178	0.616830	1.258745	0.577217	1.067908	0.941688	1.511684	0.393330	1.597711	0.477282
%RSD	1.179579	2.647721	6.64239	2.751488	5.704196	4.196081	7.887390	2.031534	8.023610	2.417245

APPENDIX III-c: Peak area ratios for the efavirenz in the mixture of PNT, CAFF, EFV, NVP, Δ^9-THC and DAM reference standards at three different concentration level.

	Day 1		Day 2		Day 3		Day 4		Day 5	
Control Level (mg/L)	**Instrument 1**	**Instrument 2**	**Instrument 1**	**Instrument 2**	**Instrument 1**	**Instrument 2**	**Instrument 1**	**Instrument 2**	**Instrument 1**	**Instrument 2**
Low (10.00)	0.357102	0.280040	0.441339	0.294272	0.468795	0.343716	0.438326	0.416999	0.474774	0.402981
	0.366222	0.301640	0.433949	0.295081	0.458873	0.383852	0.428435	0.427270	0.486530	0.374674
	0.366056	0.298306	0.402068	0.311628	0.418098	0.364369	0.446847	0.417431	0.474019	0.388640
	0.374847	0.311651	0.400811	0.307581	0.438051	0.373061	0.440458	0.416936	0.476520	0.383973
	0.365180	0.328101	0.405889	0.318166	0.439618	0.364163	0.434882	0.423855	0.473997	0.374585
Average	0.365882	0.303947	0.416811	0.305345	0.444687	0.365832	0.437790	0.420498	0.477168	0.384971
Standard deviation	0.006287	0.017688	0.019287	0.010450	0.019743	0.014756	0.006808	0.004782	0.005333	0.011755
%RSD	1.718241	5.819450	4.627339	3.422420	4.439788	4.033626	1.555125	1.137204	1.117639	3.053418
Medium (100.00)	3.956112	3.733237	3.507553	3.560770	3.964714	3.578457	4.092476	3.706317	4.075972	3.531353
	4.218690	3.768961	3.757877	3.645028	3.968935	3.623775	4.073063	3.684224	4.128173	3.588568
	3.783002	3.797261	3.810035	3.591212	3.983710	3.570657	4.105835	3.693499	4.165814	3.512752
	3.823646	3.830516	3.915074	3.603203	3.996368	3.695642	4.057216	3.680564	4.099304	3.508973
	3.884744	3.755493	3.784705	3.687790	4.068882	3.624314	3.957507	3.708841	4.186275	3.509310
Average	3.933239	3.777094	3.755049	3.617600	3.996522	3.618569	4.057219	3.694689	4.131107	3.530191
Standard deviation	0.172438	0.037805	0.150643	0.049528	0.042347	0.049762	0.058737	0.012708	0.045574	0.033910
%RSD	4.384111	1.000889	4.011740	1.369092	1.059584	1.375176	1.447715	0.343944	1.103188	0.960577
High (1000.00)	26.568443	24.377419	18.366959	22.574799	25.697171	22.657595	26.708475	21.900063	25.850054	21.935600
	27.176193	24.522525	20.837619	22.532267	26.945274	22.780787	30.201063	22.075675	27.775649	22.320532
	28.011105	25.250332	24.547839	21.615157	25.746810	23.357901	27.947567	21.949144	27.506783	22.195057
	27.871354	24.657874	24.889405	22.439169	26.198063	24.975195	27.726250	22.286790	26.899153	21.939228
	28.470661	25.018332	24.963043	21.988720	30.209341	25.616102	24.630146	21.758691	29.327888	22.248341
Average	27.619551	24.765296	22.720973	22.230022	26.959332	23.877516	27.442700	21.994072	27.471905	22.127751
Standard deviation	0.748750	0.360629	2.982066	0.415407	1.884512	1.340578	2.024439	0.199125	1.274421	0.179374
%RSD	2.710941	1.456187	13.124729	1.868674	6.990204	5.614396	7.376966	0.905358	4.638998	0.810628

APPENDIX III-d: Peak area ratios for the nevirapine in the mixture of PNT, CAFF, EFV, NVP, Δ^9-THC and DAM reference standards at three different concentration level.

	Day 1		Day 2		Day 3		Day 4		Day 5	
Control Level (mg/L)	**Instrument 1**	**Instrument 2**	**Instrument 1**	**Instrument 2**	**Instrument 1**	**Instrument 2**	**Instrument 1**	**Instrument 2**	**Instrument 1**	**Instrument 2**
Low (10.00)	0.376087	0.287256	0.429519	0.269484	0.410259	0.345909	0.383312	0.389896	0.464470	0.389479
	0.391373	0.309012	0.433021	0.275288	0.442060	0.376686	0.382436	0.400526	0.455294	0.358101
	0.382624	0.317644	0.387886	0.293429	0.442522	0.363720	0.425901	0.404763	0.441767	0.364456
	0.392654	0.319043	0.416624	0.288876	0.425396	0.378265	0.391710	0.410854	0.442417	0.352499
	0.390466	0.328141	0.406121	0.297310	0.392020	0.361535	0.411500	0.404554	0.443492	0.352795
Average	0.386641	0.312219	0.414634	0.284878	0.422451	0.365223	0.398972	0.402119	0.449488	0.363466
Standard deviation	0.007083	0.015516	0.018382	0.011965	0.021626	0.013137	0.019063	0.007765	0.010047	0.015334
%RSD	1.832001	4.969488	4.433209	4.200008	5.119104	3.597075	4.777956	1.930971	2.235134	4.218872
Medium (100.00)	3.957089	3.835855	3.639422	3.711596	3.746602	3.740380	3.845585	3.628350	3.830492	3.617428
	4.293875	3.818332	3.466810	3.710053	3.964382	3.734633	3.814163	3.722817	3.842151	3.593201
	3.868310	3.839143	3.710189	3.743729	3.865578	3.704511	3.895085	3.440703	3.798002	3.600056
	4.017936	3.839265	3.862899	3.707706	3.884312	3.714240	3.913931	3.464996	3.954141	3.671168
	3.980185	3.867318	3.719323	3.749803	3.938622	3.735841	3.719981	3.752411	3.917080	3.619412
Average	4.023479	3.839982	3.679729	3.724577	3.879899	3.725921	3.837749	3.601855	3.868373	3.620253
Standard deviation	0.160861	0.017566	0.144054	0.020415	0.084526	0.015638	0.076776	0.143789	0.064813	0.030581
%RSD	3.998046	0.457439	3.914796	0.548129	2.178556	0.419713	2.000548	3.992086	1.675464	0.844715
High (1000.00)	21.526942	24.270263	22.481111	23.664897	21.447240	19.243245	20.704230	23.154234	23.272257	23.877420
	20.693974	24.390210	27.060697	23.229126	20.942085	19.000569	24.111147	23.126971	26.104206	23.965864
	21.213598	24.289287	32.232285	23.470620	20.706654	19.319044	22.414751	22.690866	26.979662	23.853257
	21.338529	24.260745	34.599704	23.041596	20.844392	19.961700	21.403355	23.240914	24.464883	23.829313
	22.233152	24.076799	32.811688	22.513700	22.603797	19.873152	20.151652	23.126722	29.378625	23.531288
Average	21.401239	24.257461	29.837097	23.183988	21.308834	19.479542	21.757027	23.067941	26.039927	23.811429
Standard deviation	0.558401	0.113412	4.977109	0.443010	0.776034	0.417856	1.564063	0.215923	2.354512	0.164889
%RSD	2.609198	0.467533	16.680944	1.910843	3.641844	2.145104	7.188774	0.936031	9.041929	0.692478

APPENDIX III-e: Peak area ratios for the phenacetin in the mixture of PNT, CAFF, EFV, NVP, Δ^9-THC and DAM reference standards at three different concentration level.

	Day 1		Day 2		Day 3		Day 4		Day 5	
Control Level (mg/L)	**Instrument 1**	**Instrument 2**	**Instrument 1**	**Instrument 2**	**Instrument 1**	**Instrument 2**	**Instrument 1**	**Instrument 2**	**Instrument 1**	**Instrument 2**
Low (10.00)	0.135693	0.343142	0.313947	0.324425	0.277455	0.347479	0.312632	0.480403	0.305126	0.427813
	0.226430	0.359858	0.324084	0.317081	0.294915	0.386724	0.303797	0.476116	0.309002	0.403137
	0.136554	0.355234	0.310105	0.332841	0.269486	0.375259	0.330897	0.463139	0.307795	0.419281
	0.154441	0.353003	0.287452	0.324291	0.281912	0.386429	0.312706	0.465023	0.327319	0.422485
	0.210597	0.335376	0.322006	0.307103	0.254197	0.372120	0.301221	0.467958	0.317934	0.419244
Average	0.172743	0.349323	0.311519	0.321148	0.275593	0.373602	0.312251	0.470528	0.313435	0.418392
Standard deviation	0.042815	0.009902	0.014620	0.009632	0.015098	0.016000	0.011632	0.007420	0.009131	0.009216
%RSD	24.785580	2.834600	4.693047	2.999336	5.478334	4.282743	3.725076	1.576996	2.913248	2.202715
Medium (100.00)	3.425337	4.375469	3.108183	3.871580	3.235136	3.909814	3.381574	3.980373	3.205345	3.843860
	3.558560	4.127370	3.036043	3.986887	3.295702	3.814033	3.421254	4.017554	3.285105	3.948690
	3.327925	4.136878	3.211759	3.812109	3.274718	3.797802	3.362254	4.044409	3.329075	3.794063
	3.312996	4.143359	3.216321	3.757327	3.304730	3.943358	3.310087	3.975995	3.260611	3.861694
	3.293065	4.503481	3.154075	4.009304	3.265722	3.811268	3.316263	4.039381	3.320778	3.880746
Average	3.383577	4.257311	3.145276	3.887441	3.275201	3.855255	3.358287	4.011543	3.280183	3.865811
Standard deviation	0.110266	0.172434	0.075585	0.109083	0.027329	0.066471	0.046401	0.032119	0.050116	0.056432
%RSD	3.258856	4.050314	2.403134	2.806030	0.834422	1.724171	1.381680	0.800657	1.527831	1.459783
High (1000.00)	23.295575	23.704329	18.582072	21.530941	22.542302	20.959378	24.676481	21.477207	23.259907	21.210288
	23.607933	23.013136	19.225818	21.515046	23.408354	21.363509	25.454191	20.967947	24.320045	21.208589
	23.940858	23.914246	21.104901	20.336745	23.430422	21.801228	24.652688	20.961557	24.193443	21.177038
	22.755304	24.038098	22.561877	21.385897	24.363918	25.264978	26.604157	21.027949	24.617367	20.927256
	24.939399	24.473152	20.605354	21.003219	27.754181	24.077553	24.399653	20.327035	25.160959	21.186265
Average	23.707814	23.828592	20.416004	21.154370	24.299835	22.693329	25.157434	20.952339	24.310344	21.141887
Standard deviation	0.815215	0.535513	1.572820	0.504196	2.035691	1.877519	0.900193	0.410042	0.695519	0.120830
%RSD	3.438593	2.247355	7.703859	2.383413	8.377386	8.273439	3.578238	1.957022	2.861000	0.571519

APPENDIX III-f: Peak area ratios for the Δ^9-tetrahydrocannabinol in the mixture of PNT, CAFF, EFV, NVP, Δ^9-THC and DAM reference standards at three different concentration level.

	Day 1		Day 2		Day 3		Day 4		Day 5	
Control Level (mg/L)	**Instrument 1**	**Instrument 2**	**Instrument 1**	**Instrument 2**	**Instrument 1**	**Instrument 2**	**Instrument 1**	**Instrument 2**	**Instrument 1**	**Instrument 2**
Low (10.00)	0.481728	0.500942	0.519663	0.469297	0.516264	0.497842	0.562145	0.522461	0.624784	0.457317
	0.523264	0.520556	0.506688	0.474053	0.587356	0.485069	0.554269	0.503521	0.598947	0.421388
	0.477336	0.498353	0.505103	0.459989	0.566056	0.526635	0.603966	0.455985	0.579177	0.460762
	0.526794	0.515197	0.504437	0.467724	0.515765	0.521405	0.573226	0.459478	0.598980	0.427256
	0.515021	0.535709	0.508685	0.460839	0.527224	0.515248	0.574494	0.452603	0.595452	0.438993
Average	0.504828	0.514152	0.508915	0.466380	0.542533	0.509240	0.573620	0.478810	0.599468	0.441143
Standard deviation	0.023536	0.015255	0.006227	0.005932	0.032417	0.017326	0.018894	0.032006	0.016350	0.017566
%RSD	4.662089	2.967092	1.223585	1.271836	5.975052	3.402396	3.293814	6.684482	2.727363	3.981889
Medium (100.00)	5.203013	4.943507	4.433080	4.658665	5.262379	4.756247	5.043938	4.591452	4.893597	4.564618
	5.785559	4.990446	4.263918	4.670275	5.232696	4.673650	5.065020	4.652246	4.796198	4.472611
	4.887212	4.936524	4.537823	4.717166	4.918394	4.670177	5.155179	4.575116	4.854235	4.507698
	5.247997	4.959665	4.543644	4.693443	5.130358	4.667162	5.041939	4.589076	5.040483	4.533479
	5.243555	4.944483	4.535324	4.648470	5.068984	4.752294	4.986745	4.633662	4.983811	4.553603
Average	5.273467	4.954925	4.462758	4.677604	5.122562	4.703906	5.058564	4.608310	4.913665	4.526402
Standard deviation	0.323241	0.021577	0.120272	0.027736	0.138107	0.046055	0.061287	0.032898	0.098408	0.037060
%RSD	6.129573	0.435462	2.695017	0.592961	2.696054	0.979081	1.211552	0.713881	2.002738	0.818752
High (1000.00)	21.198702	29.958406	13.793885	26.004363	18.909972	27.937427	18.877530	25.687078	20.012747	26.632403
	20.533943	29.785129	15.175454	26.964262	19.357253	26.929992	21.423392	25.232655	21.344213	27.262832
	21.002180	29.575785	17.498996	26.690270	18.331637	27.482439	19.188777	26.246353	20.776741	26.701851
	20.850884	29.801564	18.411413	26.903009	19.417465	29.973125	20.726936	25.836392	20.607210	26.955375
	21.334780	29.606533	18.080014	26.488985	21.905857	29.589091	18.880923	25.772825	21.873465	26.282963
Average	20.984098	29.745483	16.591953	26.610178	19.584437	28.382415	19.819512	25.755061	20.922875	26.767085
Standard deviation	0.312148	0.156650	2.011414	0.387053	1.368658	1.332660	1.179190	0.362570	0.712474	0.366738
%RSD	1.487545	0.526636	12.122826	1.454529	6.988496	4.695372	5.949641	1.407762	3.405241	1.370108

APPENDIX IV: Ten replicate blank analyses

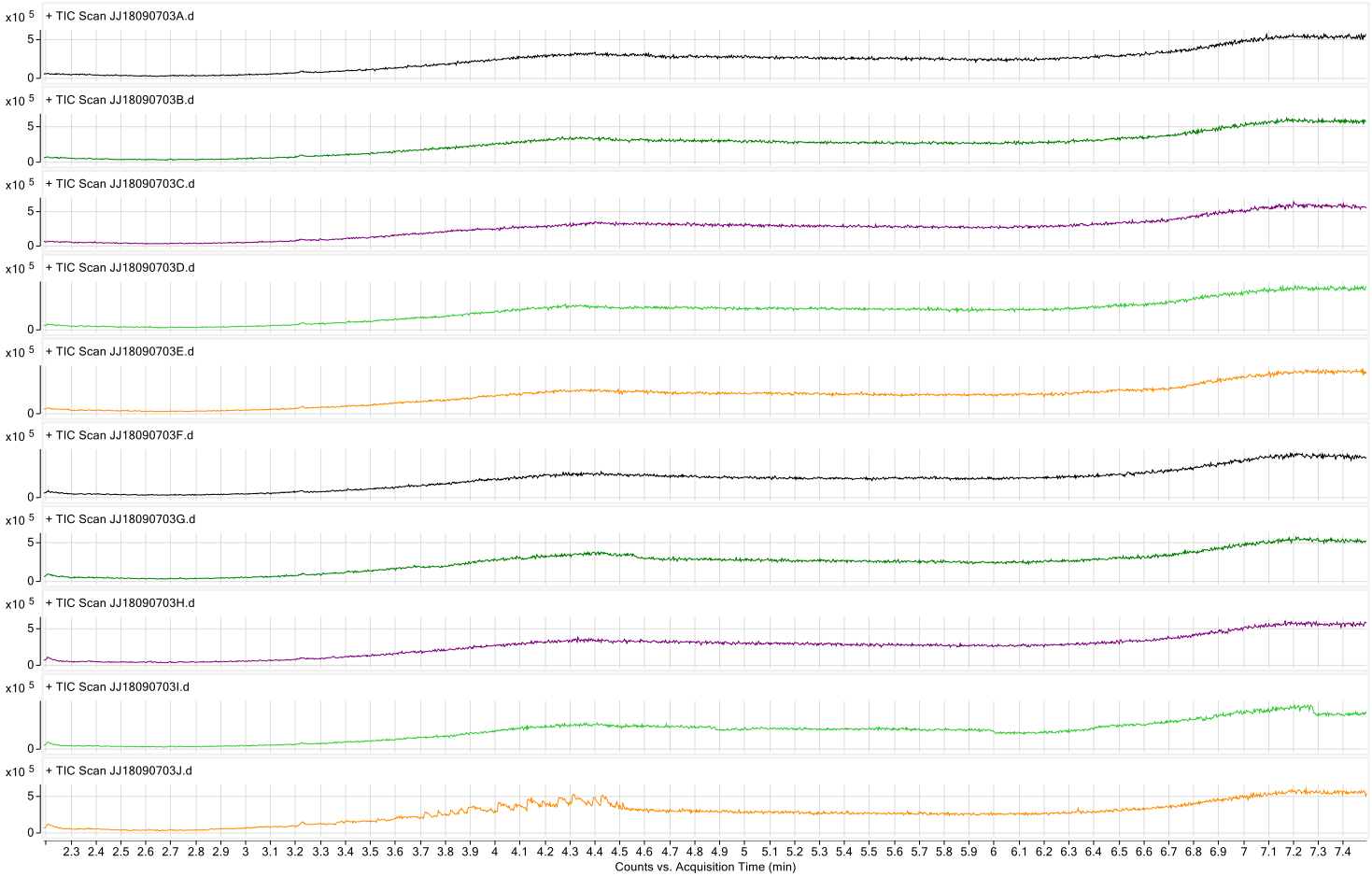

APPENDIX V EI mass spectra, molar mass and proposed fragmentation patterns of the compounds identified in both the simulated and actual seized street nyaope samples.

APPENDIX V-a: EI mass spectra, molar mass and proposed fragmentation patterns of ACA, ACOD, CAFF, CBCM, CBCN and CBD.

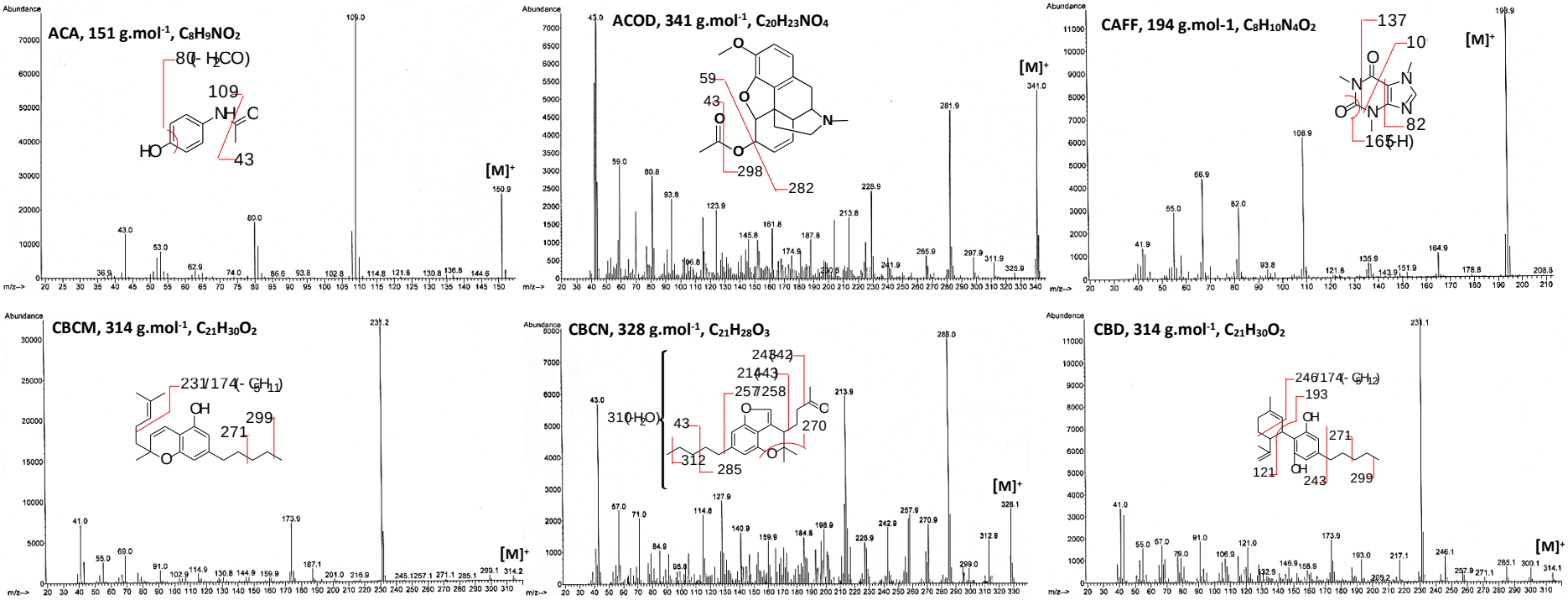

APPENDIX V-b: EI mass spectra, molar mass and proposed fragmentation patterns of CBG, CBN, COC, COD, DAM, DTM, EFV and 6-MAM

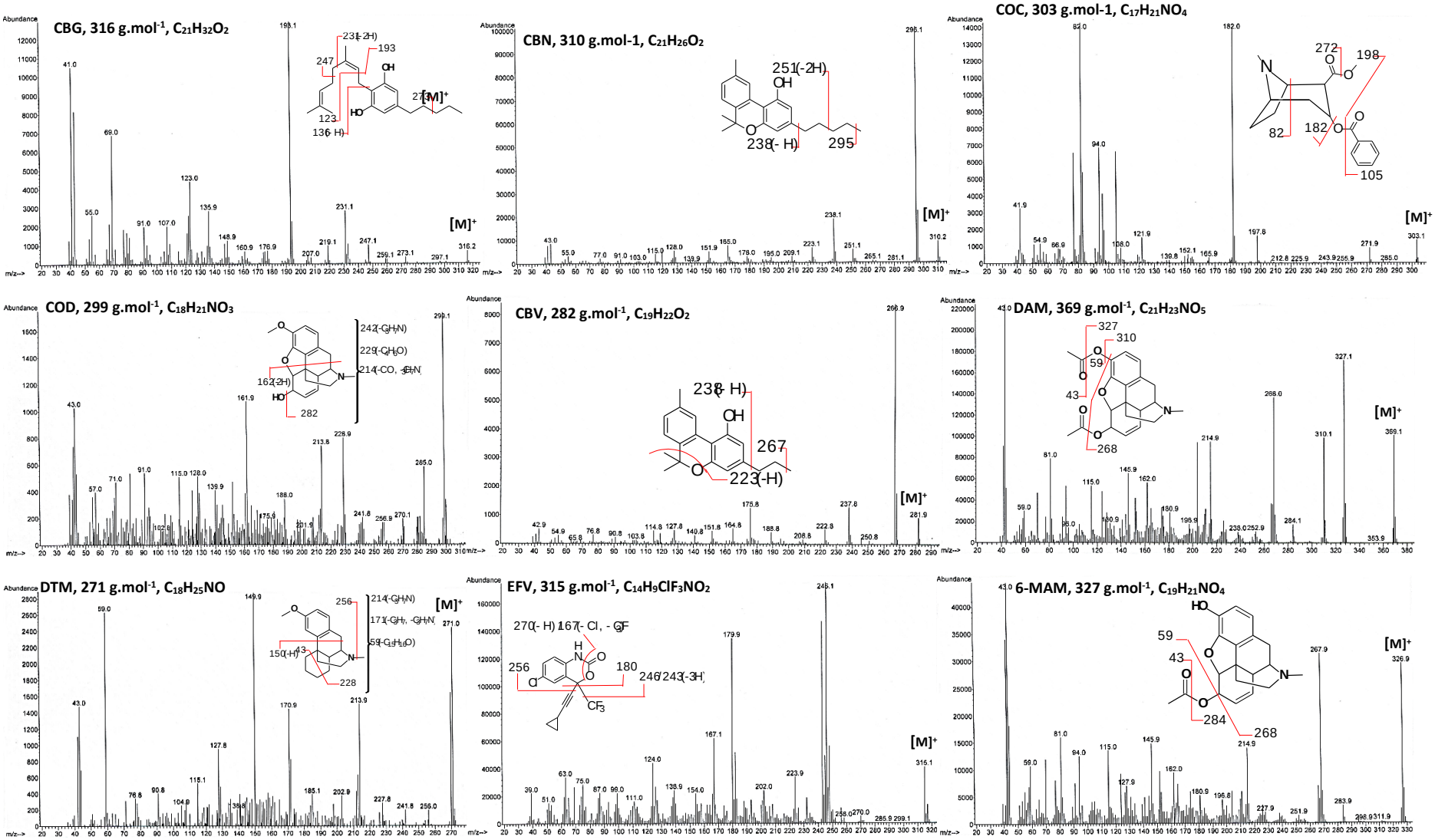

APPENDIX V-c: EI mass spectra, molar mass and proposed fragmentation patterns of MTQ, NCT, NVP, PNT, Δ^9-THV, THCV and vitamin E

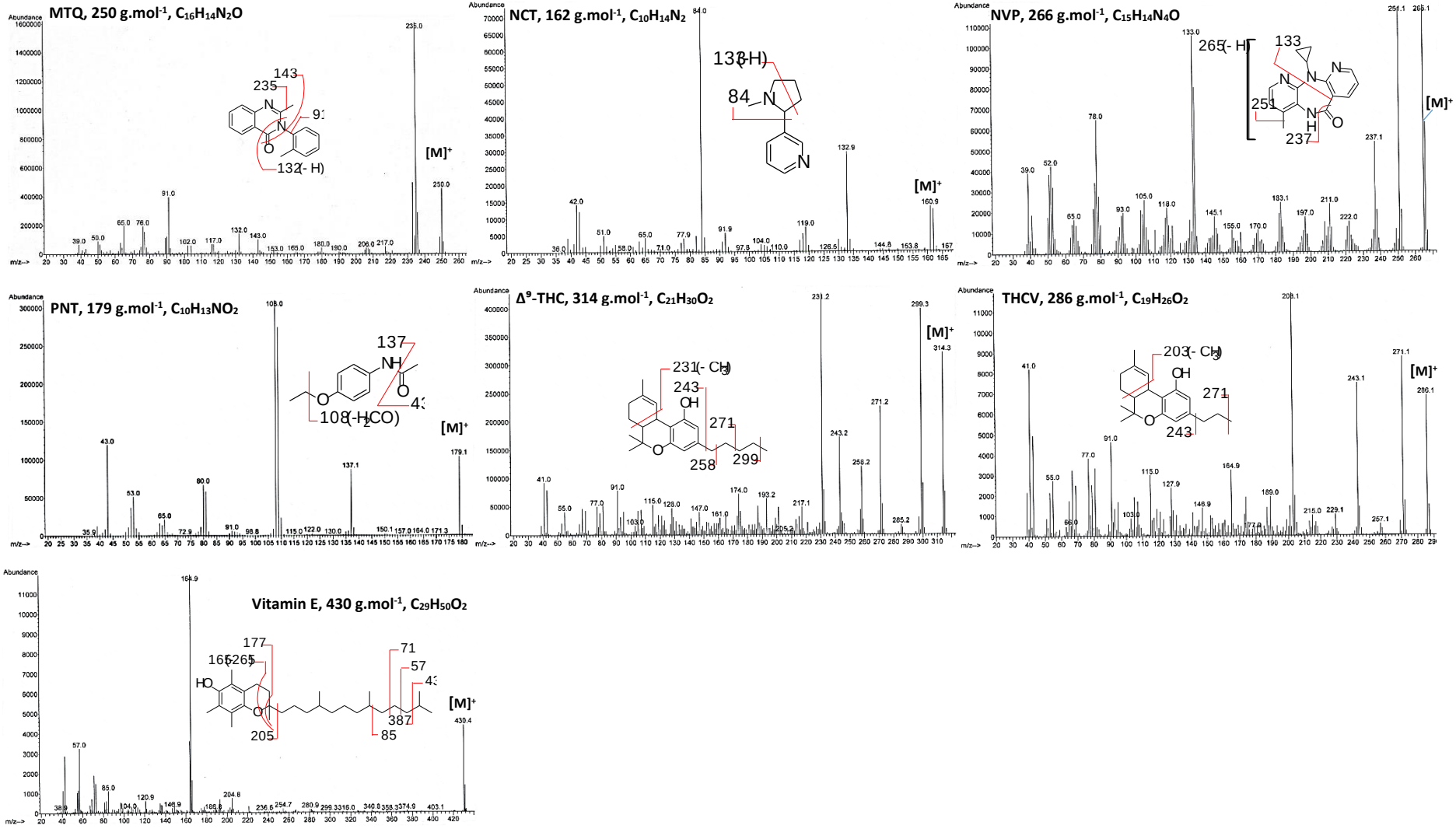

APPENDIX VI EI mass spectra of the compounds identified in both the simulated and actual seized street nyaope samples in comparison to the NIST mass spectral data.

APPENDIX VI-a: EI mass spectra of ACA, ACOD and CAFF in comparison to the NIST mass spectral data.

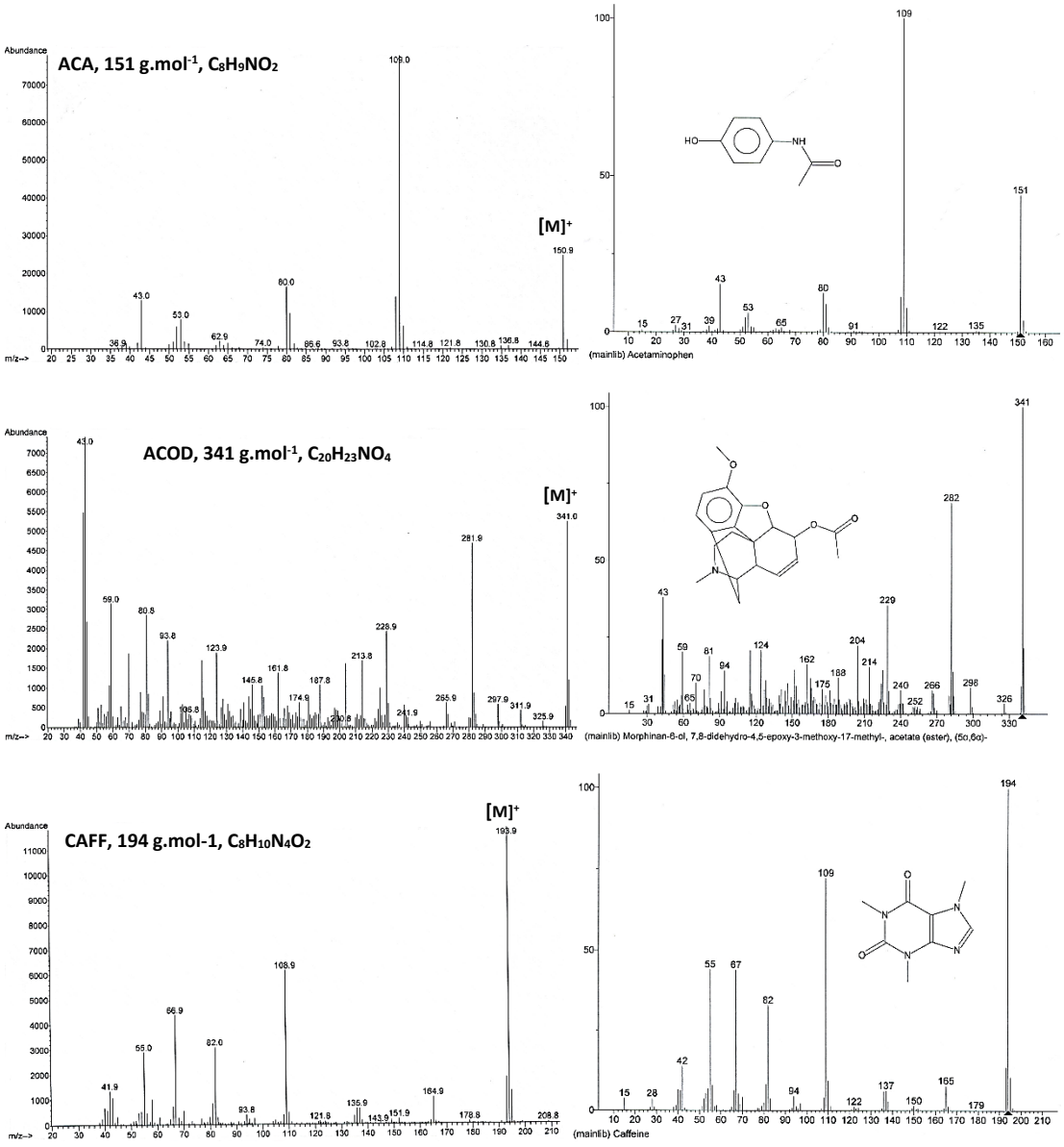

APPENDIX VI-b: EI mass spectra of CBCM, CBCN, CBD and CBG in comparison to the NIST mass spectral data.

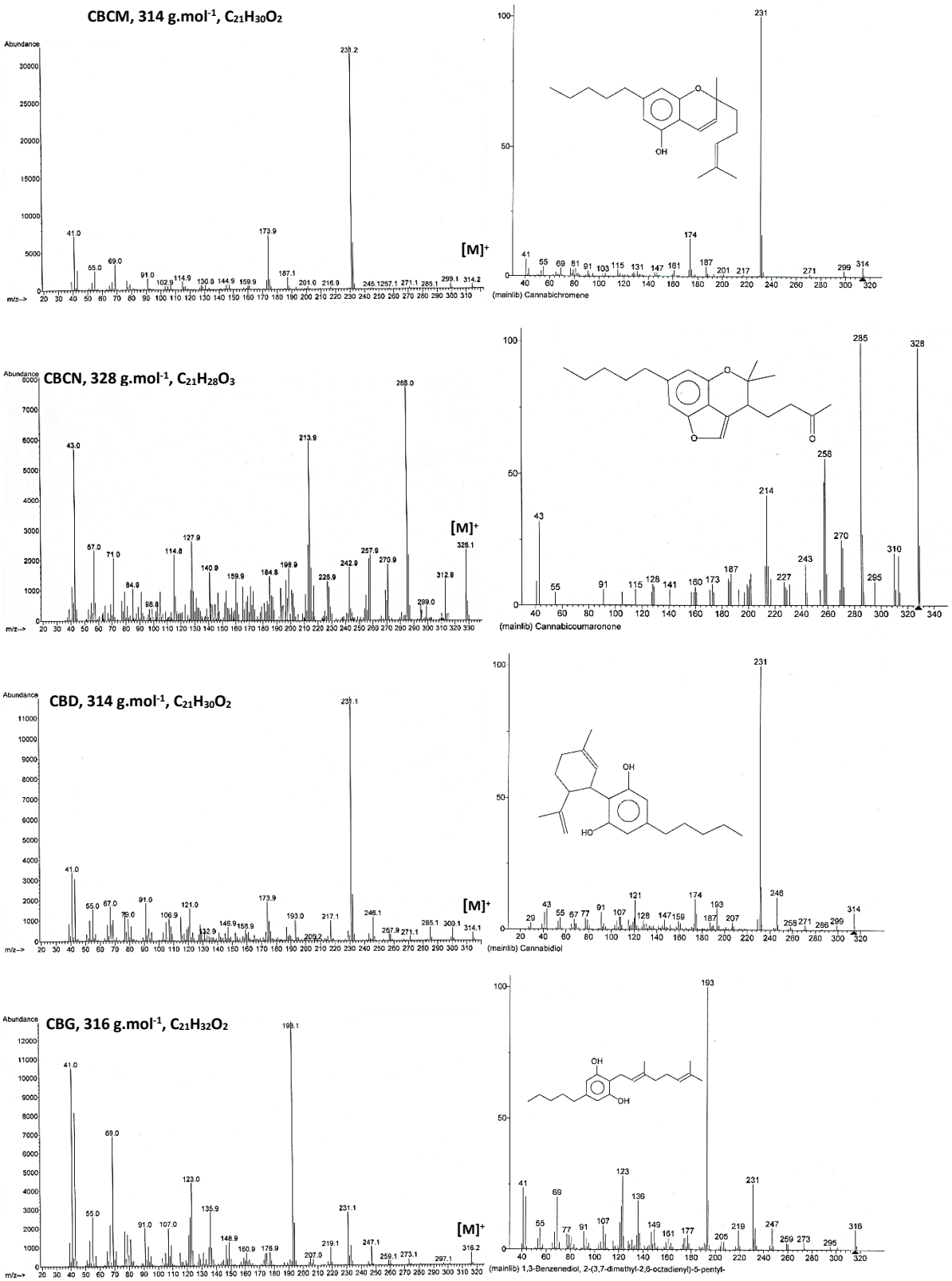

APPENDIX VI-c: EI mass spectra of CBN, CBV, COC and COD in comparison to the NIST mass spectral data.

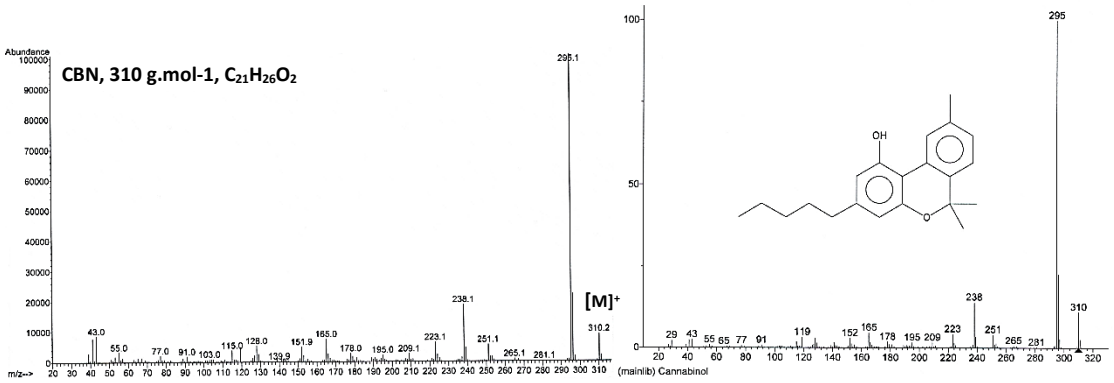

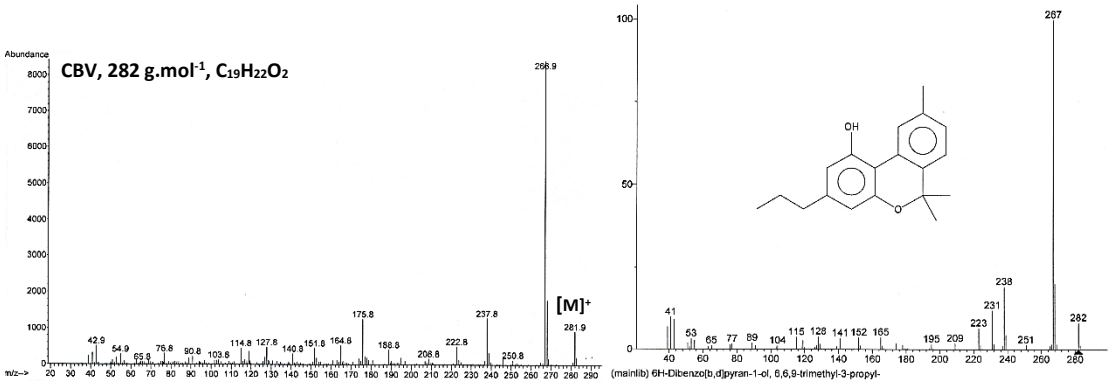

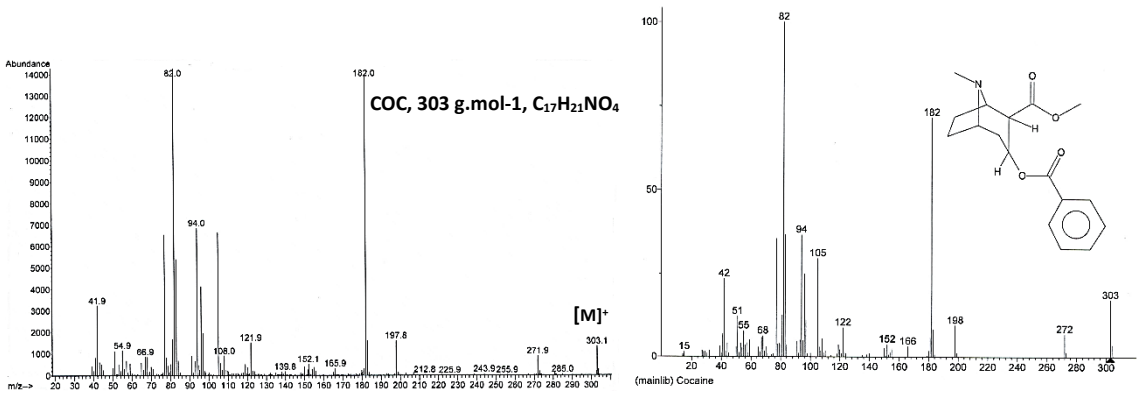

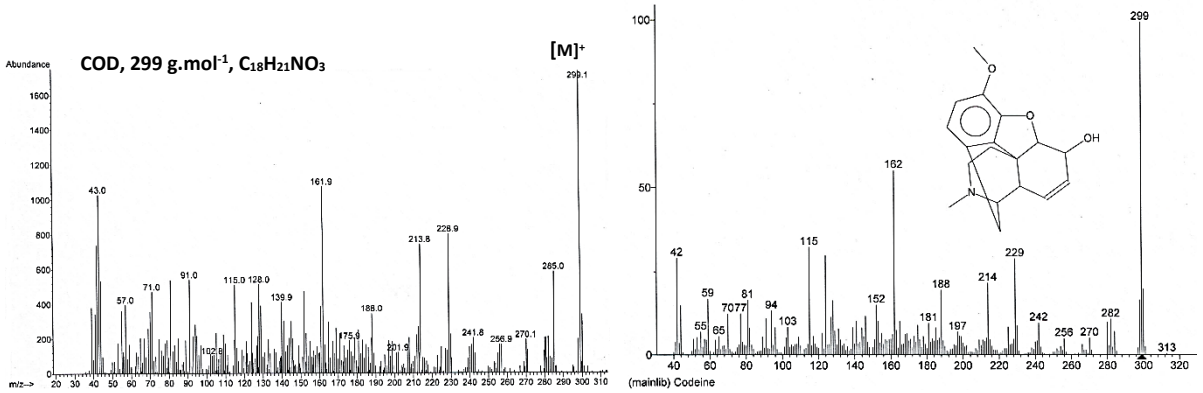

APPENDIX VI-d: EI mass spectra of DAM, DTM, EFV and 6-MAM in comparison to the NIST mass spectral data.

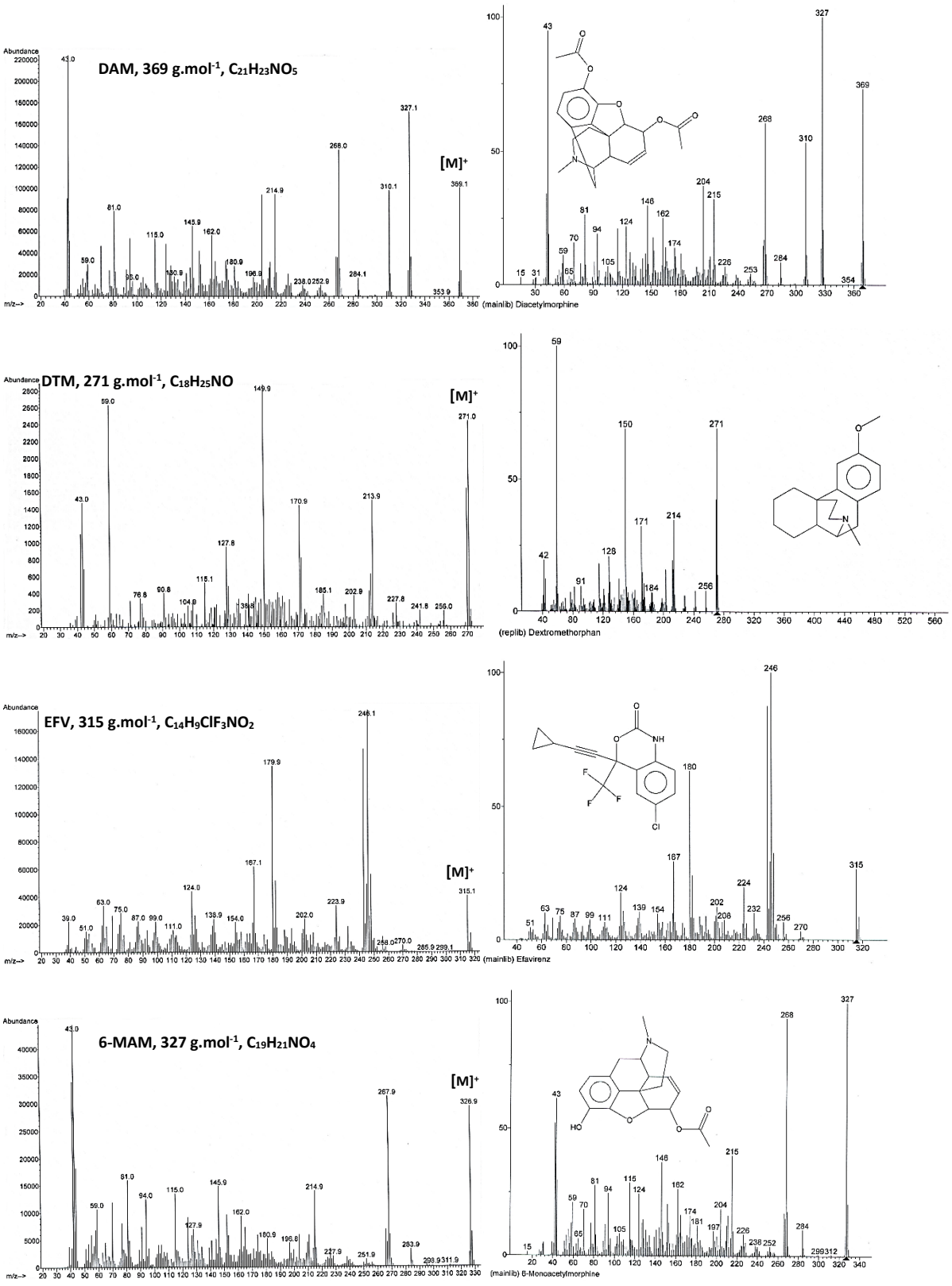

APPENDIX VI-e: EI mass spectra of MTQ, NVP, NCT, PNT and, in comparison to the NIST mass spectral data.

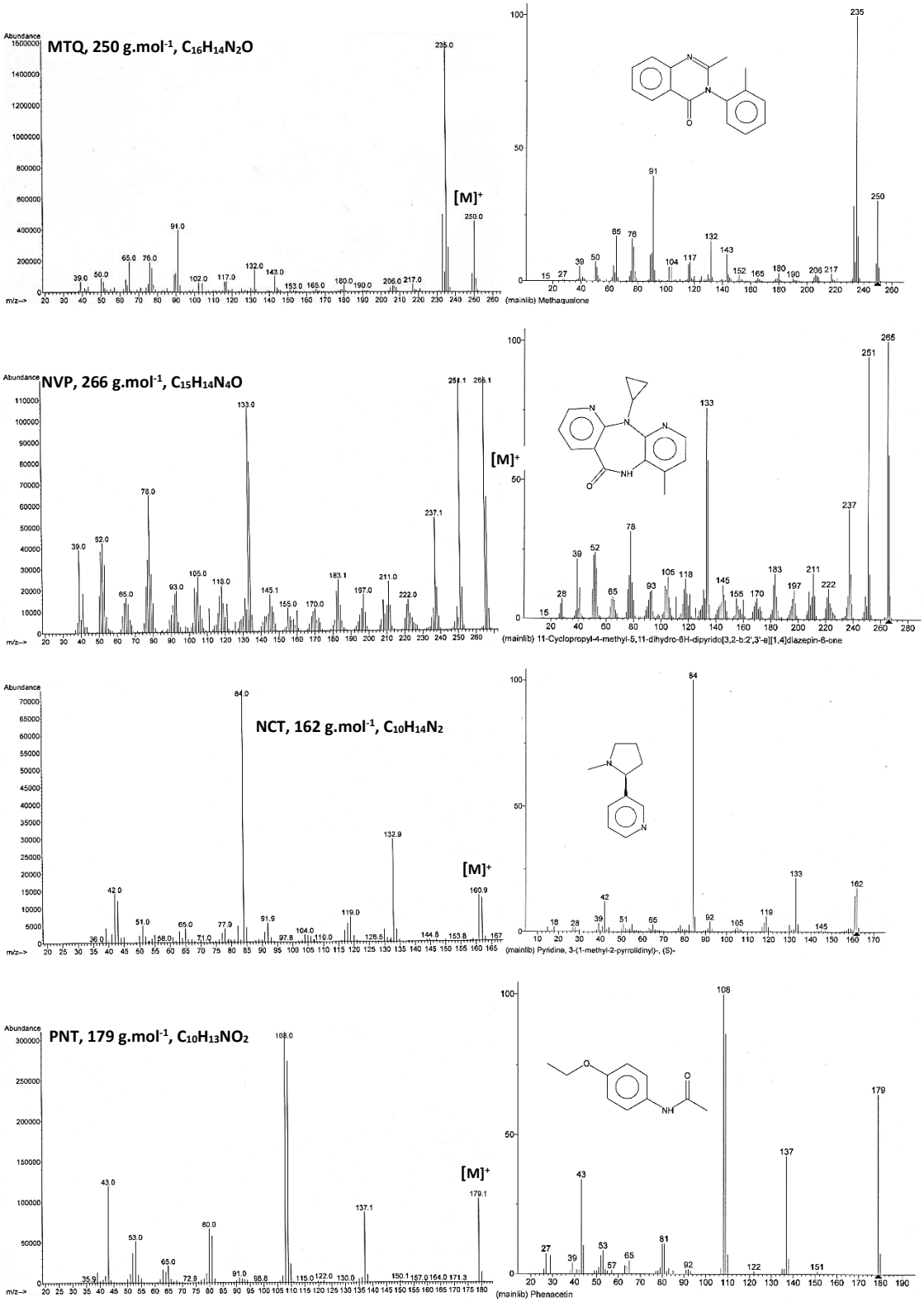

APPENDIX VI-f: EI mass spectra of Δ^9-THC, THVC and vitamin E in comparison to the NIST mass spectral data.

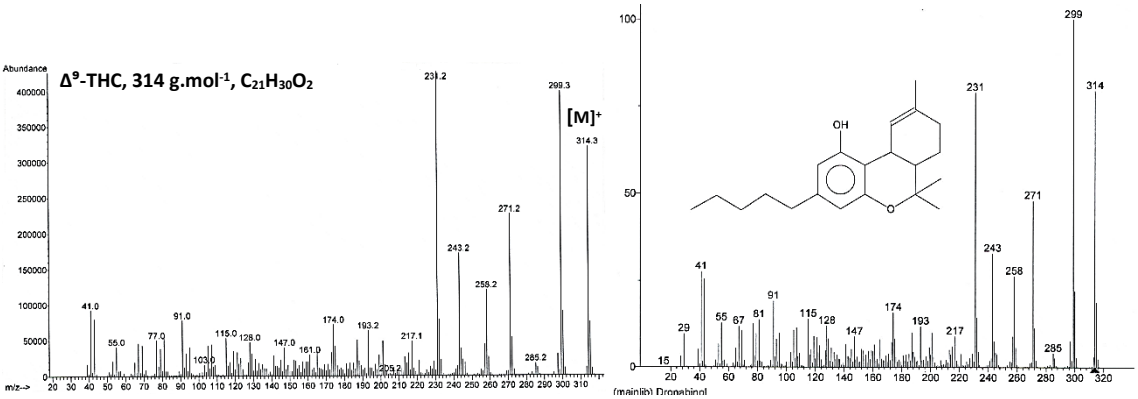

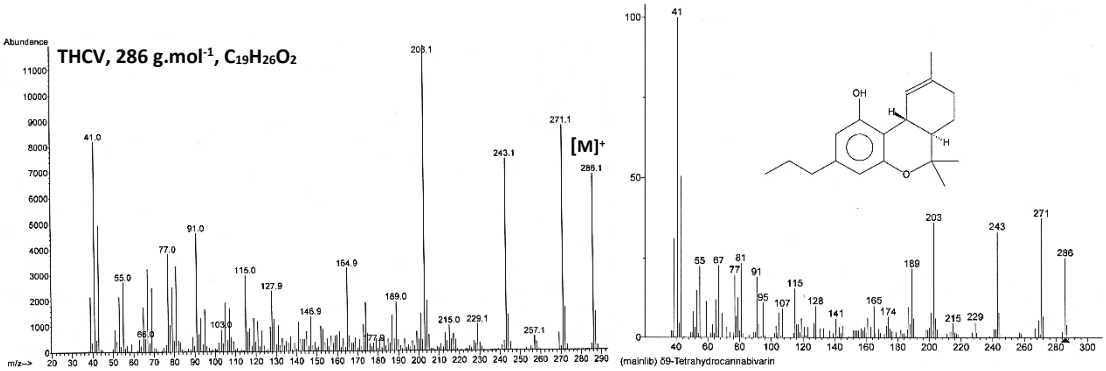

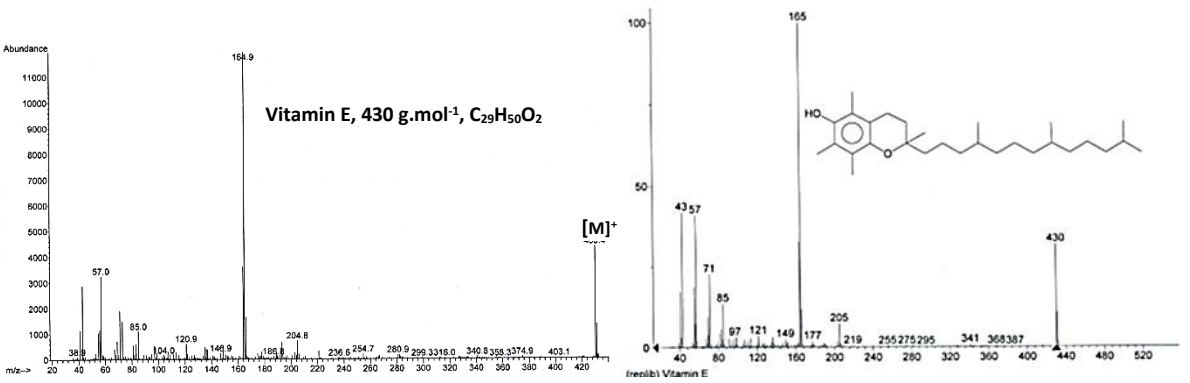

APPENDIX VII Average peak area ratios and the pooled average peak area ratios for the 18 simulated nyaope samples at t = 0, 24, 48 and 72 hours of autosampler storage.

APPENDIX VII-a: PAR and the PPAR for the simulated nyaope samples, S1, S2 and S6 at t = 0, 24, 48 and 72 hours of autosampler storage.

			S1							S2							S6				
	0	24 h	48 h	72 h	PPAR	SD	%RSD	0	24 h	48 h	72 h	PPAR	SD	%RSD	0	24 h	48 h	72 h	PPAR	SD	%RSD
PNT	1,239	1,262	1,184	1,066	1,188	0,087	7,36	1,316	1,306	1,214	1,058	1,223	0,120	9,77	1,560	1,470	1,352	1,220	1,401	0,148	10,54
CAFF	0,389	0,385	0,372	0,367	0,378	0,010	2,77	0,445	0,438	0,424	0,415	0,430	0,014	3,16	0,397	0,380	0,371	0,366	0,379	0,014	3,61
EFV	3,544	3,792	3,879	3,754	3,742	0,142	3,79	3,939	3,967	3,965	3,646	3,879	0,156	4,02	4,317	4,155	4,200	4,154	4,206	0,077	1,82
THCV	0,182	0,216	0,217	0,206	0,205	0,016	7,97	0,203	0,215	0,210	0,188	0,204	0,012	5,84	0,190	0,197	0,197	0,194	0,195	0,003	1,63
CBV	0,017	0,024	0,024	0,020	0,021	0,003	14,76	0,025	0,027	0,029	0,023	0,026	0,003	10,24	0,024	0,023	0,025	0,024	0,024	0,001	3,69
CBCM	0,062	0,084	0,084	0,073	0,076	0,011	14,18	0,088	0,097	0,094	0,079	0,089	0,008	8,64	0,081	0,091	0,087	0,085	0,086	0,004	4,61
CBD	0,044	0,051	0,053	0,055	0,051	0,005	9,65	0,052	0,053	0,052	0,052	0,052	0,001	1,55	0,045	0,047	0,047	0,054	0,048	0,004	8,14
NVP	2,491	2,713	2,658	2,520	2,595	0,107	4,13	1,520	1,560	1,488	1,357	1,481	0,088	5,94	1,461	1,449	1,422	1,397	1,432	0,029	1,99
Δ^9THC	5,727	6,134	6,574	6,504	6,235	0,390	6,25	6,003	6,184	6,496	6,134	6,205	0,209	3,37	5,781	6,012	6,285	6,396	6,118	0,277	4,53
ACOD	0,093	0,098	0,108	0,114	0,103	0,009	9,11	0,088	0,085	0,108	0,101	0,096	0,011	11,27	0,092	0,115	0,113	0,106	0,107	0,010	9,62
CBN	0,243	0,299	0,323	0,295	0,290	0,034	11,61	0,336	0,352	0,345	0,295	0,332	0,026	7,69	0,320	0,321	0,346	0,333	0,330	0,012	3,56
6-MAM	0,053	0,064	0,076	0,078	0,068	0,012	17,14	0,065	0,079	0,082	0,077	0,076	0,007	9,43	0,076	0,084	0,092	0,092	0,086	0,008	9,12
HER	1,906	2,105	2,096	1,980	2,022	0,096	4,74	2,234	2,217	2,168	2,142	2,190	0,043	1,95	2,513	2,511	2,538	2,469	2,508	0,029	1,14

APPENDIX VII-b: PAR and the PPAR for the simulated nyaope samples S7, S12 and S13 at t = 0, 24, 48 and 72 hours of autosampler storage.

			S7							S12							S13				
	0	**24 h**	**48 h**	**72 h**	**PPAR**	**SD**	**%RSD**	**0**	**24 h**	**48 h**	**72 h**	**PPAR**	**SD**	**%RSD**	**0**	**24 h**	**48 h**	**72 h**	**PPAR**	**SD**	**%RSD**
PNT	1,491	1,408	1,358	1,209	1,366	0,118	8,66	1,464	1,392	1,314	1,195	1,341	0,115	8,58	1,673	1,692	1,576	1,414	1,589	0,127	8,01
CAFF	0,398	0,376	0,368	0,341	0,371	0,024	6,40	0,414	0,391	0,379	0,367	0,388	0,020	5,17	0,428	0,424	0,412	0,411	0,419	0,009	2,13
EFV	2,747	2,660	2,691	2,612	2,678	0,057	2,12	3,700	3,565	3,635	3,534	3,609	0,074	2,06	5,431	5,327	5,382	5,289	5,357	0,062	1,16
THCV	0,222	0,229	0,232	0,226	0,227	0,004	1,88	0,197	0,212	0,204	0,201	0,204	0,006	3,12	0,178	0,195	0,188	0,190	0,188	0,007	3,61
CBV	0,027	0,028	0,030	0,028	0,028	0,001	3,76	0,025	0,025	0,026	0,024	0,025	0,001	4,12	0,021	0,024	0,024	0,023	0,023	0,002	6,54
CBCM	0,092	0,103	0,103	0,099	0,099	0,005	5,32	0,074	0,086	0,083	0,079	0,080	0,005	6,27	0,072	0,085	0,079	0,075	0,078	0,006	7,18
CBD	0,060	0,059	0,060	0,059	0,060	0,001	1,46	0,049	0,052	0,051	0,052	0,051	0,002	3,07	0,056	0,058	0,061	0,060	0,059	0,002	3,72
NVP	1,286	1,287	1,272	1,213	1,265	0,035	2,75	1,333	1,335	1,330	1,273	1,318	0,030	2,25	2,263	2,289	2,187	2,133	2,218	0,071	3,20
Δ^9THC	6,817	6,816	7,161	7,273	7,017	0,235	3,36	6,127	6,235	6,450	6,481	6,323	0,171	2,70	6,243	6,185	6,380	6,521	6,332	0,150	2,37
ACOD	0,099	0,109	0,126	0,106	0,110	0,011	10,36	0,072	0,092	0,091	0,084	0,085	0,009	11,14	0,097	0,105	0,082	0,087	0,093	0,011	11,36
CBN	0,378	0,363	0,393	0,370	0,376	0,013	3,38	0,327	0,361	0,377	0,361	0,356	0,021	5,92	0,311	0,332	0,353	0,365	0,340	0,024	7,02
6-MAM	0,071	0,069	0,090	0,092	0,080	0,012	15,35	0,062	0,083	0,086	0,091	0,080	0,012	15,54	0,069	0,081	0,089	0,090	0,082	0,010	11,86
HER	2,583	2,523	2,492	2,418	2,504	0,069	2,74	2,452	2,485	2,506	2,458	2,475	0,025	1,01	2,497	2,483	2,403	2,392	2,444	0,054	2,21

APPENDIX VII-c: PAR and the PPAR for the simulated nyaope samples S4, S9, S10, S16, S17 and S18 at t = 0, 24, 48 and 72 hours of autosampler storage.

			S3							S5							S8				
	0	**24 h**	**48 h**	**72 h**	**PPAR**	**SD**	**%RSD**	**0**	**24 h**	**48 h**	**72 h**	**PPAR**	**SD**	**%RSD**	**0**	**24 h**	**48 h**	**72 h**	**PPAR**	**SD**	**%RSD**
CAFF	0,531	0,535	0,533	0,496	0,524	0,019	3,55	0,458	0,448	0,443	0,421	0,443	0,016	3,58	0,618	0,618	0,586	0,568	0,598	0,025	4,12
EFV	7,140	7,025	7,873	7,771	7,452	0,431	5,79	4,363	4,406	4,689	4,688	4,536	0,176	3,88	7,967	7,944	8,001	7,983	7,974	0,024	0,30
THCV	0,096	0,103	0,115	0,113	0,107	0,009	8,40	0,104	0,112	0,119	0,116	0,113	0,007	6,00	0,123	0,131	0,127	0,124	0,126	0,004	2,89
CBV	0,012	0,011	0,016	0,016	0,014	0,002	17,44	0,012	0,013	0,014	0,014	0,013	0,001	7,18	0,016	0,017	0,017	0,016	0,016	0,001	4,16
CBCM	0,151	0,168	0,189	0,166	0,168	0,016	9,28	0,154	0,168	0,181	0,159	0,165	0,012	7,28	0,194	0,223	0,213	0,186	0,204	0,017	8,35
CBD	0,032	0,049	0,039	0,057	0,044	0,011	25,46	0,030	0,034	0,042	0,049	0,039	0,008	22,05	0,051	0,049	0,048	0,073	0,055	0,012	21,50
Δ^9THC	7,356	7,332	8,597	8,563	7,962	0,714	8,96	6,936	7,128	8,140	8,254	7,614	0,679	8,91	8,328	8,479	8,948	8,974	8,682	0,328	3,77
ACOD	0,091	0,094	0,105	0,086	0,094	0,008	8,37	0,091	0,074	0,114	0,083	0,090	0,017	18,71	0,092	0,097	0,107	0,135	0,108	0,019	18,01
CBN	0,718	0,776	0,925	0,926	0,836	0,106	12,64	0,698	0,805	0,876	0,825	0,801	0,075	9,34	1,044	1,087	1,027	0,981	1,035	0,044	4,25
6-MAM	0,246	0,245	0,290	0,298	0,270	0,028	10,44	0,201	0,226	0,250	0,246	0,231	0,022	9,65	0,310	0,333	0,324	0,323	0,322	0,010	2,95
HER	1,805	1,861	2,041	2,107	1,953	0,143	7,34	1,409	1,569	1,694	1,573	1,561	0,117	7,49	2,323	2,375	2,310	2,254	2,315	0,050	2,14
			S11							S14							S15				
	0	24 h	48 h	72 h	PPAR	SD	%RSD	0	24 h	48 h	72 h	PPAR	SD	%RSD	0	24 h	48 h	72 h	PPAR	SD	%RSD
CAFF	0,618	0,591	0,566	0,529	0,576	0,038	6,60	0,534	0,521	0,500	0,463	0,505	0,031	6,13	0,593	0,580	0,558	0,530	0,565	0,028	4,95
EFV	8,880	8,739	8,915	8,845	8,845	0,076	0,86	7,922	7,786	7,993	7,829	7,882	0,093	1,18	6,758	6,721	6,847	6,815	6,785	0,057	0,83
THCV	0,106	0,109	0,110	0,108	0,108	0,002	1,67	0,107	0,114	0,113	0,108	0,111	0,003	3,13	0,120	0,127	0,123	0,124	0,124	0,003	2,53
CBV	0,014	0,013	0,013	0,013	0,013	0,000	3,64	0,015	0,014	0,015	0,015	0,015	0,000	2,43	0,016	0,016	0,014	0,014	0,015	0,001	6,59
CBCM	0,171	0,189	0,182	0,164	0,176	0,011	6,26	0,167	0,197	0,182	0,174	0,180	0,013	7,13	0,191	0,209	0,193	0,199	0,198	0,008	4,07
CBD	0,036	0,046	0,046	0,054	0,046	0,007	15,82	0,041	0,046	0,045	0,057	0,047	0,007	14,42	0,038	0,040	0,044	0,045	0,042	0,003	7,75
Δ^9THC	7,684	7,794	8,348	8,542	8,092	0,418	5,16	7,794	7,900	8,414	8,608	8,179	0,394	4,82	8,435	8,531	9,228	9,326	8,880	0,462	5,20
ACOD	0,099	0,110	0,115	0,102	0,106	0,007	6,94	0,124	0,087	0,104	0,098	0,103	0,016	15,09	0,075	0,075	0,107	0,086	0,086	0,015	17,31
CBN	0,854	0,897	0,892	0,877	0,880	0,019	2,20	0,983	1,053	0,969	0,992	0,999	0,037	3,70	1,028	1,106	1,033	1,005	1,043	0,043	4,16
6-MAM	0,288	0,309	0,315	0,317	0,307	0,013	4,27	0,267	0,279	0,269	0,282	0,274	0,007	2,66	0,274	0,306	0,322	0,321	0,306	0,023	7,42
HER	2,227	2,301	2,318	2,272	2,279	0,040	1,74	1,926	1,977	1,908	1,898	1,927	0,035	1,83	2,151	2,227	2,224	2,145	2,187	0,045	2,06

APPENDIX VII-d: PAR and the PPAR for the simulated nyaope samples S4, S9, S10, S16, S17 and S18 at t = 0, 24, 48 and 72 hours of autosampler storage.

			S4							S9							S10				
	0	24 h	48 h	72 h	PPAR	SD	%RSD	0	24 h	48 h	72 h	PPAR	SD	%RSD	0	24 h	48 h	72 h	PPAR	SD	%RSD
CAFF	0,244	0,242	0,231	0,213	0,233	0,014	6,04	0,125	0,115	0,126	0,113	0,120	0,007	5,70	0,219	0,214	0,207	0,188	0,207	0,014	6,64
EFV	4,943	4,983	4,944	4,855	4,931	0,054	1,09	3,489	3,472	3,884	3,835	3,670	0,220	5,98	3,982	3,925	3,947	3,866	3,930	0,049	1,24
THCV	0,210	0,218	0,206	0,206	0,210	0,006	2,78	0,199	0,202	0,219	0,220	0,210	0,011	5,18	0,184	0,186	0,186	0,181	0,184	0,002	1,19
CBV	0,025	0,027	0,026	0,026	0,026	0,001	2,65	0,023	0,023	0,027	0,027	0,025	0,002	9,06	0,021	0,023	0,023	0,023	0,022	0,001	3,24
CBCM	0,086	0,089	0,083	0,085	0,086	0,003	2,98	0,079	0,081	0,090	0,089	0,085	0,006	6,69	0,075	0,075	0,076	0,075	0,075	0,000	0,32
NVP	2,378	2,368	2,222	2,186	2,288	0,099	4,31	1,883	1,888	2,014	1,958	1,936	0,062	3,22	1,929	1,895	1,891	1,820	1,884	0,046	2,42
Δ^9THC	3,046	3,173	2,947	3,021	3,047	0,094	3,08	2,766	2,935	3,209	3,202	3,028	0,216	7,14	2,680	2,751	2,766	2,783	2,745	0,045	1,65
ACOD	0,079	0,072	0,075	0,065	0,073	0,006	7,93	0,046	0,042	0,051	0,048	0,047	0,004	8,18	0,068	0,064	0,063	0,065	0,065	0,002	3,20
CBN	0,252	0,260	0,248	0,245	0,251	0,006	2,59	0,191	0,200	0,253	0,241	0,221	0,030	13,70	0,210	0,208	0,225	0,222	0,216	0,009	3,94
6-MAM	0,420	0,441	0,444	0,437	0,435	0,011	2,49	0,241	0,241	0,282	0,259	0,256	0,019	7,62	0,312	0,314	0,316	0,318	0,315	0,002	0,79
HER	0,670	0,675	0,655	0,636	0,659	0,018	2,66	0,307	0,300	0,345	0,334	0,322	0,022	6,69	0,564	0,553	0,567	0,570	0,563	0,007	1,28
			S16							S17							S18				
	0	24 h	48 h	72 h	PPAR	SD	%RSD	0	24 h	48 h	72 h	PPAR	SD	%RSD	0	24 h	48 h	72 h	PPAR	SD	%RSD
CAFF	0,157	0,147	0,153	0,139	0,149	0,008	5,25	0,210	0,207	0,213	0,196	0,207	0,008	3,76	0,177	0,169	0,180	0,165	0,173	0,007	4,03
EFV	3,669	3,412	3,735	3,619	3,609	0,140	3,87	5,473	5,474	5,540	5,410	5,474	0,053	0,97	4,137	4,190	4,714	4,682	4,430	0,309	6,99
THCV	0,203	0,189	0,199	0,199	0,198	0,006	3,09	0,208	0,220	0,221	0,218	0,217	0,006	2,82	0,179	0,191	0,208	0,206	0,196	0,014	7,00
CBV	0,027	0,023	0,026	0,026	0,026	0,002	6,13	0,024	0,025	0,027	0,026	0,026	0,001	4,28	0,018	0,022	0,026	0,025	0,023	0,004	15,97
CBCM	0,099	0,093	0,101	0,096	0,097	0,003	3,46	0,084	0,094	0,095	0,093	0,091	0,005	5,49	0,072	0,077	0,086	0,085	0,080	0,007	8,59
NVP	2,042	1,880	1,980	1,886	1,947	0,078	4,00	1,548	1,556	1,534	1,464	1,525	0,042	2,76	1,656	1,689	1,785	1,749	1,720	0,058	3,38
Δ^9THC	3,161	3,021	3,206	3,127	3,129	0,079	2,52	3,083	3,209	3,196	3,194	3,171	0,059	1,85	2,664	2,864	3,114	3,157	2,950	0,230	7,80
ACOD	0,059	0,054	0,056	0,056	0,056	0,002	3,61	0,054	0,058	0,078	0,065	0,064	0,010	16,06	0,052	0,057	0,058	0,055	0,056	0,003	5,22
CBN	0,239	0,217	0,256	0,238	0,238	0,016	6,66	0,244	0,250	0,255	0,250	0,250	0,004	1,75	0,188	0,198	0,234	0,242	0,216	0,027	12,39
6-MAM	0,332	0,312	0,337	0,319	0,325	0,011	3,47	0,394	0,411	0,440	0,413	0,414	0,019	4,60	0,277	0,282	0,315	0,311	0,296	0,019	6,57
HER	0,429	0,391	0,421	0,409	0,413	0,016	3,97	0,609	0,596	0,619	0,591	0,603	0,013	2,11	0,443	0,444	0,488	0,492	0,467	0,027	5,82

APPENDIX VIII Chromatograms showing the comparison of samples for S1, S17 and S14 respectively at t= 0, 24, 48 and 72 hours.

APPENDIX VIII-a: ***Chromatograms showing the comparison of samples for S1, S17 and S14 respectively at t=0 where identifications were (2.582) caryophyllene, (3.135) phenacetin, (3.536) caffeine, (4.543) efavirenz, (5.242) tetrahydrocannabivarin, (5.429) tetracosane IS, (5.733) cannabichromene, (5.948) nevirapine, (6.234) Δ⁹-THC, (6.411) cannabigerol, (6.520) cannabinol, (7.020) diamorphine, (7.520) nonacosane, (9.454) unknown, in the first chromatogram (S1)***

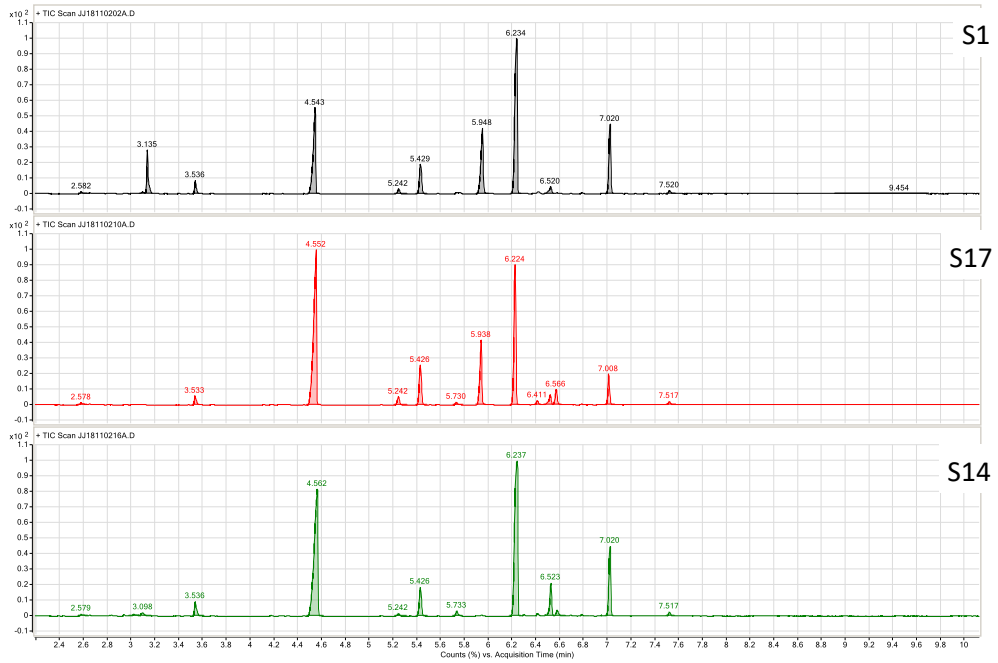

APPENDIX VIII-b: ***Chromatograms showing the comparison of samples for S1, S17 and S14 respectively at t = 24 hours Chromatograms showing the samples for S1, S17 and S14 respectively at t=0 where identifications were (2.582) caryophyllene, (3.135) phenacetin, (3.536) caffeine, (4.543) efavirenz, (5.242) tetrahydrocannabivarin, (5.429) tetracosane IS, (5.733) cannabichromene, (5.948) nevirapine, (6.234) Δ⁹-THC, (6.411) cannabigerol, (6.520) cannabinol, (7.020) diamorphine, (7.520) nonacosane, (9.454) unknown, in the first chromatogram (S1).***

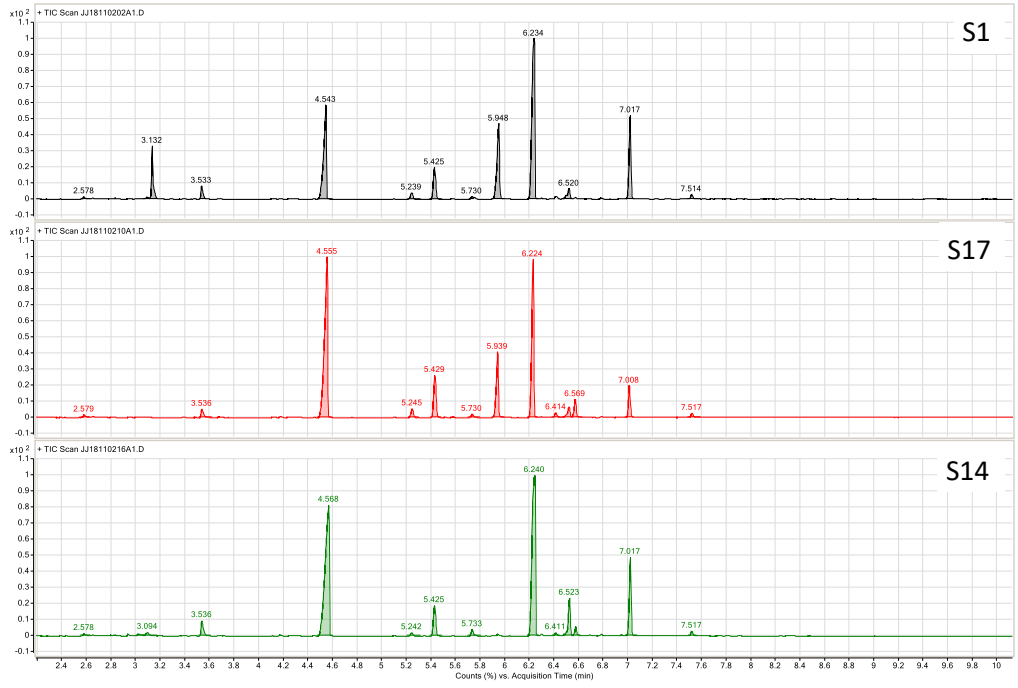

APPENDIX VIII-c: ***Chromatograms showing the comparison of samples for S1, S17 and S14 respectively at t = 48 hours Chromatograms showing the samples for S1, S17 and S14 respectively at t=0 where identifications were (2.582) caryophyllene, (3.135) phenacetin, (3.536) caffeine, (4.543) efavirenz, (5.242) tetrahydrocannabivarin, (5.429) tetracosane IS, (5.733) cannabichromene, (5.948) nevirapine, (6.234) Δ^9-THC, (6.411) cannabigerol, (6.520) cannabinol, (7.020) diamorphine, (7.520) nonacosane, (9.454) unknown, in the first chromatogram (S1).***

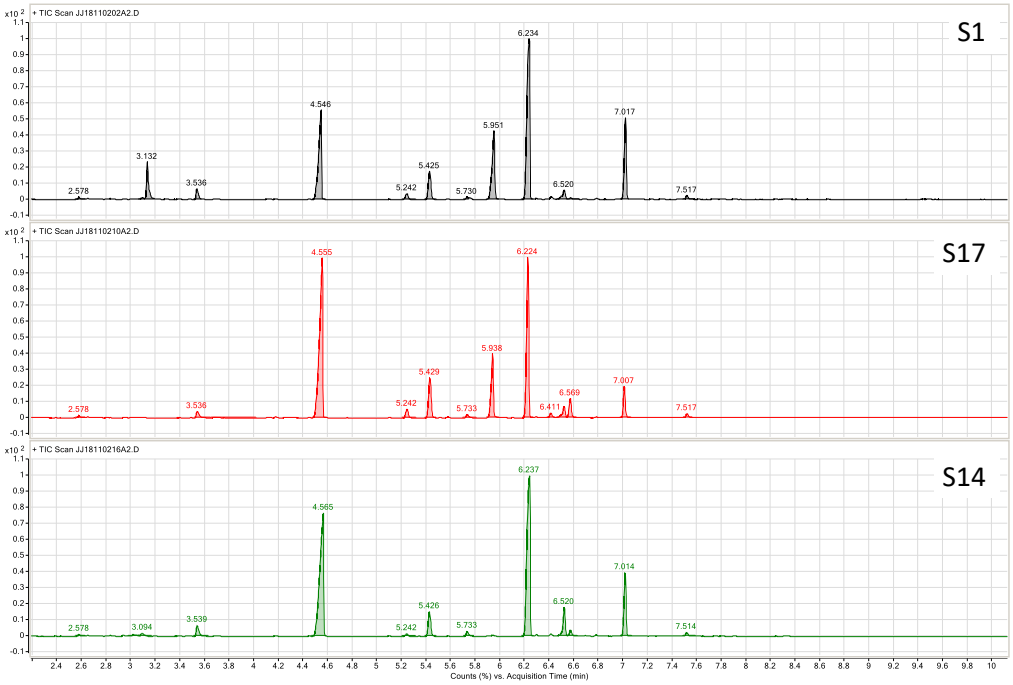

APPENDIX VIII-d: ***Chromatograms showing the comparison of samples for S1, S17 and S14 respectively at t = 72 hours where identifications were (2.582) caryophyllene, (3.135) phenacetin, (3.536) caffeine, (4.543) efavirenz, (5.242) tetrahydrocannabivarin, (5.429) tetracosane IS, (5.733) cannabichromene, (5.948) nevirapine, (6.234) Δ^9-THC, (6.411) cannabigerol, (6.520) cannabinol, (7.020) diamorphine, (7.520) nonacosane, (9.454) unknown, In the first chromatogram (S1).***

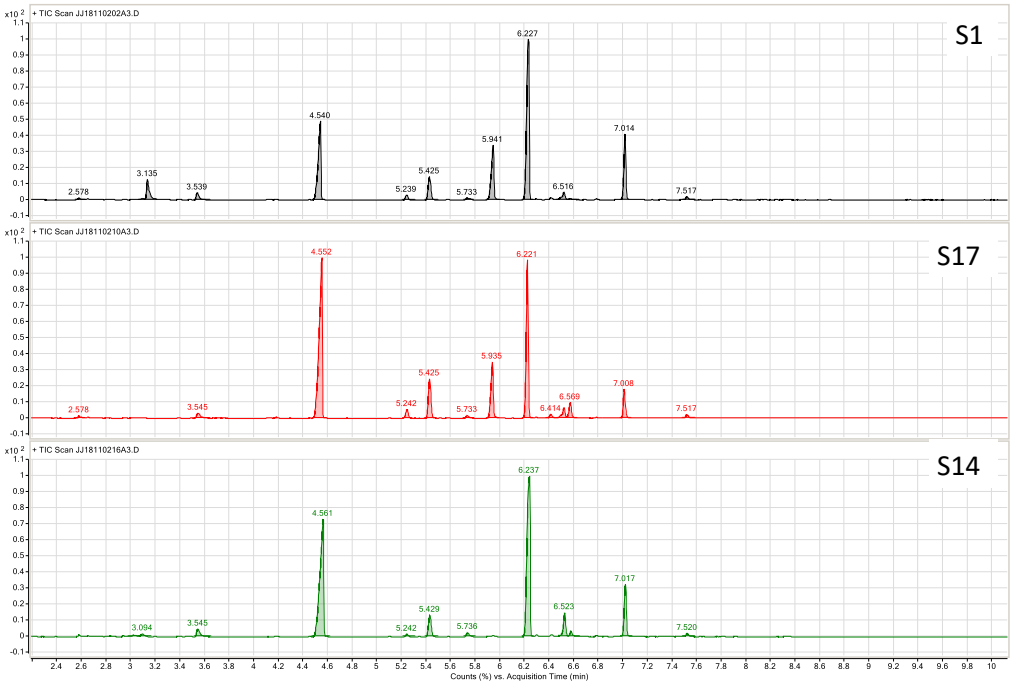

APPENDIX IX Chromatograms showing the within batch comparison of the samples from the different batches at t = 0.

APPENDIX IX-a: ***Chromatograms showing the comparison of the samples S1, S7, S13, S12, S6 and S2 respectively within the same batch at t=0 where (2.582) caryophyllene, (3.135) phenacetin, (3.536) caffeine, (4.543), efavirenz, (5.242) tetrahydrocannabivarin, (5.429) tetracosane IS, (5.733) cannabichromene, (5.948) nevirapine, (6.234) Δ^9-THC, (6.520) cannabinol, (7.02) diamorphine, (7.520) nonacosane and (9.454) unknown in the first chromatogram (S1).***

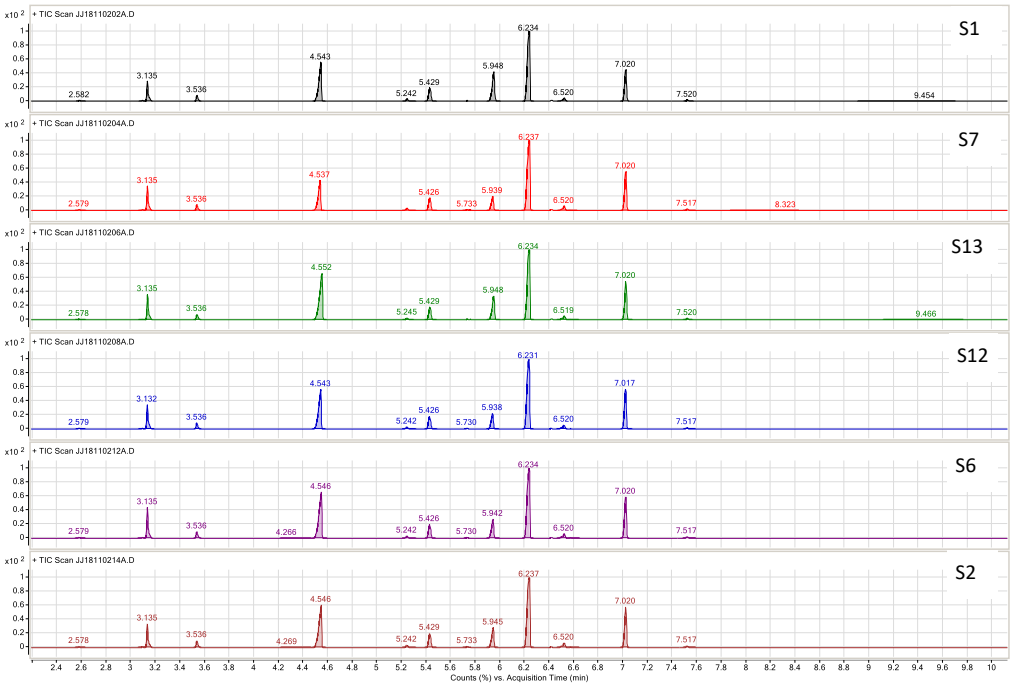

APPENDIX IX-b: ***Chromatograms showing the comparison of the samples S17, S18, S9, S16, S10 and S4 respectively within the same batch at t=0 within where caryophyllene, (3.533) caffeine, (4.552) efavirenz, (5.242) tetrahydrocannabivarin, (5.426) tetracosane IS, (5.730) cannabichromene, (5.938) nevirapine, (6.224) Δ^9-THC, (6.411) cannabigerol, (6.523) cannabinol, (6.566) 6-monoacetylmorphine, (7.008) diamorphine and (7.517) nonacosane in the first chromatogram (S17).***

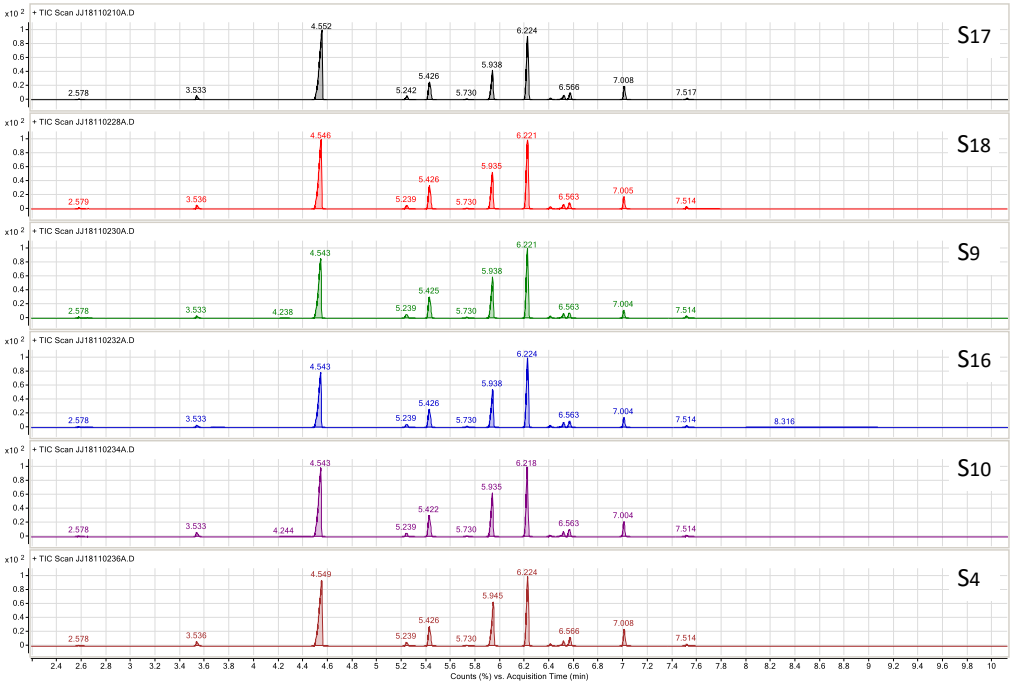

APPENDIX IX-c: ***Chromatograms showing samples S14, S8, S11, S15, S5 and S3 respectively at t=0 where (2.579) caryophyllene, (3.098) bulnesol, (3.536) caffeine, (4.562) efavirenz, (5.242) tetrahydrocannabivarin, (5.426) tetracosane IS, (5.733) cannabichromene, (6.237) Δ^9-THC, (6.411) cannabigerol, (6.523) cannabinol, (6.576) 6-monoacetylmorphine, (7.020) diamorphine and (7.517) nonacosane in the first chromatogram (S14).***

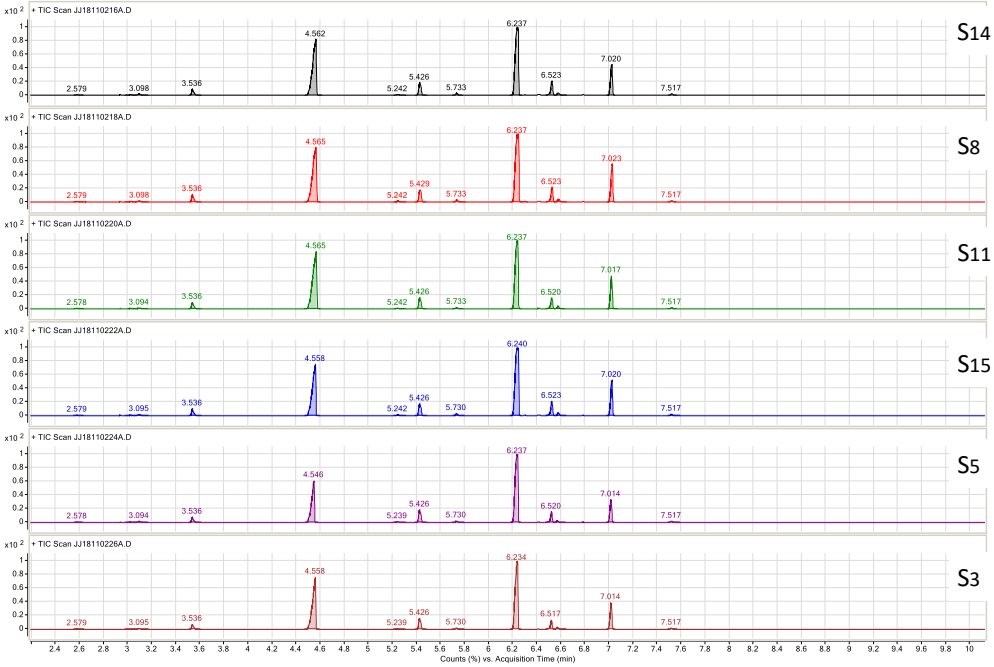

APPENDIX X Chromatograms comparing samples of S1 after 0, 24, 48 and 72 hours respectively.

APPENDIX X-a: ***Chromatograms comparing samples of S1 after 0, 24, 48 and 72 hours respectively where identification were (2.582) caryophyllene, (3.135) phenacetin, (3.536) caffeine, (4.543), efavirenz, (5.242) tetrahydrocannabivarin, (5.429) tetracosane IS, (5.733) cannabichromene, (5.948) nevirapine, (6.234) Δ^9-THC, (6.520) cannabinol, (7.02) diamorphine, (7.520) nonacosane and (9.454) in the first chromatogram (t=0)***

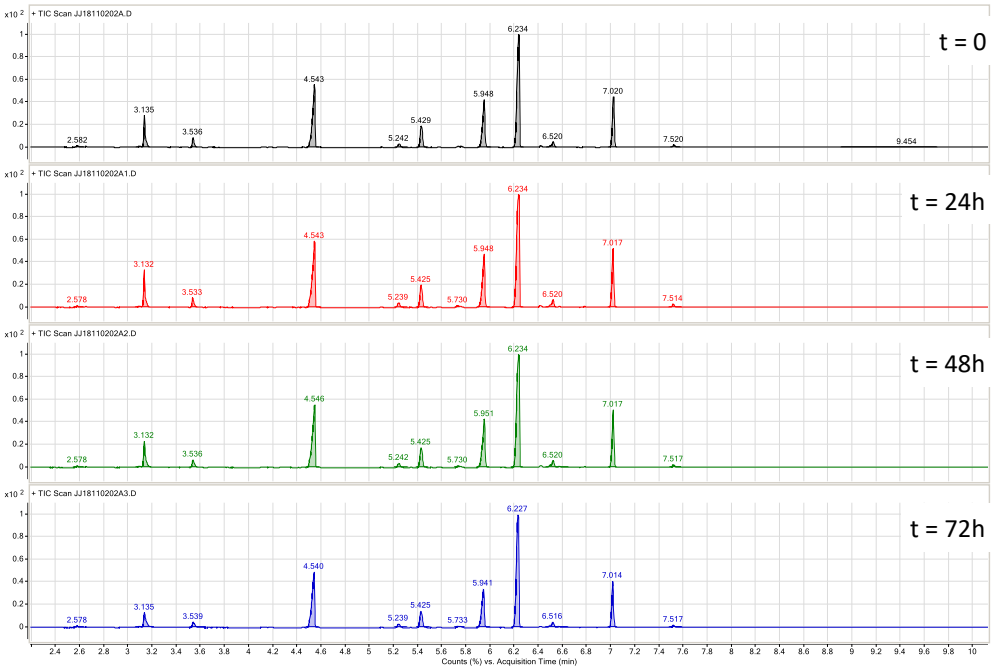

APPENDIX X-b: ***Chromatograms comparing samples of S17 after 0, 24, 48 and 72 hours respectively where identification were (2.578) caryophyllene, (3.533) caffeine, (4.552) efavirenz, (5.242) tetrahydrocannabivarin, (5.426) tetracosane IS, (5.730) cannabichromene, (5.938) nevirapine, (6.224) Δ⁹-THC, (6.411) cannabigerol, (6.523) cannabinol, (6.566) 6-monoacetylmorphine, (7.008) diamorphine and (7.517) nonacosane in the first chromatogram (t=0).***

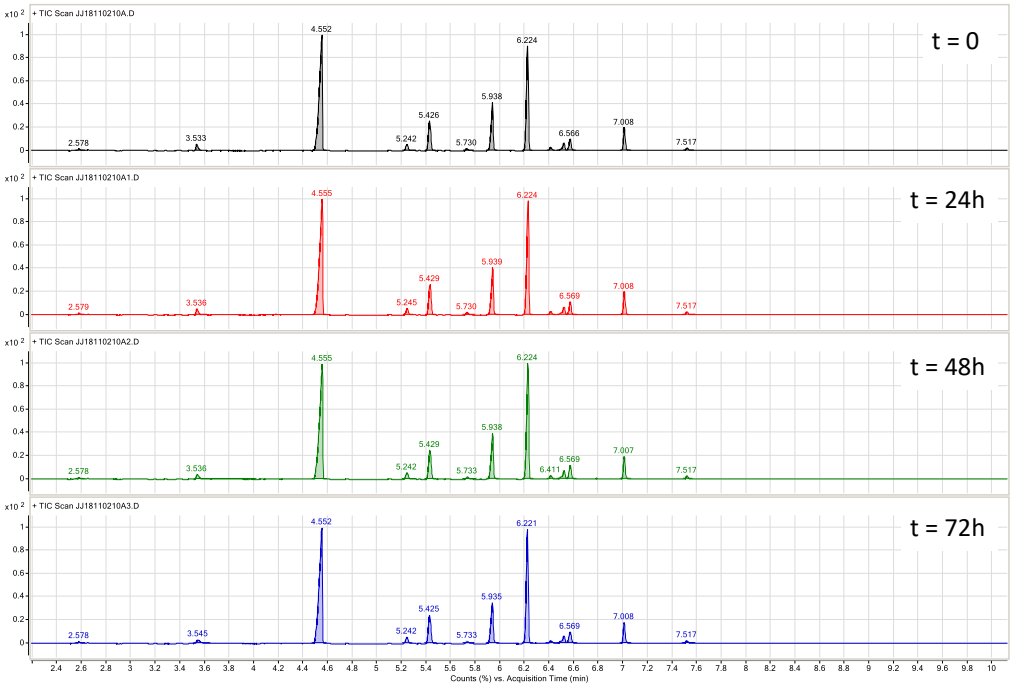

APPENDIX X-c: ***Chromatograms comparing samples of S14 after 0, 24, 48 and 72 hours respectively where identification were (2.579) caryophyllene, (3.098) bulnesol, (3.536) caffeine, (4.562) efavirenz, (5.242) tetrahydrocannabivarin, (5.426) tetracosane IS, (5.733) cannabichromene, (6.237) Δ⁹-THC, (6.411) cannabigerol, (6.523) cannabinol, (6.571) 6-monoacetylmorphine, (7.02) diamorphine and (7.17) nonacosane in the first chromatogram (t=0).***

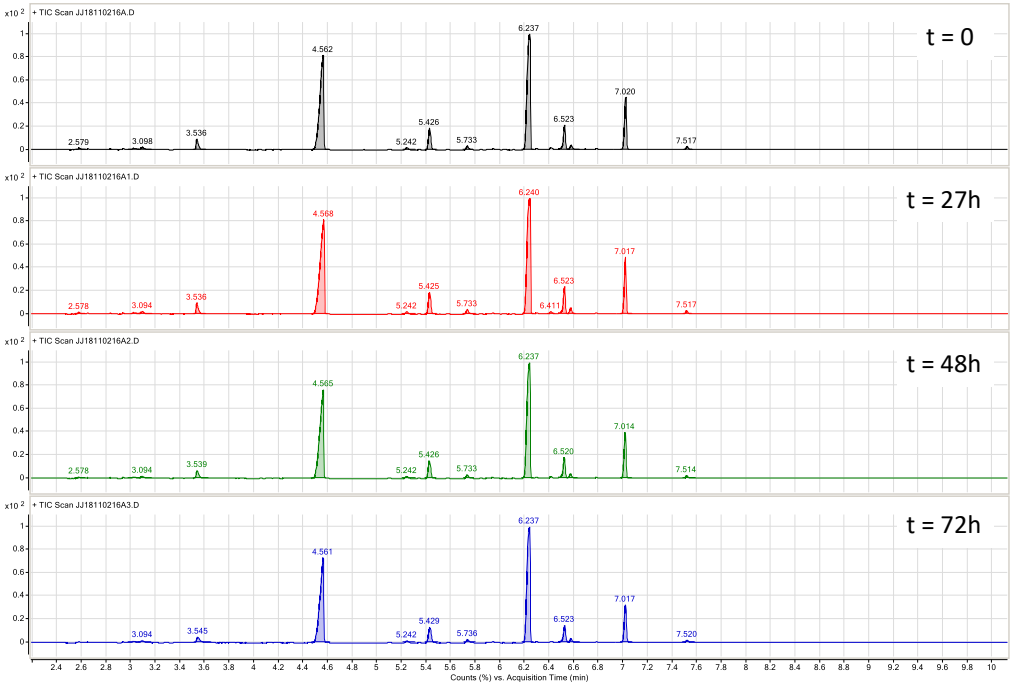

APPENDIX XI Average peak area ratios and the pooled average peak area ratios of the individual components in the 15 sub-samples from the 5 actual seized street nyaope samples at t = 0, 24, 48 and 72 hours of autosampler storage.

APPENDIX XI-a: PAR and the PPAR of the individual components in the actual seized street nyaope samples A1, A2, A3, B1, B2 and B3 at t = 0, 24, 48 and 72 hours of autosampler storage.

			A1							A2							A3				
	0	24 h	48 h	72 h	PPAR	SD	%RSD	0	24 h	48 h	72 h	PPAR	SD	%RSD	0	24 h	48 h	72 h	PPAR	SD	%RSD
NCT	0,077	0,117	0,105	0,074	0,093	0,021	22,59	0,097	0,085	0,080	0,061	0,081	0,015	18,63	0,081	0,082	0,065	0,097	0,081	0,013	15,96
ACA	0,193	0,241	0,085	0,200	0,180	0,066	36,94	0,056	0,141	0,200	0,080	0,119	0,065	54,30	0,251	0,179	0,065	0,185	0,170	0,077	45,44
CAFF	0,288	0,292	0,284	0,264	0,282	0,012	4,38	0,291	0,288	0,286	0,258	0,281	0,015	5,43	0,308	0,297	0,273	0,288	0,292	0,015	5,11
THCV	1,464	1,446	1,576	1,230	1,429	0,144	10,11	1,487	1,487	1,573	1,244	1,448	0,142	9,78	1,480	1,464	1,520	1,404	1,467	0,048	3,28
CBV	0,137	0,143	0,165	0,109	0,139	0,023	16,67	0,147	0,154	0,170	0,117	0,147	0,022	15,13	0,163	0,154	0,160	0,149	0,156	0,006	3,90
Δ^9-THC	13,089	12,655	12,850	11,073	12,417	0,913	7,35	13,481	13,456	13,067	11,171	12,794	1,098	8,58	13,395	13,192	12,749	12,260	12,899	0,505	3,91
ACOD	0,279	0,262	0,222	0,203	0,241	0,035	14,55	0,309	0,268	0,264	0,211	0,263	0,040	15,24	0,282	0,209	0,289	0,258	0,259	0,036	13,91
CBN	1,057	1,045	1,213	0,880	1,049	0,136	13,00	1,134	1,088	1,189	0,862	1,068	0,143	13,43	1,184	1,174	1,131	1,065	1,138	0,054	4,74
6-MAM	1,653	1,576	1,744	1,437	1,602	0,130	8,12	1,604	1,596	1,679	1,359	1,560	0,139	8,92	1,699	1,673	1,701	1,626	1,675	0,035	2,08
DAM	0,544	0,533	0,573	0,453	0,526	0,051	9,75	0,510	0,505	0,492	0,376	0,471	0,064	13,56	0,543	0,557	0,523	0,500	0,531	0,025	4,66
			B1							B2							B3				
	0	24 h	48 h	72 h	PPAR	SD	%RSD	0	24 h	48 h	72 h	PPAR	SD	%RSD	0	24 h	48 h	72 h	PPAR	SD	%RSD
NCT	0,224	0,248	0,237	0,234	0,236	0,010	4,27	0,226	0,213	0,229	0,216	0,221	0,008	3,56	0,242	0,244	0,244	0,234	0,241	0,005	2,09
CAFF	0,041	0,054	0,060	0,038	0,048	0,010	21,44	0,031	0,048	0,054	0,046	0,045	0,010	21,46	0,062	0,062	0,073	0,064	0,065	0,005	7,89
MTQ	0,118	0,114	0,123	0,114	0,117	0,004	3,80	0,113	0,106	0,112	0,098	0,107	0,007	6,54	0,137	0,126	0,135	0,129	0,132	0,005	4,07
CAFF	0,297	0,291	0,312	0,273	0,293	0,016	5,57	0,262	0,262	0,267	0,258	0,262	0,004	1,50	0,293	0,286	0,296	0,278	0,288	0,008	2,83
CBV	0,146	0,147	0,155	0,138	0,146	0,007	4,98	0,133	0,137	0,136	0,129	0,134	0,003	2,61	0,144	0,149	0,150	0,145	0,147	0,003	2,07
Δ^9-THC	3,131	3,087	3,209	2,839	3,067	0,159	5,20	2,884	2,855	2,836	2,756	2,833	0,055	1,93	3,136	3,069	3,133	2,917	3,063	0,103	3,35
CBN	1,964	1,930	1,890	1,745	1,882	0,096	5,11	1,773	1,800	1,779	1,714	1,767	0,037	2,10	1,891	2,004	1,887	1,841	1,906	0,069	3,63

APPENDIX XI-b: PAR and the PPAR of the individual components in the actual seized street nyaope samples C1, C2 and C3 at t = 0, 24, 48 and 72 hours of autosampler storage.

			C1							C2							C3				
	0	24 h	48 h	72 h	PPAR	SD	%RSD	0	24 h	48 h	72 h	PPAR	SD	%RSD	0	24 h	48 h	72 h	PPAR	SD	%RSD
NIC	0,012	0,008	0,008	0,008	0,009	0,002	23,74	0,014	0,013	0,013	0,012	0,013	0,001	5,80	0,017	0,024	0,017	0,019	0,019	0,003	17,54
CAFF	1,010	0,961	0,996	0,954	0,980	0,027	2,77	1,303	1,309	1,246	1,252	1,277	0,033	2,58	1,528	1,524	1,514	1,365	1,483	0,079	5,31
COC	0,103	0,094	0,101	0,102	0,100	0,004	4,28	0,110	0,113	0,104	0,101	0,107	0,005	4,99	0,204	0,206	0,203	0,186	0,200	0,009	4,65
THCV	0,061	0,053	0,066	0,059	0,060	0,006	9,21	0,087	0,080	0,088	0,077	0,083	0,005	6,33	0,089	0,098	0,101	0,077	0,091	0,011	12,02
CBV	0,021	0,023	0,024	0,022	0,023	0,001	5,52	0,027	0,030	0,034	0,033	0,031	0,003	9,87	0,031	0,035	0,035	0,028	0,032	0,003	10,39
COD	0,023	0,029	0,037	0,023	0,028	0,007	23,69	0,046	0,038	0,041	0,037	0,040	0,004	10,30	0,047	0,042	0,053	0,040	0,046	0,006	12,39
Δ^9-THC	0,957	0,854	0,947	0,886	0,911	0,049	5,40	1,172	1,136	1,156	1,107	1,143	0,028	2,45	1,265	1,285	1,361	1,105	1,254	0,107	8,56
ACOD	0,226	0,210	0,226	0,222	0,221	0,008	3,46	0,300	0,306	0,300	0,273	0,295	0,015	5,01	0,334	0,341	0,368	0,333	0,344	0,016	4,72
CBN	0,162	0,133	0,151	0,125	0,143	0,017	11,74	0,186	0,146	0,174	0,170	0,169	0,017	9,98	0,213	0,188	0,210	0,168	0,195	0,021	10,75
6-MAM	0,545	0,505	0,533	0,502	0,521	0,021	4,05	0,696	0,707	0,696	0,668	0,692	0,017	2,42	0,844	0,868	0,865	0,792	0,842	0,035	4,17
HER	3,710	3,585	3,543	3,496	3,584	0,092	2,57	4,769	4,653	4,653	4,471	4,636	0,123	2,66	5,723	5,729	5,760	4,840	5,513	0,449	8,14

APPENDIX XI-c: PAR and the PPAR of the individual components in the actual seized street nyaope samples A1, A2, A3, B1, B2 and B3 at t = 0, 24, 48 and 72 hours of autosampler storage.

			D1							D2							D3				
	0	24 h	48 h	72 h	PPAR	SD	%RSD	0	24 h	48 h	72 h	PPAR	SD	%RSD	0	24 h	48 h	72 h	PPAR	SD	%RSD
NCT	0,404	0,394	0,423	0,421	0,410	0,014	3,29	0,388	0,387	0,344	0,356	0,369	0,022	6,02	0,435	0,434	0,422	0,422	0,428	0,007	1,65
CAFF	0,586	0,637	0,505	0,797	0,631	0,123	19,51	0,532	0,566	0,540	0,775	0,603	0,115	19,11	0,536	0,566	0,527	0,759	0,597	0,109	18,32
MTQ	0,038	0,041	0,032	0,055	0,041	0,010	23,43	0,034	0,036	0,034	0,053	0,039	0,009	23,41	0,034	0,036	0,033	0,052	0,039	0,009	22,59
THCV	0,056	0,058	0,044	0,072	0,057	0,011	19,76	0,051	0,052	0,047	0,070	0,055	0,010	18,47	0,051	0,052	0,046	0,068	0,054	0,010	17,91
CBV	0,024	0,037	0,035	0,076	0,043	0,023	52,47	0,022	0,033	0,038	0,074	0,042	0,023	54,38	0,022	0,033	0,037	0,074	0,042	0,022	53,66
COD	0,015	0,013	0,010	0,014	0,013	0,002	18,81	0,014	0,012	0,010	0,014	0,012	0,002	14,52	0,014	0,011	0,010	0,014	0,012	0,002	15,15
Δ^9-THC	1,450	1,503	1,127	1,877	1,489	0,307	20,62	1,317	1,335	1,201	1,827	1,420	0,278	19,56	1,327	1,336	1,174	1,793	1,407	0,268	19,02
ACOD	0,217	0,239	0,124	0,274	0,214	0,064	30,04	0,197	0,212	0,136	0,266	0,203	0,054	26,37	0,198	0,212	0,130	0,261	0,200	0,054	26,91
CBN	0,312	0,354	0,248	0,268	0,296	0,047	16,05	0,289	0,312	0,268	0,259	0,282	0,023	8,33	0,294	0,311	0,260	0,252	0,279	0,028	9,94
6-MAM	0,262	0,221	0,156	0,372	0,253	0,091	35,92	0,233	0,199	0,168	0,364	0,241	0,086	35,75	0,234	0,202	0,163	0,359	0,239	0,085	35,52
DAM	2,540	2,719	2,194	3,320	2,693	0,471	17,49	2,305	2,413	2,346	3,224	2,572	0,437	16,99	2,321	2,412	2,288	3,159	2,545	0,412	16,21
TOCO	0,051	0,067	0,050	0,087	0,064	0,017	27,37	0,046	0,059	0,053	0,084	0,061	0,017	27,54	0,046	0,059	0,051	0,082	0,060	0,016	26,47
			E3							E2							E3				
	0	24 h	48 h	72 h	PPAR	SD	%RSD	0	24 h	48 h	72 h	PPAR	SD	%RSD	0	24 h	48 h	72 h	PPAR	SD	%RSD
NCT	0,088	0,082	0,101	0,090	0,090	0,008	8,64	0,096	0,107	0,103	0,100	0,101	0,005	4,53	0,10	0,11	0,10	0,10	0,10	0,01	5,87
CAFF	1,074	1,006	1,034	1,078	1,048	0,034	3,27	0,962	0,984	1,097	1,173	1,054	0,099	9,39	0,94	0,97	1,04	1,10	1,02	0,07	6,98
THCV	0,009	0,008	0,008	0,009	0,009	0,001	10,27	0,008	0,007	0,009	0,010	0,009	0,001	14,26	0,01	0,01	0,01	0,01	0,01	0,00	11,44
COD	0,027	0,021	0,018	0,026	0,023	0,004	16,55	0,024	0,021	0,020	0,028	0,023	0,004	16,49	0,02	0,02	0,02	0,03	0,02	0,00	15,43
Δ^9-THC	0,384	0,349	0,348	0,369	0,363	0,017	4,70	0,344	0,341	0,370	0,402	0,364	0,028	7,72	0,34	0,34	0,35	0,38	0,35	0,02	5,36
ACOD	0,348	0,314	0,310	0,313	0,321	0,018	5,69	0,312	0,306	0,329	0,341	0,322	0,016	4,88	0,31	0,30	0,31	0,32	0,31	0,01	2,36
6-MAM	0,806	0,720	0,702	0,686	0,729	0,054	7,37	0,722	0,704	0,744	0,747	0,729	0,020	2,78	0,71	0,70	0,71	0,70	0,70	0,01	0,84
DAM	3,927	3,693	3,748	3,886	3,813	0,111	2,91	3,518	3,612	3,976	4,230	3,834	0,330	8,60	3,45	3,57	3,78	3,97	3,69	0,23	6,17
TOCO	0,053	0,054	0,058	0,063	0,057	0,005	8,03	0,047	0,053	0,061	0,069	0,057	0,009	16,44	0,05	0,05	0,06	0,06	0,06	0,01	14,09

APPENDIX XII Chromatograms showing the samples for A1, B1, C1, D1 and E1 respectively at t=0, 24, 48 and 72 hours.

APPENDIX XII-a: ***Chromatograms showing the samples for A1, B1, C1, D1 and E1 respectively at t=0 where identifications were For A1: (3.194) acetaminophen, (3.564) caffeine, (5.242) tetrahydrocannabivarin, (5.429) tetracosane IS, (5.730) cannabichromene, (6.234) Δ^9-THC, (6.411) cannabigerol, (6.517) cannabinol, (6.563) 6-monoacetylmorphine, (6.681) unknown, (7.001) diamorphine and (7.514) nonacosane; For B1: (2.411) nicotine, (3.098) bulnesol, (3.616) caffeine, (4.754) methaqualone, (5.242) tetrahydrocannabivarin, (5.426) tetracosane IS, (5.575) cannabivarin, (5.733) cannabichromene, (5.935) cannabicoumaronone, (6.212) Δ^9-THC, (6.411) cannabigerol, (6.513) cannabinol, (6.681) unknown, (6.933) unknown, (7.517) nonacosane; For C1 (3.558) caffeine, (4.891) cocaine, (5.245) tetrahydrocannabivarin, (5.429) tetracosane IS, (5.736) cannabichromene, (5.935) cannabicoumaronone, (6.212) Δ^9-THC, (6.489) acetylcodeine, (6.554) 6-monoacetylmorphine, (7.004) diamorphine; For D1 (2.407) nicotine, (3.390) unknown, (3.561) caffeine, (4.198) unknown, (4.937) methaqualone, (5.242) tetrahydrocannabivarin, (5.425) tetracosane IS, (5.755) cannabidiol, (5.948) codeine, (6.209) Δ^9-THC, (6.485) acetylcodeine, (6.554) 6-monoacetylmorphine, (7.001) diamorphine, (7.520) nonacosane, (8.332) unknown, (8.683) unknown, (9.581) unknown; For E1 (2.411) nicotine, (3.396) unknown, (3.558) caffeine, (4.941) methaqualone, (5.426) tetracosane IS, (6.209) Δ^9-THC, (6.551) 6-monoacetylmorphine, (7.001) diamorphine.***

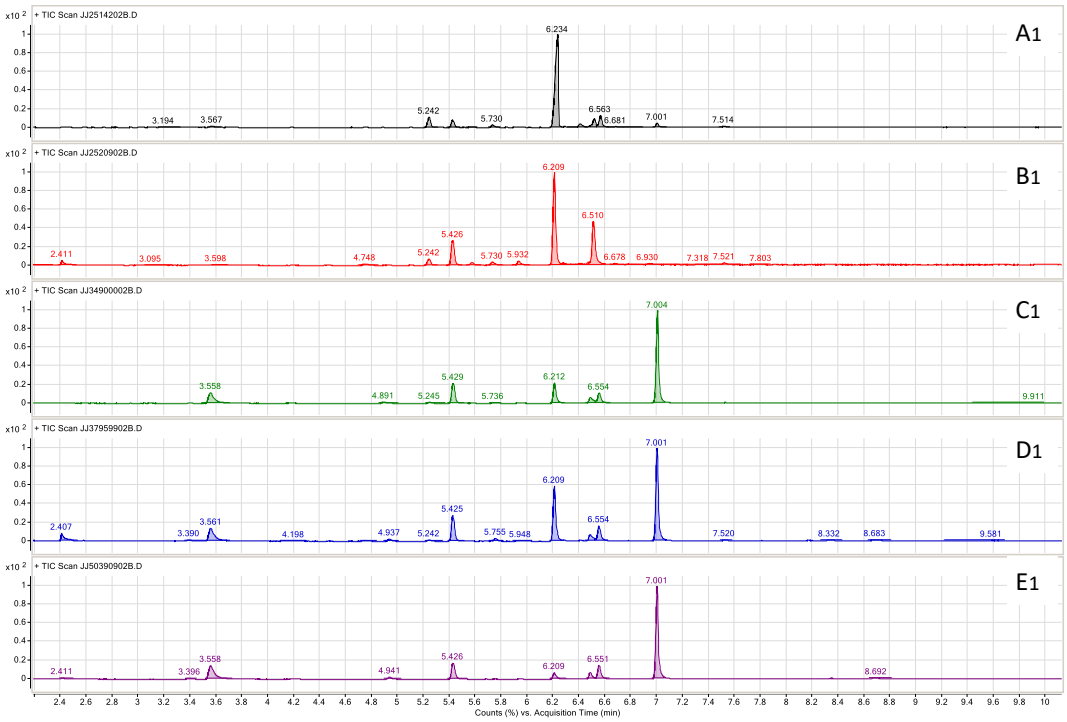

APPENDIX XII-b: Chromatograms showing the samples for A1, B1, C1, D1 and E1 respectively at t=24 hours

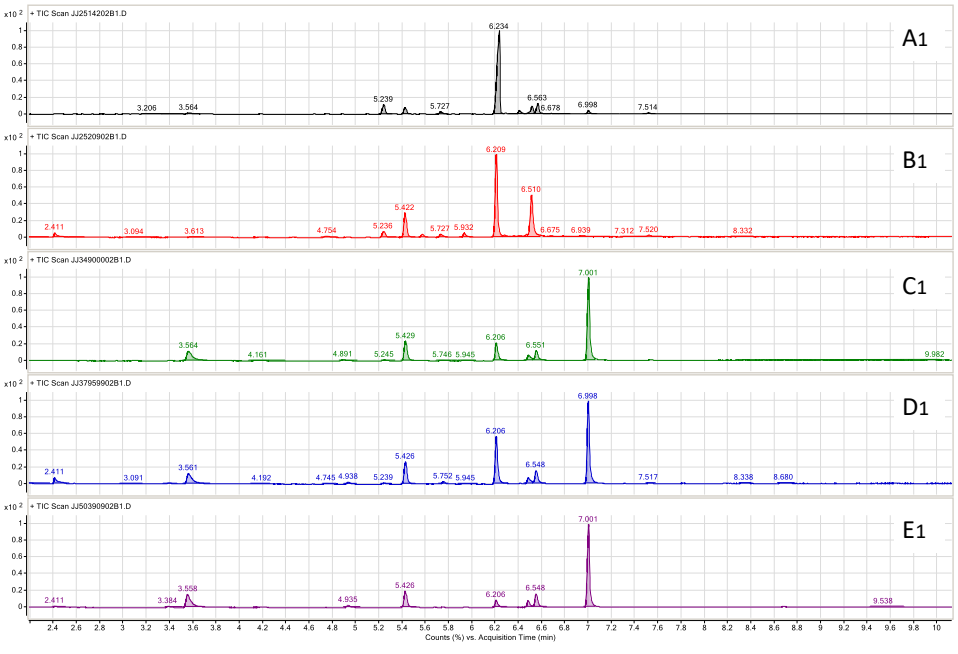

APPENDIX XII-c: Chromatograms showing the samples for A1, B1, C1, D1 and E1 respectively at t=48 hours

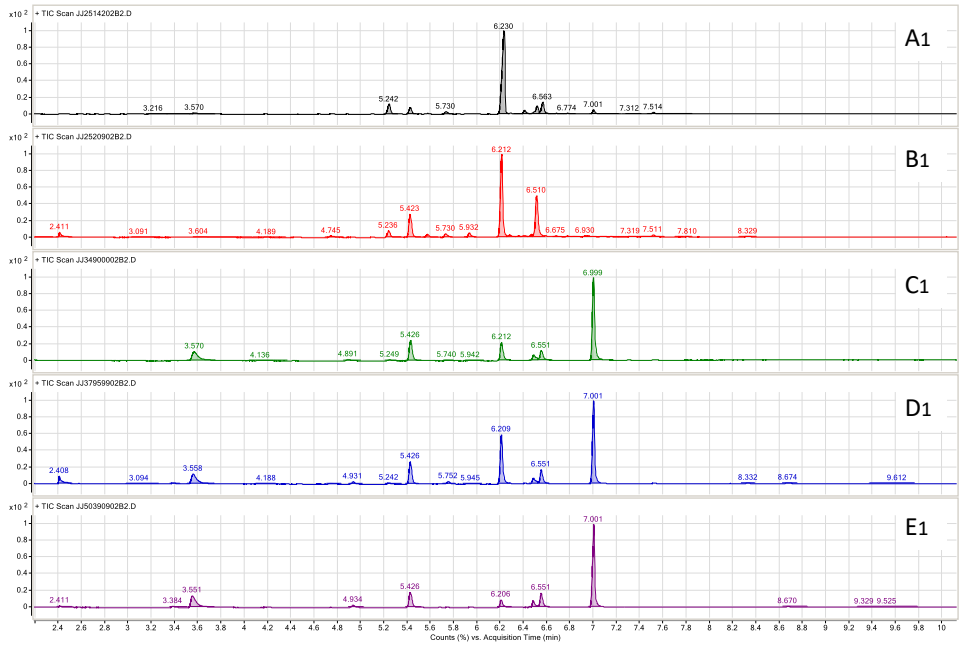

APPENDIX XII-d: Chromatograms showing the samples for A1, B1, C1, D1 and E1 respectively at t = 72 hours

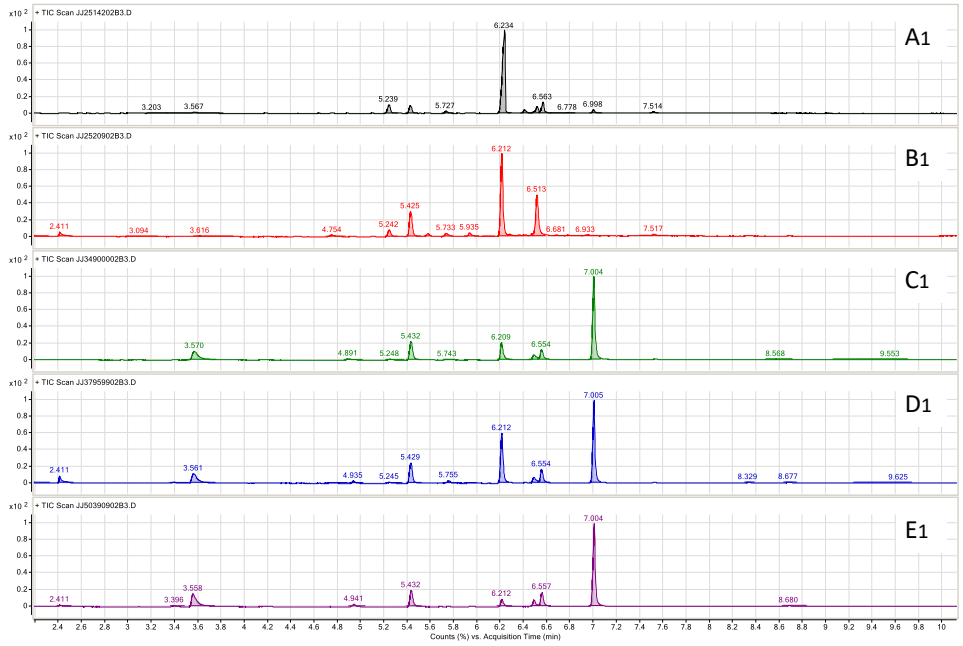

APPENDIX XIII Chromatograms showing the three sub-samples for sample A, B, C, D and E respectively at t = 0

APPENDIX XIII-a ***Chromatograms showing the three sub-samples for sample A (A1, A2, A3) at t = 0 where identifications were: (3.209) acetaminophen, (3.567) caffeine, (5.242) tetrahydrocannabivarin, (5.429) tetracosane IS, (5.733) cannabichromene, (6.234) Δ⁹-THC, (6.408) cannabigerol, (6.517) cannabinol, (6.566) 6-monoacetylmorphine, (6.681) unknown, (7.001) diamorphine and (7.517) nonacosane in the first chromatogram (A1).***

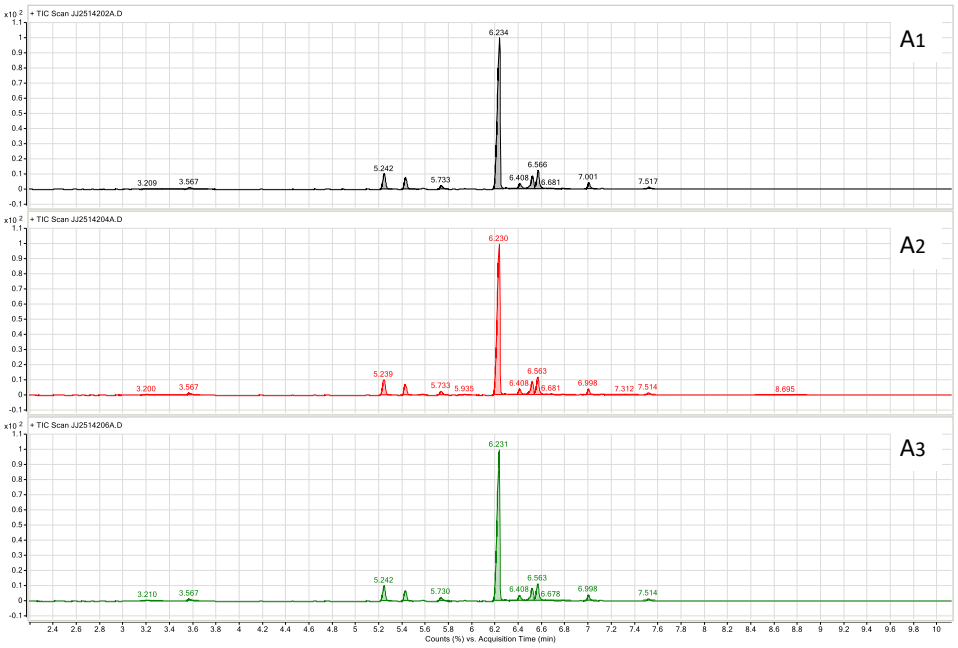

APPENDIX XIII-b: ***Chromatograms showing the three sub-samples for sample B (B1, B2, B3) at t=0 where identifications were (2.408) nicotine, (3.091) bulnesol, (3.610) caffeine, (4.748) methaqualone, (5.239) tetrahydrocannabivarin, (5.426) tetracosane IS, (5.575) cannabivarin, (5.730) cannabichromene, (5.932) cannabicoumaronone, (6.212) Δ⁹-THC, (6.411) cannabigerol, (6.510) cannabinol, (6.681) unknown, (6.933) unknown, (7.517) nonacosane in the first chromatogram (B1).***

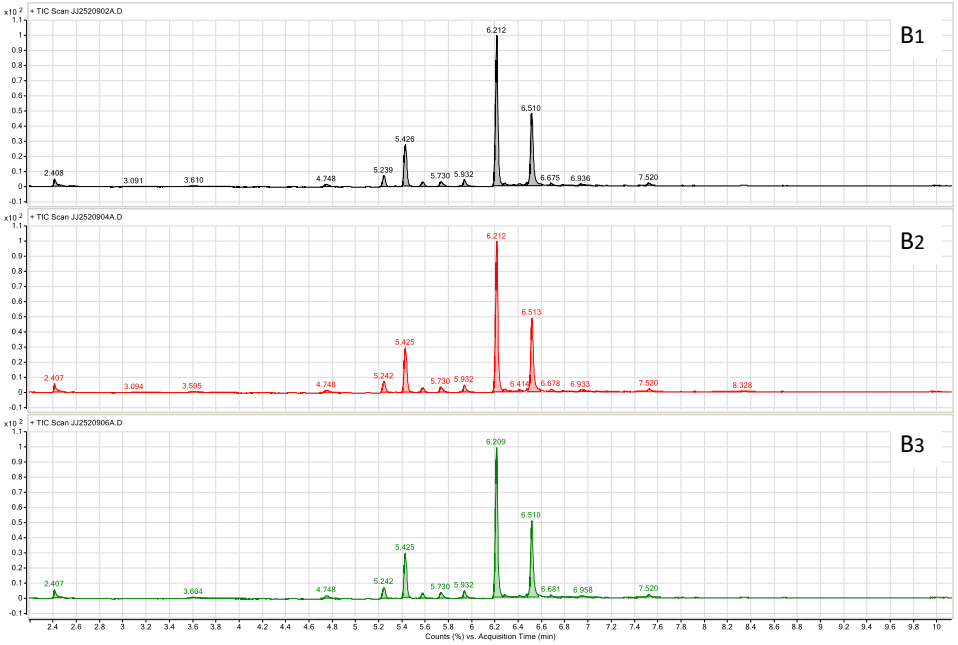

APPENDIX XIII-c: ***Chromatograms showing the three sub-samples for sample C (C1, C2, C3) at t=0 where identifications were (3.558) caffeine, (4.891) cocaine, (5.245) tetrahydrocannabivarin, (5.429) tetracosane IS, (5.736) cannabichromene, (6.212) Δ⁹-THC, (6.489) acetylcodeine, (6.554) 6-monoacetylmorphine, (7.004) diamorphine in the first chromatogram (C1).***

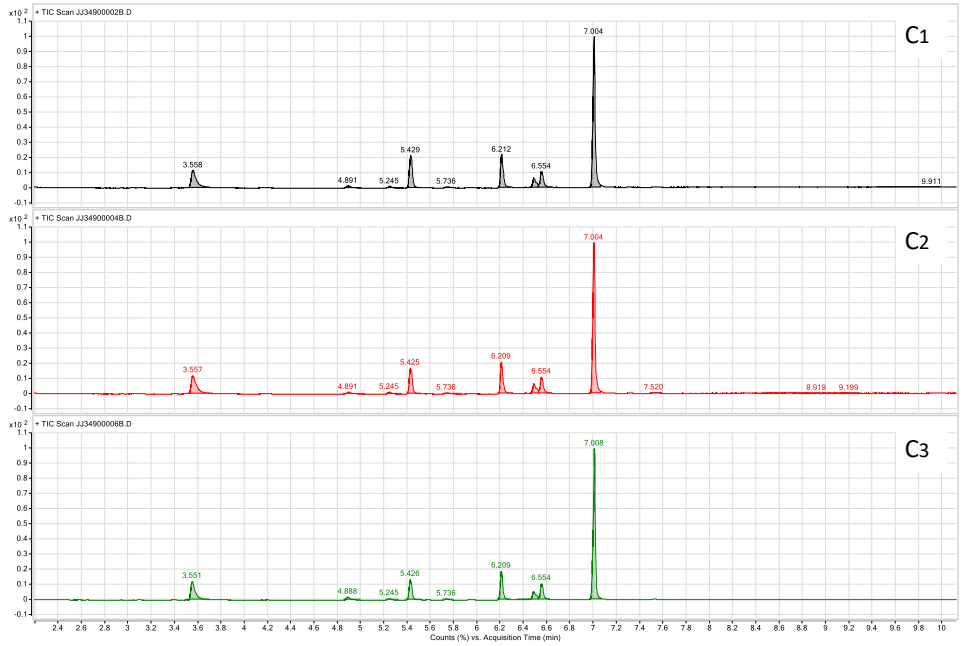

APPENDIX XIII-d: ***Chromatograms showing the three sub-samples for sample D (D1, D2, D3) at t = 0 where identifications were (2.411) nicotine, (3.091) bulnesol, (3.396) unknown, (3.561) caffeine, (4.934) methaqualone, (5.245) tetrahydrocannabivarin, (5.426) tetracosane IS, (5.755) cannabidiol, (6.209) Δ⁹-THC, (6.485) acetylcodeine, (6.551) 6-monoacetylmorphine, (7.001) diamorphine, (7.524) nonacosane, (8.338) unknown, (8.683) unknown in the first chromatogram (D1).***

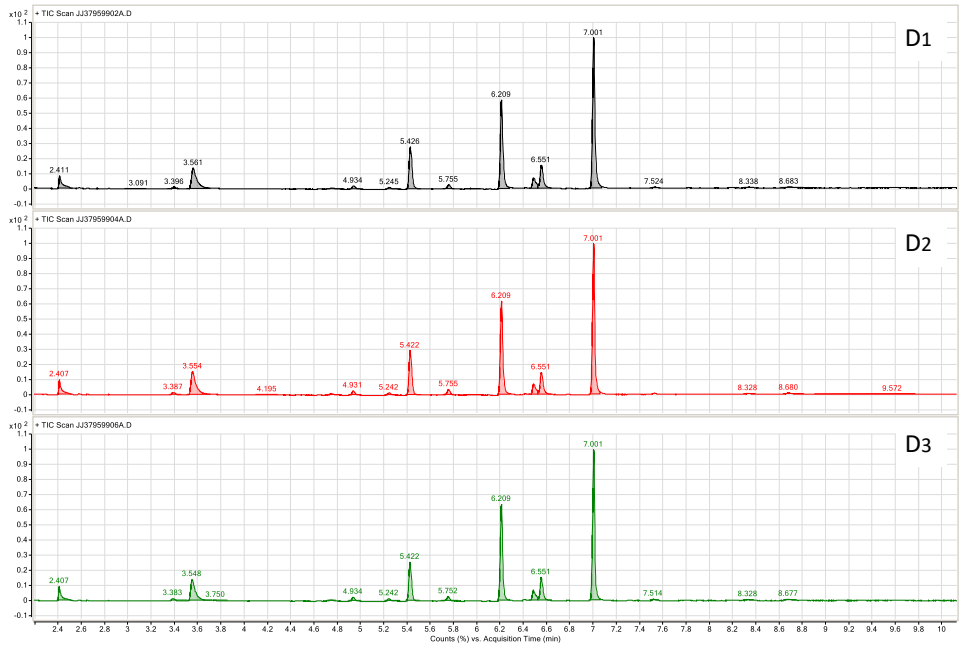

APPENDIX XIII-e: ***Chromatograms showing the three sub-samples for sample E (E1, E2, E3) at t = 0 where identifications were (2.414) nicotine, (3.399) unknown, (3.557) caffeine, (4.941) methaqualone, (5.429) tetracosane IS, (6.212) Δ^9-THC, (6.551) 6-monoacetylmorphine, (7.001) diamorphine, (8.686) unknown and (9.553) unknown in the first chromatogram (E1).***

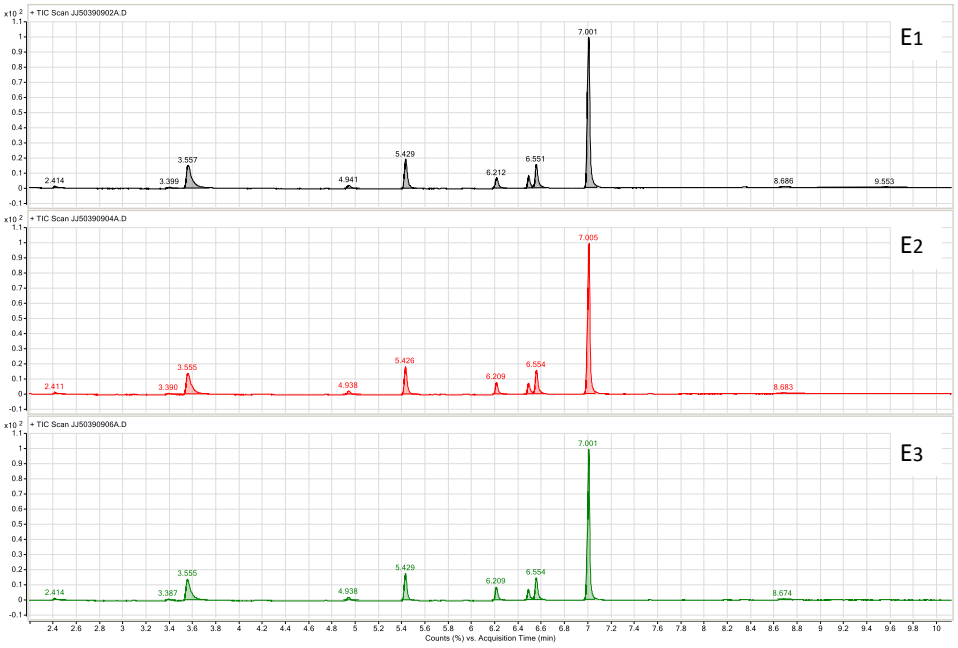

APPENDIX XIV Chromatograms for samples A, B, C, D and E after 0, 24, 48 and 72 hours respectively.

APPENDIX XIV-a: ***Chromatograms for sample A after 0, 24, 48 and 72 hours respectively where identifications were: (3.194) acetaminophen, (3.567) caffeine, (5.242) tetrahydrocannabivarin, (5.429) tetracosane IS, (5.730) cannabichromene, (6.234) Δ^9-THC, (6.408) cannabigerol, (6.517) cannabinol, (6.563) 6-monoacetylmorphine, (6.681) unknown, (7.001) diamorphine and (7.514) nonacosane in the first chromatogram (t = 0)***

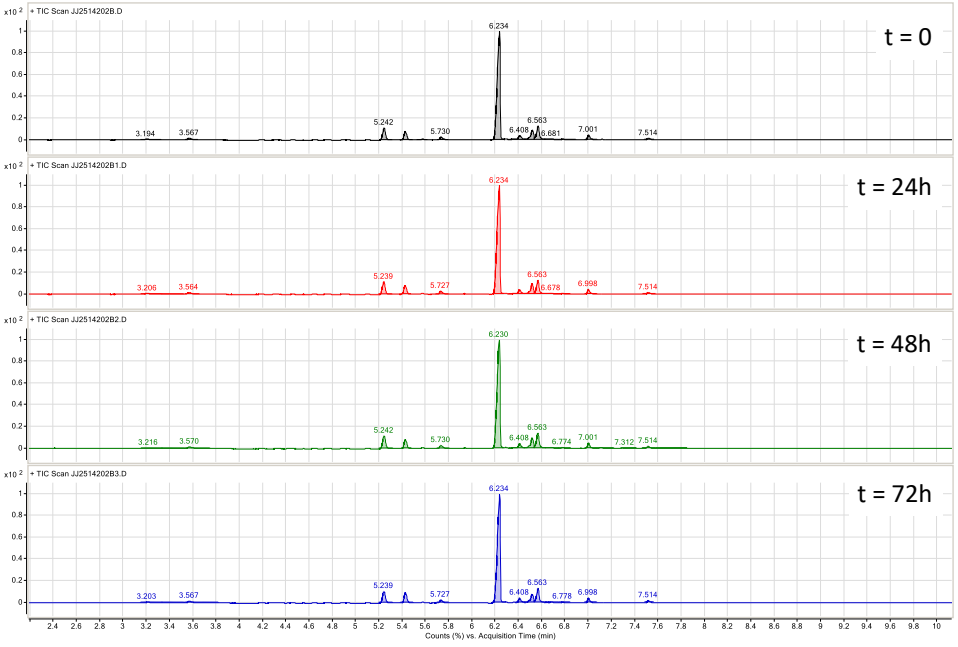

APPENDIX XIV-b: ***Chromatograms for sample B after 0, 24, 48 and 72 hours respectively where identifications were(2.411) nicotine, (3.095) bulnesol, (3.598) caffeine, (4.748) methaqualone, (5.242) tetrahydrocannabivarin, (5.426) tetracosane IS, (5.572) cannabivarin, (5.730) cannabichromene, (5.932) cannabicoumaronone, (6.212) Δ9-THC, (6.510) cannabinol, (6.678) unknown, (6.930) unknown, (7.318) unknown, (7.521) nonacosane, (7.803) unknown in the first chromatogram (t = 0).***

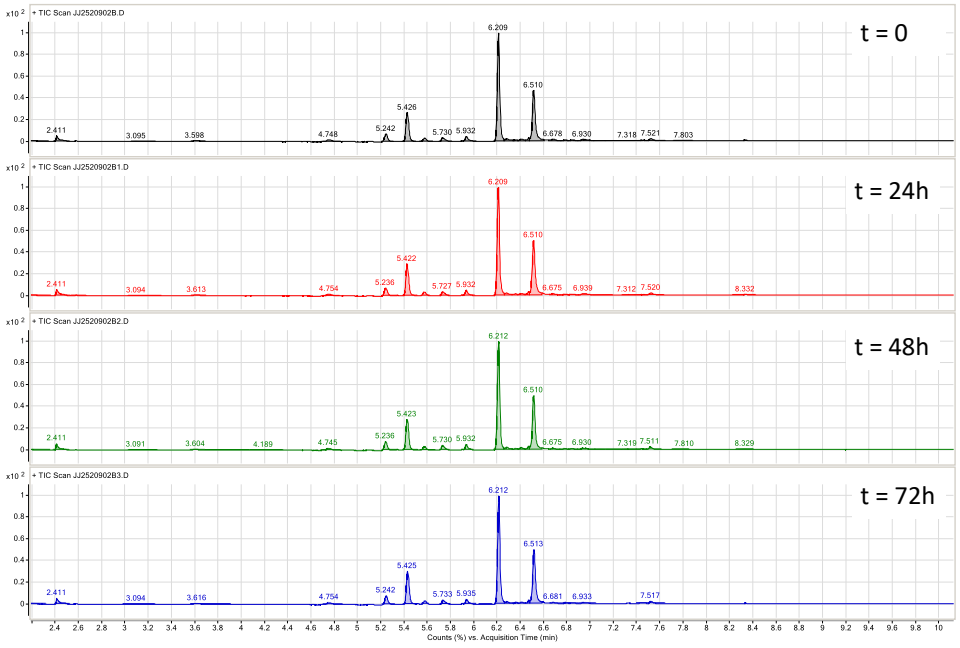

APPENDIX XIV-c: ***Chromatograms for sample C after 0, 24, 48 and 72 hours respectively where identifications were (3.558) caffeine, (4.891) cocaine, (5.245) tetrahydrocannabivarin, (5.429) tetracosane IS, (5.736) cannabichromene, (5.935) cannabicoumaronone, (6.212) Δ^9-THC, (6.489) acetylcodeine, (6.554) 6-monoacetylmorphine, (7.004) diamorphine in the first chromatogram (t = 0).***

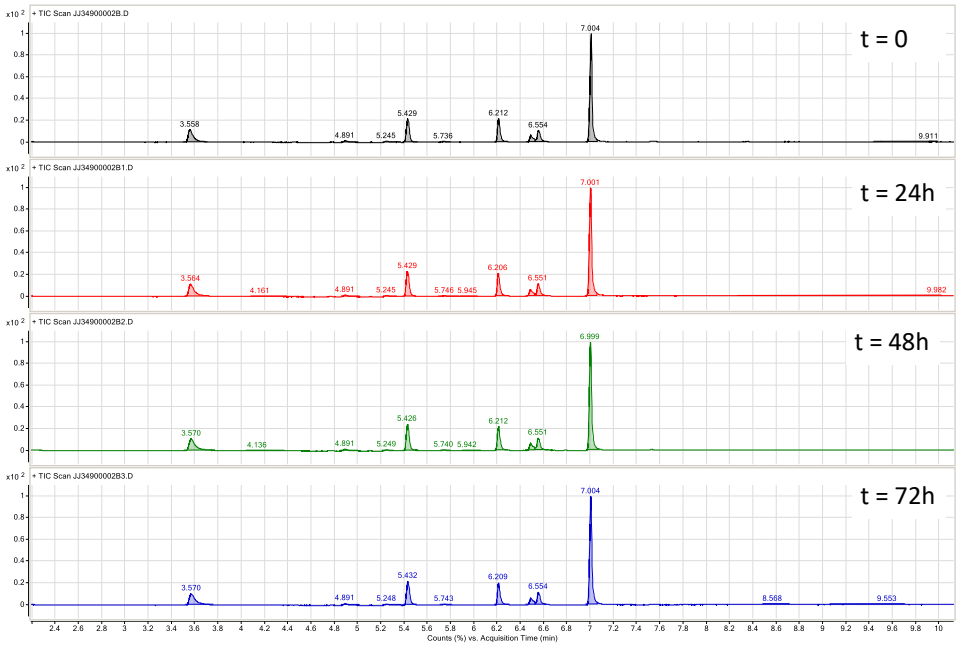

APPENDIX XIV-d: ***Chromatograms for sample D at after 0, 24, 48 and 72 hours respectively where identifications were (2.407) nicotine, (3.390) unknown, (3.561) caffeine, (4.198) unknown, (4.937) methaqualone, (5.242) tetrahydrocannabivarin, (5.425) tetracosane IS, (5.755) cannabidiol, (5.948) codeine, (6.209) Δ⁹-THC, (6.485) acetylcodeine, (6.554) 6-monoacetylmorphine, (7.001) diamorphine, (7.520) nonacosane, (8.332) unknown, (8.683) unknown, (9.581) unknown in the first chromatogram (t = 0).***

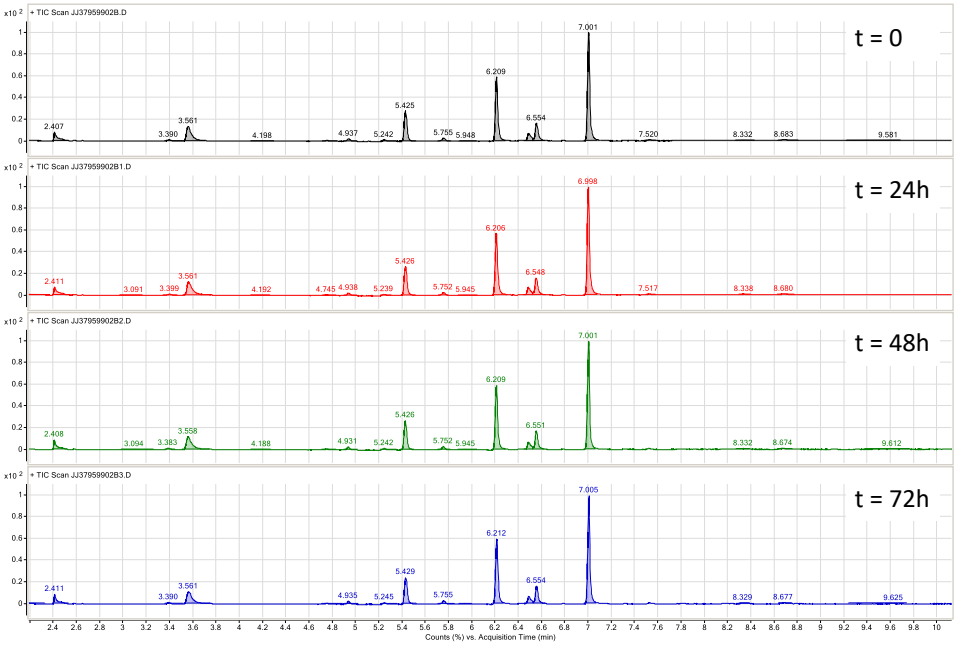

APPENDIX XIV-e: ***Chromatograms for sample E after 0, 24, 48 and 72 hours respectively where identifications were (2.411) nicotine, (3.396) unknown, (3.558) caffeine, (4.941) methaqualone, (5.426) tetracosane IS, (6.209) Δ9-THC, (6.551) 6-monoacetylmorphine, (7.001) diamorphine in the first chromatogram (t = 0).***